

# COASTAL ENVIRONMENTS

NE MASSACHUSETTS  
and  
NEW HAMPSHIRE



FIELD TRIP  
EASTERN SECTION  
SOCIETY of ECONOMIC  
PALEONTOLOGISTS and MINERALOGISTS

MAY 9 - 11, 1969

COASTAL RESEARCH GROUP  
DEPT. OF GEOLOGY  
UNIV. OF MASSACHUSETTS



CONTRIBUTION No. 1 - CRG

Geology Department  
University of Massachusetts  
Amherst, Mass.

FIELD TRIP GUIDEBOOK  
COASTAL ENVIRONMENTS OF NORTHEASTERN  
MASSACHUSETTS AND NEW HAMPSHIRE

May 9-11, 1969

by

COASTAL RESEARCH GROUP  
UNIVERSITY OF MASSACHUSETTS

Contributors:

Fayez S. Anan  
Jon C. Boothroyd  
Joan M. DaBoll  
Stewart C. Farrell  
Victor Goldsmith

Sharon A. Greer  
Allan D. Hartwell  
Miles O. Hayes  
C. Larry McCormick  
Barry S. Timson

Pleistocene Studies:

Frederick D. Larsen  
Joseph H. Hartshorn (editorial consultant)

## ACKNOWLEDGMENTS

The bulk of the work presented in this guidebook was carried out as thesis and class projects by graduate and undergraduate students of the Department of Geology, the University of Massachusetts. The work on estuaries was supported by Project No. 388-084 (Contract N00014-67-A-0230-0001) with the Office of Naval Research (Geography Branch). Work on the beaches was supported by the Coastal Engineering Research Center, U.S. Army Corps of Engineers (Contract DACW72-67-C-0004).

Permission was granted by the Parker River National Wildlife Refuge to conduct studies within the Refuge boundaries. Refuge personnel have been most helpful. The New England Division of the U.S. Army Corps of Engineers has supplied various types of information. Access to the Crane Beach area was granted by the supervisors of the Crane Beach Reservation. Art Moon, harbor master for Ipswich, was helpful with the logistics for our work in the Parker River and Essex estuaries.

In addition to the contributors to this guidebook, many students in the Department of Geology at the University have contributed generously of their time, energy, and know-how. Our special thanks go to Albert C. Hine, Robert N. Bozeman, Victoria Byrne, Eugene Rhodes, John Gifford, Walter Handy, Karl Geller, Kathryn Gray, Gail Ashley, Linda Sandanato, Paul Pinet, Peggy Losee, Philip Durgin, Dennis O'Brien, and Carl Hobbs. The help of summer field assistants Jack Cysz, Allen Mytkowitz, David Reynolds, and Greg Field is duly acknowledged.

The compilation of this guidebook would have been impossible without the expert secretarial and editorial efforts of Mrs. Judy Timson. Dick Brown and Stewart Clark contributed greatly to the task of drafting the figures. Dennis Wilkins is acknowledged for his long hours in the photo darkroom.

The encouragement and support of the Department of Geology, University of Massachusetts, including Mrs. Carol Kirkpatrick, Departmental Secretary, and Mr. James Terrell, Technical Assistant, have been very helpful in the past few years.

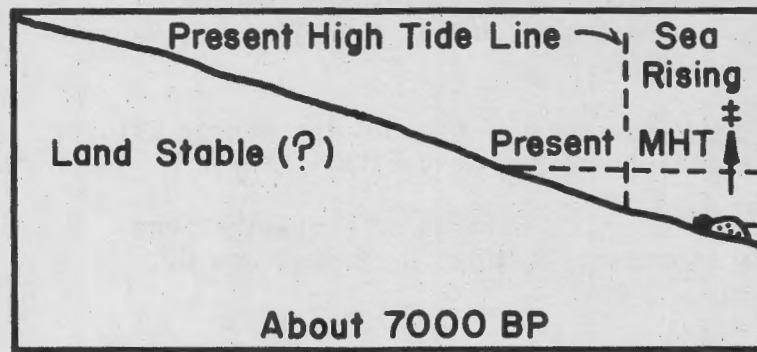
With respect to the field trip itself, Bill Forward of the Parker River National Wildlife Refuge has agreed to furnish vehicles for the first day's trip and Mr. Robert Smith, of the Massachusetts Beach Buggy Association, has helped organize our tour down Crane Beach.

## TABLE OF CONTENTS

ACKNOWLEDGEMENTS	
INTRODUCTION	1
ROAD LOG	7
First Day	7
Second Day	18
Third Day	31
STOP DESCRIPTIONS	34
1. Joppa Flat, Merrimack River Estuary	34
2. Erosion Zone, Northern Plum Island	36
3. Profile PLA	44
4. Profile PLB	50
5 & 6. Profiles PLC and PLD	58
7. Plum Island Spit	59
8a. Mussel Bank, Parker River Estuary	61
8b. Central Point Bar, Parker River Estuary	65
9. Cape Merrill	68
10. Bar Head Drumlin, South End Plum Island	73
11a. High Tide Beach	76
11b. Plum Island Dunes	78
12. Plum Island Marsh	80
13. Rye Gravel Beach, Rye, New Hampshire	82
14. Hampton Beach, N. H.	83
15. Hampton Harbor Estuary	92
16. Middle Ground, Parker River Estuary	108
17. Ebb Spit, South End of Plum Island	115
18. Essex Bay Sand Bodies, a Preliminary Report	128

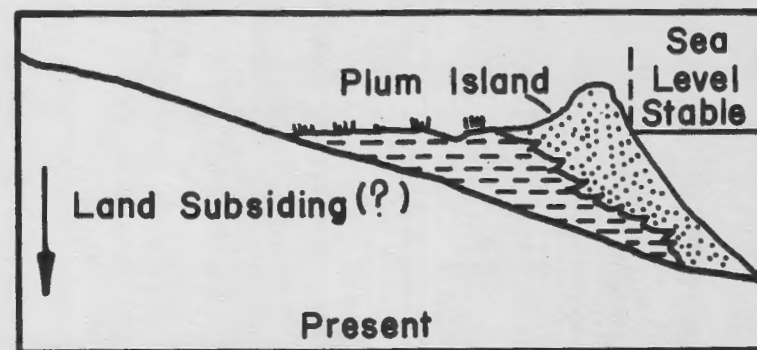
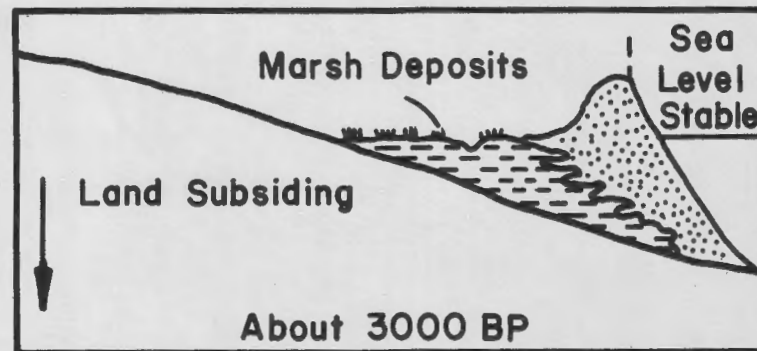
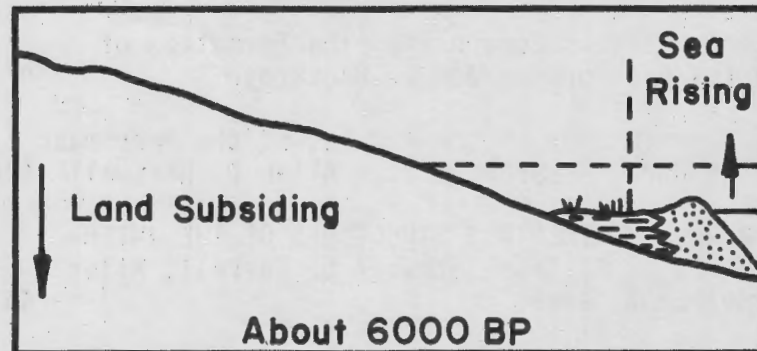
19. Crane Beach	146
20. Bull Brook Site, Paradise Road	174
21. Nourse Cemetary Grave] Pits	174
22. High Tide Hydrography, Merrimack River Estuary	176
23. Woodbridge Island Marsh	178
24. Parker River Estuary Marsh	180
25. Flights	183
26. Tidal Delta, Merrimack River Estuary	185
27. Clam Flat and Mussel Banks, Merrimack River Estuary	204
28. Woodbridge Island Point Bar	209
29. Plum Island River Point Bar	215
CONTRIBUTIONS	218
Hydrography of the Merrimack River Estuary, Massachusetts - Allan D. Hartwell and Miles O. Hayes	218
Storms as Modifying Agents in the Coastal Environment - Miles O. Hayes and Jon C. Boothroyd	245
Grain-size Parameters of the Beach and Dune Sands, Northeastern Massachusetts and New Hampshire Coasts - Fayez S. Anan	266
Offshore Bars at Plum Island, Massachusetts - Victor Goldsmith	281
Sediment Dispersal Trends in the Littoral Zone; A Problem in Paleogeographic Reconstruction - Miles O. Hayes, Fayez S. Anan, Robert N. Bozeman	290
Growth Cycle of a Small Recurved Spit, Plum Island, Massachusetts - Stewart C. Farrell	316
Holocene Sediments of the Parker River Estuary, Massachusetts - Joan M. DaBoll	337
Eolian Sand Transport on Plum Island, Massachusetts - Frederick D. Larsen	356
Holocene Stratigraphy of the Marshes at Plum Island, Massachusetts - C. Larry McCormick	368

Post-storm Profile and Particle-Size Changes of a New Hampshire Gravel Beach: A Preliminary Report - Barry S. Timson	391
Sedimentary Mineralogy of the Hampton Harbor Estuary, New Hampshire and Massachusetts - Sharon A. Greer	403
Diagnostic Primary Structures of Estuarine Sand Bodies (Abstract) - Miles O. Hayes, Jon C. Boothroyd, Albert C. Hine	415
Forms of Sand Accumulation in Estuaries (Abstract) Miles O. Hayes	416
Hydraulic Conditions Controlling the Formation of Estuarine Bed Forms - Jon C. Boothroyd	417
Holocene Stratigraphy of the Marshes of the Merrimack River Estuary, Massachusetts - Allan D. Hartwell	428
GLOSSARY OF PRIMARY SEDIMENTARY STRUCTURES OF THE INTER- TIDAL ZONE - Fayez S. Anan, Stewart C. Farrell, Miles O. Hayes, Sharon A. Greer	441
GLOSSARY OF TERMS	455
REFERENCES CITED	458



West

East



‡ Mean High Tide

FIGURE I-1

## INTRODUCTION

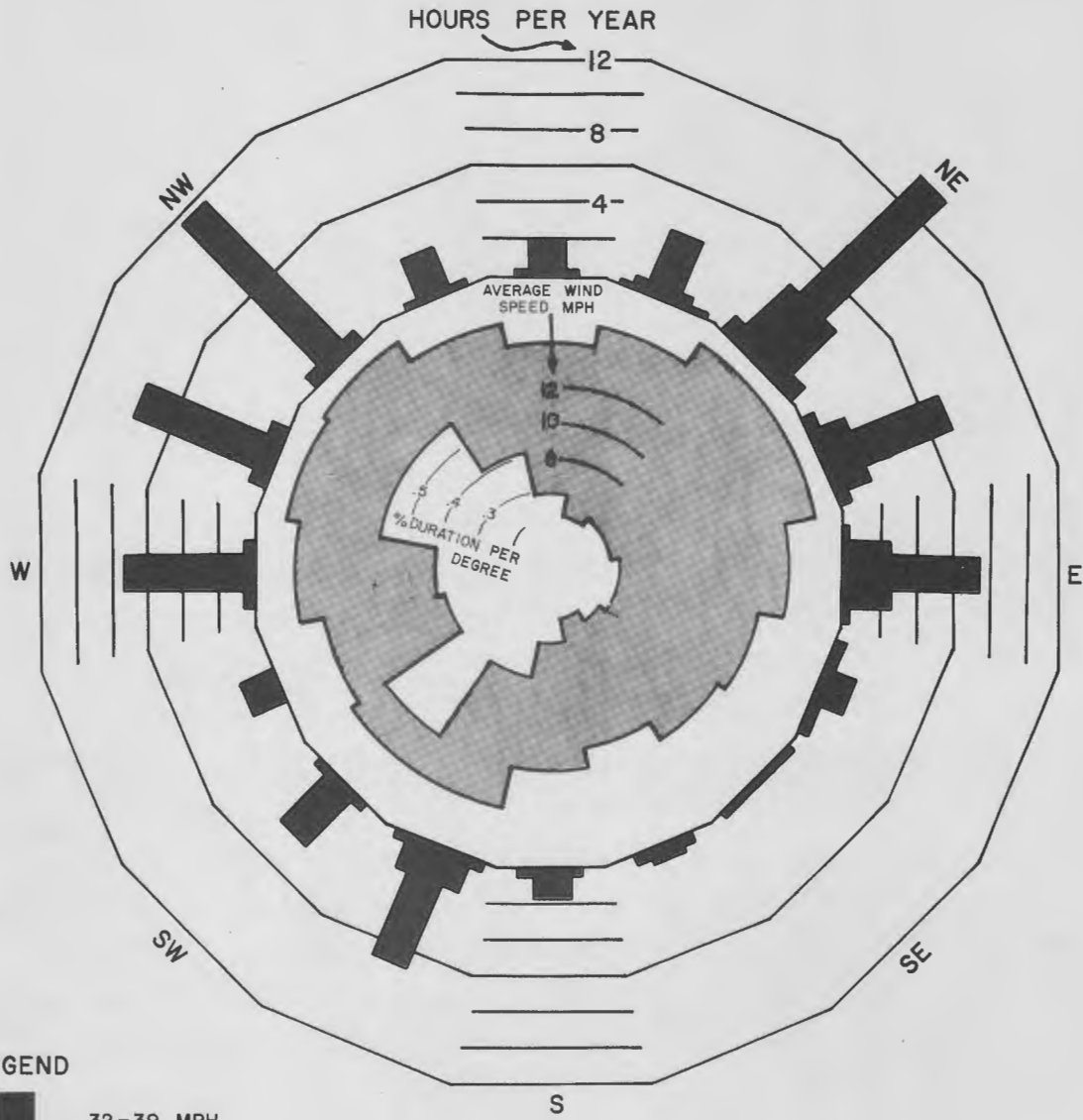
The large tidal range and relatively clear coastal waters of the northern New England shoreline afford an extraordinary opportunity to study intertidal environments. This three-day field trip will concentrate on a small depositional shoreline located between the granitic headland of Cape Ann, Massachusetts, and the rocky shores of the northern New Hampshire coast. A major theme of the trip will be the inspection of the large intertidal sand bodies that abound in the area, but all of the other intertidal environments in the area will be visited.

### Sea-Level Changes

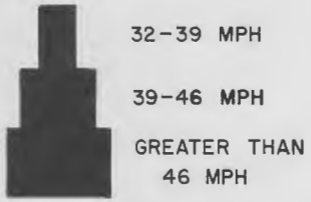
The relative sea-land relationships through the Holocene Epoch have been very complex in this area because there has been (1) a period of continental rebound subsequent to retreat of continental glaciers, (2) general subsidence of the land after the initial rebound and (3) eustatic rise of sea level accompanying ice melt (McIntire and Morgan, 1963, p. 1). Stated simply, before 10,500 B.P. the land mass in the field-trip area was under an ice load and the land was generally subsiding. Between 10,500 B.P. and 7500 B.P. land rebound was more rapid than sea-level rise. At approximately 6300 B.P., the land began to subside again and, hence, a relative sea-level rise was initiated. Around 3500 B.P., the present stillstand of sea level was attained, but the land continued to subside, even up to the present (McIntire and Morgan, 1963). Following this hypothesis for sea-level changes, McIntire and Morgan derived a simple pattern for the origin of the barrier islands of the field-trip area (shown in Figure I-1). This simplified picture of sea-land relationships in northern New England is not accepted by all workers; the problem is still under intense study.

---

Figure I-1. History of the development of Plum Island (modified from McIntire and Morgan, 1963).



**LEGEND**



**WIND ROSE**  
**LOGAN AIRPORT, BOSTON, MASS.**  
 OCTOBER 1949 - SEPTEMBER 1959

DURATION FOR EACH RANGE OF WIND SPEEDS IS MEASURED OUTWARD FROM TOP OF UNDERLYING BAR GRAPH.

PERCENT DURATION PER DEGREE IS THE AVERAGE PERCENT DURATION OBSERVED FOR EACH 16 POINTS OF THE COMPASS DIVIDED BY 22 1/2 DEGREES.

**FIGURE I-2**

## Coastal Processes

Winds play a primary role in coastal processes in this area. A wind rose summarizing data for a ten-year period at Logan Airport, Boston, is given in Figure I-2. This diagram shows that the prevailing winds blow offshore, but that the strongest winds blow from the northeast and from the northwest. These northerly winds are related to the passage of low-pressure centers along the southern New England coast. These low-pressure systems, locally referred to as "nor'easters", are primary factors in generating cycles of erosion and deposition on the beaches of the field trip-area (discussed in paper by Hayes and Boothroyd, p.245 in this guidebook).

In comparison with the mid-Atlantic and Gulf Coast states, areas where considerable coastal research is being carried out, one of the most unique features of this area is the large tidal range. At the entrance to the Merrimack River, the mean tidal range is 8.0 feet, and the spring range is 9.3 feet. At the south end of Plum Island, the mean range is 8.7 feet and the spring range is 9.9 feet. The tidal curve for the spring of 1969 is given in Figure I-3. Although there is a distinct diurnal inequality of the tides in this area, the inequality is small. Wave conditions are generally mild, because the area is sheltered from the open ocean and because the prevailing winds blow offshore. However, 10-15 ft. waves commonly occur during northeasters.

Many of the terms used in this guidebook as well as in our field discussions will undoubtedly be unfamiliar to many of the field trip participants. For purposes of clarification, a glossary of tentative terms has been prepared (p.455 ).

---

Figure I-2. Summary of wind data for ten-year period at Logan Airport, Boston (after U.S. Army Corps of Engineers, N.E. Division, unpublished report).

# TIDE CURVE FOR PLUM ISLAND 1969

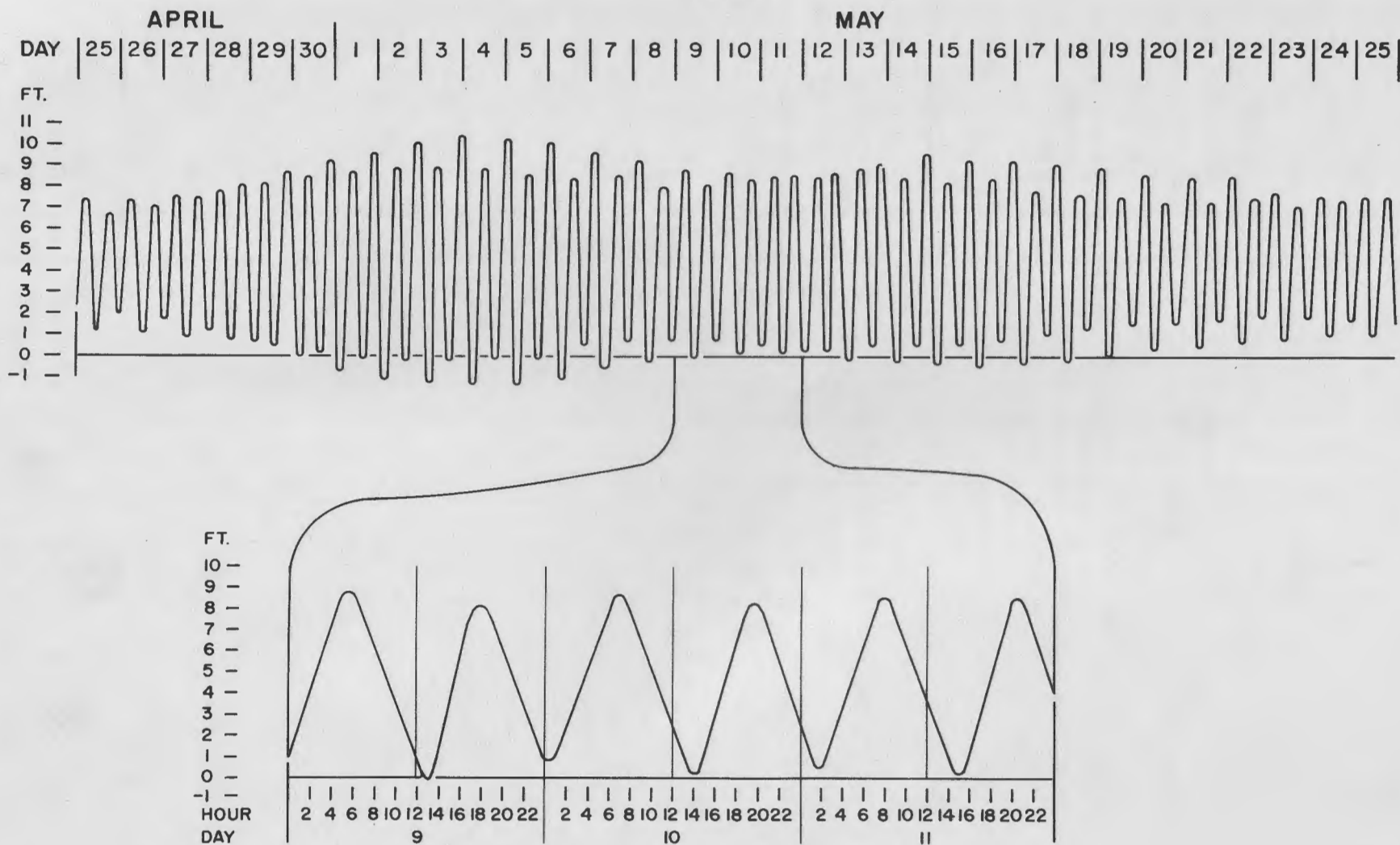
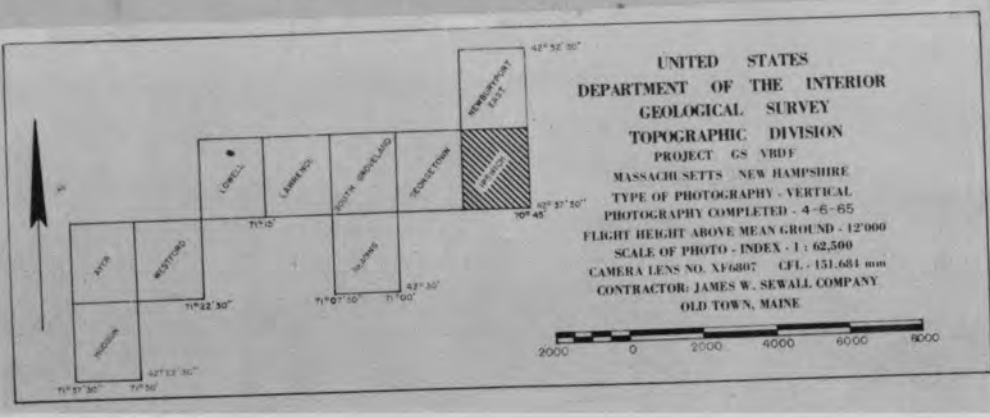


FIGURE I-3

Figure I-3. Tidal curve for spring of 1969 at Plum Island, Mass.  
Blow-up shows tidal curves for days of field trip.



FIGURE RL - I LOCATION MAP FOR FIELD TRIP STOPS IN MASSACHUSETTS  
 12 = STOP LOCATION



ROAD LOG - FIRST DAY

May 9, 1969

Assemble in parking area of Chalet Motor Lodge, Amesbury, Massachusetts. The general locations of the stops visited on the first day are shown on Figure RL-1.

\*\*\*\*\*

<u>Total Mileage</u>	<u>Distance From Last Reading</u>	
00.00	00.0	Leave Chalet Motor Lodge parking area. Turn right (east) on Route 110.
00.10	00.1	Intersection with Interstate 95. Continue straight ahead on Route 110.
00.30	00.2	Intersection. Continue straight ahead.
02.00	01.7	Cross over railroad.
02.20	00.2	Intersection. Continue straight through in an easterly direction.
02.30	00.1	Intersection with U.S. Route 1-A. Turn right (south).
02.60	00.3	To the right is the salt water marsh of the Merrimack River estuary.
02.85	00.25	Tidal creek in Merrimack River estuary. The road runs along the margin of the high salt marsh. A number of fresh-water sedges grow around the border of the marsh.
03.20	00.35	Crossing bedrock outcrop (Newburyport quartz diorite, Dev.).
03.60	00.4	Marsh on the left.
04.10	00.5	Crossing Merrimack River bridge. Note that the tide is now ebbing; ebb currents sometimes attain velocities of 4 to 5 feet/sec. under the bridge. Average annual discharge of the river is approximately 7000 c.f.s. Note also that the river is highly polluted with industrial wastes.

<u>Total Mileage</u>	<u>Distance From Last Reading</u>	
04.30	00.2	Bear right off the main highway onto Route 1-A.
04.40	00.1	Intersection. Turn left under overpass and continue straight east through the business district of Newburyport.
04.55	00.15	To the left is the Newburyport harbor, an important sports fishing center.
04.85	00.3	Turn left at intersection and follow the waterfront road. Newburyport was an important Revolutionary and post-Revolutionary port, especially during clipper ship days.
05.55	00.7	Merrimack River estuary on left. Note broad expanse of the exposed mud flat. This area is known as Joppa Flat and is highly polluted, because as fresh water stands over this area at high tide slack large quantities of the voluminous suspended pollutants settle to the bottom. Details of the hydrography of this estuary will be discussed at the next stop.
05.90	00.35	Marsh growth is beginning to cover the upper reaches of the mud flat at this point. The dominant marsh plant is <u>Spartina alterniflora</u> . This is a zone of accumulation of rafted ice blocks during winter storms.
06.25	00.35	Turn left into parking area of Sportsmen's Lodge.  <u>Stop 1</u> - Joppa Flat, Merrimack River estuary (see stop description on p.34 ).  Continue east on Plum Island Turnpike.
06.70	00.45	Plum Island Airport on right.
07.30	00.6	Both to the left and to the right of the highway is the high salt marsh of the Merrimack River estuary, which is populated predominantly by <u>Spartina patens</u> , <u>Juncus gerardi</u> , and other marsh grasses.
07.40	00.1	Visible to the southeast across the marsh are the high barrier dunes of Plum Island.

<u>Total Mileage</u>	<u>Distance From Last Reading</u>	
07.70	00.3	Crossing Plum Island River, a tidal creek that connects the Merrimack River estuary with the Parker River estuary to the south.
08.10	00.4	Intersection. Continue straight ahead. The highway to the south closely follows the boundary between the dunes on the back side of Plum Island and the high salt marsh.
08.30	00.2	Take a sharp left.
08.50	00.2	This part of the island is subject to severe erosion during northeasterly storms. Piles of sand are blown and washed into the streets; some houses have been lost from the seaward side of the island.
08.90	00.4	Church. This location marks the southern margin of the main channel of the Merrimack River during the middle 1800's. (Fig. 2-1 ).
09.40	00.5	Turn right and drive to Coast Guard Station.
09.60	00.2	Coast Guard Station parking area.
<p><u>Stop 2</u> - Erosion zone, northern Plum Island (see stop description on p.36 ).</p> <p>At this stop, walk out to the jetties north of the Coast Guard Station where a lecture will be given by Mr. Cecil K. Wentworth of the New England Division of the U.S. Army Corps of Engineers on the problems of maintaining this stretch of beach. After the lecture, walk south along the groin field to the area where several houses have been lost by erosion, approximately one-quarter mile south. Return to Coast Guard parking area.</p> <p>Leave Coast Guard Station and drive back to the main road.</p>		
09.80	00.2	Turn right (north) on main road.
10.10	00.3	Headquarters of Parker River National Wildlife Refuge. Turn left into parking area. At this point we will board 4-wheel drive vehicles furnished by the Wildlife Refuge for trip down

<u>Total Mileage</u>	<u>Distance From Last Reading</u>
--------------------------	---

Plum Island. As you leave the parking area, turn right (south).

11.10	01.0
-------	------

There is an open area in front of the cottages along here on the left. This is due to severe erosion during Hurricanes Carol and Diane in 1954, when the front row of cottages on the foredune ridge were lost.

11.50	00.4
-------	------

Turn left into parking area and drive onto beach.

CAUTION: This is not an open beach! In order to drive beach buggies on this beach, permission and a permit must be secured from the main office of the Parker River National Wildlife Refuge, Newburyport, Massachusetts.

11.60	00.1
-------	------

Stop 3 - Profile PLA (see p.44 ).

Continue south along beach.

11.90	00.3
-------	------

Leaving groin field.

12.40	00.5
-------	------

Entering Parker River National Wildlife Refuge.

12.60	00.2
-------	------

The particular beach features that you see along this stretch of beach will be dependent upon the storm and wave conditions during the few days prior to your trip. You can normally see a variety of forms, including well-developed berms, ridge-and-runnel systems, welded berms, berm-ridges, and numerous other features. If there has been a storm recently, the beach profile will be very flat and featureless.

The dune scarp on the right is the result of erosion during repeated northeasters. The last major erosion that occurred in these dunes prior to the time of writing (April 7, 1969) was during several storms in February, 1969. These dunes have not retreated very far, but there has been a net loss in the range of around 5 to 10 feet during the last three years.

13.80	01.2
-------	------

Stop 4 - Profile PLB (see p.50 ).

Continue south along beach.

<u>Total Mileage</u>	<u>Distance From Last Reading</u>	
14.00	00.2	If the weather is clear, you will be able to look to the southeast and see the granitic headland of Cape Ann, Mass., projecting out into the sea.
14.50	00.5	You will detect a change in grain size as you move south along the beach, as the sediment gradually becomes finer grained.
15.50	01.0	<u>Stop 5</u> - Profile PLC (see p.58 ). Proceed south along beach.
16.10	00.6	Camp Sea Haven, a summer camp for crippled children. Notice that in this general area there is an abundance of red heavy minerals (predominantly garnet) along the face of the dunes and at the back of the berm. This garnet accumulation is concentrated on the back-beach during northeasters.
16.55	00.45	A large dune lobe projects onto the backbeach. These dune lobes build onto the beach in winter between storms as a result of strong north-westerly winds that build up during periods of high atmospheric pressure over the northeastern U.S. These northwest winds sometimes attain velocities of 40 to 50 mph. You will probably notice that the dune lobes contain a strong component of high-angle crossbedding dipping offshore (Fig. 116-1, p.78 ), which is unusual for barrier foredune crossbedding.
17.65	01.1	<u>Stop 6</u> - Profile PLD (see p.58 ). Continue south along beach.
18.25	00.6	Emerson's Rocks on left. This is the remnant of an eroded drumlin.
18.65	00.4	Eroded drumlin on right. This will be stop 10. Continue southwest along beach.
18.75	00.1	On the left is the inlet into the Parker River estuary. The bars offshore are part of the

<u>Total Mileage</u>	<u>Distance From Last Reading</u>
--------------------------	---

ebb tidal delta. Across the inlet to the left is Crane Beach, which will be visited on the second day of the trip.

19.35	00.6
-------	------

Stop 7 - Plum Island spit (see p.59 ).

Across the Parker River estuary (southwest) are three large drumlin complexes with wave-cut cliffs on their eastern borders. Boulder pavements face the predominant wave direction, northeast. Across the channel to the south is a dune field composed of fine-grained quartz sand.

Turn around and drive back up spit.

19.75	00.4
-------	------

Turn left across sand onto dirt road at the west end of the drumlin.

19.95	00.2
-------	------

Intersection. Turn right. This area at the intersection is in Plum Island State Park.

The ponds on the left are breeding ponds for water fowl. Plum Island is one of the major nesting places for Canada Geese on the north-south flyway.

20.10	00.15
-------	-------

Turn left onto Wildlife Refuge road.

20.60	00.5
-------	------

These breeding ponds are maintained artificially by dams built by Wildlife Refuge personnel.

20.70	00.1
-------	------

The high dunes on the right are part of the foredune ridge.

21.00	00.3
-------	------

The large hill straight ahead and to the left was mapped by Sammel (1963) as a drumlin.

21.10	00.1
-------	------

Crossing drumlin.

21.20	00.1
-------	------

Heavy vegetation.

21.30	00.1
-------	------

To the left, between the road and the main channel of the Parker River, is a hill called Grape Island, which is composed of sand and gravel. This hill was mapped by Chute and Nichols (1941) as outwash, but Sammel (1963) mapped the bulk

<u>Total Mileage</u>	<u>Distance From Last Reading</u>
--------------------------	---

of the hill as "marine and estuarine deposits" which are attached to a small segment of ground moraine on the southern end of the hill.

21.50	00.2
-------	------

Note that the roadway at this point is following the contact between the high salt marsh and the back-island dunes.

21.70	00.2
-------	------

To the left is a panorama of the salt marsh of the Parker River estuary. In the far background are numerous drumlins.

22.45	00.75
-------	-------

Take a left.

22.55	00.1
-------	------

Vegetated dunes on left.

22.65	00.1
-------	------

Dike built for retaining breeding ponds. Proceed west across dike onto the salt marsh.

22.95	00.3
-------	------

Assembly point for boarding boats to visit tidal flats in Parker River estuary. A location map for this segment of the trip is given in Figure RL-1, p.7. Once in boats, head in a southwesterly direction across the main channel.

23.15	00.2
-------	------

Land boats on point bar and walk to Stop 8a - Mussel bank, Parker River estuary (see p.61).

Either walk or take boat around the margin of the point bar in a northerly direction.

23.25	00.1
-------	------

Stop 8b - Central point bar, Parker River estuary (see p.65).

Board boats. Boats will follow the main channel north and land on the western edge of the Cape Merrill mud flat.

25.25	02.0
-------	------

Stop 9 - Cape Merrill mud flat (see p.68).

Walk up onto marsh for orientation lecture before visiting mud flat.

Return to boats and head south back to original point of departure.

27.25	02.0
-------	------

Land boats and return to vehicles.

Turn around and drive back out to main road.

<u>Total Mileage</u>	<u>Distance From Last Reading</u>	
27.75	00.5	Intersection. Turn right.
30.05	02.3	Leaving Wildlife Refuge.
30.10	00.05	Park on left and walk east approximately 500 feet to the large wave-cut cliff.  <u>Stop 10</u> - Bar Head drumlin (see p.73 ).  Turn around and drive back up the island (north).
32.45	02.35	Intersection with road leading to stops 8 and 9. Continue north.
32.55	00.1	Fields on left are plowed regularly and planted with grain for the wild fowl.
32.85	00.3	Observation tower on left.
33.25	00.4	Pull into parking lot on left. From this point walk east into the dunes. Walk approximately 2000 feet to the beach where dynamic beach processes occurring during a rising tide will be observed. This is <u>Stop 11a</u> - High tide beach (see p.76 ).  Walk back through the dunes toward the vehicles. On the way back we will stop to examine dune morphology and dune sediments; <u>Stop 11b</u> - Plum Island dunes (see p.78 ).  Return to the vehicles and drive north.
34.10	00.85	Sub-headquarters for the Refuge. Bear right.
34.50	00.4	<u>Stop 12</u> - Plum Island marsh (see p.80 ).  Continue north.
35.00	00.5	Road is now at contact between high salt marsh and back-island dunes. Across the marsh to the left, the small island that protrudes through the marsh (Pine Island) is composed of bedrock.
35.80	00.8	On the left is the main channel of the Plum Island River.

<u>Total Mileage</u>	<u>Distance From Last Reading</u>	
36.20	00.4	The channel on the left has large-scale bedforms composed of sand that extend most of the distance across the channel. They appear to have a preferred flood orientation along this stretch of the channel.
36.50	00.3	Leaving Wildlife Refuge; proceed straight ahead.
37.05	00.55	Intersection with Plum Island Turnpike. Turn left.
37.45	00.4	Crossing Plum Island River.
38.60	01.15	Sportsmen's Lodge. On the right you will see the Merrimack estuary at high tide. Contrast this with its appearance when we stopped earlier this morning.
39.30	00.7	Some of the houses along this street date from colonial times.
39.70	00.4	We begin the tour through scenic downtown Newburyport.
40.40	00.7	Major intersection. Bear right.
40.70	00.3	Intersection. Proceed straight ahead under overpass; do not turn.
40.90	00.2	On the right is the main channel of the Merrimack River. At this point the tidal influence is still very strongly felt.
42.25	01.35	We just came up onto a high-level pitted outwash plain. This area is underlain by Newburyport quartz diorite.
42.75	00.5	Intersection. Turn right.
42.95	00.2	Bridge over the Merrimack River; this point is still well below the upper limit of tidal influence.
43.10	00.15	Intersection. Bear right.
43.30	00.2	Outcroppings of bedrock. This is just east of the contact between the Newburyport quartz diorite and the Dedham granodiorite (Dev.).

<u>Total Mileage</u>	<u>Distance From Last Reading</u>	
43.90	00.6	Intersection with Route 110; turn left and pass under Route 95 bridge.
44.20	00.3	Turn left into Chalet Motor Lodge parking area.

END OF FIRST DAY

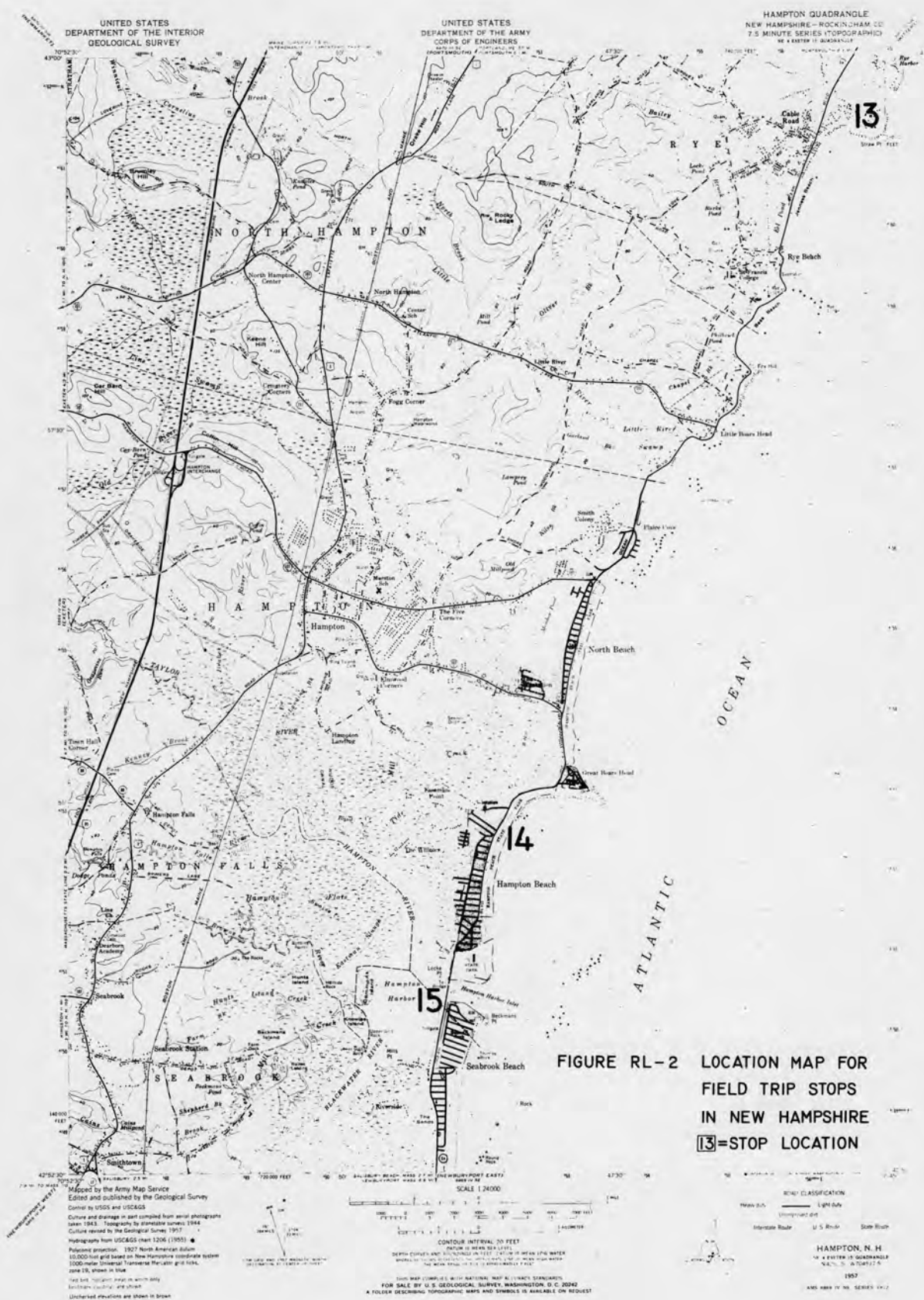


**FIGURE RL-2 LOCATION MAP FOR  
FIELD TRIP STOPS  
IN NEW HAMPSHIRE  
13=STOP LOCATION**

UNITED STATES  
DEPARTMENT OF THE INTERIOR  
GEOLOGICAL SURVEY

UNITED STATES  
DEPARTMENT OF THE ARMY  
CORPS OF ENGINEERS

HAMPTON QUADRANGLE  
NEW HAMPSHIRE—ROCKINGHAM CO.  
7.5 MINUTE SERIES TOPOGRAPHIC  
NO. 4487 (II) QUADRANGLE

Mapped by the Army Map Service  
Edited and published by the Geological Survey  
Control by USGS and USCGS  
Culture and drainage in part compiled from aerial photographs  
taken 1943. Topography by aneroid survey 1944.  
Culture revised by the Geological Survey 1957.  
Hydrography from USCGS chart 1206 (1953).  
Datum: geoid. 1927 North American datum.  
10,000-foot grid based on New Hampshire coordinate system.  
1000-meter Universal Transverse Mercator grid ticks  
every 10,000 feet in both.  
The 1000-foot map is shown only  
for reference. The 1000-foot  
contour interval is shown.  
Unclassified elevations are shown in brackets.

SCALE 1:24,000  
CONTOUR INTERVAL 20 FEET  
DEPTH CURVES AND SOUNDINGS IN FEET (FATHOMS IN BRACKET)  
FOR SALE BY U.S. GEOLOGICAL SURVEY, WASHINGTON, D.C. 20542  
A FOLDER DESCRIBING TOPOGRAPHIC MAPS AND SYMBOLS IS AVAILABLE ON REQUEST

ROAD CLASSIFICATION  
Interstate Route U.S. Road State Road  
HAMPTON, N.H.  
NO. 4487 (II) QUADRANGLE  
1957  
AND PART OF NO. SERIES 44-2

ROAD LOG - SECOND DAY

May 10, 1969

Assemble in parking area of Chalet Motor Lodge, Amesbury, Massachusetts. Today's stop locations are shown on Figures RL-1 and RL-2.

\*\*\*\*\*

<u>Total Mileage</u>	<u>Distance From Last Reading</u>	
00.00	00.0	Leave Chalet Motor Lodge parking area. Turn right on Route 110 and proceed straight ahead under Route 95 overpass.
00.20	00.2	Turn left onto Interstate 95 and head north.
07.80	07.6	Turn right on exit 2. Leave Route 95.
08.10	00.3	Toll Booth. Turn right (east) at next intersection and drive toward Hampton Beach. This is the Exeter-Hampton Expressway.
09.25	01.15	Hampton Harbor estuary marsh on right.
10.00	00.75	Intersection with Route 1. Continue straight ahead over bridge.
10.35	00.35	To the south is the high salt marsh of the Hampton Harbor estuary.
10.65	00.3	Intersection. Continue straight ahead.
11.15	00.5	Crossing tidal creek of Hampton Harbor estuary.
11.85	00.7	Continue straight ahead toward beach, into town of Hampton Beach.
12.15	00.3	Intersection with Route 1A. Turn left (north).
12.25	00.1	Hampton Beach is one of the most important recreation beaches on the northern New England coast. Northeasterly storms severely erode the northern end of this beach; hence, it has to be nourished frequently with new sand, which is usually obtained in the inlet of the Hampton Harbor estuary. Hampton Beach is discussed further under the description of Stop 14, p. .

<u>Total Mileage</u>	<u>Distance From Last Reading</u>	
12.70	00.45	The sea wall on the right has an important bearing on the erosion problem on Hampton Beach, because waves reflect off the sea wall during high storm tides, such that a strong southerly current is set up. This current apparently aids in removing sand from the northern end of the beach.
12.90	00.2	Great Boar's Head, a rock-cored drumlin, on the right.
13.40	00.5	North Beach on the right. During high storm tides, spectacular displays of waves breaking against this sea wall can be watched. Frequently large pebbles are thrown over the sea wall into the street.  This is the first of a sequence of gravel beaches that extend from North Beach through the whole state of New Hampshire and into Maine.
14.20	00.8	Offshore to the right is the Isle of Shoals.
15.00	00.8	Plaice Cove headland. Note erosional boulder rampart.
15.30	00.3	Houses on right sit on crest of foredune ridge.
15.95	00.65	Approaching Little Boar's Head straight ahead and to the right.
16.05	00.1	Sharp bend to the right. As we pass around the leading edge of the Little Boar's Head, a rock-cored drumlin, look to the south and note the retreating erosional remnants of other rock-cored drumlins. Notice that the sediment on the beaches appears to come directly out of the eroding drumlins. A small tombolo is located a few hundred feet to the south. Further south the headland that protrudes furthest out into the Gulf is Great Boar's Head, which is the northern limit of the depositional shoreline that the UMass Coastal Research Group is concentrating on. In the very far distance, if the weather is clear, you will be able to see the large granitic headland of Cape Ann, Massachusetts, approximately 25 miles to the south.

<u>Total Mileage</u>	<u>Distance From Last Reading</u>	
16.35	00.3	On the right are some small pocket beaches of gravel that overlie outcrops of bedrock, the Rye Schist (Ord.).
16.65	00.3	On the right is a gravel sea-wall type beach. This is typical of the gravel beaches of the northern New England shore.
16.85	00.2	Sharp left. Straight ahead is another of the large, well-developed gravel beaches. These gravel ridges normally fill in lows in the topography and shelter the marsh from sea wave action. In very active storms, gravel is washed up across the ridge crest into the street.
17.55	00.7	Inasmuch as the tide is high, you will probably notice a distinct wave refraction pattern on the right. There is a remnant of a rock-cored drumlin approximately 300 feet offshore, around which the waves usually refract.
17.70	00.15	The house on the left is a remodeled coastal watch station, a remnant from World War II.
18.05	00.35	Beginning of Jenness Beach. This beach is the major New Hampshire surfing locality. Waves are usually small but are generally better formed here than at sand beaches further to the south. Wave height on a good surfing day is about 2 feet.
19.00	00.95	Intersection. Turn right on Old Beach Road.
19.40	00.4	Intersection. Turn right on Locke Road.
19.70	00.3	Park just off the road in the vicinity of the gazebo.  This is <u>Stop 13</u> - Rye Gravel Beach, New Hampshire (see p.82 ).  Continue around circle and exit following the same route.
20.00	00.3	Intersection. Turn left onto Old Beach Road.
20.40	00.4	Intersection with Route 1A. Turn left (south).

<u>Total Mileage</u>	<u>Distance From Last Reading</u>	
		Follow Route 1A back to Hampton Beach.
		The small, brightly colored buoys you see just off the rocky sections of the shore are buoys for lobster pots. Lobster fishing is a major industry along the northern New England coast.
26.00	05.6	Intersection. Bear left on Route 1A.
27.10	01.1	Pull into parking area. <u>Stop 14</u> - Hampton Beach, New Hampshire (see p. 83 ).
		Continue south along Route 1A.
27.25	00.15	Bear left on Route 1A.
27.75	00.5	There will probably still be piles of sand left in the parking area on the left. This sand is blown into the area during northeasterly storms.
28.30	00.55	Hampton State Park on left.
28.50	00.2	Crossing bridge over Hampton Harbor estuary.
28.70	00.2	Pull off to right, just across bridge.
		<u>Stop 15</u> - Hampton Harbor estuary (see p. 92 ).
		Continue south along Route 1A.
28.90	00.2	Harbor on right. This part of the Hampton Harbor estuary is the only place in New Hampshire where clams may be taken. There is no commercial clamming industry in New Hampshire; it is all done by private license by New Hampshire residents.
29.40	00.5	Vegetated dunes on right.
30.15	00.75	Intersection. Turn right on Route 86.
30.45	00.3	Bridge of Blackwater River. Notice the strong tidal currents under the bridge that result from the shortening of the width of the channel. Gravel bars have been deposited on both sides of the bridge.

<u>Total Mileage</u>	<u>Distance From Last Reading</u>	
30.65	00.2	Note outcrops of the Newburyport quartz diorite in the marsh on the right. This marsh continues to the south and joins the marsh of the Merrimack River estuary.
32.20	01.55	Intersection. Go straight ahead.
33.00	00.8	Intersection. Turn left (south) on Route 1.
33.65	00.65	Intersection. Bear left.
35.15	01.5	Intersection (Salisbury). Bear left on Route 1-1A.
35.40	00.25	Ann's of Salisbury.
37.05	01.65	Merrimack River Bridge.
37.25	00.2	Bear right; follow Route 1A.
37.35	00.1	Intersection. Continue straight ahead on Route 1A.
37.55	00.2	Intersection. Turn left on Route 1A-113.
37.75	00.2	Kettle hole on right.
37.95	00.2	Intersection. Continue straight ahead on Route 1A. The houses in this part of Newburyport were captains' homes during the clipper ship days. On the roofs of most of these houses there is either a cupola or a fenced-in area; these are the well-known "widow's walks" where the wives waited for their husbands to come home from the sea.
39.35	01.4	To the left you can see across the Merrimack River estuary to the north end of Plum Island.
40.00	00.65	The dunes of Plum Island can be seen to the left.
40.80	00.8	Another vista of the Parker River estuary and Plum Island to the left.
41.40	00.6	This small green is the center of the town of Old Newbury, the first settlement in this area.

<u>Total Mileage</u>	<u>Distance From Last Reading</u>	
		It was settled in the year 1635 by people from Plymouth.
41.75	00.35	Parker River bridge. The Parker River is the major fresh-water stream entering the Parker River estuary.
42.55	00.8	High salt marsh of the Parker River estuary. The rectangular pattern of trenches you see in the marsh were dug for mosquito control in hopes that better drainage would cut down the number of ponded areas. Trenches have been dug periodically since colonial times, but a major amount of this work was done by the CCC in the depression days. The latest diggings are part of a project to control the green-head fly.
45.55	03.0	Rowley. Continue straight ahead through intersection.
48.55	03.0	Railroad bridge. Entering the business district of the town of Ipswich.
48.85	00.3	Intersection. Continue straight ahead; do not turn right. Leave Route 1A.
49.15	00.3	Here again is a section of old houses, Revolutionary and pre-Revolutionary. Many of these houses have been rebuilt or restored by the Ipswich Historical Society.
49.55	00.4	Intersection. Turn left and bear right at the next intersection.
49.85	00.3	Ipswich River on right.
50.00	00.15	Intersection. Bear left.
50.30	00.3	To the right, several drumlins can be seen protruding from the salt water marsh.
51.00	00.7	High salt marsh of the Parker River estuary to the left. Several large drumlins, the Great Neck complex, are straight ahead.
51.20	00.2	High salt marsh on the right.

<u>Total Mileage</u>	<u>Distance From Last Reading</u>	
51.60	00.4	Drumlin topography. Note that some of the drumlins are eroded. This occurs during storm surges of northeasterly storms, hence the wavecut cliffs are generally on the north-easterly sides of the drumlins.
51.75	00.15	Intersection; bear left. As you go up the drumlin around the eastern side, you have an overview of the whole Parker River estuary.
52.00	00.25	<p>Pull over for a brief <u>stop</u>. Straight east is a section of marsh in the middle of the channel known as Middle Ground, which sits atop a large flood tidal delta. Around Middle Ground is a complex of sandy depositional environments that will be visited on today's trip (Stop 16).</p> <p>Looking up the channel, in a more northerly direction, observe that the channel curves around back toward the east and that a large point bar is developed on the western side of the channel. Meandering of the main channel continues further to the northwest. If the tide is low enough, you will be able to see mud flats, clam flats, and mussel banks exposed.</p> <p>Directly across the estuary are some wavecut cliffs in glacial till. These cliffs were presumably cut by the northwesterly winds that blow during periods of high pressure over the continent.</p> <p>Looking northeast across the island, you can see Camp Sea Haven boys' camp which is located approximately one-half mile south of profiling station PLC (Stop 5).</p>
52.50	00.5	Another overview. Looking in a southeasterly direction, you can see the spit at the south end of Plum Island that was visited on the first day (Stop 7). Looking in a more north-easterly direction you see a large sand spit (ebb spit) trailing away from the main mass of the flood-tidal delta. We will visit this spit at the next stop. Further to the south is the quartzose sand beach, Crane Beach, that will be visited later in the afternoon today.

<u>Total Mileage</u>	<u>Distance From Last Reading</u>
--------------------------	---

52.70	00.2
-------	------

Turn left to parking area of Ipswich Bay Yacht Club.

Board boats at Ipswich Bay Yacht Club pier for transportation over to the ebb spit on the flood-tidal delta of the Parker River estuary (a distance of approximately .45 mi.).

Stop 16 - Middle Ground, Parker River estuary (see p.108 ).

From the ebb spit, walk up to the southern edge of the marsh on Middle Ground. Then walk west to the large clam flat on the western border of the marsh.

After visiting the clam flat, board boats for trip south to the next stop (a distance of approximately 1.25 mi.).

Stop 17 - Ebb spit, southern end of Plum Island (see p.115 ).

Board boats again for trip directly across main channel. Land on north end of Crane Beach (approximately .8 mi.). At this point, we will change to 4-wheel drive vehicles for trip down Crane Beach.

---

While Stops 16 and 17 are being visited, the vehicles left behind at the Ipswich Bay Yacht Club will have to be moved to Crane Beach. This can be done by members of our group. The following is the road log to be followed in making this transfer of vehicles to Crane Beach.

---

Turn around in parking lot of Ipswich Bay Yacht Club and exit the same way you came in.

53.65	00.95
-------	-------

Intersection. Bear right.

54.15	00.5
-------	------

The sand dunes on the north end of Crane Beach can be seen to the left.

55.35	01.2
-------	------

Intersection. Bear right.

<u>Total Mileage</u>	<u>Distance From Last Reading</u>	
55.75	00.4	Complex intersection. Bear left.
55.90	00.15	Pass straight ahead through intersection.
56.05	00.15	Ipswich River.
56.20	00.15	Church on right. Intersection. Go straight ahead.
56.30	00.1	Turn left; follow signs to Crane Beach.
57.00	00.7	This is drumlin topography in part, which has been mantled up to a level of 50 feet by marine blue clay.
58.20	01.2	Intersection. Bear left.
59.60	01.4	High salt marsh of the Essex Bay estuary.
59.80	00.2	Large drumlin on right (Hog Island).
60.00	00.2	Dunes of Crane Beach visible on right. Highest dune is a mantled drumlin.
60.25	00.25	The Crane estate. The entire Castle Neck-Crane Beach area was once owned by Richard T. Crane and was given by him to the Commonwealth of Massachusetts for use as a state park.
60.60	00.35	Bear left, avoiding the main entrance gate to the Crane Beach reservation.
60.95	00.35	Drive onto beach and go north.  CAUTION: This beach is not open to beach buggies under normal conditions, so in no case should you ever drive onto this beach without first checking with the Crane Reservation people at the main parking area.
61.55	00.6	Point of intersection of sand beach and drumlin face. This is the landing point for the boats transporting people from Stop 17. Board trucks at this point and drive down Crane Beach. <u>Drive very carefully along the beach.</u>
62.15	00.6	This is the public beach for the town of Ipswich.

<u>Total</u> <u>Mileage</u>	<u>Distance</u> <u>From Last</u> <u>Reading</u>
--------------------------------	---

You will note that the sand of Crane Beach is considerably finer grained than that at Plum Island. It is composed largely of quartz. We are now in Ridge Zone North (Fig.19-2), which is characterized during constructional periods by well-developed ridge-and-runnel systems. Constructional features probably will not be as well developed on Crane Beach as they are on Plum Island, because the waves are smaller here, due to the broad, flat topography offshore, and also evidently because of the finer grain size.

62.45      00.3

This area has suffered a large amount of erosion during the winter of 1968-69. The dune scarps have much greater relief than they had in prior years.

62.50      00.05

Profile CBA (Fig.19-2, p.147 ).

62.60      00.1

Entering the Accretional Zone on Crane Beach (Fig.19-2). You will notice that there is a very wide flat area in front of the dunes. There is no actual foredune ridge on this portion of the beach.

62.70      00.1

Straight ahead is the granitic headland of Cape Ann.

63.00      00.3

Profile CBB.

63.30      00.3

Entering Ridge Zone, South (Fig.19-2), an area with a very wide low-tide terrace and large, low-amplitude ridges during constructional periods.

63.60      00.3

Profile CBC.

64.00      00.4

Dune lobes building out from a former scarp on the foredune ridge.

64.35      00.35

Profile CBD. We are now entering the Essex Delta Zone (Fig.19-2) of Crane Beach, a broad sand-flat area which is influenced in part by tidal currents that sweep into Essex Bay inlet.

Straight ahead is the Essex Bay inlet. This

<u>Total Mileage</u>	<u>Distance From Last Reading</u>	
		inlet cannot migrate further south, because of bedrock on the southern side.
64.75	00.4	A recurved spit at the south end of Crane Beach, somewhat similar to the spit at the south end of Plum Island. At this locality we will debark from the trucks and get in small boats to visit several localities that make up <u>Stop 18</u> - Essex Bay (see p.128 ).  After visiting Stop 18, board the trucks for transportation back up Crane Beach.  <u>Stop 19</u> - Crane Beach (see p.146 ) - will be at the position along the beach that appears most interesting on the day of the trip.  Continue north.
67.35	02.6	Drive off beach into parking area, and continue out of the Crane Beach area.
67.70	00.35	Bear right at intersection.
70.10	02.4	Bear right at intersection.
72.00	01.9	Intersection. Turn right (northeast) on Route 1A.
72.10	00.1	Intersection. Bear left on Route 1A.
72.35	00.25	Ipswich River and major intersection in center of Ipswich. Continue straight through intersection.
72.90	00.55	Complex intersection. Continue north on Route 1A.
73.20	00.3	Cross over railroad.
74.35	01.15	Turn right on Paradise Road.
74.95	00.6	Bear left at intersection.
75.15	00.2	<u>Stop 20</u> - Bull Brook gravel pit (see p.174 ).  Return to Route 1A.

<u>Total Mileage</u>	<u>Distance From Last Reading</u>	
75.95	00.8	Intersection with Route 1A. Go <b>right</b> (north).
76.30	00.35	Turn right on small dirt road.
76.40	00.1	<u>Stop 21</u> - Nourse Cemetery gravel pit (see p.174 ). Back out dirt road to main highway.
76.50	00.1	Continue north on Route 1A.
78.05	01.55	Intersection in Rowley. Continue on Route 1A.
81.85	03.8	Parker River.
82.60	00.75	Drumlins on left.
84.85	02.25	Entering Newburyport.
85.70	00.85	Turn right on Route 1A.
85.80	00.1	Go straight through intersection.
85.90	00.1	Turn left under overpass.  Now follow road log for the FIRST DAY from mileage <u>40.70</u> to <u>44.20</u> .
89.40	03.5	Chalet Motor Lodge parking area.

END OF SECOND DAY

ROAD LOG - THIRD DAY

May 11, 1969

Assemble in parking area of Chalet Motor Lodge. Today's stop locations are shown on Figure RL-1.

\*\*\*\*\*

<u>Total Mileage</u>	<u>Distance From Last Reading</u>	
00.00	00.0	Leave Chalet Motor Lodge parking area and follow exactly the same route as the FIRST DAY from mileage <u>00.00</u> to <u>09.40</u> .
09.40	09.4	Road to Coast Guard Station on northern Plum Island. Continue straight ahead.
10.00	00.6	Bear right into parking area and park near Coast Guard boat house. Walk down to dock. At this point, we will board boats and go to <u>Stop 22</u> - High-tide hydrography, Merrimack River estuary (see p.176 ).  From Stop 22, which is approximately .8 miles from the landing (near center of main channel), go south to Woodbridge Island.  <u>Stop 23</u> - Woodbridge Island marsh (see p.178 ).  After examining cores from the marsh of Woodbridge Island, board boats and return to landing (approximately 1.0 mi.).  Return to vehicles and drive back down main road.
10.10	00.1	Wildlife Refuge Headquarters. Continue south.
10.85	00.75	Church on right. Observe the water level in the basin behind the church. This has been dry most of the other times we have been by it. This basin was created as a result of the extension of the northern end of the island by spit growth in the interval between 1827 and 1851.
11.40	00.55	Intersection. Turn right.

<u>Total Mileage</u>	<u>Distance From Last Reading</u>	
11.60	00.2	Intersection. Go straight ahead.
12.05	00.45	Plum Island River.
13.05	01.0	Airport on left.
13.55	00.5	Turn left at intersection.
14.15	00.6	Intersection. Turn left on Route 1A.
16.85	02.7	Parker River.
18.50	01.65	Turn left on dirt road.
18.70	00.2	Bear right at fork.
19.60	00.9	Entrance to Parker River National Wildlife Refuge.
20.20	00.6	<u>Stop 24</u> - Parker River estuary marsh (see p.180 ).  The hill we are parked on was mapped by Sammel (1965) as "marine and estuarine deposits."
20.40	00.2	Drive east 0.2 miles and turn around. Go back to Route 1A the same way you came in.
22.30	01.9	Intersection with Route 1A. Turn right (north).
23.95	01.65	Parker River.
26.65	02.7	Traffic signal. Turn right.
27.25	00.6	Turn right at intersection.
27.75	00.5	Plum Island Airport. Park vehicles. This is <u>Stop 25</u> - Flights (see p.183 ).

While the flights are in progress, an alternate trip will be run to demonstrate the environments of the Merrimack River estuary that are exposed at low tide. This part of the trip will be done in rotation; that is, as soon as your flight is completed, you will be shuttled to the north end of Plum Island where you will board a boat to get into rotation to visit Stops 26, 27, 28, and 29. Details of this rotation system will be explained in the field.

<u>Total Mileage</u>	<u>Distance From Last Reading</u>
--------------------------	---

In order to begin the tour of Stops 26-29, leave airport parking area and drive east toward Plum Island.

28.75	01.0
-------	------

Plum Island River.

29.40	00.65
-------	-------

Turn left.

30.80	01.4
-------	------

Park vehicles near Coast Guard boat house and walk to dock.

You will be transported by boat to the following stops:

Stop 26 - Tidal delta, Merrimack River estuary (see p.185 ).

Stop 27 - Clam flat and mussel banks, Merrimack River estuary (see p.204 ).

Stop 28 - Woodbridge Island point bar (see p.209 ).

Stop 29 - Plum Island River point bar (see p.215 ).

Detailed locations for these stops are shown on Figure .

From Stop 29, walk along the edge of the marsh to the bridge across the Plum Island River. From this point, you will be transported back to the airport.

33.85	03.05
-------	-------

Airport parking area. Final assembly.

END OF TRIP

STOP DESCRIPTIONS

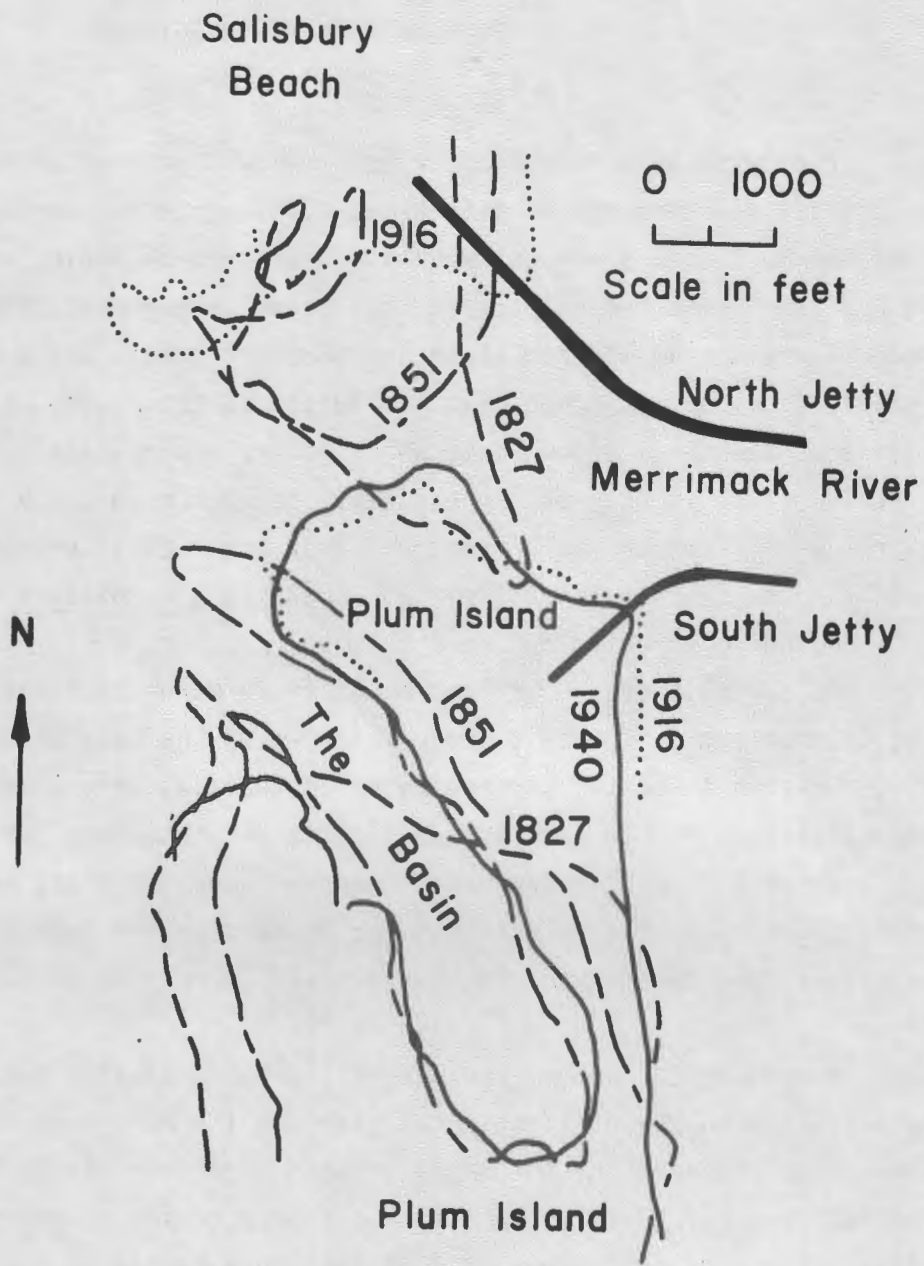
## STOP 1 - JOPPA FLAT, MERRIMACK RIVER ESTUARY

Miles 0. Hayes

The purpose of this stop is to provide a general orientation to the coastal environments in this area. Looking to the north, you will see the Merrimack River estuary at mid-tide (tide ebbing). The bottom profile across the estuary at this point is asymmetrical, with the deep channel being located along the northern margin and a broad, very gently sloping flat (Joppa Flat) situated to the south. At this stage of the tide, Joppa Flat, which covers approximately 300 acres at low tide, is only partly exposed. Sediments on Joppa Flat range from muddy sand to mud in size and they are rich in organic content. Around the margin of the flat, Spartina alterniflora marsh grass is beginning to build out over the mud.

As a result of the deflection of fresh water to the south side of the estuary as the salt wedge intrudes up the main channel during the rising tide, the surface water on the flat very seldom attains salinities higher than 10 to 15 parts per thousand. At high-water slack, this "fresh" water mass is ponded over the flat; hence, suspended pollutants tend to settle. For details on the hydrography of the estuary see paper by Hartwell and Hayes (p.218 ) in this guide-book.

According to Jerome, and others (1965), pollution has had a severe influence on the utilization of clams in the Merrimack River estuary. Over 500 acres of the estuary contain a potentially harvestable clam population, but 82.1% of this area has been closed to the taking of shellfish because of pollution. All of the Joppa Flat area that you see to the north is labeled as a "grossly contaminated area" and is closed to all digging of clams for human consumption. A small acreage in the estuary is available for taking of shellfish provided that they are conditioned at the Shellfish Purification Plant in Newburyport prior to being marketed



**Shore Lines at Mean High Tide**

- 1827, U.S. Army Engineers
- - - - 1851, U.S. Army Engineers
- ..... 1916, U.S. Army Engineers
- ~~~~~ 1940, R.L. Nichols (Plum Island only)

**FIGURE 2-1**

## STOP 2 - EROSION ZONE, NORTHERN PLUM ISLAND

Miles 0. Hayes

Plum Island is a barrier island 8.4 miles long and, in most places, between one-half and one mile wide. Its southern end is attached to a drumlin complex. According to McIntire and Morgan (1963), the island first came into existence between 6000 and 7000 B.P.

At this stop, we will see the northern tip of the island, which has undergone remarkable changes both in size and in shape during the last 150 years. These changes, which are illustrated in Figure 2-1, were described by Nichols (1964, p. 32) as follows:

In 1827 the northern end of Plum Island was not forked. Between 1827 and 1851 the eastern side retrograded about half a mile southward. The western side was modified later to form the western prong. Following this period of retrograding southward, a spit, attached to the eastern side, prograded northward, so that by 1851 it was more than a mile long. Since 1851 this spit, the eastern prong, has greatly increased in size. In 1942 it had an area of approximately .3 sq. mile.

This stop will begin at the parking area of the Coast Guard station (Fig. 2-2). The sand in this area, which frequently attains granule size, is the coarsest on the island. It is very rich in yellow-orange feldspar grains.

The history of the development of this part of the island is closely related to the offshore bottom topography. The complex topography off the mouth of the Merrimack River is shown by the bathymetric diagram on Figure 2-3. Note the large lunate bar (ebb-tidal delta) off the river mouth. Also observe the alignment of the northwest side of the ebb-tidal delta perpendicular to the predominant northeasterly winds. During northeasterly storms, waves refract around the offshore bar such that they approach the north end of Plum Island from the southeast. This angle of

---

Figure 2-1. Changes in the shorelines of the north end of Plum Island and the south end of Salisbury Beach from 1827 to 1940 (from Chute and Nichols, 1941, Pl. 3).

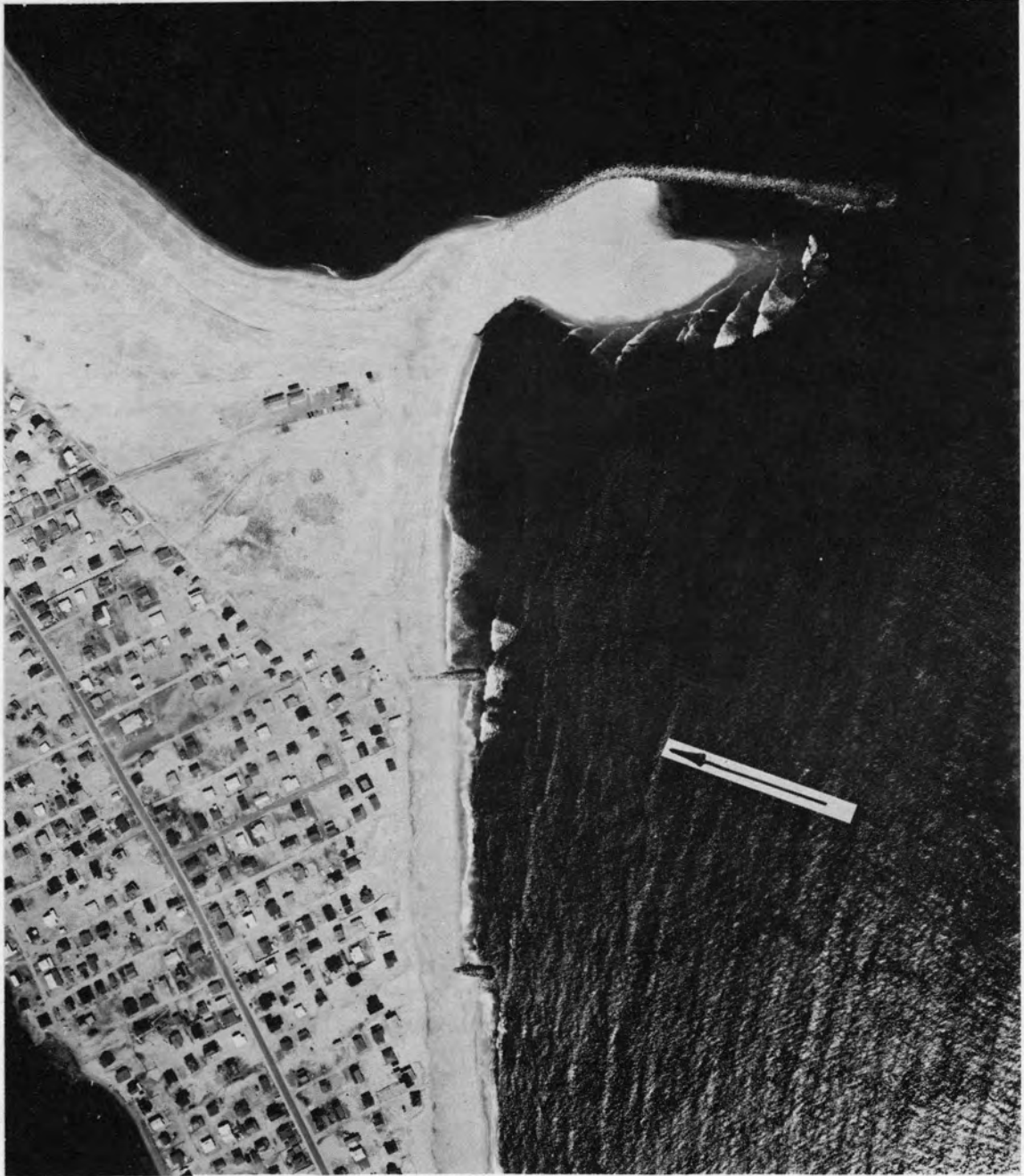


FIGURE 2-2

wave approach is illustrated on the aerial photograph of Figure 2-2. This pattern of wave refraction around the ebb-tidal delta brings about accretion of sand on the south side of the numerous groins on this part of the island, as well as growth of spits that parallel the south jetty (Fig. 2-2).

During the past winter, the north end of Plum Island underwent severe erosion, especially in the vicinity of the Coast Guard station. A very slow-moving storm during February 24 to 27 caused the bulk of the damage. The erosion near the Coast Guard station (Fig. 2-4) was rather freakish, inasmuch as it occurred inside the inlet mouth. Waves washed across the north jetty and struck the north end of Plum Island inside the jetties, cutting back a northwest-southeast trending scarp.

The erosion problem is even more acute further south along the beach. The problem area was described by the New England Division, U.S. Army Corps of Engineers in a preliminary report (1967), as follows:

This erosion is particularly severe during major storms resulting in losses of cottages, serious reduction in lot sizes, and total loss of some seaward lots. Many cottages have been moved landward as far as possible and are now bordering the boulevard. Normal high tides now approach backshore dunes and embankments along much of the problem area, which is becoming more and more vulnerable to storm erosion.

This area is still under study by the Corps of Engineers. A Beach Erosion Control Report for northern Plum Island was completed in 1952 and is published as House Document No. 243, 83rd Congress, 2nd Session. A further preliminary study was completed in October, 1967 (unpublished). The data in these two reports and later findings will be discussed in the field by C. K. Wentworth of the New England Division, Corps of Engineers, Waltham, Massachusetts.

---

Figure 2-2. Vertical aerial photograph of the north end of Plum Island (18 April, 1968). Coast Guard station is indicated by letters CG. Note the wave approach from the southeast (arrow). Photo courtesy of the U.S. Army Corps of Engineers.



Figure 2-3. Bottom topography of the nearshore area off the mouth of the Merrimack River estuary. Note asymmetry of the ebb-tidal delta, with the northwest-southeast orientation of the northern side of the offshore bar that results from the predominant northeasterly wave direction of major storms. Contours based on data of the U. S. Coast and Geodetic Survey, Hydrographic Survey No. 8096 (July, 1953 - November, 1954). Constructed by Jon C. Boothroyd.



FIGURE 2-4

Figure 2-4. Erosion on north side of Plum Island Coast Guard station by slow-moving northeasterly storm of 24 to 27 February, 1969. This erosion occurred inside the inlet as a result of waves breaking across the north jetty (refer to Fig. 2-2). Photo courtesy of the Boston Globe.

# EFFECT OF 25-26 MAY 1967 STORM

## STATION PLA, PLUM ISLAND NEWBURY, MASS.

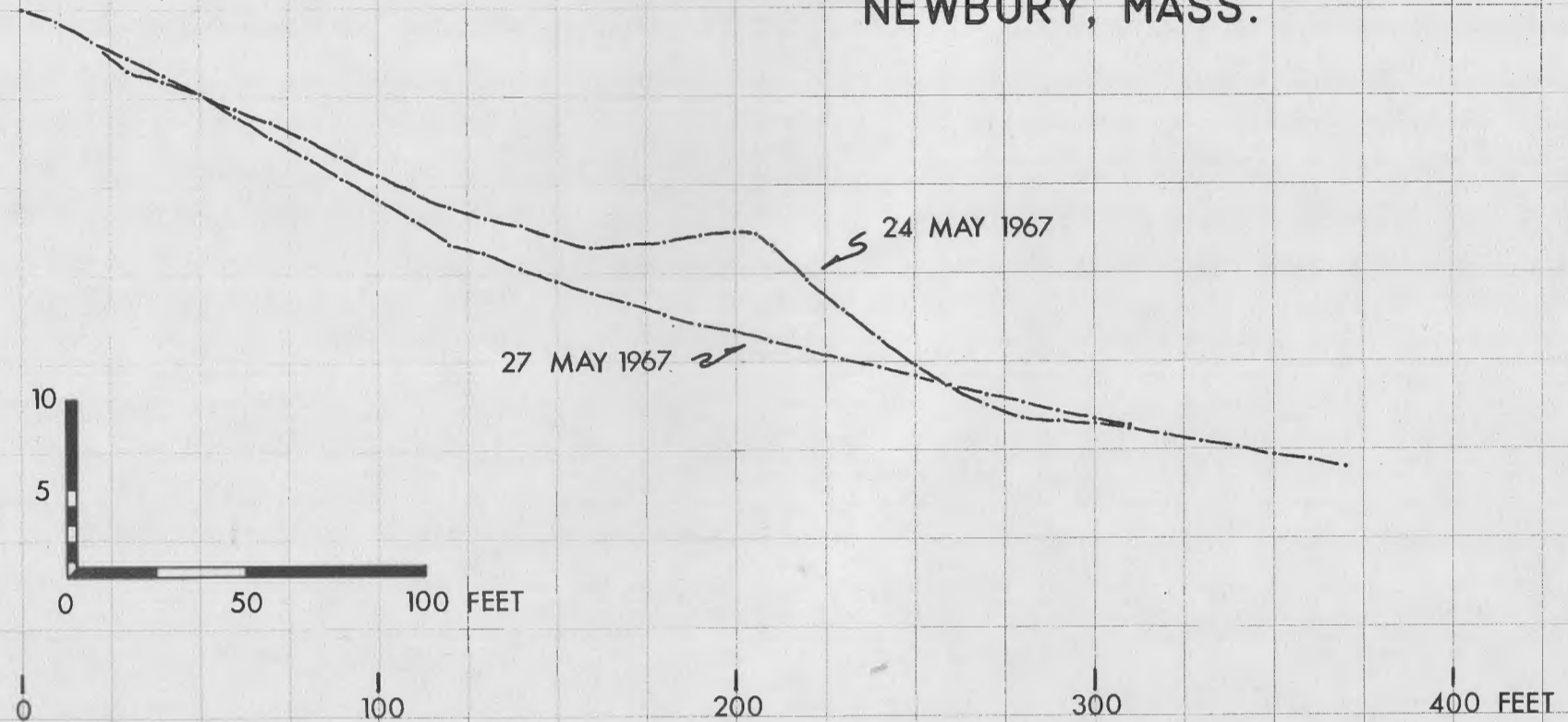


FIGURE 3-1

### STOP 3 - PROFILE PLA

Miles O. Hayes

Fayez A. Anan

Victor Goldsmith

This is one of four permanent profiling localities on Plum Island that our group has been surveying since September, 1965. Over 100 profiles have been run at this locality at approximately 2-week intervals. PLA is different from the other three profiles to the south in that it is generally coarser-grained, the beach face is considerably steeper, and the recovery rate is very rapid. Cusps are very common features along this stretch of the beach.

Two profiles typical of this station are given in Figure 3-1. During constructional periods a broad berm develops that produces a convex upward profile (profile of 24 May, 1967; Fig. 3-1). After storms, the profile is very flat and featureless (see profile of 27 May, 1967; Fig. 3-1). Photographs showing two contrasting profiles are given in Figures 3-2 and 3-3.

Figure 3-4 is a scatter plot of samples collected at the four profiling stations on Plum Island. The average mean size of six samples from station PLA is  $1.23\phi$  (0.42 mm). The six PLA samples were collected from the beach face at different times of the year. The difficulties involved in sampling beach sediments will be discussed in the field by Anan (see his paper on the grain size parameters of Plum Island sediments, p.266 , of this guidebook).

The nature of the bar offshore from this profile is discussed by Goldsmith (p.281 , of this guidebook).

---

Figure 3-1. Profiles at station PLA on Plum Island showing the effect of the 25 to 26 May, 1967, northeaster. These two profiles are typical erosional and constructional profiles for station PLA.

Figure 3-2. Profile PLA on 18 December, 1966. Erosional scarp in the middle of the profile was cut by a north-easter in November. A large neap berm had developed on the seaward side of the scarp.

Figure 3-3. Typical post-storm profile at station PLA (27 May, 1967). Compare photograph with the measured profile in Figure 3-1.



**FIGURE 3-2**



**FIGURE 3-3**

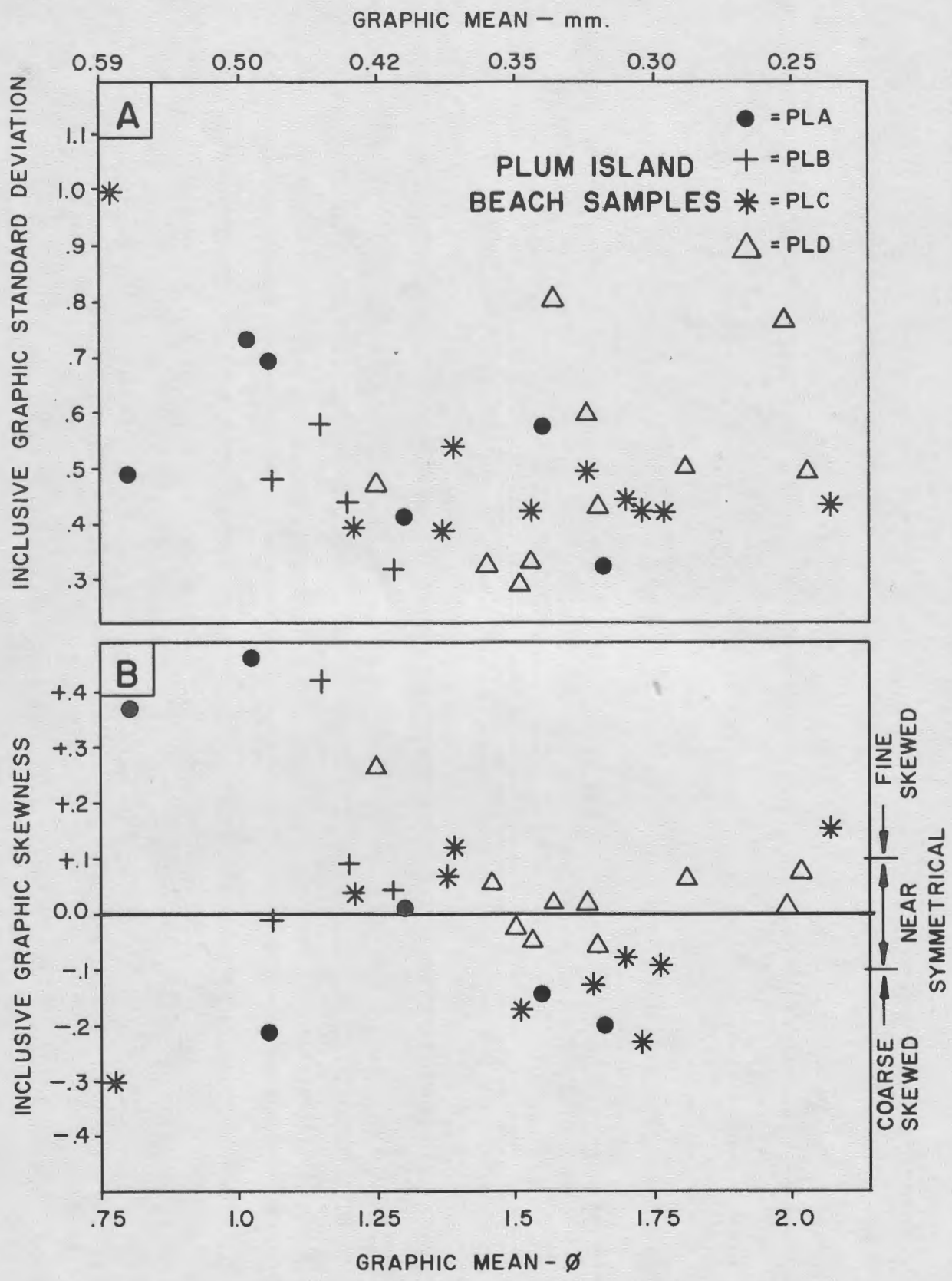


FIGURE 3-4

Figure 3-4. Scatter plots of graphic mean versus inclusive graphic standard deviation (A) and inclusive graphic skewness (B) for 30 beach samples collected at the 4 profiling stations on Plum Island. Samples were collected by scraping the top one-eighth inch of sand from the beach surface. Samples were taken at different times of the year, mainly from the beach face.



FIGURE 4-1



FIGURE 4-2

## STOP 4 - PROFILE PLB

Miles 0. Hayes

This profile and the two others to the south follow a similar pattern of erosion and construction in response to northeasterly storms. The measurement of over 100 profiles over a period of three years at this station yields the following pattern with respect to beach erosion and accretion:

- (1) post-storm profile - flat to concave upward, generally smooth and uniformly medium-grained. A typical example is given in Figure 4-1.
- (2) Early accretion - formation of ridge-and-runnel system that migrates toward the backbeach. Illustrated in Figure 4-2.
- (3) Welded ridge - the landward-migrating ridge is welded onto the backbeach. See Figure 4-3.
- (4) Late accretionary berm - a broad, convex upward berm formed by welding of the ridge with beach-face accretion building the berm seaward. See Figure 4-4 for example. Recovery is rapid on this profile, as is demonstrated in Figure 4-5.

Aerial views of a post-storm profile and an early accretionary profile are given in Figures 4-6 and 4-7. The response of the beach profile to northeasterly storms is discussed in greater detail by Hayes and Boothroyd on p.245 of the guidebook, and Hayes, and others (p.290 ) consider the role of these profile changes in the formation of primary structures in the beach zone.

The mean grain size of four samples collected from the PLB profile at different times (see scatter plot, Fig. 3-4) is  $1.16 \phi$  (0.443 mm).

---

Figure 4-1. Flat, post-storm profile at station PLB on 9 Nov., 1968.

Figure 4-2. Ridge-and-runnel system near profile PLB on 1 Aug., 1966.  
View looking north along the beach face.



**FIGURE 4-3**



**FIGURE 4-4**

Figure 4-3. View looking north from approx. 300 feet south of profiling station PLB on 22 July, 1967. The large ridge in foreground had welded against the backbeach at the point just south of the profile.

Figure 4-4. Large accretionary berm at profile PLB on 26 Jan., 1967. This berm was removed by the northeaster of 27 to 28 Jan., 1967.

# POST-STORM ACCRETION 27 MAY - 14 JUNE 1967

STATION PLB, PLUM ISLAND  
NEWBURY, MASS.

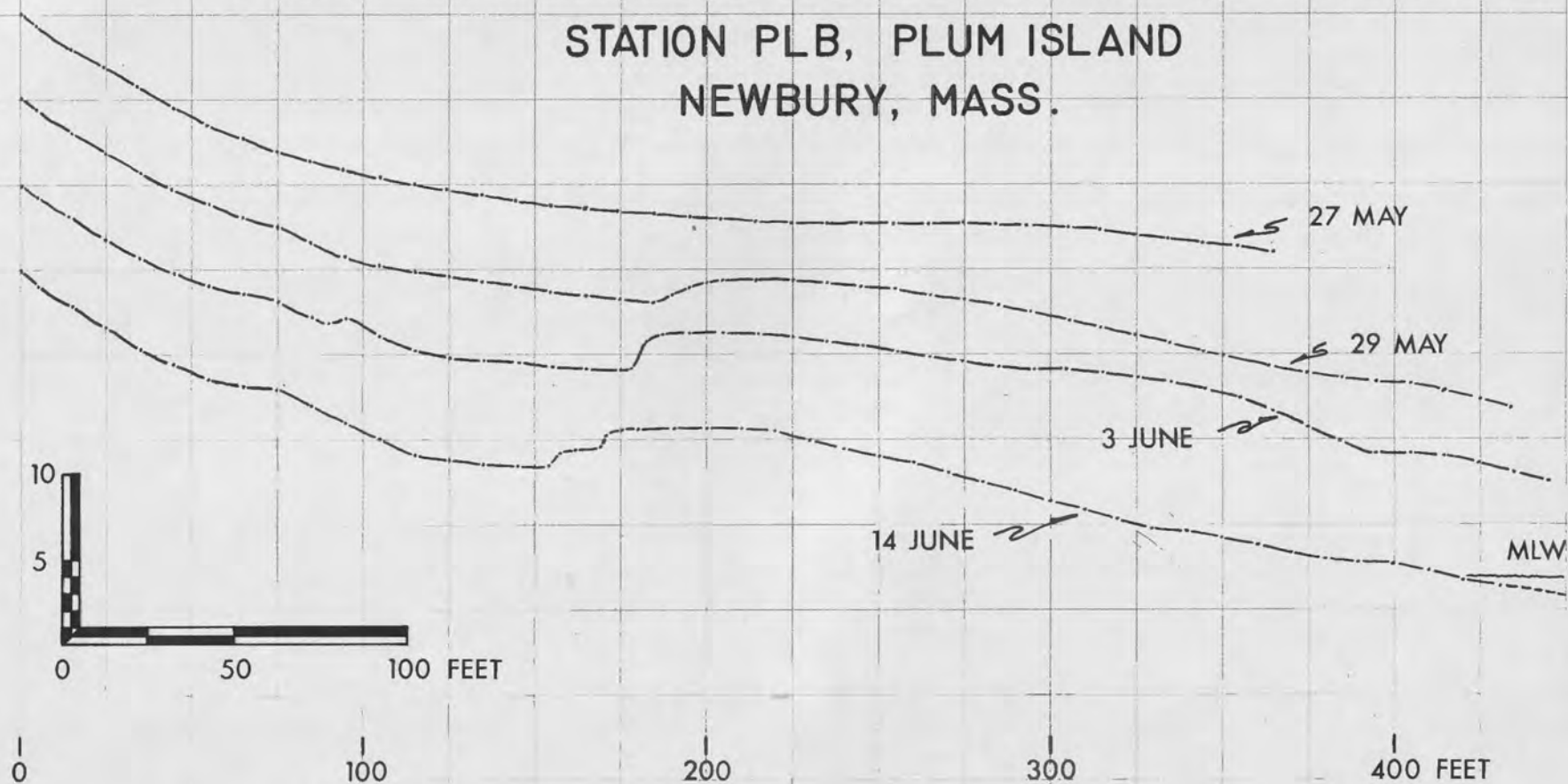


FIGURE 4-5

Figure 4-5. Profiles illustrating a typical recovery period after erosion by northeasterly storm.



FIGURE 4-6

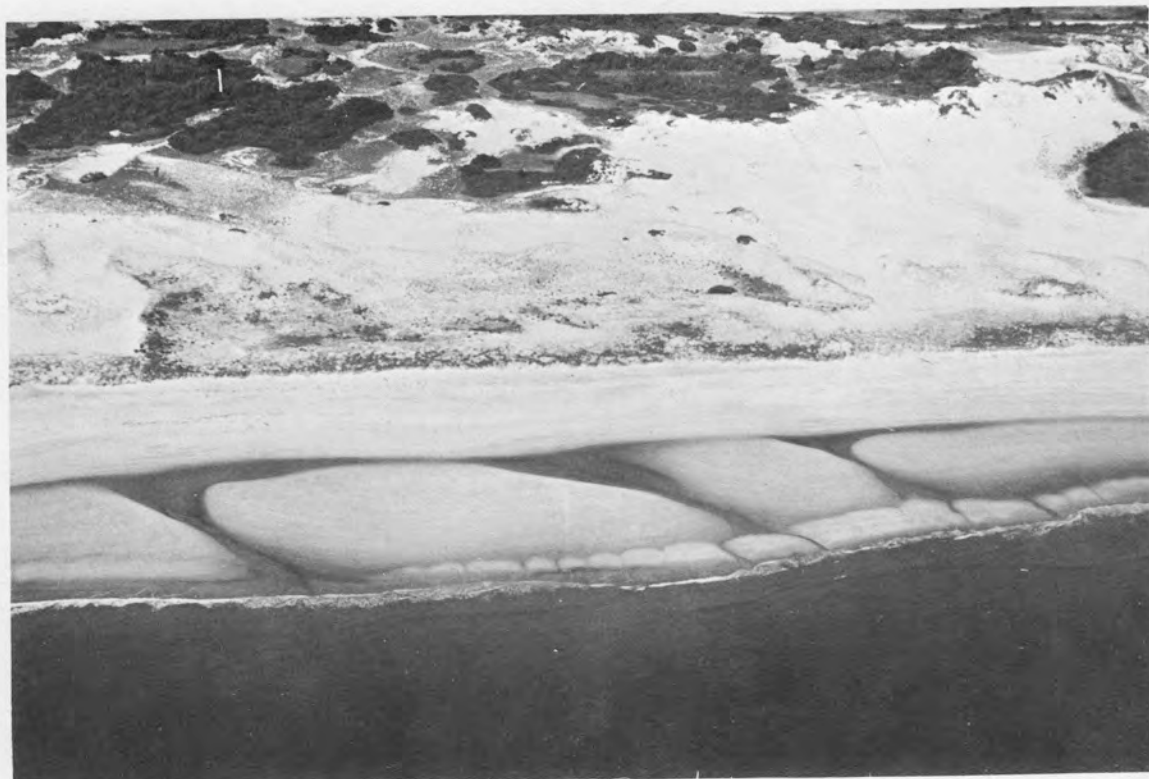


FIGURE 4-7

Figure 4-6. Aerial view of flat post-storm beach cut by northeaster in April, 1967.

Figure 4-7. Aerial view of accretionary beach profile on August, 1967. Note development of two distinct ridge-and-runnel zones.

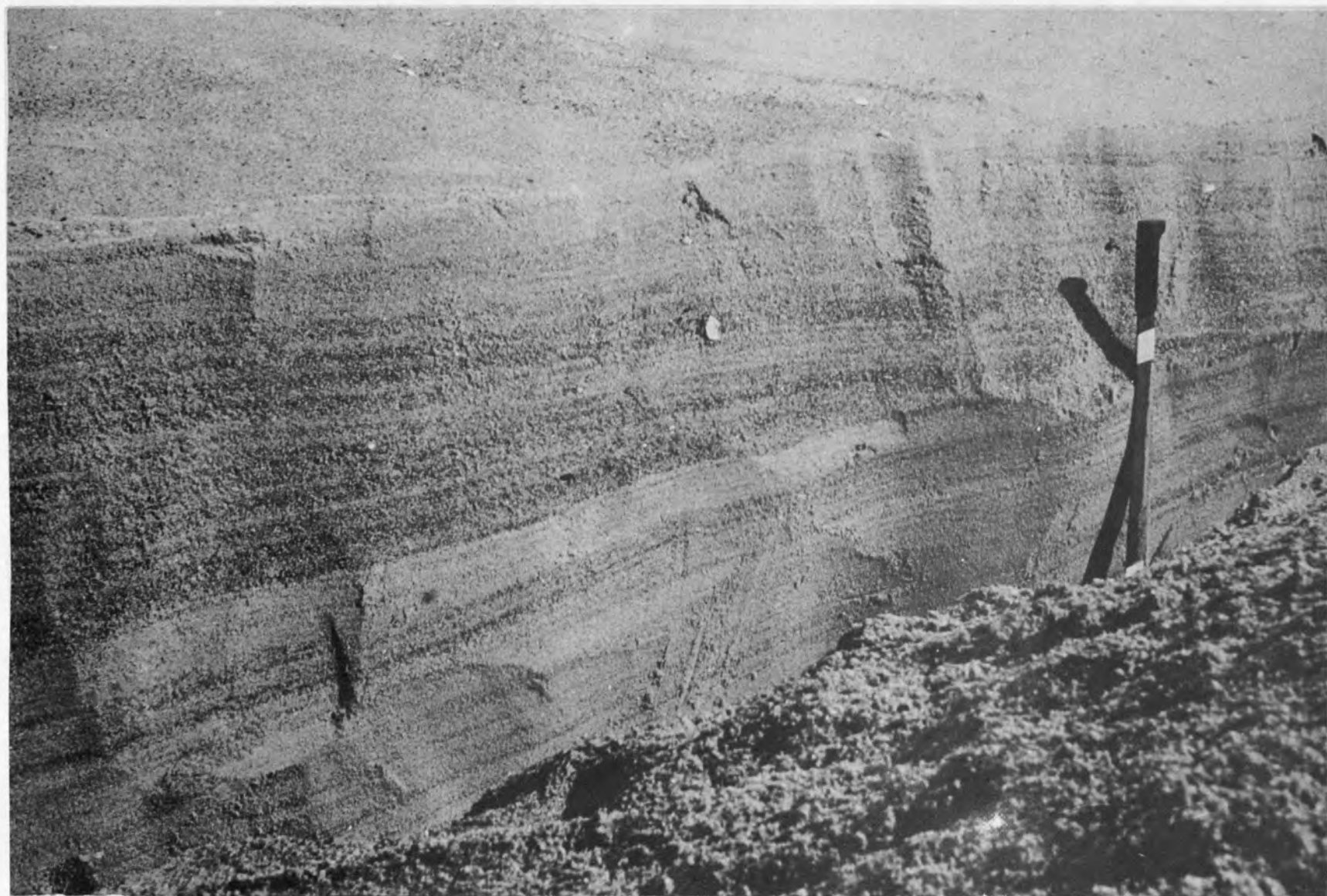


FIGURE 5-1

## STOPS 5 and 6 - PROFILES PLC AND PLD

### Miles 0. Hayes

Measurement of over 80 profiles at each of these stations revealed an erosion-accretion cycle similar to that found at station PLB. There are some subtle differences among the profiles that will be discussed in the field.

The average grain size of 10 samples collected on different dates from profile PLC is  $1.51\phi$ ; the average size for 10 samples from profile PLD is  $1.64\phi$ .

A large trench dug through the beach face of a broad accretionary berm at profile PLC on 22 July, 1966, is illustrated in Figure 5-1.

---

Figure 5-1. Beach-face bedding in trench dug near profile PLC on 22 July, 1966.

## STOP 7 - PLUM ISLAND SPIT

Stewart C. Farrell

The Plum Island sand spit in the Parker River estuary is the largest sand body of its type in the region covered in this field guide. From April, 1965, to April, 1969, a body of sediment 2,000 feet long, 600 feet wide, and 7 feet thick was deposited on the sand flats and in the channel of the Parker River (Farrell, p.316 , elsewhere in this guidebook). The south end of Plum Island can be subdivided into three general sedimentation provinces. The drumlin and the beach trending southwest from it make up the first province. If there is sufficient swell running, the pattern of wave refraction, reinforcement, and destructive interference in the entrance of the Parker River will be observable. The second province is the foreland cusp. This extension of the southwest-trending beach into the main channel is a prominent feature that played an important role in the development of the spit (Farrell, p.316 ). The third region is the spit and basin area. The nose of the spit became attached to the Plum Island shore in January, 1969, and the basin is now an enclosed pond. Cores and trenches in the beach face and backside of the spit illustrate the sedimentary structures of past periods of deposition.



## STOP 8a - MUSSEL BANK, PARKER RIVER ESTUARY

Joan M. DaBoll

A location map showing the route to be taken at this stop is shown in Figure 8a-1. Mussel banks cover some large areas and many small ones in the southern part of the Parker River estuary. They are composed of an uneven surface of live mussels, Mytilus edulis, over a thin layer of shells of dead mussels. Mixed with and below the shells are soft, black, very fine-grained sediment and waste material from the mussels. There are no remains of mussel shells at depth because the shells decompose in the organic acid-rich sediment. Below the black, fine-grained deposit, at depths ranging from 2 inches to 2 feet, is a firm foundation of sand or gravel upon which the mussels originally established themselves. Where the foundation is fine-grained gray sand, such as is under the mussel banks on Middle Ground or along much of the eastern boundary of the estuary, it contains numerous fragments of clam shells, Mya arenaria (Fig. 8a-2). In these areas productive clam flats border the mussel banks and clammers periodically employ various methods to try to keep the mussel banks from encroaching further onto the productive areas.

In the southern half of the estuary, where mussels are abundant, salinity varies between 28.5 and 31.9‰. Maximum flood currents in these areas are around 3.5 ft./sec. and maximum ebb currents around 2.5 ft./sec.

The process of accumulation of fine-grained sediment on banks made up of sessile, benthic communities of filter-feeding molluscs was termed "biodeposition" by Haven and Morales-Alamo (1969). On the mussel banks in the Parker River, suspended sediment is extracted from the water by the mussels. Feces and pseudo-feces lumps composed of organic-rich, black mud accumulate around the living mussels. Thus, fine-grained black mud deposits are accumulating in areas exposed to fairly high current

---

Figure 8a-1. Location map of the Parker River estuary. The routes for two stops, 8 and 16, are shown. Stop 9, Cape Merrill, is located at the confluence of the Parker and Plum Island Rivers.



A



B



C

FIGURE 8a-2

velocities because of this unique combination of biodeposition and the baffle effect of the living mussel shells.

---

Figure 8a-2.

A. Photograph of mussel bank which has grown over a clam flat. The surface is covered with an uneven layer of mussels. The depressions are filled with water.

B. Box sample showing mussels and underlying clam flat deposits. The fine-grained, black sediment under the mussels was compressed during sampling.

C. Box sample showing mussels over thin bed of fine-grained sand. Below the sand is a bed of very fine-grained black sediment with a few small fragments of mussel shells, indicating the presence of an earlier mussel bank.

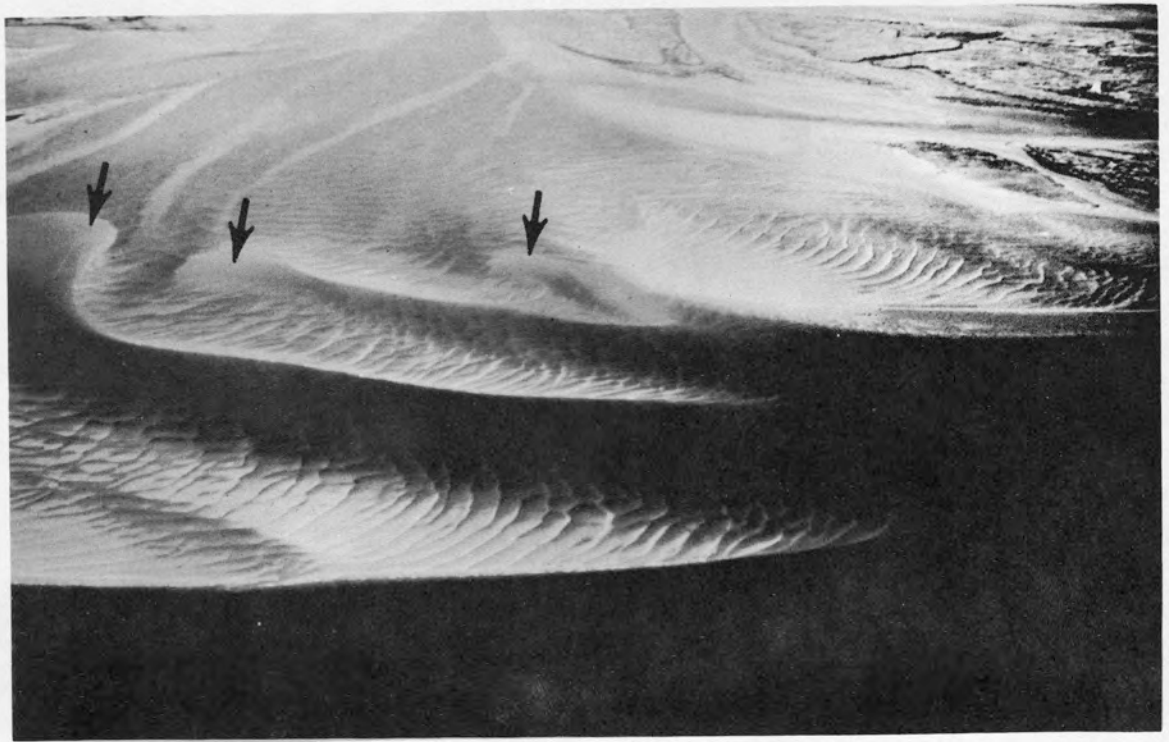


FIGURE 8b-1



FIGURE 8b-2

## STOP 8b - CENTRAL POINT BAR, PARKER RIVER ESTUARY

Joan M. DaBo11

There are three large point bars in the main body of the Parker River estuary and a complex of smaller point bars at the confluence of the Parker and Plum Island Rivers. A progressive change occurs in these point bars from the mouth of the estuary to its head. The point bar to be visited at this stop is located directly north of Middle Ground (Fig. 8a-1).

A large flood bifurcation off the main channel and several smaller ebb channels dissect the flat into elongated segments whose configurations are shown on the aerial photograph, Figure 8b-1. In the flood bifurcation and on the highest parts of the flat, large flood-oriented sand waves are the dominant bedforms. In the main channel to the east and on the lower parts of the flat, ebb-oriented sand waves occur. Superimposed on the large flood sand waves are ripples which usually show ebb orientations at low tide. Explanation of the sand wave pattern by the time-velocity asymmetry of the flood and ebb currents is given in "Holocene Sediments of the Parker River Estuary" (this guide-book; p.337 ).

Samples from the sand bodies of this flat have graphic means between  $1.65$  and  $2.9\phi$ . The coarsest sand is in the flood bifurcation and on those parts of the flat directly in line with it. The finest sand occurs on the outer margin near the main channel and along the western margin near the marsh.

The next point bar northeast of Stop 8b, which you will pass by in the boats, differs from the one at Stop 8b in that it is triangular in shape and is not highly dissected by flood and ebb channels (Fig. 8b-2).

---

Figure 8b-1. Aerial view looking southwest over the point bar at stop 8b. Note the dissection by flood and ebb channels and the lobes of sand deposited at the heads of the ebb channels (arrows). On the exposed parts of the flats, flood-oriented sand waves are the dominant features (flood currents flow from left to right). Close to the marsh, sand waves are not present, due to the dying out of the currents on the shallow portion of the bar.

A single ebb channel cuts across its point, isolating a small flat. This point bar has a slightly elevated ridge which extends from the ebb lobe of sand at the end of the ebb channel to the center of the flat. This ridge acts as an ebb shield. Flood-oriented sand waves have developed to the south of this area and smaller ebb-modified sand waves to the north. Graphic means of sediment samples from this point bar average 1.8 to 2.3 $\phi$ . The coarsest sand is on the highest area of the flat.

The complex of point bars at the head of the estuary (including Cape Merrill, Stop 9) vary greatly in size, morphology, bedforms and grain size. Those on the western side of the estuary are composed of fine-grained sand with graphic means averaging 2.6 $\phi$ ; small flood sand waves have formed on some flats. The point bars on the eastern side of the estuary are very fine-grained sand flats and mud flats, having graphic means which average 4 $\phi$ .

---

Figure 8b-2. Point bar northeast of Stop 8b; view looking west. This point bar is not highly dissected by channels, only one ebb channel cuts across it near its point (see upper right of photograph). An ebb lobe of sand has formed at the head of the channel. Cutting half-way across the flat, near its center, is an ebb shield with ebb-modified sand waves to the north of it and larger, flood-oriented sand waves to the south.

# CAPE MERRILL

PARKER RIVER ESTUARY

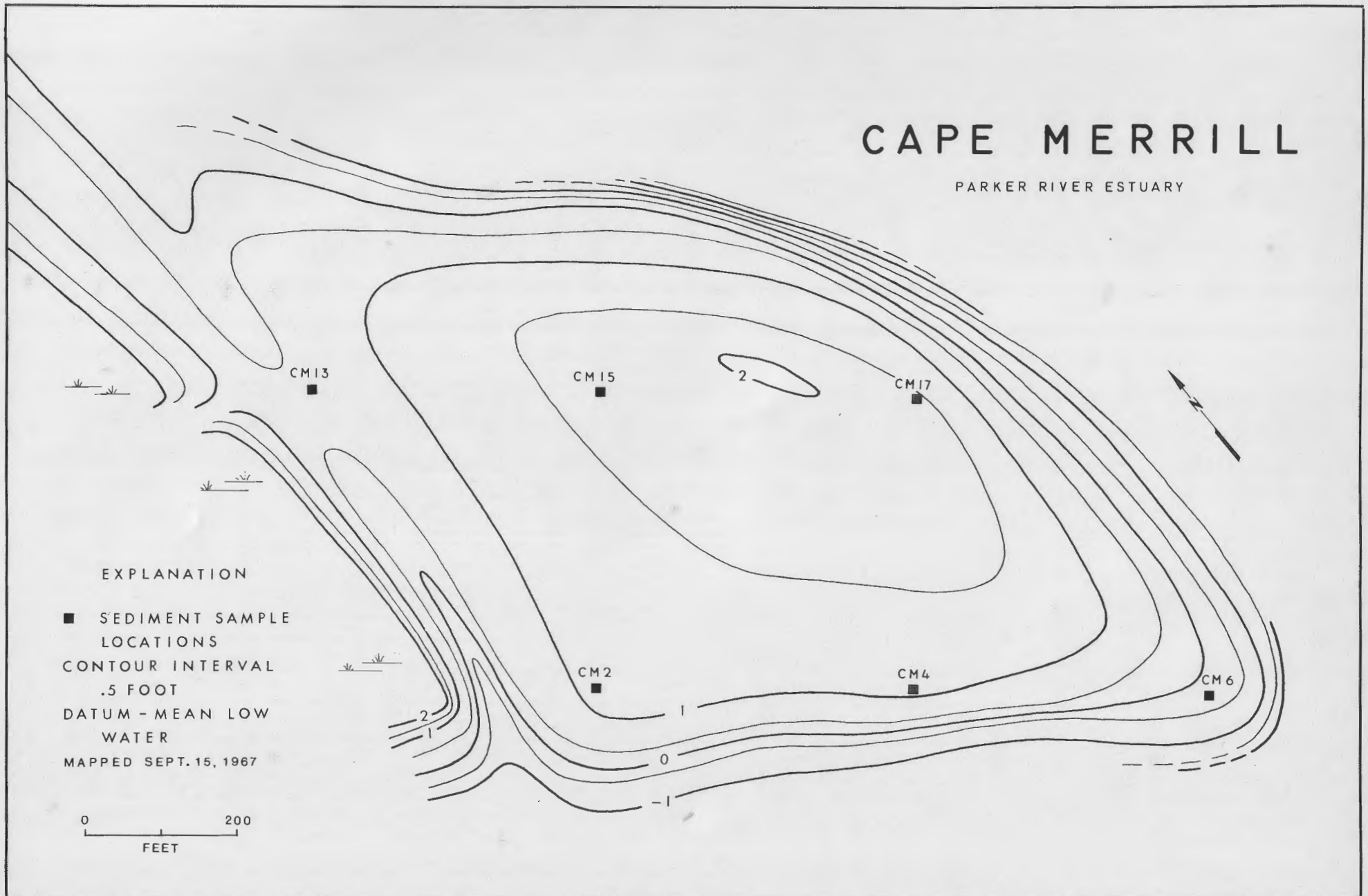


FIGURE 9-1

## STOP 9 - CAPE MERRILL

Joan M. DaBoll

Cape Merrill is typical of the broad mud flats in the large tidal creeks of the Parker River estuary. It is located at the junction of the Plum Island and Parker Rivers. The contour map (Fig. 9-1) shows the relief of the flat to be barely two feet at mean low water.

The flat covers an area of 6400 square feet, and slopes gently away from a central high to the margins, where the gradient increases. A small drainage channel almost isolates the flat from its western marsh bank at low tide.

The surface of the flat is nearly smooth, with only slight undulations and small irregularities. Infauna are abundant and cause some of the surface features such as mounds of sediment or coiled castings around worm burrows and small depressions over razor clam burrows.

Salinity values at Cape Merrill range from 24 to 29.6<sup>0</sup>/oo. Current velocity reaches a flood maximum of 2.1 ft./sec. and an ebb maximum of 1.6 ft./sec.

The sediment is coarsest toward the channels, decreases in grain size upslope toward the center, and then increases slightly on the topographic high. Graphic means of samples near channels average 3.5 $\phi$  (.090mm). Those from the central part of the flat average 4.4 $\phi$  (.048mm). Cumulative weight-percent curves for three representative samples are shown in Figure 9-2.

The substrate is dark brown and is usually shot through with numerous worm burrows. Occasional beds of shell fragments occur in some areas. Worms are the dominant infaunal organism over most of the flat. Razor clams and moon snails are present in fewer numbers.

Photographs of several box samples from this area are included in Figure 9-3.

---

Figure 9-1. Contour map of Cape Merrill.

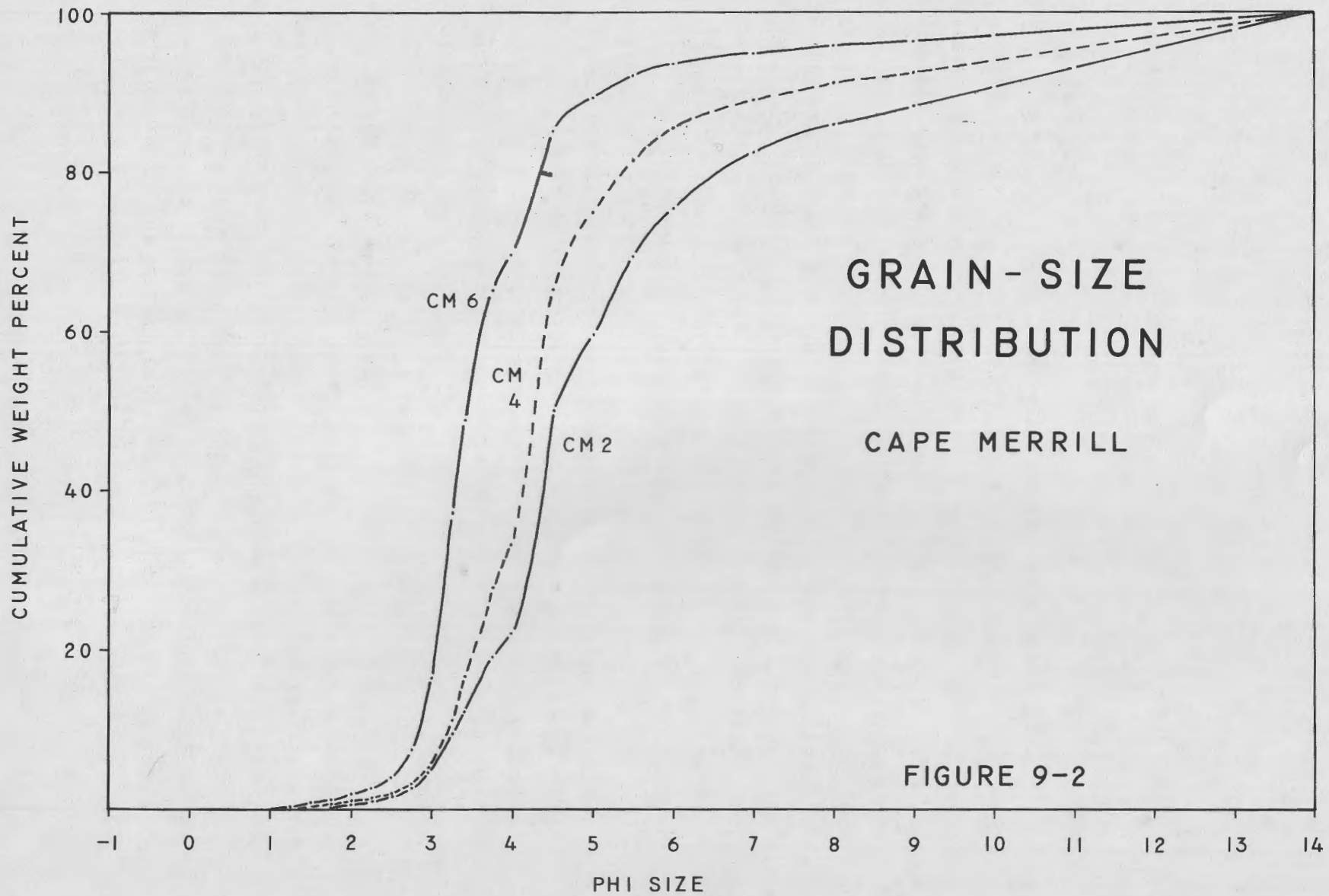
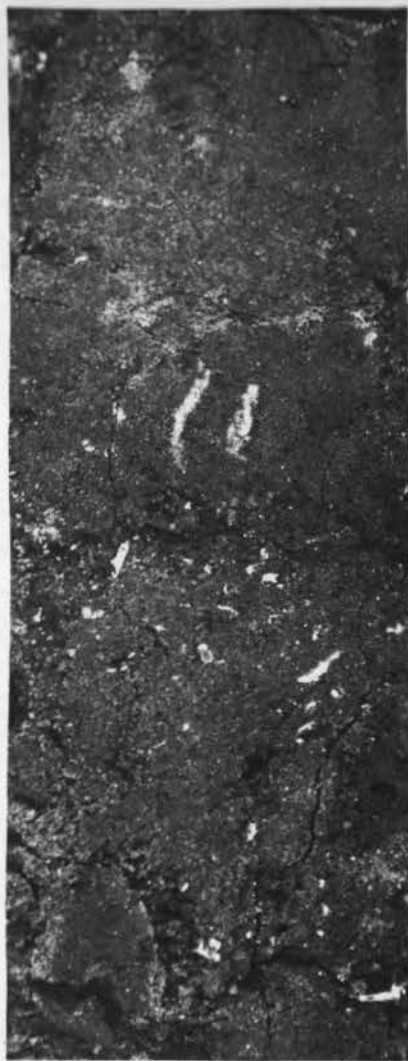


Figure 9-2. Cumulative weight-percent curves of sediment samples from Cape Merrill. Grain size increases and sorting improves along a traverse from the marsh toward the channel. Sample CM2, taken near the marsh, has a graphic mean of  $5.17\phi$  and a standard deviation of  $2.04\phi$ . CM6, taken near the channel, has a graphic mean of  $3.62\phi$  and standard deviation of  $1.05\phi$ .

5C



CM13



5<sub>3</sub>



0 1  
INCH

FIGURE 9-3

Figure 9-3. Box samples from mud flats.

5C This sample shows a discontinuous shell rich bed, one large worm burrow and several small worm burrows filled with light-colored sediment (fine sand).

CM13 Box sample from Cape Merrill showing shell fragments and small worm burrows filled with light-colored fine sand.

5<sub>3</sub> Sample illustrating bedding disrupted by burrowing.

## STOP 10 - BAR HEAD DRUMLIN, SOUTH END OF PLUM ISLAND

Joseph H. Hartshorn

Although the absolute age of the drumlins of the Boston area is unknown (that is, in radiocarbon years), most local glacial geologists attribute them to the next-to-last advance of the ice. The reasoning involves distribution of the drumlins, their orientation, their fossil content, their composition, and the degree of alteration of the original gray till. A later advance of the ice deposited a till of different texture and color, which has not yet been altered, or weathered, in a macroscopic sense. This drumlin cut gives us a chance to see both types of till.

### Section (all thicknesses variable):

Modern soil, dark gray, sandy, little humus.

Modern windblown sand, gray. This sand is still accumulating on top of the drumlin, and the soil profile at the surface is barely able to keep pace with the upbuilding of the sand. The sources include both nearby dunes and beaches.

Paleosol, fine sand to silty clay, black to dark brown, very little recognizable plant material.

Eolian mantle, fine sand through very fine sandy silt with some clay, yellow brown. After the withdrawal of the last ice sheet, the largely unvegetated areas of till and stratified drift were prime sources for windborne sand and dust. Much of southern New England is covered with a few inches to as much as five feet of this kind of fine-grained eolian material. Ventifacts are common in the mantle, although they are probably scarce or absent here.

Till, light gray, sand matrix, numerous clasts. Those who have not worked in New England or some Arctic areas will find it hard to accept this as a till. To Midwesterners, to whom till generally is a silty clay with few clasts, this probably looks like a "gravel". However, its characteristics are similar to tills found in proper topographic positions and

with properly oriented till fabrics over much of New England. Thus till may have some stratification and small laminations of well-sorted sand, but generally it is structureless. It has a wide range of grain sizes with, however, very little clay, contains angular clasts that have the appearance of having been freshly broken from bedrock or other angular fragments, and contains few striated clasts. Many clasts have silt caps on the tops or sides; this phenomenon does not occur in deposits known from other criteria to be of stream-laid origin and thus is used by local geologists - with care and with trepidation - as a criterion for till. This is the upper or "new" till.

Till, olive brown or dark yellow brown, very fine sand to clay matrix, with as much as 15 to 20 percent clay. Clasts are scarcer than in the upper till. The till is compact, difficult to dig, stands well in vertical faces (except during periods of freeze and thaw), contains numerous subangular to subrounded striated clasts, and commonly exhibits a horizontal fissility that resembles a well-made Danish pastry. The cause of the fissility is debatable.

#### Slump.

The beach displays a well-washed assortment of rock types from the north and west, including volcanics, granites, gabbro-diorites, rhyolites, breccias, metamorphosed sediments, and others. Striations are particularly visible on these boulders and cobbles. Some wind etching can be seen on a large granite boulder; the time of the wind cutting is under discussion.



FIGURE IIA-1A



FIGURE IIA-1B

## STOP 11a - HIGH TIDE BEACH

Miles 0. Hayes

At this stop, you will observe the hydrodynamic processes generated by the tide rising over sand bodies on the beach. Unless there has been a recent storm, there should be several localities along the central part of Plum Island where large ridges are in the process of building and migrating landward. We will stop at the point where the ridges are best developed on the day of the trip. Observe the differentiation of types of flow across the various subdivisions of the beach. As the water first rises, sheet flow (upper flow regime) will move across the crest of the ridge in response to wave uprush (Fig. 11a-1a). It is probable that you will observe antidunes in the process of formation and self-destruction across the top of the ridge. Another important process is the flow separation that takes place along the top of the ridge slip face. At the point of flow separation (Fig. 11a-1b), sediment cascades down the slip face. You can also observe the formation of ripples and megaripples in the runnel as strong currents flow parallel with the ridge crest. Thus, there are three basic types of flow in the beach zone during the rising tidal stage: (1) shallow sheet flow across the ridge crest, which forms plane beds and antidunes on the ridge surface; (2) a zone of flow separation at the top of the slip face where sediment avalanching down the slip face creates high-angle crossbedding; and (3) unidirectional currents flowing in the runnel under lower flow regime conditions that form ripples and megaripples.

---

Figure 11a-1. Tide rising over a ridge on central Plum Island.

A. View looking south down the crest of the ridge. Runnel (on the right) is approximately 2-1/2 feet deep. Note grain lamination (to the left) formed by shallow sheet drainage across the ridge surface.

B. View looking north along a ridge (tide higher than at A). Note zone of flow separation in the foreground. The top of the ridge slip face lies directly under this zone. Upper flow regime conditions exist to the right of the flow separation zone.



FIGURE 11B-1A



FIGURE 11B-1B

## STOP 11b - PLUM ISLAND DUNES

Fayez S. Anan - Miles O. Hayes - Frederick D. Larsen

At this stop we will walk though the dunes to the beach and back. On the way different morphological zones of the barrier island will be observed (details of the dune morphology are given in Larsen's paper on p. 356 of this guidebook). The problem of sampling barrier island sediments and details of the grain-size parameters of the dune sand will be discussed (a description of the texture of Plum Island dune and beach sand is given by Anan on p. 266 of this guidebook).

If the weather conditions are right, you will be able to see exposures of dune crossbedding. Although we have never made a systematic statistical study of the crossbedding in these dunes, our general observations indicate that a crossbedding orientation diagram would show a wide scatter. It is also clear that the fore-dune ridge contains an abundance of high-angle crossbedding that dips offshore (Fig. 11b-1). This crossbedding is formed by migrating dune lobes under the influence of strong northwesterly winds (refer to wind rose, Fig. I-2). We will probably be able to see dune lobes growing landward from the back-island dune ridge. These dune lobes are formed during northeasterly storms.

---

Figure 11b-1. Crossbedding in foredune ridge along the central part of Plum Island.

A. Crossbedding exposed in wavecut cliff on foredune ridge near middle of Plum Island. View looking southwest. High-angle crossbeds in center of photograph were formed by slip-face migration of a dune lobe built by northwest winds.

B. Crossbedding exposed on landward side of foredune ridge near profiling locality PLB. Dune face was scalloped by strong northeasterly winds. View looking southwest. Crossbeds formed by northwest winds.



FIGURE 12-1 A

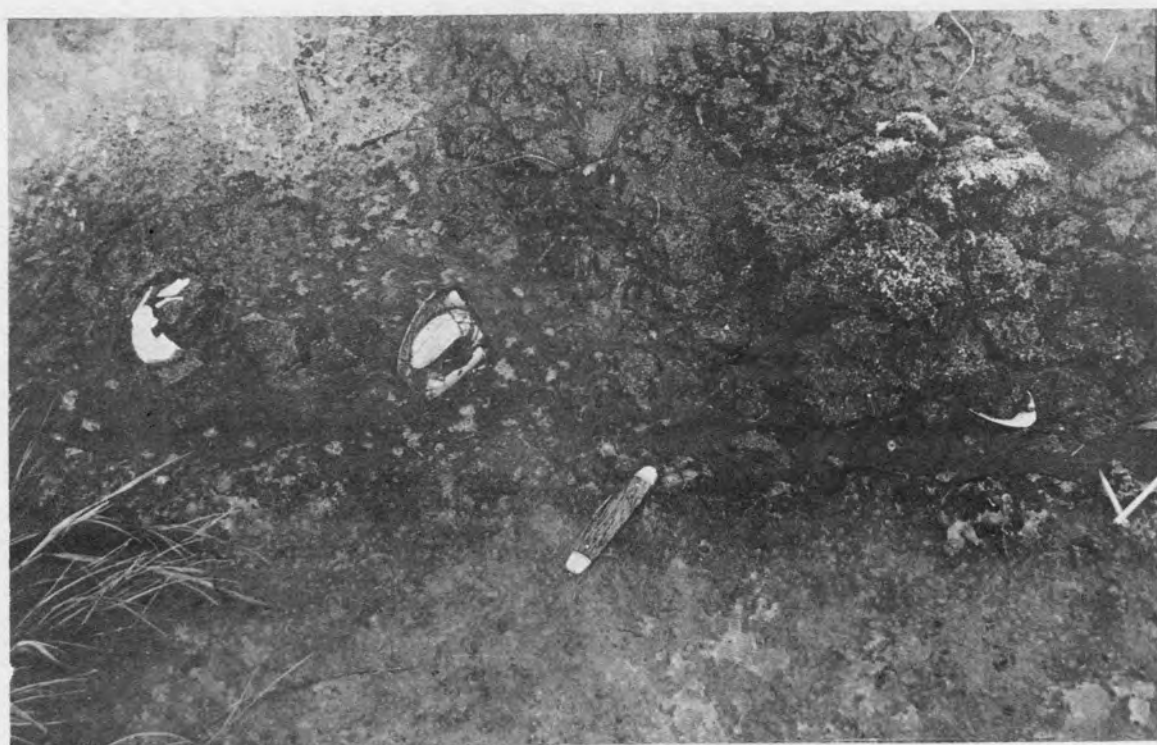


FIGURE 12-1B

## STOP 12 - PLUM ISLAND MARSH

Miles O. Hayes

The high salt marsh forms a flat plain that adjoins the western boundary of the dunes on Plum Island. The most common grasses that make up the dense mat of vegetation you will walk over include Spartina patens, Juncus gerardi, Distichlis spicata, and others. The high salt marsh is the most nearly planar marsh environment and the most densely populated with floral elements.

The general stratigraphic column of Holocene sediments at this stop is as follows:

<u>Thickness</u>	<u>Description</u>
7 to 10 ft.	High salt marsh peat; brown to yellow brown, composed of roots of high salt marsh plants, fine textured, average organic content - 23%.
0 to 2 ft.	<u>Spartina alterniflora</u> peat; gray brown, composed almost exclusively of remains of <u>S. alterniflora</u> and silt.
?	Eastern coarse-grained facies (of McCormick); gray, fine to very fine-grained sand, moderately to poorly sorted.

This stop is located near the eastern border of cross-section B-B' (Fig. 4) in McCormick's paper (p.368, in this guidebook). McIntire and Morgan (1963) had a radiocarbon date of 680 years B.P. for the base of the peat near this locality; therefore, the peat deposit east of the main channel of the estuary is thought to be considerably younger than

---

Figure 12-1.

- A. Blocks of ice carried out of the main channel of the Plum Island River during a spring tide. Note dark laminations of mud in the ice.
- B. Close-up of mud deposit left by melted ice block. Note Mya arenaria shells.

that on the western side (McCormick). The total thickness of the eastern coarse-grained facies is uncertain, inasmuch as McCormick's cores never completely penetrated it. It appears to be in the vicinity of 30 feet thick on the basis of data of McIntire and Morgan.

If you examine the peat closely, you will detect layers of mud mixed with the organic layers. Ice rafting accounts for the accumulation of at least some of this mud. During extended periods of sub-freezing temperatures, the surface of the estuary freezes at high tide. As the tide ebbs, blocks of ice drop to the surface of the mud flats. Layers of mud are then frozen to the bottom of the ice blocks. As the tide floods again, the blocks float off, carrying a coating of mud. This process is repeated numerous times and the blocks become filled with laminations of mud. During storm surges and exceptionally high spring tides, the sediment-laden blocks are transported out of the channels onto the marsh where many are stranded. When the blocks melt, a mud layer, sometimes as much as 2 to 3 inches thick, is deposited. Figure 12-1a shows ice blocks stranded on the edge of the Plum Island River channel. The muddy sediment carried onto the marsh by the blocks commonly contains shells of Mya arenaria and other infauna (Fig. 12-1b).

## STOP 13 - RYE GRAVEL BEACH, RYE, NEW HAMPSHIRE

Barry S. Timson

This stop at Rye Gravel Beach provides an opportunity to investigate gravel beach morphology and particle-size and shape distribution and to make comparisons with Plum Island beaches.

The sequence of beach forms, from land, seaward, is: (1) wash-over fan (absent at south end of beach); (2) storm ridge; (3) berms; (4) beach face; and (5) beach step. The number of berms varies with tidal and weather conditions. The berms are usually cusped, and include both erosional and constructional varieties at different periods.

Particle-size distribution generally decreases both landward and seaward from the storm-ridge crest. Large discoidal pebbles generally constitute ridge and berm frameworks. Large spherical pebbles usually accumulate on berm surfaces while smaller spheres and rod-shaped pebbles constitute the base of the beach face.

Variation in morphologic development and particle-size distribution occurs during post-storm recovery (Timson, p.391 of this guidebook).

Comparisons between Plum Island beach forms, growth rates, and particle-size distributions resulting from storm erosion and subsequent recovery and those of Rye Gravel Beach will be discussed in the field.

## STOP 14 - HAMPTON BEACH, N.H.

Miles O. Hayes

Hampton Beach is one of the most important recreational beaches on the northern New England coast (Fig. 14-1). Thousands of tourists, especially from the Canadian provinces, come to the area each summer. A perennial problem on this beach is the loss of sand from the northern end. Hence, corrective measures are taken periodically to keep a wide sand beach available for the tourists in the summer. The Corps of Engineers has had the area under surveillance for several years (see House Documents Nos. 325 and 416).

A report dated 1953 by the Corps of Engineers (House Document 325) recommended improvement of the beach in front of and north of the business district by placing 101,000 cu. yds. of sand on the beach. The project was carried out in 1955. Subsequent studies showed that during the period December, 1955 to January, 1959, about 80,000 cu. yds. of fill above mean low water had been lost, an annual loss of approximately 26,000 cu. yds. (Byrne, 1966). The process was repeated in the fall of 1965 when approximately 250,000 cu. yds. of sand, dredged from the harbor, was placed on the beach in the vicinity of this stop location. American Dredging Co., using a 20 inch hydraulic dredge, did the work under state and federal supervision. Pipe was laid for about 2-1/2 miles. Filling began at the southern end of the fill area, worked north to about the middle of the bend in the shore, and then progressed southward. The dredging operation was completed on December 1, 1965.

Our group began observing this beach on 30 September, 1965, the day that the fill operation began (Fig. 14-2). The profile for that day is shown in Figure 14-3. Since the beginning of our study, 94 beach profiles have been measured at this stop locality at approximately 2-week intervals. Several stations on Hampton Beach also have been monitored. As shown in Figure 14-3, in the interval between 18 November, 1965, and 1 March, 1969, most of the sediment originally implaced at the stop locality (station HBB) has been lost. This loss is dramatically shown in the photographs of Figures



FIGURE 14-1

28 MARCH, 1967



FIGURE 14-2

30 SEPTEMBER, 1965

14-4 and 14-5. Practically all the loss of sand from this beach took place during northeasterly storms. In intervals between storms, a small amount of sand returned to the beach, but not nearly as much as had been lost in the preceding storm. Most of the sand that is carried offshore during storms is transported to the south by long-shore currents generated by the waves from the northeast. Wave reflection from the seawall on the north end of the beach (Fig. 14-7) appears to augment the long-shore drift.

The beach survived the first year without much loss of sand. However, erosion during the second winter was very severe. During the spring of 1967 the beach face retreated progressively landward toward the seawall (Fig. 14-6). Note the meagre efforts of the beach to recover between storms. The recovery material is indicated by the shaded portions of the profiles for 9 March, 1967, and 24 May, 1967 (Fig. 14-6). The storm of 25 to 26 May, 1967, was very severe and a large volume of sediment was lost. The last period of severe erosion was during February, 1969, which produced the profile of March, 1969 (Fig. 14-3).

Figure 14-7 is a scatter plot of mean grain size versus inclusive graphic standard deviation and inclusive graphic skewness for 15 samples collected at profile HBB at different times of the year and on different parts of the profile. The samples average  $1.59\phi$  in mean grain size and  $.57$  in inclusive graphic standard deviation. Most of the samples are near symmetrical; 4 are coarse skewed and 2 are fine skewed.

As you stand at the seawall, look seaward across the large rocks now protruding through the short, steep beach profile. Try to imagine a sand berm the width of a football field between the seawall and the high-tide mark and you will have reconstructed the beach as it was in late fall, 1965.

---

Figure 14-1. Hampton Beach, N. H., on 28 March, 1967. Arrow points to stop location. Compare this view with the profile in Figure 14-6.

Figure 14-2. View looking north along Hampton Beach on 30 September, 1965, the day the fill operation began. Station HBB is approximately 100 feet from the end of the pipe (see profile (Fig. 14-3) for this date).

Figure 14-3. Changes in profile HBB, Hampton Beach, N. H., in the interval from 30 September, 1965, to 1 March, 1969.

BEACH PROFILES  
STATION HBB, HAMPTON BEACH  
HAMPTON, N.H.

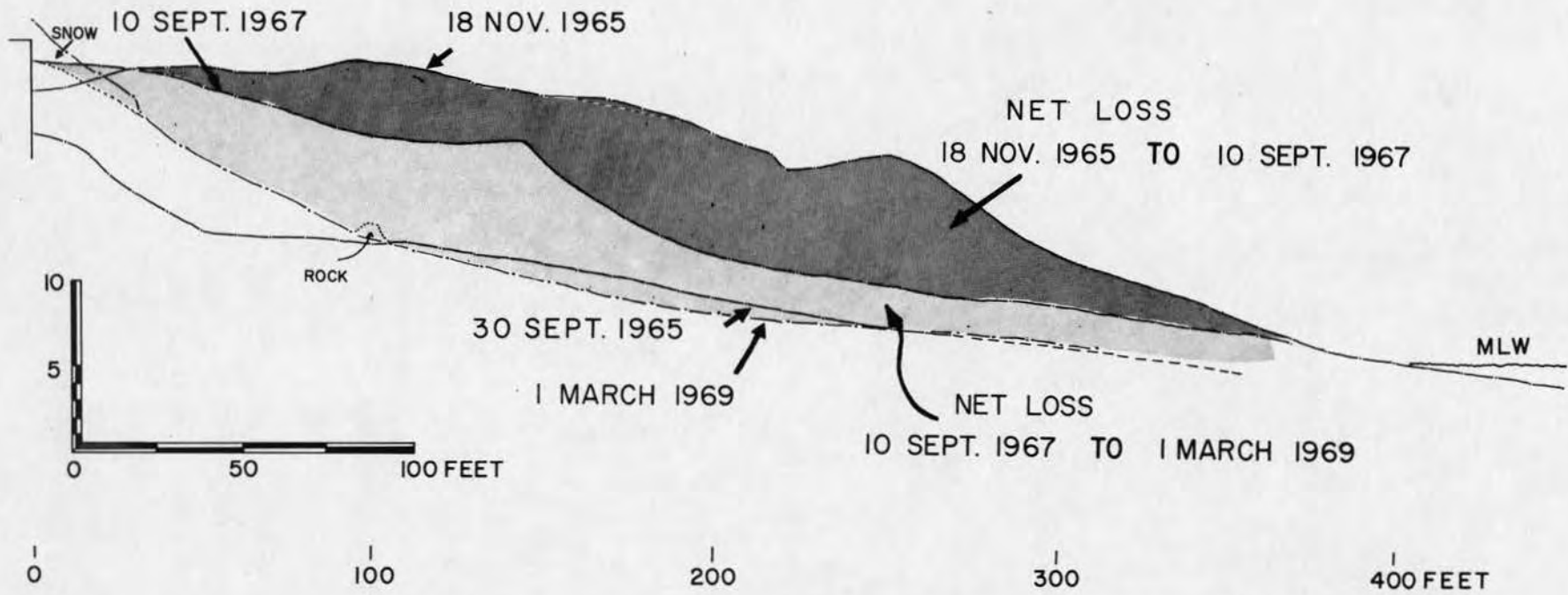


FIGURE 14-3



**FIGURE 14-4**      **18 NOVEMBER, 1965**



**FIGURE 14-5**      **11 FEBRUARY, 1969**

Figure 14-4. Profile HBB, Hampton Beach, N. H., on 18 November, 1965.

Figure 14-5. Same view as Figure 14-4 on 11 February, 1969. Compare these photographs with the beach profiles in Figure 14-3.

Figure 14-6. Changes in the beach profile at station HBB, Hampton Beach, N. H., in the spring of 1967.

# SPRING 1967 PROFILES

STATION HBB, HAMPTON BEACH  
HAMPTON, N. H.

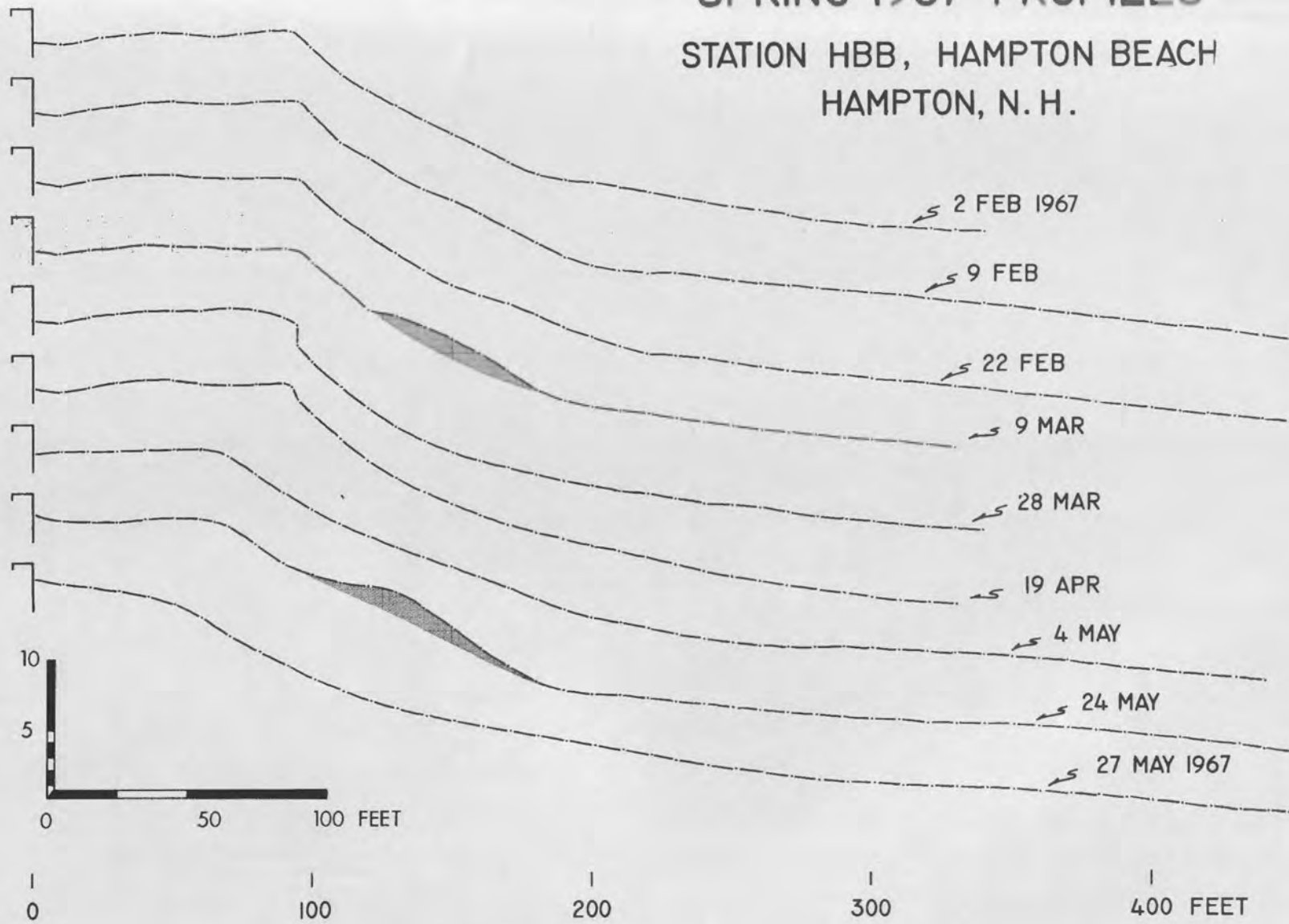


FIGURE 14-6

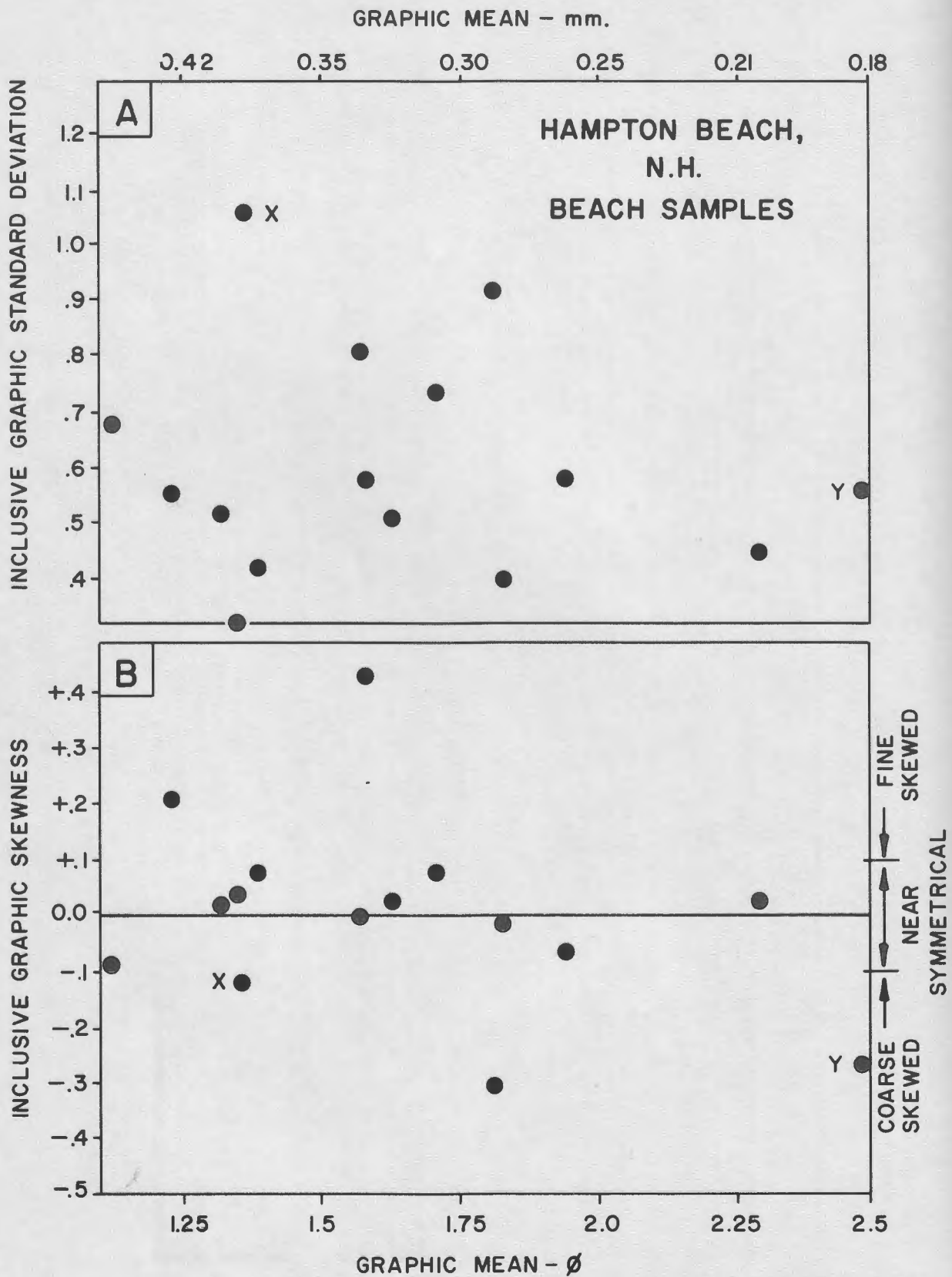


FIGURE 14-7

Figure 14-7. Scatter plots of graphic mean versus inclusive graphic standard deviation (A) and inclusive graphic skewness (B) for 16 samples collected at profile HBB. Sample x was collected from material coming directly from the dredge pipe and sample y was a beach-face sample collected on 30 September, 1965, before the fill operation began.

## STOP 15 - HAMPTON HARBOR ESTUARY

Sharon A. Greer

Hampton Harbor is the northernmost estuary in the field trip area (Fig. RL-2). It has a mean tidal range of 8.3 feet and a spring range of 9.1 feet. The estuary is partially mixed; the fresh water influx is minute compared to the volume of sea water exchanged during a tidal cycle.

Detailed field study of this estuary during the summer and fall of 1967 showed that the estuarine environment could be divided into six distinct subenvironments.

**SALT MARSH:** This is the most extensive environment (Fig. 15-1). The higher parts of the marsh are populated by Spartina patens, Juncus gerardi, and other species in minor amounts. The intertidal marsh is almost exclusively Spartina alterniflora. The thickness of the marsh is irregular, but detailed stratigraphy has not been done.

**SMALL TIDAL CHANNELS AND MUD FLATS:** In the Hampton estuary, the mud flats are associated exclusively with the smaller tidal channels. They are located between the peat banks and the channel proper and contain approximately 80 percent fine sand and 20 percent silt and mud.

The small tidal channels typically have one of two cross-sectional profiles, either flat-bottomed or containing a large sand body, the mid-channel bar (Fig. 15-2).

In the channels that contain mid-channel bars, the high shallow channel carries the highest velocity flood currents, and the deep channel carries the highest velocity ebb currents. Thus the bar migrates in the flood direction and usually has a high slip face oriented in the landward direction. The reason for the migration in the flood direction is that by the time ebb velocities are strong enough to transport sand, the water

---

Figure 15-1. Salt marsh and meandering tidal channel of the Taylor River, Hampton Harbor estuary.



FIGURE 15-1

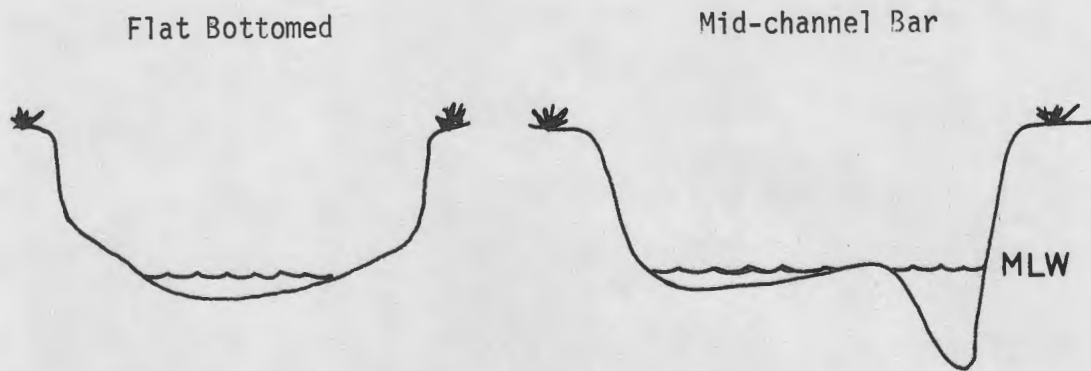


FIGURE 15-2

level is so low that it is confined to the deep, outside channel.

**LARGE TIDAL CHANNELS AND SAND FLATS:** The large tidal channels are typically broad and shallow and are bordered by wide intertidal sand flats (Fig. 15-3). The floor is usually covered with linear megaripples, peat blocks, and shell hash. Where the large channels enter the inlet, the dominant ebb currents have built ebb lobes, analogous to Price's crescentic terminal bars (Price, 1963).

The bordering sand flats are composed of fine-grained (approximately  $3.25\phi$ ) quartz sand. The bedforms on the flats are predominantly ripples or current shadows. The internal structure of these flats has nearly been destroyed by the burrowing of *Mya arenaria* (soft-shell clam) and numerous species of worms. In places, laminations formed by filamentous algal mats have been preserved.

**INLET:** The inlet area (Fig. 15-4) contains a diversity of sand body types and bedform varieties. The sand body types include a flood and ebb delta, several spits, ebb lobes, ridge-and-runnel systems, and large migrating transverse bars.

The floor of the inlet is completely covered with bedforms. The area between the jetties has large, migrating, ebb-oriented bars with a wavelength of 100 to 300 feet. These bars are built by ebb currents which attain a velocity in excess of 3.0 feet per second at the floor of the inlet.

---

Figure 15-2. Cross-sectional profiles of a flat-bottomed tidal channel and of a tidal channel containing a mid-channel bar.



FIGURE 15-3A



FIGURE 15-3 B

The bars retain their ebb orientation during flood, but have small flood-oriented megaripples superimposed on them.

Landward from the bridge, the floor of the inlet is covered with flood-oriented bedforms throughout the tidal cycle in response to high velocity flood currents and the topographically high position of this part of the inlet. Some of these flood-oriented megaripples and sand waves grade into washed-out dunes, apparently a transition to the upper flow regime (Simons and others, 1965). The deeper channels on either side of this central area have bedforms which change their orientation with the changing tide.

Data on the orientation of the bedforms in the inlet were collected at high and low water slack during a period of mean tidal range. The rose diagrams in Figure 15-5 show the slip face orientations of these bedforms

The flood tidal delta has been studied by numerous University of Massachusetts students. A composite of the observations and data from these studies is presented in the following section.

**FLOOD TIDAL DELTA:** The flood tidal delta is a major form of sand accumulation in estuaries. Because this sand body is mainly intertidal and migrates away from the basin center, it is most important in paleogeographic reconstruction of shallow-water marine sedimentary environments (see paper by Hayes and others, p.290 of this guidebook).

The Hampton Harbor flood tidal delta has been built onto a large clam flat by tidal currents flowing into the inlet and then diverging into the main tidal channels. At all stages of the tide, most of the delta surface is covered with linear flood-oriented sand waves which have a complex criss-cross pattern (Fig. 15-6). Current flow studies provide little insight into the cause of the criss-cross pattern, but it is probably the result of a subtle shift in flow direction as the water level rises.

---

Figure 15-3. View down Blackwater River tidal channel showing a main tidal channel and associated environments.



FIGURE 15-4 A



FIGURE 15-4 B

The flood delta is somewhat modified by the strong ebb currents which flow in the channels on either side of the sand body. On the south side a long, trailing ebb spit is built by the ebb current in the Blackwater River channel. At low-water slack, this spit is covered with ebb-oriented scour-megaripples (Fig. 15-7) and some sand waves with scour pits (similar scour-megaripples are seen at Stop 17). The migrating scour pits and planar slip faces produce festoon and planar cross-bedding. Festoon crossbeds form where scour pits are migrating and planar crossbeds where a plane slip face is moving up the stoss side of the preceding bedform.

Occasionally these scour-megaripples become washed out (or planed off) when the water is very shallow, but the current velocity still quite high (3.2 ft./sec). Apparently at that time the flow is near the upper boundary of the lower flow regime (Simons and others, 1965); see also discussion by Boothroyd, p.417 of this guidebook. At times, a large standing wave develops over the spit until the flow either stops (dunes exposed as during ebb tide) or the water becomes so deep that the flow drops well into the lower flow regime and normal avalanche slip faces reappear (as during flood tide).

Several maps of the tidal delta were made in the spring of 1967. Work includes current velocity and direction studies by P. Pinet, measurement of structure orientations by J. Boothroyd, and topographic and grain size maps by W. Handy and K. Geller, respectively.

The topographic contour map in Figure 15-8 delineates the largest features on the delta, two flood-oriented bars. The large westernmost bar is presently being destroyed by a small channel draining the clam flat. Apparently, the sand supply to the bar is too little to maintain the slip face position. The grain-size distribution (Fig. 1509) shows that the sediment becomes progressively finer toward the highest part of the sand body. This is apparently a reflection of the distance from the source, the sub-tidal inlet floor.

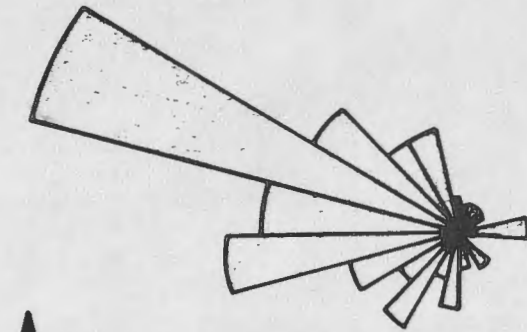
Bedform orientations taken at low tide during the spring of 1967 (Fig. 15-10) show the general fanning out of the sand waves across the delta.

---

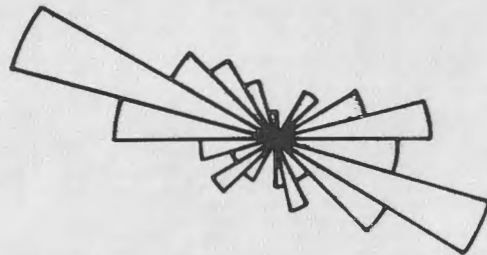
Figure 15-4. Hampton Harbor estuary inlet.

# SLIP FACE ORIENTATIONS

## HAMPTON HARBOR INLET



HIGH TIDE SLACK  
57 READINGS



LOW TIDE SLACK  
62 READINGS

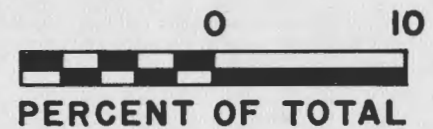


FIGURE 15-5

The map also shows that the megaripples on the ebb spit are oriented obliquely to the trend of the spit. The oblique trend is caused by the tide falling rapidly in the center of the inlet, producing a gradient toward the center of the inlet; thus the water flows obliquely across the spit. As the water level continues to fall, the current becomes confined to the channel and flows parallel to the spit in the latter stages of ebb flow. As the tide floods it piles up in the inlet and then flows obliquely across the spit, producing obliquely oriented flood megaripples.

---

Figure 15-5. Rose diagram showing slip face orientations of bedforms in the Hampton Harbor inlet. Readings were taken during a period of mean tidal range.

Figure 15-6. The Hampton Harbor flood tidal delta showing the criss-cross sand wave pattern and trailing ebb spit.

Figure 15-7. Scour-megaripples on the ebb spit of the flood tidal delta.

Figure 15-8. Topographic contour map of the flood tidal delta of the Hampton Harbor estuary.



FIGURE 15 - 6



FIGURE 15 - 7

# HAMPTON HARBOR TIDAL DELTA

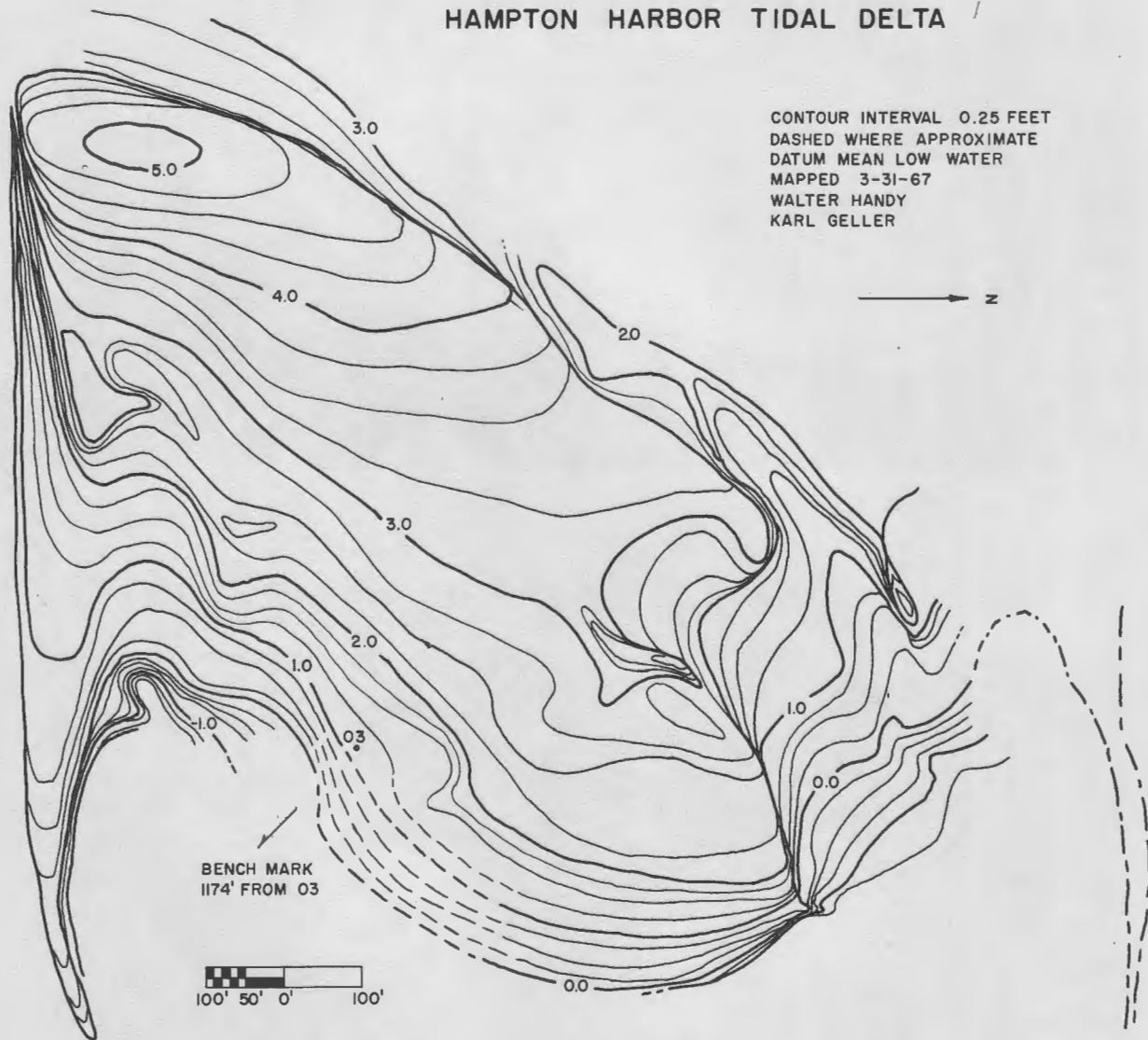


FIGURE 15-8

Figure 15-9. Grain size distribution of sand on the flood tidal delta. Map based on 23 samples spaced evenly over the delta.

Figure 15-10. Bedform orientations at low tide on the flood tidal delta of the Hampton Harbor estuary showing the fanning out of the sand waves across the main body of the delta and the oblique orientation of the megaripples on the ebb spit.

# HAMPTON HARBOR TIDAL DELTA SEDIMENT DISTRIBUTION MAP

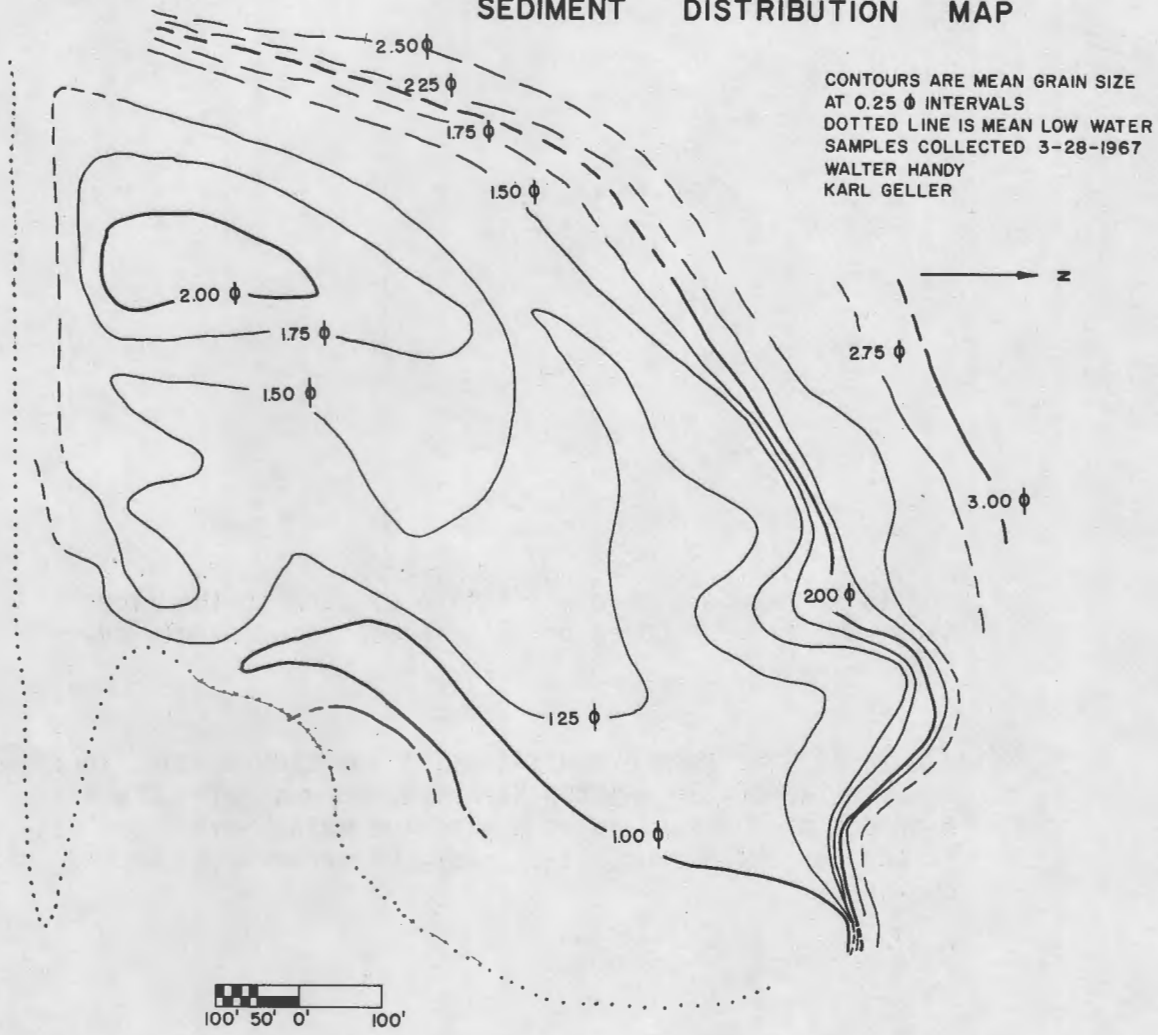


FIGURE 15-9

SEDD WAVE AND MEASURED ORIENTATIONS  
HAMPTON HARBOR TIDAL DELTA

HAMPTON HARBOR TIDAL DELTA

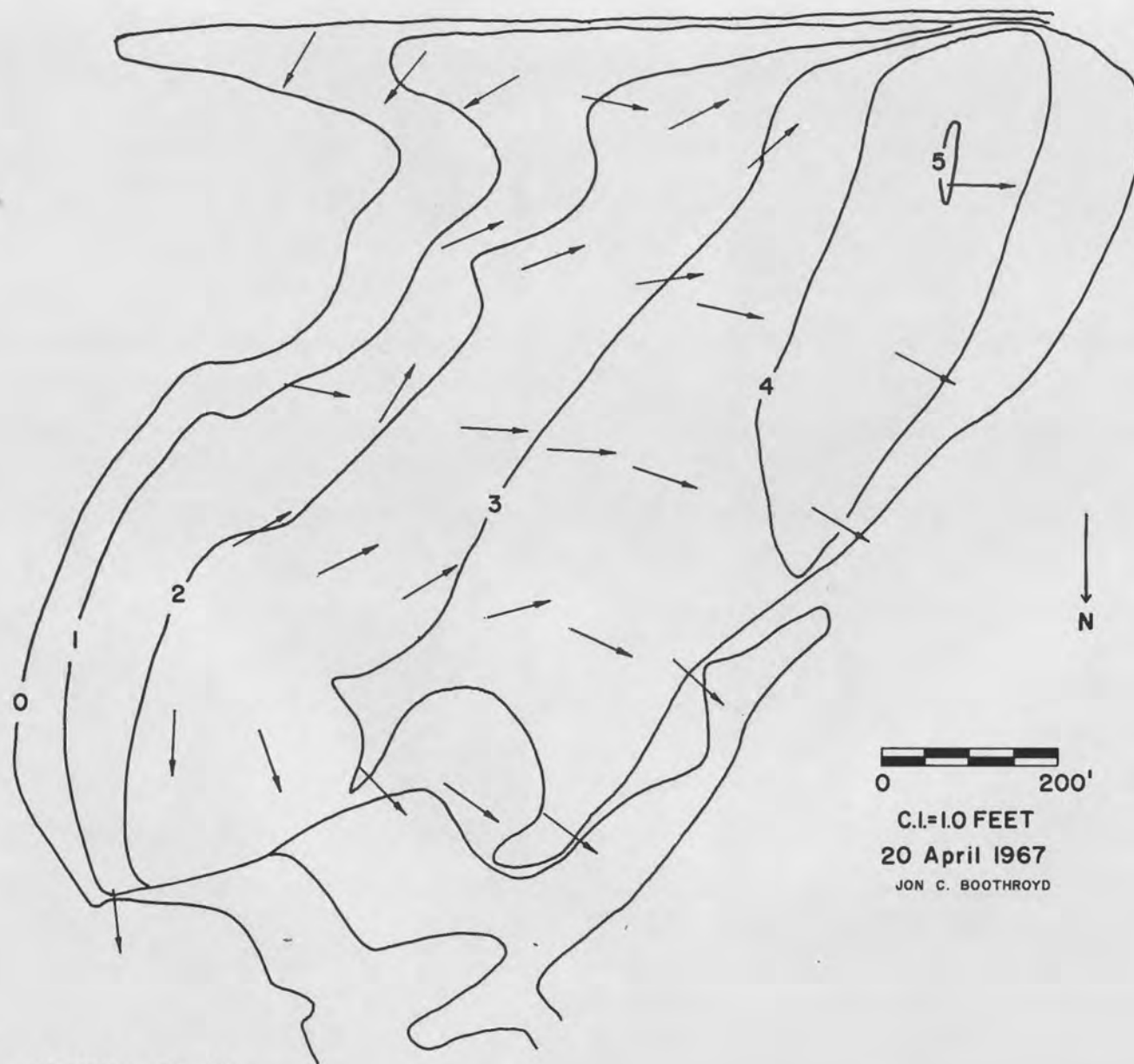
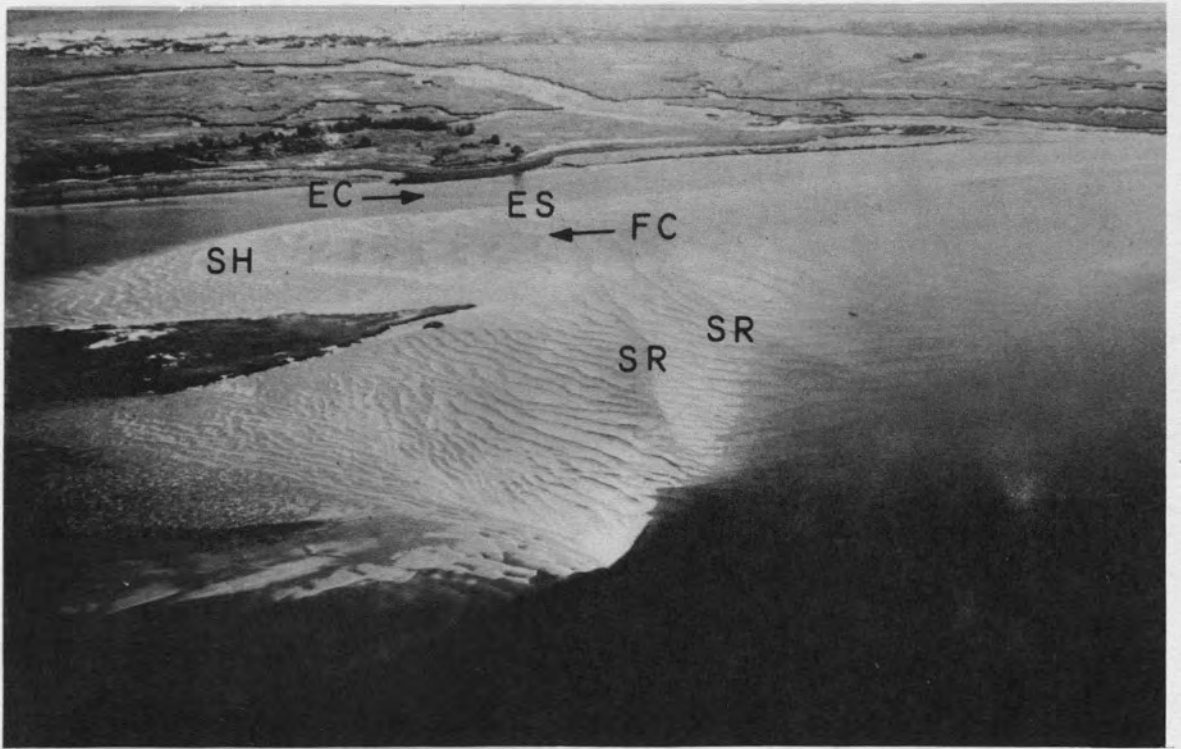


FIGURE 15-10



A



B

FIGURE 16-1

## STOP 16 - MIDDLE GROUND, PARKER RIVER ESTUARY

Joan M. DaBo11

The purpose of the traverse to be made at this location (Fig. 8b-1) is to provide the opportunity to observe some of the significant features of the flood tidal delta system of the Parker River estuary; an ebb spit, flood channel with ebb shield near its upcurrent margin, and a broad flat, covered by flood-oriented sand waves which are superimposed upon a series of sand ridges of low amplitude but very great wave length (Fig. 16-1(A)).

Ebb-oriented scour-megaripples, 2 to 7 feet in length and 6 to 12 inches in height, are the dominant features on the southern portion of the ebb spit, which is situated along the eastern margin of the flat (Fig. 16-1(A)). The megaripples are formed during the ebb period by strong currents which flow obliquely across the spit in a southerly direction. At the northern end of the spit there are sand waves, 30 to 50 feet in length and 12 inches in height, which show both flood and ebb features due to the proximity of a flood channel on the west and an ebb channel on the east. Their shape at low tide indicates a general flood orientation, but ebb currents have rounded their crests and formed small, ebb-oriented slip faces (Fig. 16-1(B)).

---

Figure 16-1(A). View looking southeast across the southern end of Middle Ground. Long, narrow sand form on the distant edge of the sand flat (labeled ES) is an ebb spit of the flood tidal delta complex. Beyond it is an ebb channel (labeled EC; arrow indicates ebb current direction). On the west side of spit is a flood channel (labeled FC; arrow indicates flood current direction) with a well developed ebb shield (labeled SH) at its head. A less well-developed ebb shield has formed on the near side of the flat. Two large, flood-oriented sand ridges (labeled SR) have formed across the exposed part of the flat. A third can be seen below water level at far center right. Wave lengths of these features average 500 feet and, where exposed, heights average 1.2 feet. The flat is dominated by flood-oriented sand waves, 30-60 feet in length and averaging 7 inches in height, with smaller ebb-oriented sand waves, 15-25 feet in length and 4 inches in height, occurring north of the shields.

(B). Closer aerial view of the southern end of Middle Ground showing eastern ebb shield (SH), flood channel (FC), and one of the sand ridges. Note the predominance of flood-oriented sand waves.

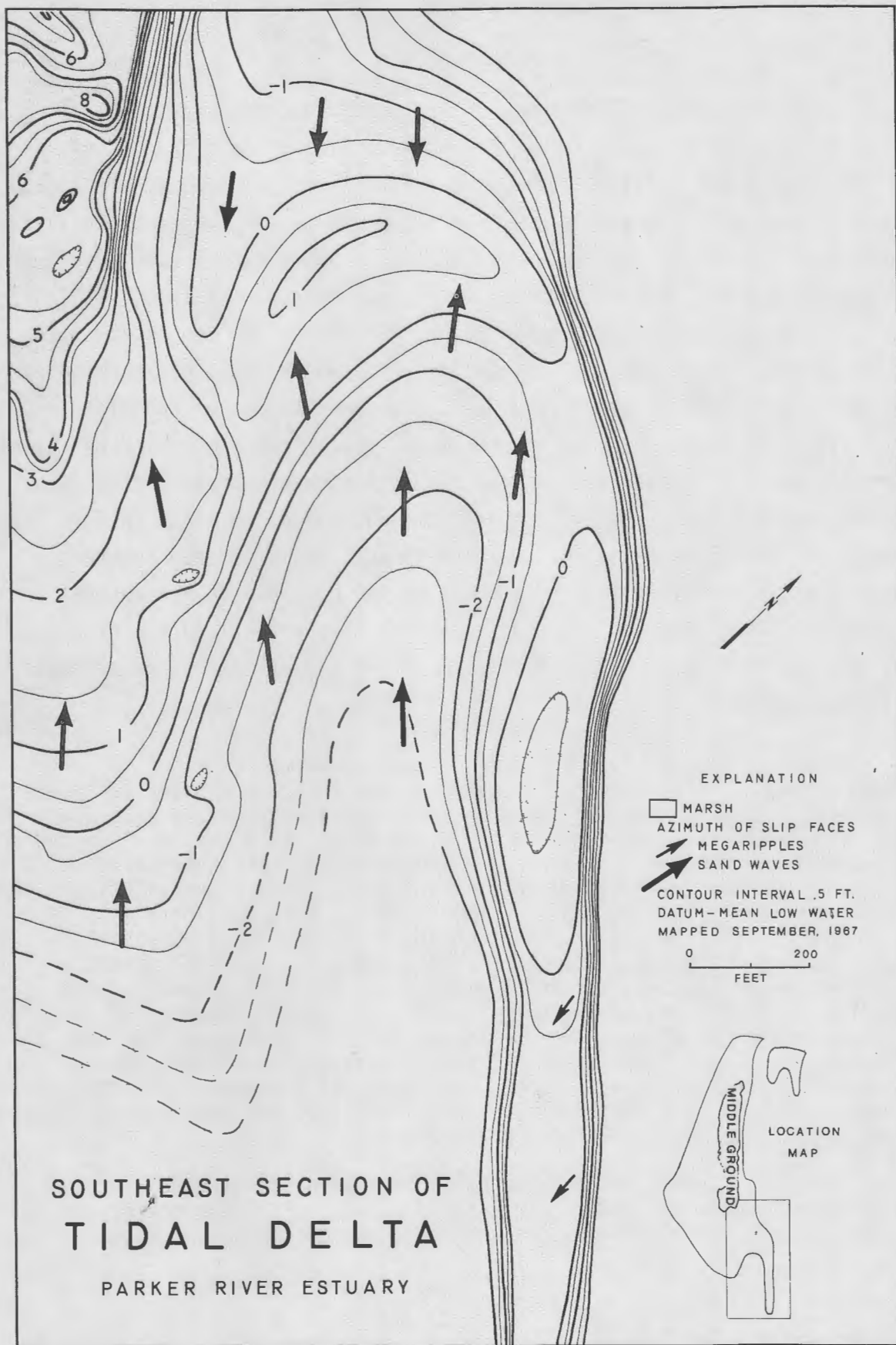


FIGURE 16-2

To the west of the spit, a flood channel cuts into the flat (Fig. 16-2). An ebb shield is situated near the head of the flood channel. South of this shield, flood sand waves, 20 to 60 feet in length and 4 to 9 inches in height, dominate the flat. Smaller, ebb-oriented sand waves, 15 to 30 feet in length and 4 inches in height, dominate to the north. The coarsest sand in this area, averaging around  $1.35\phi$ , occurs in the flood channel and on the extreme northern end of the spit. The graphic mean of sediment on the shield is slightly finer,  $1.6\phi$ , because strong ebb currents carry finer material high on the ebb shield due to its low gradient.

The broad flat west of the flood channel on the southwest side of the tidal delta system (Fig. 16-3) has a low ebb shield along its northern boundary, separating this flat from the finer grained clam flat to the north. In this area (at low tide), small ebb-oriented sand waves, 15 to 25 feet in length and 4 inches in height, are sometimes present north of the shield, whereas larger flood-oriented sand waves, 30 to 60 feet in length and 6 to 9 inches in height, are present south of the shield. Trending obliquely to the sand waves, but not interrupting their continuity, are three large sand ridges with wavelengths averaging 500 feet and measured heights up to 1.2 feet where exposed at low water (Fig. 16-1(B)). Grain size on this flat ranges between  $1.5$  and  $1.8\phi$ . The coarsest sand is on the ebb shield.

Box samples from the sand flats along the southern portion of the tidal delta system show both horizontal bedding and crossbedding. The crossbedding dips northwest, reflecting the dip of the slip faces of the sand waves. In areas where ripples retain constant trends throughout the tidal cycle, small-scale crossbedding is preserved (Fig. 16-4).

---

Figure 16-2. Contour map of the southeastern section of Middle Ground showing the ebb spit, ebb shield and flood channel. The eastern ends of the exposed sand ridges are shown. Sand wave orientations are superimposed on the map.

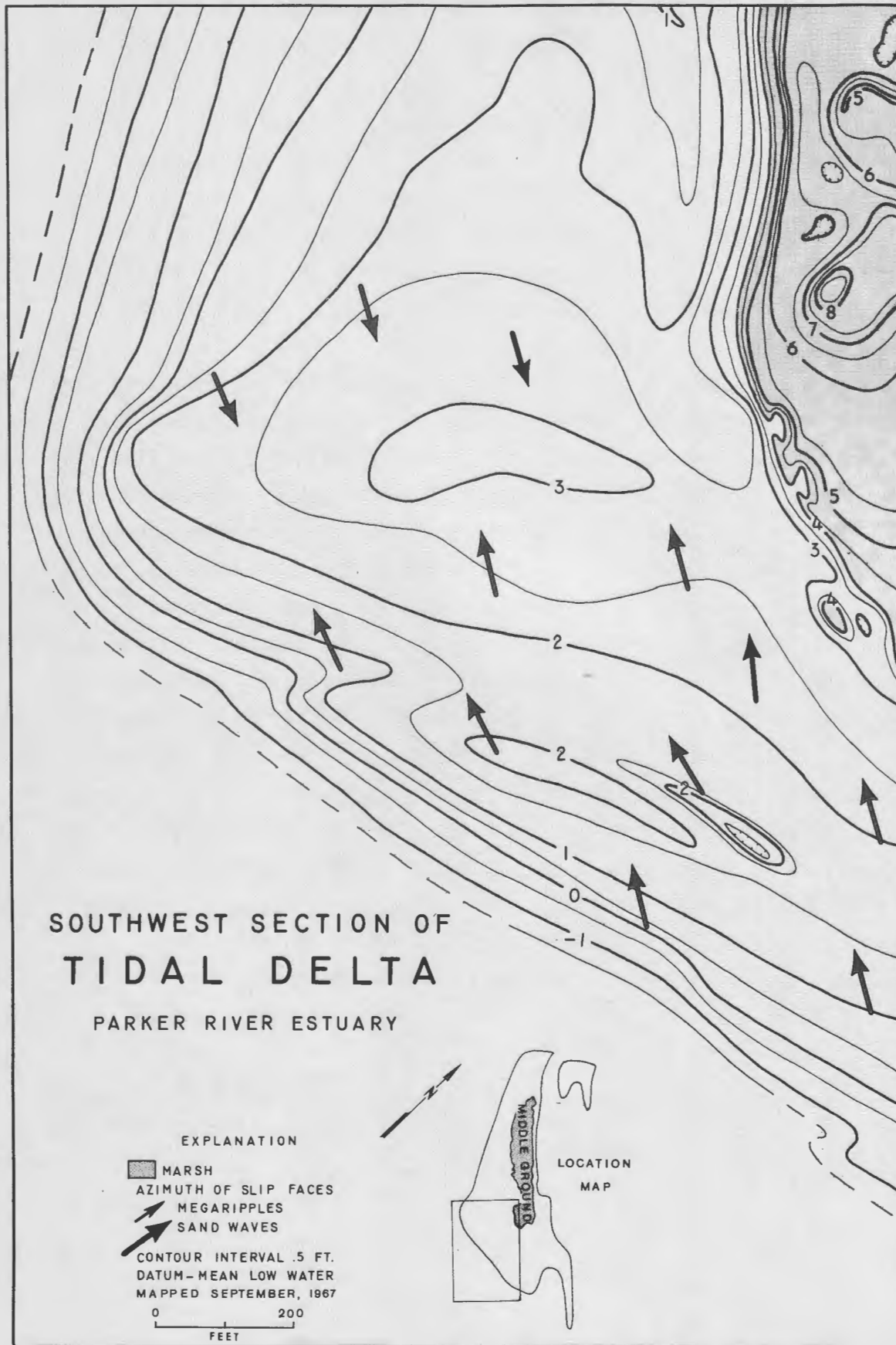


FIGURE 16-3

Figure 16-3. Contour map of the southwestern section of Middle Ground.  
A poorly developed ebb shield occurs on the northern half of map. Note the large flood-oriented sand ridges that cut across this part of the tidal delta.

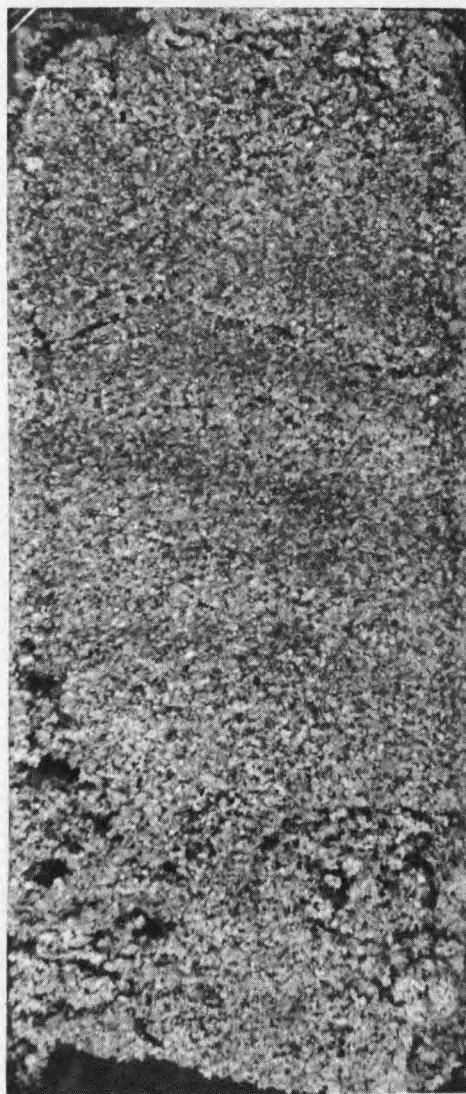
Figure 16-4. Photographs of representative box samples from the sand flats surrounding Middle Ground.

- 13E Sample from the southwestern section of Middle Ground just west of the marsh. Sand waves are poorly developed in this area and horizontal bedding is preserved.
- 51 Sample from the southeastern section of Middle Ground, south of the ebb shield. Crossbedding is preserved in this sample with a dip direction paralleling that of the slip faces of the sand waves.
- 26 Biogenic structure in sample from small ebb-dominated depression directly east of Middle Ground marsh.

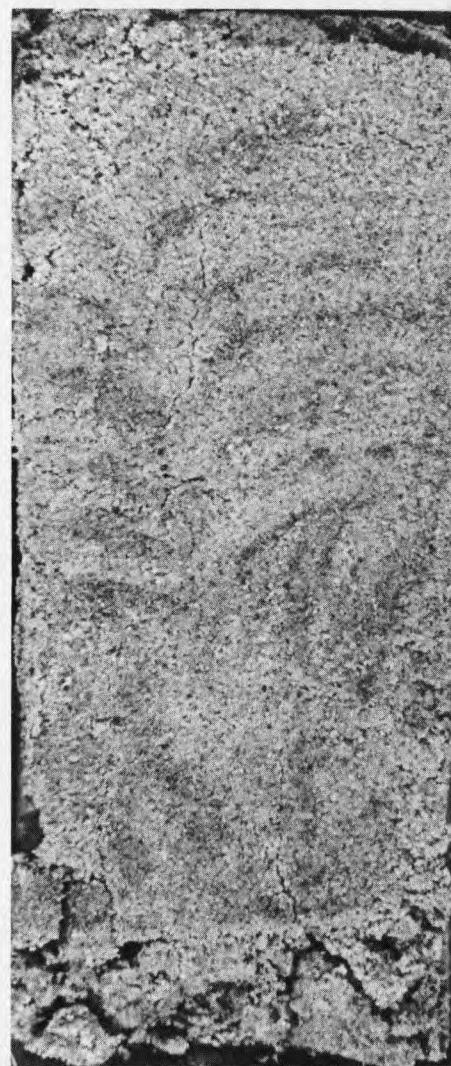
13E



51



26



0 1  
INCH

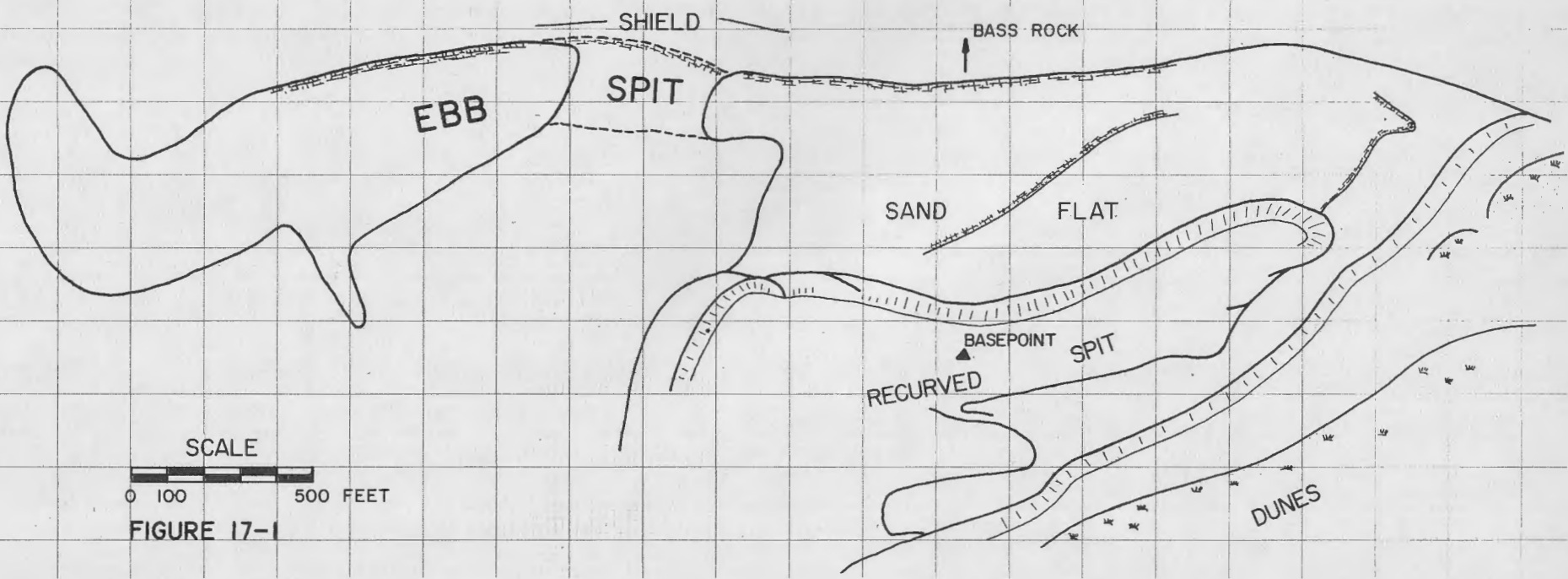
FIGURE 16-4

# EBB SPIT AREA

SOUTH END, PLUM ISLAND  
IPSWICH, MASS.



PARKER RIVER CHANNEL



SCALE  
0 100 500 FEET  
FIGURE 17-1

## STOP 17 - EBB SPIT, SOUTH END OF PLUM ISLAND

Jon C. Boothroyd

### GENERAL ORIENTATION

The intertidal area at the southwestern end of Plum Island consists of a spit formed by waves and tidal currents, which curves into the Parker River estuary, a small sand flat, and an ebb spit trailing southeast from the sand flat (Fig. 17-1). Both the sand flat and the ebb spit possess a well-developed ebb shield, measuring 4000 feet long and trending roughly N45W. The ebb spit is approximately 2500 feet long but is totally exposed only at spring low water. Areas of special interest referred to in the following discussion are numbered on Figure 17-2.

### TOPOGRAPHY AND BEDFORMS

The ebb spit rises abruptly some 25 feet from the Parker River channel bottom to the intertidal ebb shield, then slopes away perpendicular to the channel to below mean low water (Fig. 17-3). Along the long axis of the spit, the area nearest the sand flat (location 1 on Fig. 17-2) is the highest above mean low water; then the surface slopes down to near or below mean low water at location 4 (Fig. 17-2), and up again to location 6.

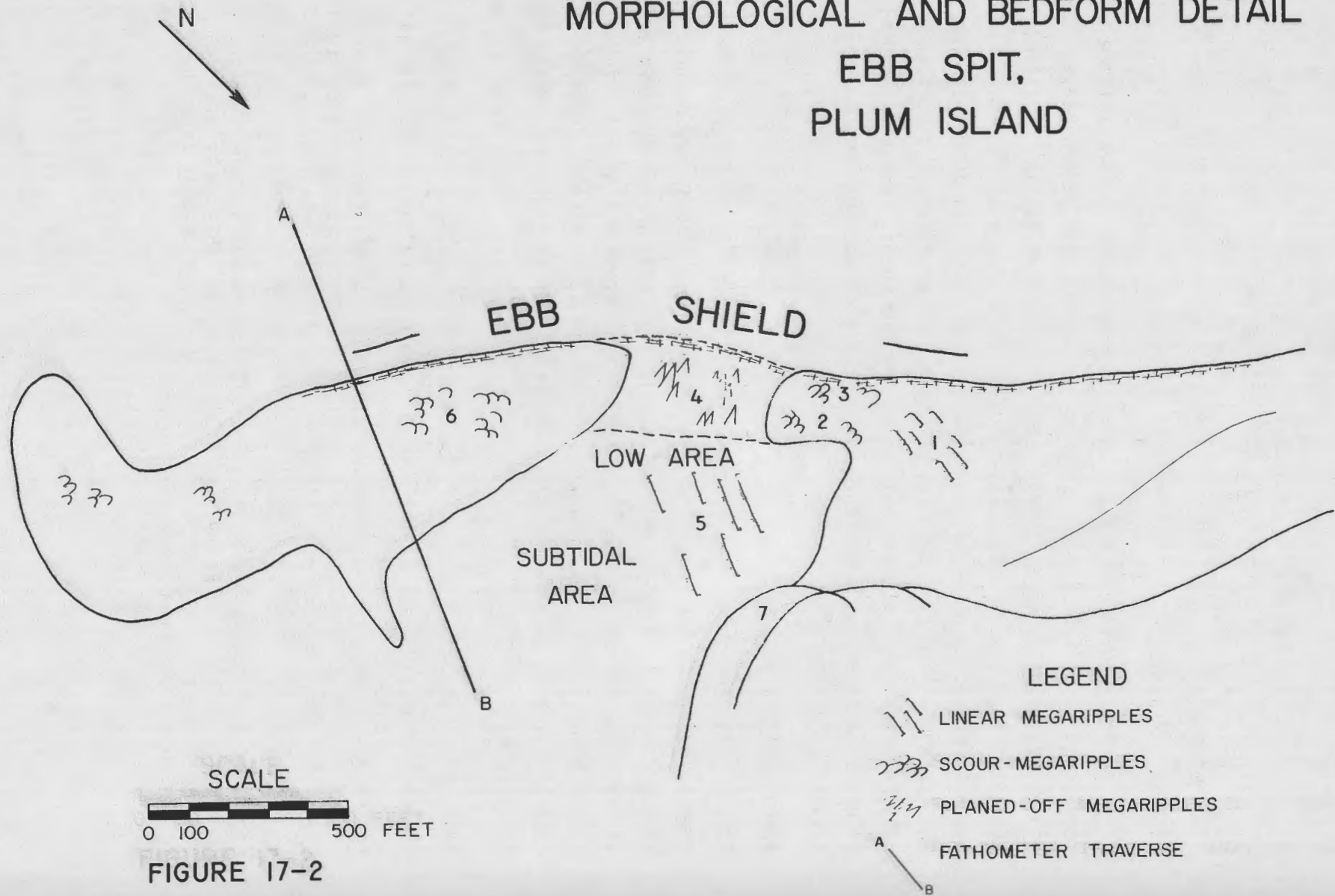
---

Figure 17-1. Index map of the ebb spit area, south end of Plum Island.

Figure 17-2. Morphological and bedform detail of the ebb spit, south end of Plum Island. Note the areas where various types of megaripples occur. The numbered localities are discussed in the text. Line A-B indicates the fathometer traverse shown in Fig. 17-3.

Figure 17-3. Cross profile of the ebb spit, south end of Plum Island. Profile obtained by fathometer traverse along line A-B (Fig. 17-2) at high water. Note the slope of the spit surface away from the ebb shield and the Parker River channel.

# MORPHOLOGICAL AND BEDFORM DETAIL EBB SPIT, PLUM ISLAND



EBB SPIT, CROSS-PROFILE  
PLUM ISLAND

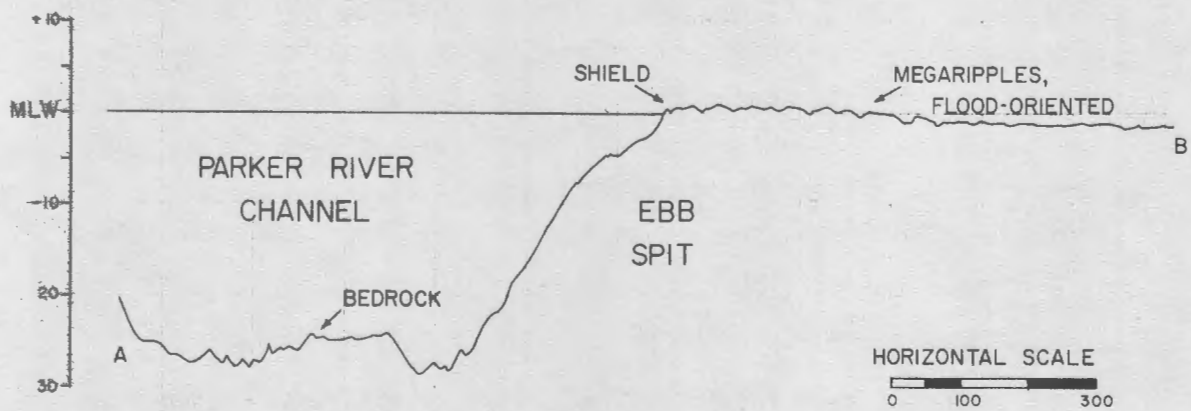


FIGURE 17-3

The most abundant type of bedform exposed on the ebb spit is megaripples. The megaripples vary from linear to planed-off but scour-megaripples are the most common type. The backs of the megaripples sometimes are covered with lunate-linguoid ripples. At low tide the megaripples are ebb-oriented in response to ebb currents but they do change to flood orientation during flooding tides. Observations of scour-megaripple migration rates through the tidal cycle at locality 2 (Fig. 17-2) show, however, that dominant migration is in the ebb direction.

Figure 17-4 shows the slip-face orientations of the megaripples at low tide. The variations in mean azimuth between mainland and extension localities (Fig. 17-4) reflect ebb-tidal current flow during different parts of the ebb cycle. During early ebb tide, water flows unhindered across the spit and a southwesterly slip-face orientation results. Later in the ebb cycle, the ebb shield serves to channelize flow and protect the mainland megaripples from a change in orientation. Just before the ebb shield becomes emergent along the lower end of the spit, water spills over the shield almost perpendicular to the spit long axis and the extension orientations result.

Figure 17-5 shows histograms of wave length and amplitude of the low-tide megaripples.

#### VARIATION IN MEGARIPPLE FORM IN RESPONSE TO FLOW CONDITIONS

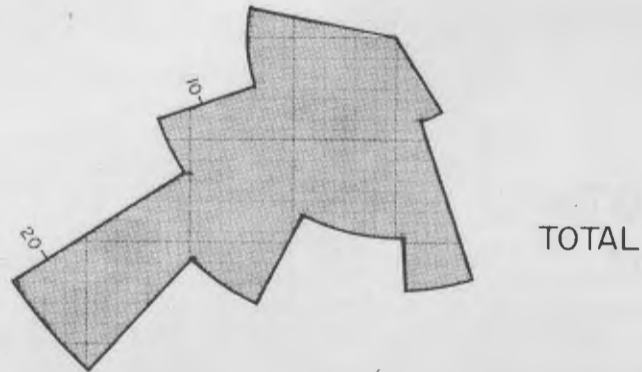
A walk from locality 1 to 4 shows an important sequence of bedforms. At 1 the megaripples have linear crests and moderate wave lengths

---

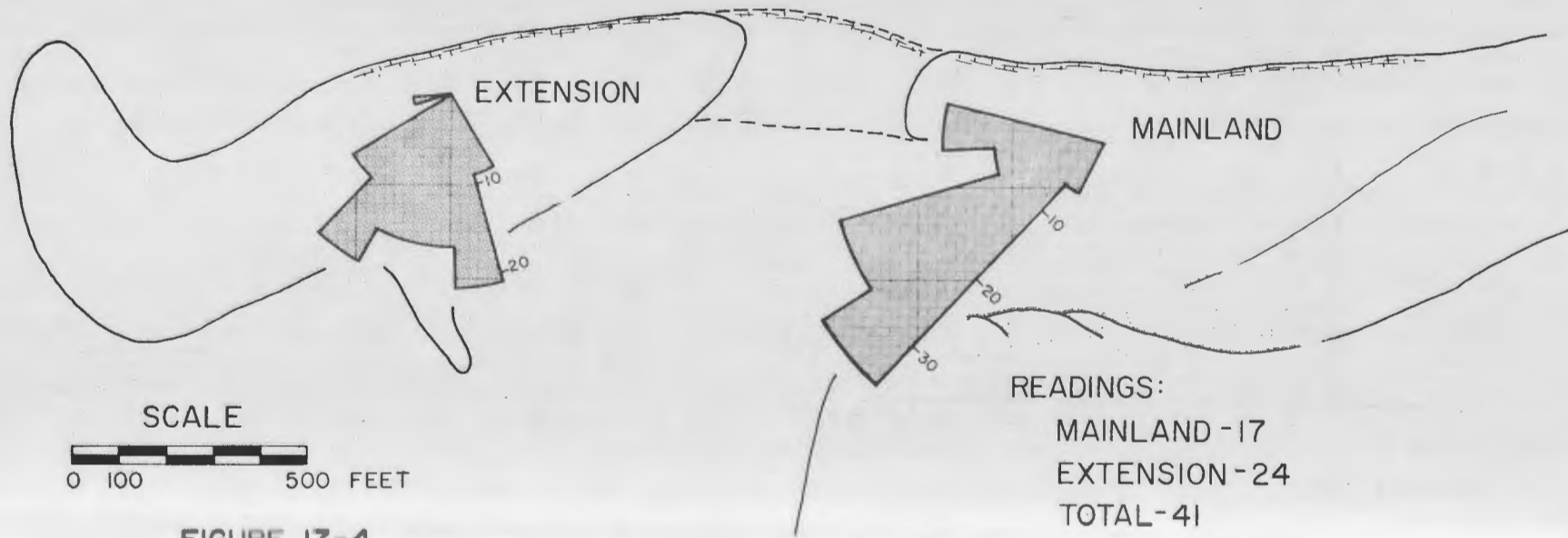
Figure 17-4. Azimuths of slipface orientations of megaripples on the ebb spit, south end of Plum Island. Readings were obtained at mean low water on a 100 x 200 foot grid system. Note the difference in orientation of megaripple slip faces on the two sections of the ebb spit. This difference is discussed in the text.

Figure 17-5. Megaripple scale, ebb spit at south end of Plum Island. Megaripples of largest wave length and amplitude are found at the ebb shield (locality 3, Fig. 17-2).

# MEGARIPPLE ORIENTATION EBB SPIT PLUM ISLAND



TOTAL



EXTENSION

MAINLAND

SCALE



READINGS:

MAINLAND - 17

EXTENSION - 24

TOTAL - 41

FIGURE 17-4

MEGARIPPLE SCALE  
EBB SPIT, PLUM ISLAND

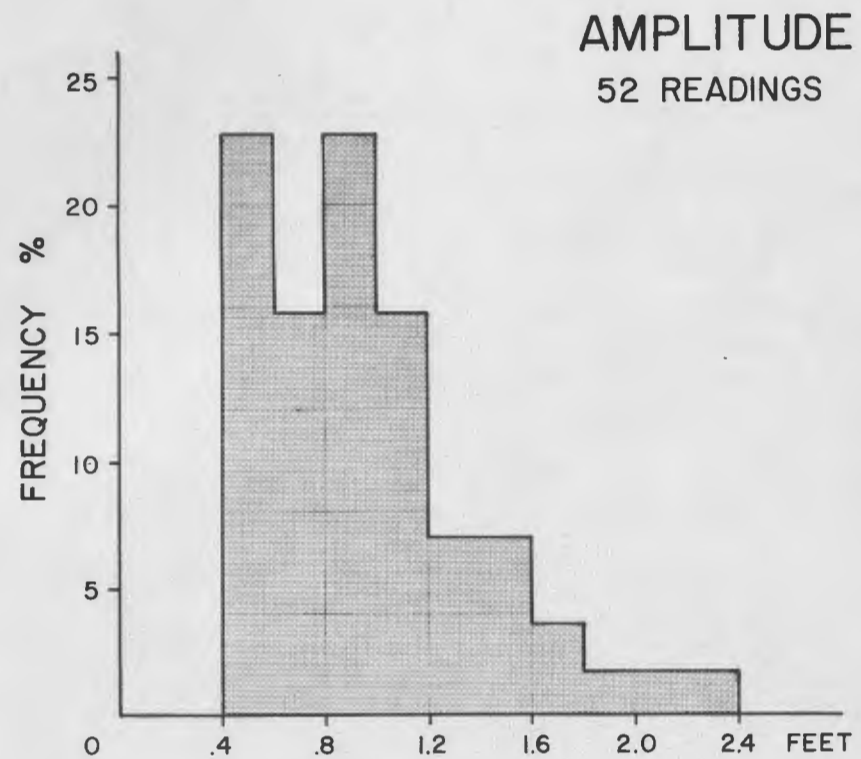
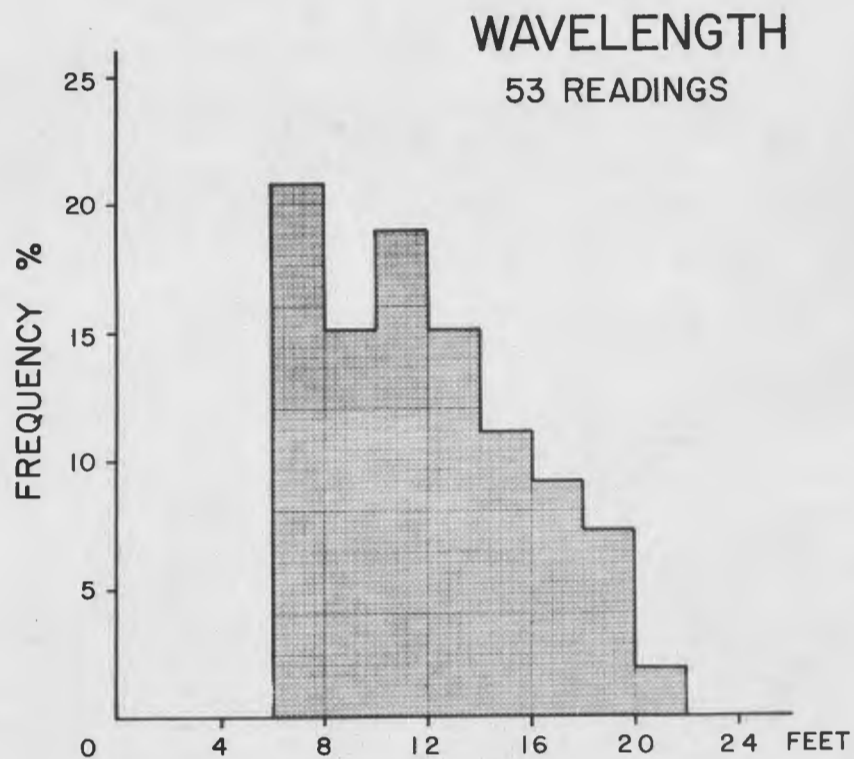


FIGURE 17-5

and amplitudes. Scour pits are moderately to poorly developed. Bedforms at 2 have larger wave lengths and amplitudes and scour pits are better developed. They also show a decrease in linearity of crests. At 3, on the ebb shield, megaripples of greatest amplitude and with best-developed scour pits are found. Finally, at 4 the megaripples are planed-off and much decreased in amplitude.

This change in external form is due to changes in flow conditions. Qualitative observations indicate that strengths of flow, and thus Froude number values, increase from locality 1 to locality 4. Maximum flow over the megaripples at locality 1 was measured at a maximum Froude number of .36 (Table 2, p.422 in this guidebook). This agrees quite well with values obtained by Guy, Simons, and Richardson (1966) for megaripple formation in a flume. The megaripples at locality 4 are interpreted as being planed-off by increasing velocity in shallowing depths of flow. Hence they would be high lower flow regime to transition-zone bedforms with Froude values approaching 1.0. Megaripples at localities 2 and 3 represent intermediate stages between 1 and 4.

The above sequence of bedforms shows quite clearly on the aerial photograph (Fig. 17-6). In addition, linear megaripples also are present (locality 5). These linear megaripples are entirely subtidal. Their external form is a response to still lower strengths of flow than for those megaripples at locality 1.

#### MEGARIPPLE CROSSBEDDING

Megaripple migration produces undulatory to trough crossbedding in sections cut horizontal to bedding and planar to festoon crossbedding

---

Figure 17-6. Aerial photograph of a portion of the ebb spit and sand flat, south end of Plum Island, showing bedform response to flow conditions. Bedforms are ebb-oriented in this photograph taken at mean low water. Strongest flow occurs at locality A. At locality 5, which is subtidal, deeper water and ebb shielding cause lower strengths of flow.

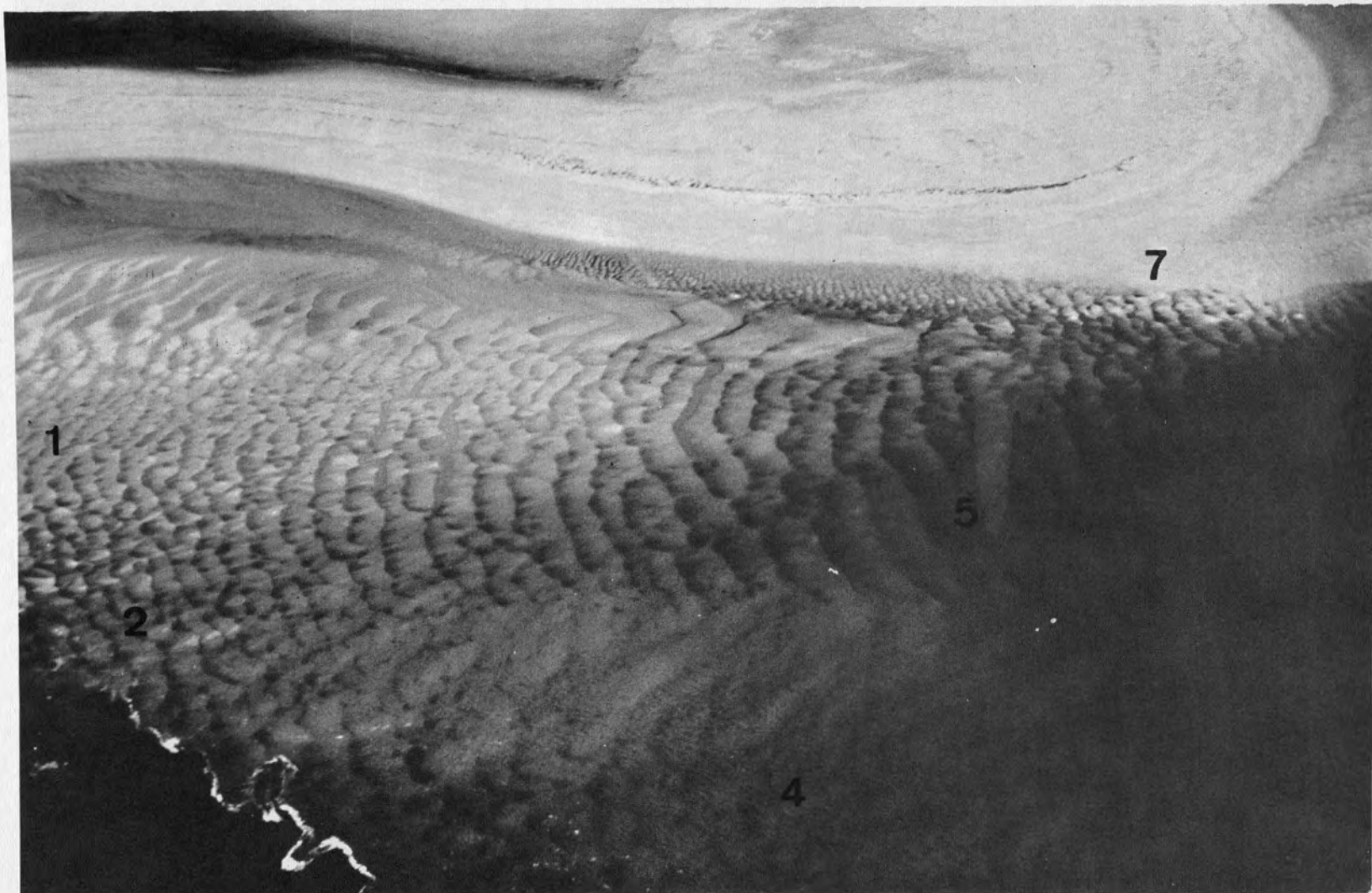


FIGURE 17-6

in sections transverse to megaripple crests (Figs. 17-7 and 17-8). Those megaripples examined in Figures 17-7 and 17-8 were at locality 7 and usually form only during spring tides. Due to a high groundwater table the internal structure of megaripples at localities 1 to 4 are difficult to examine. Under some conditions, megaripples in this area exhibit bimodal crossbedding in cuts transverse to crests (Fig. 17-9).

This interpretation of mode of formation of festoon crossbedding disagrees with views of Harms and others (1963) and Harms and Fahnestock (1965), but is in agreement with ideas and data presented by Allen (1966) and Williams (1968). A speculative interpretation of the type of crossbedding formed by megaripples at locality 4 points to increasing concavity of the festoon crossbeds as seen in a transverse section. This idea is supported by work by Jopling (1965), in which he found increasing concavity of the crossbeds with decreasing depths and increasing strengths of flow (Fig. 17-10).

---

Figure 17-7. Megaripple crossbedding at locality 7 (Fig. 17-2), south end of Plum Island. Crossbedding is undulatory to trough in this section cut horizontal to bedding surface and festoon in the section cut transverse to the slip face.

Figure 17-8. Sketch of trough or festoon crossbedding in a section cut horizontal to megaripple bedding surface. Cut at locality 7, south end of Plum Island.

Figure 17-9. Bimodal festoon crossbedding in a section cut transverse to megaripple slip face, on the sand flat near locality 1, south end of Plum Island. Bimodal crossbedding originates as the megaripple migrates in response to both flood- and ebb-tidal currents. The bedform is ebb-oriented in the photograph.

Figure 17-10. Crossbedding variation. Modified from Jopling (1965).

- A. Variation of crossbedding with change in nature of basal contact, and depth-ratio.
- B. Relationship between crossbedding and depth-ratio.

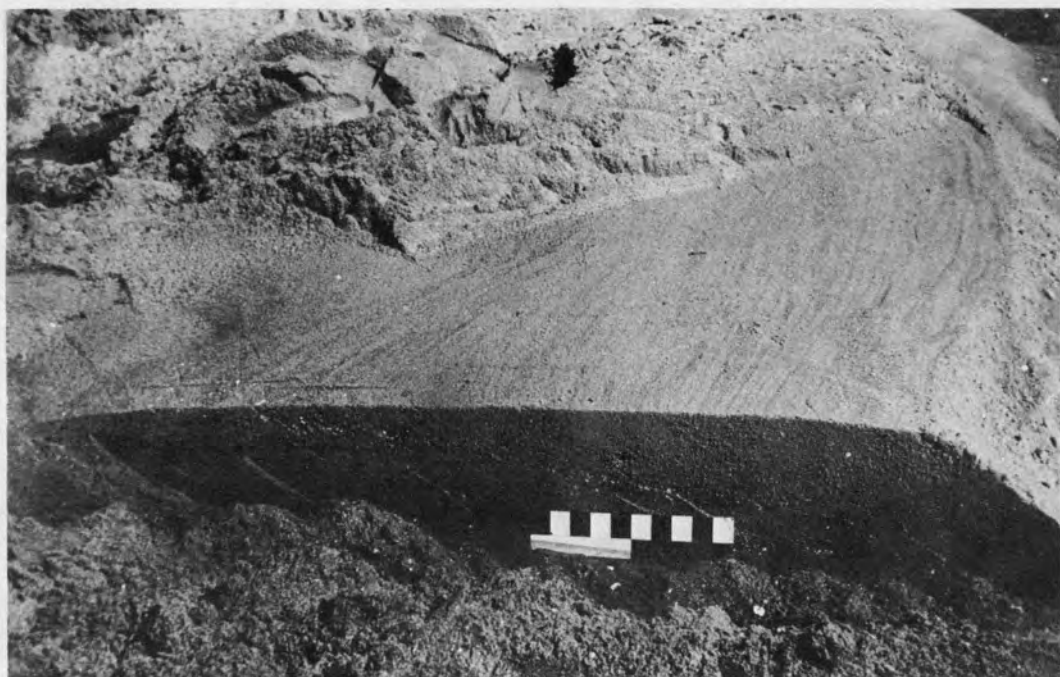


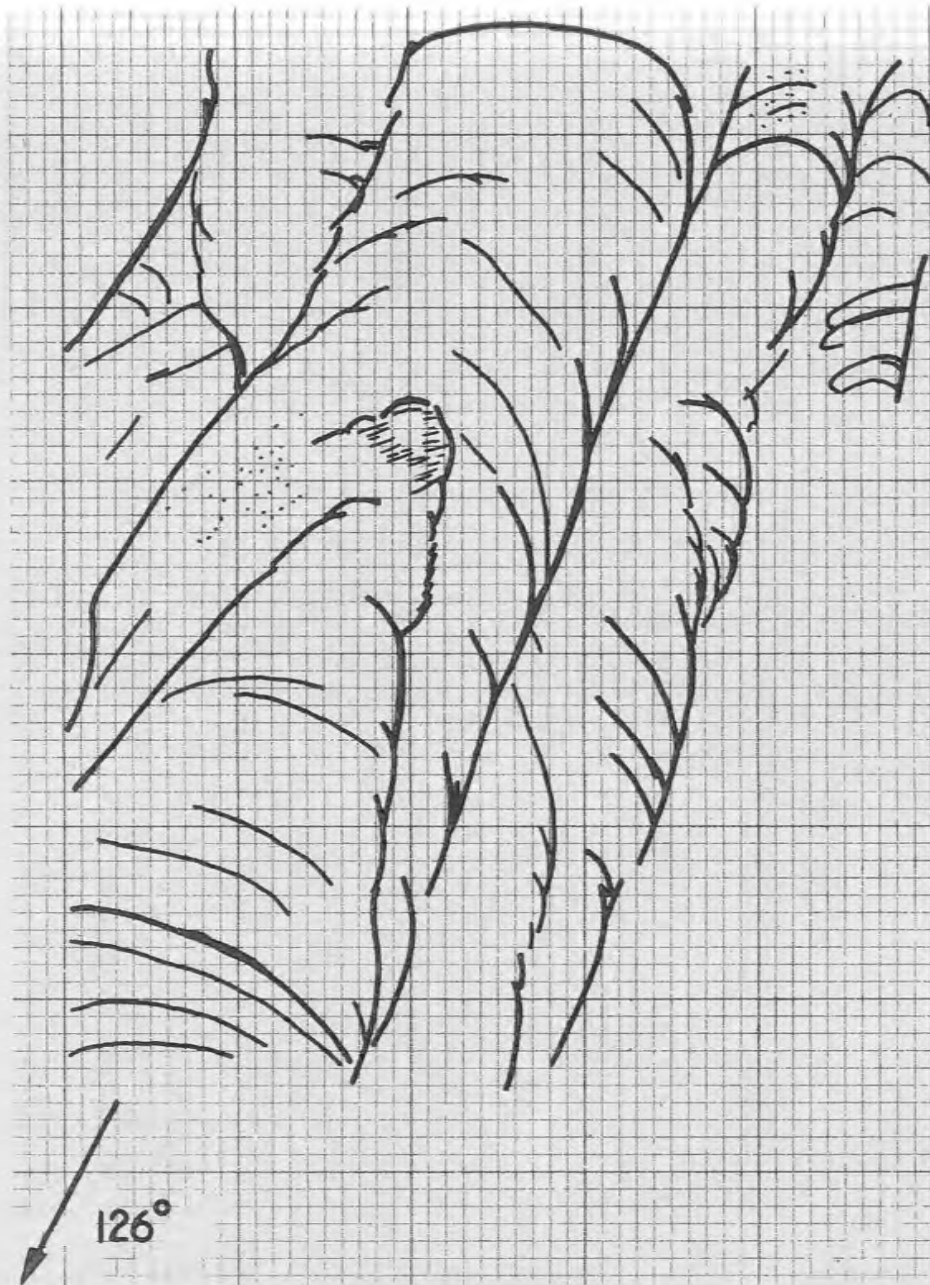
FIGURE 17-7



FIGURE 17-9

# MEGARIPPLE CROSS-BEDDING

EBB SPIT AREA,  
PLUM ISLAND



SCALE



FIGURE 17-8

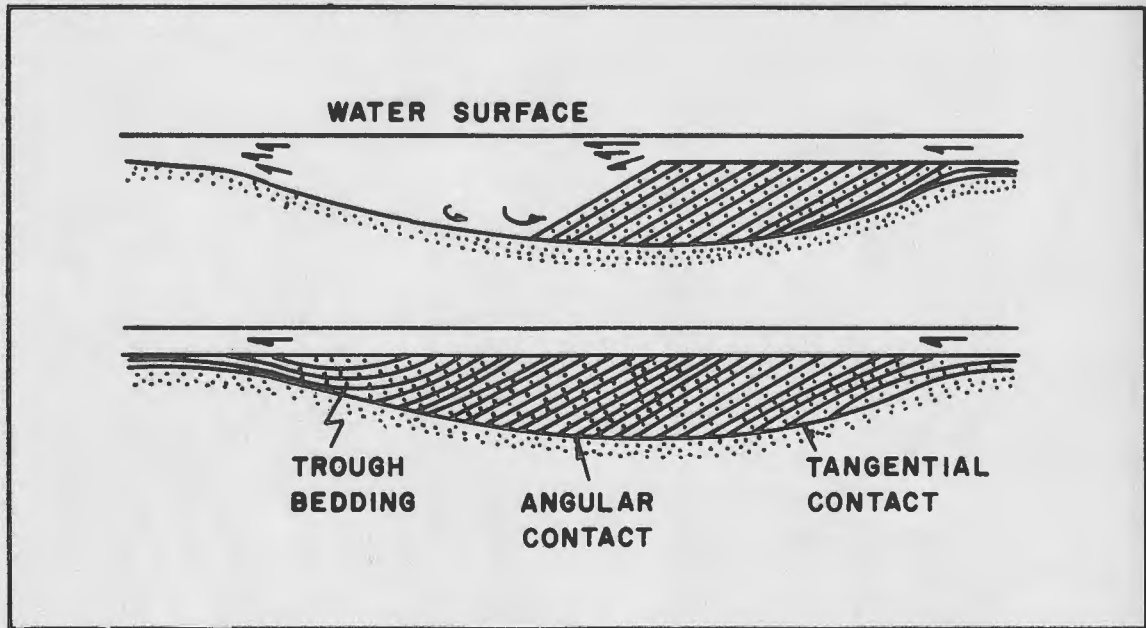
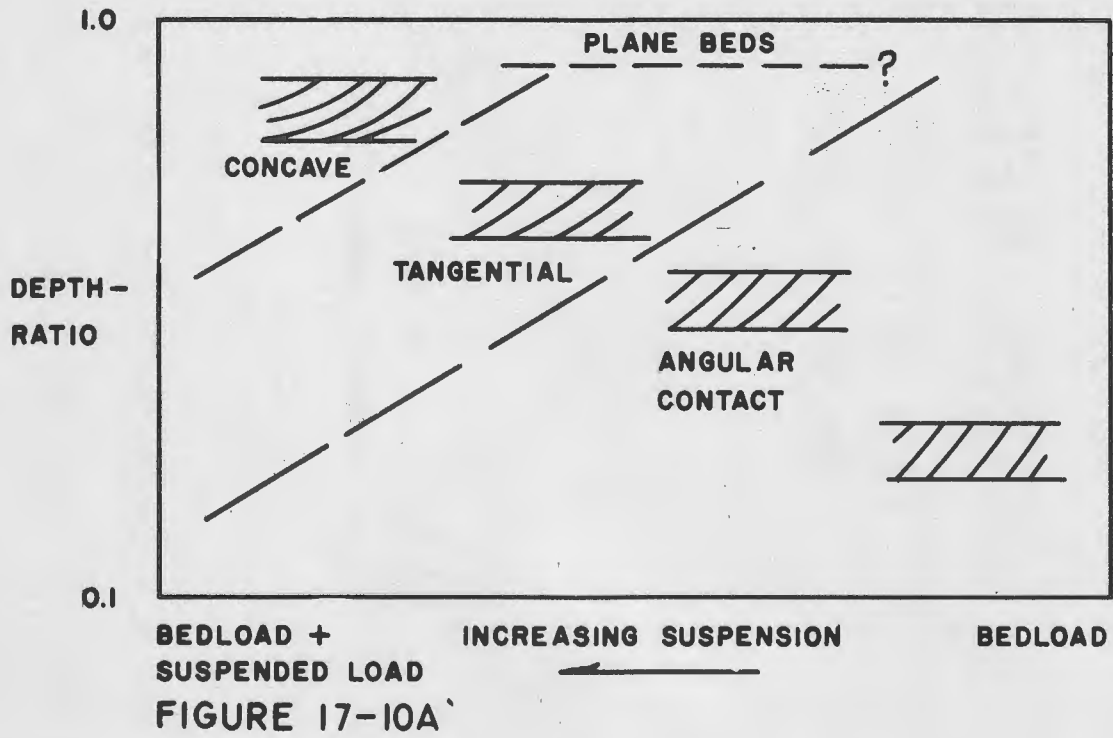
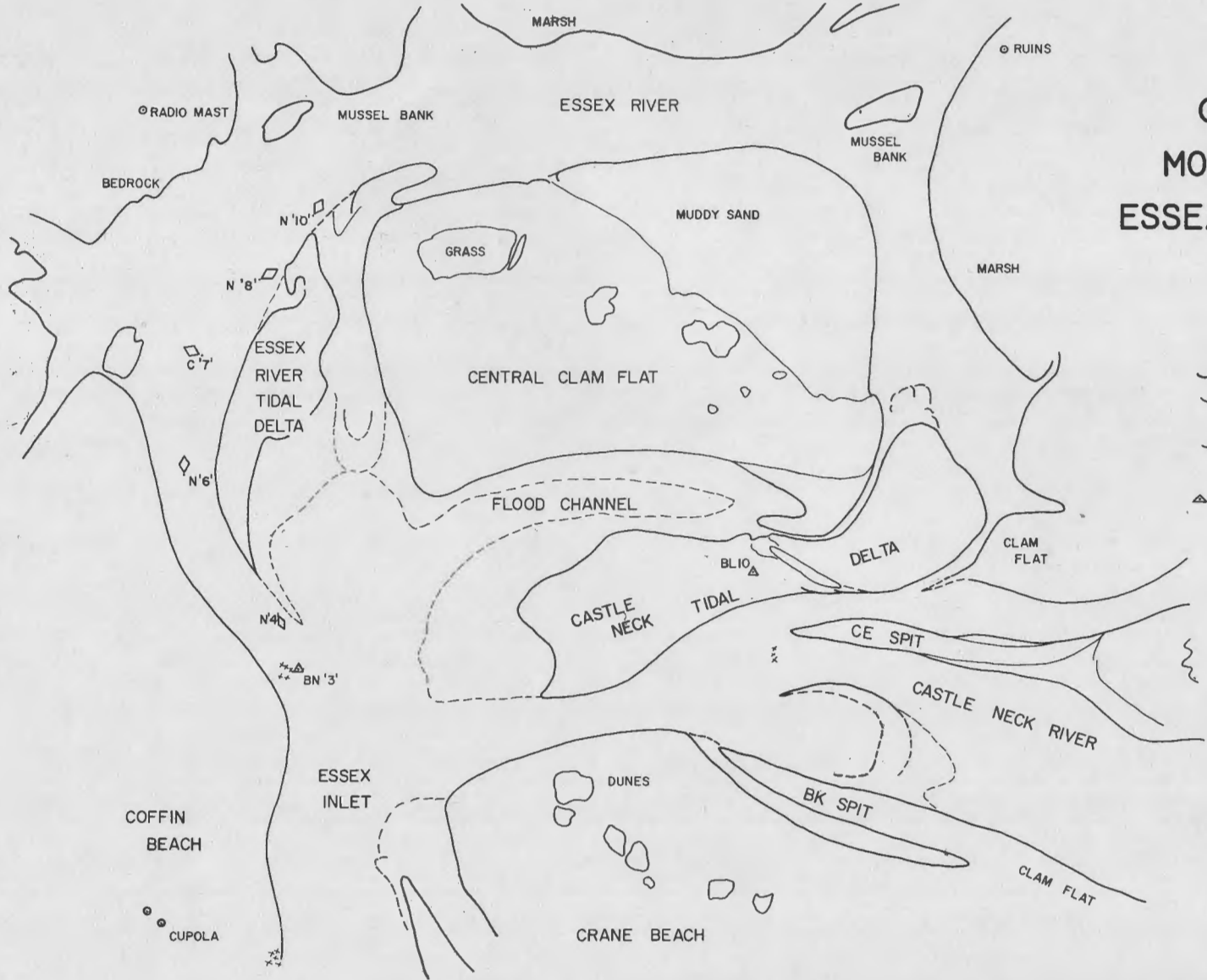


FIGURE 17-10B

# GENERAL MORPHOLOGY ESSEX BAY AREA



- LEGEND
- MEAN LOW WATER
  - - - INTERTIDAL MORPHOLOGIC SUBDIVISIONS
  - - - SUBTIDAL MORPHOLOGIC SUBDIVISIONS
  - △ ○ ORIENTATION MARKERS

SCALE  
0 400 FEET



FIGURE 18-1

## STOP 18 - ESSEX BAY SAND BODIES

### A PRELIMINARY REPORT

Jon C. Boothroyd

#### GENERAL ORIENTATION

The Essex estuary is the southernmost of the series under study that begins with Hampton estuary on the north (Fig. RL-1). This estuary, measuring 3 1/2 miles long by 2 1/2 miles wide, is situated behind the Castle Neck barrier island and Coffin Beach, a barrier beach (Fig. 18-1). The major sand-depositional area, Essex Bay, measures 1 1/2 miles long by 1 mile wide, and is bounded by Castle Neck, Cross Island (a rock-cored drumlin), and by several bedrock knobs (Fig. 18-1).

Two main tidal channels carry both flood and ebb flow, the Castle Neck River, which trends directly behind Castle Neck, and the Essex River, which runs behind Cross Island and extends to the town of Essex. Other less well-defined channels carry mainly flood flow. Very little fresh water enters the estuary; the little that is present is in the upper reaches of the Essex River.

The estuary is quite shallow and abounds with large, intertidal sand flats. Deepest depths are in the two main tidal channels and in the inlet. The inlet is free from artificial constrictions but cannot migrate southwest, the direction of dominant longshore drift, because it is bounded by bedrock on the south side of the channel. The channel is 50 feet deep at this constriction, with maximum recorded current velocities of up to 4.0 feet per second.

#### INTERTIDAL SAND BODIES

The major intertidal sand bodies are located in the Essex Bay area. The most important features are indicated by number on Figure 18-2, an oblique aerial photograph looking NNW across Essex Bay. Briefly, these features are: (1) clam flats, (2) tidal deltas, (3) ebb spits, and

---

Figure 18-1. Index map of the Essex Bay area. The large intertidal sand bodies are indicated by name, and major reference points are located. Refer to this map for field orientation.

(4) other spits. This is not a complete list but indicates areas of concentrated study. Work is not yet complete in this area and only preliminary interpretations are offered.

Sand-body external form can be delineated in part by fathometer profiles run transverse to major trends. Figure 18-4 shows a series of fathometer profiles run from Castle Neck, across the northern tidal delta (Castle Neck delta, Fig. 18-2), through a large flood channel, to the wide central clam flat. These profiles also include several spits in the Castle Neck tidal channel. Profile locations are shown in Figure 18-3.

The Castle Neck and Essex River tidal deltas are lobes of the central sand body which fills most of Essex Bay. They represent the latest stage of major intertidal sand accumulation, occurring after deposition of the central lobe. This central lobe is now an extensive clam flat.

#### LARGE-SCALE BEDFORMS (INTERTIDAL AND SUBTIDAL)

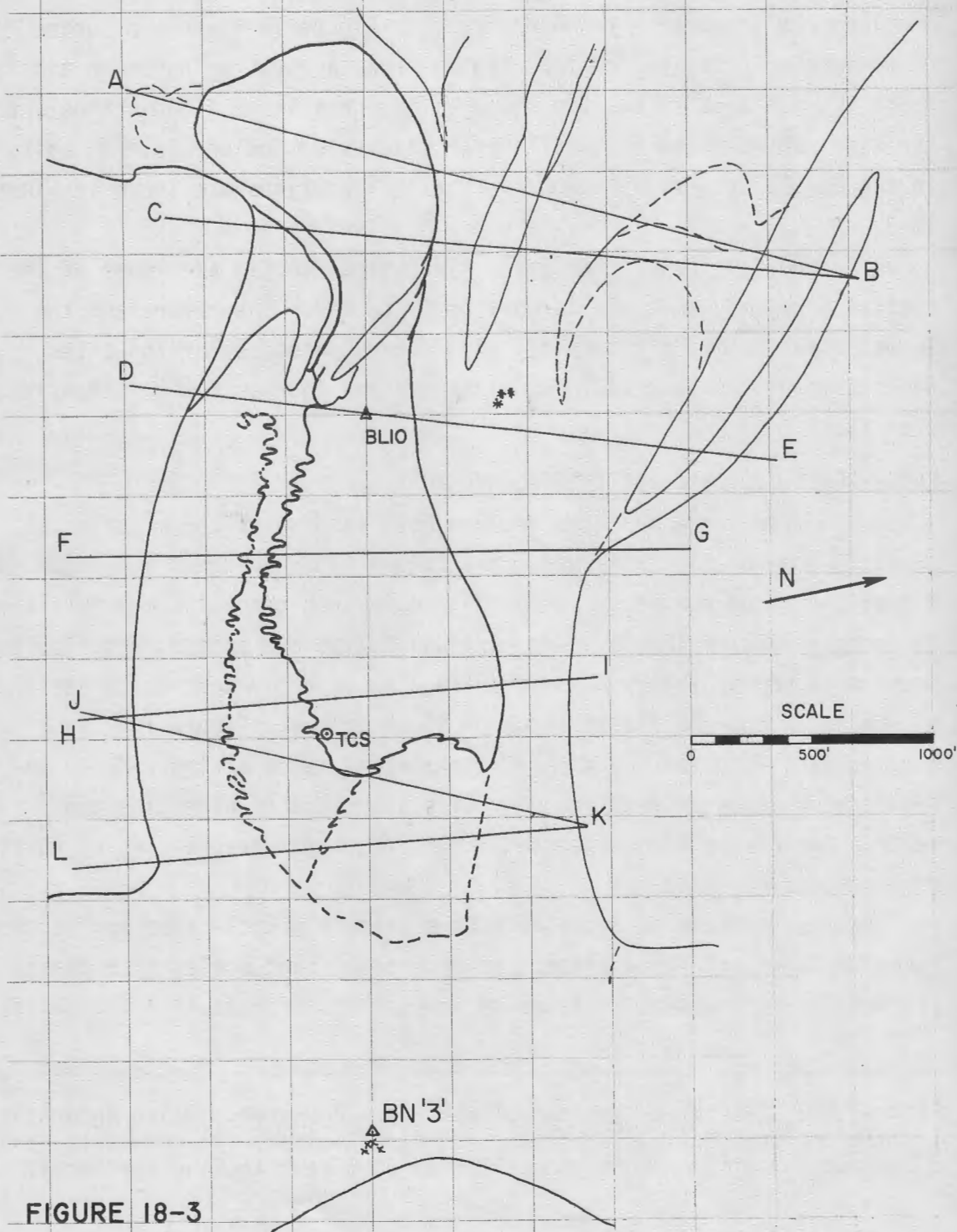
Large-scale bedforms include both sand waves and megaripples (Fig. 18-5 a and b). Sand waves are mainly flood-oriented and occur subtidally in flood channels, in some flood-and-ebb channels, and intertidally on topographically low portions of tidal deltas and spits. Megaripples occur on topographically high intertidal to slightly subtidal areas such as ebb spits and ebb shield areas on tidal deltas. Figure 18-6 indicates sand wave and megaripple orientations taken at low tide on the Castle Neck delta. Preliminary studies show that at high tide the megaripples become flood-oriented, while the sand waves would, of course, remain flood-oriented.

As tide conditions change in a bimonthly cycle from spring to neap, zones of flood and ebb dominance on intertidal sand bodies also change (as defined by bedforms at times of low water). Figure 18-7 indicates the

---

Figure 18-2. Aerial photograph of the Essex Bay area. Major intertidal features are : (1) clam flats, (2) tidal deltas, (3) ebb spits, and (4) other spits. Photograph taken at 3500 feet looking northwest.

# FATHOMETER TRAVERSES CASTLE NECK DELTA ESSEX BAY



relative increase of ebb dominance with a change from neap through mean to spring tide conditions. The major large-scale bedforms found in zones of flood dominance are sand waves, and in zones of ebb dominance, megaripples. Current velocities are higher over the flats during spring tides because a larger volume of water must be exchanged during the tidal cycle. During these times of higher flow velocity, megaripple fields increase in area.

Figure 18-8 a and b are histogram plots of the wavelengths of flood and ebb-oriented large-scale bedforms measured on the intertidal sand bodies of the Essex Bay area. Note that most flood-oriented bedforms are sand waves and that most ebb-oriented bedforms are megaripples, as defined in the UMass Coastal Research Group classification system (p. 455, this guidebook). Figure 18-9 a and b gives amplitudes of flood- and ebb-oriented bedforms, but shows no general trend.

#### SAND-WAVE ORIENTATIONS AS PALEOCURRENT INDICATORS

Intertidal sand-wave orientations are indicated in Figure 18-10 for various sand bodies in Essex Bay. These orientations are, in all cases, in a flood direction. Figure 18-11 is a summation of orientations for all the sand bodies. The rose diagram shows a bifurcating pattern of flow around the large central clam flat.

As discussed earlier (p. 417, this guidebook), sand-wave migration produces large-scale planar crossbedding. In Essex Bay, this crossbedding has a dominant landward orientation even though there is a large parallel component.

Figure 18-12 extends the overall view of bedform orientation to include the subtidal environment. Bedform orientations were obtained from an uncontrolled aerial mosaic obtained during flights in September, 1968, in cooperation with Long Island University marine engineers.

---

Figure 18-3. Location map for fathometer traverses across the Castle Neck tidal delta. Outline of the tidal delta is the mean-low-water line. Refer to Figure 18-4 for topography along the traverses.

# TRANSVERSE PROFILES CASTLE NECK TIDAL DELTA ESSEX BAY

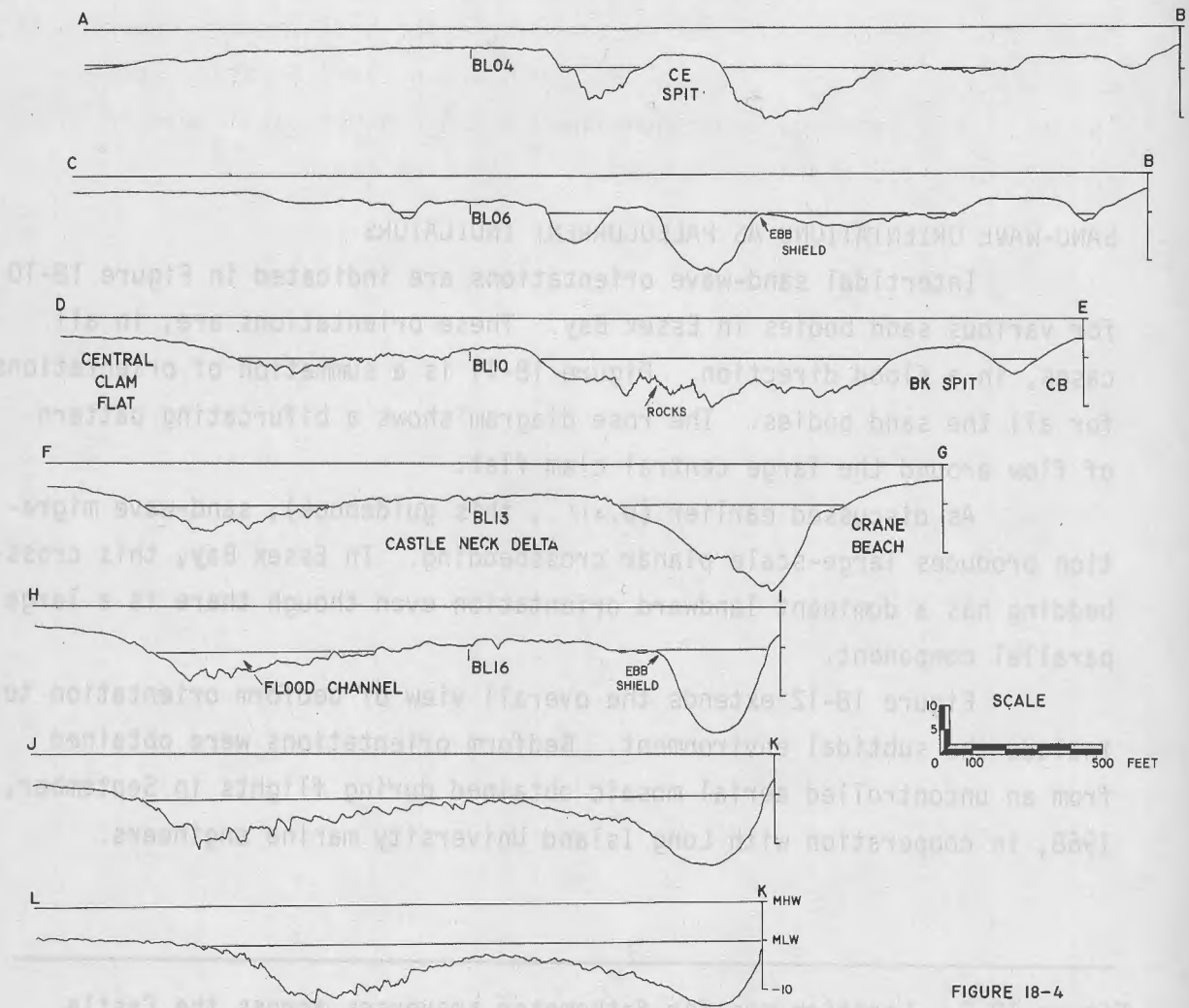


FIGURE 18-4

## CONCLUSION

The foregoing discussion is a brief look at some aspects of estuarine sand bodies and bedforms. It is by no means a complete presentation. Further topics and questions can be discussed in the field.

---

Figure 18-4. Topographic cross profiles of the Castle Neck tidal delta and surrounding features. Refer to Figure 18-3 for exact locations of the profiles. Note the deep channel of the Castle Neck River, which carries both flood and ebb flow, as opposed to the shallow flood channel southwest of the tidal delta. Note also the high relief of the intertidal sand bodies.

Figure 18-5.

A. Sand waves on the Castle Neck tidal delta, Essex estuary. These bedforms are flood-oriented with wavelengths of 30 to 50 feet. Note the sinuosity of the crests.

B. Megaripples on the Castle Neck tidal delta, Essex Bay. These bedforms are scour-megaripples developed during spring tide on the ebb-dominated area of the tidal delta. The megaripples are ebb-oriented in this photo taken at mean low water.

Figure 18-6. Sand wave and megaripple orientations on the Castle Neck tidal delta, measured during a mean tide at mean low water. The sandwaves are generally oriented with the axis of the flood channel (Fig. 18-1) while the megaripple orientation reflects the spilling of ebb currents over the ebb shield (Fig. 18-4).

Figure 18-7. Zones of flood and ebb dominance on the Castle Neck tidal delta. Zones are defined by the type of large-scale bedform present at mean low water. Note that the ebb zone increases in size during spring tides.

Figure 18-8. Wavelengths of flood-and-ebb oriented large-scale intertidal bedforms, Essex Bay. Note that most flood-oriented bedforms are sand waves and most ebb-oriented bedforms are megaripples. Measurements made at mean low water.

Figure 18-9. Amplitudes of large-scale, flood-oriented and ebb-oriented bedforms, Essex Bay. Refer to Fig. 18-8 for notes on bedform type.



FIGURE 18-5A



FIGURE 18-5B

# ORIENTATION OF LARGE-SCALE BEDFORMS CASTLE NECK DELTA ESSEX BAY

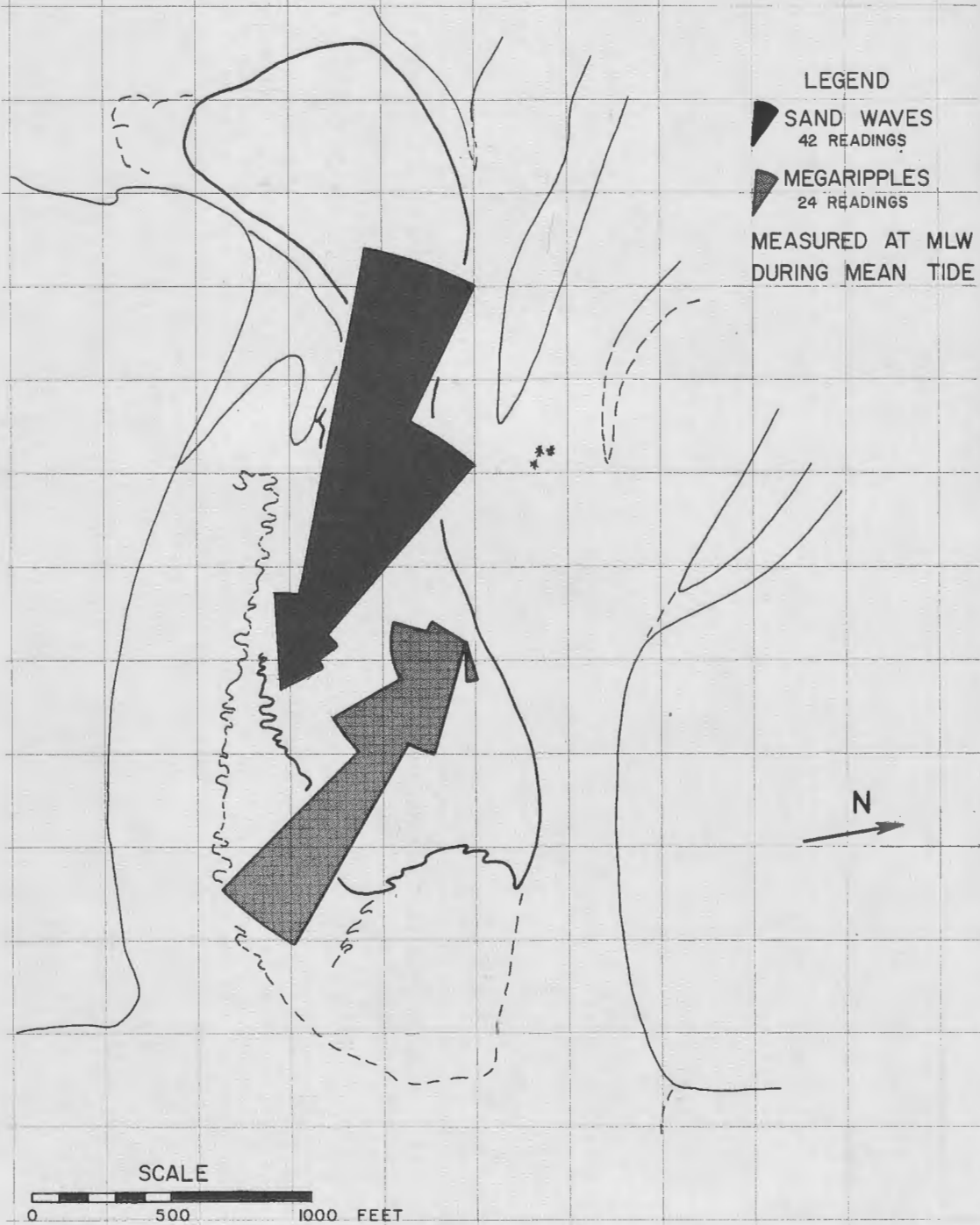
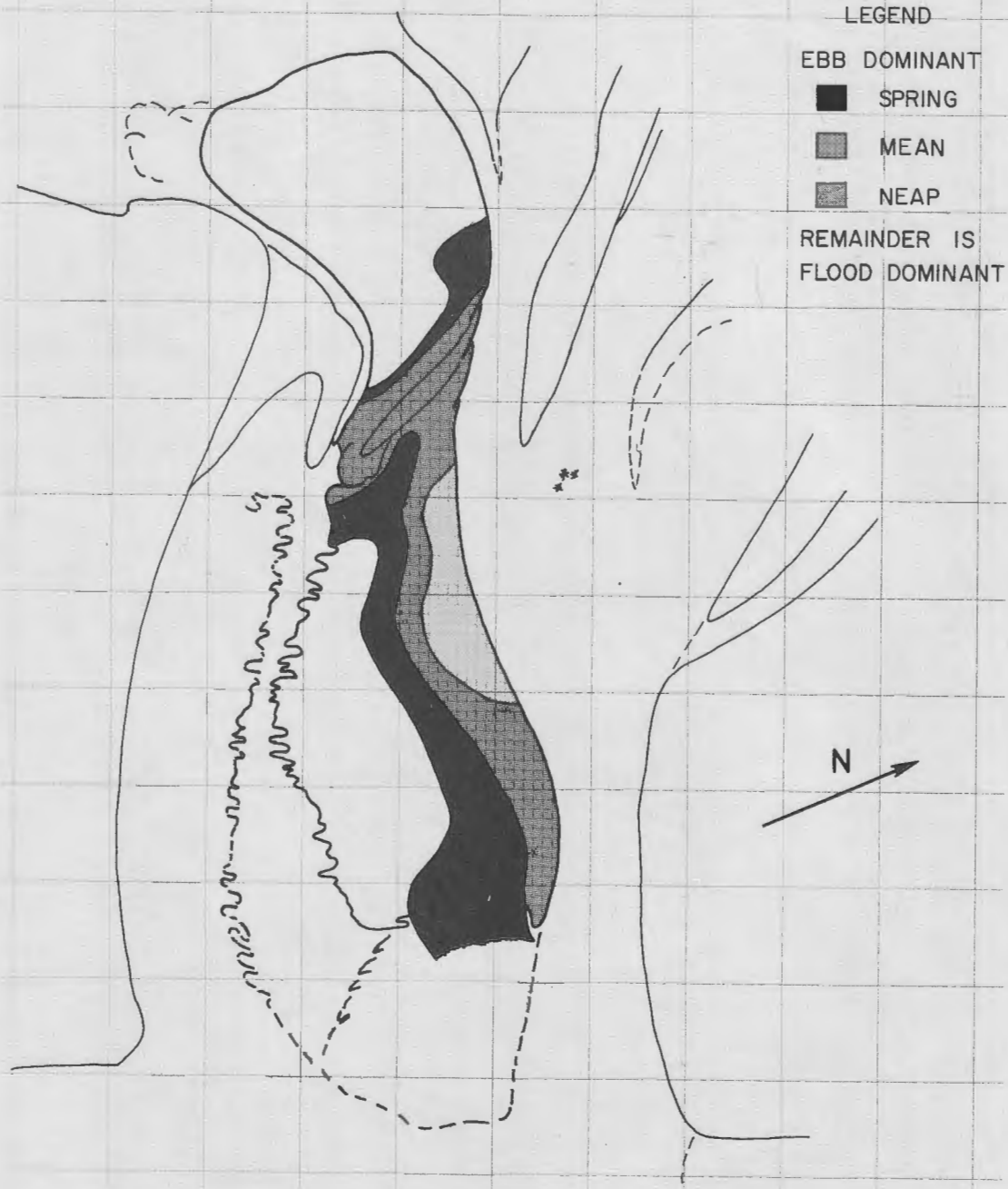


FIGURE 18-6

# FLOOD VS. EBB DOMINANCE CASTLE NECK DELTA ESSEX BAY



LEGEND

EBB DOMINANT

■ SPRING

▨ MEAN

▩ NEAP

REMAINDER IS  
FLOOD DOMINANT

SCALE



FIGURE 18-7

WAVELENGTHS OF  
LARGE-SCALE BEDFORMS  
ESSEX BAY AREA

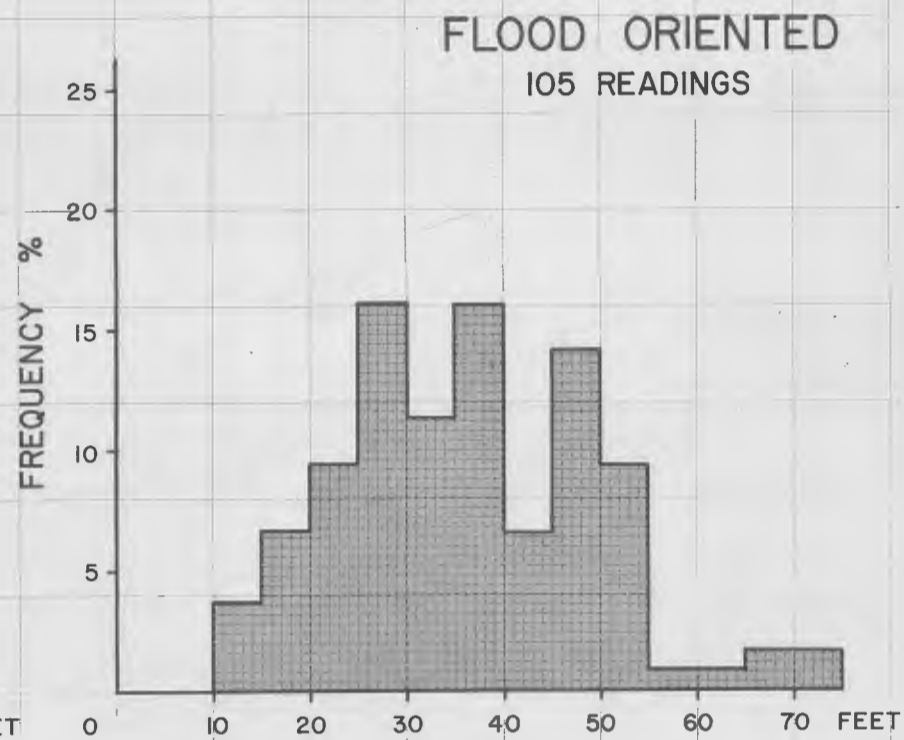
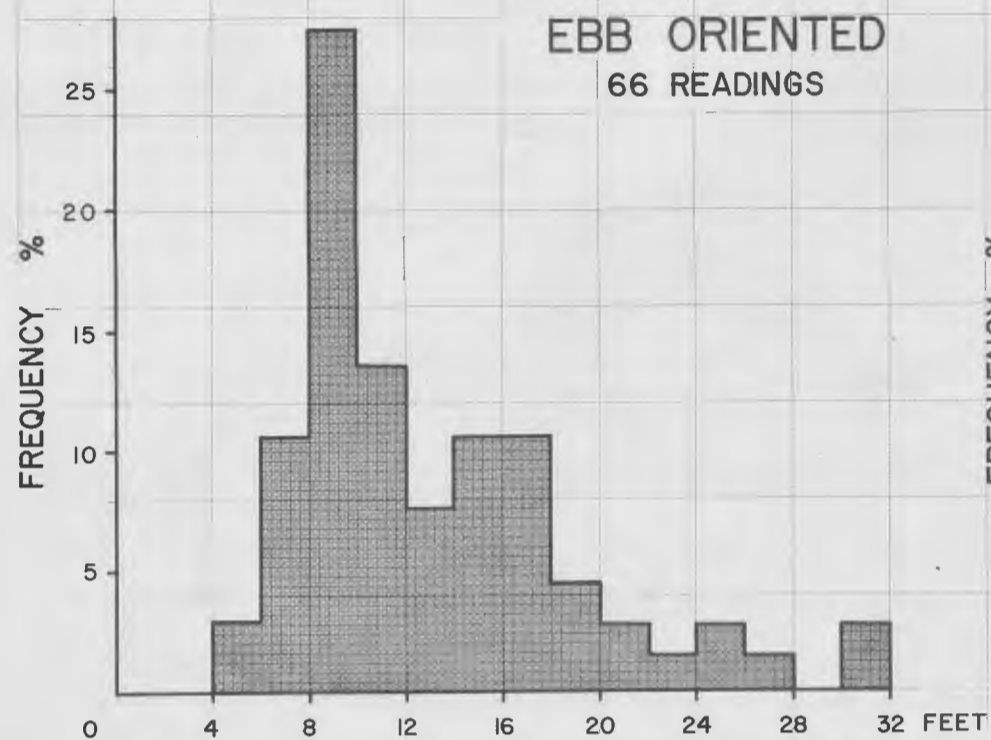


FIGURE 18-8

# AMPLITUDES OF LARGE-SCALE BEDFORMS ESSEX BAY AREA

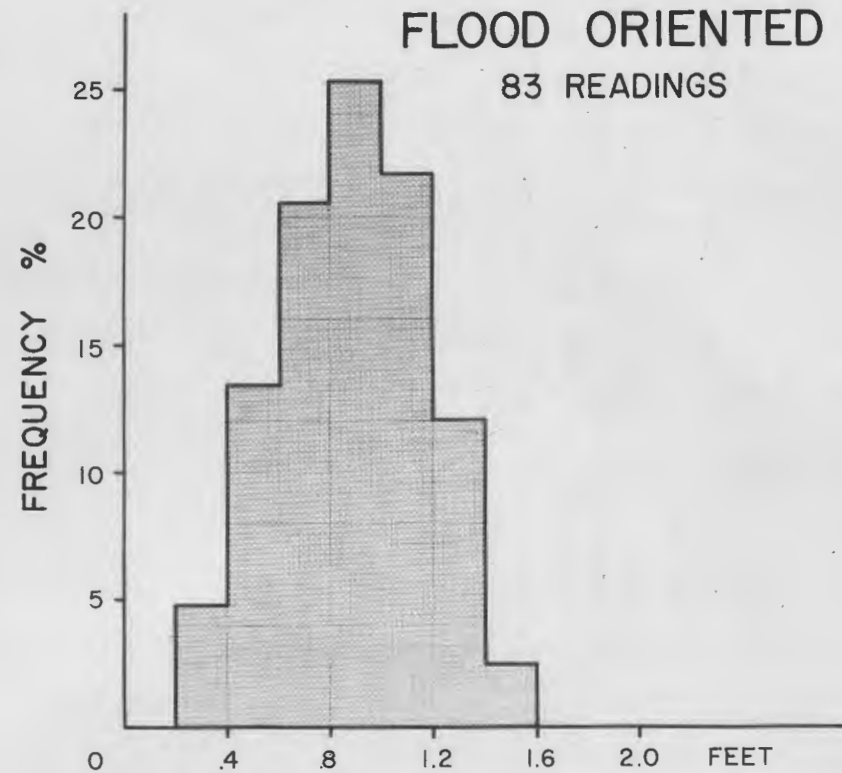
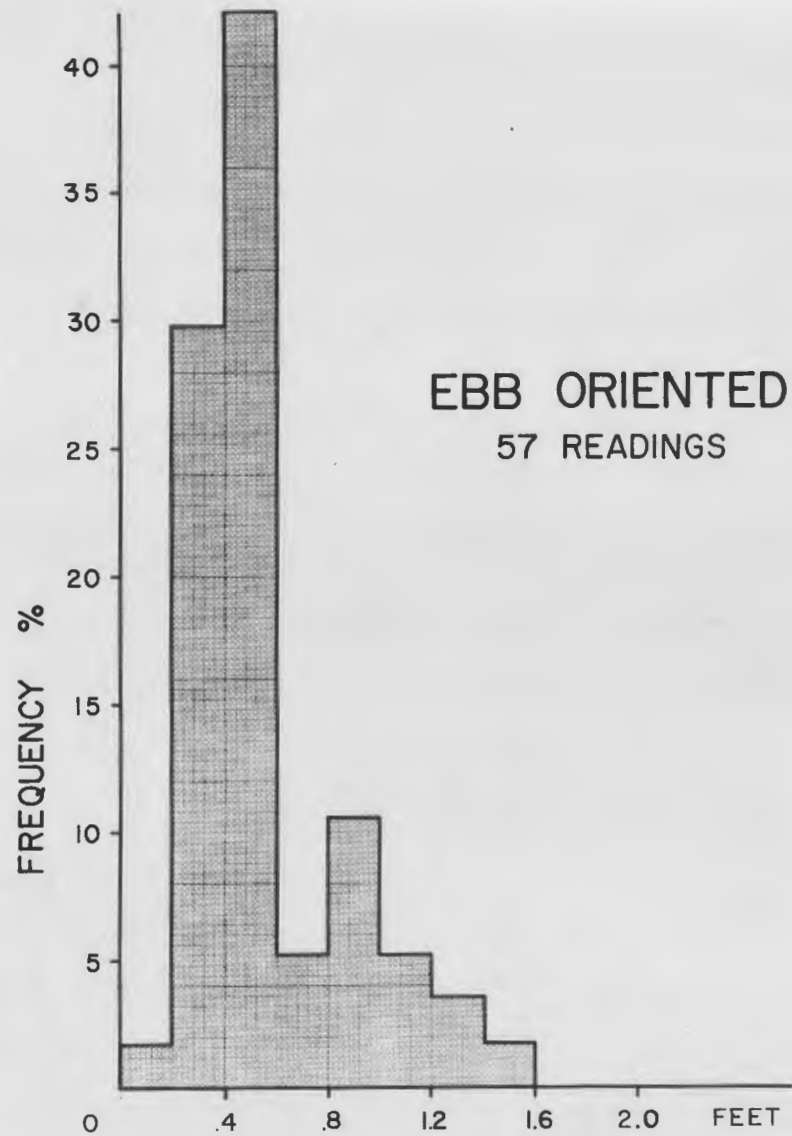


FIGURE 18-9

Figure 18-10. Orientations of sand waves on the major intertidal sand bodies, Essex Bay. Note the dominant flood orientation pattern. Sand waves measured at mean low water.

Figure 18-11. Summary of intertidal sand wave orientations, Essex Bay. The dominant orientation is landward with a strong component parallel to the shoreline.

Figure 18-12. Orientations of large-scale bedforms, Essex Bay. Measurements from vertical aerial photographs taken at mean low water. Note that intertidal and shallow subtidal bedforms are flood-oriented while deep channel bedforms are ebb-oriented in part.

# INTERTIDAL SAND WAVE ORIENTATIONS ESSEX BAY AREA

LEGEND  
NOTE: ROSE PLOTS ARE NOT  
TO SCALE

SCALE  
0 400 FEET

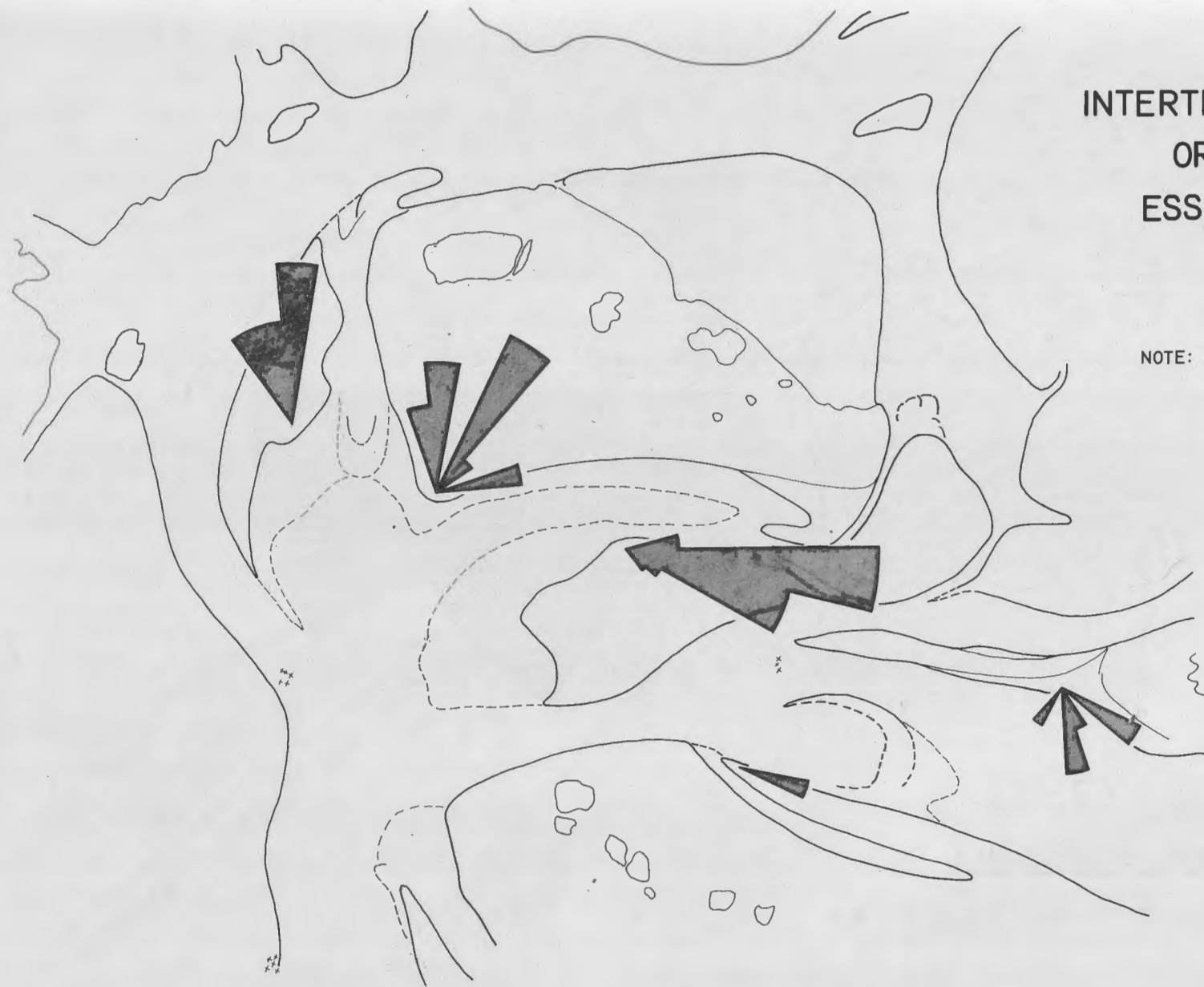


FIGURE 18-10

INTERTIDAL SAND WAVE  
ORIENTATIONS  
ESSEX BAY

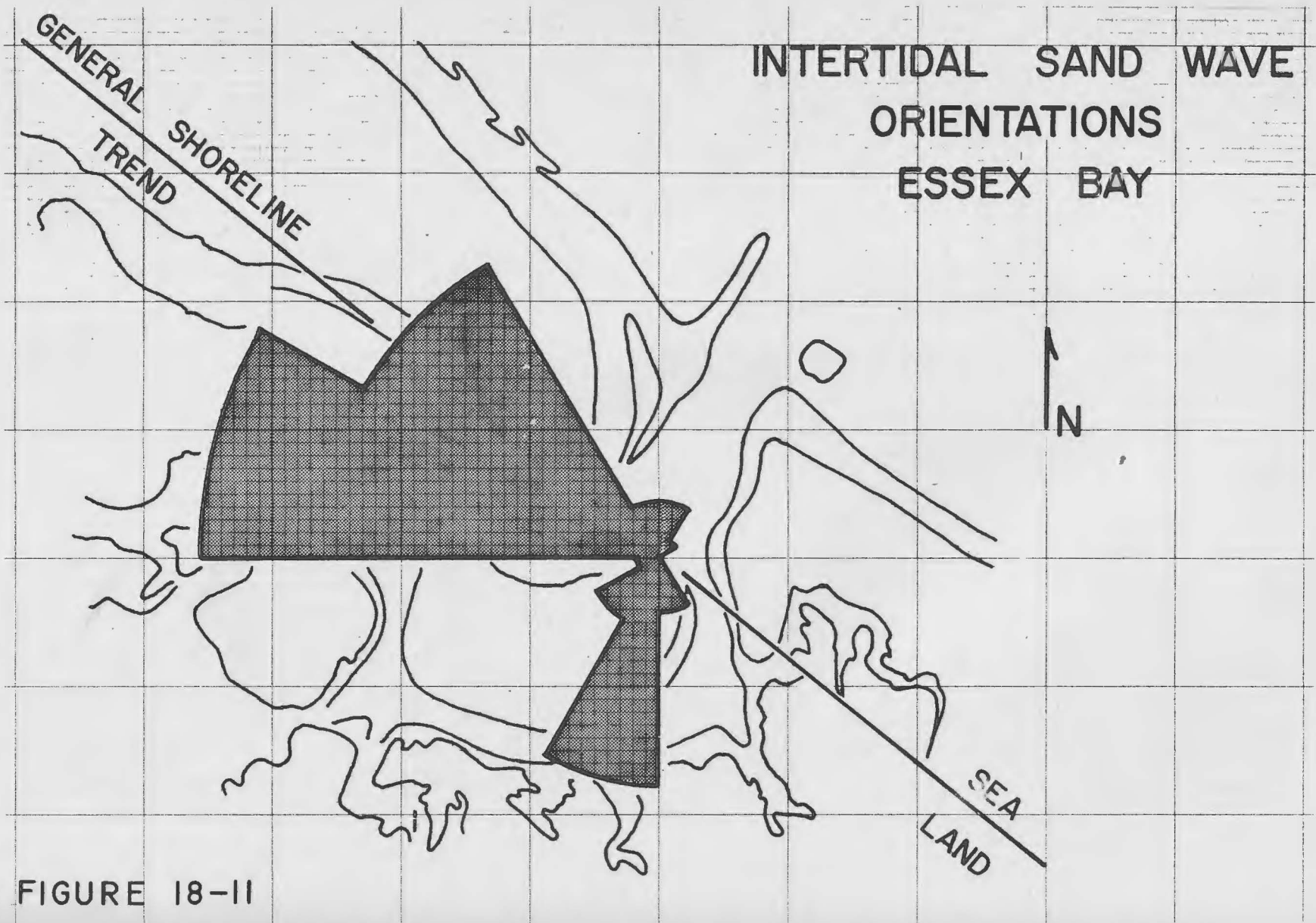
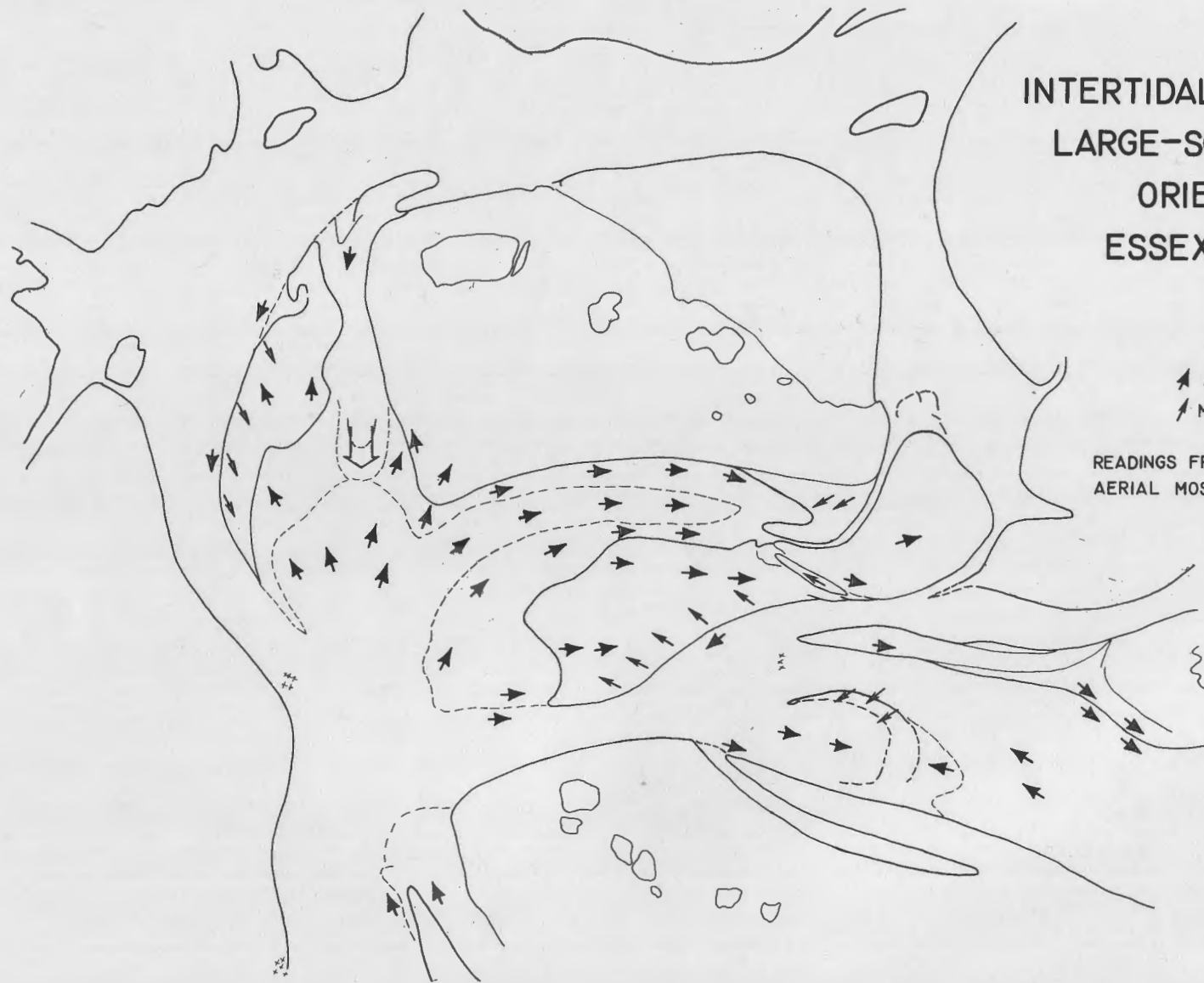


FIGURE 18-II

# INTERTIDAL AND SUBTIDAL LARGE-SCALE BEDFORM ORIENTATIONS ESSEX BAY AREA



## LEGEND

- ▲ SAND WAVES
- ▬ MEGARIPPLES

READINGS FROM UNCONTROLLED  
AERIAL MOSAIC, FLOWN 14 SEPT. 1968

## SCALE

0 400 FEET

FIGURE 18-12

CRANE BEACH  
ESSEX ESTUARY AREA  
IPSWICH - ESSEX, MASS.



FIGURE 19-1

## STOP 19 - CRANE BEACH

Jon C. Boothroyd

### GENERAL ORIENTATION

Castle Neck is the southernmost barrier island on the northeast Massachusetts coast. The barrier trends southeast approximately three miles from Castle Hill and Steep Hill, rock-cored drumlins that anchor Castle Neck near its northern extremity (Figs. RL-1 and 19-1). Note the profile locations (Fig. 19-1); they will be referred to in the following text.

### CRANE BEACH MORPHOLOGY

The shore front of Castle Neck, called Crane Beach, can be divided into 4 distinct constructional phase zones on the basis of beach morphology. Data obtained from pace and Brunton mapping of 13,000 linear feet of beach dune at low tide during the summer of 1967, show the following pattern (Fig. 19-2): a northern ridge zone, a central accretion zone, a southern ridge zone, and a zone dominated by the Essex tidal delta. The morphology of a fifth zone, not shown, is controlled in large part by Essex inlet tidal currents.

#### Ridge Zone, North

The northwesternmost part of the beach mapped, including the Crane Reservation swimming area, is characterized by a well-developed ridge-and-runnel system and a small berm quite close to a scarped fore-dune ridge (Fig. 19-3, a and b). The ridge trends 2500 feet southeastward roughly parallel to the foredune ridge, is up to 200 feet wide and has a landward-oriented slip face ranging up to 2.5 feet in amplitude. The ridge has become welded to the berm in places.

The runnel is narrow (10 to 100 ft. wide), may contain standing water, and is floored with well-developed linear ripples. The small berm is also narrow (50 ft. wide) and not more than 5 feet high, usually less.

---

Figure 19-1. Index map of Crane Beach - Essex Bay area, Ipswich-Essex, Massachusetts. Note the profile localities.

CONSTRUCTIONAL PHASE MORPHOLOGY  
CRANE BEACH, SUMMER 1967

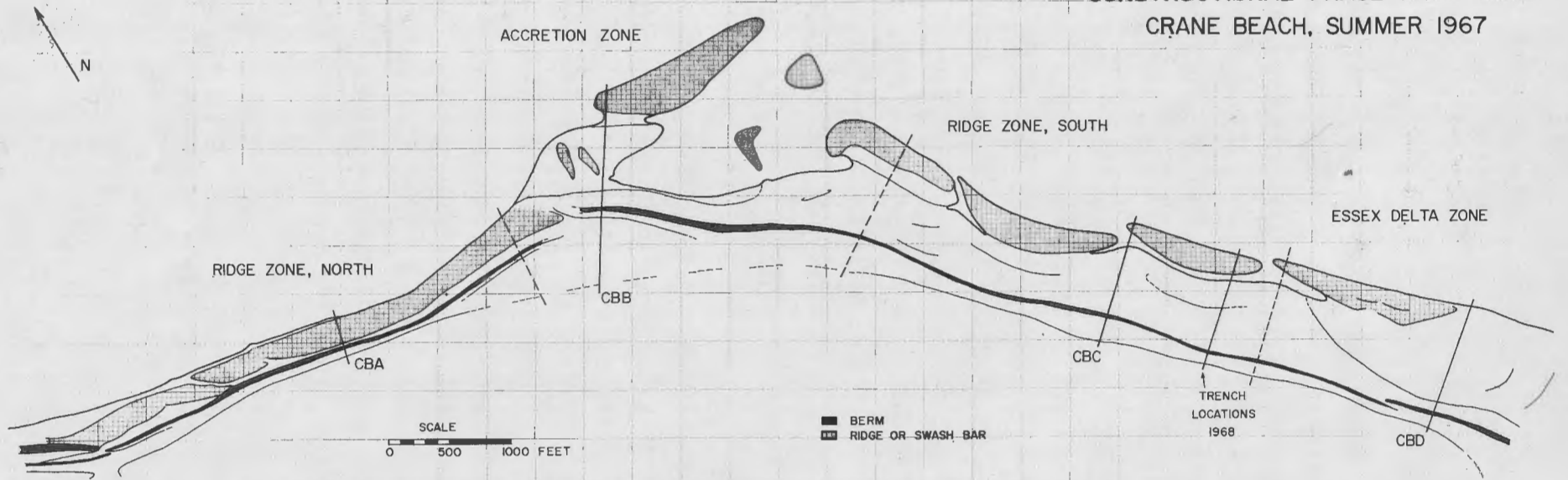


FIGURE 19-2

### Accretion Zone

The next beach zone, to the southeast, is a wide accretional area (Fig. 19-4 a and b) with nearshore swash bars, a small sand flat, and a large berm-ridge. Beach morphology in this area is controlled in part by the Parker River tidal currents as well as by wave action. The dune line is well inshore, as much as 600 feet from the crest of the berm-ridge. The intervening area is flooded only by high storm tides and thus vegetation is becoming well established.

The swash bars are varied in length (100 to 1200 ft.) and have slip faces that range from 0 to more than 4 feet. Slip face orientation is quite variable. The larger swash bar, as well as the sand flat, are covered with linear ripples of varying orientation (Fig. 19-4a). The large berm-ridge is best developed landward of the sand flat. It changes to a ridge configuration northward and tapers downward in size to the south.

### Ridge Zone, South

South of the accretion zone the beach trend swings rather abruptly to a more southerly direction, the sand becomes finer, and beach morphology changes markedly. This area is characterized by a very small berm and an extremely wide low-tide terrace with isolated ridges advancing across it (Fig. 19-5 a and b). There is a low, relatively unscarped fore-dune ridge just landward of the berm.

The isolated ridges are slightly cusped, with the horns pointing seaward. They measure 800 to 1200 feet long, up to 200 feet wide, with slip face amplitudes as much as 2.5 feet. There is no runnel system comparable to the Ridge Zone, North; the ridges sit as discrete units on the wide, flat, low-tide terrace. Linear ripples are present just landward of the ridges but most of the low-tide terrace has a plane bed surface.

---

Figure 19-2. Crane Beach morphological zonation for a constructional period. Based on pace and Brunton mapping done at low tide during the summer of 1967.

RIDGE ZONE, NORTH - AREA 4  
CRANE BEACH

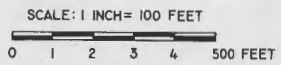
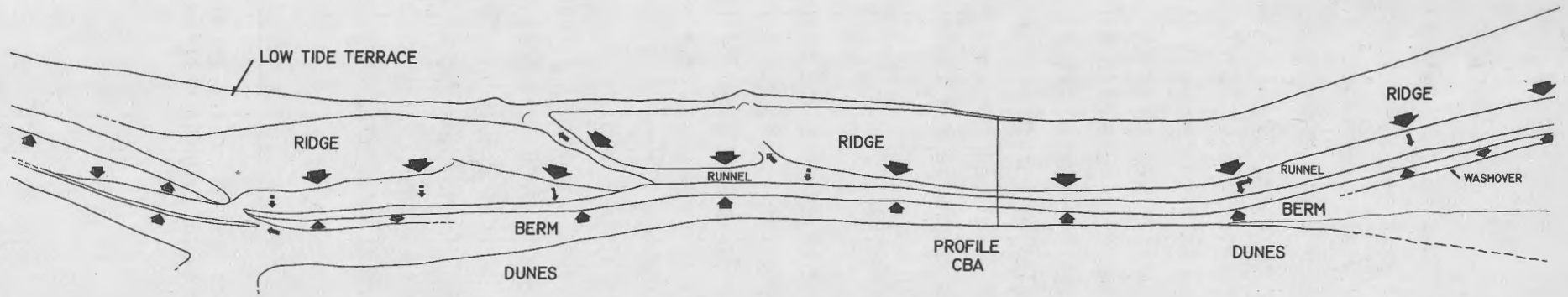


FIGURE 19-3A



FIGURE 19-3B

## Essex Delta Zone

Beach morphology in this southernmost area is determined partly by tidal current distribution of sand around the mouth of the Essex inlet. The largest feature is a sand flat up to 800 feet wide covered with well-developed, land-oriented, linear ripples (Fig. 19-6 a and b). A moderate sized berm-ridge 5 feet high lies close to a scarpred foredune ridge.

The large isolated ridges to the north decrease in amplitude and die out in this area, but a complex swash bar-ridge system begins just south of this zone. The swash bar-ridge complex is not included in this part of the beach study.

## BEACH STRUCTURES, BEDFORMS, AND CROSSBEDDING

### Beach Profiles

Topographic beach profiles show large-scale structures and morphology quite well. Four profiling stations (Fig. 19-2) were established on Crane Beach, and profiles were run at 4- to 7-day intervals, from May to September, 1967, Figure 19-7 illustrates a representative profile from each locality, obtained in late summer during the maximum constructional period. (For a complete discussion of beach structure genesis, see p. 245 this guidebook).

### Ridge, Berm, and Berm-ridge Form and Crossbedding

During any constructional period, but especially in the summer, on Crane Beach, ridges may migrate landward across a low-tide terrace. Ridge slip faces are, of course, landward-oriented, and migration of these slip faces forms large-scale planar crossbedding in the ridge. Figure 19-8 illustrates just such ridge migration at profile CBA during the summer of 1967.

---

Figure 19-3. Ridge Zone North, Crane Beach.

- A. Pace and Brunton map showing a well-developed ridge-and-runnel system with some ridge welding. Note area covered by aerial photograph (Fig. 19-3 b).
- B. Aerial photograph of portion of Ridge Zone, North, Crane Beach. Note the well-developed ridge that is welded to the berm at the top right and lower left of the photograph.

The external form of the ridge can be seen in Figure 19-9 a, a view across one of the isolated ridges of Ridge Zone, South (see Fig. 19-2 for location). Figure 19-9 b is a closeup of the slip face of the same ridge. Note the plane-bed top surface and linear ripples landward of the slip face. The color variations parallel to, and just back of, the ridge-slip face crest are interpreted as antidunes (p.76 , this guidebook).

Crossbedding in the above ridge is illustrated in Figure 19-10, a drawing of crossbedding exposed in a trench wall cut transverse to the slip face. Note the high dip angle (up to  $28^\circ$ ) and the scale (as much as 1.0 ft.) of the planar crossbeds. Note also the climbing effect of the crossbedding, as the ridge grows in amplitude and migrates shoreward. This mode of migration allows preservation of ridge bedforms in the internal structure. All ridges on the low-tide terrace examined by the Coastal Research Group showed this bedding configuration.

Berm form and internal structure are also shown in Figure 19-10. Berm bedding is commonly flat (reflecting berm-top surface form) to gently seaward dipping ( $5^\circ$  to  $10^\circ$ , reflecting beach-face surface slopes). However, many berms examined by the Coastal Research Group exhibit landward-dipping planar crossbeds (Fig. 19-10) interpreted as having formed by ridge migration shoreward, after which burial and the subsequent formation of a berm obscures all traces of the former ridge (see p. , this guidebook). If the ridge is large, berm-type sedimentation will modify only the seaward portion of the ridge and a unique external form (the berm-ridge) will result (Fig. 19-7, profile CBB). Landward-dipping crossbeds will be more pronounced, as illustrated by Figure 19-11.

### Linear Ripples

Linear ripples in the beach environment are formed by swash-driven currents landward of the wave break-point. They are asymmetrical,

---

#### Figure 19-4. Accretion Zone, Crane Beach.

- A. Pace and Brunton map showing a large berm-ridge and a swash bar - ridge complex with multidirectional slip faces.
- B. Aerial photograph of a part of the Accretion Zone.

ACCRETION ZONE - AREA 3  
CRANE BEACH

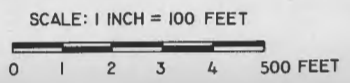
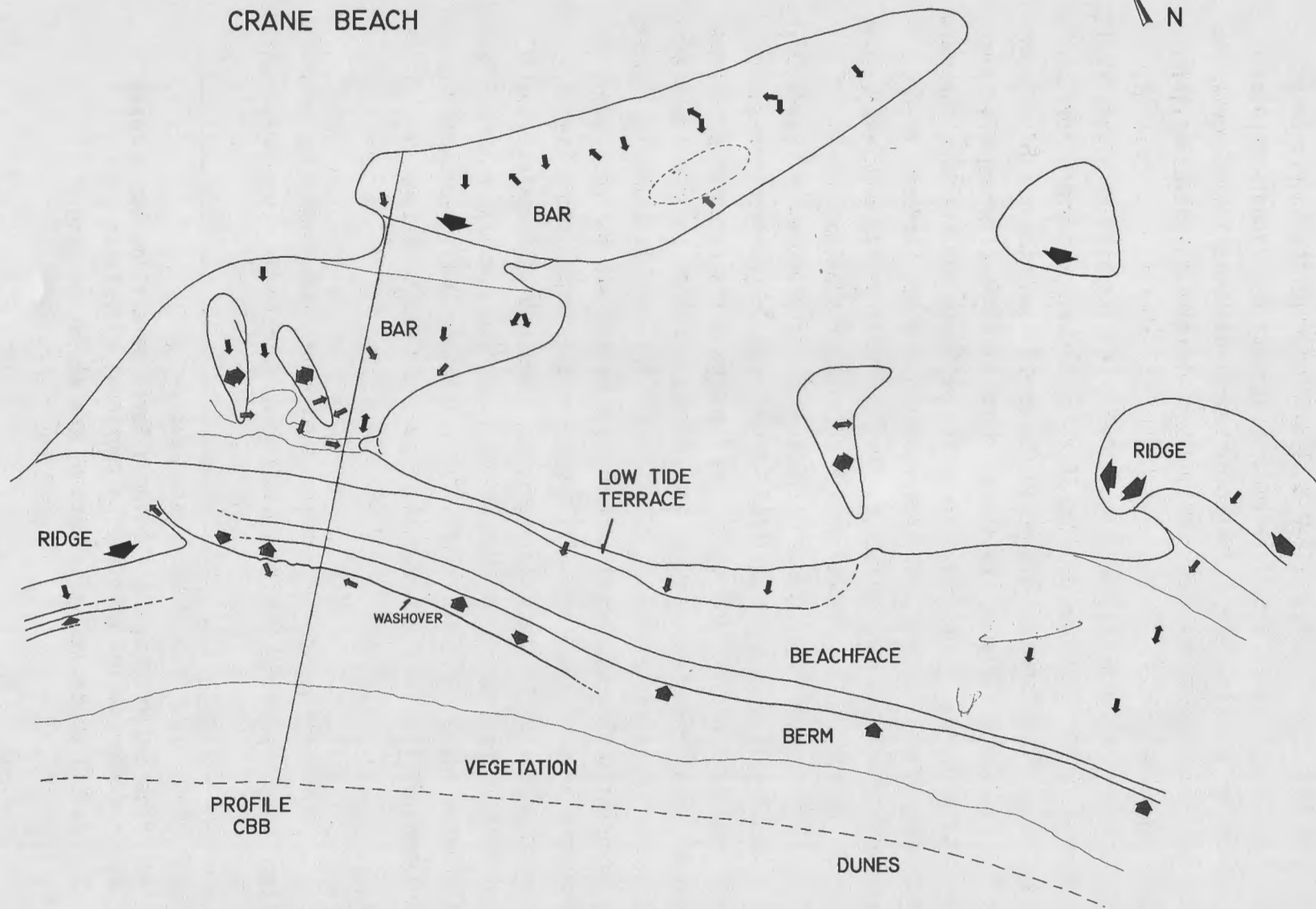


FIGURE 19-4A



FIGURE 19-4B

# RIDGE ZONE, SOUTH - AREA 2

CRANE BEACH

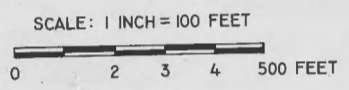
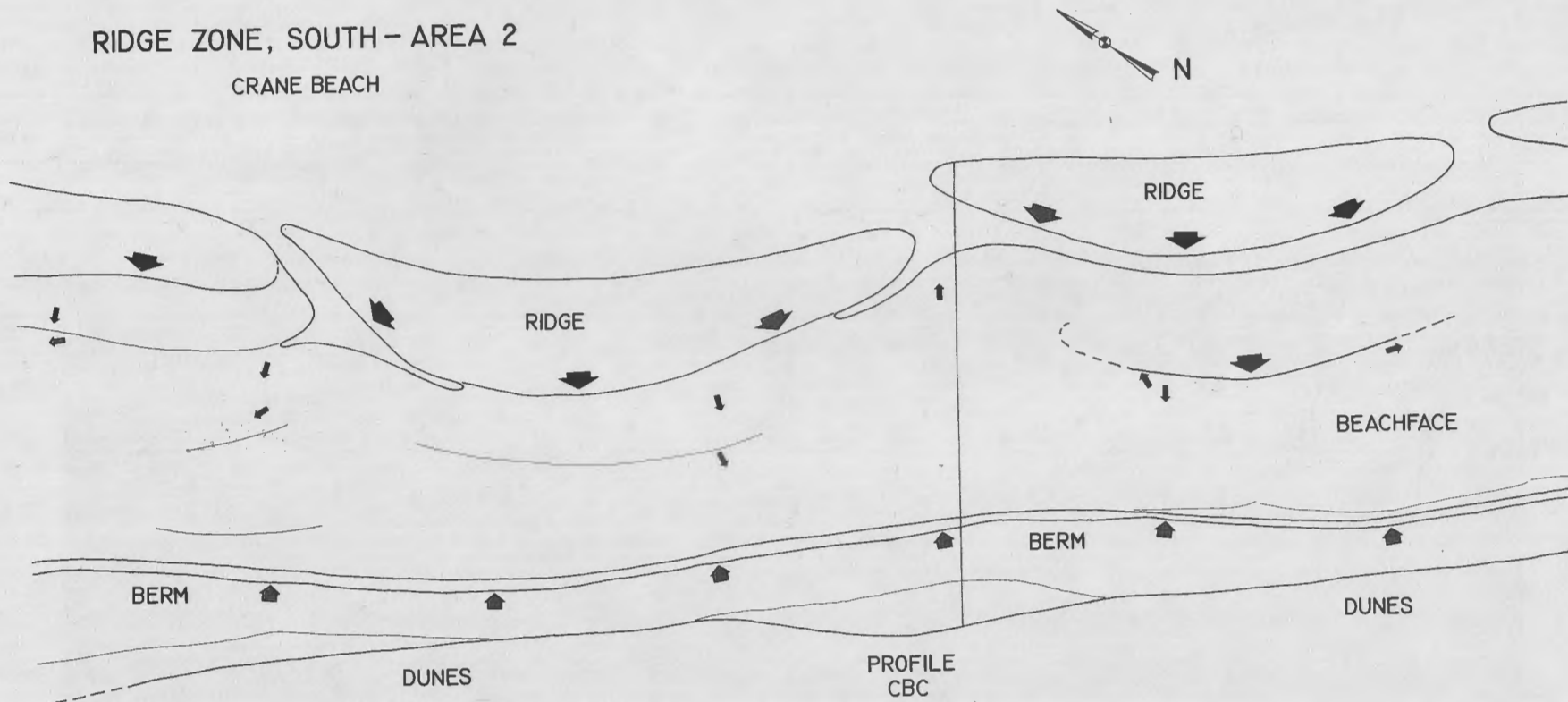


FIGURE 19-5A

with landward-oriented slip faces (Fig. 19-12). Linear ripples may be modified by backwash or waves and the slip face obscured or destroyed, but the primary form was asymmetrical landward. As discussed elsewhere in the text (p. 417), linear ripples form under very low strengths of flow. They are found on the beach on very low-gradient low-tide terraces; on the backs of very large ridges or swash bars, again with low gradients; and in runnels, which are protected areas behind ridges. Very low gradients are needed because swash energy necessary to push water up steeper gradients will cause the bed to plane out.

Harms (1969) shows that linear ripple wavelength and amplitude increase, and crest linearity decrease, with increased current energy. This concept is illustrated in Figure 19-13, a view of linear ripples just landward of the ridge discussed above (Figs. 19-9 and 19-10). The bottom component of flow strengthens away from the ridge slip face (see p. 76, this guidebook), causing the change in form of the linear ripples.

An increase in grain size also increases linear ripple wavelength and amplitude (Harms, 1969). The distribution of ripple scale shown in Figure 19-14 is due to variations in both grain size and swash energy.

#### Plane Beds

Plane beds, which are uncommon in the estuarine environment, are quite common on the beach. Berm tops, beach faces, most ridge surfaces, as well as large areas of low-tide and beach-face terraces, are plane beds. It is very important to make a distinction between plane beds and flat beds. Plane beds, a reflection of flow-regime condition, may be either horizontal or inclined. Flat beds may or may not be plane beds, but certainly are plane beds in the beach environment.

Plane beds in the beach environment are formed by shallow-swash sheet-flow under upper flow regime conditions, such as across a ridge surface or up a beach face. The horizontal bedding seen in the ridge (Fig. 19-10) is plane bedding, as is the seaward-dipping and horizontal bedding

---

Figure 19-5. Ridge Zone, South, Crane Beach.

A. Pace and Brunton map showing cusped isolated ridges on a wide low-tide terrace.

B. Aerial photograph of a portion of Figure 19-5 A.

of the berm. Measurements in the Accretion Zone, Crane Beach, indicate that plane beds make up over 50 percent of beach bedding (see following section).

#### Beach Crossbedding as a Paleocurrent Indicator

On the basis of pace and Brunton mapping, the Accretion Zone (Fig. 19-4) showed the greatest complexity of structures and the greatest variations in crossbedding. For this reason it was chosen as a model to illustrate bedding found in the beach environment.

Crossbedding azimuths were measured on a 100 x 100-foot grid system; crossbedding or bedding was inferred from external form. The azimuths for the various types of structures are shown in Figure 19-15. Ripple crossbedding is small-scale planar and festoon and landward-oriented; ridge crossbedding is large-scale planar and landward-oriented; and berm crossbedding is inclined seaward at low dip angles. Beds dipping less than  $5^{\circ}$  were classified as flat. A summation of azimuths for all structures is illustrated in Figure 19-16.

It is significant to note that horizontal beds (plane beds) constitute almost 50 percent of beach bedding at this locality. Berm bedding is also plane, but the seaward-dipping aspect is important to this immediate discussion.

The important point is that bedding and crossbedding shows a dominant landward dip. Only 6.8 percent of the beds measured indicate a seaward dip.

It is evident from the foregoing discussion that: (1) beach bedding is over 50 percent planar and formed under upper flow-regime conditions; (2) crossbedding formed under low-regime conditions is also important, with both large-scale and small scale planar crossbedding present;

---

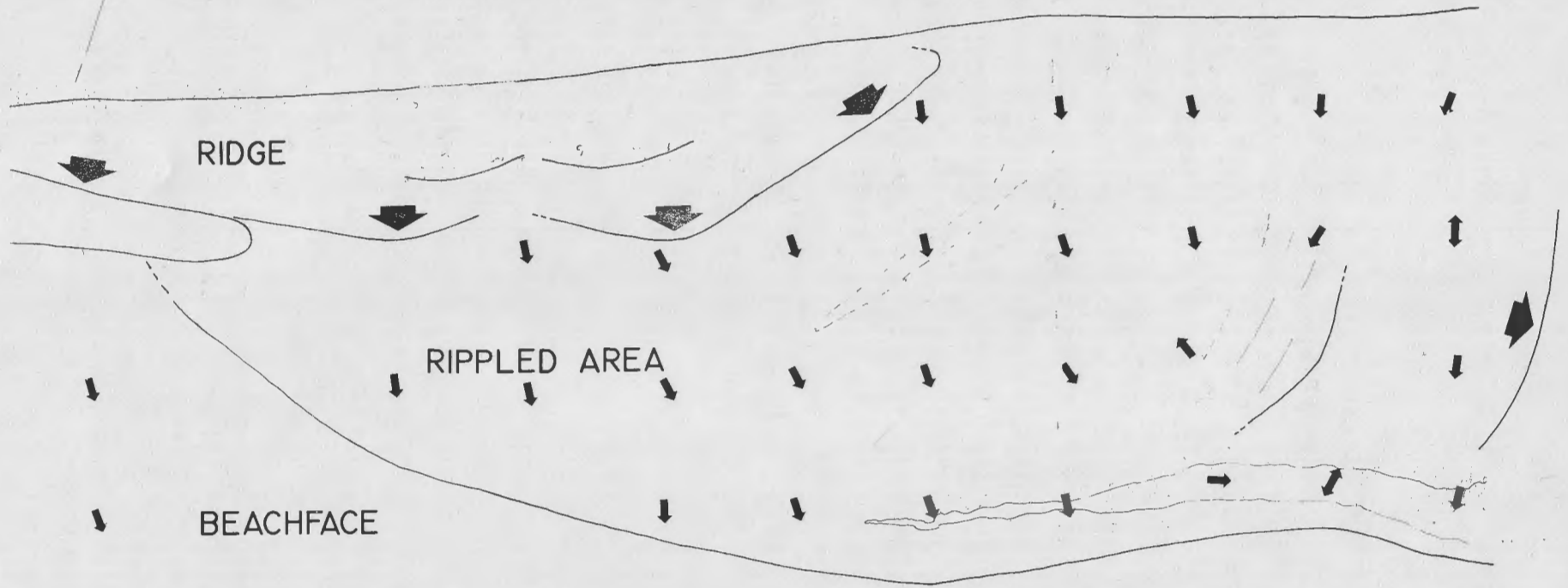
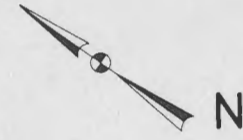
Figure 19-6. Essex Delta Zone, Crane Beach.

A. Pace and Brunton maps showing the large sand flat with linear ripples. The large ridge to the left is low in amplitude. Features to the right are dominated by Essex tidal currents.

B. Aerial photograph of part of Figure 19-6 A. Note the wide sand flat and offshore swash bar. Area to the right in the photo is not a part of Essex Delta Zone.

# ESSEX DELTA ZONE - AREA I

CRANE BEACH



RIDGE

RIPPLED AREA

BEACHFACE



DUNES

BERM

PROFILE  
CBD

SCALE: 1 INCH = 100 FEET



FIGURE 19-6A



FIGURE 19-6B

(3) crossbedding, both small and large-scale, shows a persistent landward dip; (4) gently seaward-dipping beds make up less than 10 percent of total beach bedding. Crossbedding trend is, then, perpendicular to general beach trend, and dominantly up the regional "paleoslope".

---

Figure 19-7. Constructional beach profiles, August, 1967, Crane Beach, Massachusetts. The profile from each locality shows the major structures representative of that zone.

# CONSTRUCTIONAL PROFILES

## CRANE BEACH

22 AUGUST 1967

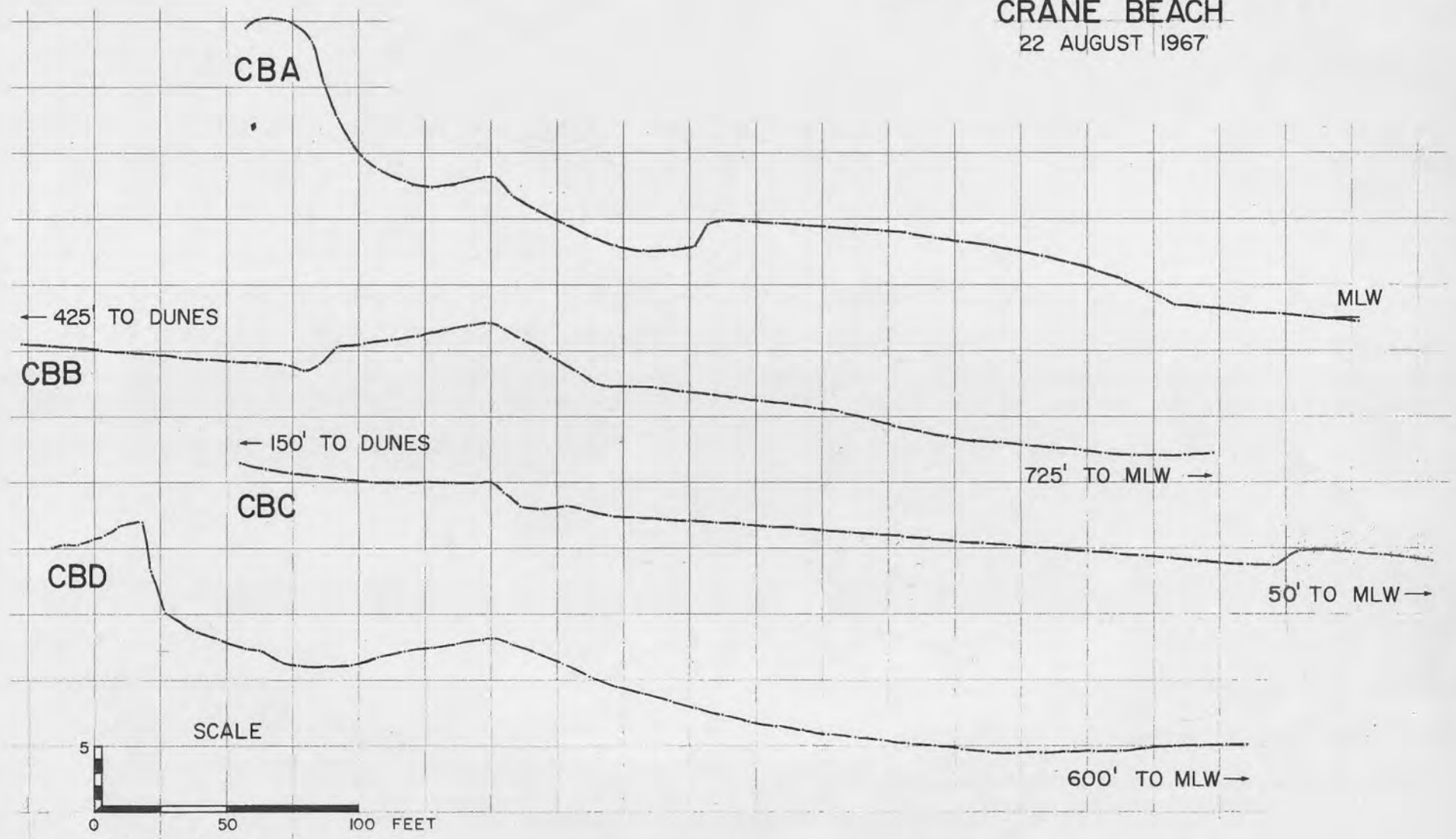


FIGURE 19-7

Figure 19-8. Summer accretion, profile CBA, Crane Beach, Ipswich, Massachusetts. Note the landward ridge migration and development of a ridge-and-runnel profile.

Figure 19-9A. External form of isolated ridge, Ridge Zone, South, Crane Beach, Massachusetts. Ridge is sitting on a very wide linear-rippled low-tide terrace. Shovel just landward of slip face is 3.5 feet high.

Figure 19-9B. Closer view of ridge slip face of Figure 19-9A. Note the plane-bed top surface and linear ripples landward of the ridge. Stake at slip face is 3.5 feet high.

Figure 19-10. Internal structure of berm and ridge in Ridge Zone, South, Crane Beach, Massachusetts. For location see Figure 19-2. Note large-scale, land-oriented planar crossbeds in the ridge, and flat to gentle seaward-dipping beds in the berm with some landward dips at the base. Trenches dug 3 to 5 August, 1968.

10  
5  
0

FIGU

# SUMMER ACCRETION 29 MAY-7 SEPT 1967

STATION CBA, CRANE BEACH  
IPSWICH, MASS.

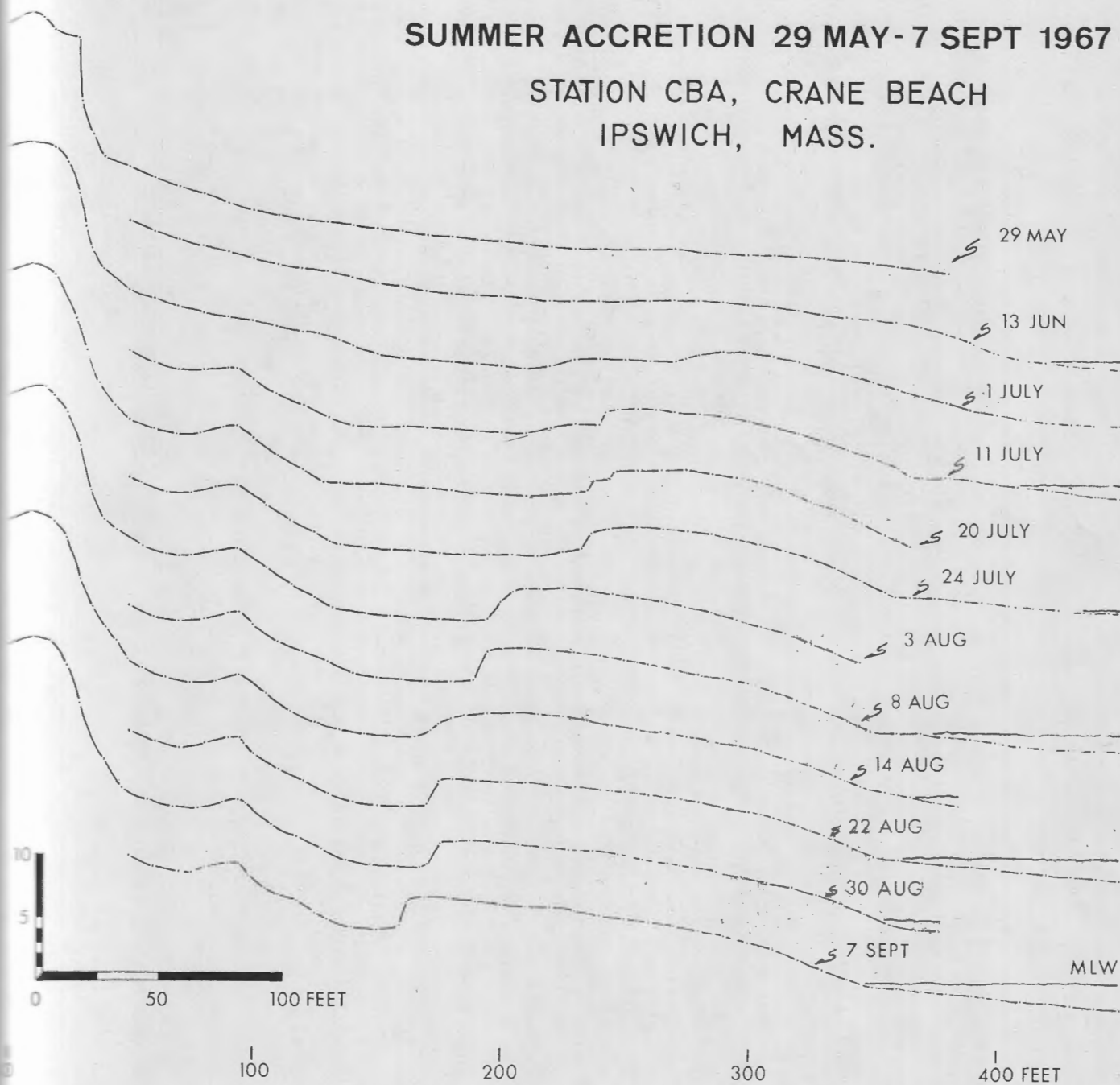


FIGURE 19-8



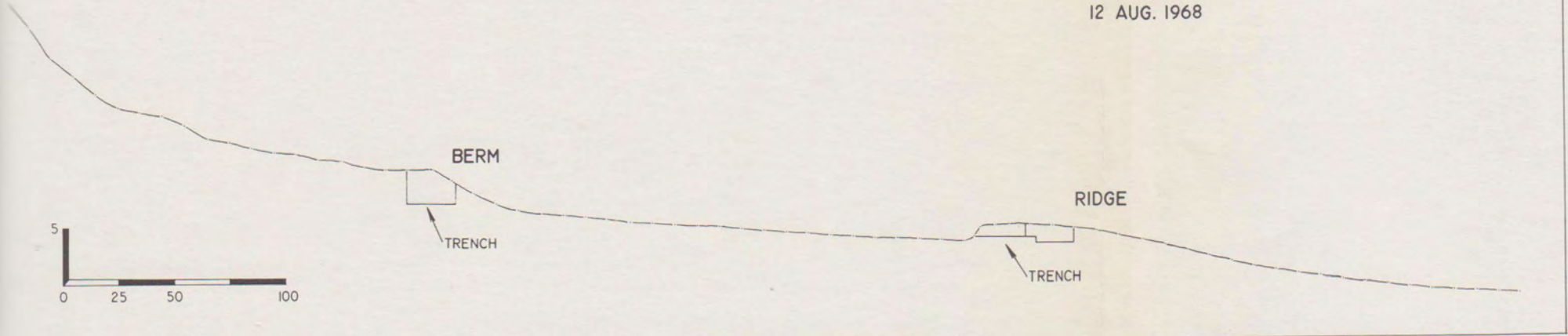
FIGURE 19-9A



FIGURE 19-9B

PROFILE CBS, CRANE BEACH

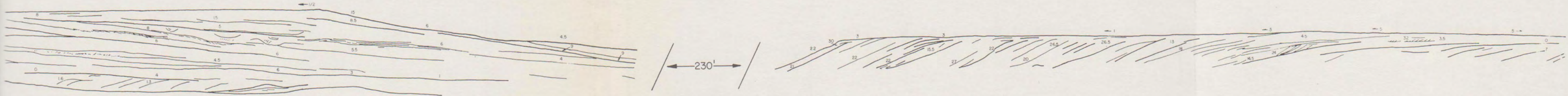
12 AUG. 1968



BERM AND RIDGE STRUCTURE  
RIDGE ZONE, SOUTH  
CRANE BEACH

BERM

RIDGE



250 FEET TO MEAN LOW WATER →

FIGURE 19-10

Figure 19-11. Berm-ridge cross section, profile CBD, Crane Beach, Massachusetts. Profiles in box at the upper left illustrate ridge configuration of 13 July, with later modification to berm-ridge form. Note the landward-oriented, steeply dipping crossbedding topped by shallow seaward-dipping beds.

Figure 19-12. Linear ripples, Crane Beach, Massachusetts. Note the asymmetrical landward-oriented slip faces and the excellent linearity of crests.

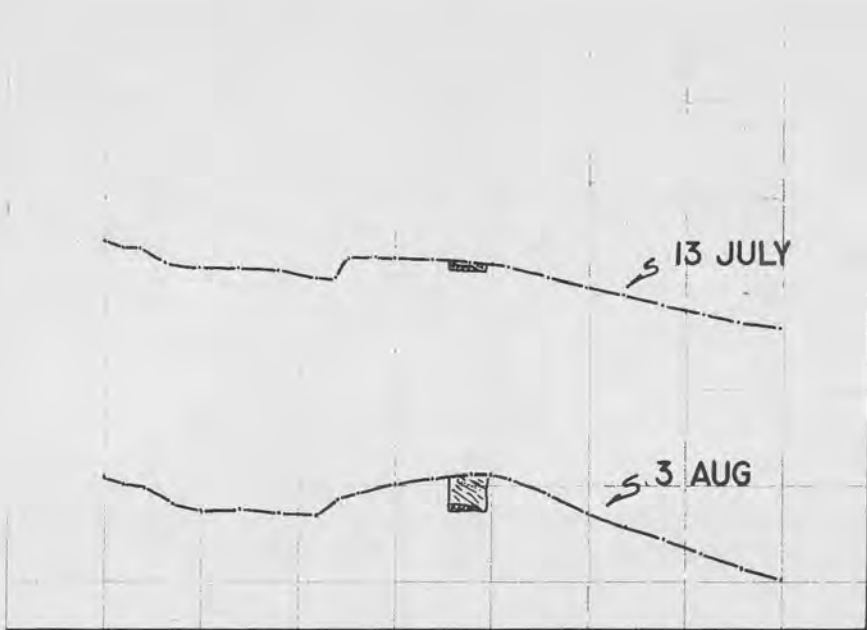
Figure 19-13. Linear ripples landward of ridge of Figures 19-9 and 19-10. Note the increase in wavelength and decrease in linearity away from the ridge slip face indicating increasing hydraulic energy. Scale is 1 foot long.

Figure 19-14. Linear ripple scale, Crane Beach, Massachusetts.

# BERM-RIDGE CROSS-SECTION

## 3 AUG, 1967

STATION CBD, CRANE BEACH  
IPSWICH, MASS.



SCALE: ONE INCH = ONE FOOT  
HORIZONTAL AND VERTICAL

FIGURE 19-II



FIGURE 19-12

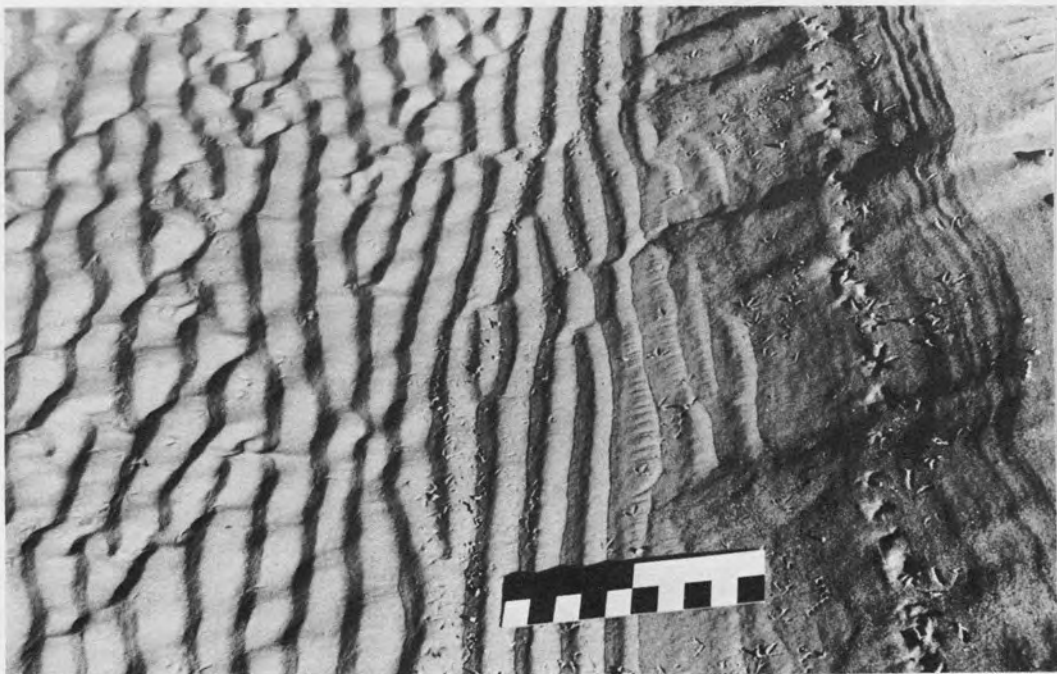


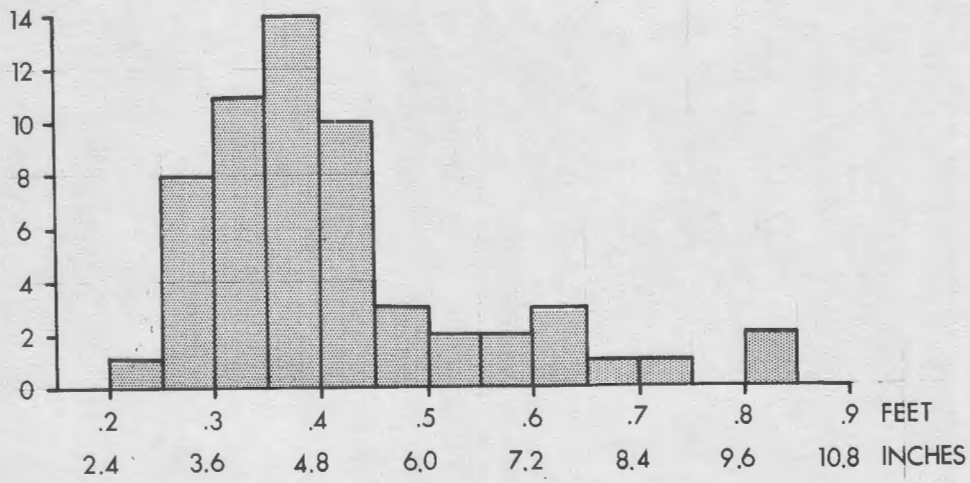
FIGURE 19-13

# RIPPLE SCALE

CRANE BEACH, IPSWICH, MASS.

## WAVELENGTH

58 READINGS



## AMPLITUDE

58 READINGS

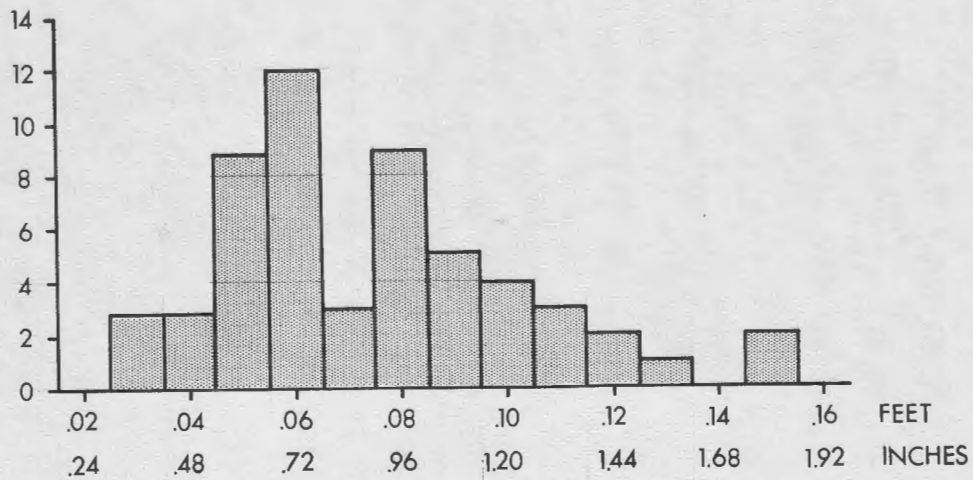


FIGURE 19-14

Figure 19-15. Crossbedding azimuths, Accretion Zone, Crane Beach, Massachusetts. Ripples show small-scale planar and festoon crossbedding, ridges show large-scale planar crossbedding, and berms show gentle dips (5 to 15°). Note the major orientation pattern for each structure.

Figure 19-16. Summation of crossbedding azimuths for Accretion Zone, Crane Beach, Massachusetts. Note the persistent landward dip of the crossbedding.

# CROSSBEDDING AZIMUTHS

ACCRETION ZONE - AREA 3

CRANE BEACH, IPSWICH, MASS.

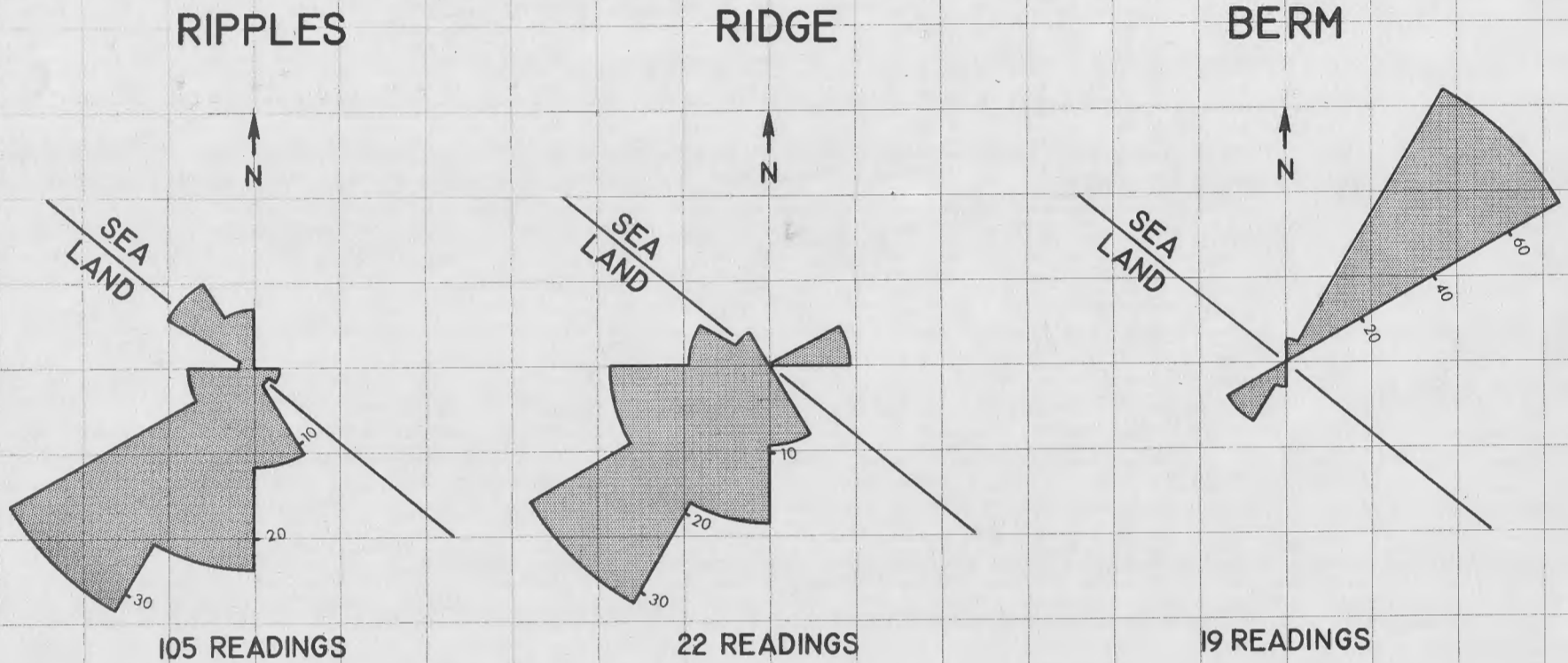
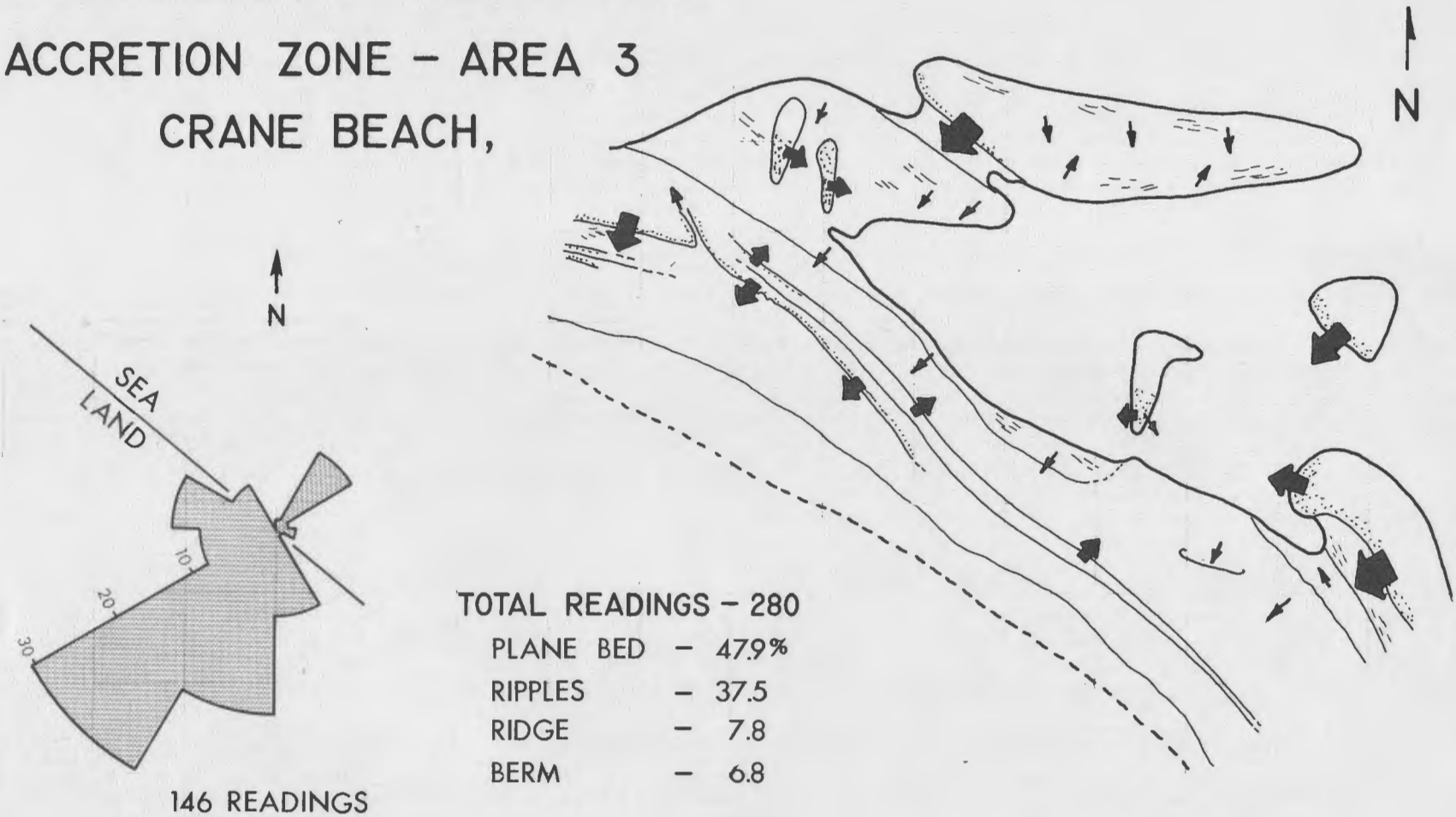


FIGURE 19-15

# CROSSBEDDING AZIMUTHS

ACCRETION ZONE - AREA 3

CRANE BEACH,



TOTAL READINGS - 280

PLANE BED - 47.9%

RIPPLES - 37.5

RIDGE - 7.8

BERM - 6.8

146 READINGS

FIGURE 19-16

## STOP 20 - BULL BROOK SITE, PARADISE ROAD

### IPSWICH

Joseph H. Hartshorn

When the soil was being stripped from the south side of the area prior to beginning sand removal, some sharp-eyed bulldozer operators, who were also amateur archaeologists, found some fluted points of a kind never seen before in Massachusetts. These Clovis-type points were in dubious association with disseminated chunks of charcoal in what may have been a living horizon. A radiocarbon date of about 9300 years B.P. (before the present) is now generally accepted by archaeologists for the paleo-Indian culture at this site.

Why the paleo-Indians lived at this spot is an interesting question, and what physical conditions were in that stage of local post-glacial history may hold part of the answer. However, no recent geologic study has tried to fit all the geologic and radiocarbon data together.

The Bull Brook site lies on an almost isolated flat-topped plain. It has been called a kame plain or a kame delta. The sedimentary structures seen in the sides of the pit at different periods of excavation have included plane bedding, planar foresets, large-scale deltaic beds, scour-and-fill structures, and ripple marks. Rhythmic graded beds that look like coarse-grained varves may still be visible. Smooth, flat, rounded pebbles, cobbles, and boulders are isolated in the sand in the southwest side of the pit; the source is unknown, the environment of deposition has been mapped as marine (Sammel, 1963).

On the east side of the sand pit, beyond the grading and loading machinery, is a trench in marine clay. Pebbles, cobbles, and boulders are scattered throughout. The upper part of the clay is oxidized to a dark yellow brown or brown and is fissile. Other outcrops in deeper excavations show that an unaltered gray clay underlies this upper weathered portion. No marine fossils have been collected from this formation, perhaps because no really systematic, detailed search has been made.

The clay laps up on the side of the sand plain. A bore hole 75 feet deep in the bottom of the sand pit showed only 30 feet of sand (Sammel, 1962).

## STOP 21 - NOURSE CEMETERY GRAVEL PITS

Joseph H. Hartshorn

Because of time limitations, this stop may not be made. Two sand and gravel pits at the base of Jewett Hill show a thin (2 to 6 foot) layer of clay interbedded with glacial stratified drift. The contact between the clay and stratified drift is irregular. The geology is more complex than indicated by Sammel (1963), who mapped the area as marine and estuarine deposits.

## STOP 22 - HIGH TIDE HYDROGRAPHY, MERRIMACK RIVER ESTUARY

Allan D. Hartwell

Miles O. Hayes

The Merrimack River estuary is a classic example of a Type B estuary (Pritchard, 1955) and is generally well-stratified (see Merrimack hydrography paper, p.218 ). If discharge is greater than about 3000 c.f.s., a sharp, slightly tilted, boundary develops between the intruding salt-water mass and the overriding fresh-water mass. During the flood period, salt water from the ocean is deflected to the north or right side of the estuary, whereas fresh river water ponds up on the south side over Joppa Flat. A significant amount of the sediment suspended in the fresh water, as well as of the pollutants the river carries, is deposited on Joppa Flat.

This stop will consist of a boat trip from the northern end of Plum Island into the lower portion of the Merrimack River estuary. An attempt will be made to point out the location of the surface expression of the salt water - fresh water interface during the flood tide and to delimit the hydrography across the boundary with in-situ salinometer measurements. Fathometer records will be available to demonstrate bottom topography and bedforms in the main channel.

Sediment samples from the channel bottom will be taken with a grab sampler. These sediments are coarse grained (mean about 0.5-1.0  $\phi$ ) and are composed of quartz (35-40%), rock fragments (25-40%), yellow-orange feldspar (20-30%), and traces of coal. Clam and mud flats along the estuary margins are finer grained (mean about 3-4  $\phi$ ) with quartz (85-90%) and mica. The Merrimack sediments contrast sharply with those found in the Plum Island River and channels in the Salisbury Marsh. The latter are mostly fine-grained gray sand with a notable absence of yellow-orange feldspar. The reason for this contrast in sediment mineralogy is uncertain at this time, but it may reflect differences in sediment source area or the effects of chemical weathering.

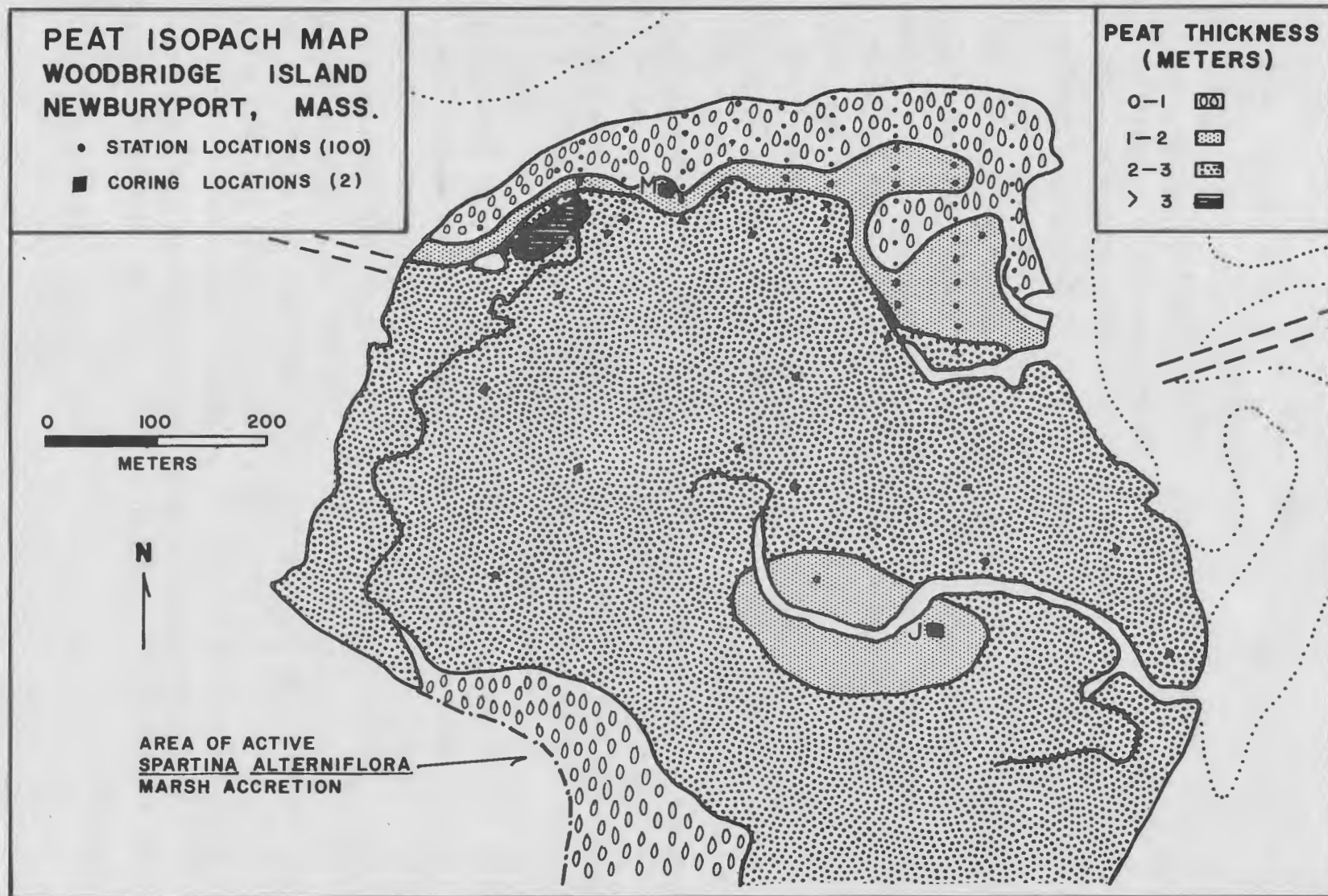


FIGURE 23-1

## STOP 23 - WOODBRIDGE ISLAND MARSH

Allan D. Hartwell

This will be a brief stop to examine the Holocene stratigraphy of the salt marsh on Woodbridge Island. The relation of this marsh to the rest of the salt marsh complex of the Merrimack River estuary is discussed in greater detail elsewhere in this guidebook (see p.428 ). Details of the peat thickness and geometry of the Woodbridge Island marsh are shown on Figure 23-1. The general stratigraphic sequence from top to bottom includes: (1) living high salt marsh dominated by Spartina patens; (2) high salt marsh peat; (3) sand to muddy low salt marsh peat with abundant roots of Spartina alterniflora; and (4) gray silty to sand intertidal facies believed to be analogous to the clam flat and tidal channel sediments in the present estuary. The north end of Woodbridge Island is underlain by an elongate curving sand body composed of reworked glaciofluvial sediments similar to that found under the marshes south of the Plum Island Turnpike. Angular cobbles were unearthed in several holes. Origin of this sand mass is still uncertain. It could be either an old tidal delta complex built when the river mouth was further south than at present or a deposit of glaciofluvial material. A Spartina alterniflora marsh appears to have started on the south side of the sand body when mean sea level was 1 to 2 meters lower than present. This marsh gradually accreted vertically and laterally until it was high enough for the present high salt marsh community, dominated by Spartina patens, to establish itself.

---

Figure 23-1: Peat isopach map of Woodbridge Island.



FIGURE 24-1

## STOP 24 - PARKER RIVER ESTUARY MARSH

Miles 0. Hayes

At this stop we will visit several localities on the salt marsh north of the Rowley River in the Parker River estuary. This is the area illustrated in Figures 7 and 9 of McCormick's paper on the Parker River marshes (p.368, in this guidebook). The pre-Holocene topography in this area is very irregular, therefore the Holocene thicknesses are quite variable and the Holocene facies relationships are very complex.

As pointed out by McCormick, an arm of the eastern coarse-grained facies, thought to represent an open main tidal channel deposit, protrudes in a westerly direction under the Rowley River area. The subsurface contact between the eastern coarse-grained facies and the western fine-grained facies is reflected by a small surficial topographic break. The eastern coarse-grained facies is covered by Spartina alterniflora marsh which is slightly lower in elevation than the high salt marsh that overlies the western fine-grained facies. If time permits, we will visit this contact and extract cores from the two zones.

The Holocene section at the first point we will visit after leaving the vehicles is as follows (from top to bottom):

<u>Thickness</u>	<u>Description</u>
12 ft.	High salt marsh peat
1.5 ft.	<u>S. alterniflora</u> peat
7.5 ft.	Western fine-grained facies
1 ft.	Black peat
1.5 ft.	Weathered zone
?	Blue clay

---

Figure 24 - 1. View looking west along the Rowley River. Much of the marsh along the margins of the main channel is dominated by S. alterniflora. This marsh is apparently very young and is rapidly accreting over what was recently a broad expanse of sand flats. The points to be visited at this stop are located in the upper right-hand portion of the photograph.

Inasmuch as the Holocene facies vary markedly over this area, we will take as many cores as time permits. An aerial view of the marsh in the Rowley River area is shown in Figure 24-1.



FIGURE 25-1

## STOP 25 - FLIGHTS

Miles O. Hayes

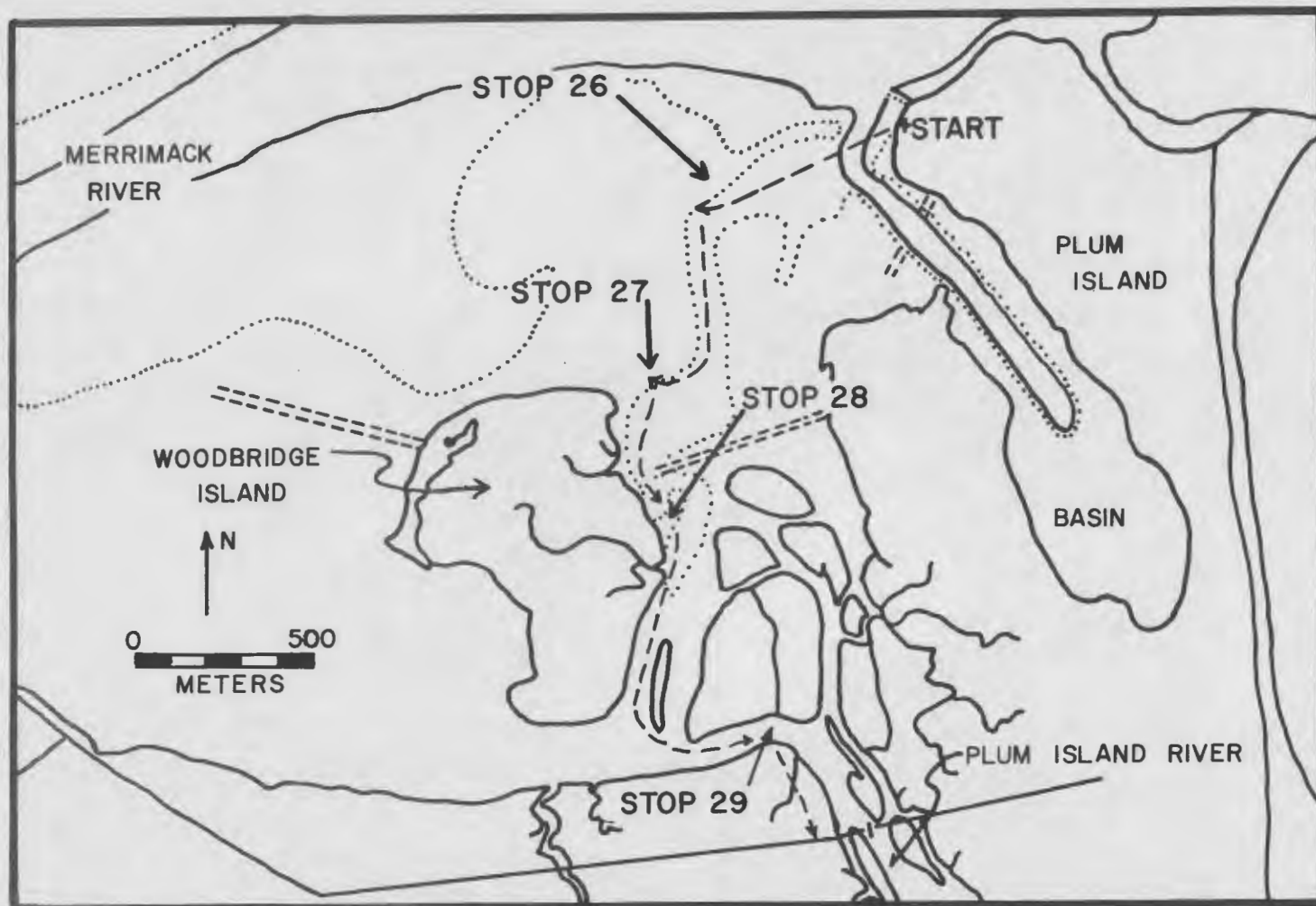
Immediately upon take-off from the Plum Island Airport, assuming good weather, you will be in good viewing area for the intertidal environments visited on the field trip. The flight plan is first to circle the inlet of the Merrimack River estuary so that the flood-tidal delta and the intertidal mud flats of the lower estuary can be viewed. From that point, we will fly a zigzag pattern down Plum Island and Crane Beach so as to view the beach zone. The end point of the beach overflight will be Coffin Beach. After viewing Coffin Beach, we will circle over the intertidal sand bodies of the Essex Bay area, fly over the landward side of Crane Beach, and then spend the remainder of the flight making passes over the inlet and main channel of the Parker River estuary. An attempt will be made to provide each passenger with good viewing of every environmental type present in the area.

One of the more fascinating spectacles from the air in this area are the large intertidal sand bodies. A typical view of one of the Parker River sand bodies is shown in Figure 25-1. If viewing conditions are good, you should be able to discern a sharp differentiation in bedform orientations between the high-level intertidal zones and the sub-tidal channels. The intertidal zones contain sand waves that are dominantly flood-oriented, whereas the sub-tidal channels, although complex, contain a significantly higher amount of ebb-oriented features.

We will fly at low tide. Each flight will last approximately 30 to 45 minutes.

---

Figure 25-1. Small sand body located northeast of Middle Ground in the Parker River estuary. The estuary mouth is to the right. Note large flood-oriented sand waves over the surface of the flat, the well-developed ebb shield at the left-hand margin of the flat, and the curving spill-over lobe, built by ebb currents, on the upper right-hand portion of the sand body.



**MERRIMACK RIVER ESTUARY LOCATION MAP**  
**FIGURE 26-1**

## STOP 26 - TIDAL DELTA, MERRIMACK RIVER ESTUARY

Allan D. Hartwell

Stops 26 to 29 are located in close proximity, thus their locations are shown on a single map (Fig. 26-1); stops 26 to 28 are shown on aerial photograph (Fig. 26-2).

The flood tidal delta of the Merrimack River estuary (Figs. 26-1 and 26-2) is similar in morphology and structure to those previously visited in the Parker River and Essex estuaries. One important difference is that this delta is subject to marked fluctuations in fresh water discharge into the estuary (refer to the Merrimack hydrography paper by Hartwell and Hayes on p.218 of this guidebook). At this stop, we will examine a variety of bedforms and how they are related to the pattern of tidal circulation around and over the delta. The aerial photograph (Fig. 26-3) and plane table map (Fig. 26-4) show the main features of the delta, which include a large ebb spit, flood sand-wave field, ebb shield, and northwest sand lobe area. The ebb shield forms a topographic high 1.0-1.3 m below mean sea level. The entire southwestern and western portions of the delta are covered with mussel banks.

During the summer of 1968, the tidal delta was visited 23 times at low tide to observe bedforms, sedimentary structures, sediment distribution, infauna, and migration of sand waves. In late June, an east-west range line was established and a plane table map prepared (Fig. 26-4). About every 6 days for the rest of the summer, bedform azimuths, wavelengths, and amplitudes were measured at low tide on a 100-foot (30.4 m) grid across most of the delta. An attempt was made to gather data representative of spring, normal, and neap tides and high and low discharge conditions. The delta was remapped at the end of the summer and the location of each flood-oriented sand wave determined.

The rose diagram in Figure 26-5 (left) shows the distribution of

---

Figure 26-1. Map showing location of stops 26 to 29.

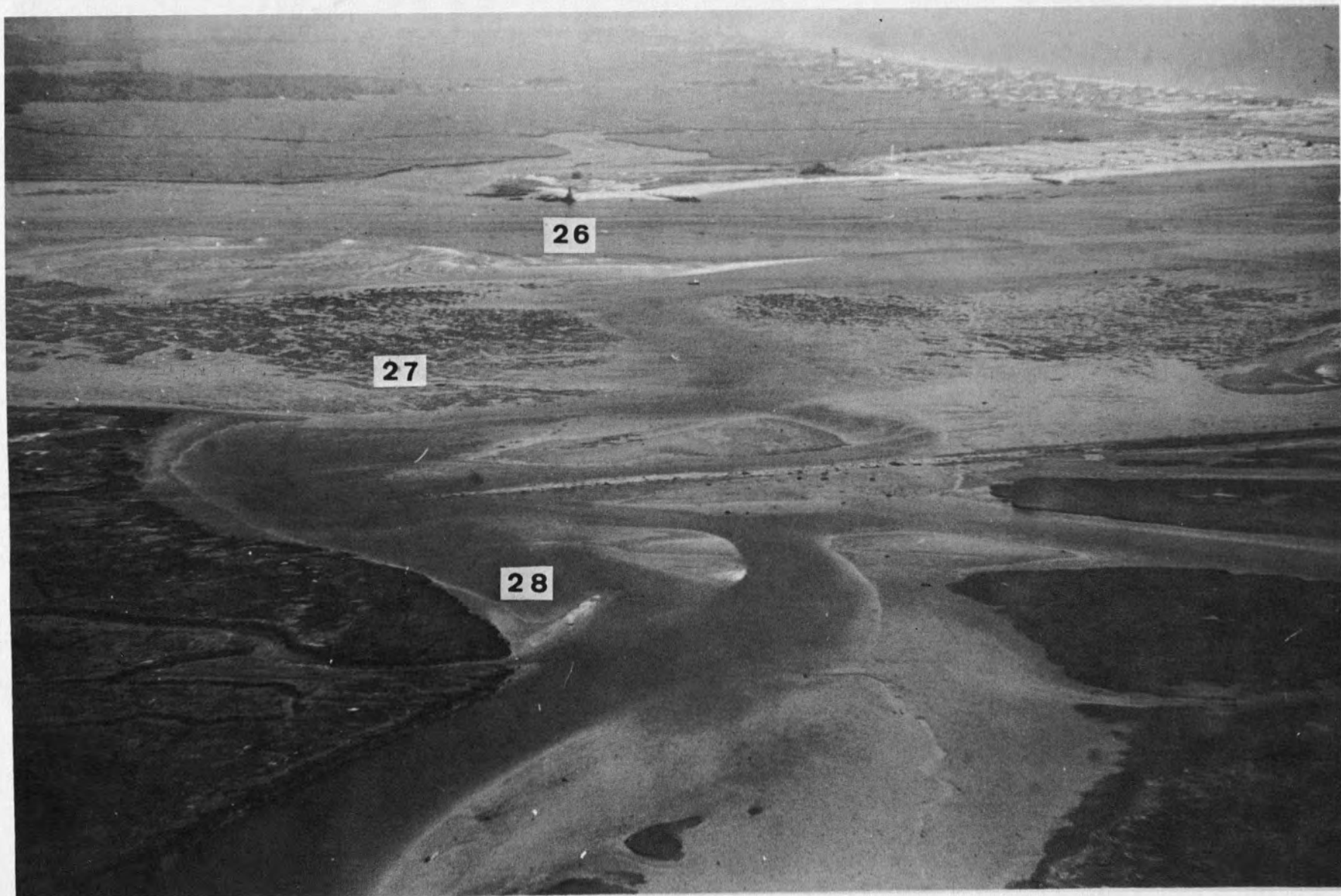


FIGURE 26-2

Figure 26-2. Lower Merrimack River estuary at low tide (looking north). Note location of Stops 26, 27, and 28.

Figure 26-3. Vertical aerial photograph of flood tidal delta of Merrimack River estuary. Note the exceptionally large ebb shield on western side of delta (estuary mouth is to the right). Compare photograph with plane table map of Figure 26-4. Photograph taken on 18 April, 1968; courtesy, U.S. Army Corps of Engineers.

Figure 26-4. Plane table map of flood-tidal delta of the Merrimack River estuary. Compare with aerial photograph of Figure 26-3. Datum is mean sea level.



FIGURE 26-3

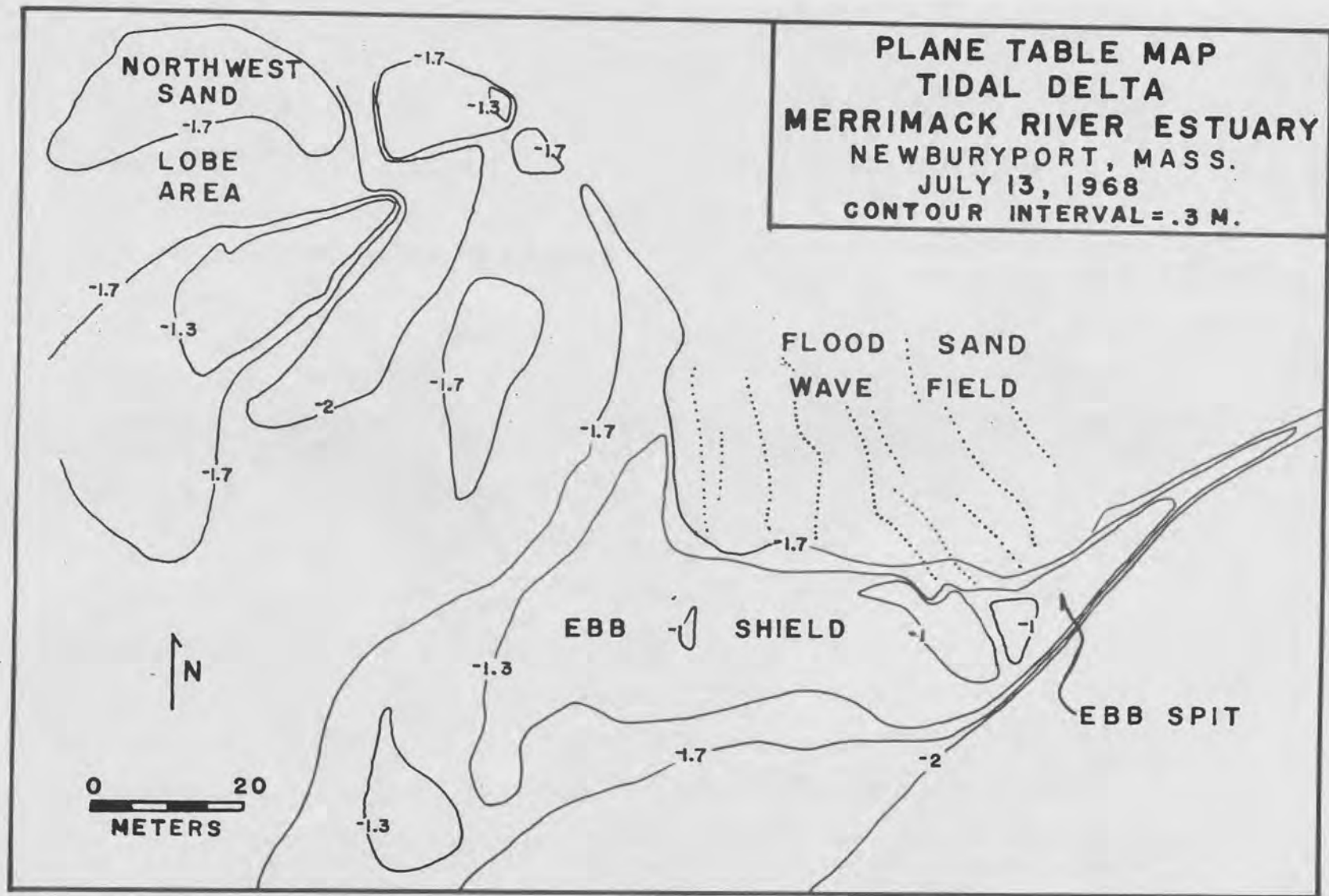


FIGURE 26-4

# SLIP FACE AZIMUTHS

## MERRIMACK RIVER TIDAL DELTA

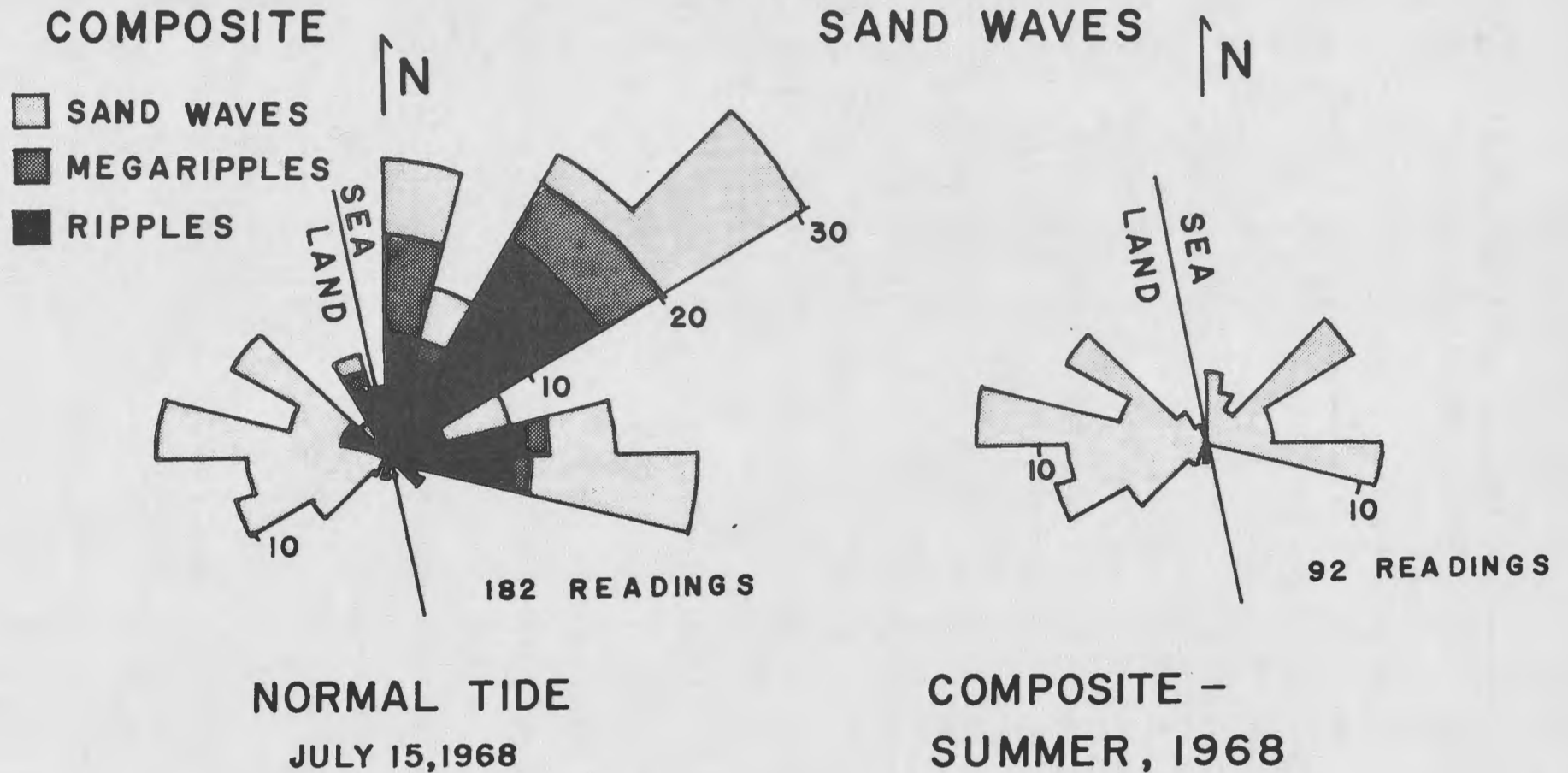


FIGURE 26-5

Figure 26-5. Compilations of slip-face azimuths at low tide for bedforms on the Merrimack River flood-tidal delta.

(Left) Rose diagram of azimuths of 182 slip-face orientations of sand waves, megaripples, and ripples combined. Data collected during a normal tide on 15 July, 1968.

(Right) Composite rose diagram summarizing sand-wave azimuths collected at low tide during spring, neap, and normal tides (total of 92 readings).



**FIGURE 26-6**



the azimuths of slip-face orientations on bedforms during a normal low tide. Ripples and megaripples show ebb orientation toward the northeast; whereas sand waves are bimodal, reflecting the flood dominance on the larger sand waves northeast of the delta and the influence of ebb currents during a falling tide on the smaller ones on the ebb shield (see aerial photograph, Fig. 26-2). The azimuths of sand wave slip-face orientations from the whole delta are plotted together on Figure 26-5 (right).

One of the most striking aspects of the tidal delta is the response of bedforms to neap, normal, and spring tide conditions. The normal tidal range is 2.50 m (8.2 ft.), spring tides reach 3.56 m (11.7 ft.), and neap tides may be as little as 1.53 m (5.0 ft.). During normal tides, the bulk of the ebb shield is covered with ripples and sand waves while the ebb spit and the north end of the ebb shield have megaripples and scour-megaripples. During spring tides, larger volumes of water enter the estuary, so currents are stronger. The resulting low-tide bedforms are large megaripples and scour-megaripples across most of the ebb shield (Fig. 26-6). In contrast, the small water volume of neap tides forms small ripples (Fig. 26-7) on the ebb shield with megaripples being almost nonexistent (at low tide).

Details of these responses to tidal range and water volume are documented in Figures 26-8 to 26-11. All of the ripples measured (Fig. 26-8) show ebb dominance at low tide but those formed during spring and normal tides are more bimodal than those formed during neap tides. The histograms of wavelength (Fig. 26-9) show that neap tide ripples have the longest

---

Figure 26-6. View looking northwest across the central portion of the ebb shield on the flood tidal delta of the Merrimack River estuary (low tide). Spring tide, 13 June, 1968.

Figure 26-7. Approximately the same view as Figure 26-6 during a neap tide, 22 July, 1968.

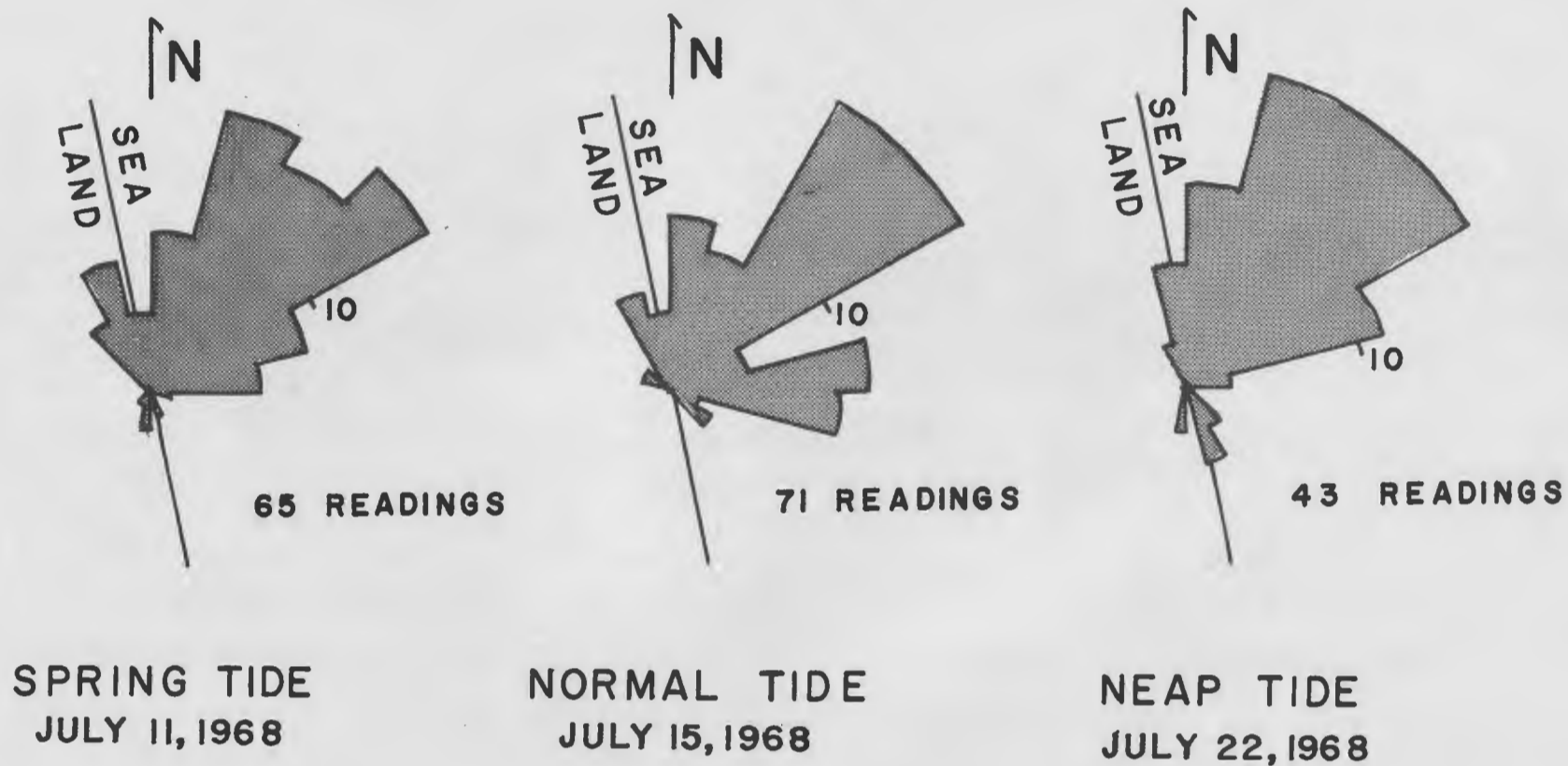
Figure 26-8. Rose diagrams showing slip-face azimuths of ripples measured at low tide on the flood tidal delta of the Merrimack River estuary during three tidal phases (spring; normal; neap).

Figure 26-9. Histograms showing wavelengths (ripple spacing) for ripples occurring on the Merrimack flood-tidal delta during three tidal phases (spring; normal; neap - at low tide). This is a composite diagram of all the ripples measured.

Figure 26-10. Rose diagrams showing slip-face azimuths of megaripples measured at low tide on the flood-tidal delta of the Merrimack River estuary during three tidal phases (spring; normal; neap).

# RIPPLE SLIP FACE AZIMUTHS

## MERRIMACK RIVER TIDAL DELTA



### FIGURE 26-8

# RIPPLE SCALE

WAVELENGTH

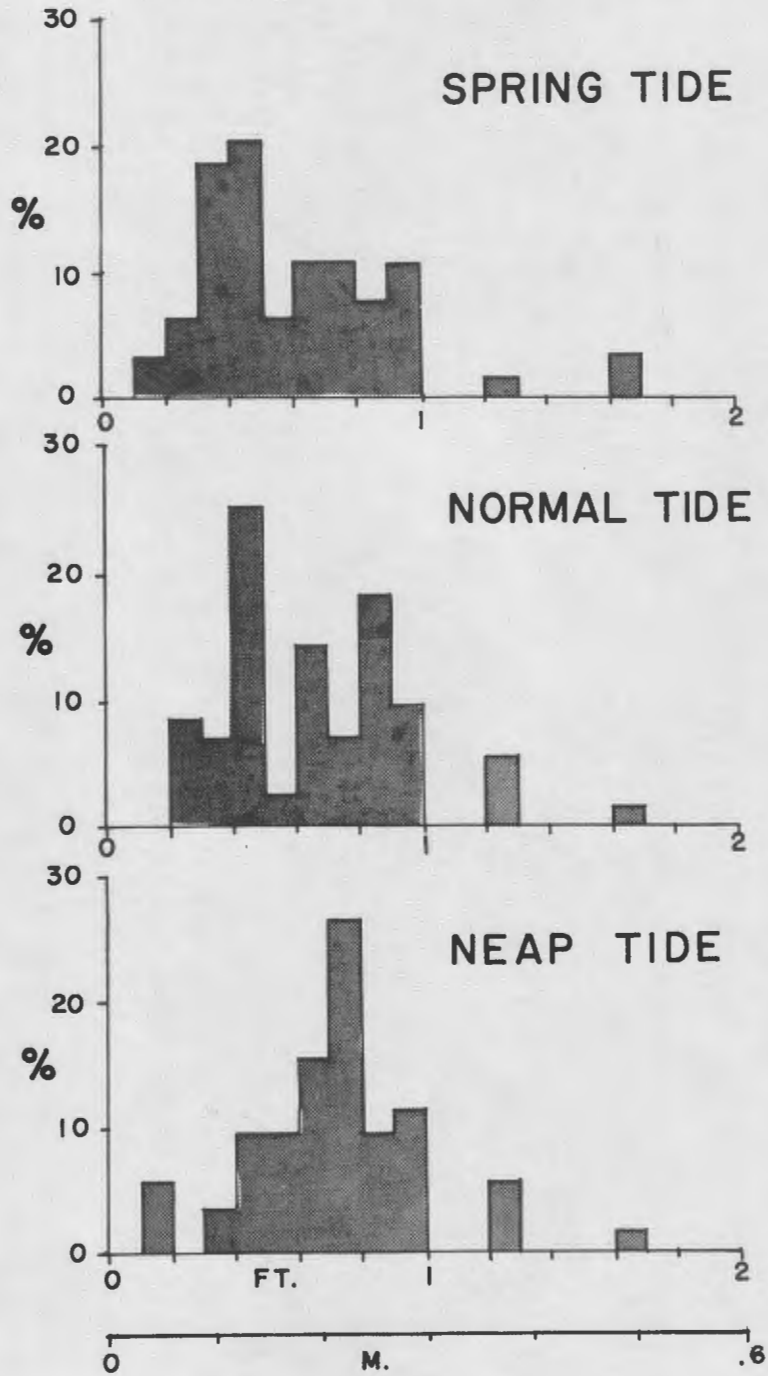


FIGURE 26-9

# MEGARIPPLE SLIP FACE AZIMUTHS

## MERRIMACK RIVER TIDAL DELTA

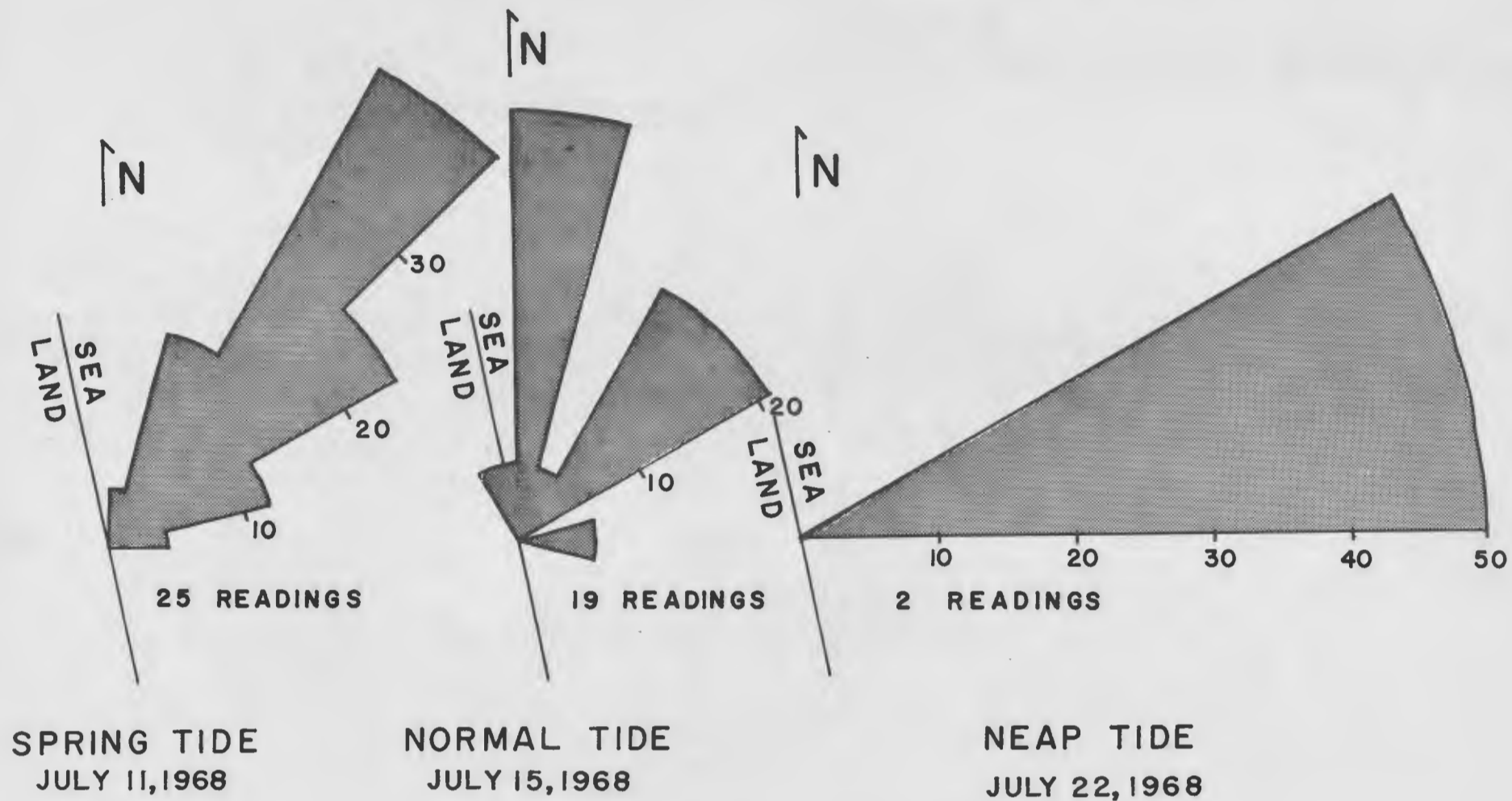


FIGURE 26-10

# MEGARIPPLE SCALE

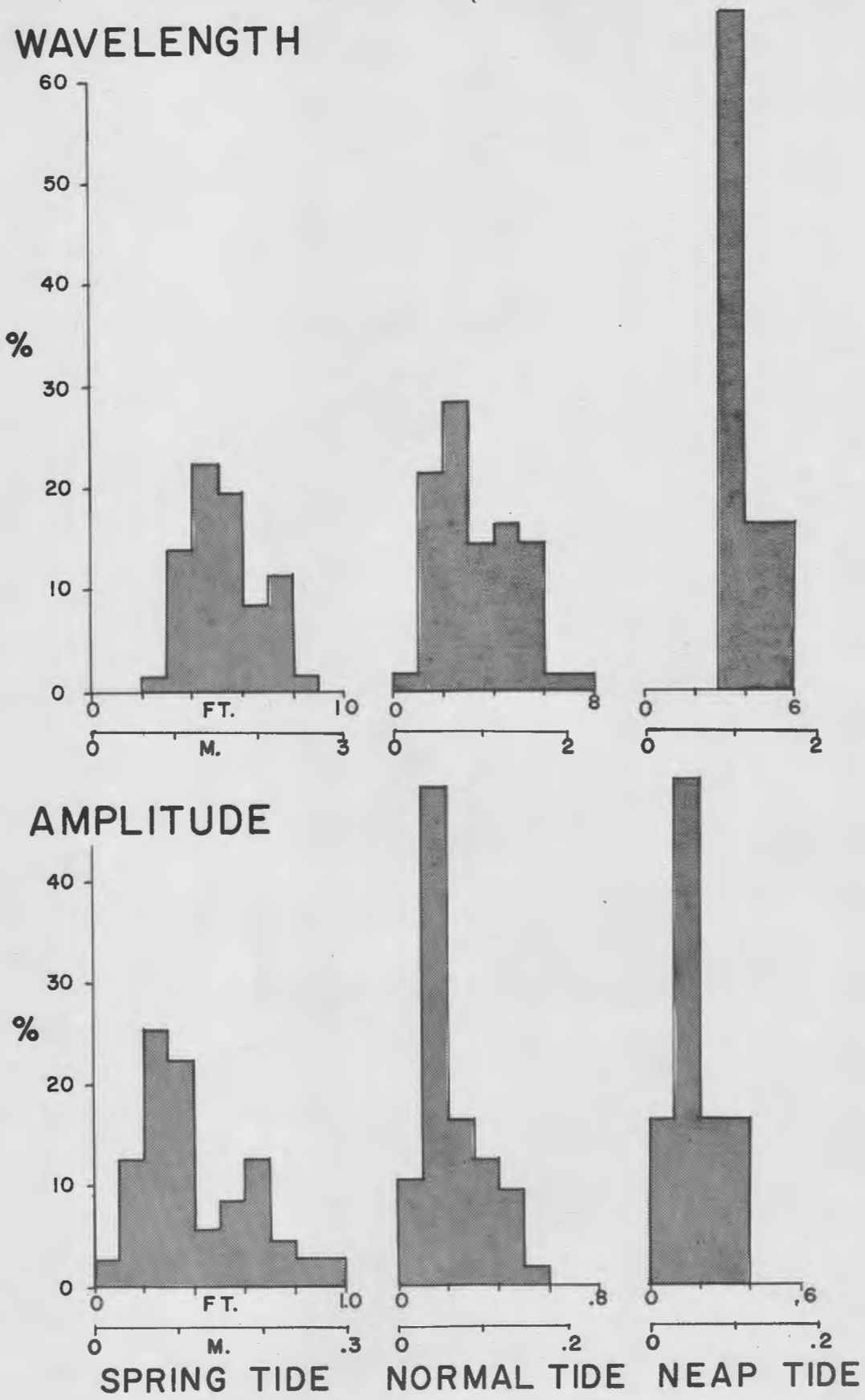


FIGURE 26-II

wavelengths, with 27 percent in the 21.3 to 24.4 cm (.7 to .8 ft.) class. Ripples formed during normal and spring tides show 3 peaks in wavelength (Fig. 26-9) at 9.2 to 15.2 cm (.3 to .5 ft.), 18.3 to 24.4 cm (.6 to .8 ft.), and 24.4 to 30.5 cm (.8 to 1.0 ft.). The ripples represented by the first and third peaks probably were formed under higher flow strength in the scour pits of the megaripples. The middle peak corresponds to the neap tide ripples that develop on the ebb shield.

Rose diagrams of megaripple slip-face azimuths (Fig. 26-10) reveal that spring and neap-tide azimuths are nearly uniformly oriented to the northeast. During normal tides, a distinct bimodality is evident, reflecting current flow to the north across the ebb spit and to the northeast across the north end of the ebb shield (Figs. 26-3 and 26-4). Histograms of wavelength (Fig. 26-11) show that spring tide megaripples are largest (.6 to 3.0 m; 2 to 10 ft.) but 3 peaks occur. Normal tide megaripples are smaller with 2 peaks at .6 to .9 m (2 to 3 ft.) and 1.2 to 1.5 m (4 to 5 ft.). Megaripples are rare during neap tides but 66 percent of the wavelengths measured are .9 to 1.2 m (3 to 4 ft.). Histograms of amplitudes (Fig. 26-11) reveal a similar trend; that is, spring tide megaripples are largest with two peaks at 6.1 to 9.2 cm (.2 to .3 ft.) and 18.3 to 21.3 cm (.6 to .7 ft.). During normal and neap tides, peak amplitudes are only 3.0 to 6.1 cm (.1 to .2 ft.).

In addition to these changes in bedform azimuth and magnitude, striking changes in morphology of the delta and migration rates of sand waves were observed during the summer of 1968. A series of stakes were placed at slip-face bases of selected bedforms. Figure 26-12 shows a photo sequence illustrating the migration rate of a flood-oriented sand wave. During a 45-day period, it moved more than 8.5 m, with greatest migration occurring during spring tides (Fig. 26-13).

---

Figure 26-11. Histograms showing wavelengths and amplitudes of megaripples occurring on the Merrimack flood tidal delta during three tidal phases (spring; normal; neap - at low tide). This is a composite diagram of all the megaripples measured.

A



B



C



D



E



F



FIGURE 26-12

A rapid decrease in fresh water discharge in early July had profound effects on large bedforms and ebb shield morphology. During late June, discharge was 2 to 3 times above the annual mean of 7000 c.f.s. The ebb shield had numerous sand waves on it which showed ebb orientations at low tide with active slip faces migrating northeastward. During the first 10 days of July, discharge dropped from 21,300 to 5760 c.f.s. and flood currents began to dominate the whole delta. The old slip faces were largely destroyed and in many places westward-migrating ones were built that remained through the ebb period and were, hence, still flood-oriented at low tide. Many large sand waves with a former ebb orientation at low tide began to retreat and assumed a flood asymmetry, indicating dominance of flood currents as transporting agents over the delta. Additional work is necessary to monitor these changes on an annual basis.

Different parts of the tidal delta show variations in grain size and mineralogy. Most of the ebb shield, ebb spit, and flood sand wave field consist of coarse- to medium-grained sand similar to that in the main channel of the estuary. Mineral composition of the sand averages 50 percent quartz, 30 percent yellow-orange feldspar, 12 percent gray to white feldspar, and 8 percent rock fragments. The sand on the southwest portion of the delta is finer grained with more quartz (62 percent), less feldspar (18 percent yellow and 15 percent gray), 5 percent rock fragments, and a

---

Figure 26-12. Series of photographs (taken at low tide) illustrating the rate of movement of the slip face of a flood-oriented sand wave with respect to a permanent stake placed in the flood sand wave field of the Merrimack flood-tidal delta (Fig. 26-3). All photographs were taken looking northwest. Observations were made during the summer of 1968; specific dates for each photograph are:

- |            |             |
|------------|-------------|
| A. 25 June | D. 13 July  |
| B. 8 July  | E. 31 July  |
| C. 11 July | F. 8 August |

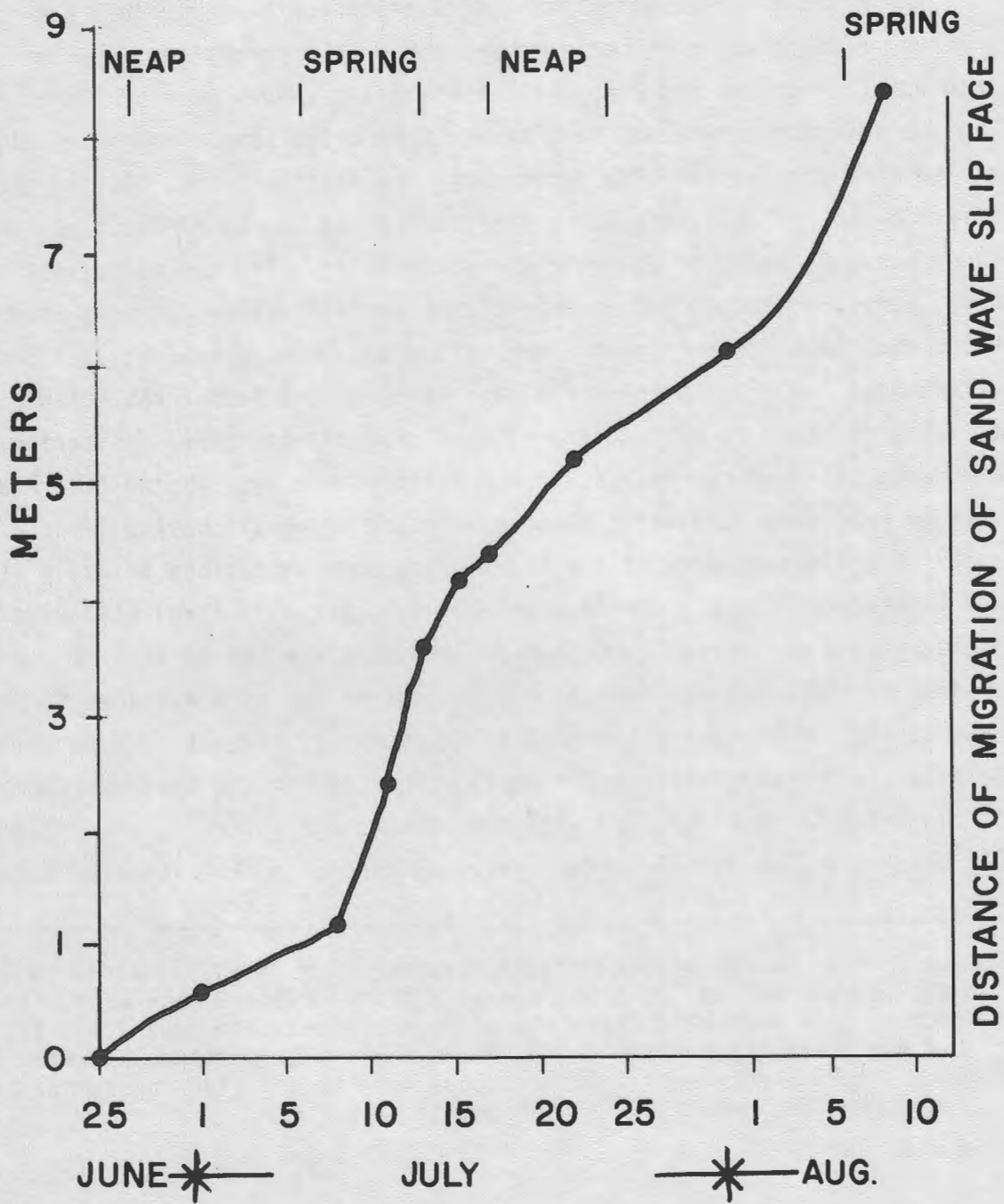


FIGURE 26-13

trace of garnet. Grain-size analysis is incomplete at this time, but this distribution of size and mineral composition over the delta appears to be the result of size-sorting by currents across the delta. An additional factor is the presence of two apparently different types of sand in the area. The channel sediments of the Merrimack are coarse grained with abundant yellow-orange feldspar and rock fragments. Sand under the Salisbury and Newbury marshes and in the Plum Island River is finer grained with abundant quartz, some gray to white feldspar, rock fragments, and garnet, but very little yellow-orange feldspar. These two sand populations are either derived from two different sources or have different post-depositional chemical weathering histories (for further discussion of this problem, see paper by Greer, p.403 of this guidebook).

---

Figure 26-13. Relation of distance of migration of the slip face of the flood-oriented sand wave illustrated in Figure 26-12 to tidal phase. Migration rates were greatest during the intervals 8 to 13 July and 5 to 8 August, periods of spring tide.

## STOP 27 - CLAM FLAT AND MUSSEL BANKS

### MERRIMACK RIVER ESTUARY

Allan D. Hartwell

At this stop a muddy to sandy clam flat that grades northward into mussel banks will be examined. This area is typical of much of the intertidal zone of the lower estuary. Common sedimentary structures include clam and worm burrows (Fig. 27-1) and small black hydrogen sulphide cells. Common fauna include the soft clam (Mya arenaria), clam worm (Nereis virens), duck clam (Macoma balthica), blue mussel (Mytilus edulis), and the bloodworm (Glycera dibranchiata). Note the change in mineralogy from a muddy brown sand on the surface (mean about  $0.5\phi$ ) with trace amounts of yellow-orange feldspar to a better sorted, finer grained grayish-white sand (mean 1.0 to  $1.5\phi$ ) at depth. In places, buried mussel banks and buried clam flats with abundant large Mya arenaria in life position are present from 75 cm downward.

Figure 27-1. X-ray radiographs showing sedimentary structures typical of the clam flats of the Merrimack River estuary. Photographs are contact prints of x-ray negatives made from 1 cm. thick slices from oriented box samples.

A. (Sample 279) Muddy, sandy, clam flat area near Stop 27. Small clam worm (Nereis virens) burrows and duck clam (Macoma balthica) in life position near top.

Coarser grained sand at depth but no soft clams (Mya arenaria) exposed in sample. Sample is mottled with numerous black hydrogen sulphide cells.

B. (Sample 2116) Mud flat near west end of Joppa Flat. Well-developed burrowing by small worms (probably N. virens) near top and large M. arenaria in life position at the bottom.

C. (Sample 2122) Mud flat south of breakwater on Joppa Flat west of Woodbridge Island. Two sizes of worm burrows are well-exposed at top (worm species uncertain). Coarser grained muddy-sand at depth with M. balthica in life position.

D. (Sample 838-F) Rhythmite sample from mud flat on point bar on Plum Island River near Parker River National Wildlife Refuge boat ramp. Sand layers or rhythmites (Reineck, 1967) probably formed during storms by wave action that carried sand out of channel bottoms onto mud flats.

5 cm 0



FIGURE 27-1

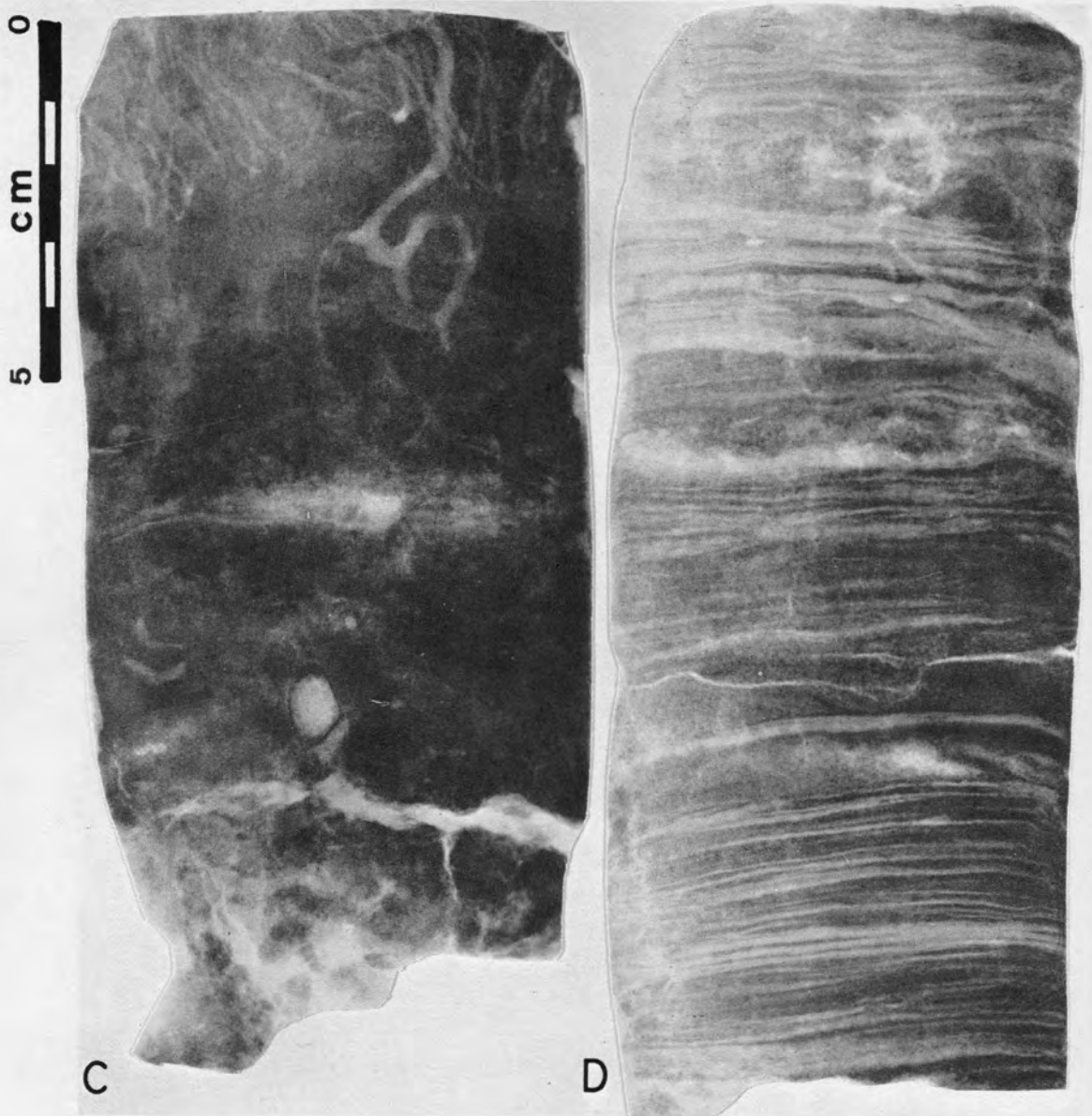


FIGURE 27-1

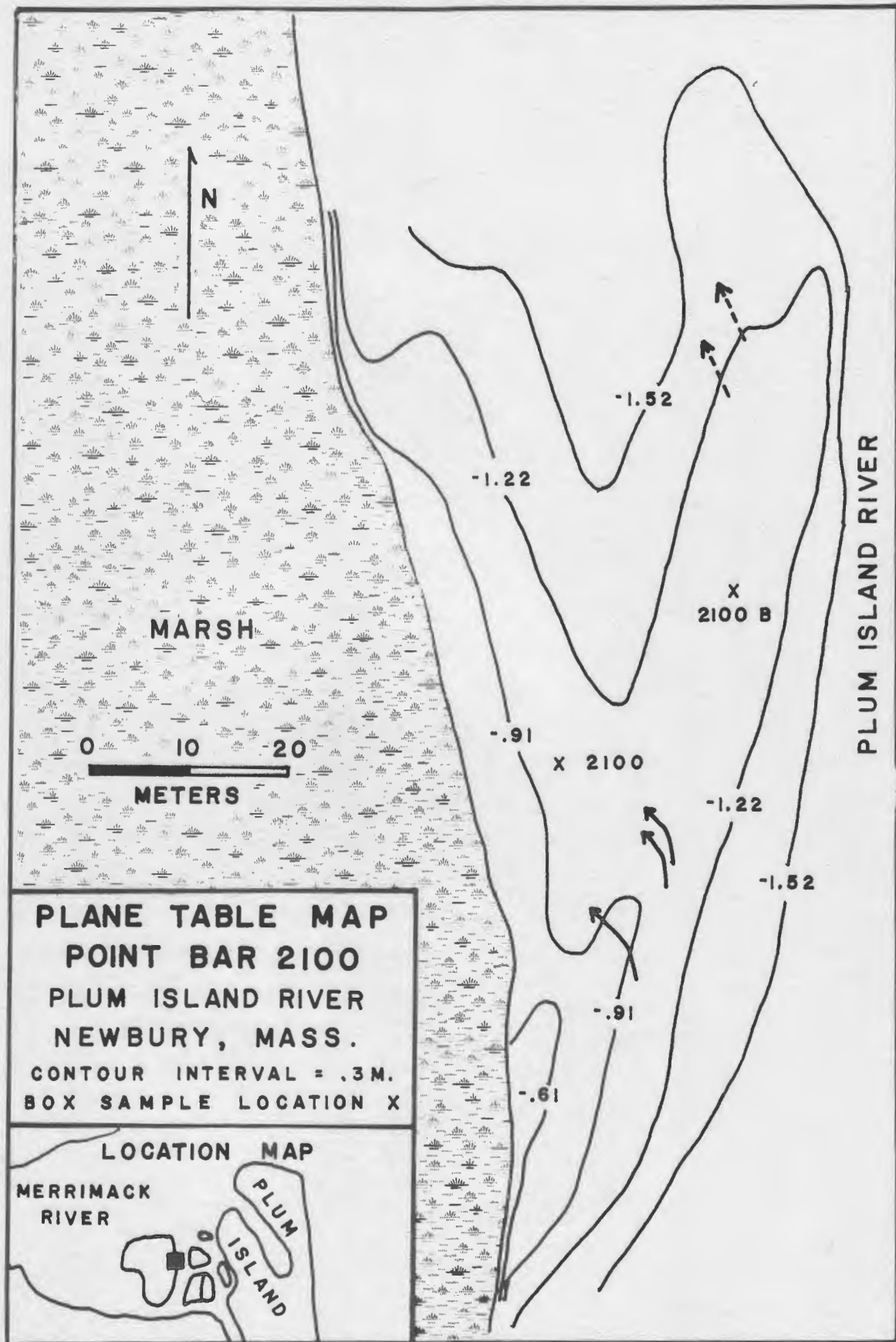


FIGURE 28-1

## STOP 28 - WOODBRIDGE ISLAND POINT BAR

Allan D. Hartwell

This point bar is similar to several in the smaller tidal channels in the northern Plum Island area. The dominant feature is a large northerly-trailing ebb spit which protects a muddy to sandy clam flat on the western side of the spit (see plane table map, Fig. 28-1). During flood tide, currents funnel south across the clam flat and plane off the top of the ebb spit, building a southeasterly migrating slip face which deposits low-angle crossbeds. In general, ebb currents appear to be stronger than flood currents across this point bar. As the tide level drops, ebb currents sweep across the crest of the spit, forming upper flow-regime planar beds on the leading edge of the spit. Behind the spit crest, scour-megaripples form as a result of a drop in flow-regime with increasing water depth (Fig. 28-2). Pronounced current lineation develops on top of the spit (illustrated in Fig. 28-3). This lineation shows a drastic change in orientation from parallel with trend of spit on the up-channel margin to almost perpendicular to the spit on the west. This change in orientation is probably related to early drainage of the clam flat as the tide level drops while water tends to pond to the southeast behind the spit. Thus, water flowing across the spit will take the shortest distance to the lower level clam flat behind, producing the perpendicular trend in lineation. Other sedimentary structures include worm burrows and clam burrows on the clam flat and herringbone crossbeds on the spit (Fig. 28-4).

---

Figure 28-1. Plane table map of point bar on eastern edge of Woodbridge Island, Merrimack River estuary, at low tide. Datum is mean high water. Dashed arrows near end of spit give orientation of the ebb-oriented megaripples shown in Figure 28-2. Solid, curved arrows near base of spit show surface lineation patterns formed by ebb currents (lineation shown in Figure 28-3).

Figure 28-2. View looking south-southeast, up the main trend of the Woodbridge Island point bar. Orientation of the scour-megaripples in the foreground is shown in Figure 28-1.

Figure 28-3. Lineations on surface of Woodbridge Island point bar formed by ebb currents (orientation given in Fig. 28-1). Note imbrication of shells and current shadows behind coarse fragments. Current was flowing from bottom to top of photograph.



FIGURE 28-2

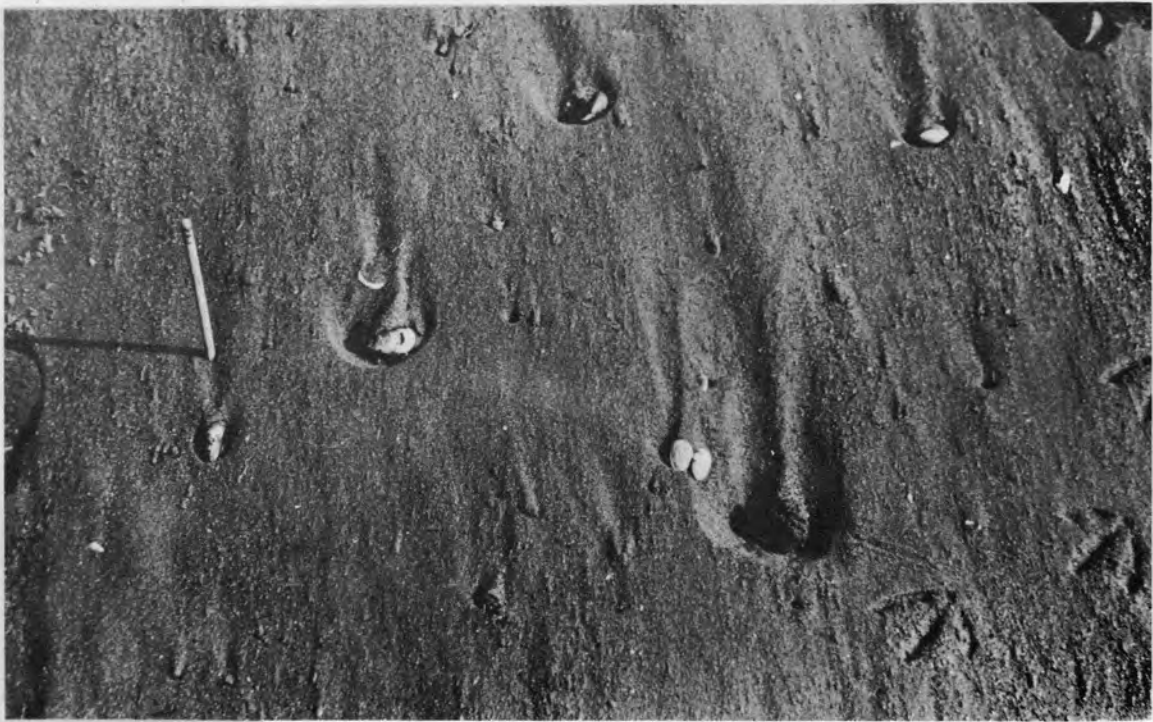


FIGURE 28-3

Figure 28-4. X-ray radiographs of sedimentary structures from point bar 2100 (Fig. 28-1).

A. (Sample 2100) Sandy clam flat with large Nereis virens burrow lined with brown oxidized layer. Mya arenaria in life position at bottom.

B. (Sample 2100-B) Herringbone crossbeds developed in the ebb spit. Upper portion of the sample shows flood crossbeds dipping about 20° S36E that overlie lower angle (10°) ebb crossbeds with an azimuth of N54W.

0  
5 cm



A



B

FIGURE 28-4

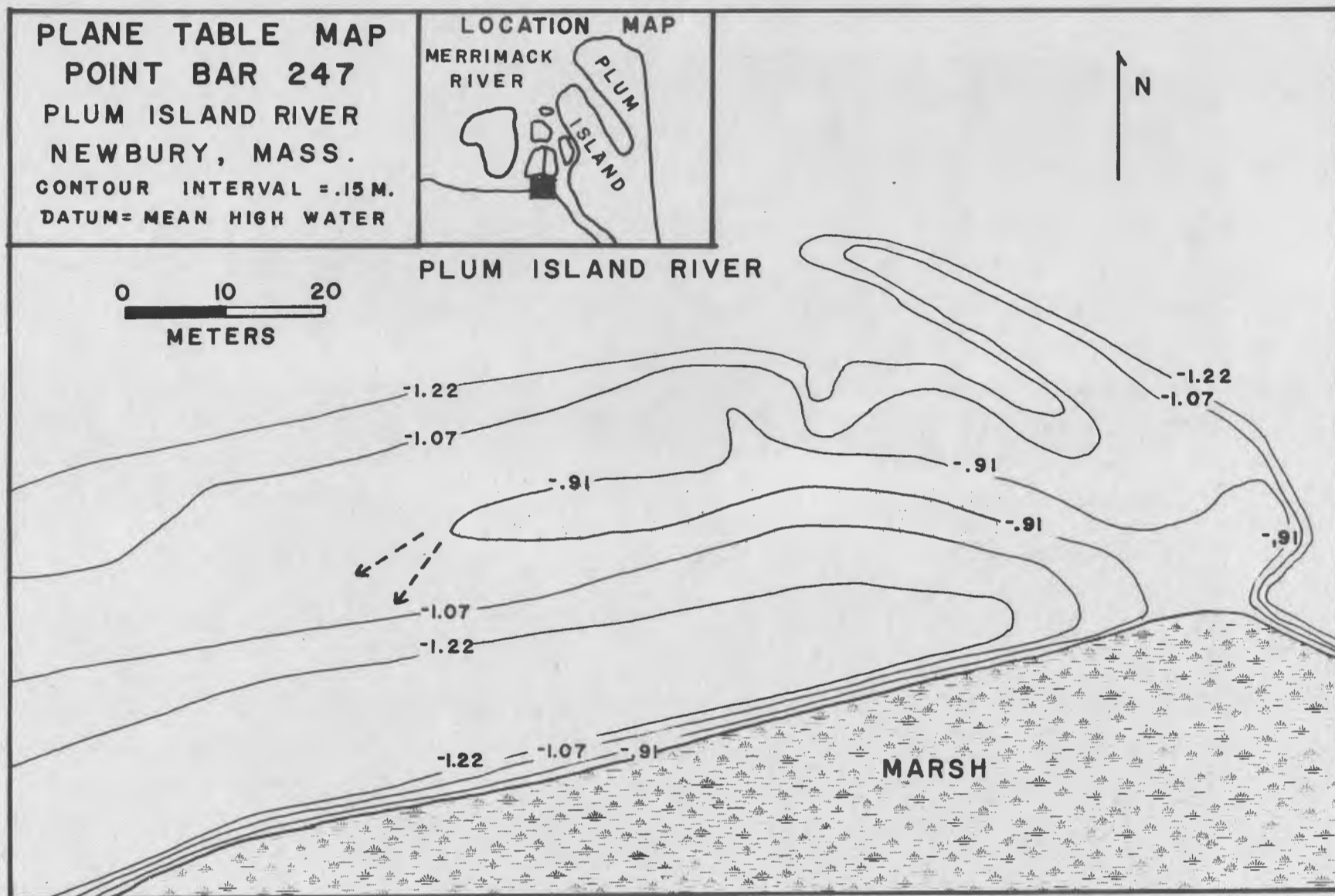


**FIGURE 29-1**

## STOP 29 - PLUM ISLAND RIVER POINT BAR

Allan D. Hartwell

This point bar is similar to the one described at Stop 28, but it shows more flood influence. The general morphology of the bar is dominated by a large ebb spit oriented toward the northwest (see plane table map, Fig. 29-1 and photograph, Fig. 29-2). At low tide the spit is generally covered with scour-megaripples, but a well-developed slip face is active on the eastern margin during flood tide. On the western end of the point bar, two current lineations (S38°W and S58°W) are evident at low tide. These represent different stages in the draining of the clam flat. Sedimentary structures include clam burrows and worm burrows on the flat, low-angle crossbeds on the ebb spit, and higher-angle planar crossbedding on the flood slip face. Note the distinct change in grain size, with coarsest sediments occurring on the spit and muddy sand occurring on the clam flat. The sand contains abundant quartz, gray to white feldspar, rock fragments, and some garnet, but yellow-orange feldspar is almost completely absent. This sand appears to be derived from a local deposit of glaciofluvial material that lies under the marsh south of the Plum Island Turnpike.

---

Figure 29-1. Plane table map of Plum Island River point bar at low tide. Dashed arrows show current lineation on western end of the point bar.



FIGURE 29-2

Figure 29-2. Plum Island River point bar, looking northwest  
across the eastern margin of the bar.

CONTRIBUTIONS

## HYDROGRAPHY OF THE MERRIMACK RIVER ESTUARY

Allan D. Hartwell

Miles O. Hayes

Abstract: The Merrimack River estuary is a classic example of a Type B estuary (Pritchard, 1955); it is usually well-stratified. If discharge is greater than about 3000 c.f.s., a sharp, slightly tilted boundary develops between the intruding salt-water mass and the overriding fresh-water. During the flood period, salt water from the ocean is deflected to the north, or right side, of the estuary, whereas the fresh river water ponds up on the south side over Joppa Flat. A significant amount of the sediment suspended in the fresh water, as well as some of the pollutants the river carries, is deposited on Joppa Flat.

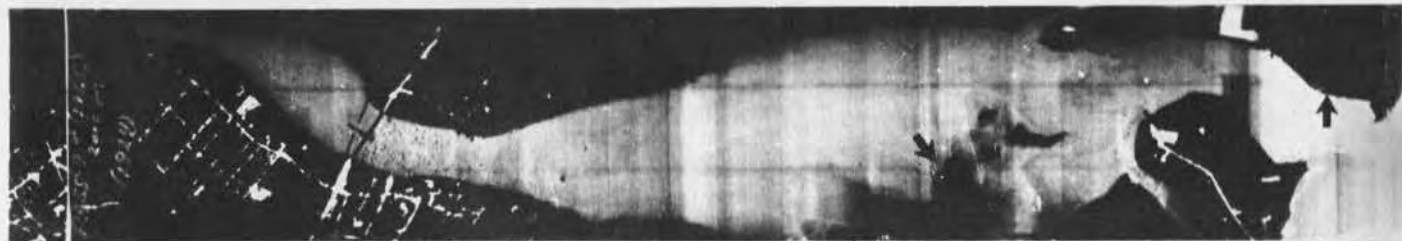
### INTRODUCTION

Hydrography of the Merrimack River estuary is of considerable interest from both the practical and scientific points of view. Inasmuch as the Merrimack River is highly polluted, the zones of maximum pollution within the estuary are determined by the circulation pattern. From a scientific standpoint, this estuary is a classic type B estuary of Pritchard (1955), which develops a sharp, slightly tilted boundary between the salt water wedge and surficial fresh water as the tide floods. The Coastal Research Group of the University of Massachusetts has made periodic studies of the circulation pattern of the estuary since the fall of 1965. A concentrated study in July of 1967 delineated the three-dimensional picture of circulation through a complete tidal cycle. Data collected by Hartwell in the summer of 1968 contrasted the effect of large and small freshwater runoff on the general circulation pattern of the estuary.

An excellent general summary of the hydrography of the Merrimack River estuary is given by Jerome and others (1965). The surface circulation pattern was clearly shown on infrared imagery maps reported by Wiesnet and Cotton (1967) (Figs. 1 and 2).



EBB



LOW



FLOOD



HIGH

FIGURE 1

The Merrimack River is the fourth largest river in New England after the Connecticut, Penobscot, and St. John. The drainage basin of the river occupies an area of 12,970 sq. km. (5,010 sq. mi.); the river descends 77.3 m. (254 ft.) at a generally uniform slope along its 186 km. (116 mi.) path from Franklin, N. H., to Plum Island. Average daily discharge is about 7,000 c.f.s., ranging from over 23,000 c.f.s. in the spring to about 1,700 c.f.s. in the fall. The lower 35.4 km. (22 mi.) of the channel are tidal, with a mean tidal range varying from 2.5 m. (8.2 ft.) at the mouth to 1.5 m. (5.1 ft.) at Haverhill. During mid-summer at least 12.9 km. (8 mi.) of the lower river is intruded by salt water, but this intrusion probably goes further upriver during periods of lower discharge.

---

Figure 1. Infrared imagery of the lower part of the Merrimack River estuary, from Plum Island to Newburyport. Upstream is to the left. For orientation, see jetties on the right of the upper diagram and the city of Newburyport on the lower left of the lower diagram.

(Ebb) Outgoing tide at 0335h, 29 Sept., 1966. Whole estuary is full of light-colored, warm, low-salinity water.

(Low) Low tide at 1922h, 28 Sept., 1966. Note uniform tone of the warm estuarine water throughout the entire length of the estuary.

(Flood) Incoming tide at 2205h, 28 Sept., 1966. Note the surface expression of the salt water (cold water) interface. Arrow on left points to leading nose of the salt water wedge.

(High) High tide at 0037h, 29 Sept., 1966. Note the spreading of warm (light-colored) estuarine water over the cold ocean water, especially in the area of Joppa Flat.

From Wiesnet and Cotton, 1967, Figure 2. Disregard arrows.



FIGURE 2

## SURFACE CIRCULATION PATTERN

The surface circulation of the Merrimack estuary is clearly delineated by infrared imagery obtained in August and September, 1966, by Don Wiesnet and John Cotton of the Water Resource Division, U. S. Geological Survey, Boston, Mass. Figures 1 and 2 show the imagery at ebb tide, low-water slack, flood tide, and high-water slack. The imagery shows that the estuary is filled with high-temperature, low-salinity water at low tide and that as the tide begins to flood, a wedge of cold salt water moves up the north side of the estuary over Joppa Flat. At high-water slack and early into the ebb period, the ponded fresh water on Joppa Flat streams toward the northeast over the main channel of the estuary such that at approximately mid-tide the whole surface of the estuary is covered with low-salinity river water.

## STRATIFICATION AND THREE-DIMENSIONAL CIRCULATION

In order to relate the three-dimensional circulation of the estuary to the surface pattern depicted by the infrared imagery (above), a detailed sampling program was undertaken on 7 and 8 July, 1967. A total of 34 sampling stations were established (at high tide). Each of these stations that were not uncovered were sampled at two-hour intervals through a complete tidal cycle. Samples were taken from the surface to the bottom at 1 m. (3 ft.) intervals. This was accomplished with four field crews in small boats that attempted to collect a 'simultaneous' sample over a time span of twenty minutes at the indicated two-hour intervals. The lower half of the estuary was sampled on 7 July, 1967, and the upper half sampled one hour later at each designated interval on 8 July, 1967.

---

Figure 2. Close-up of the flood-tide infrared imagery of Figure 1. Cold, highly saline ocean water on the right (dark) and warm, low salinity river water on the left (light).

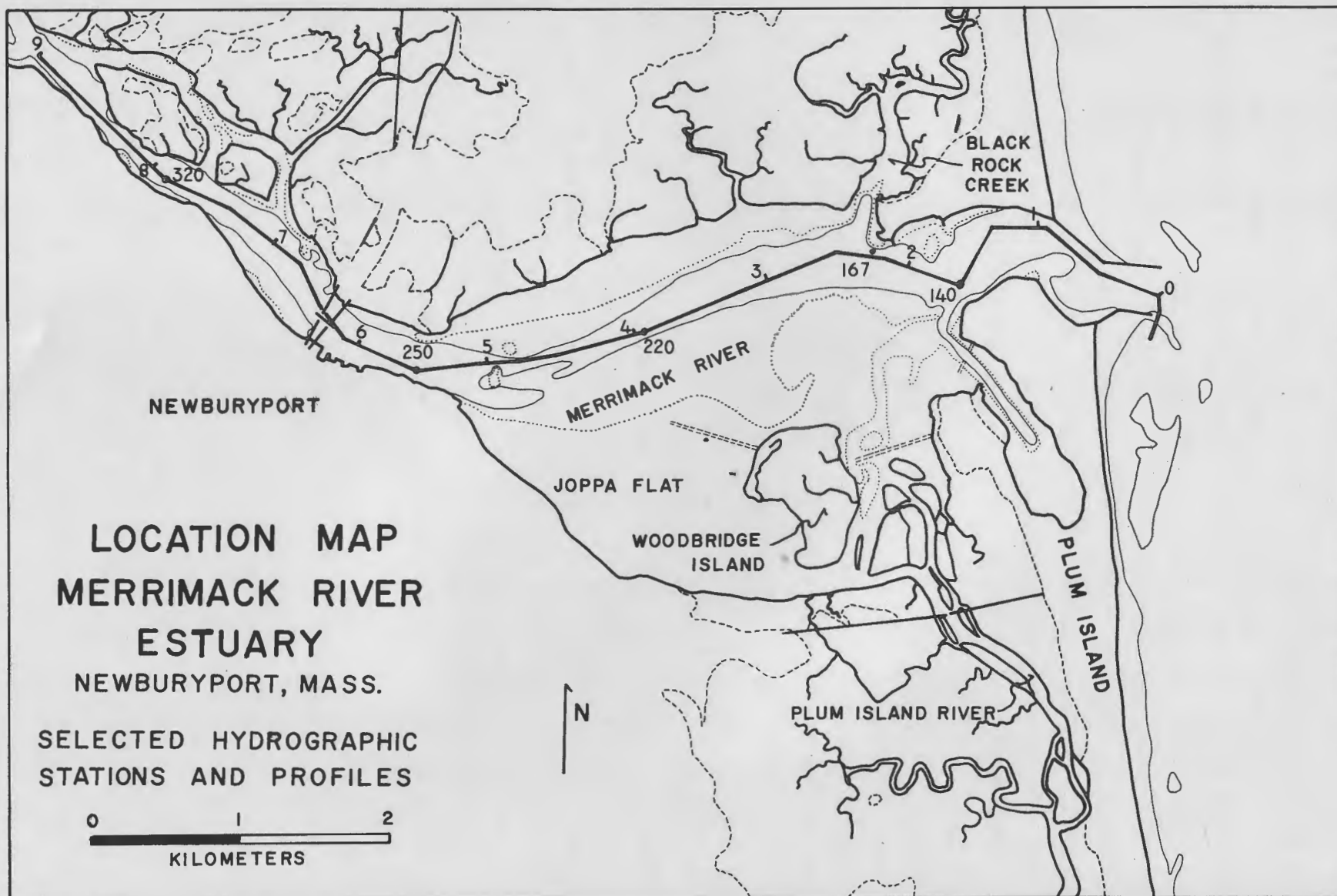


**FIGURE 3**

From this data it was possible to construct a vertical longitudinal cross-section depicting the circulation of the estuary from the mouth to 9 kilometers upstream (Figs. 3 and 4a, b).

The longitudinal channel section showing salinity through a complete tidal cycle on 7 to 8, July, 1967, clearly depicts the three-dimensional pattern of flow along the main channel of the estuary. This data was collected when the river discharge was nearly normal, about 6300 c.f.s. At low-water slack (Fig. 4a, b), most of the estuary was fresh water. During early flood the salt water at the mouth began to intrude upstream along the channel bottom. Two hours after low-water slack, the 5 ‰ isohaline had moved more than 3 kilometers upstream and some horizontal stratification had developed in the lower estuary. Four hours after low-water slack, the whole upper estuary had a well-developed horizontal stratification, whereas the lower estuary was almost entirely salt water. The fresh water-salt water interface was well-developed at high water slack; however, once the damming effect of the flood current was removed, the boundary moved rapidly seaward and stratification was destroyed. By low-water slack, nearly all of the salt water had been flushed out of the main channel.

The entire three-dimensional framework of salinity structure in the estuary at two hours before high-water slack is shown in Figure 5. This diagram indicates that the salt water-fresh water interface is slightly tilted toward the south; hence, the estuary falls into the Type B class of Pritchard (1955). The three-dimensional salinity structure of the estuary is shown further in the series of diagrams in Figure 6. Note the close agreement between the surface salinity data of Figure 6 and the

---

Figure 3. Location map for hydrographic stations and profiles in the Merrimack River estuary.

# MERRIMACK RIVER ESTUARY LONGITUDINAL CHANNEL SECTION SALINITY ‰

JULY 7-8, 1967

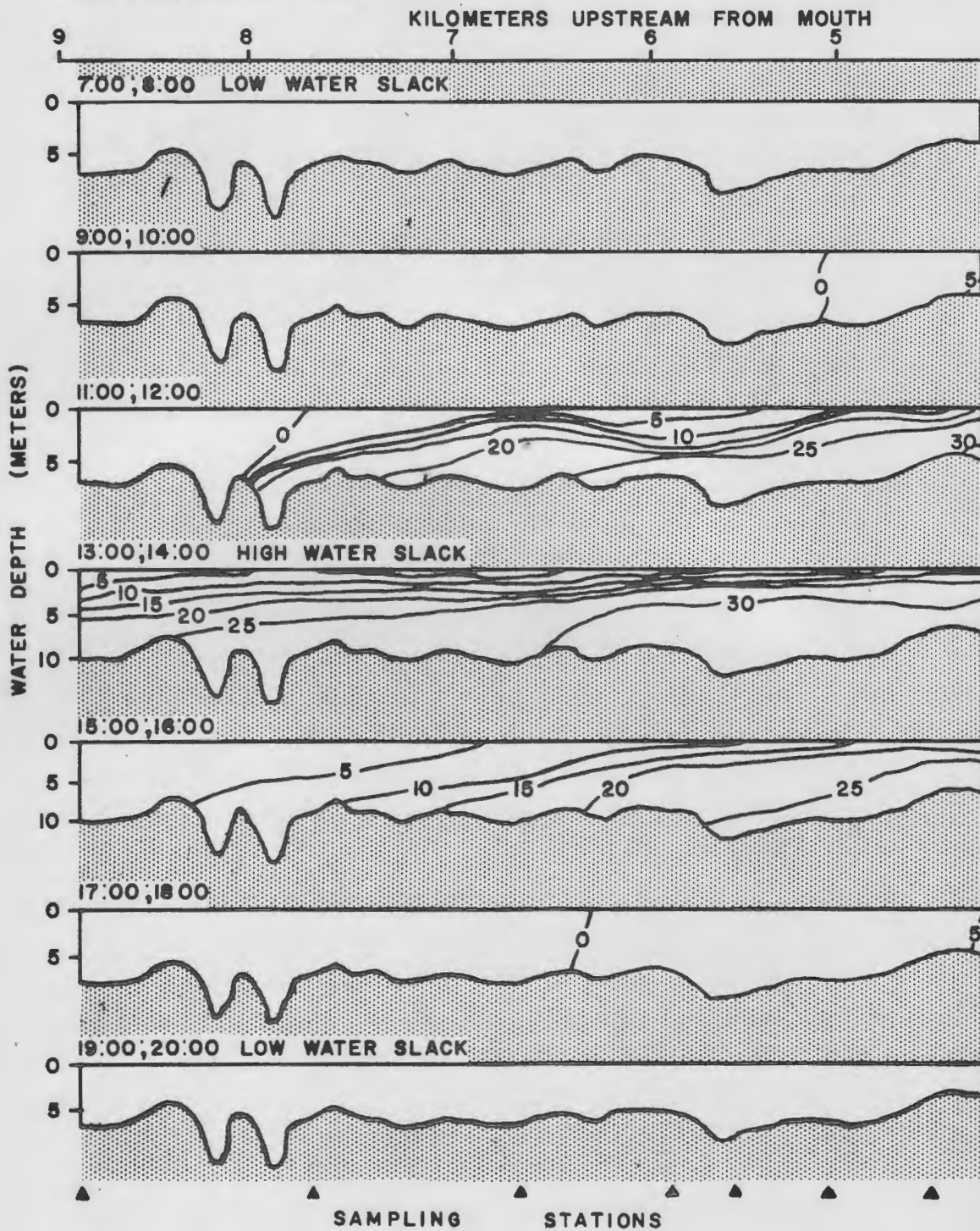


FIGURE 4A

# MERRIMACK RIVER ESTUARY LONGITUDINAL CHANNEL SECTION SALINITY ‰

JULY 7-8, 1967

KILOMETERS UPSTREAM FROM MOUTH

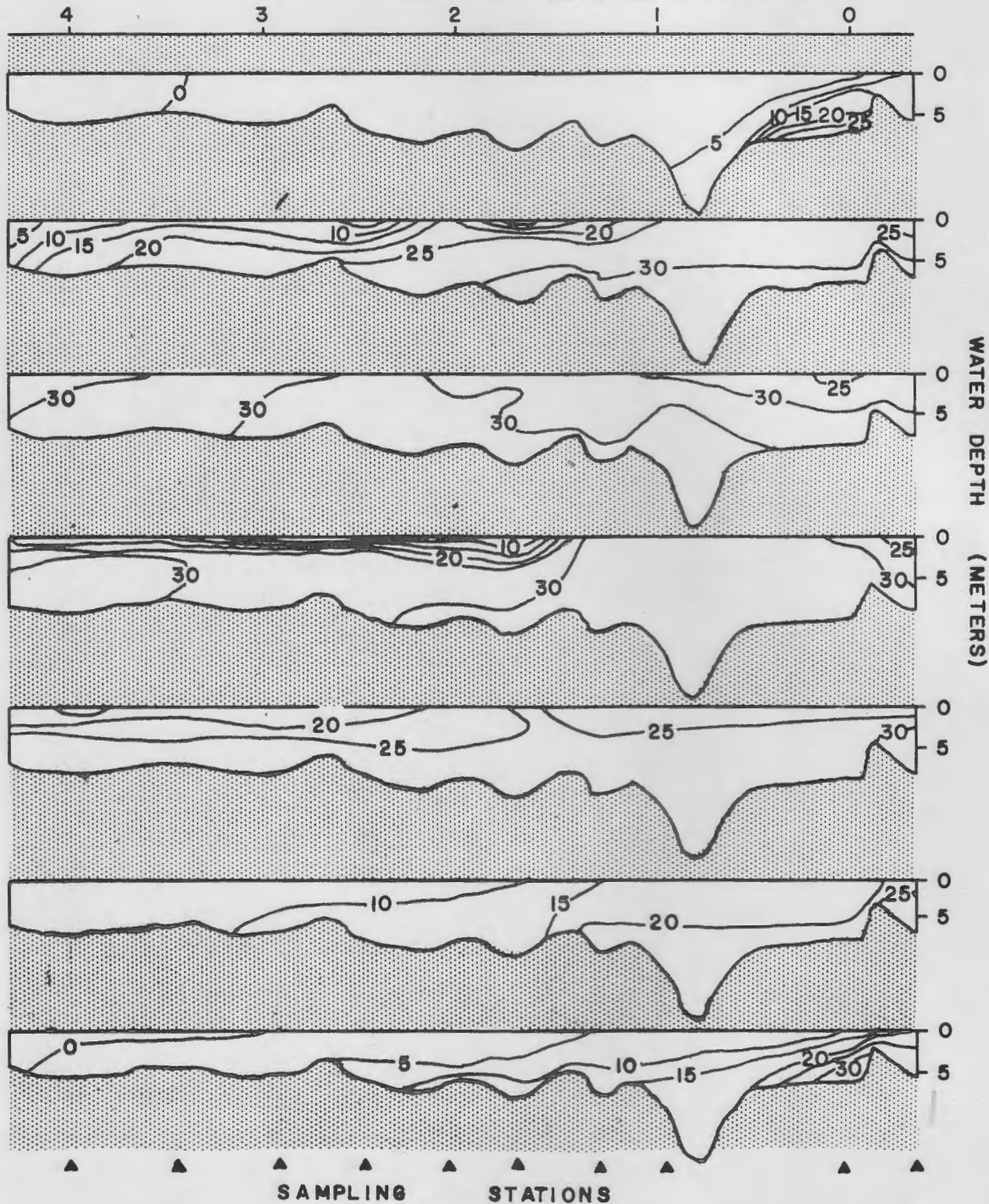


FIGURE 4B

Figure 4 a,b. Longitudinal cross-section of the main channel of the Merrimack River estuary showing vertical changes in salinity through a complete tidal cycle. The location of this section, which is along the middle of the main channel of the estuary, is shown in Figure 3.

# MERRIMACK RIVER ESTUARY NEWBURYPORT, MASS

2 HOURS BEFORE HIGH WATER SLACK  
JULY 7, 1967 11:00  
JULY 8, 1967 12:00

## SALINITY ‰

- 0-10 ‰ 
- 10-20 ‰ 
- 20-32 ‰ 

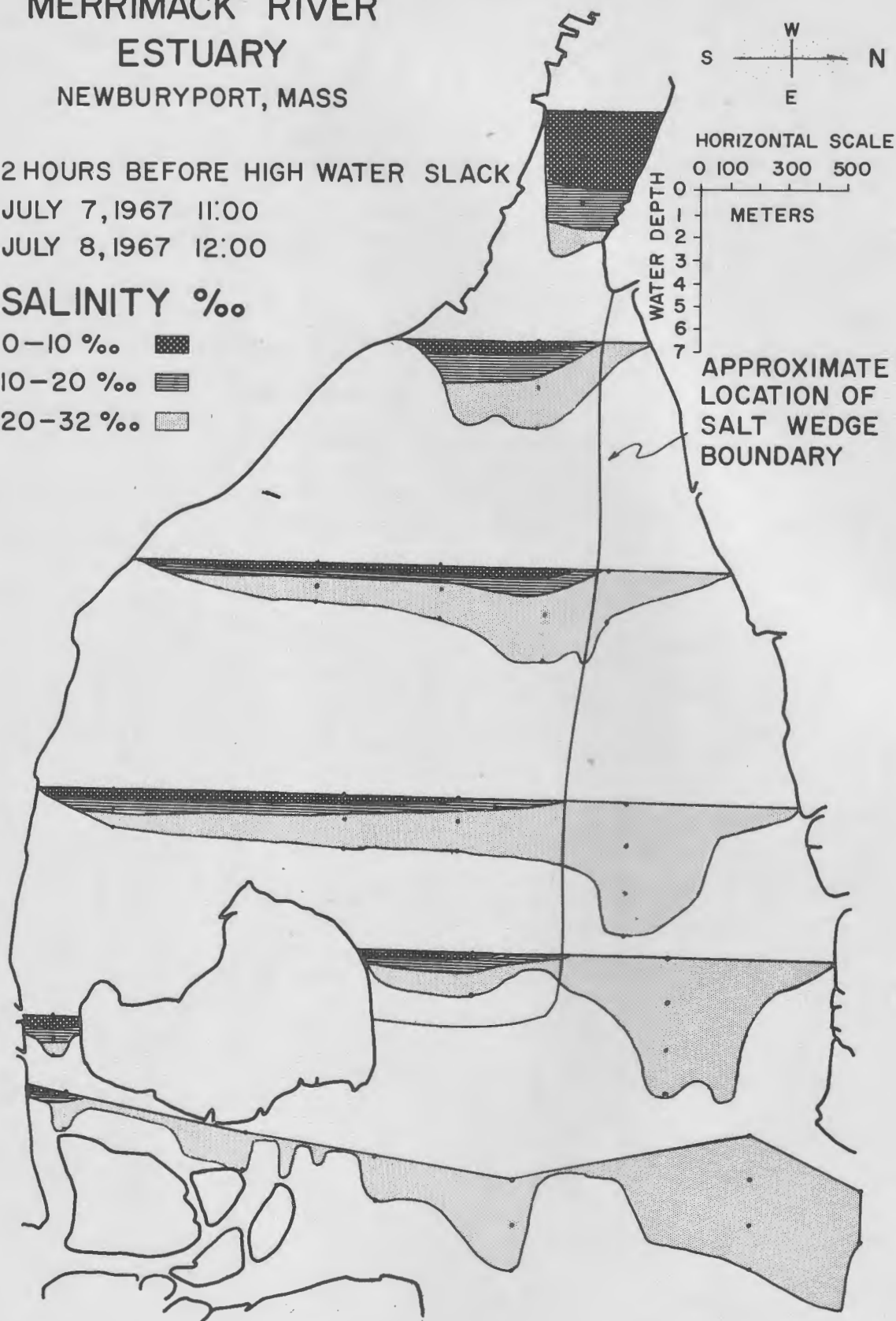


FIGURE 5

Figure 6. Variation of salinity with depth in the Merrimack River estuary through a complete tidal cycle. Data collected on 7 and 8 July, 1967.

- A. Low-water slack. Note the complete absence, at any depth, of saline water in the estuary.
- B. Flood, two hours after low-water slack. Compare the surface water salinity pattern in this diagram with the infrared imagery of Figure 2. Note the intrusion of the salt wedge up the main channel in the northeast section of the estuary.
- C. Flood, two hours before high-water slack. At this stage, the salt wedge has completely intruded the lower half of the estuary. Compare this data with Figure 5; both diagrams are based on the same sampling period.
- D. High-water slack. Note that at this stage, the fresh water had already begun to drain over the surface of the estuary, even though the lower portions of the water column were still completely marine.
- E. Ebb, four hours after high-water slack. At this stage, the stratification was almost completely destroyed and most of the marine water had been pushed out of the estuary.



# FLOOD

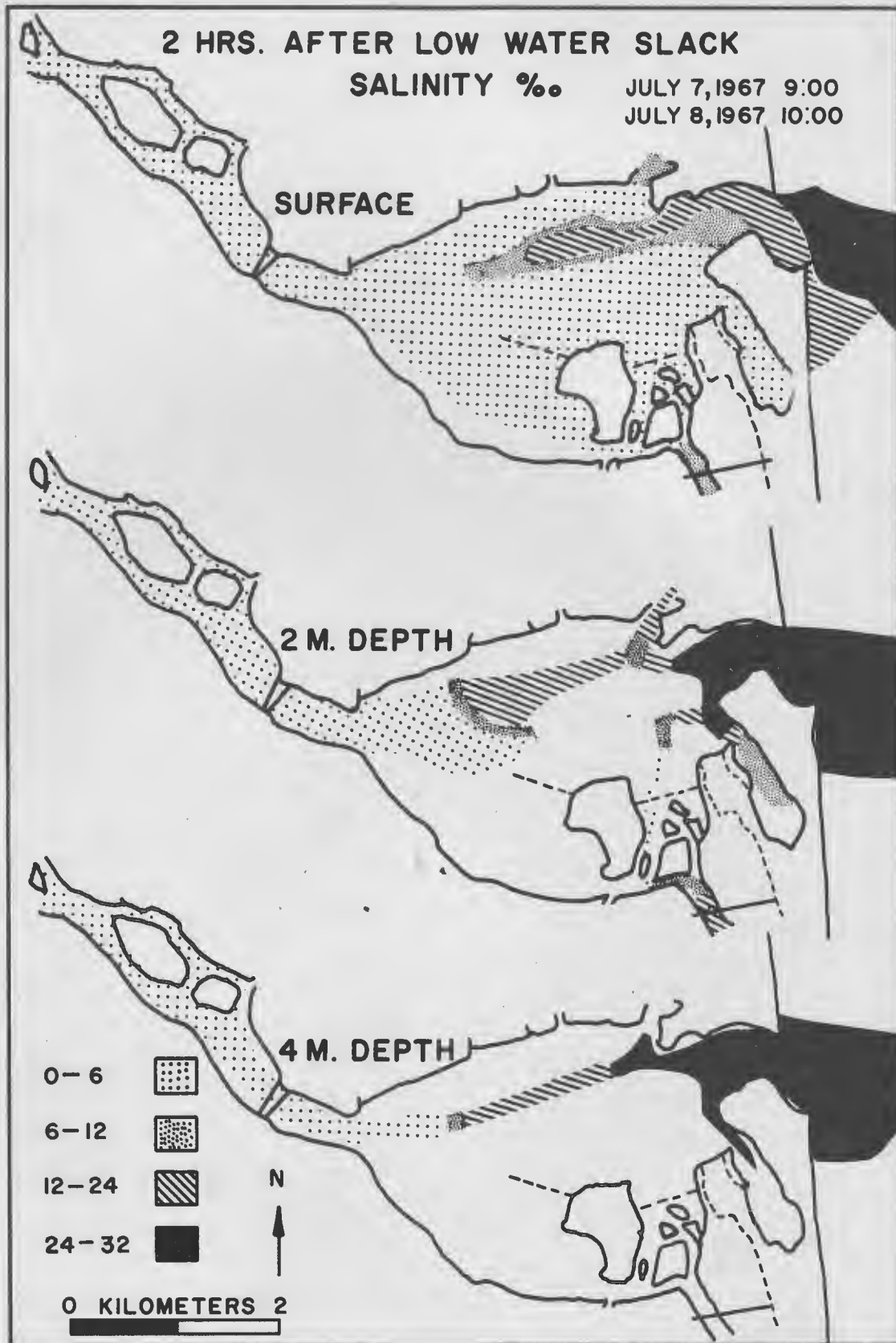


FIGURE 6B

# FLOOD

2 HRS. BEFORE HIGH WATER SLACK

SALINITY ‰

JULY 7, 1967 11:00

JULY 8, 1967 12:00

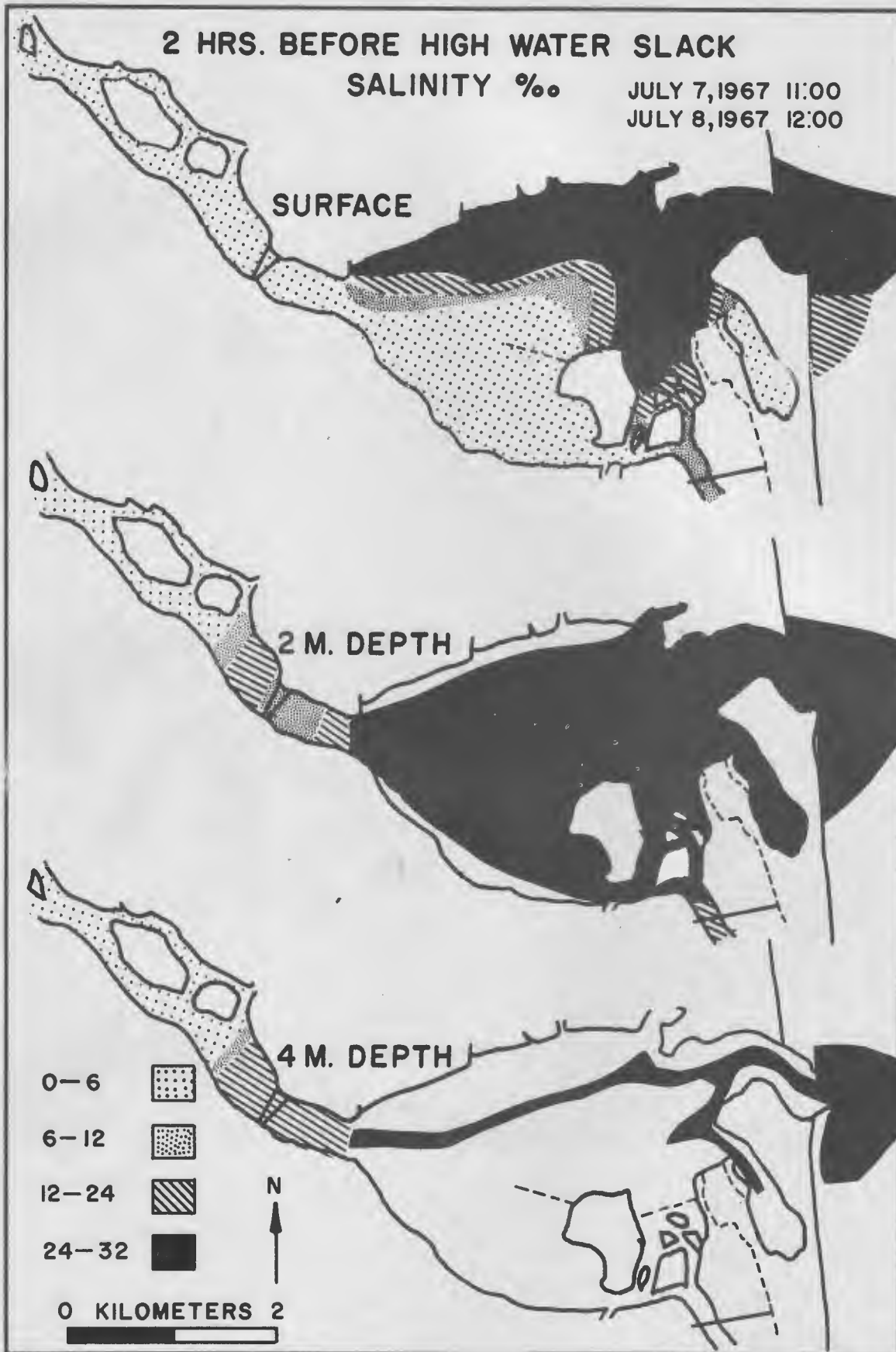


FIGURE 6C

# HIGH WATER SLACK

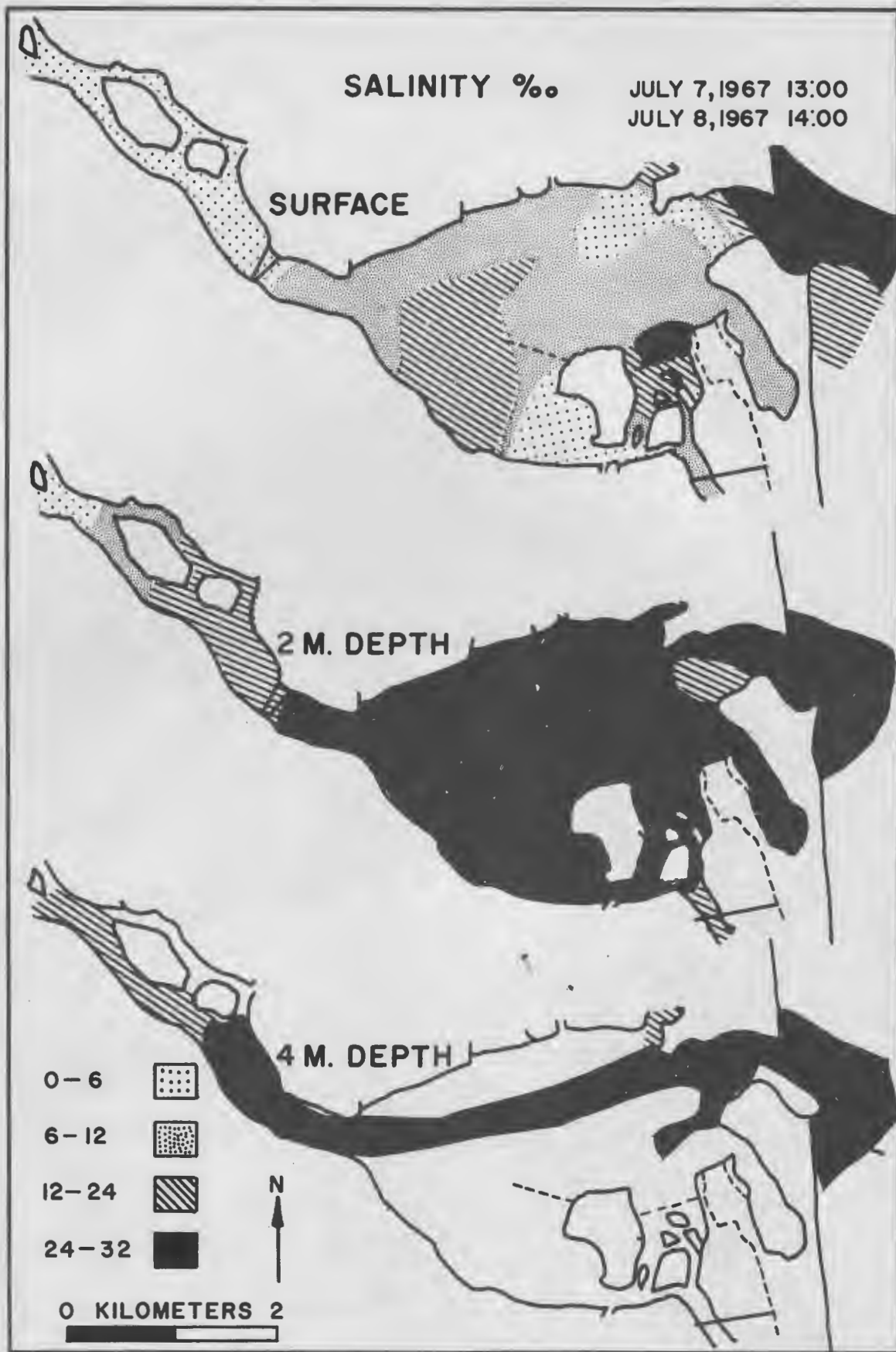


FIGURE 6D

EBB

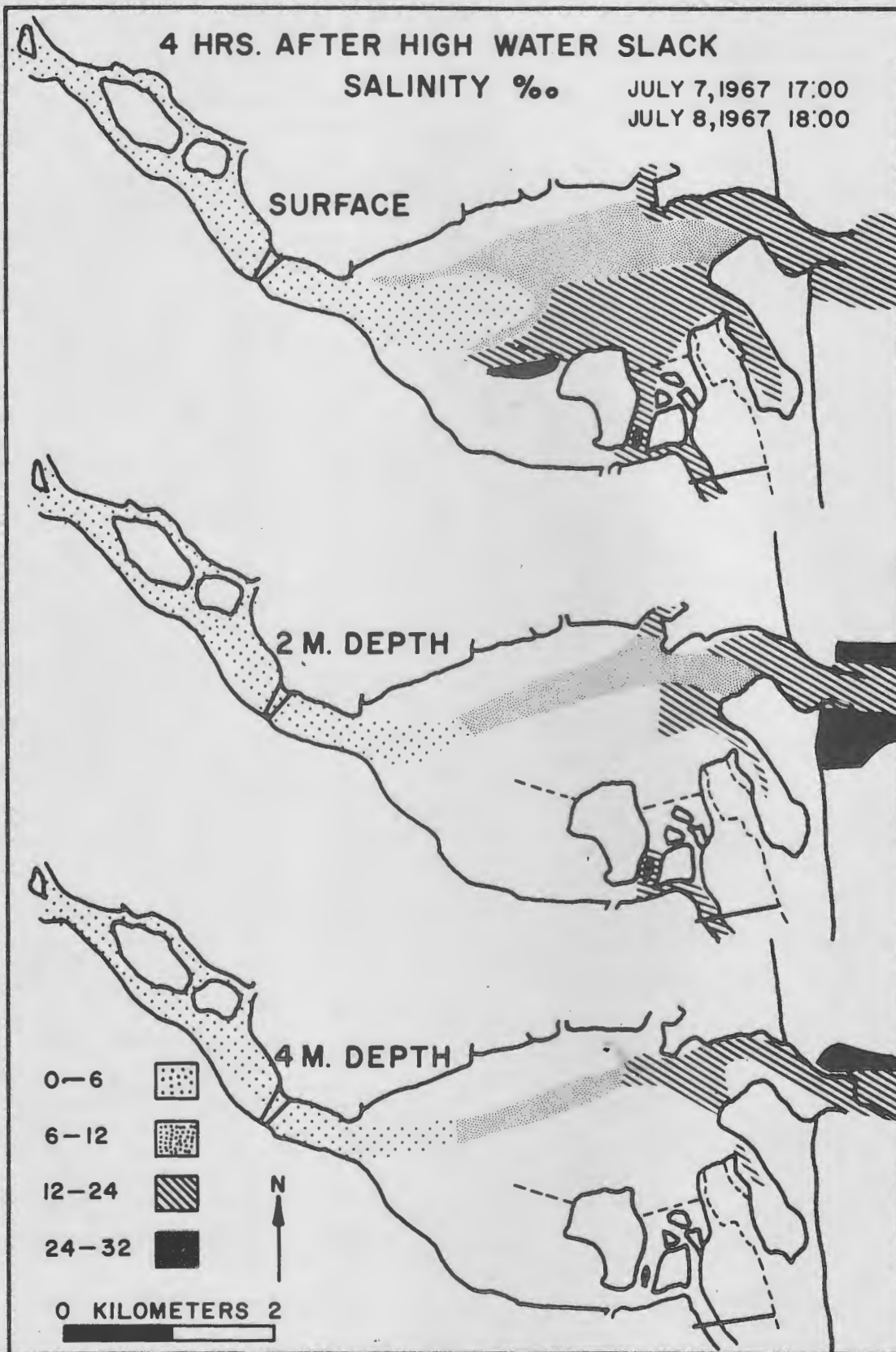


FIGURE 6E

# MERRIMACK RIVER ESTUARY LONGITUDINAL CHANNEL SECTION SALINITY ‰

AUG. 26, 1968

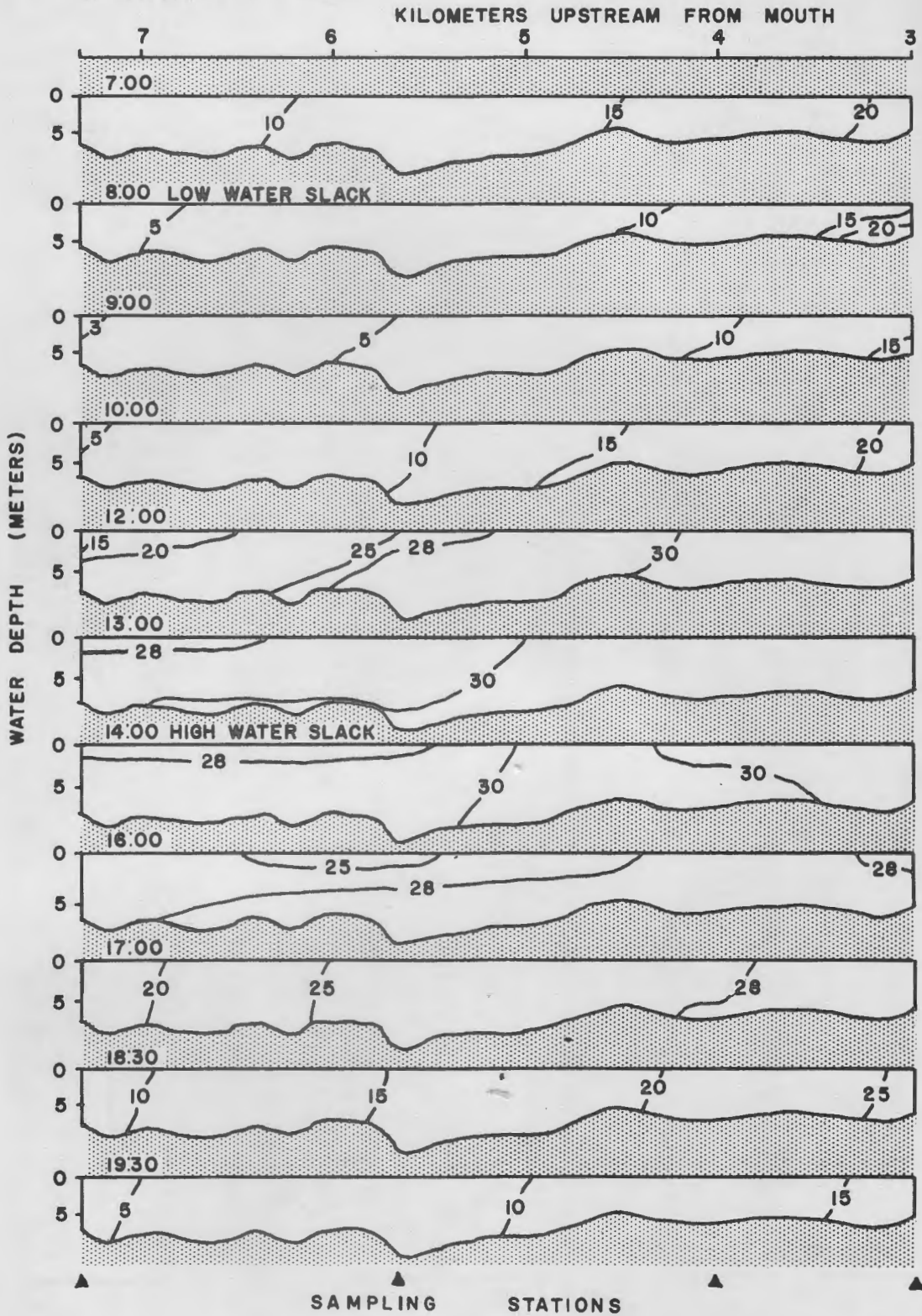


FIGURE 7A

# MERRIMACK RIVER ESTUARY LONGITUDINAL CHANNEL SECTION TEMPERATURE °C

AUG. 26, 1968

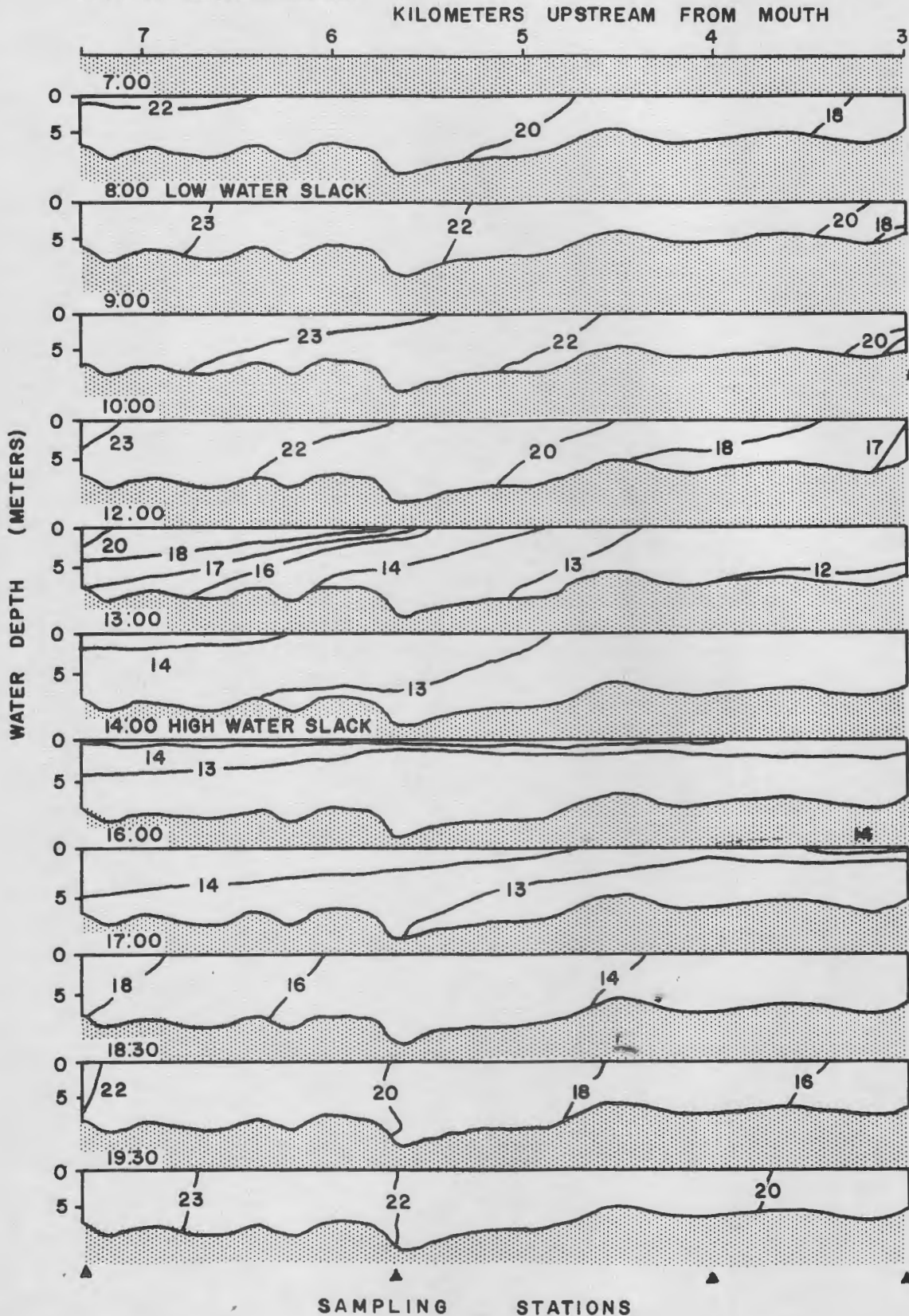


FIGURE 7B

Figure 7 a,b. Vertical variation of salinity (A) and of temperature (B) along the central portion of the Merrimack River estuary main channel through a complete tidal cycle. These samples were collected during a period of extremely low discharge (1900 c.f.s.). Note the lack of well-developed stratification of the type that occurred in July, 1967 (Fig. 4 a,b).

infrared imagery data of Figures 1 and 2. The high-salinity water of Figure 6 correlates with the cold-water in Figures 1 and 2. A significant difference between the two sets of data is that the three-dimensional salinity data shows that the entire southern portion of the estuary is filled with salt water at two meters depth and deeper during the interval between about mid-tide and high-water slack. Thus, although fresh water stands over Joppa Flat in the latter stages of flood and at high water slack, a wedge of salt water moves under this fresh-water mass. Current data show that near high-water slack these two masses flow in opposite directions.

The occurrence of a modest dry spell during late summer of 1968 allowed a comparison of the July, 1967 data with a period of low discharge. On 26 August 1968 data was collected through the tidal cycle at five stations along the main channel. On the date of sampling, river discharge was far below normal (about 1900 c.f.s.). During this tidal cycle, only slight stratification developed (Fig. 7 a,b). The isohaline boundaries determined during this survey are nearly vertical as compared with the nearly horizontal isohalines of Figure 4. From this data, it is evident that there is a critical runoff value at some point between 1900 c.f.s. and 6300 c.f.s. at which the stratification in the estuary begins to improve.

Details of thirty-minute changes in tide level, current velocity, salinity, temperature and suspended sediments through the entire vertical column at a single station during a complete tidal cycle are plotted in Figure 8. This diagram shows that during flood tide, salinity rises sharply while temperature and

---

Figure 8. Changes in current velocity, salinity, temperature, and suspended sediments through a complete tidal cycle at a single anchor station (2.4 km. upstream from the mouth) in the main channel of the Merrimack River estuary.

# MERRIMACK RIVER ESTUARY AUGUST 25, 1968

ANCHOR STATION 2.4 KM UPSTREAM OF MOUTH

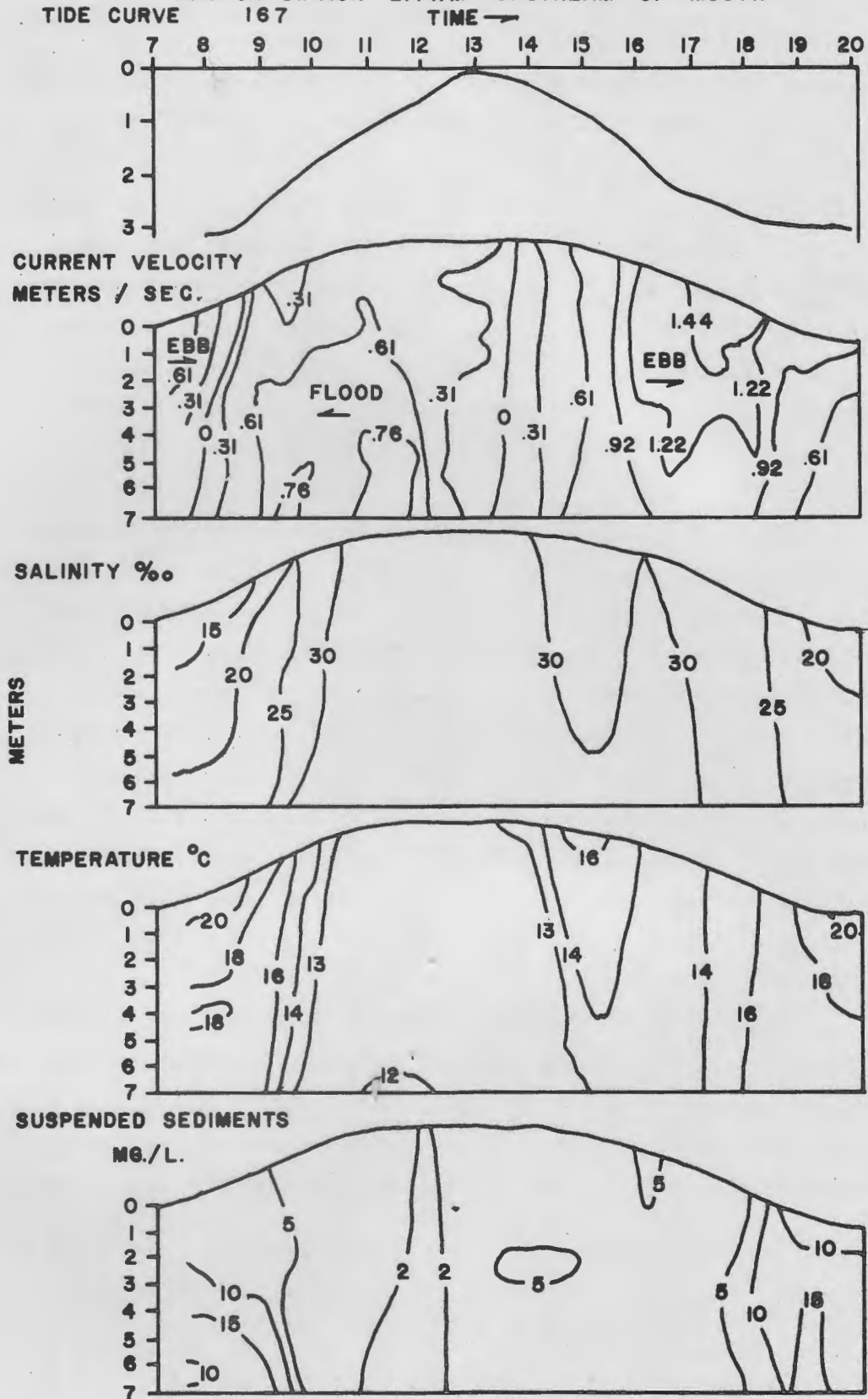


FIGURE 8

suspended sediments decrease to minimum values about one hour before high- slack. Changes in temperature and salinity during the ebb period are complicated at the sampling station because of the influence of a small tributary channel to the north. Current velocity data reveals that peak flood velocities occur in pulses along the bottom whereas maximum ebb flow is in the upper part of the water column. Time-velocity asymmetry of tidal currents is also evident in that maximum flood velocities occur two-thirds of the way through the flood period and maximum ebb velocities occur three-quarters of the way through the ebb period. Low- and high-water slack generally occur from 30 to 45 minutes later than their respective minimum and maximum points on the tide curve at this one particular location.

Figure 9 a,b shows current velocity profiles for four stations along the length of the estuary. In general, maximum flood velocities occur near the bottom, whereas maximum ebb velocities, which are frequently twice as fast as the flood velocities, occur near the surface.

Suspended sediment samples collected in late August, 1968, contain concentrations up to 19 mg/liter in the fresh river water, whereas the ocean water contains less than 3 mg/liter. Data on suspended load, measured by the Geological Survey at Lowell, Massachusetts., during 1967, ranged from an average of 2860 tons/day in April to 46 tons/day in September (Water Resources Data, U.S.G.S., 1967). In view of the estuarine circulation pattern, it is probable that a significant quantity of this sediment load is deposited on Joppa Flat. In recent years, rapid shoaling of the channel south of Woodbridge Island has been observed. Spartina alterniflora has been accreting over this accumulating muddy sediment. Much of this sediment appears to be pollutants from the river and possibly effluent from the Newburyport Sewage Plant.

# MERRIMACK RIVER ESTUARY — CURRENT VELOCITY PROFILES

STATION:	320	250	220	140
KILOMETERS UPSTREAM	7.7	5.6	3.9	1.7
DATE	JUNE 24, 1967	JUNE 24, 1967	JUNE 27, 1967	JUNE 23, 1967

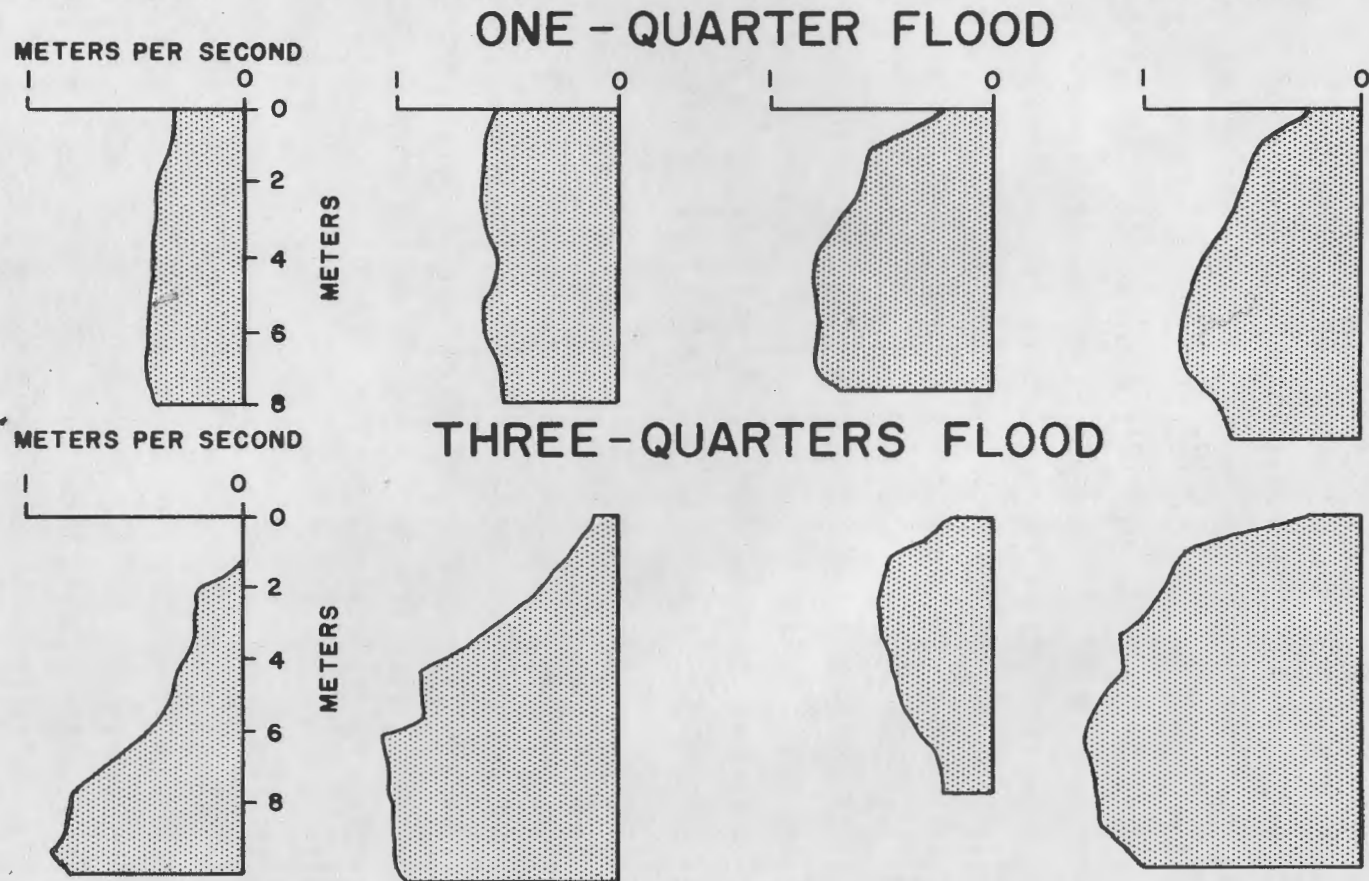


FIGURE 9A

# MERRIMACK RIVER ESTUARY — CURRENT VELOCITY PROFILES

STATION: 320  
 KILOMETERS 7.7  
 UPSTREAM

250  
 5.6

220  
 3.9

140  
 1.7

DATE JUNE 24, 1967

JUNE 24, 1967

JUNE 27, 1967

JUNE 23, 1967

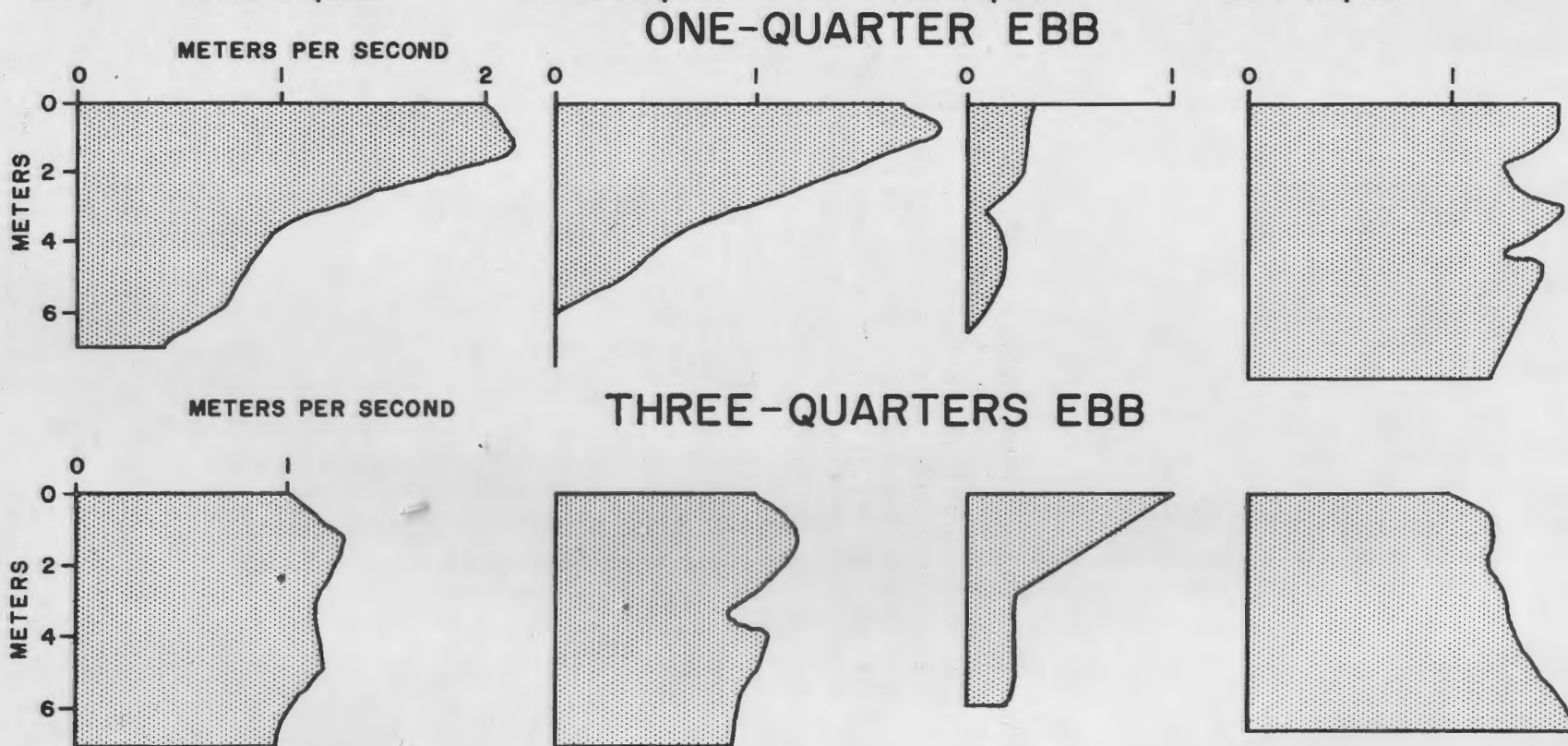


FIGURE 9B

Figure 9 a,b. Current velocity profiles through a complete tidal cycle at four stations in the main channel of the Merrimack River estuary. Note that maximum flood velocities generally occur near the bottom, whereas maximum ebb velocities, which sometimes double maximum flood velocities, occur near the top of the water column.

## SUMMARY

Data on infrared imagery (Wiesnet and Cotton, 1967) and from a three-dimensional survey of the water structure of the estuary, conducted in July, 1967, indicate that the Merrimack River estuary is a Type B estuary in the classification scheme of Pritchard. During periods of normal and high runoffs, the estuary is well-stratified; however, when the discharge drops to around 3000 c.f.s., the stratification disappears and the estuary becomes partially mixed. Ebb currents are generally stronger than flood currents in the estuary, sometimes attaining velocities greater than 1.5 m./sec. (5 ft./sec.). In general, maximum ebb velocities are concentrated in the upper portion of the water column and maximum flood velocities in the lower portions. Suspended sediment loads up to 19 mg/liter are carried by the river water, whereas the ocean water averages less than 3 mg/liter. The general circulation pattern of the estuary plays a primary role in the distribution of pollutants within the estuary system.

## STORMS AS MODIFYING AGENTS IN THE COASTAL ENVIRONMENT

Miles O. Hayes

Jon C. Boothroyd

Abstract: Northeasterly storms play a dominant role in the generation of cycles of erosion and deposition on the beaches of New Hampshire and northeastern Massachusetts. Measurement of bimonthly, and often closer-spaced, beach profiles at 8 stations from September, 1965, to April, 1969, revealed the following stages of low-tide beach morphology relative to storm occurrences:

- (1) Early post-storm (up to 3 or 4 days after storm) - Profile is flat to concave and beach surface is generally smooth and uniformly medium grained. Severest storms leave erosional dune scarps.
- (2) Early accretion (usually 2 days to 6 weeks after storm) - Small berms, beach cusps, and ridge-and-runnel systems are quick to form.
- (3) Late accretion, or maturity (6 weeks or more after storm) - Landward-migrating ridges weld onto the backbeach to form broad, convex berms. On some beaches, welding does not occur and gigantic ridges (up to 4 feet in height) lie between the backbeach and the low-tide terrace.

No stage is unique to any particular season and the cycle is frequently interrupted by recurring storms.

During the period of observation, over 20 moderate to severe northeasters affected the study area. The role of these storms as geological agents was controlled by (1) size and intensity of storm; (2) speed of storm movement; (3) tidal phase (i.e., spring or neap tide); (4) path of storm with respect to beach; and (5) time interval between storms.

## INTRODUCTION

The importance of coastal storms in shoreline processes is now widely recognized (Blumenstock and others, 1961; Stoddart, 1962; Hayes, 1967). Observations of the effects of over 20 northeasterly storms during the past four years indicate that these storms are the dominant factor controlling cycles of erosion and deposition of the sand beaches of northern New England. The "northeaster", which develops as a low-pressure center over the southwestern or southeastern U.S. and swings in a northeasterly course along the Atlantic coast, is the most important storm affecting the northern New England coast. Tracks of some of the major storms that occurred during the interval between 7 August, 1966 and 29 May, 1967 are shown in Figure 1. Because of the counterclockwise rotation of winds around these low-pressure centers, strong northeasterly winds blow against the northern New England coast as the storm center swings over the continental shelf east of southern New England. During the span of our observations, September, 1965 to April, 1969, no major hurricanes have passed through the area. Figure 1 shows the track of Hurricane Faith in late August, 1967. This hurricane generated large, long-period waves which had only a minor erosional effect on the northern New England coast.

## THE BEACH PROFILE

The measurement of over 600 beach profiles at 8 permanent beach profiling localities in northeastern Massachusetts and New Hampshire reveal a consistent recurrence of three basic beach profiles: (a) early post-storm (up to three or four days after storm); (b) early accretion (usually two days to six weeks after storm); and (c) late accretion, or maturity (six weeks or more after storm)

---

Figure 1. Tracks of major storm centers for the period 27 August, 1966, to 29 May, 1967. The most effective storms occurring during this interval were the storms labeled 25 January and 21 May. The track of Hurricane Faith is the easternmost track.

# TRACKS OF MAJOR STORMS

27 AUG 1966 - 29 MAY 1967

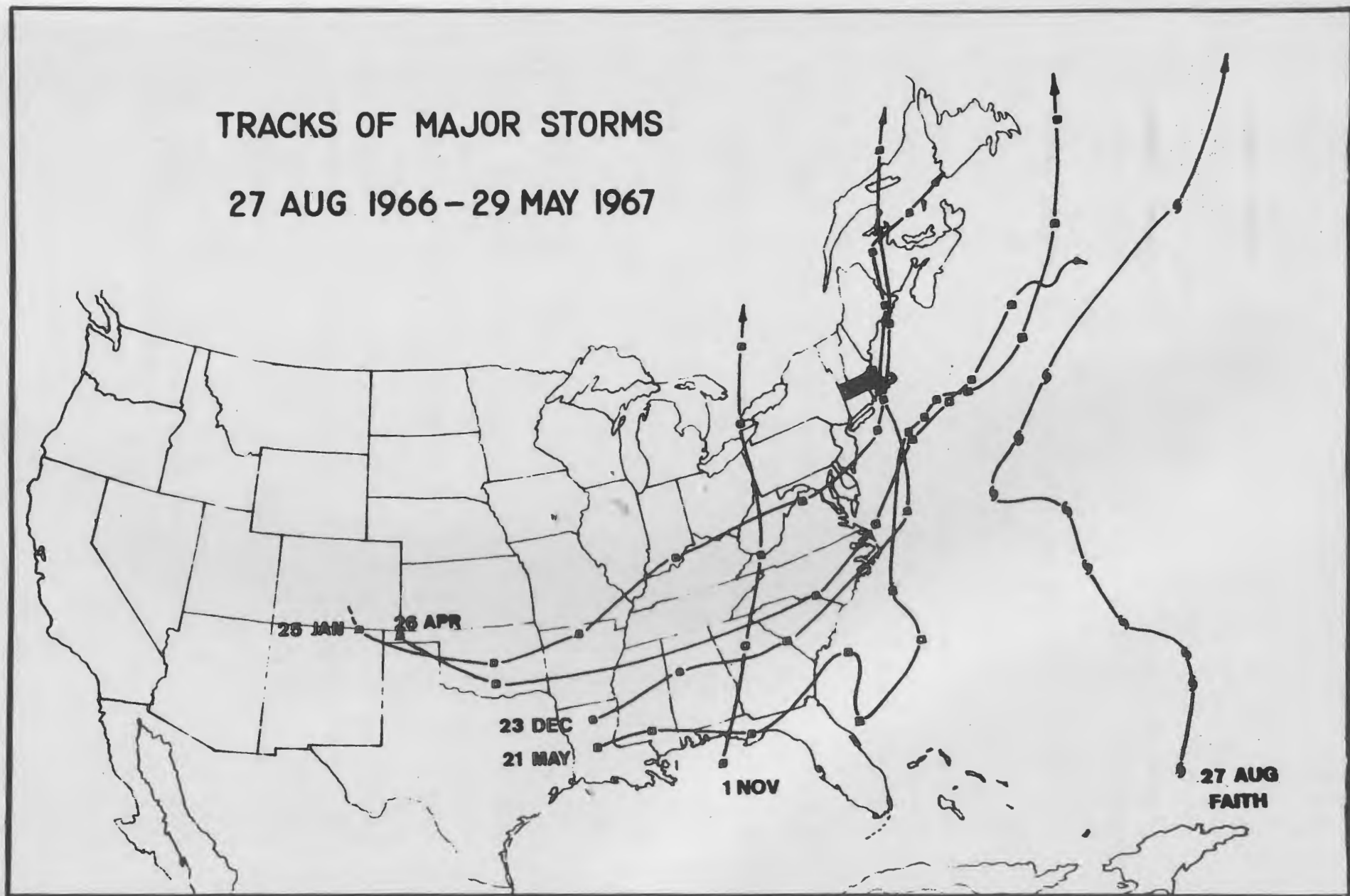


FIGURE 1

The early post-storm profile is flat to concave-upward and the beach surface is generally smooth and uniformly medium grained. The most severe storms leave erosional dune scarps. An example of such a profile is shown in Figure 2, which was taken on the day following the major northeasterly storm of 25-26 May, 1967. Two views of the beach profile cut by that storm are shown in Figure 3.

Typically, the constructional beach profile (Fig. 4) consists of a ridge-and-runnel system, sometimes accompanied by a small, incipient berm. The ridge grows in size through the constructional period and will eventually weld to the backbeach if the interval between storms is long enough. This cycle of beach accretion is further illustrated in the descriptions for Stops 4 and 19 (this guidebook).

After welding of the ridge, the beach continues to accrete on the beach face, forming a broad depositional berm that is convex-upward. This is the mature profile. The profile for 10 September, 1967, in Figure 5 is a typical example of such a profile. During the development of the mature profile, beach cusps are very common along the beach face. Our observations indicate that at least 90 percent of the cusps we have observed were formed during the constructional phase of beach development and are, hence, depositional features.

Therefore, the cycle of erosion and deposition of the sand beaches of Mass. and N.H. is a cycle related directly to storm activity. Although storms are most common during the months of December to March, no single erosional or accretional stage is unique to any particular season. The cycle is frequently interrupted by recurring storms.

There is no distinct "summer beach" or "winter beach". The profiles on Figure 5 show that summer beach profiles can be either of the extreme end members of the erosional-accretional cycle on northern New England beaches. Figure 6 illustrates the rapid rate with which sediment can accumulate on the beach during the winter. In a period of only 18 days,

---

Figure 2. A typical post-storm beach profile on Plum Island (Profile PLC). This profile was cut by the major northeaster of 25 to 26 May, 1967. Profile measured on 27 May.

# POST-STORM BEACH PROFILE

STATION PLC, PLUM ISLAND  
NEWBURY, MASS.

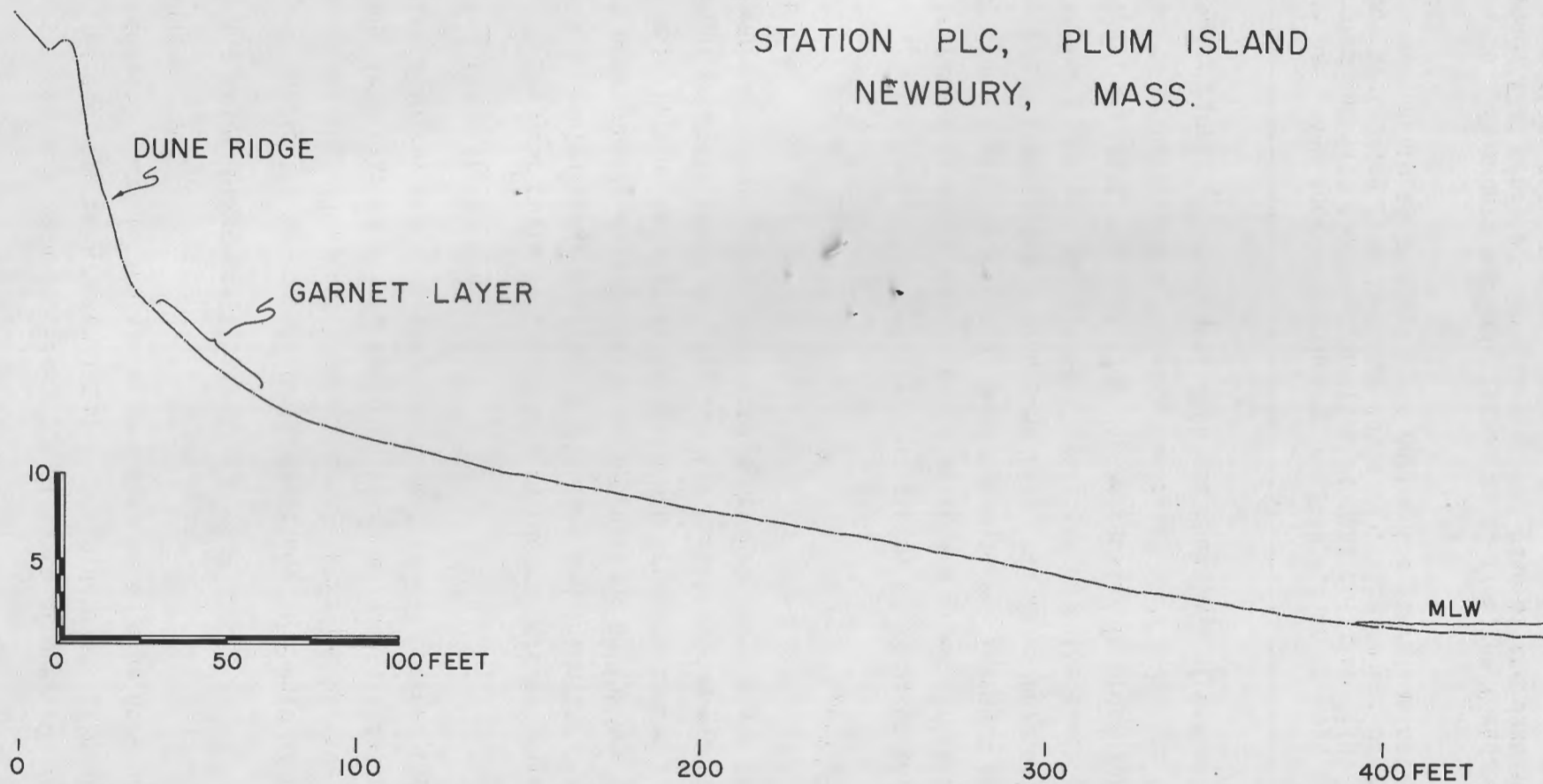


FIGURE 2

the high-tide mark advanced seaward a distance of over 100 feet, and a large, welded neap berm accumulated in the middle of the beach profile. This sediment accumulation was eroded away by a large northeaster of 27-28 January, 1967.

#### IMPORTANT STORM CHARACTERISTICS

During the period of our observations, the role of northeasterly storms as geological agents appears to be controlled by five factors-- size and intensity of storm, speed of storm movement, tidal phase, path of storm with respect to beach, and time interval between storms.

##### Size and Intensity of Storm

The most obviously important characteristic of a storm with respect to geological processes is its size and intensity. Northeasterly storms occasionally attain hurricane proportions on the New England coast. Northeasterly wind velocities of 50-60 mph are very common. These storms sometimes generate storm surges, but the surges seldom exceed 3 feet. An example of a very large and intense northeasterly storm is shown in Figure 7.

##### Speed of Storm Movement

Regardless of the size of the storm, if it moves through an area so fast that winds cannot build up from a given direction for several hours, then it will be of only minor importance. Inasmuch as most erosion on the beach takes place during high tide, the waves have only approximately four to six hours per day to effectively cut back the beach profile. Generally, at least two high tides are necessary in order for beach erosion to be very severe. During the first high tide, the beach profile is usually simply smoothed out, with not much loss of sediment. It is

---

Figure 3a. View looking north from Profile PLC on 27 May, 1967. Compare photograph with the beach profile at that position (Fig. 2). Note logs protruding from the wave-cut scarp. The amount of retreat of the dune scarp at this position during the storm was between 5 and 10 feet.

Figure 3b. Same date and orientation as a, from the foredune ridge. Note broad, flat profile. Dark zone at the base of the dune scarp is a garnet-rich, heavy mineral deposit.



FIGURE 3A



FIGURE 3B

during the following high tides that the beach begins to cut down and back (Fig. 8).

A fast-moving storm can easily pass completely through the New England area within a 24-hour period. The two storms that have been most effective during our period of observation, the storms of 25 to 26 May, 1967, and 24 to 27 February, 1969, have both been very slow-moving storms. Note the almost stationary position of the 25 to 26 May, 1967, storm off Nantucket for a period of two full days (Fig. 7).

#### Tidal Phase

Whether the storm occurs during the spring or neap tide is another important consideration. Even if a storm surge of 3 feet accompanies a neap tide, the high-water mark will only reach its normal level (M.H.T.) during the storm. If, however, the storm occurs during a spring tide and a minor surge is added to the high-water mark, then the dunes and the back-beach are exposed to intense wave erosion (Fig. 9). Most of the very effective northeasters we have observed occurred during spring tides.

#### Path of Storm with Respect to Beach

When a storm is centered offshore from Nantucket, northeasterly winds blow directly across the Gulf of Maine with a very long fetch. Hence, large waves can be formed. If a storm passes to the west of the northern New England coast, or far offshore, then winds will approach the shore from a different angle, usually at smaller velocities, and the resultant waves will be relatively small. Therefore, the path followed by storms that are the most effective is in a northeasterly direction across the continental shelf off southeastern New England (Fig. 1), just east of the island of Nantucket.

#### Time Interval Between Storms

One of the most effective deterrents against dune erosion or loss of shore property is a large mass of sand on the beach profile itself. Much of the erosive energy of the storm waves may be used up in removing this sand.

---

Figure 4. Typical constructional beach profile for the coast of northeastern Massachusetts and New Hampshire. This profile was measured at profiling station CBA at the north end of Crane Beach on 22 August, 1967.

# CONSTRUCTIONAL BEACH PROFILE

STATION CBA, CRANE BEACH  
IPSWICH, MASS.

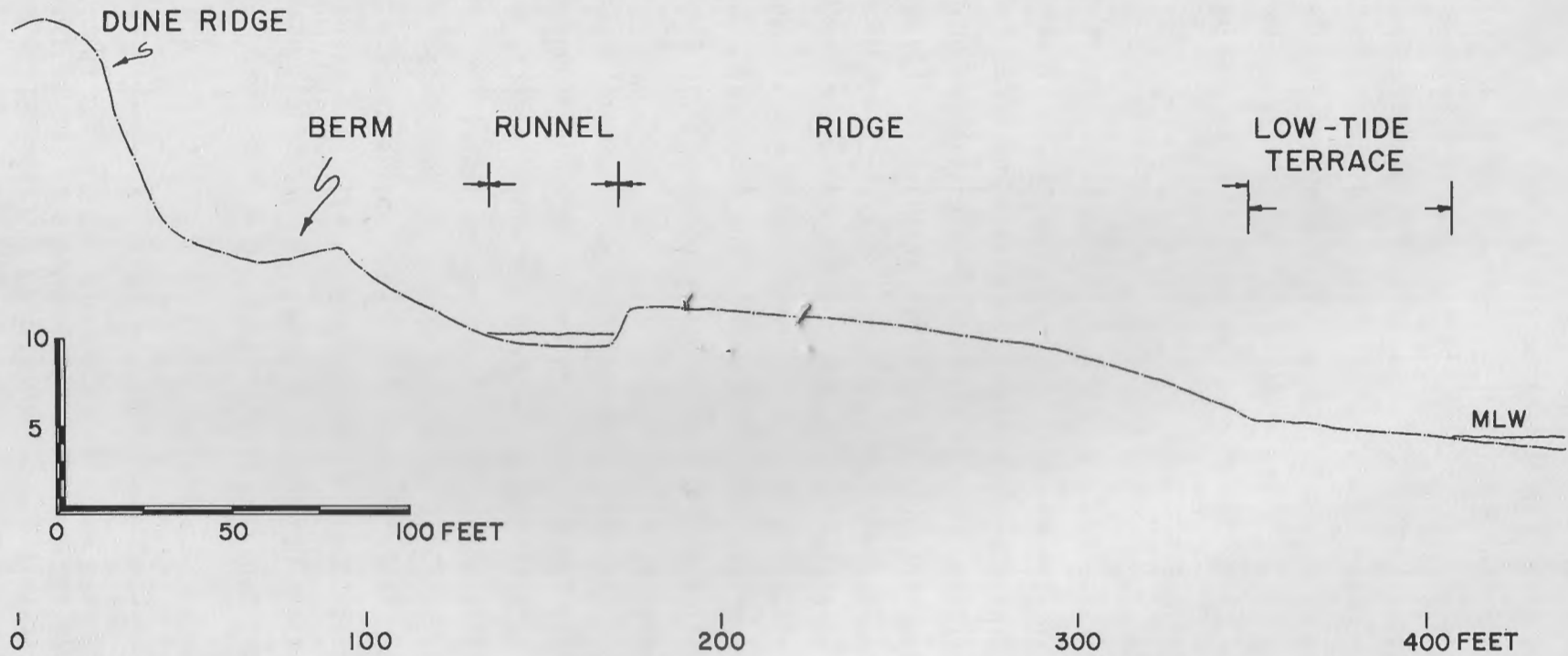


FIGURE 4

An example of the protective effect of a broad berm is illustrated in Figure 10. A relatively severe storm of 3 November, 1966, cut away approximately two-thirds of the berm at profiling station PLB. The profile was left with a high beach scarp; however, there was no erosion below the normal storm profile or into the dunes. Figure 11 has three photographs illustrating the destruction of the berm by this storm. If, on the other hand, storms follow each other very closely, without an interim period for sand to return to the beach, erosion will be much greater than normal.

#### CONCLUSIONS

1. The cycle of erosion and deposition on the sand beaches of New Hampshire and northeastern Massachusetts is closely related to the periodic northeasterly storms that pass through New England. The cycle consists of three stages: (1) an early post-storm profile that is flat to concave-upward; (2) an early accretionary profile which normally consists of a ridge-and-runnel system, with the ridge migrating toward the backbeach area; (3) a late accretionary or mature profile that occurs after the ridge has welded to the backbeach and a broad berm has developed. On some beaches, welding does not occur and gigantic ridges (up to 4 feet in height) lie between the backbeach and the low-tide terrace (Figs. 12 and 13).

2. The concept of "winter" and "summer" beach profiles does not hold true in this area. Although there is a general tendency for storms to be most frequent during the winter months, and for accretion to be slightly more prevalent during the late summer months, any of the three basic profiles can occur during any particular season.

3. The role of northeasterly storms as geologic agents is apparently controlled by size and intensity of the storm, speed of storm movement, tidal phase (i.e., spring or neap tide), path of storm with respect to beach, and time interval between storms.

---

Figure 5. Summer profiles at station PLB on Plum Island. These profiles represent the two extreme end members of the erosional-accretional cycle, post-storm (22 June, 1967) and late accretion (10 Sept., 1967).

# SUMMER BEACH PROFILES

STATION PLB, PLUM ISLAND  
NEWBURY, MASS.

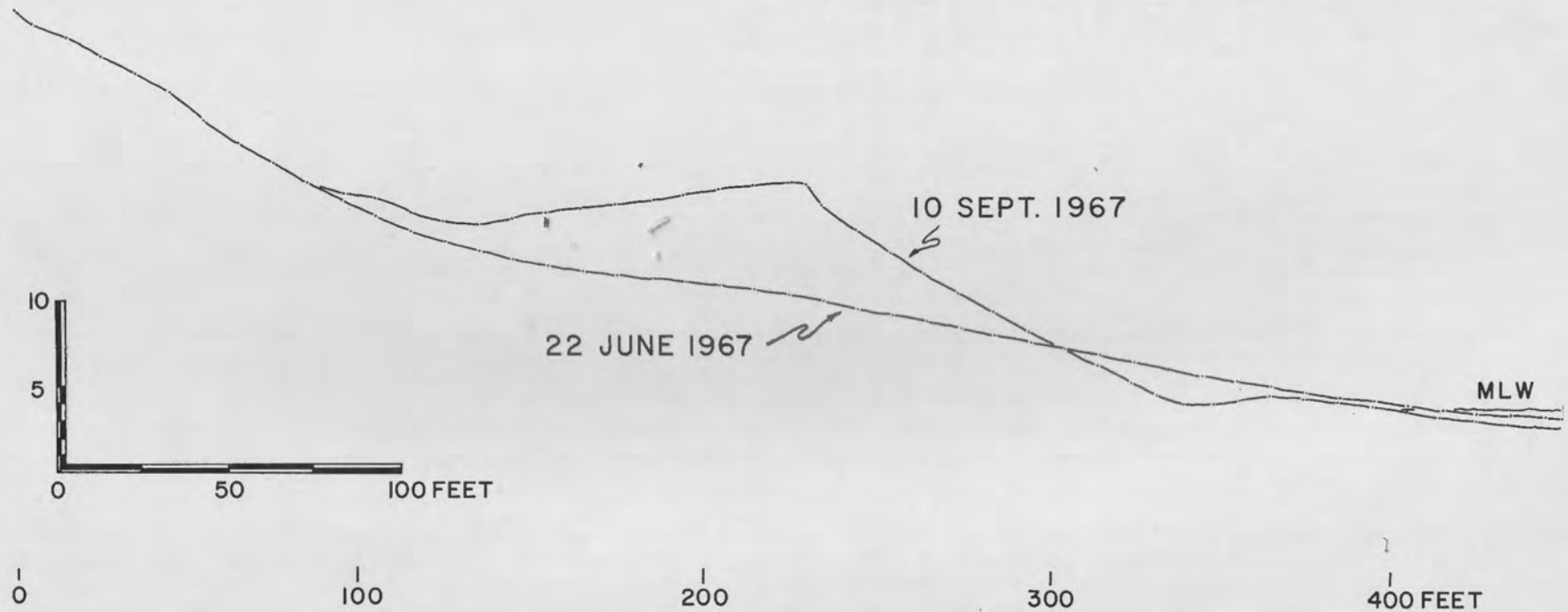


FIGURE 5

Figure 6. Profiles depicting winter accretion at station PLC, Plum Island, for the period 5 to 23 January, 1967. During this 18-day period, the high-tide mark advanced seaward over 100 feet, and a large neap berm (arrow) developed.

Figure 7. Location of a large northeasterly storm at 1:00 A.M. on Friday, 26 May, 1967. The track of this storm is shown by the dashed line. The distance between blocks along the track represents the distance the storm center has traveled within a 12-hour interval. This is one of the largest storms to affect the study area during the last four years. Note the slow progress of the storm once it reached a position directly offshore from the southeast coast of Massachusetts. It was practically stationary for a period of two full days.

Figure 8. Profiles illustrating the erosional effect of the 27 to 28 January, 1967, storm at profiling station PLC on Plum Island. Most of the month of January had been very mild, as indicated by the large accumulation of sediment shown on the 23 January profile. Compare these profiles with those in Figure 6. Strong winds from the northeast first started blowing on the morning of 28 January. Our first profile, at low tide in the late afternoon of 28 January, showed that the waves had simply rearranged the sand on the beach into an extremely flat, featureless profile. The profile measured at low tide the next morning showed that the whole beach profile had been eroded downward a vertical distance averaging around 3 feet. This fast-moving storm left the area on Saturday, 28 January, and erosion of the profile ceased.

Figure 9. Storm Waves.

- A. The erosion zone on northern Plum Island.
- B. Dune erosion near profile PLB.

Figure 10. Profiles illustrating the erosional effect of the 3 November, 1966, storm at station PLB on Plum Island. The main effect was the removal of approximately two-thirds of the large mature berm that had been deposited during the late summer and early fall months and months and the carving of a steep beach scarp.

# WINTER ACCRETION 5-23 JAN 1967

STATION PLC, PLUM ISLAND  
NEWBURY, MASS.

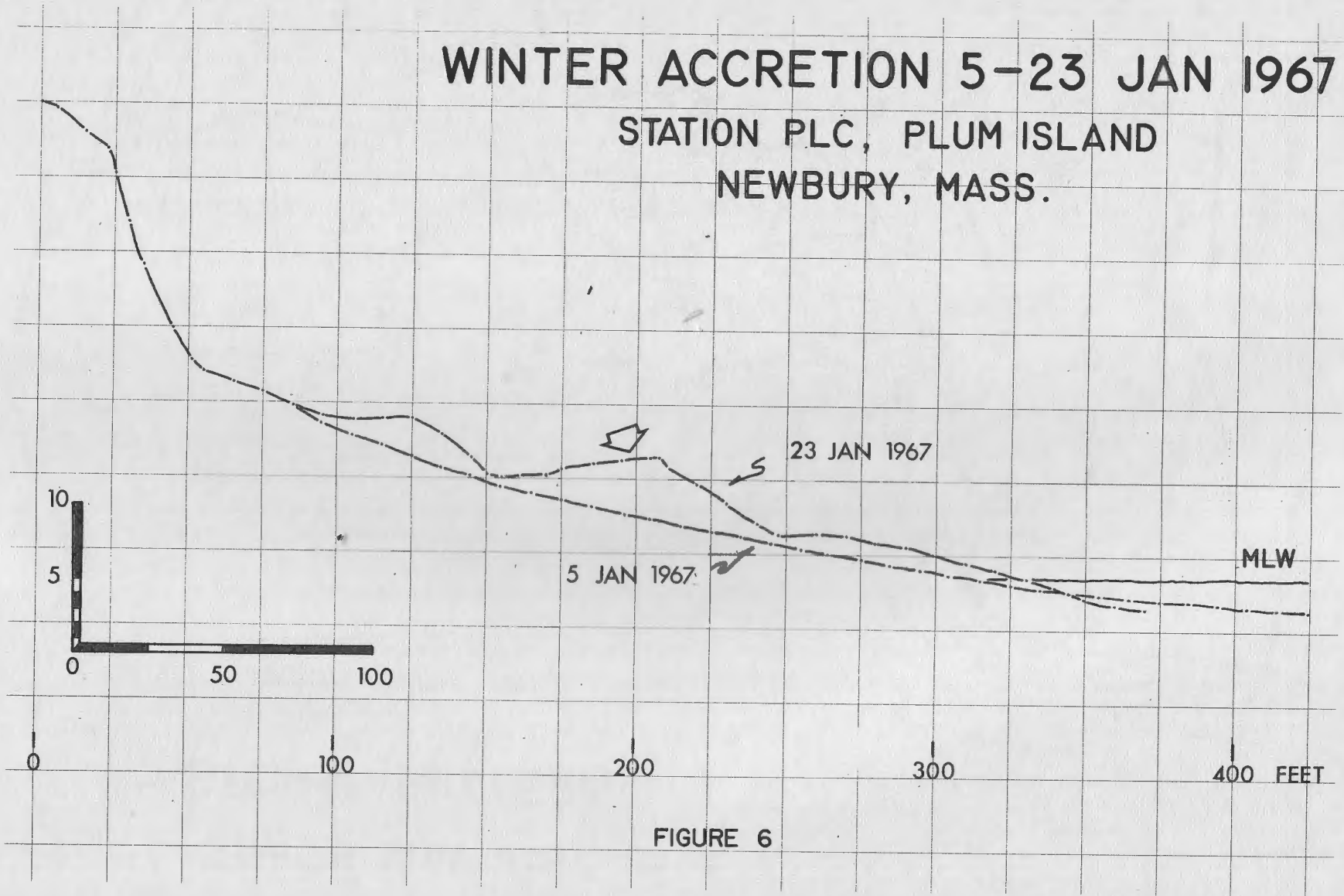


FIGURE 6

# 25-26 MAY 1967 STORM PATTERN

POSITION GIVEN FOR  
1<sup>00</sup>AM FRI 26 MAY

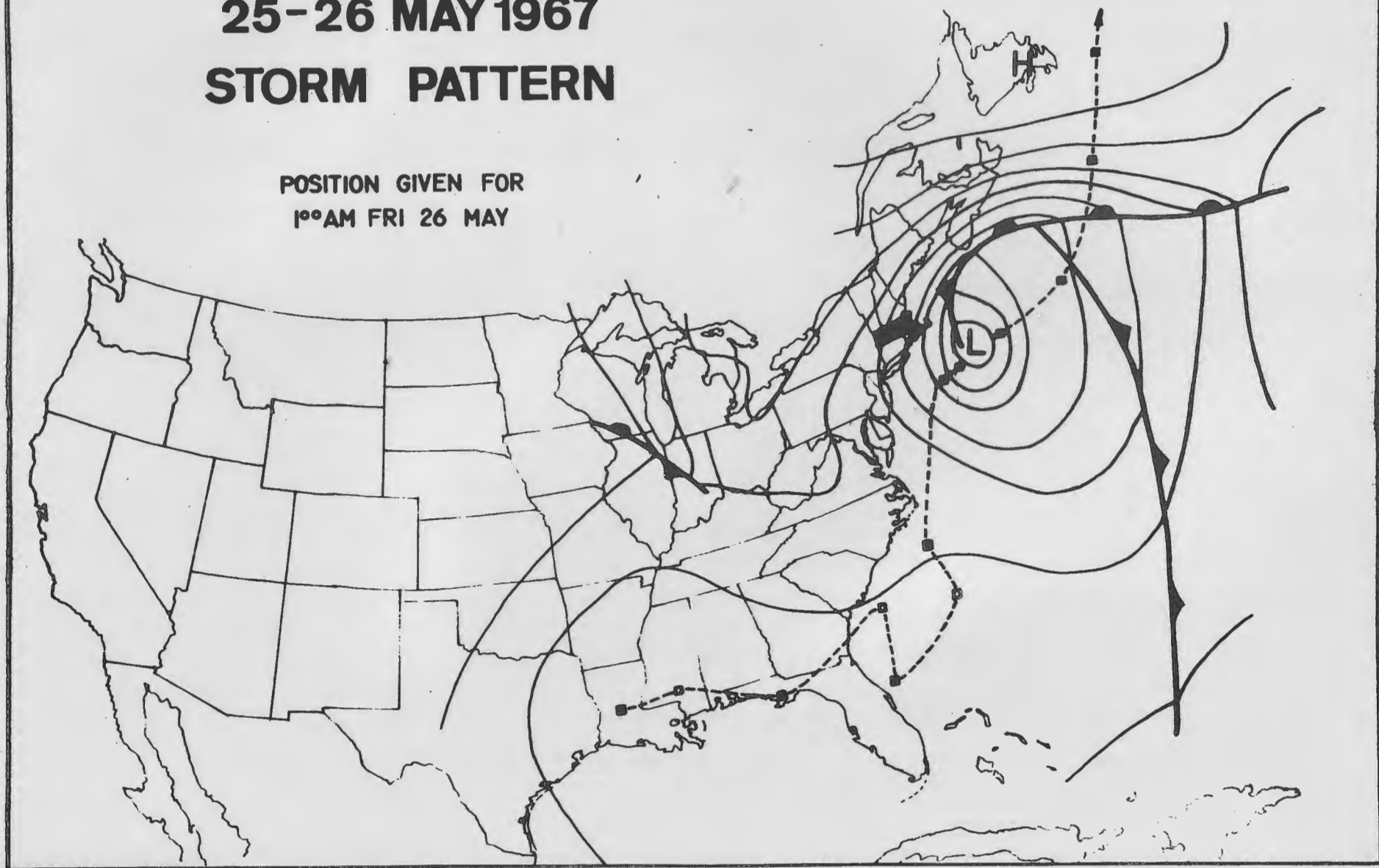


FIGURE 7

# EFFECT OF 27-28 JAN 1967 STORM

STATION PLC, PLUM ISLAND  
NEWBURY, MASS.

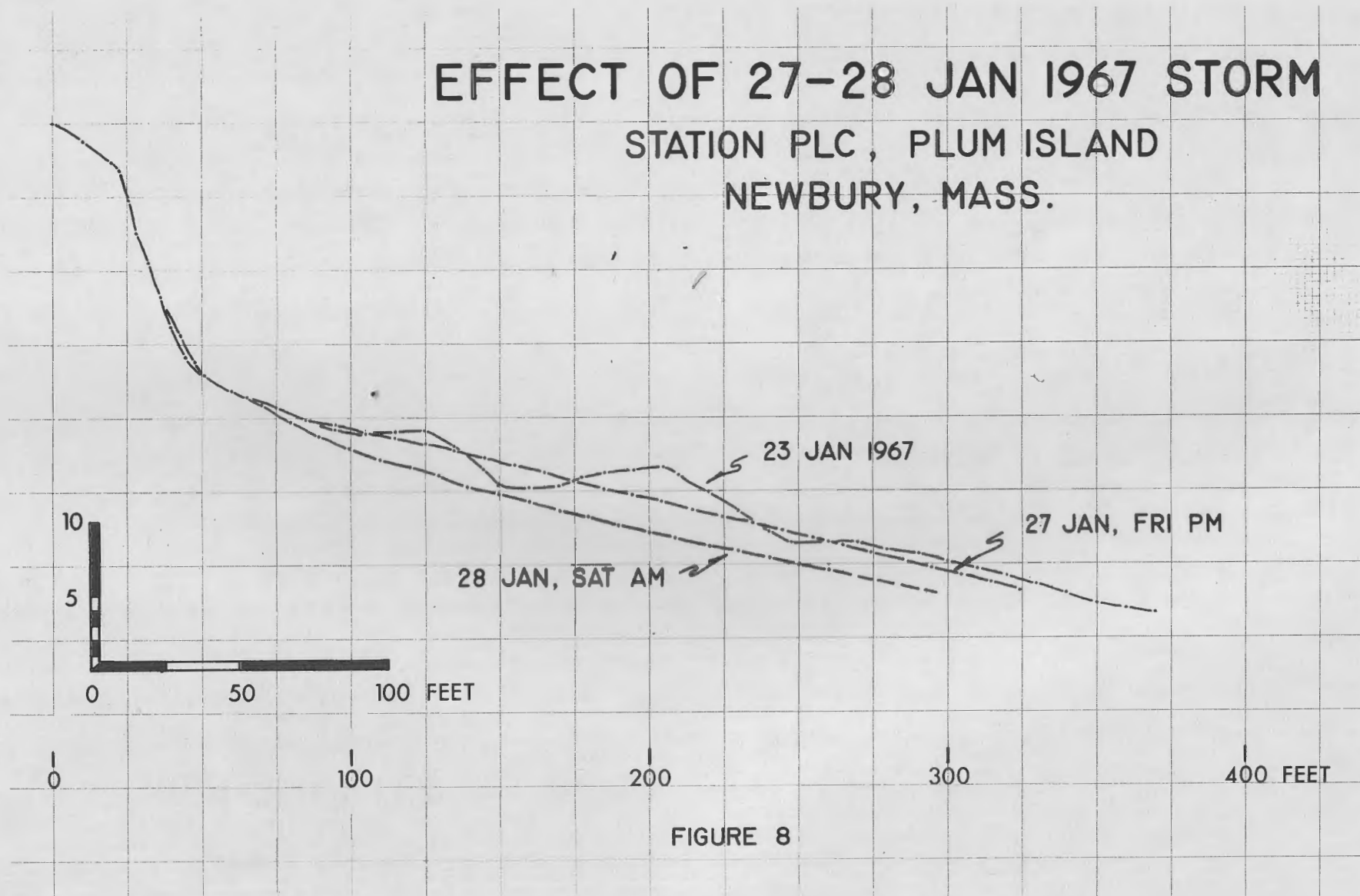


FIGURE 8



FIGURE 9A



FIGURE 9B

# EFFECT OF 3 NOV 1966 STORM

STATION PLB, PLUM ISLAND  
NEWBURY, MASS.

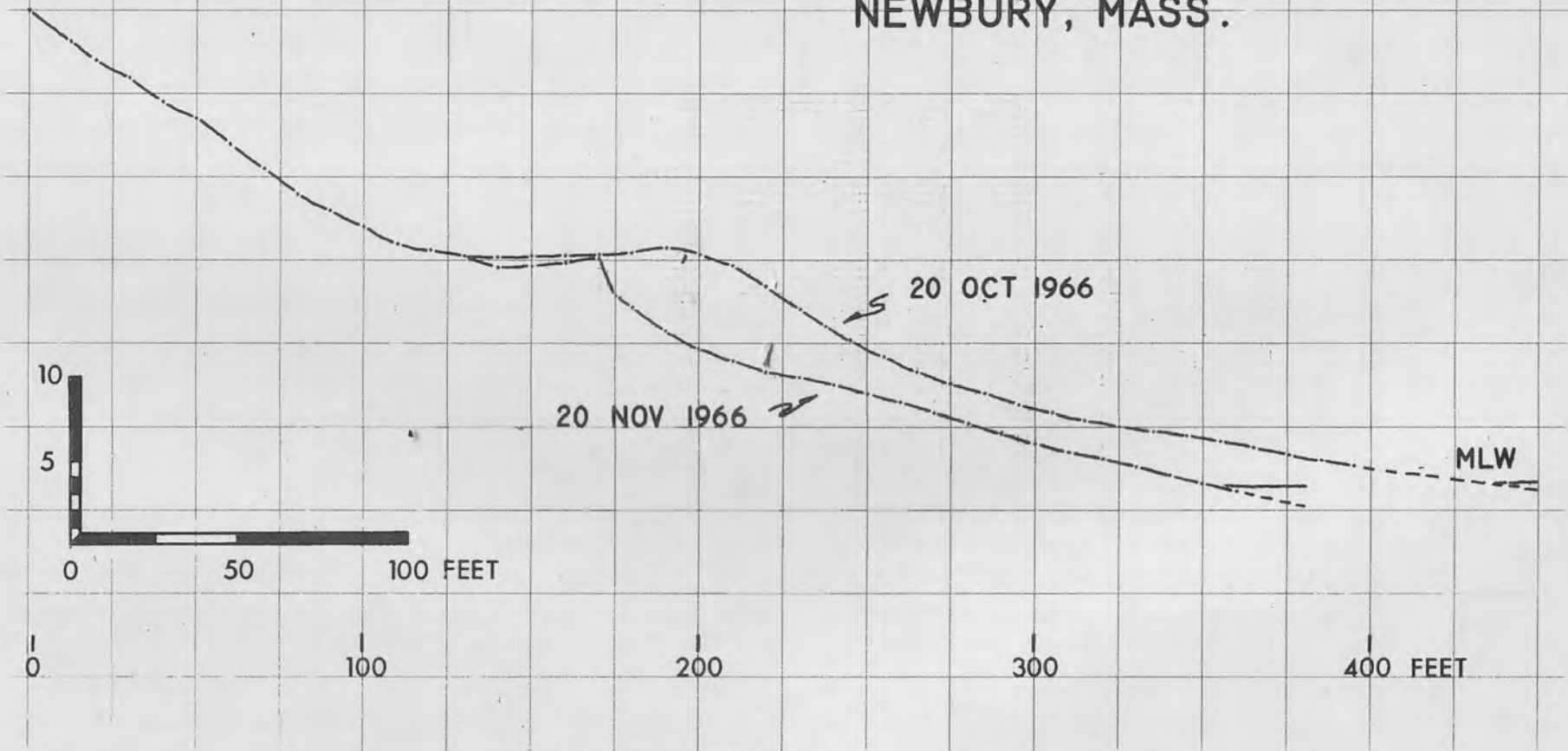


FIGURE 10

Figure 11. Observations during the northeaster of 3 November, 1966.  
A. and B. Wave attack at high tide on the beach at the north end of Plum Island.  
C. Destruction of the berm (at high tide) on central Plum Island.

Figure 12. Accretional and post-storm profiles at station CBA on Crane Beach. The 20 December, 1966, profile was measured the day following a mild, fast-moving northeaster. The 21 July, 1966, profile was measured after a long period of mild weather. Ridges developed on this profile migrate very slowly and, hence, very seldom weld to the back-beach.

Figure 13. Views from profile CBA at the time of measurement of the profiles shown in Figure 11. Both views look southeast and were taken from the dune crest at approximately the same position.  
A. 21 July, 1966.  
B. 20 December, 1966.



FIGURE 11

POST-STORM AND ACCRETION  
PROFILES  
STATION CBA, CRANE BEACH

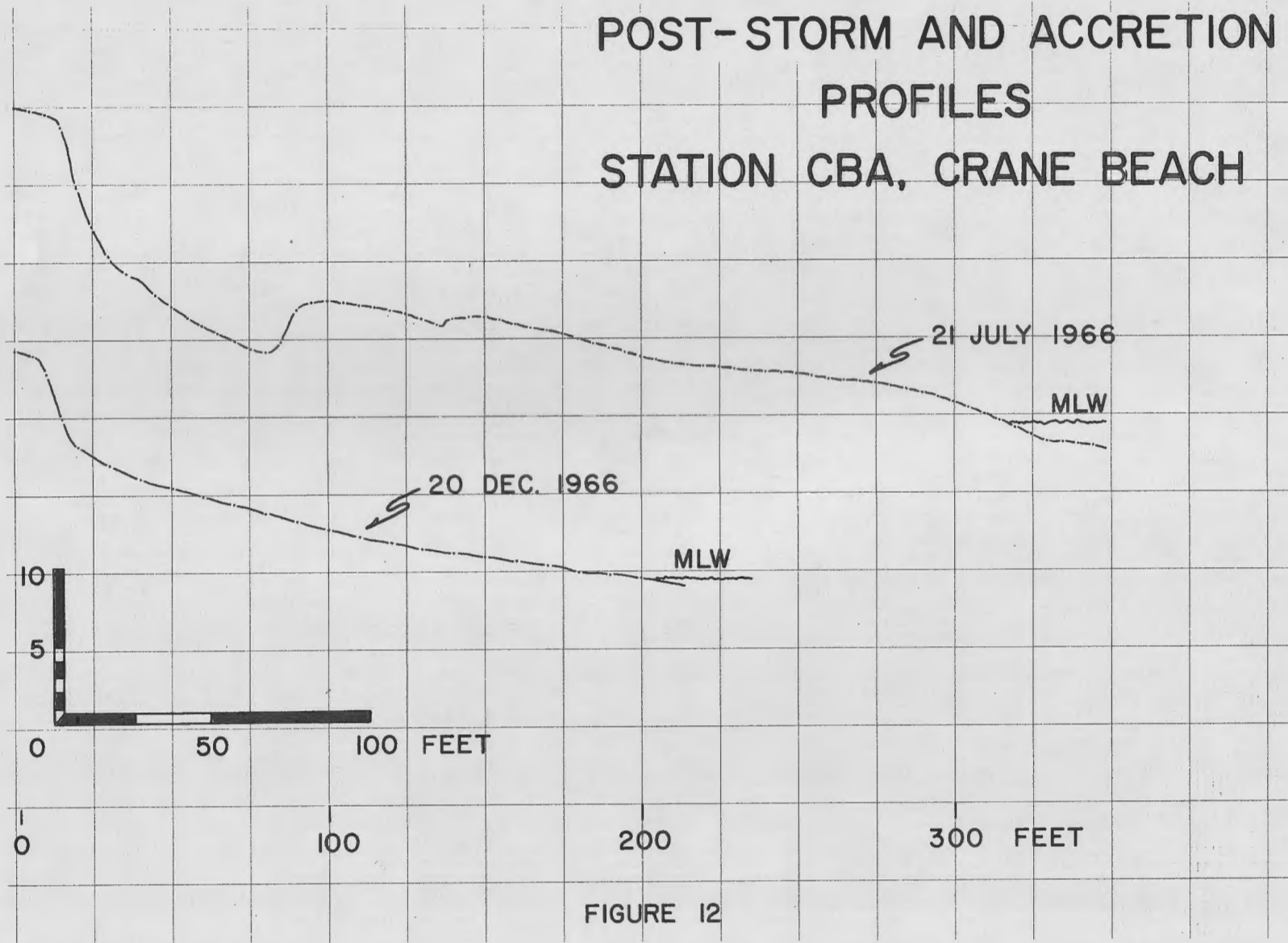


FIGURE 12



FIGURE 13A



FIGURE 13B

GRAIN-SIZE PARAMETERS OF THE BEACH AND DUNE SANDS,  
NORTHEASTERN MASSACHUSETTS AND NEW HAMPSHIRE COASTS

Fayez S. Anan

Abstract: A total of 159 samples were collected, using different sampling techniques, from modern beaches and coastal dunes of the northeastern Massachusetts and southern New Hampshire coasts. Statistical parameters of the grain-size distribution indicate that a meticulous and consistent sampling of one sedimentation unit is an essential step in obtaining adequate and consistent results.

A comparison of the method of moments with Folk and Ward's (1957) graphical method for deriving statistical parameters shows the moment method to be superior to the graphical method, especially when skewness and kurtosis are used. Scatter plots of first moment versus second moment, second moment versus third moment, and third moment versus fourth moment provide fairly good separation between beach sands (type B samples) and coastal dune sands.

Beach sands are better sorted than dune sands from the same area. Most of the beach and dune sands are positively skewed. Two different populations of grain-size distribution occur in the dunes. Samples from the upper part of the dune slip faces are characteristically positively skewed whereas samples from the lower part are dominantly negatively skewed.

#### INTRODUCTION

The economic importance of environmental discrimination and paleogeographic reconstruction has led to an intensive search for criteria inherent in the sediments, that uniquely characterize the different environments. Initial work on grain-size distribution and derived parameters by Udden (1914), Wentworth (1929), Otto (1939), and Doeglas (1946) provided great promise.

Inconsistent results of recent investigations using statistical parameters (mean, standard deviation, skewness, and kurtosis) have led to conflicting opinions regarding the sensitivity of these parameters to the transporting agents and environment of deposition. Inman and

TABLE 1. A BRIEF SUMMARY OF THE STEPS INVOLVED IN DERIVING STATISTICAL PARAMETERS.

SAMPLING	SEPARATION OF SAMPLE COMPONENTS INTO CLASSES	DERIVATION AND COMPUTATION OF STATISTICAL PARAMETERS
<p>1. UNCONTROLLED SAMPLING</p> <p>a. Stratigraphic Noncontrol: The sample is part of one or more sedimentational units.</p> <p>b. Spatial Noncontrol: The sample is obtained from the lower, middle, or upper part of the beach face, from the low-tide terrace, or from the back beach.</p> <p>c. A combination of Stratigraphic and Spatial Noncontrol.</p> <p>2. CONTROLLED SAMPLING</p> <p>Stratigraphic and Spatial Control: Samples consist of one sedimentation unit, and are obtained consistently from the same position.</p>	<p>1. SIEVING</p> <p>Separation into discrete classes according to intermediate axis.</p> <p>2. SETTLING TUBE (sic)</p> <p>Continuous distribution according to hydraulic equivalent (that is, settling velocity).</p>	<p>1. GRAPHIC</p> <p>Using subjectively selected parts of the size distribution. Calculation by using Inman (1952) or Folk and Ward (1957) formulas.</p> <p>2. MOMENT</p> <p>Using the total distribution. Calculation by using moment formulas.</p>

Chamberlin (1955), Folk and Ward (1957), Mason and Folk (1958), Harris (1957, 1959), Friedman (1961), Duane (1964), Chappell (1967), Hails (1967), Moiola and Weiser (1968), and others found that a scatter plot of a combination of some two of the statistical parameters is effective in differentiating between some environments. Mason and Folk (1958) found a plot of skewness against kurtosis to be effective in differentiating between beach and coastal dune environments, but Friedman (1961) found a plot of skewness against standard duration more reliable in differentiating between the same two environments. On the other hand, Shepard and Young (1961), Schlee and others (1964), Gees (1965), and Hayes (1965) concluded that statistical parameters are unreliable for distinguishing between different environments.

#### DISCUSSION OF THE PROBLEM

The theoretical explanation of the usefulness of statistical parameters in environmental discrimination is that the grain-size distribution (and the derived statistical parameters) reflects the mode and energy of transportation and the environment of deposition. For example, the wind has a limited competence as to the largest grain it will transport, whereas wave action tends to eliminate the finer grains through the action of swash and backwash. The result, theoretically, is a positively skewed grain-size distribution for dune sands and a negatively skewed distribution for beach sands. However, the sensitivity of statistical parameters to the environment and transporting agent has been supported as well as disputed by equally competent geologists.

Seeking an explanation for this conflict necessitates an analysis of the total processes used in determining the statistical parameters.

The following steps are usually involved:

1. Collection of samples.
2. Separation of the sample components into classes according to some property, such as size, nominal diameter, or hydraulic equivalent. (This factor has not been evaluated yet, and will be discussed in a later publication.)
3. Derivation and computation of statistical parameters.

A brief summary of some of the possible means used in accomplishing each of these steps is shown in Table 1.

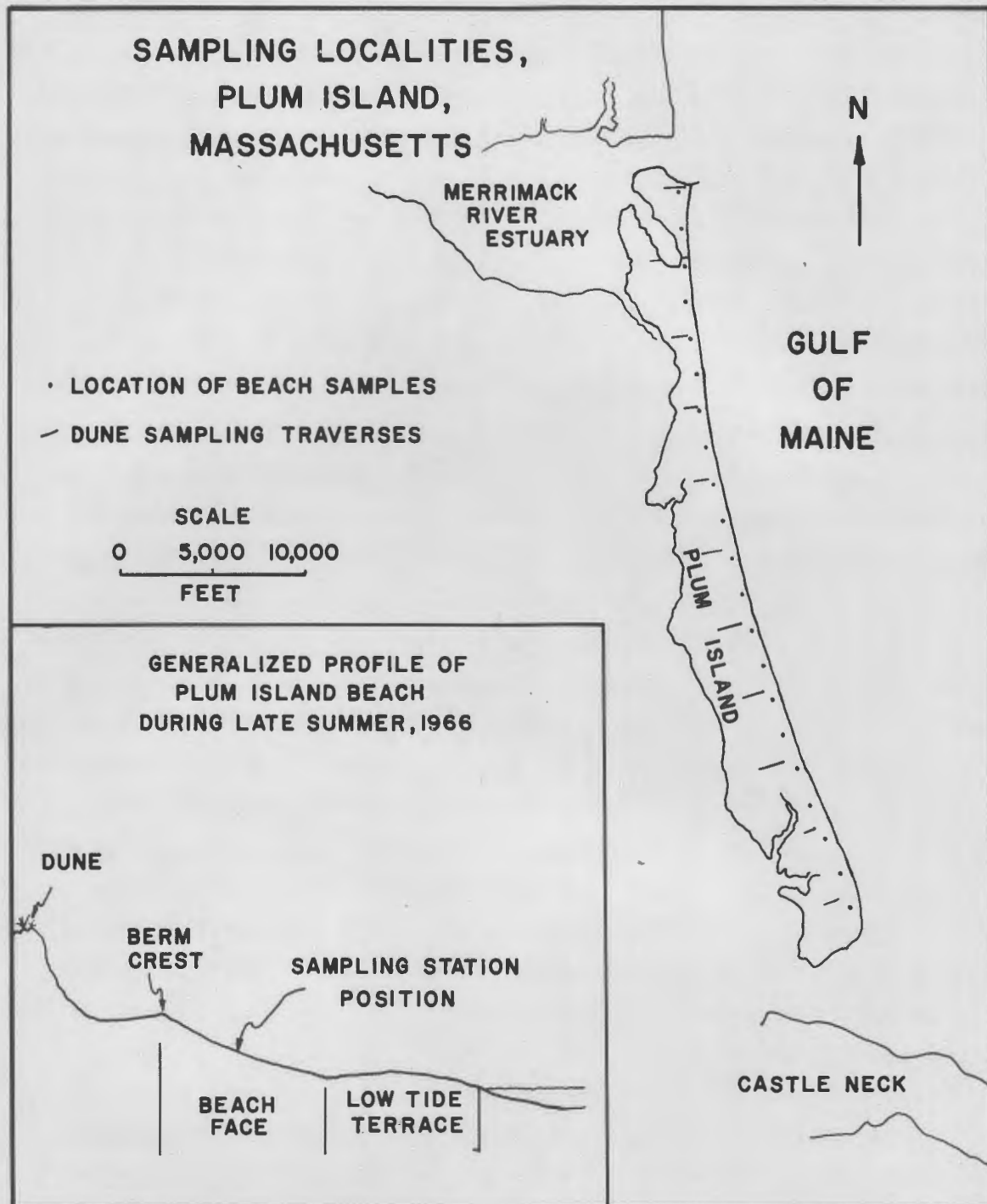


**FIGURE 1**

The conflicting results and opinions as to the effectiveness of statistical parameters in environmental discrimination could be attributed to inconsistency or inadequacy of one or all of the three steps involved in obtaining the statistical parameters.

One of the purposes of this study is to evaluate separately the effect of sampling techniques, size-analysis (sic) techniques, and computational methods on statistical parameters.

At this point, I would like to emphasize that this report is written primarily for this field trip guide book. The data are incomplete, and the conclusions will be tentative until such time as the rest of the data have been worked out.

## PROCEDURE

### Field Procedure

Data from only 159 samples are presented in this report. The samples were collected in the summer of 1966 from coastal dunes and beaches along the northern part of the Massachusetts coast and the southern part of the New Hampshire coast.

**BEACH SAMPLES:** Fifty-five samples were collected from the Plum Island beach. Sampling stations were spaced at intervals of two thousand feet along the beach, starting at the northern end of the island (next to the southern jetty of the Merrimack River). All stations considered in this report were located on the beachface, halfway between the berm crest and the landward limit of the low-tide terrace (Fig. 1). At each station three samples were collected, designated by the letters A, B, and C.

Sample A. At each station, the uppermost layer, one to two grains thick, was carefully scraped off, using the edge of a three-inch piece of a plastic ruler, and placed in a plastic bag. The area from which the sample was collected was approximately one foot wide and three feet long, and was oriented parallel to the shoreline.

Sample B. After collecting sample A, a layer one grain thick was scraped off and discarded. Then a layer one to two grains thick was scraped off and placed in another plastic bag.

Sample C. One foot south of the collection site for samples A and B, a core 15 inches long was taken and placed in a plastic bag. The core was taken with a plastic tube two inches in diameter.

The beach samples presented in this report are part of an extensive sampling system, which will be reported on in a later publication. DUNE SAMPLES: From a series of 104 samples collected from the dunes, 15 samples were collected from the Salisbury, Mass. - Seabrook, N.H., area, 60 samples from Plum Island, and 29 samples from the Castle Neck area.

Eighty samples were collected along traverses perpendicular to the dune belt (Fig. 1). The number of samples per traverse was a function of the width of the dune belt in that area. Collection of samples was from active slip faces near the top of the dune whenever possible. A layer one-eighth of an inch thick and parallel to the dune surface was collected using a flat-bottomed scoop. When the station occurred in a vegetated area, the sample was collected from a hole two to three feet deep, below the root zone. Samples collected along these traverses are designated as sample E.

During later visits to the area, the writer observed that grains in the lower part of all active dunes are coarser than grains in the upper part of the same dune. Consequently, 24 additional samples were collected from the Plum Island dunes. Two samples were collected from the modified slip face of each of 12 active dunes. All slip faces are modified due to the variable wind direction.

Sample F. A layer one-eighth of an inch thick was collected from the upper one-third of the dune slip face using a flat-bottomed scoop.

Sample G. Using the same technique, these samples were collected one to two feet above the inflection point at the base of the slip face.

#### Lab. Procedure

All samples were washed with warm water several times and oven-dried. A sample split of 40 to 50 grams was sieved for 20 minutes with a Ro-Tap machine using eight-inch diameter sieves at one-quarter phi ( $\phi$ ) intervals. Fractions retained on each sieve were weighed on an electric Mettler Precision Balance to 0.0001 grams.

Statistical parameters used to describe the grain-size distribution were derived by two different methods. One set of statistical parameters was derived using the formulas proposed by Folk and Ward (1957). The other set of statistical parameters was derived using the moment

method. A computer program for calculation of graphic as well as moment parameters was prepared by E. G. Rhodes at the Department of Geology, University of Massachusetts. The percentiles for the graphic method are located by linear interpolation. No interpolation is used for the moment method. For the moment method, the fine tail of the grain-size distribution was arbitrarily terminated at six phi ( $\phi$ ). A CDC 3600 computer was used in calculating all parameters.

## RESULTS

For both the graphic and the moment methods, scatter plots of mean against standard deviation, mean against skewness, standard deviation against skewness, and skewness against kurtosis have been constructed using the phi ( $\phi$ ) scale. However, only those plots of importance to this discussion will be presented.

### Effect of Sampling Techniques on Statistical Parameters

BEACH ENVIRONMENT: Figure 2 is a plot of the first moment against the second moment for beach samples of type A, B, and C. Type C samples are the coarsest, with a grand mean size of 1.023  $\phi$  (0.499 mm), are randomly distributed through the scatter plot, and have the poorest sorting. Type B samples are the finest, with a grand mean-size of 1.589  $\phi$  (0.34 mm), and have the best sorting. Type A samples, with a grand mean-size of 1.157  $\phi$  (0.45 mm), have an intermediate sorting. Thus, for the three types of samples, the sorting improves as the mean size becomes finer. However, within each suite of type A and type B samples, the sorting improves as the mean size becomes larger. Type C samples do not show any relationship between mean size and sorting, which is explained as being due to the presence of many sedimentational units as well as lag deposits in each of the type C samples. In addition, the relative amounts of each of the sedimentational units would probably vary from one station to the next. The fact that type A samples are consistently coarser than type B samples is explained by the fact that type A samples include a lag deposit of coarse grains, a one grain-thick layer, left behind by

---

Figure 2. Scatter plot of the first moment (mean) against the second moment (sorting) for beach samples. Moment Method.

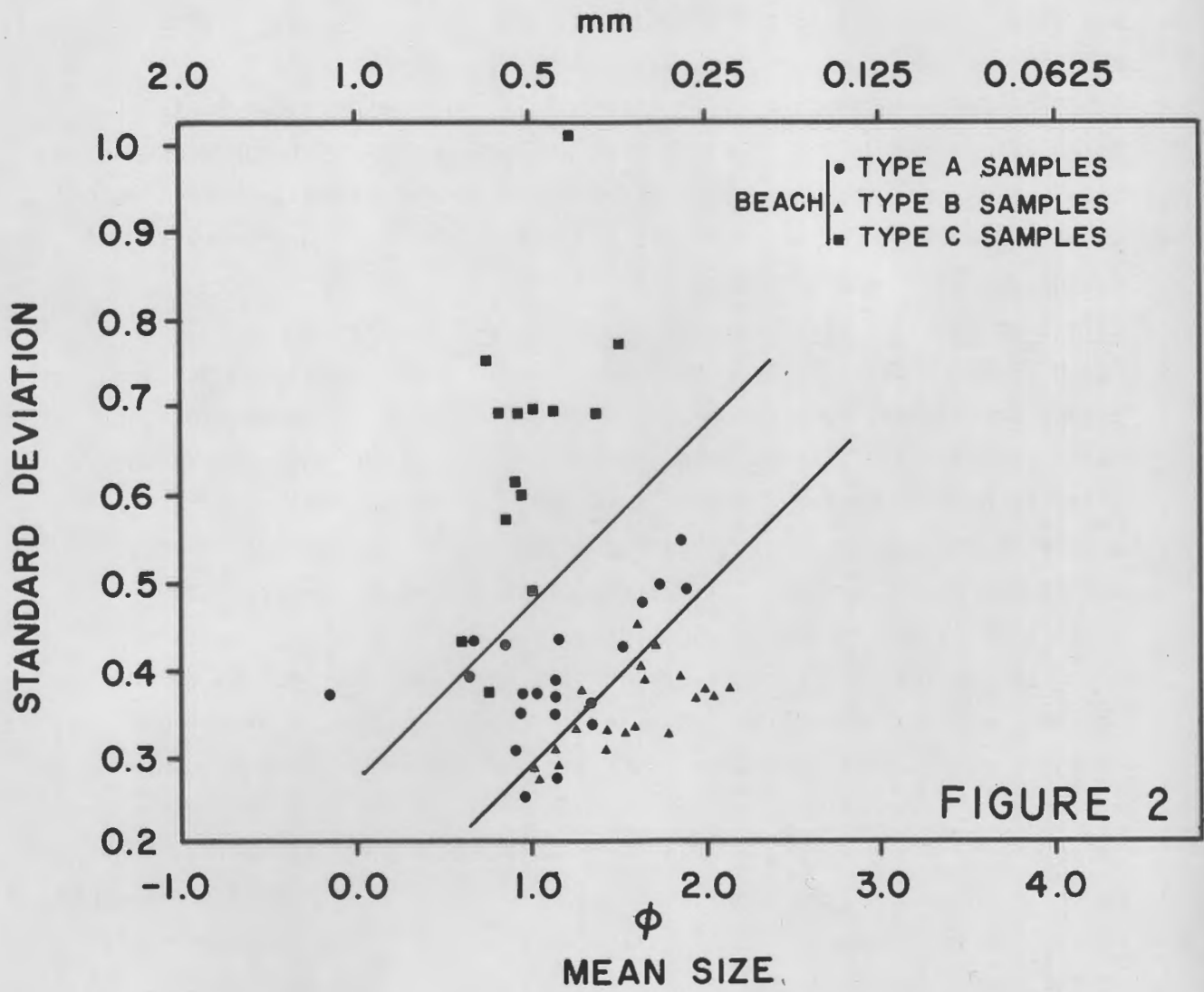


FIGURE 2

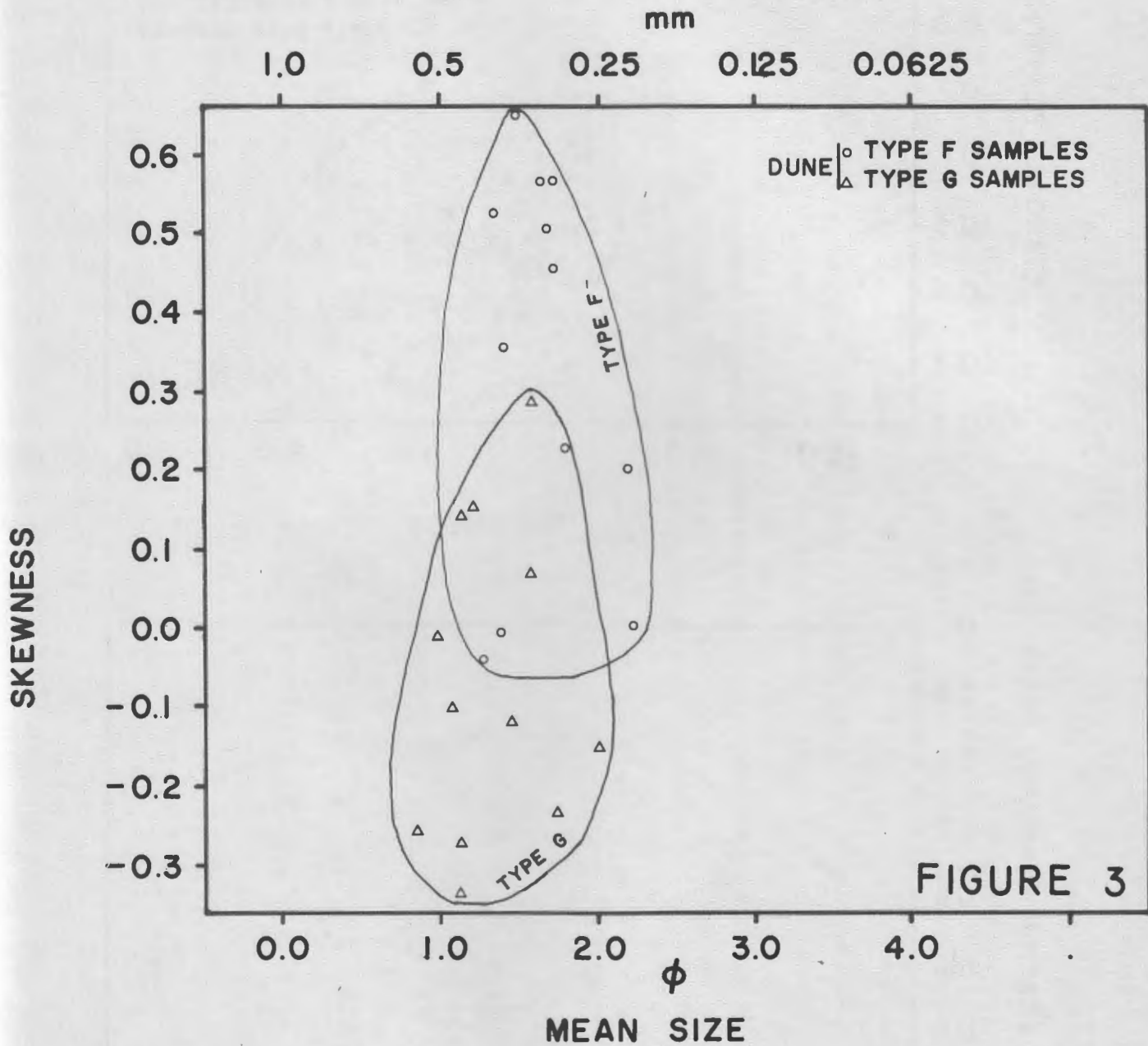
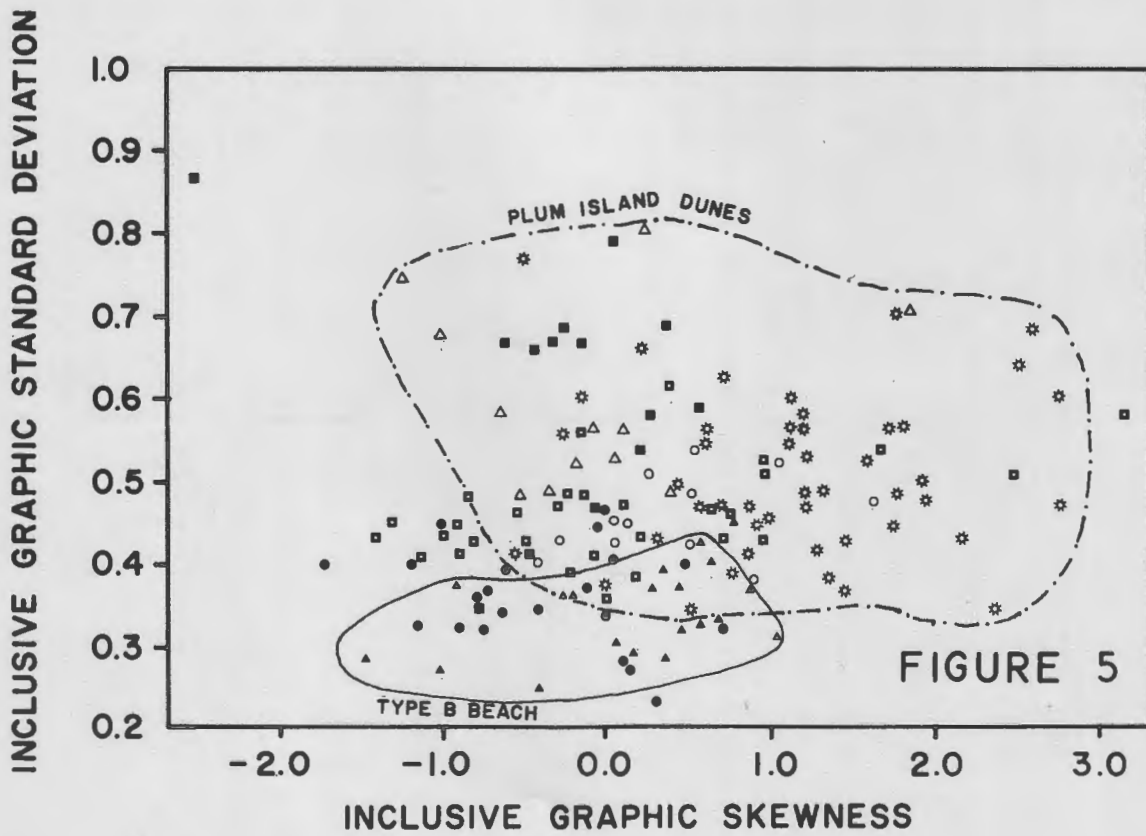
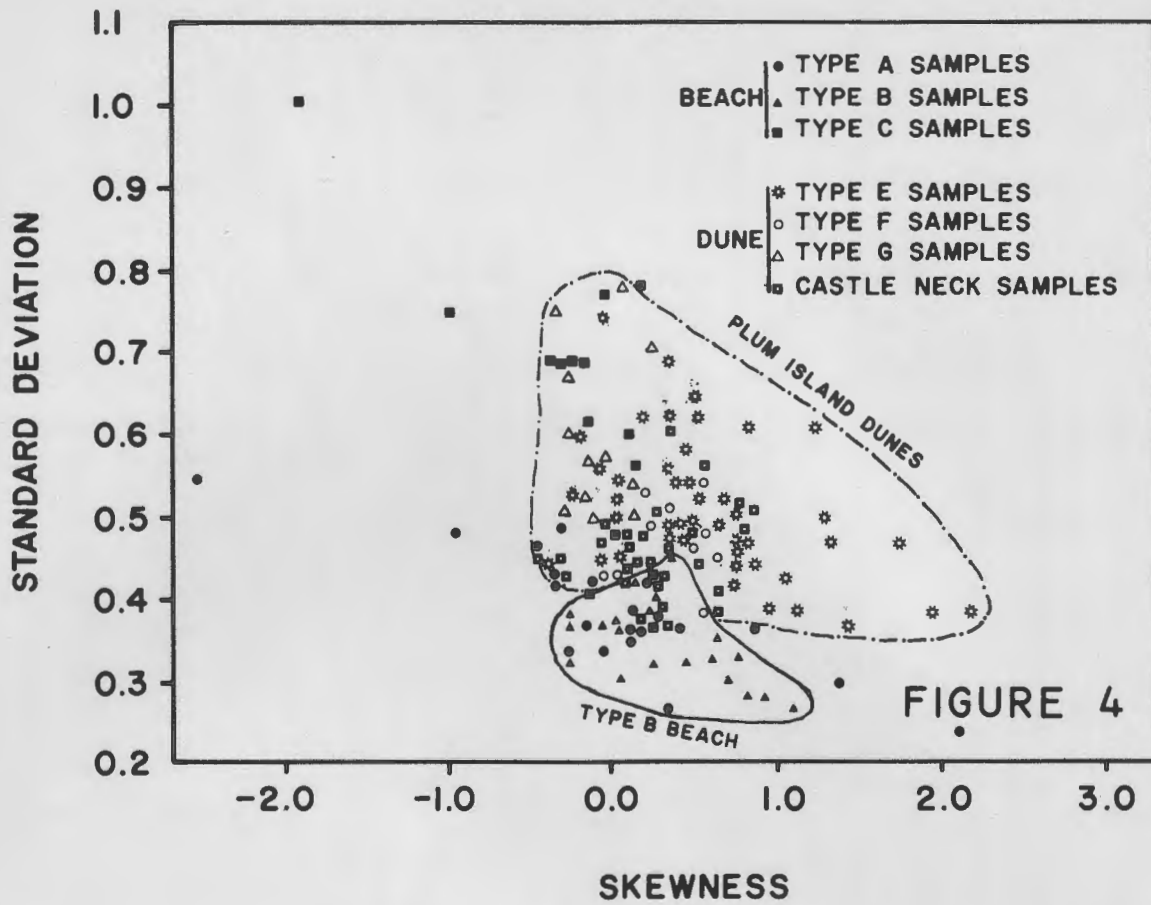


FIGURE 3



the higher regime swash of the last waves to reach the sampling position as the tide receded. Type B samples represent depositional material in the strict sense, which has not been modified by swash action.

DUNE ENVIRONMENT: Figure 3 is a plot of the first moment against the second moment for dune samples of type F and G. All type F samples, except two, are positively skewed. Two-thirds of the type G samples are negatively skewed, and have a mean size slightly coarser than type F samples. As expected, the coarsest grains deposited in the upper part of the dune roll down slope under the force of gravity, thus the lower part of the dunes is enriched in the coarse grains. In addition, during periods when the wind blows from other directions, coarse grains which are transported close to the ground surface will be deposited in the lower parts of the modified slip face. The result is positively skewed grain-size distribution in the upper part of the dune from which the coarsest grains have been lost, and negatively skewed distribution of sand in the lower part of the dune, the site of accumulation of the small tail of coarse grains.

#### Effect of Computation Methods on Statistical Parameters

Figure 4 is a scatter plot of the second moment against the third moment for all the beach and dune samples. If only type B beach samples are considered, which are the samples considered most adequate with respect to sampling techniques (discussed below), the separation between beach and dune samples is excellent. The little overlap is mainly due to dune samples from the Castle Neck area. Contrary to the findings of most workers, type B beach samples are better sorted than dune samples. However this trend will be evident only when one sedimentational unit

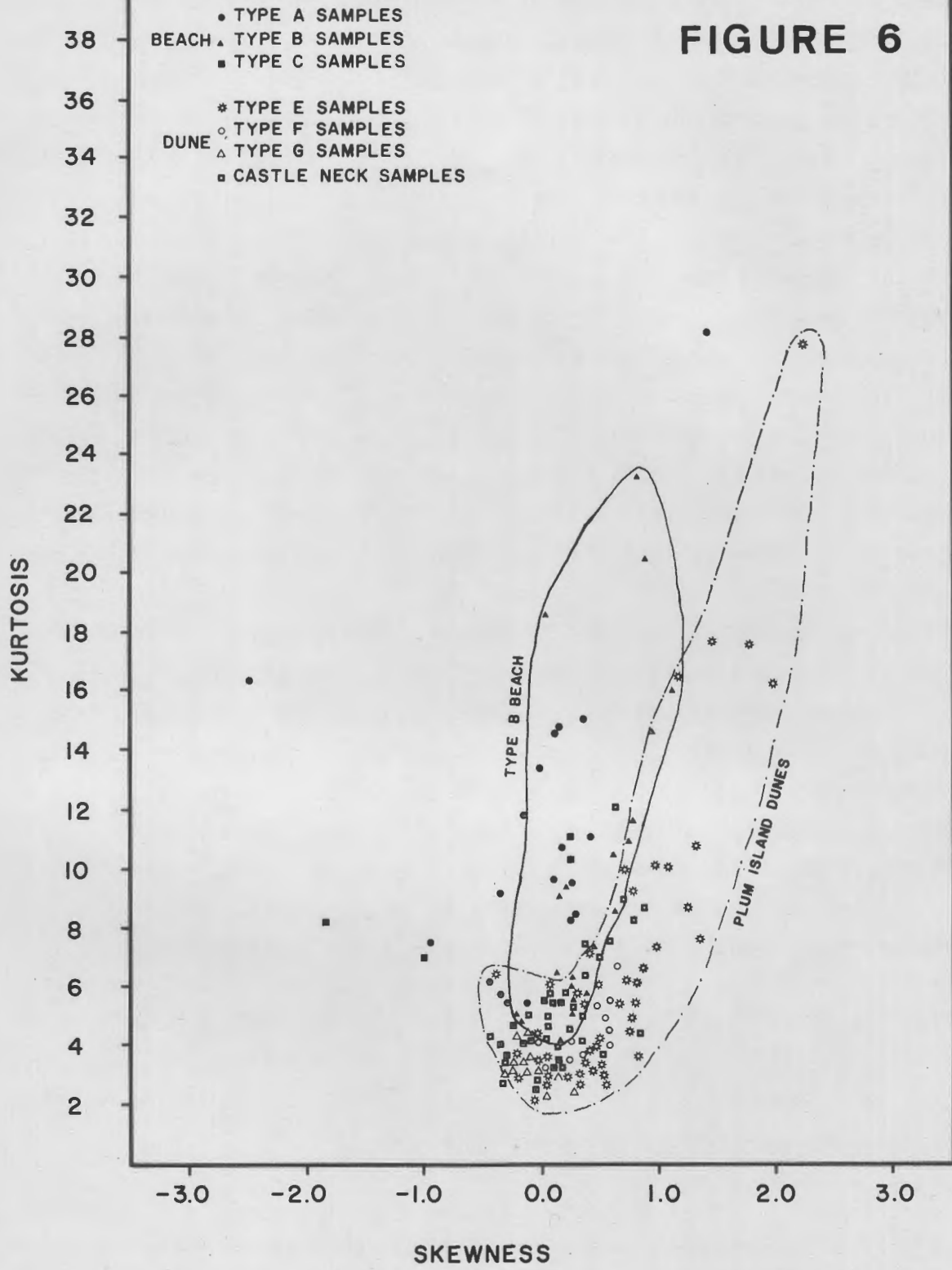
---

Figure 3. Scatter plot of the first moment (mean) against the third moment (skewness) for dune samples. Moment Method.

Figure 4. Scatter plot of the second moment (sorting) against the third moment (skewness) for beach and dune samples. Moment Method.

Figure 5. Scatter plot of the inclusive graphic standard deviation against the inclusive graphic skewness for beach and dune samples. Graphic Method.

FIGURE 6



is sampled, as indicated by the poor sorting of type C beach samples. The relatively poorer sorting in the dunes is explained by the fact that in the Plum Island area a wide range of grain sizes is available, and coarser grains, deposited during high velocity winds become mixed with existing finer grains in the dunes due to slumping and dune migration. In addition, sampling of the dune sands was not as well controlled as sampling the beach sands due to the difficulty of defining the sedimentation unit on the dunes.

Inspection of Figures 4 and 5 shows that, using the method of moments, six dune samples from Castle Neck are negatively skewed and twenty-three are positively skewed. On the other hand, when the graphical method (Folk and Ward, 1957) is used on the same samples, seventeen samples are negatively skewed and twelve samples are positively skewed. In addition, Figures 6 and 7 demonstrate adequately that a scatter plot of skewness against kurtosis determined by the method of moment provides a better separation of beach samples from dune samples than when skewness and kurtosis are determined by the graphic method. Note that statistical parameters derived by the method of moments have different values from equivalent parameters derived by the graphical method. This difference becomes more pronounced in the higher moments (that is, skewness and kurtosis).

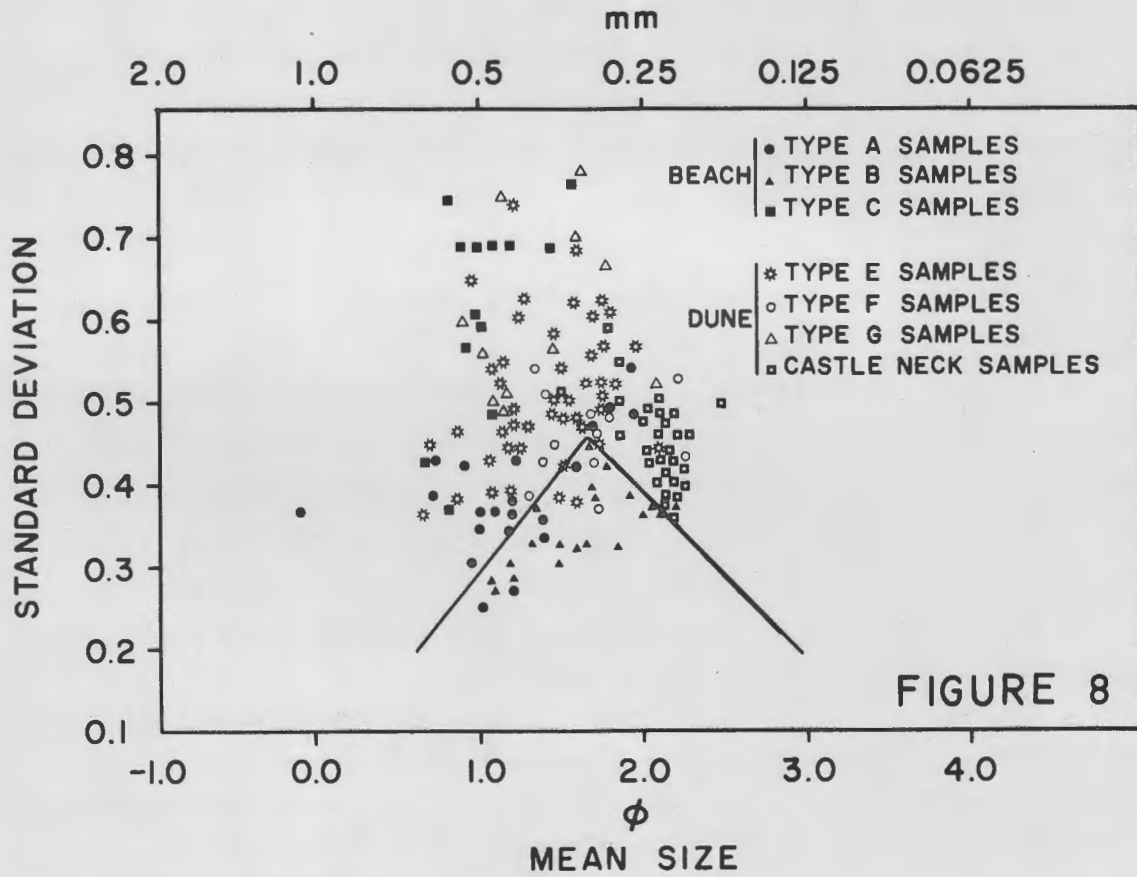
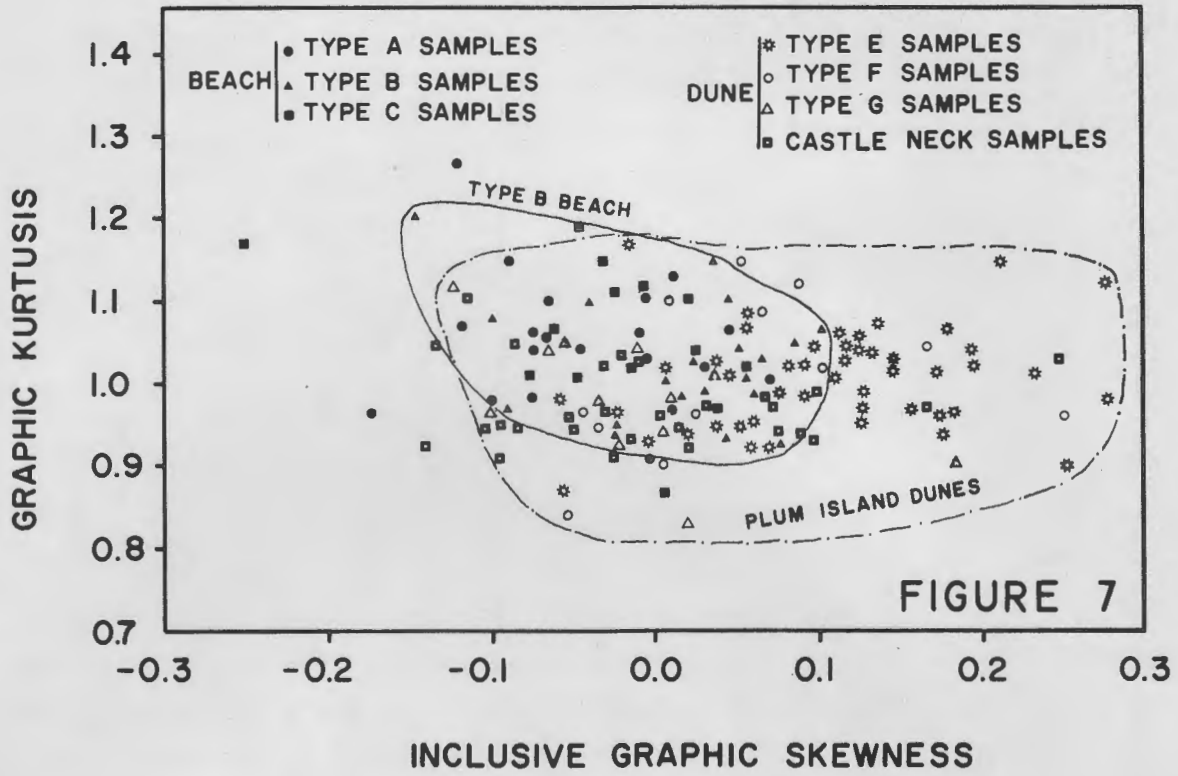
#### CONCLUSIONS

The data presented in this report support the following tentative conclusions:

1. The concept of a sedimentation unit is an important one in sampling the beach environment. Stratigraphic as well as spatial control of sampling is an essential step in obtaining uniform and consistent data. Lag deposits should be excluded from the samples. Type B samples, those collected after scraping off the surficial lag deposit, and consisting of one sedimentation unit, are considered the most adequate representation of the beachface depositional environment.

---

Figure 6. Scatter plot of the third moment (skewness) against the fourth moment (kurtosis) for beach and dune samples. Moment Method.



2. Beach sands (except samples C) are better sorted than dune sands. The finer dune sands from the Castle Neck area are better sorted than the Plum Island dune sands, but not as well sorted as Plum Island beach sands. Thus, when the source provides a wide range of sizes, the beach environment proves to possess a superior sorting mechanism to the dunes.
3. The majority of the type B beach samples are positively skewed, rather than negatively skewed, as has been reported by most workers.
4. Two populations of sand distribution occur in the Plum Island dunes. The upper part of the dune's modified slip face is characterized by a positively skewed population. The lower part of the dune's modified slip face is generally characterized by a negatively skewed population, which is also the coarsest of the two populations.
5. The moment method is more useful than the graphical method for determination of statistical parameters.
6. Statistical parameters of grain-size distribution are a useful tool in differentiating between dune and beach environments (Fig. 4, 6, and 8) if proper sampling techniques are employed.

---

Figure 7. Scatter plot of the inclusive graphic skewness against graphic kurtosis for beach and dune samples. Graphic Method.

Figure 8. Scatter plot of the first moment (mean) against second moment (sorting) for beach and dune samples. Moment Method.

## OFFSHORE BARS AT PLUM ISLAND, MASSACHUSETTS

Victor Goldsmith

Abstract: Bottom profiles were run across subaqueous bars offshore from two localities on Plum Island, Massachusetts, at four widely-spaced intervals over a period of 16 months. The offshore bar at profile PLB displays changes in size and location which do not appear to correlate with cycles of storm erosion and recovery on the adjacent beach. The offshore bar at profile PLA showed a constant growth during the 16-month period. In an earlier study, ten profiles were run within a one-year period over an inshore bar at profile PLA. The inshore bar at PLA appeared to respond to seasonal cycles of erosion and deposition on the adjacent beach. The different response of these bars indicates that the situation is quite complex and that no simple correlation exists between offshore bar growth and subaerial beach erosion on Plum Island.

### INTRODUCTION

The relationship between the size and location of offshore sand bars and wave conditions has been recognized by many workers (Keulegan, 1948; King and Williams, 1949; Shepard, 1950; and Sonu, McCloy, and McArthur, 1966). Shepard (1950, p. 11), has shown that in Southern California deeper longshore bars and deeper longshore troughs occurred on days when the waves were larger. He used the ratio of trough depth to bar depth as a means of comparing offshore bars from different areas. Keulegan (1948) made an experimental study of offshore sand bars and noted that, for constant water depths, the position of the bar formed by a single system of waves is a function of wave height and wave steepness. Keulegan also noted that the form of the bar is independent of the size of the generating waves and of wave steepness. Sonu, McCloy, and McArthur (1966) studied the relations between nearshore topography, longshore currents, and waves on the Outer Banks of Cape Hatteras. They noted that both

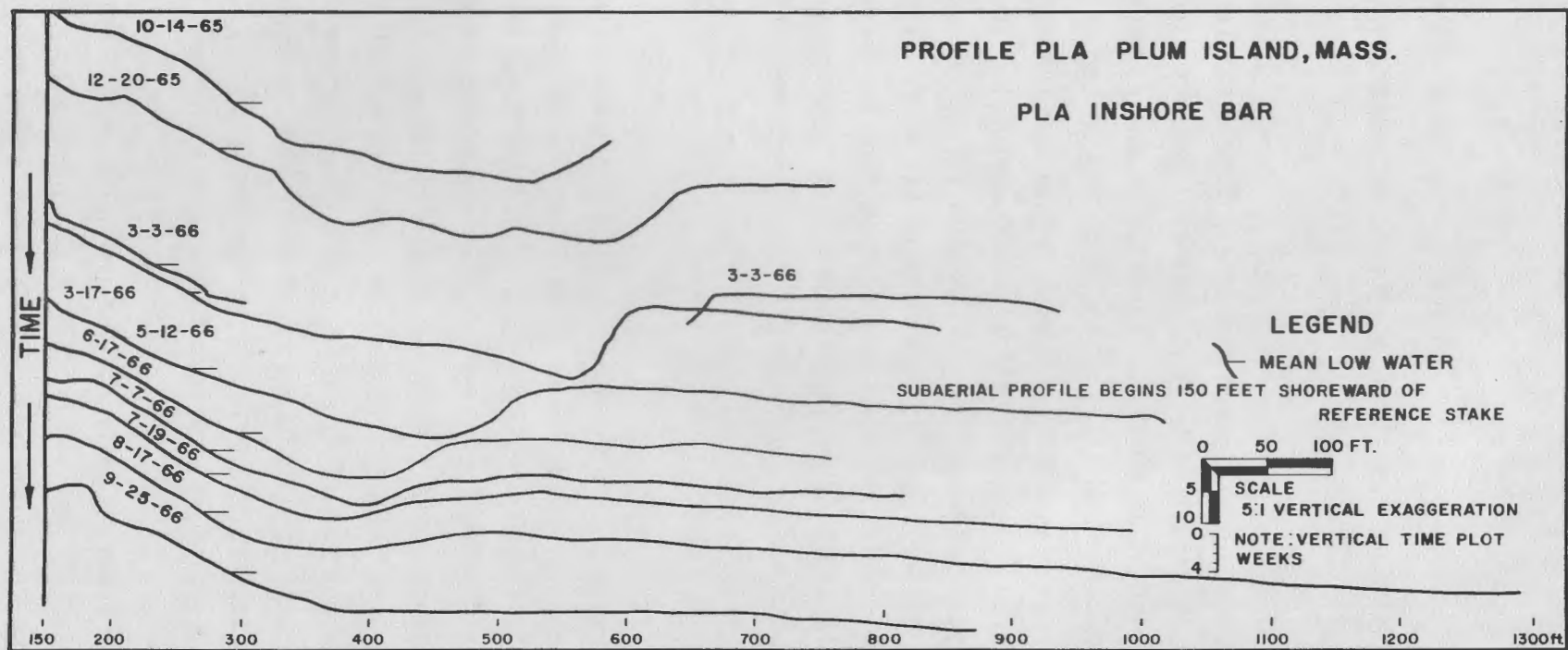


**FIGURE I**

seasonal and regional effects were large compared to the variables analyzed (longshore current velocity, angle of wave incidence, wind velocity, wave height and period, and bedslope).

A preliminary study was made of three subaqueous bars offshore from terrestrial profile stations PLA and PLB at Plum Island, Massachusetts (Fig. RL-1). The objectives were to determine the relation between changes in the subaerial profile and changes in the offshore topography, and the relations between the size of the offshore bars and general variations in wave conditions. Thus, this study was designed to determine if sand eroded from the beach during storms aided in the growth of offshore sand bars, and if this sand returned to the beach during calmer periods.

Ten subaqueous profiles were run within a one-year period (October 14, 1965 to September 25, 1966) over an inshore bar, located between the subaerial portion of the beach and the offshore bar, at profile PLA. Four subaqueous profiles were run at widely-spaced intervals within a period of 16 months (November 11, 1967 to January 29, 1969) over the bars offshore from profiles PLA and PLB. The earlier set of ten subaqueous profiles were run opposite PLA with a plane table, alidade, and a swimmer with a 20-ft. pole. The more recent subaqueous profiles were made over the offshore bars opposite PLA and PLB with a Raytheon fathometer. Subaerial profiles (from the permanent marker to M.L.W.) were run simultaneously with the measurement of each subaqueous profile. In addition, general observations of wave conditions were made.

#### PLA INSHORE BAR

The PLA inshore bar was first observed in October, 1965 about

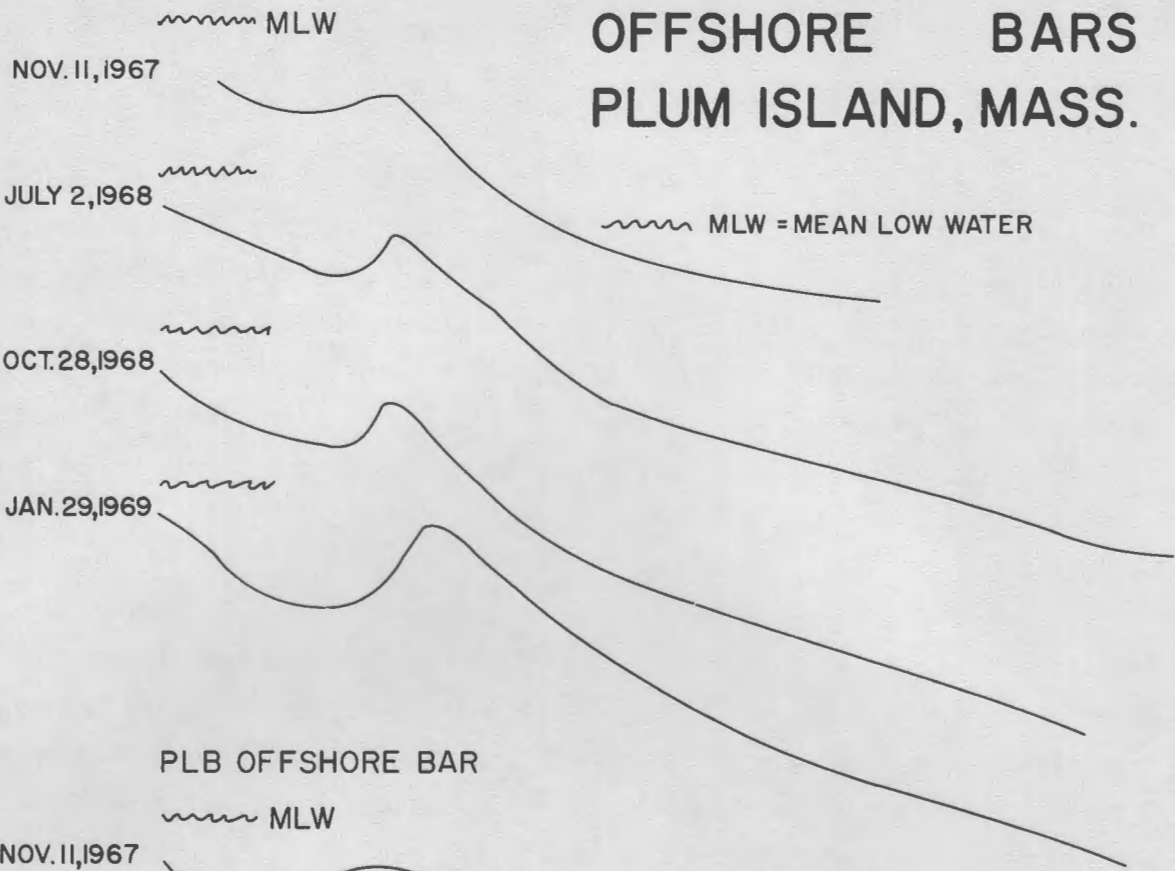
---

Figure 1. PLA inshore bar. Subaqueous profiles depicting the growth and migration of an inshore bar seaward of the PLA profile between October 14, 1965, and September 25, 1966.

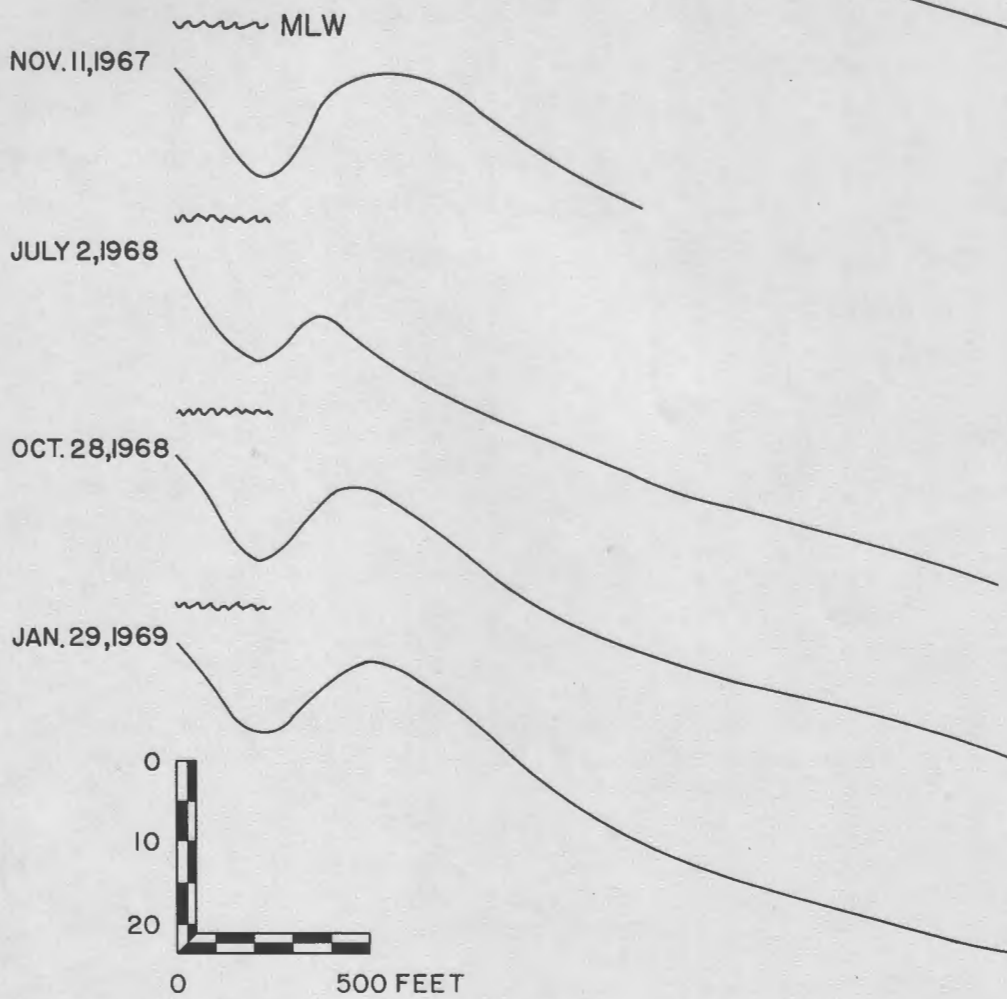
PLA OFFSHORE BAR

FIGURE 2

# OFFSHORE BARS PLUM ISLAND, MASS.



PLB OFFSHORE BAR



350 feet from the mean low water mark on the PLA subaerial profile, and within a year it had migrated inshore and welded onto the beach (Fig. 1). When first discovered, the bar was at a depth of six feet at mean low water (MLW) and was separated from the shore by a trough with a maximum depth of 16 feet below MLW. During the next six months, the bar grew on the seaward side as the shoreward slope steepened, but remained in the same relative position. During the period from March, 1966, through June, 1966, the inshore bar migrated approximately 250 feet shoreward, while retaining the same basic shape. During the summer of 1966 it welded onto the beach. Thereafter, the large mass of sand that had welded to the beach was transformed into a spit that migrated along the beach to the north, off the PLA profile. The spit then doubled back to trend in a southerly direction offshore from the PLA subaerial profile until it finally lost its identity as a distinct sand body. In general, the inshore bar had its largest growth during the winter months when storms with steeper waves were more frequent and while the adjacent beach was undergoing a net loss of sand.

#### PLA OFFSHORE BAR

The PLA offshore bar grew steadily from November, 1967, through February, 1969, while remaining in the same relative location approximately 650 feet seaward of the mean low water mark on the PLA subaerial profile (Fig. 2). On November 11, 1967, the relief of the bar was two feet and the trough/bar ratio was only 1.21 (Table 1). The PLA subaerial profile indicated that the beach had largely recovered from a storm that had occurred eight days previously. That is, a large portion of the sand which had been eroded from the beach during the storm had already returned to the beach.

On July 2, 1968, the bar was larger, with a relief of 5.3 feet

---

Figure 2. Offshore bars at Plum Island, Massachusetts. Subaqueous profiles depicting the changes in two offshore bars located seaward of the PLA and PLB profile locations, between November 11, 1967, and January 29, 1969.

Table 1

<u>Profile</u>	<u>Date</u>	<u>Subaerial Profile</u>	<u>Bar Depth*</u>	<u>Trough Depth</u>	<u>Relief</u>	<u>T/B</u>
			(feet below MLW) B	(feet below MLW) T		
PLA	11/11/67	Recovery	9.7	11.7	2.0	1.2
	7/2/68	Post-storm	8.7	14.0	5.3	1.6
	10/28/68	Between storms	9.3	15.3	6.0	1.7
	1/29/69	Between storms	7.2	15.2	8.0	2.1
PLB	11/11/67	Recovery	3.9	15.9	12.0	4.0
	7/2/68	Post-storm	10.5	16.8	6.3	1.6
	10/28/68	Between storms	8.0	16.6	8.6	2.1
	1/29/69	Post-storm	5.0	14.0	9.0	2.8

\* For vertical distance from top of:

PLA stake - add 27.78 ft.

PLB stake - add 30.22 ft.

and trough/bar ratio of 1.61. The terrestrial portion of the profile was largely erosional as the beach had only partially recovered from a severe storm that had occurred four days before, during which 8-to 10-foot waves had been observed.

On October 28, 1968, the bar was approximately the same size as shown on the previous subaqueous profile (July 2, 1968), while the PLA subaerial profile indicated a between-storm accretionary profile.

The January 29, 1969, subaqueous profile indicated a continued growth of the PLA offshore bar as well as a seaward migration of approximately 100 feet. The subaerial profile was again largely accretionary, as the area had undergone a relatively calm, storm-free period for the previous two months. However, during the time that this profile was being run, a severe northeaster was just beginning, and the waves were quite steep, with short periods and heights of about five feet.

On the days that the first two subaqueous profiles were run, long-period and low-amplitude waves were observed. However, in both these instances, the profiles were made shortly after storm conditions with accompanying steep waves of short periods and high amplitudes. The last two profiles followed extended periods of relative calm. Despite changes in the wave conditions and in the subaerial profiles, the PLA offshore bar displayed continued growth.

#### PLB OFFSHORE BAR

This offshore bar was located about 500 feet seaward of the mean low water mark on the PLB subaerial profile at the time of the first survey, November 11, 1967. The bar was quite large, with a depth of only 3.9 feet at the crest, and a trough/bar ratio of 4.0 (Table 1). The subaerial portion of the profile indicated that the beach had recovered from a storm which had occurred eight days before.

The subaqueous profile made on July 2, 1968, indicated that the bar had greatly diminished in size. The crest of the bar was 10.5 feet below the water surface at mean low water and the trough/bar ratio was reduced to 1.6. Also, the bar had migrated about 100 feet shoreward. The subaerial portion of the PLB profile was erosional and was just beginning

to recover from a severe storm which had occurred four days previously.

On October 28, 1968, the bar had migrated 100 feet seaward to its previous position and had grown up to within eight feet of the surface, with a trough/bar ratio of 2.1. The beach was largely accretional.

Three months later, on January 29, 1969, the bar was still larger, having a depth of only 5.0 feet at the crest and a trough/bar ratio of 2.8. The subaerial profile was largely erosional, having shown little recovery from an earlier storm.

Though the PLB offshore bar displays changes in size and in location, these changes do not correlate with changes in the subaerial profiles nor with changes in the wave conditions immediately preceding the running of these profiles.

#### TEMPORARY BARS

During periods of exceptionally heavy storm activity, when substantial amounts of sand are removed from the beach, large temporary sand bars form offshore. In February, 1969, during the course of four back-to-back northeasters, a large continuous bar was formed along the total length of Plum Island. The bar disappeared with the return of normal wave conditions and the recovery of the beach in March.

#### CONCLUSIONS

Based upon these limited data, it would appear that there is no obvious correlation between the size and location of these offshore bars and the cycle of storm erosion and recovery immediately preceding the running of these profiles. Therefore, two widely-spaced, subaqueous profiles are not sufficient to determine sand movement between bars and the adjacent beaches.

Other studies of the beaches on Plum Island indicate that the zones of most severe erosion and of most rapid recovery after storms slowly migrate down the beach over a period of years (M.O. Hayes and J. Boothroyd, personal communication, 1969). It is possible that the offshore bars also migrate along the beach and are in some way related to the observed shifting of zones of maximum erosion and accretion. The detailed studies of the PLA inshore bar indicate that migration of large volumes of sand

parallel to the beach does take place.

On an overall seasonal basis, the Plum Island bars tend to have their largest growth during the winter months when short-period, steep waves predominate and the beaches are undergoing a net loss of sand.

SEDIMENT DISPERSAL TRENDS IN THE LITTORAL ZONE; A PROBLEM  
IN PALEOGEOGRAPHIC RECONSTRUCTION<sup>1</sup>

Miles O. Hayes

Fayez S. Anan

Robert N. Bozeman<sup>2</sup>

Abstract: One of the most utilized methods for interpretation of ancient sedimentary basins is the reconstruction of basin paleogeography by means of paleocurrent analysis. This procedure requires the assumption that paleocurrent patterns trend down the depositional slope, delineating the dispersal trends of sediment into the basin.

Studies conducted along the northern New England coast show that this assumption is not always a safe one, particularly for estuarine and littoral environments on a coast with a large tidal range. Three major depositional regimes--ridge-and-runnel beaches, recurving spits at estuary mouths, and sand waves on estuarine sand flats--produce abundant crossbedding trending landward, or up the "depositional slope" away from the "basin" center.

Data collected on large-scale sand waves (wave length avg. 50-60 ft.; max. 143 ft.) on several intertidal sand flats show that the slip faces of these sand waves are oriented landward during both ebb and flood tides. This is brought about by the occurrence of stronger flood-tidal currents than ebb-tidal currents on the flats.

Major directional sedimentary structures (in the intertidal zone) that trend seaward are limited to beach-face deposits and to megaripples (wave length avg. 3-8 ft.) that occur predominantly near the estuary mouths and on spits marginal to tidal deltas.

---

<sup>1</sup> Abstract printed in Program, 1967 Ann. Mtg., Geol. Soc. America, Nov. 20-22, 1967, New Orleans, La., p. 93-94.

<sup>2</sup> Present address: 321 So. Sunset Canyon Drive, Burbank, California

Thus, an ancient equivalent of the depositional basin under study, which is located directly north of Cape Ann, Massachusetts, and consists of four estuary-barrier island systems, would show a complex paleocurrent pattern with a significant amount of the large-scale crossbedding trending away from the center of the basin.

#### INTRODUCTION

Paleocurrents have been used with much success as paleoslope indicators in ancient sedimentary basins, especially in studies of fluvial sediments. As Reineck (1963), Klein (1967), and others have pointed out, however, marine sediments present many difficulties with respect to prediction of paleoslope from paleocurrent analysis.

Discussion in this paper is restricted to the distribution of directional structures on the intertidal sand bodies of a small depositional area located between Cape Ann, Massachusetts, and the central coast of New Hampshire. Environments considered include estuarine sand flats, recurved spits at estuary mouths, and the ridge-and-runnel beaches of Plum Island and Crane Beach, Massachusetts. One of the earliest observations made in our studies of this shoreline was the fact that bedforms on many of the intertidal flats show a predominant landward orientation at all stages of the tide. This paper, which was presented orally before the Geological Society of America in New Orleans on 22 November, 1967, gives some of our earlier ideas on the subject. Since the original presentation, much more data has been collected and many refinements have been added to the overall scheme. However, the general conclusions of the original paper, most of which are repeated here, are still valid.

It is important to note that this paper is based primarily on intertidal zone structures. Later studies of the subtidal zone indicate that the pattern of orientation of sedimentary structures is much more complex in that environment.

#### ESTUARINE SAND FLATS

In the study area, large-scale bedforms are abundant on the intertidal sand flats of several flood-tidal deltas and on the large point bars of the Parker River estuary. A preliminary study of sand waves on the flood-tidal delta and central point bar of the Parker River estuary was conducted by the writers in August, 1966. Three

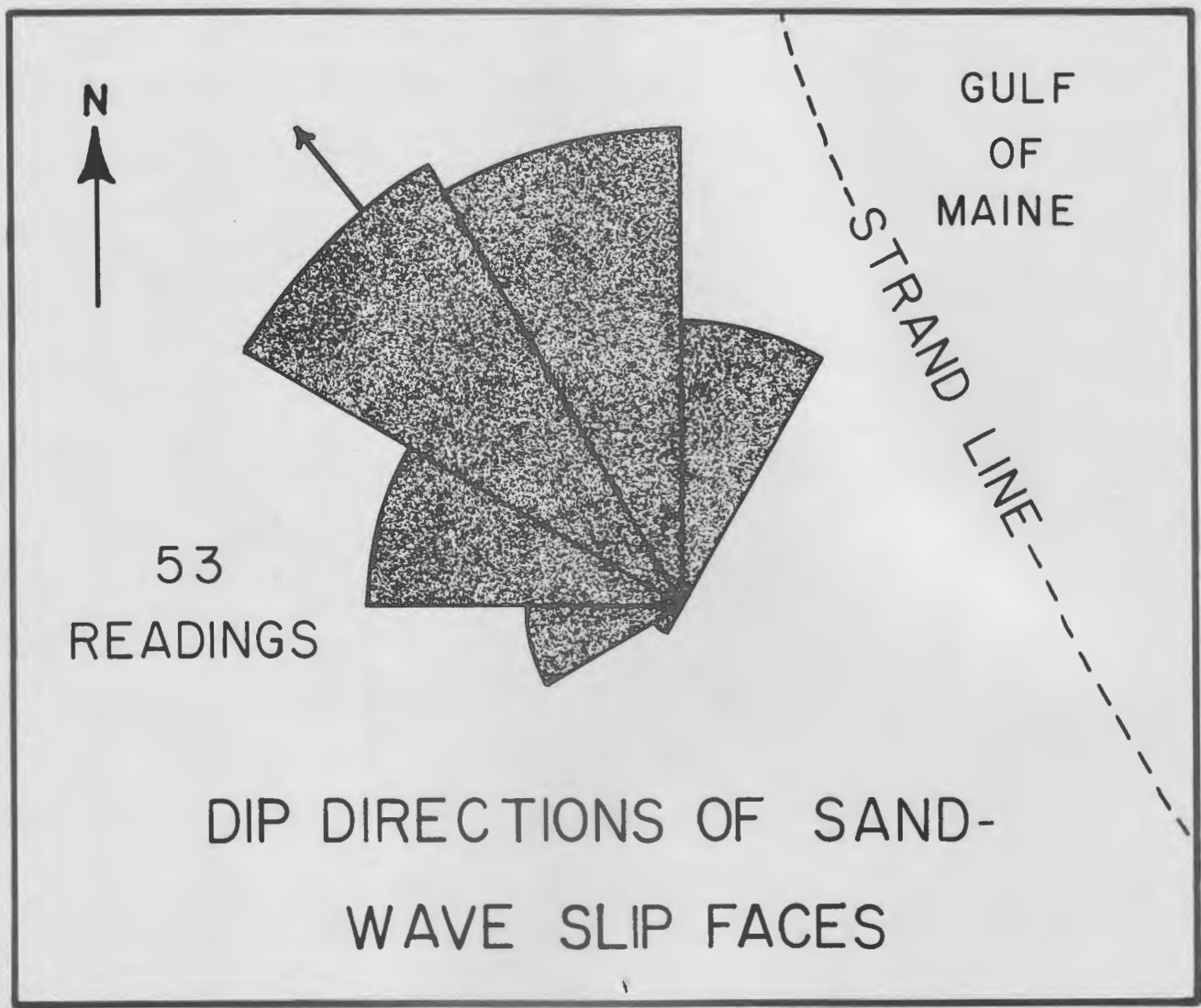
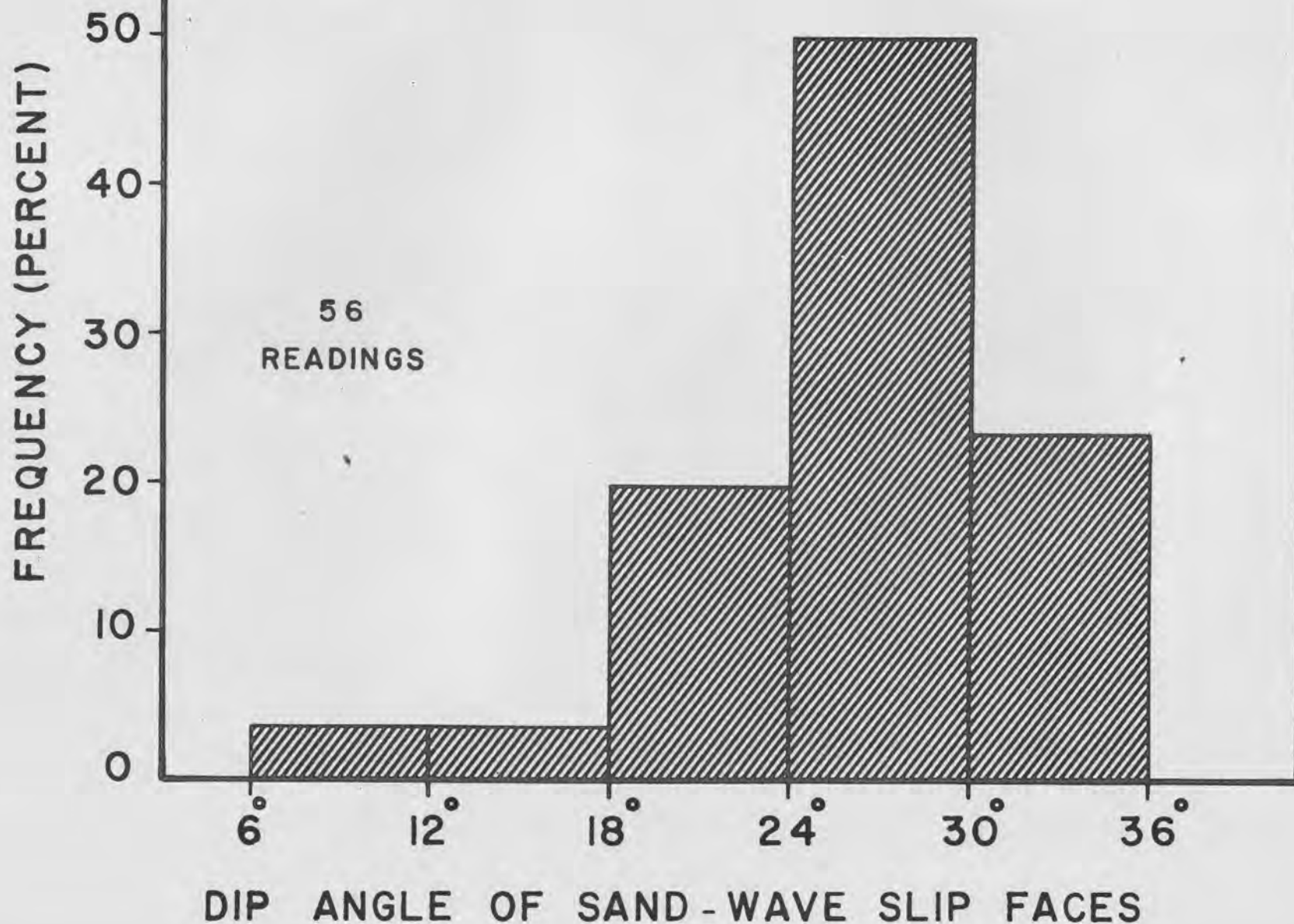


FIGURE 1

FIGURE 2



transect lines were established, two on the flood-tidal delta and one on the central point bar. Along each transect, the wave length, amplitude, dip angle of the slip face, and slip-face orientation for each sand wave was determined. All measurements were taken at low tide, yet the sand waves measured showed a 100 percent orientation in the flood direction. The rose diagram in Figure 1 summarizes the azimuths of the sand-wave slip faces. The modal angle of dip of the sand-wave slip faces was flood-oriented between  $24^{\circ}$  and  $30^{\circ}$  (avg.  $26^{\circ}$ ; Fig. 2), which indicates that there was very little modification of the flood-oriented slip faces by ebb currents.

Since this work was completed, the intertidal sand bodies of the Parker River estuary, as well as several other estuaries, have been investigated in much greater detail. This later work is summarized in the descriptions of Stops 8b, 15, 16, 17, 18, and 26 by DaBoll, Greer, Boothroyd, and Hartwell.

Our initial conclusion, then, which has been verified by later studies, was that sand waves on the intertidal sand bodies of the four estuaries under study are dominantly land-oriented. The complexities and modifications of this general scheme are discussed elsewhere in this guidebook.

The dominance of flood currents over the intertidal sand flats in these estuaries is apparently related to three primary factors:

(1) Time-Velocity Asymmetry of Tidal Currents

Inspection of over 100 tidal-current velocity curves measured in the four estuaries under study indicates that there is a general time-velocity asymmetry of tidal currents. That is, the maximum flood velocity

---

Figure 1. Dip directions of sand-wave slip faces for 53 sand waves measured at low tide along 3 transects in the Parker River estuary. The estuary mouth is located to the southeast. Note the complete dominance of flood orientations for these sand waves.

Figure 2. Histogram summarizing dip angles of sand-wave slip faces collected along the same transects as the measurements for Figure 1.

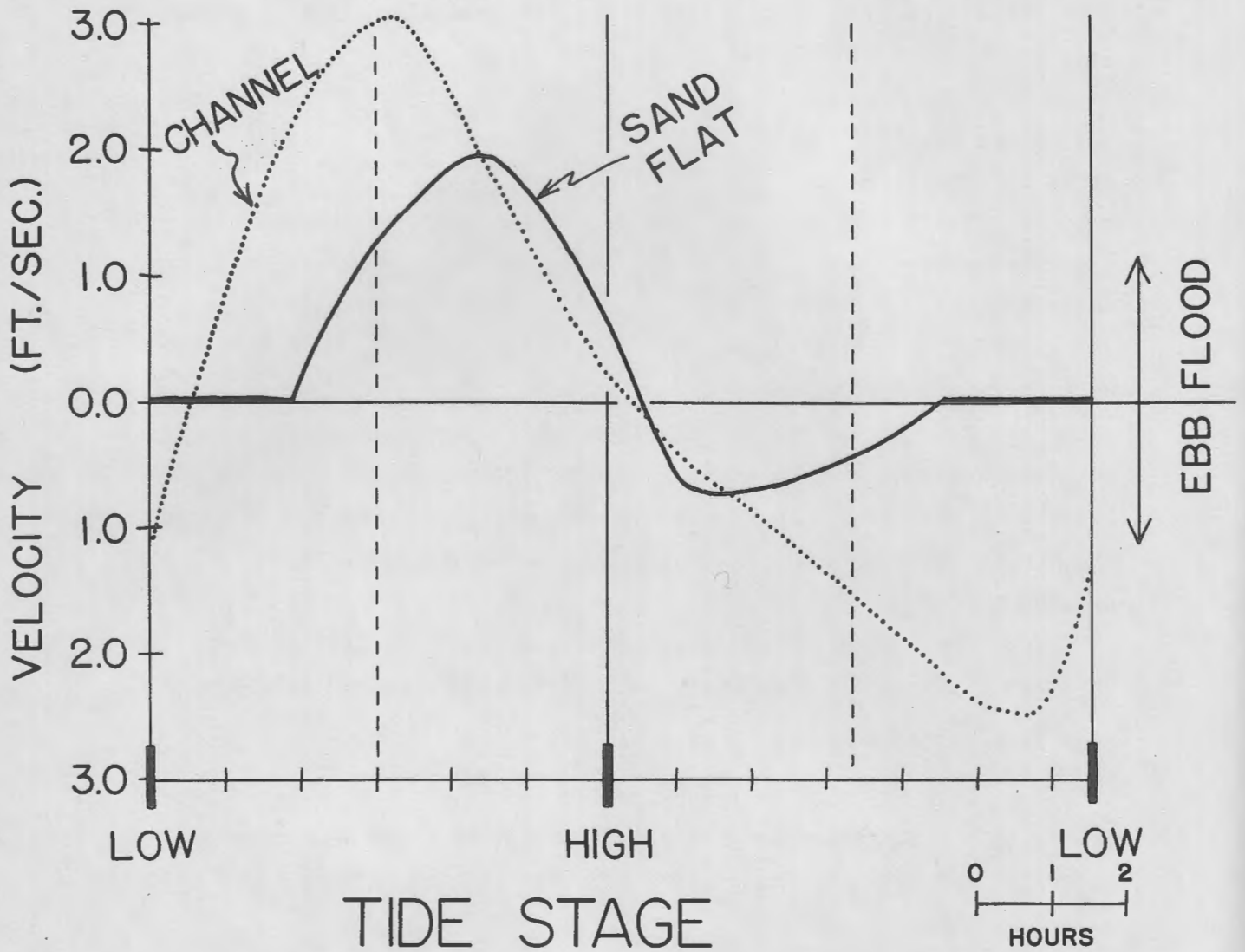


FIGURE 3

normally occurs sometime after mid-tide, or closer to high tide than to low tide, and the maximum ebb velocity occurs late in the ebb period near low water. Two typical tidal-current velocity curves are shown in Figure 3. These two curves were measured at stations located in the vicinity of the flood-tidal delta of the Parker River estuary. One station was located on an intertidal sand flat and one in a nearby large channel. Note that flood currents are much stronger than ebb currents over the flat. On the diagram (Fig. 3), the horizontal, zero-velocity zones indicate parts of the cycle during which the flat was uncovered. The important point about the channel curve (Fig. 3) is that maximum ebb velocities occur late in the cycle, near low tide. Therefore, maximum ebb velocity occurs when the sand flat is completely uncovered. The time-velocity asymmetry of tidal currents in estuaries is discussed at length by Postma (1967).

### (2) Shielding of Flats by Elevated Up-Current Margins

As sediment is transported onto flood-tidal deltas and up the flood bifurcations off the main tidal channels, mounds of sand tend to accumulate around the delta margins and at the up-current ends of the flood bifurcations. During the ebb period, maximum ebb velocity is not attained until after the water level drops below the crest of the sand mounds, hence ebb currents are diverted around the boundary of the flats. Thus, the flood waves formed by flood currents are shielded from modification by ebb currents. These mounds of sand that accumulate on the up-current margins, in the flood sense, of the sand bodies are referred to as ebb shields in the classification scheme of the Coastal Research Group (Univ. Mass.).

### (3) Residual Currents in Major Tidal Channels

Early in the flood stage, a residual ebb flow remains in the large channels; therefore, early flood currents follow paths of least resistance across the sand flats, insuring an early movement of sand in the flood, or landward, direction.

---

Figure 3: Curves of surface current velocity through a complete tidal cycle at 2 stations near the flood-tidal delta of the Parker River estuary. The solid horizontal portion of the sand-flat curve indicates the periods during which the flat was uncovered. Note the extreme asymmetry of the ebb-velocity curve for the channel station.



FIGURE 4

## RECURVED SPITS

Recurved spits are commonly attached to the ends of barrier beaches and barrier islands at estuary mouths. An excellent example of such a recurved spit occurs at the south end of Plum Island (Fig. 4). Details of the growth and history of change of this spit are presented by Farrell elsewhere in this guidebook (p.316 ). The end of the Plum Island spit projects in a landward direction, as a result of the thrust of wave motion into the Parker River estuary. At high tide, the spit migrates by building an accretionary slip face that dips in a landward direction. The high-angle, land-oriented bedding formed by the migration of this spit is illustrated in Figure 5.

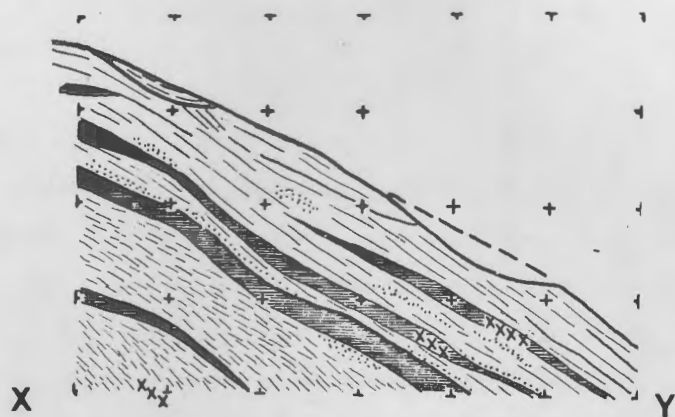


Figure 5: Internal structure of trench dug along "x-y" through the end of the recurved spit on Plum Island (Fig. 4). These high-angle, planar crossbeds dip landward. Crosses delineate one-foot squares.

---

Figure 4: Recurved spit at southern end of Plum Island, Massachusetts (20 August, 1966). Trench dug along line x-y is shown in Figure 5.

## BEACH ZONE

Because of the large tidal range and the broad exposure of the beach zone at low tide in northern New England, it is possible to examine in detail the internal structures of sand bodies deposited on the beach. The construction of sand bodies on the beaches is related closely to storm activity (see paper on storms elsewhere in the guidebook, p.245 ). The constructional profile on northern New England beaches consists of the following subdivisions: (a) a low-tide terrace; (b) a ridge which builds up rapidly in the interim between storms and migrates landward; (c) a runnel that forms behind the ridge; and (d) a small berm that develops on the backbeach (the "incipient berm"). As time passes, the ridge migrates landward, eventually welds onto the backbeach, and is finally molded into a broad, convex-upward profile. The primary sedimentary structures that form in each of the subdivisions of the constructional profile will next be considered.

### Low-Tide Terrace

Although our studies of the low-tide terrace are somewhat limited, two types of primary structures appear to dominate, horizontal lamination and festoon crossbedding. Plane beds and other upper flow-regime structures are formed near the low-water stage of the tidal cycle under conditions of sheet flow across the low-tide terrace. Antidunes have been observed on the low-tide terrace numerous times and they are commonly left preserved at low tide (Fig. 6). In addition to the upper flow regime structures, which are usually formed near low tide, festoon crossbedding is developed by the migration of scour-megaripples across the low-tide terrace during periods of high water. These scour-megaripples have been observed many times, but, as yet, we have not discerned any consistent pattern in their orientation. Thus, trenches dug in the low-tide terrace frequently reveal parallel laminations, formed in the upper flow regime during sheet flow across the terrace, interlayered with festoon crossbedding (Fig. 7).



FIGURE 6

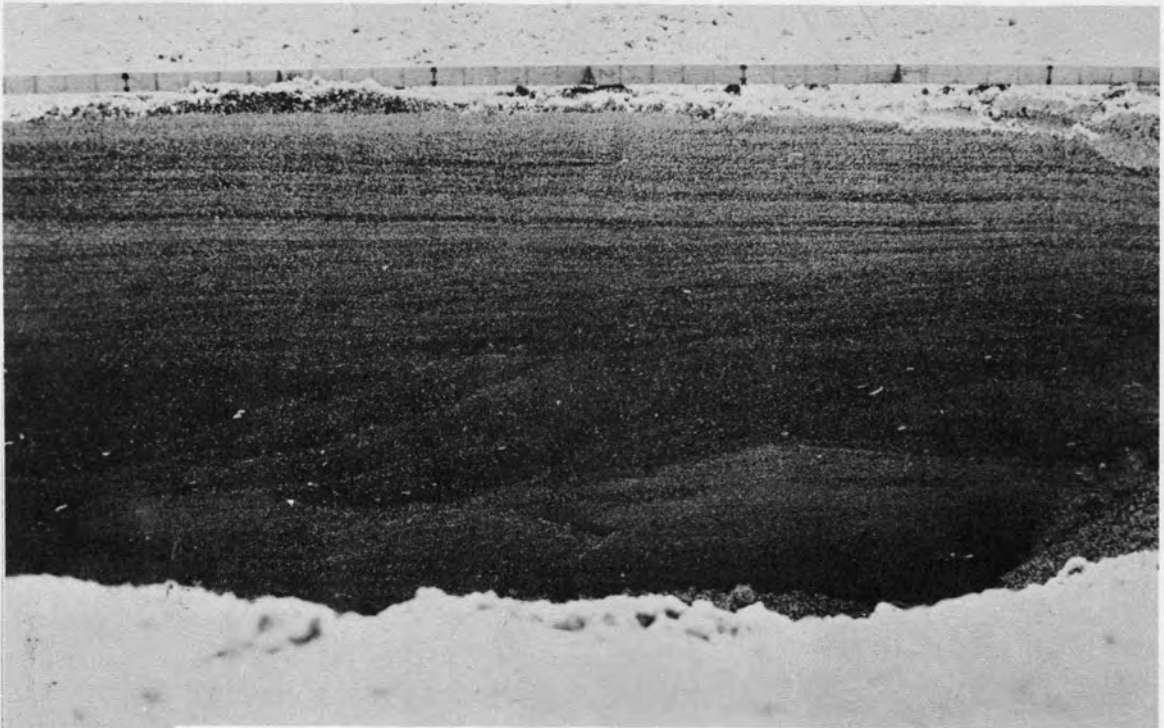


FIGURE 7

# RIDGE CROSS-SECTION

21 JULY, 1966

SOUTH OF STATION CBA, CRANE BEACH  
IPSWICH, MASS.

← 200' TO DUNES



0 1 2 3 4 5 FEET

SCALE: ONE INCH = ONE FOOT  
HORIZONTAL AND VERTICAL

FIGURE 8

## Ridge

Ridge structures are clearly revealed in trenches dug through the ridges at low tide. Figure 8 is based on a trench dug at Crane Beach on 21 July, 1966. A sketch of structures in the trench (Fig. 8) shows the typical high-angle, land-oriented crossbedding that formed as a result of migration of the ridge toward the backbeach. These ridges grow both by foreset accumulation in the landward direction as the ridge migrates and by vertical accretion of horizontal beds, especially on the seaward side.

## Runnel

Formation of a large ridge, such as the one shown in Figure 8, creates a trough (runnel) behind the ridge that runs parallel with the beach, sometimes for hundreds of feet. As the tide level drops, or as waves overtop the ridge, the return flow is blocked by the ridge and channeled parallel with the beach until an outlet is reached. Currents generated by this process form ripples and megaripples that are oriented parallel with the main strike of the beach (Fig. 9). Also, waves overtopping the ridge sometimes form asymmetric ripples oriented toward the land. Commonly, small ripples are superimposed on the backs of the larger, wave-generated ripples during late-stage draining of the runnel (Fig. 10). Therefore, three primary directions of orientation are present in the runnel, landward, and in two directions parallel with the beach.

---

Figure 6: Antidunes preserved on the low-tide terrace (at low tide) at Old Orchard Beach, Maine.

Figure 7: Typical primary structures preserved on the low-tide terrace on the Plum Island beach. Note interlayering of planar beds, formed by sheet flow near the low-water stage of the tidal cycle (upper flow regime) and festoon crossbeds, formed by migrating scour-megaripples during periods of high water level.

Figure 8: Internal structure of a large ridge located south of profiling station CBA (Crane Beach) on 21 July, 1966. The left portion of the ridge (as revealed in a trench cross-section) contains mostly high-angle crossbeds dipping landward that were formed by the migration of the ridge slip face as waves overtopped the ridge crest at high tide. The right portion contains abundant horizontal bedding that formed in the plane bed phase of the upper flow regime.

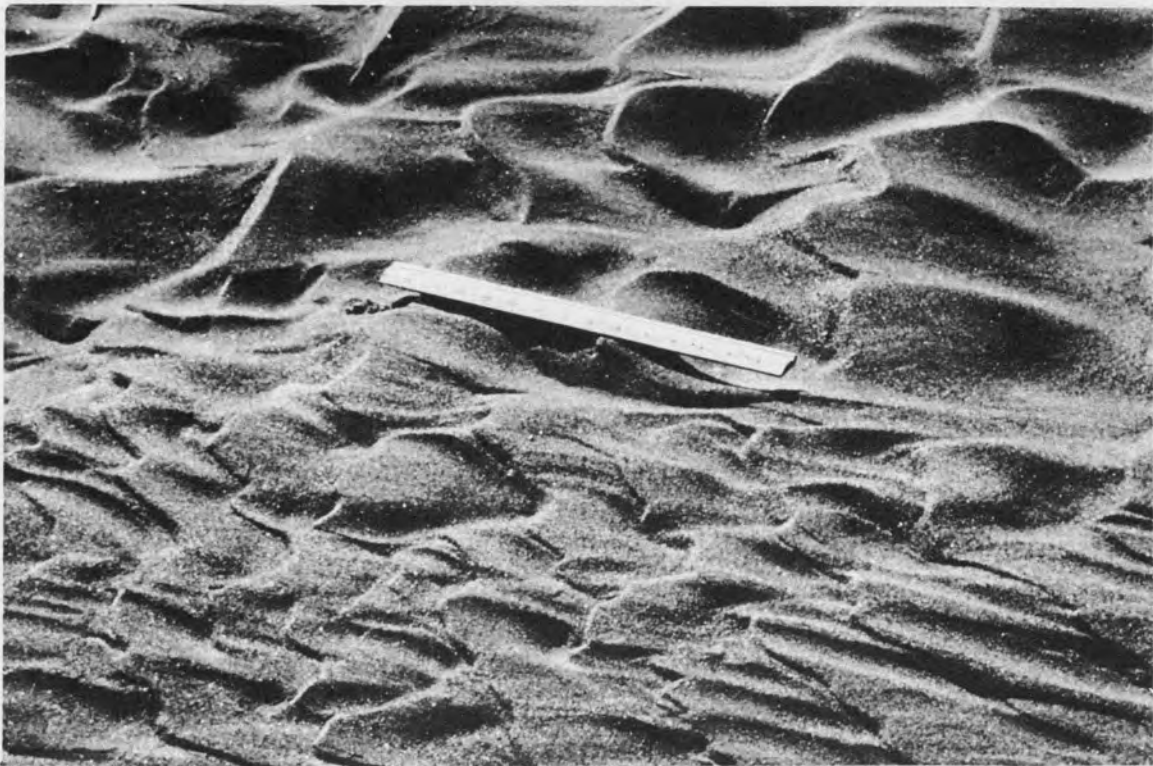


FIGURE 9A



FIGURE 9B

### Incipient Berm

As the ridge migrates toward the backbeach, gently dipping, seaward-oriented bedding accretes on the beach face of the small incipient berm. These beds generally dip at angles between  $5^{\circ}$  and  $15^{\circ}$ .

### Welded Berm

As the ridge grows, it commonly welds onto the backshore to form a wide, stable profile. This happened near Camp Sea Haven in late August, 1967 (Fig. 11). Photographs in Figures 12 and 13 illustrate the nature of internal structures in the large welded berm. At the time of observation, the beach face had been modified by neap-tide erosion and by the draping of beach face deposits across the erosion surface, which dipped seaward at an angle of  $13\ 1/2^{\circ}$ . Vertically downward below the crest of the beach face, the bedding changed from seaward-oriented (low angle) at the top, to parallel lamination in the middle, to planar crossbeds dipping landward at angles of  $30^{\circ}$  at the base (Fig. 11). Further landward, toward the middle of the berm, a deep trench revealed abundant landward-dipping, high-angle crossbedding. The photographs in Figure 13a,b illustrate these structures. Again, the high-angle, land-oriented crossbeds that made up the bulk of the Camp Sea Haven welded berm deposit were generated by the migration of ridge slip faces in the land direction (Fig. 14).

### Summary

To summarize beach structures, we have constructed a hypothetical stratigraphic sequence of sediments deposited by beach subenvironments

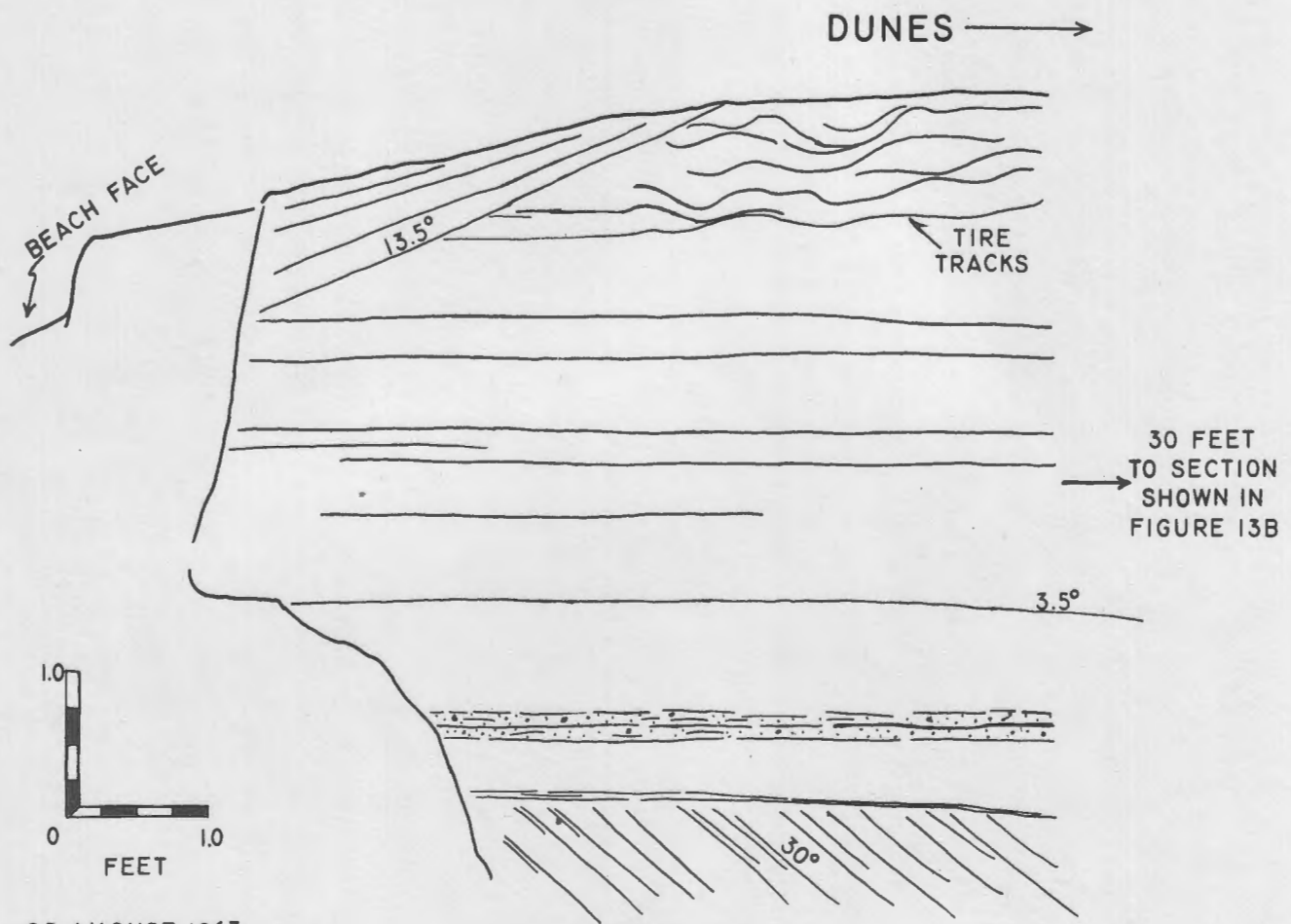
---

Figure 9. Typical ripples (A) and megaripples (B) formed in the runnel on the Plum Island beach. In (A) the view is toward the sea and in (B) the view is toward land. Ripple crests are oriented perpendicular to the strike of the beach in both photographs. Scale is a fifteen-inch ruler.

Figure 10. Land-oriented, asymmetric ripples formed by wave-generated currents. Location is in the runnel on central Plum Island beach (photo taken at low tide). Beach face is on the right. Note ladder-backing effect formed by runnel drainage from top to bottom of the photograph as a result of falling tide level.



FIGURE 10



23 AUGUST 1967

FIGURE II

during a transgressive cycle (Fig. 16). Hypothetical rose diagrams indicate predicted paleocurrent trends for each environment. Land lies to the left of the hypothetical strand line shown on the figure. This sequence is based on inspection of over 100 trenches dug in the various subenvironments of the beach zone.

At the base of the proposed transgressive sequence would be low-angle, seaward-dipping beds (Unit A). They are usually medium grained and well sorted and frequently contain abundant heavy minerals. These are the beds deposited on the flat, post-storm profile (Fig. 15).

Beds in the next unit, Unit B, dip seaward at higher angles than A, and the sediment is relatively fine grained. This is the incipient berm deposit; it may be absent in some places.

Unit C represents runnel deposits. They would consist of ripples and crossbedding of different scales, oriented both parallel with and perpendicular to the beach. Some ripples in the runnel would show a dominant land orientation. This deposit would yield a trimodal rose diagram for directional structures.

Unit D is the ridge-formed unit. These beds, formed by the ridge as it migrates over the runnel, are primarily parallel and landward-dipping. A rose diagram of crossbed azimuths would show a primary landward orientation. Crossbeds usually dip between 20° and 30°.

Overlying the ridge deposits would be beach-face sediments, Unit E, which dip seaward at angles from 5° to 15°. They would produce a unimodal rose diagram for crossbed dip azimuths.

---

Figure 11. Internal structure of seaward edge of a welded berm at Camp Sea Haven, Plum Island, on 23 August, 1967. The three major types of bedding are: (a) Low-angle seaward-dipping beds formed by on-lapping of layers over an erosional surface that dips seaward at an angle of 13 1/2°; (b) Horizontal bedding, which occupies most of the central part of the trench, formed by the vertical upbuilding of a large ridge as it migrated landward. These beds are plane beds in the flow regime scheme; hence, they are formed under conditions of relatively shallow, very high velocity flow; and (c) Landward-oriented, high-angle (30°) crossbeds at the base. These crossbeds are formed by landward migration of the ridge in its initial stages of development.



FIGURE 12A



FIGURE 12B

The uppermost sediments, Unit F, are low-tide terrace and surf-zone deposits which would probably show a random orientation pattern for directional structures. They are made up of festoon crossbeds and interlayered planar beds. Presumably, antidune structures could be present, but we have not observed any in the trenches we have examined.

#### CONCLUSIONS

An ancient equivalent of this depositional basin would show a complex paleocurrent pattern. Surprisingly, a high percentage of the large-scale crossbedding would trend away from the center of the basin, or up the "paleoslope." This study is based entirely on intertidal-zone sand bodies, so the application of this model should be restricted to that zone. Details on the subtidal environment and more elaboration on the intertidal environment are given in Stop descriptions and papers by Boothroyd, DaBoll, Greer, and Hartwell, elsewhere in this guidebook.

---

Figure 12. Photographs of the trench illustrated in Figure 11.

A. Upper portion of trench.

B. Lower portion. The coarse layer at the level of the top of the machete handle is indicated by an arrow on photograph A. Note the high-angle crossbeds at the base of the trench that dip landward at an angle of approximately 30°.



FIGURE 13A



FIGURE 13B

Figure 13.

A. View of the middle portion of the trench at Camp Sea Haven, looking south. Note the abundant landward-dipping crossbedding in the middle of the trench.

B. Close-up of the middle portion of the trench shown in photograph A. Note the landward and upward growth of the crossbedding formed by the advancing slip face of the migrating ridge.



FIGURE 14

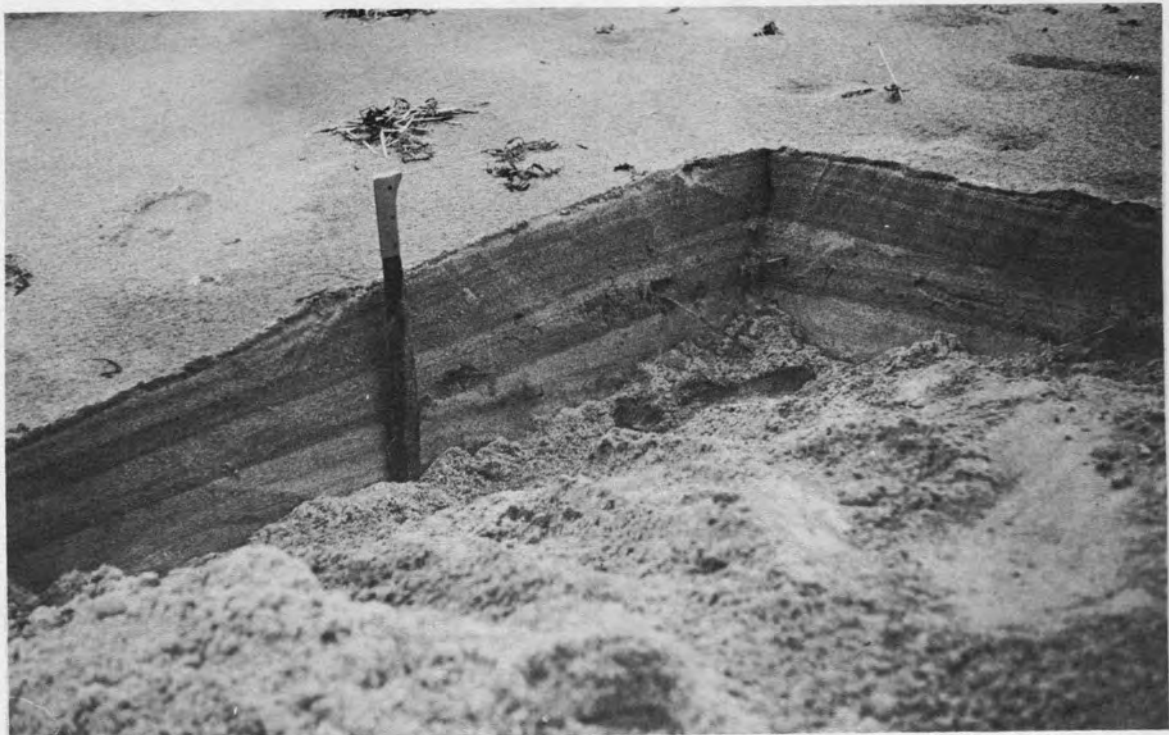


FIGURE 15

Figure 14. Internal structure of a typical ridge, showing high-angle, landward-oriented crossbedding. Compare this photograph with the one in Figure 13B.

Figure 15. Typical beach bedding on a post-storm beach. Photograph taken on 27 May, 1967, following an intense northeasterly storm. The dark beds are concentrations of heavy minerals (predominantly garnet).

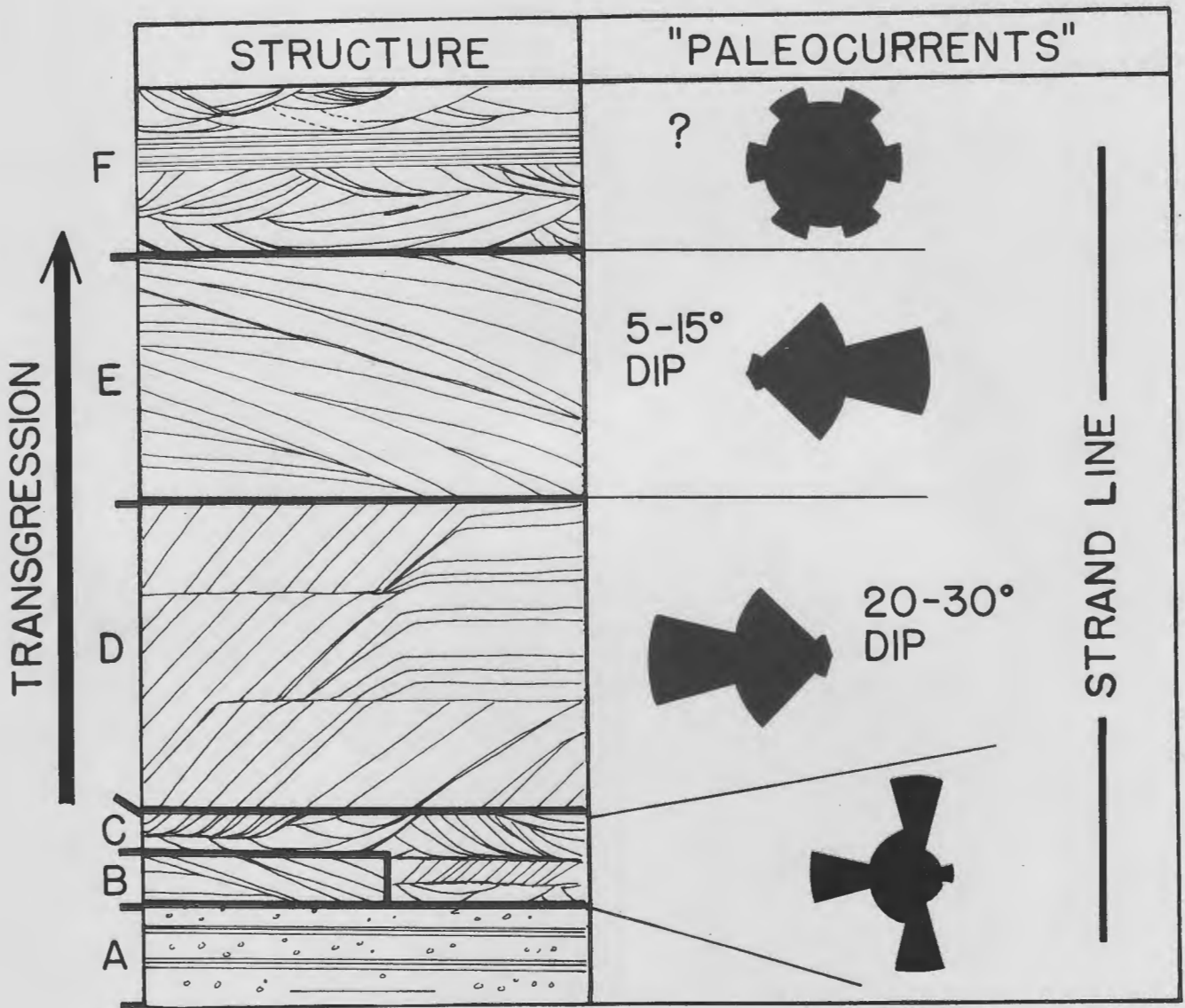


FIGURE 16

Figure 16. Hypothetical vertical sequence of primary structures formed by the transgression of the beach subenvironments of northern New England over a fixed position. Land lies to the left of the hypothetical strand line.

GROWTH CYCLE OF A SMALL RECURVED SPIT,  
PLUM ISLAND, MASSACHUSETTS

Stewart C. Farrell

Abstract: Successive increments in the growth of a small spit on the south end of Plum Island, Massachusetts, were observed by using aerial photographs taken periodically from April 4, 1965, to September 12, 1968. After April 4, 1965, growth began from a foreland cusp, with the resulting transportation and deposition of 368,000 cu. yds. of sand to form a double hooked spit by March, 1969.

Analysis of 17 surface samples shows a bimodal sediment distribution separable into a windblown fine fraction ( $2.75\phi$ ), which is dominant on that portion of the spit that is built above mean high water, and a coarse waterborne fraction ( $1.5\phi$ ) dominant on the spit beach face. These two modes are mixed in several samples from transitional areas.

Twenty-five short sand cores demonstrate transgression of the spit, by wave overwash at high tide, over lagoonal organic deposits. The slip-face sands and organic deposits are intertongued, which suggests that spit deposition occurred in pulses followed by periods of quiescence.

INTRODUCTION

This study is concentrated on the details of the growth cycle of a small, recurved spit attached to the south end of Plum Island (for location see Fig. RL-1, p.7 of this guidebook). The ocean-facing beach of Plum Island ends at a drumlin at its southernmost point. From there the beach curves west around and into the Parker River estuary. On this south-facing shore, sand accumulates by beach drift, and a combination of refracting waves and flood-tidal currents shape it into the spit form.

This discussion has three main facets. First is the examination of a series of low-altitude aerial photographs which give a pictorial history of changes in the spit over a period of four years. Second, the details of growth and sand movement are portrayed in six maps prepared between March 23, 1967, and May 29, 1967. Sediment analysis provides information regarding mode and origin of transported materials. Third, a method to discover and delimit older spit and lagoonal organic deposits is derived through correlation of sand cores.

## LONG-TERM CHANGES

The first photograph, taken April 4, 1965, is the base map to which all other changes are referred (Fig. 1). The south end of the island is divisible into three provinces: the drumlin and ocean-facing beach; the cusped north shore of the estuary channel; and the old, narrow spit and lagoonal area up-channel from the cusp. The photographs of Figures 1 to 8 focus on events occurring in the second province as growth was initiated on the landward side of the cusp.

By August 20, 1966, a new spit had grown as a long, curved finger of sand, forming a lagoon behind it (Fig. 2). The lagoonal area is termed the basin in this paper.

The photograph in Figure 3 was taken April 20, 1967, on the same weekend that the map of April 22, 1967, was surveyed. From November, 1966, to November, 1967, most of the sand transported around the drumlin was deposited on the seaward side of the foreland cusp. This created a wide beach off the cusp, but there were no major advances of the spit itself. However, after April 20, 1967, a small lobe began to grow from a point indicated in Figure 9 by an X. Accelerated deposition here resulted in the formation and rapid growth of a second hooked spit from August, 1967 (Fig. 4), to April, 1968 (Fig. 5).

The length of the first hook was 785 feet. Using it as a scale, an approximation of the rate of deposition of the second hook can be made. Visually comparing the two spits in Figure 5, the second one can be estimated to be about 1200 feet in length. The growth of the second spit occurred over a period of 239 days, an average rate of 5.2 ft./day. The first hooked spit, still present in muted form, appears in all subsequent photographs.

The growth of the second hook continued through the spring and summer of 1968, as shown in Figures 6 and 7. The final photograph on September 12, 1968, shows the second spit to be about 2000 feet long and 600 feet wide. The thickness of these deposits was found to be about 7 feet. Calculations yield volumes of 57,000 cu. yds. for the first hook and 311,000 cu. yds. of sand in the second hook. These are minimum quantities, since counting sand transported up into the estuary may well give a total of up to half a million cubic yards of sediment.

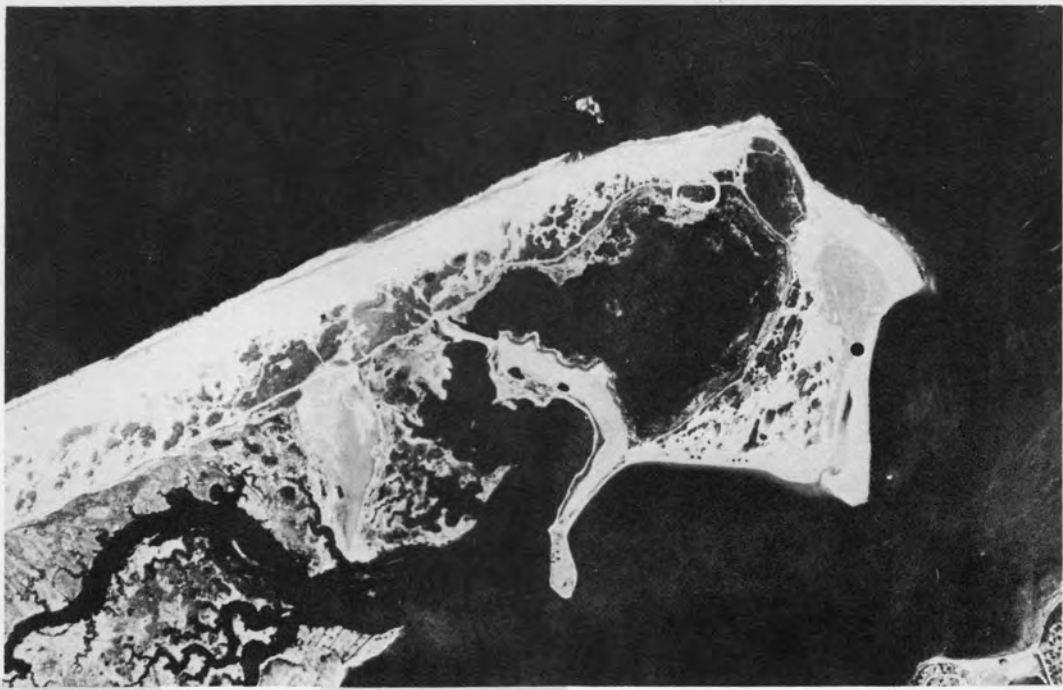


FIGURE 1

APRIL 4, 1965



FIGURE 2

AUGUST 20, 1966

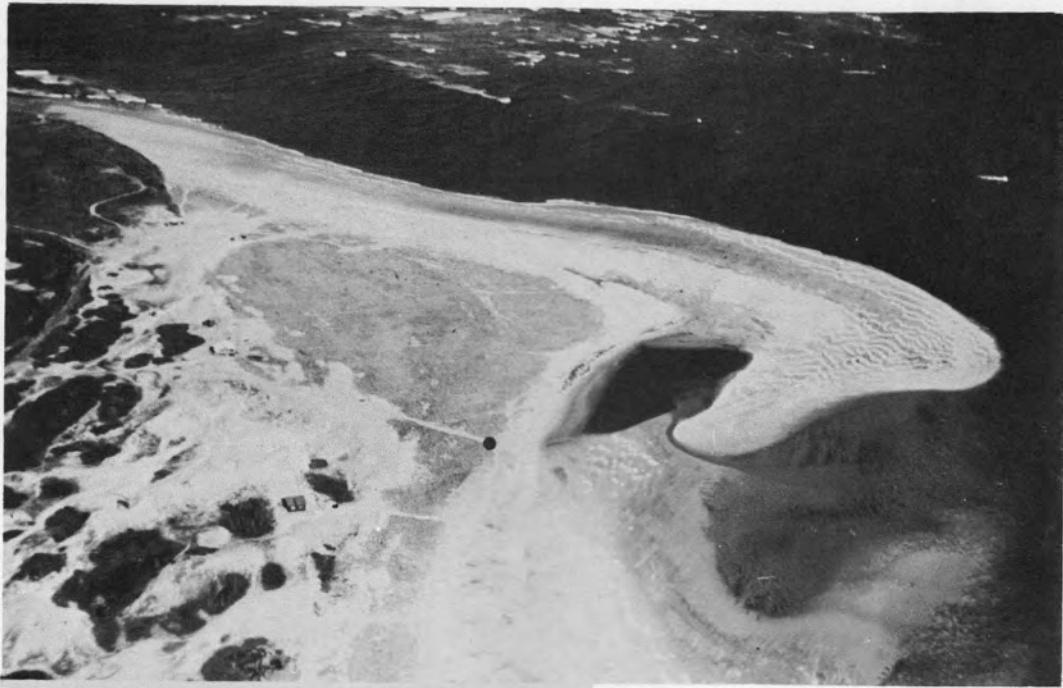


FIGURE 3      APRIL 20, 1967



FIGURE 4      AUGUST 24, 1967

Figure 1. United States Geological Survey photograph at 1:24,000 scale showing the entire south end of Plum Island. The small black dot in each photograph is included as a reference point.

Figure 2. The first curved finger of sediment was built rapidly up-channel. The organic layer deposited behind this spit was later discovered during coring operations.

Figure 3. The spit was photographed two days before it was surveyed April 22, 1967. Note the wind-created dunes on the surface of the spit and the linear streaks of sand on the sand flats.

Figure 4. Deposition during the summer of 1967 was primarily on the seaward side of the cusp, building a wide beach. The lobe on the channel side was the site of rapid deposition during the following winter.



FIGURE 5                      APRIL 19, 1968



FIGURE 6                      JUNE 15, 1968



FIGURE 7                      SEPTEMBER 12, 1968



FIGURE 8                      AUGUST 24, 1967

Figure 5. The second hook built rapidly up-channel during a 239-day period from August 24, 1967, to April 19, 1968. The rate of advance averaged 5.2 feet per day.

Figure 6. The second hook continued to advance across the sand flat in late spring and early summer, 1968, growing both longer and wider. The partly vegetated ridge, in the lower left, was originally the end of the spit on April 20, 1965.

Figure 7. Since this photograph was taken, the end of the spit advanced to and welded onto the Plum Island beach face, establishing an unbroken shore.

Figure 8. Multiple ridges advancing up onto the cusp beach face. The ridges orient themselves parallel with the wave trains striking the beach and reflect the dynamic tendency of a beach to lie perpendicular to wave orthogonals. The whole spit area for this date is shown in Figure 4.

In Figure 6, the remnants of the April 4, 1965, spit can be seen supporting dune growth and vegetation.

During the four years of observations in this area, an accretionary cycle was observed. Sand transported around the drumlin does not sweep directly into the upper estuary, but builds a cusped foreland by extending the trend of the beach to the southwest (Fig. 1). This construction takes the form of wave-built ridge-and-runnel structures which are beautifully displayed in Figure 4 and in greater detail in the close-up of the cusped foreland taken the same day (Fig. 8). The cusp results from the tendency for a beach to align itself perpendicular to the wave orthogonals approaching it. The northeast-southwest trend in this instance is the result of refraction of the waves around the eroded boulder platform directly offshore from the remaining part of the drumlin. As the cusp builds into the estuary channel, the flooding current carries sand around the tip and deposits it in the upstream current shadow, initiating the formation of the spits.

During the period of accretion of a spit, the rate of growth is a function of neap tides, spring tides, and storms. The rate increases approximately in the ratio of 1:2:10x for the above agents.

At the southwest corner of Plum Island, the Parker River turns north-northwest. When the nose of the accreting spit reached this point, it became welded to the shore of Plum Island, because the north-northwest shift in the current direction carried sand across the tip of the spit, turning it inward and against the shore. Storm overwash also aided this process by depositing material in avalanche slip faces along the inside margin of the spit. The period of observation has spanned one complete growth cycle. Figures 1 and 7 are approximately in the same position on the cycle.

A possible mechanism for the cyclic nature of spit growth may lie in a dynamic equilibrium between the tidal-water prism volume of the Parker River estuary and sedimentation rates in the estuary proper. As the estuary fills with sediment and marsh growth, the tidal volume decreases and consequently so does the size of the channel needed to carry the flow. The prograding series of welded spit ridges keeps pace with this decreasing channel cross section.

PLUM ISLAND SPIT  
MAP OF MARCH 23, 1967

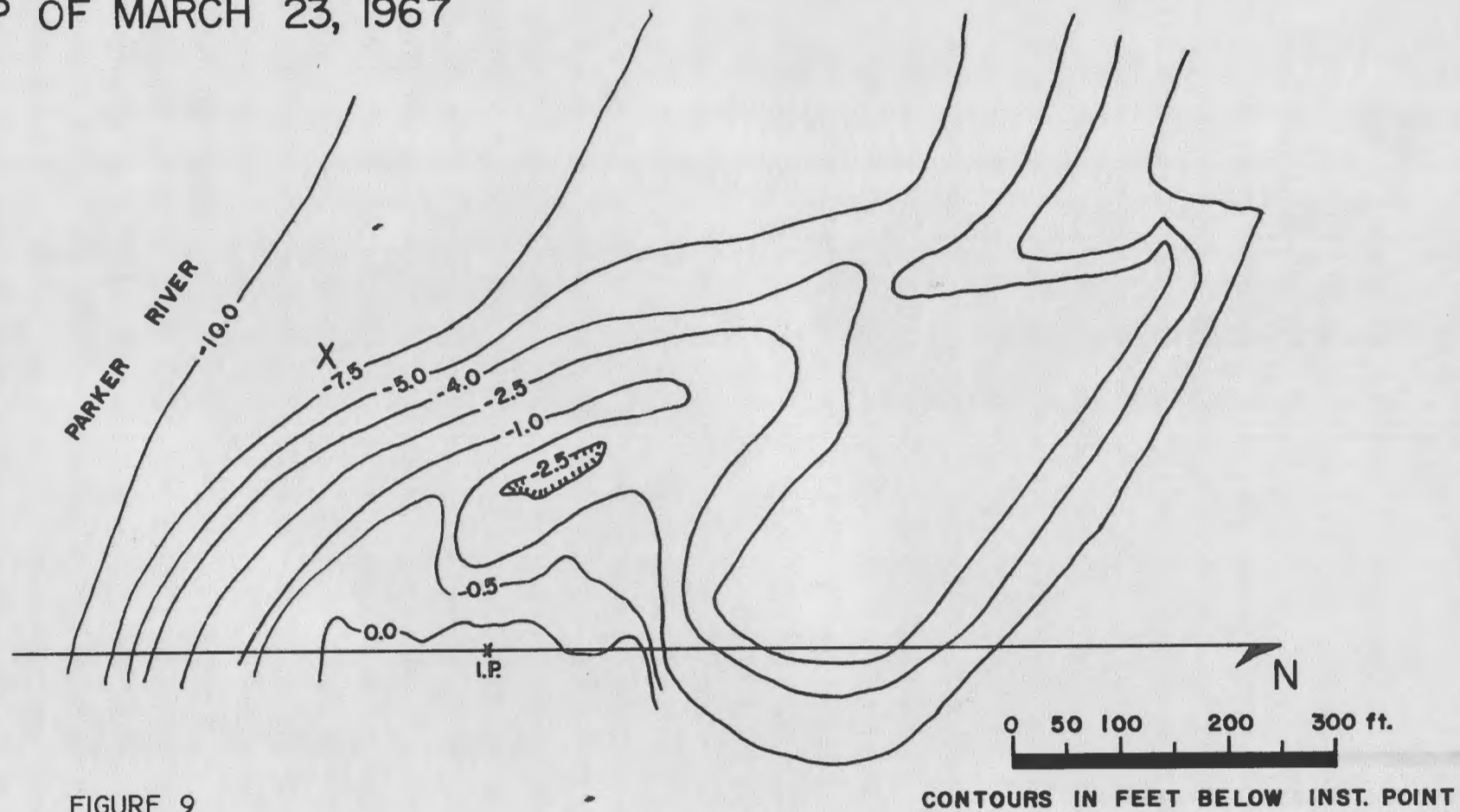


FIGURE 9

## SHORT-TERM CHANGES

In order to examine the details of spit growth and migration, the sand body was mapped by planetable methods on a bimonthly schedule during the spring of 1967. Figures 9 and 10 show the first and fifth maps in this series. The first is of March 23, 1967, and shows a simple curved spit trending northwest. By May 4, 1967, the picture was complicated by the appearance of the lobe which ultimately became the second hook. On May 25, 1967, an intense northeast storm caused this new lobe to advance 75 to 100 feet up-channel. The advance effectively blocked sediment transport to the nose of the original spit, and it stopped growing. The new lobe continued to expand and ultimately became the major feature. Figure 11 is a composite of the twelve weeks of observation. It can be seen how accretion was confined to one hook during the first six weeks. After the lobe appeared, accretion continued at both sites until May 29, when the shielding effect of the secondary lobe stopped further development of the original spit.

## GRAIN SIZE

On April 9, 1967, surface samples were collected at each control locality. Three groupings can be made from the resulting size analyses: (1) the lagoonal margin; (2) the spit beach face and; (3) the spit surface above mean high water. Table I gives the graphic mean, standard deviation, skewness, and kurtosis of 17 samples.

The most striking result from plotting cumulative curves and frequency distributions is the bimodal character of the lagoonal margin and spit-face sands. The best examples are samples 7 and 8 (Fig. 12). The fine mode ( $2.75\phi$ ) is 90 to 95 percent quartz sand. The coarse mode ( $1.0\phi$ ) is made up of 20 to 40 percent feldspar, 60 to 40 percent quartz, and 20 percent mica and rock fragments. Samples from the spit top surface, on the other hand, do not have the bimodal character, have a far lower feldspar content, and an average graphic mean size of  $2.0\phi$ . This sand originated in two ways, either by deposition over an advancing slip

---

Figure 9. March 23, 1967, map, the first in a series of six maps, showing progressive bimonthly advances of the recurved spit. The X denotes the position where the second hook began to form after April 20, 1967.

PLUM ISLAND SPIT  
MAP OF MAY 18, 1967

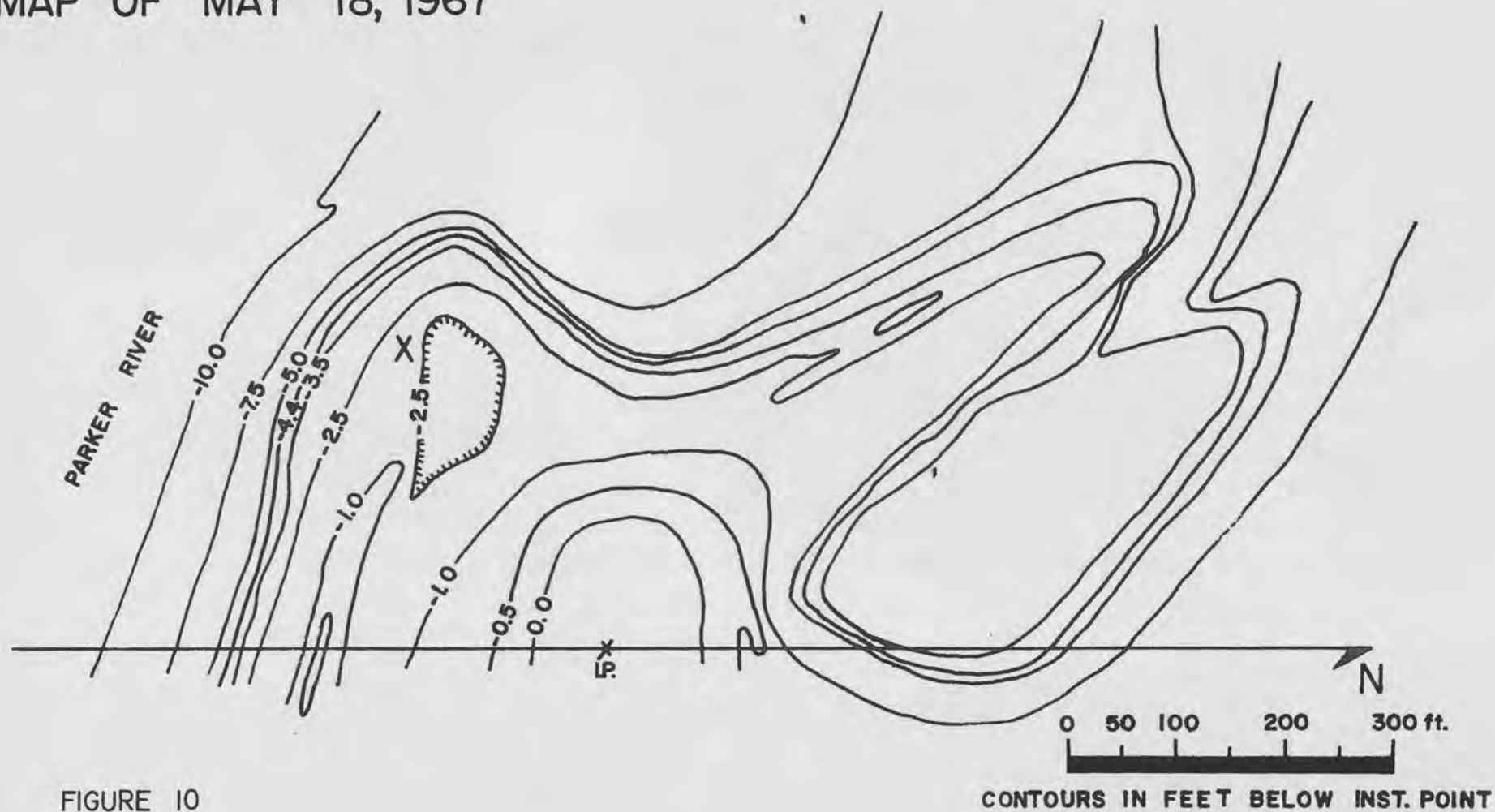


FIGURE 10

CONTOURS IN FEET BELOW INST. POINT

TABLE 1. CALCULATED GRAPHIC GRAIN-SIZE PARAMETERS FOR  
16 SPIT SAMPLES AND ONE DUNE SAMPLE COLLECTED APRIL 9, 1967

		$M_z$	$\sigma_I$	$SK_I$	$K_G$	
Lagoonal Margin	1.	2.17	0.42	+0.004	1.10	
	2.	1.81	0.60	-0.010	0.89	
	3.	2.18	0.49	+0.014	0.93	
	4.	1.89	0.43	-0.006	1.00	
	5.	2.27	0.44	-0.450	1.00	
	6.	<u>1.81</u>	<u>0.52</u>	+0.150	<u>0.93</u>	
		2.02	0.46		0.98	Average
Spit Beach Face	7.	0.87	0.59	+0.217	1.47	
	15.	1.76	0.76	-0.005	0.85	
	12.	1.67	0.78	+0.074	0.67	
	18.	1.33	0.70	+0.470	1.27	
	16.	<u>2.13</u>	<u>0.51</u>	-0.025	<u>0.89</u>	
		1.55	0.67		1.03	Average
Spit Sur- face >MHW	10.	1.84	0.34	+0.160	0.97	
	11.	1.81	0.29	+0.124	1.02	
	13.	1.98	0.29	+0.180	1.05	
	14.	2.25	0.37	+0.017	0.95	
	17.	<u>2.03</u>	<u>0.36</u>	+0.110	<u>1.02</u>	
		1.98	0.33		1.00	Average
Dune Sand		2.15	0.38	+0.253	0.99	

face or by an upbuilding of successive layers as waves washed over the spit. The wind became influential after the deposit was built up above mean high water.

On April 20 to 22, 1967, strong northeast winds moved large quantities of fine sand off the drying intertidal flats and out of the island dunes onto the spit. The resulting dune pattern on the spit surface is visible in Figure 3. The top surface sediment, after a long period of non-flooding, has grain-size parameters similar to those of a dune sample collected in the Plum Island dunes immediately inland from the spit. Features such as shape, polish, frosting, roundness, and mineralogy also were similar. Good grouping of the surface and dune samples is evident in a plot of mean size vs. standard deviation (Fig. 13).

Figure 10. Map of May 18, 1967, showing the net change since March 23, 1967. The lobe at the X on Figure 9 had developed and by April, 1969, had grown into spit containing 311,000 cu. yds. of sediment.

BIMONTHLY OF GROWTH  
OF  
SOUTHERN PLUM ISLAND SAND SPIT

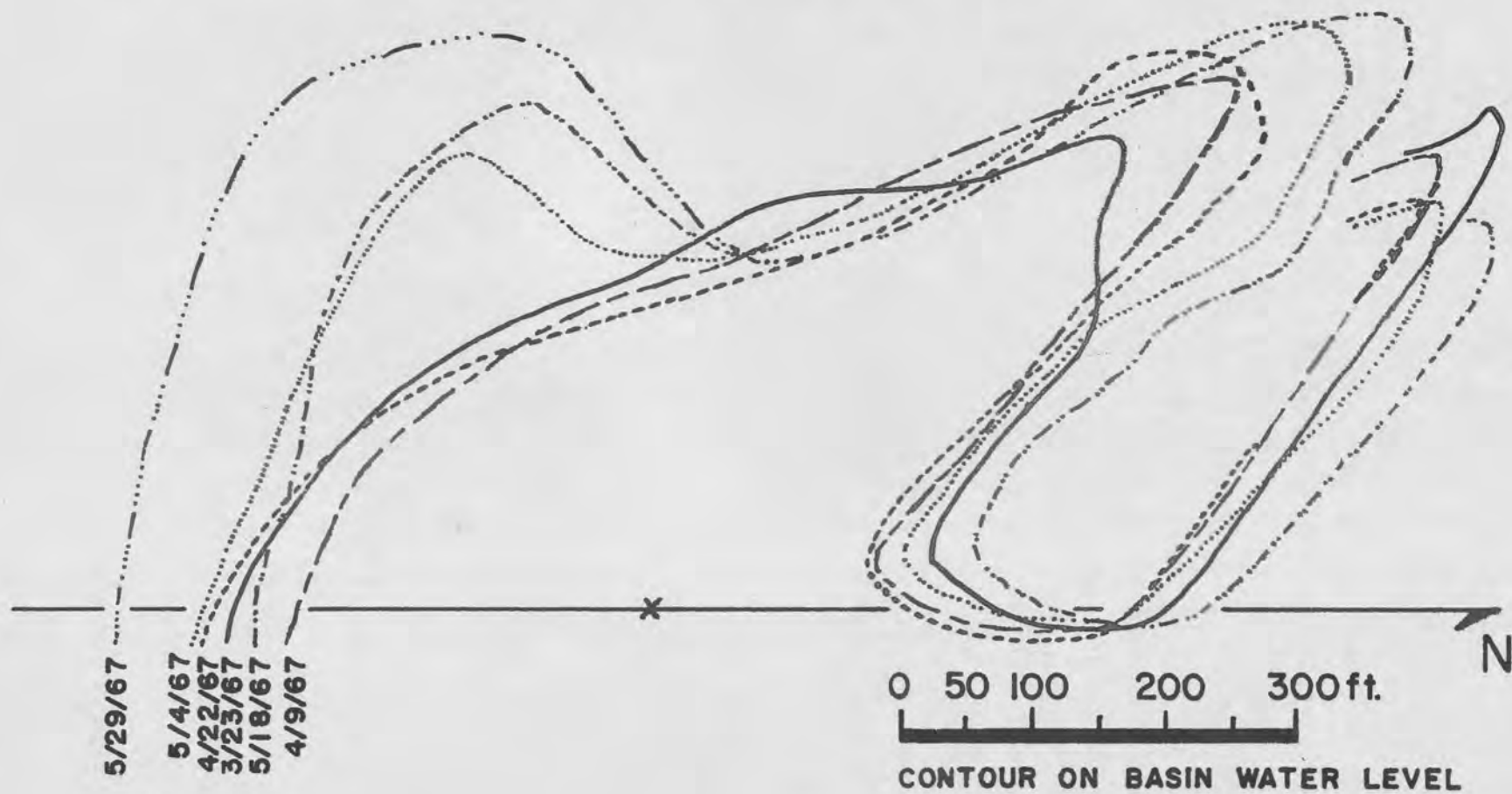


FIGURE II

Spring tide or storm overwash reversed this wind-sorting process by adding the coarser beach-face fractions.

The coarser beach-face samples are bimodal, perhaps due to selective wave sorting or addition of fines by the wind from the spit surface.

Another important fact was that the distribution of grain sizes became coarser toward the nose of the spit. Sample seven was collected at the very end of the spit and was from sediment deposited during the last flood tide before collection. The plot of position vs. grain size shows a coarsening trend toward the nose of the hook (Fig. 14).

Sand was transported along the beach face by two agents. One was the flood current, which swept past at from 0.5 to 2 feet per second. The second was the refracted waves, which curved in, striking the shoreline at an angle, resulting in net transport toward the nose. An up-rushing wave transports quantities of material in the upper flow regime. Since its effectiveness is many times that of a 2 ft./sec. tidal current, the distribution of mean sizes, perhaps, is a function of the relative rates of transportation of large vs. smaller grains by the upper flow-regime currents. The coarsest fractions outran the mean size and formed the initial slip-face deposit. When the nose advanced farther the smaller sizes added to the initial deposit and buried it with material of normal distribution.

#### CORE STRATIGRAPHY

A thick organic mat of marsh grasses covered the bottom of the basin behind the spit. During periods of spring tides or storm surges, dead grasses were rafted off the marsh and transported down the Parker River. The west and northwest winds drifted this debris over the submerged spit, where it piled up in the basin and on the flats. In April, 1967, 25 cores were hand driven into the flats, spit, and basin. The coring device consisted of a two-inch, clear, plastic pipe, a three-

---

Figure 11. Bimonthly growth of the first hook of the Plum Island spit during a twelve-week period from March 23, 1967, to May 29, 1967. Lines represent an approximate M.S.L. contour taken directly from the 6 base maps.

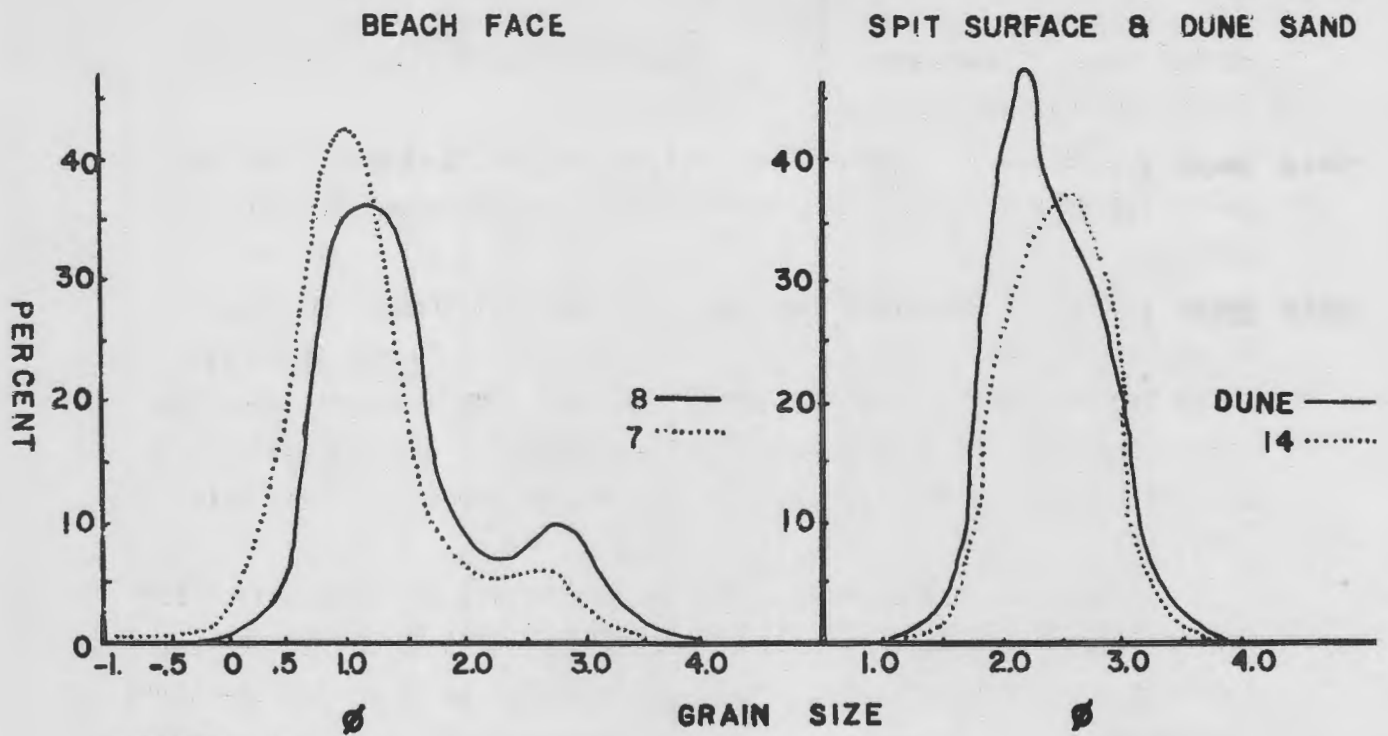


**FIGURE 12**

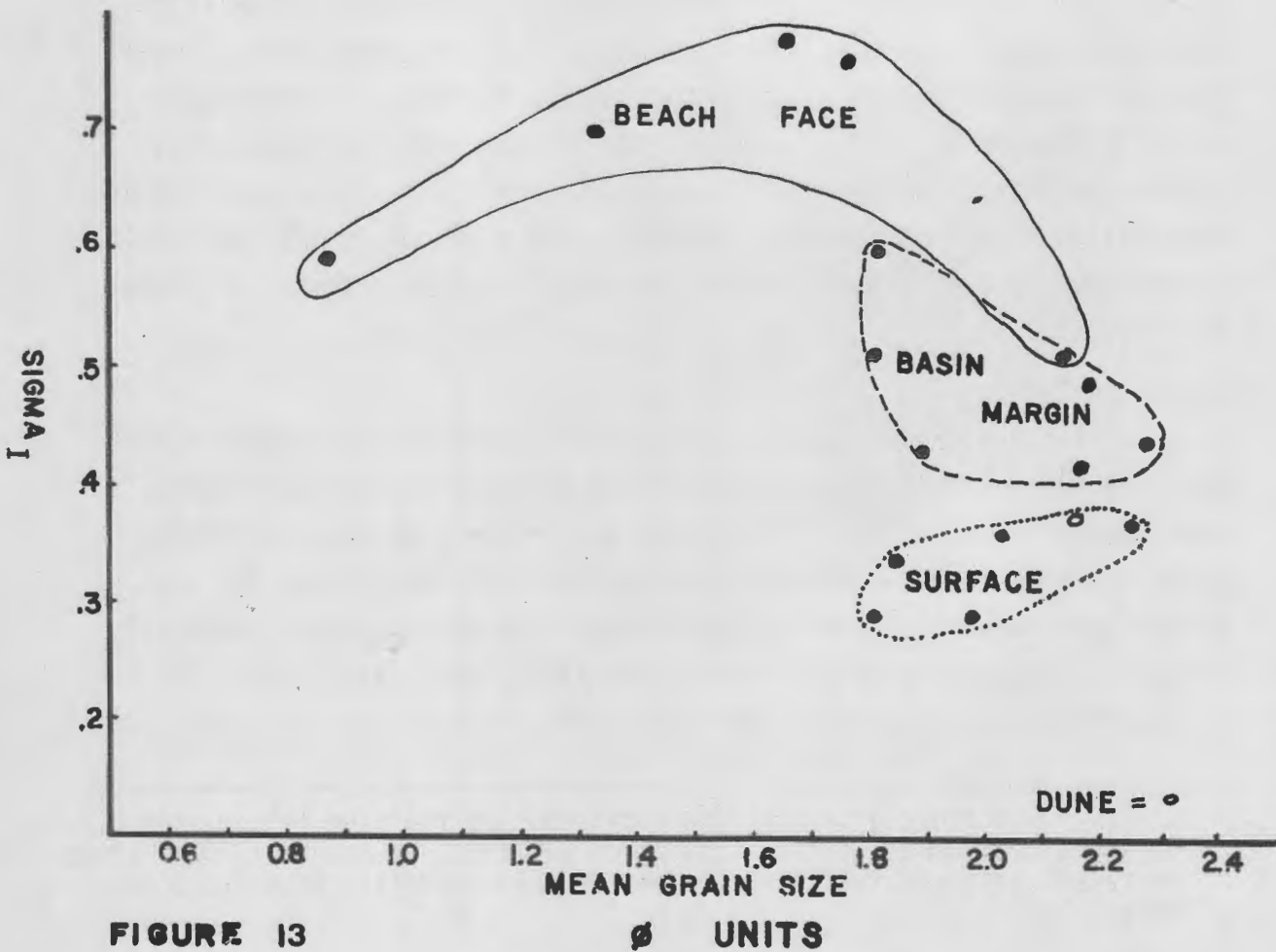


**FIGURE 13**

pound hammer, and a wood striking block. The pipe was driven to refusal, corked, and hand-extracted. The core was not extruded. All cores were measured for bed thickness and depth to various organic layers. The fence diagram (Fig. 15) is constructed from data obtained from both cores and trenches. The former basin layer is shown in Figure 2.

Other features developed on the spit during the twelve-week period were:

1. Neap-tide ridge-and-runnel systems like the one shown on the May 18, 1967, map.
2. A miniature flood-tidal delta built into the basin from its outlet.
3. A heavy mineral, halite-cemented crust was later covered by 20-foot-wavelength and 3-inch-amplitude sand dunes built by a strong northwest wind on April 20 to 22, 1967 (visible in Fig. 3).

#### CONCLUSIONS

1. Beach drift and tidal currents built a double hooked spit into the Parker River estuary over a period of four years. The growth rate was fastest during storm periods. The cyclic nature of spit development may be a complex function of tidal prism volume, tidal channel cross-sectional area requirements, decreasing estuary volume, and southerly migration of Plum Island.

2. Wind and water sorting work separately to modify the spit sands. The grain-size data show the separation between them.

3. Grain size increases toward the hook end, indicating differential movement rates of larger-sized grains under upper flow-regime conditions.

---

Figure 12. Frequency distributions of the spit beach face and basin margin sands compared to the spit top surface and Plum Island dune sand.

Figure 13. Poor sorting of the sand on the beach face is a reflection of its bimodal character. The wind has modified the surface material and those samples plot close together with the dune sample.

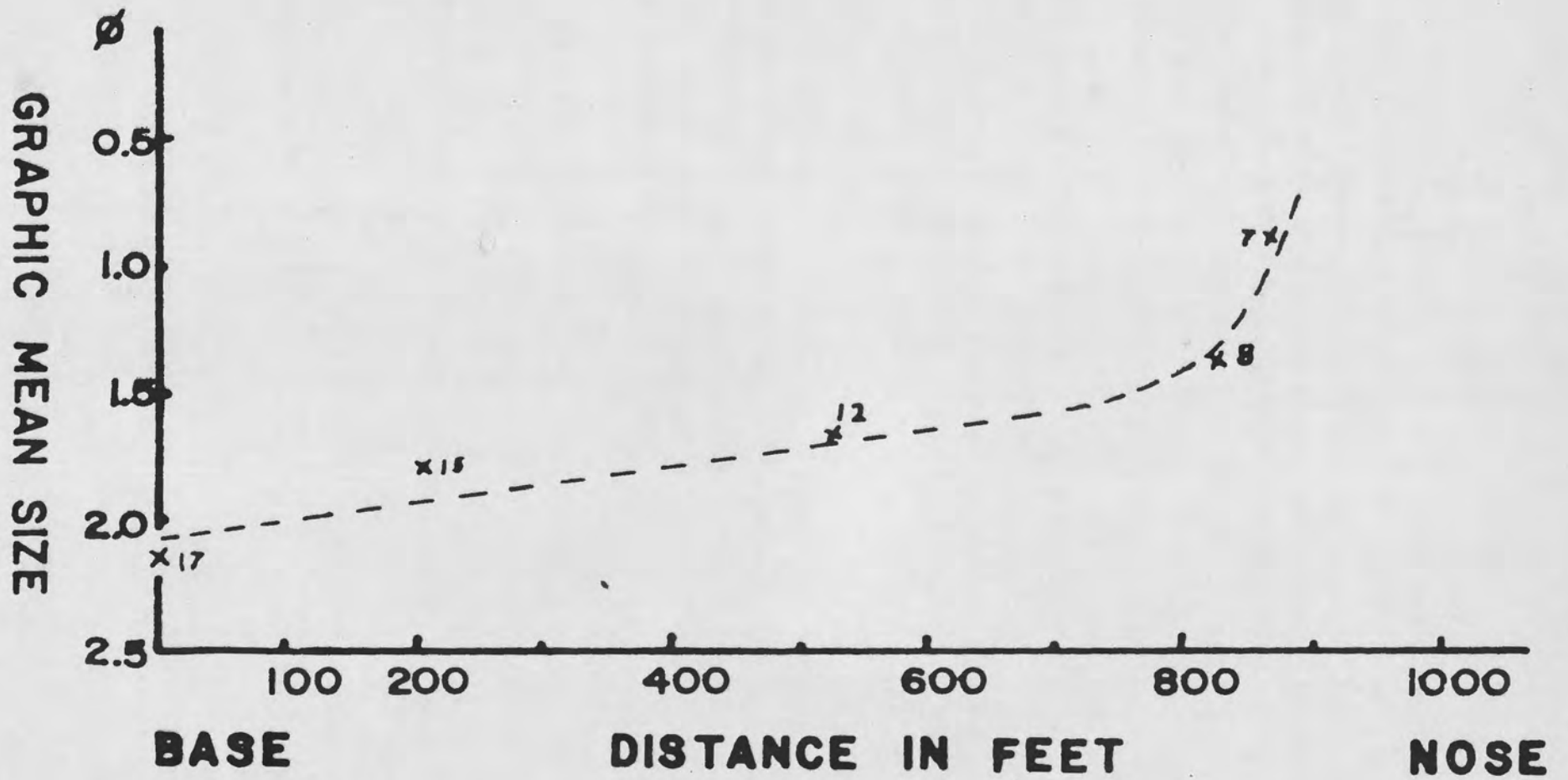


FIGURE 14

4. Vegetation debris rafted off the salt marsh becomes trapped in the basin and acts as a distinctive marker bed showing inter-tonguing of sand and black organic material. Core stratigraphy and its correlation point to pulses of sand deposition followed by relatively long periods of organic accumulation.

---

Figure 14. Plotting graphic mean size vs. distance from the base to the nose of the spit shows an increase in size toward the nose reflecting differential transportation rates of sizes by upper-flow regime swash currents.

FENCE DIAGRAM FOR THE SPIT BASED ON  
CORES TAKEN ON APRIL 9 & 22, 1967

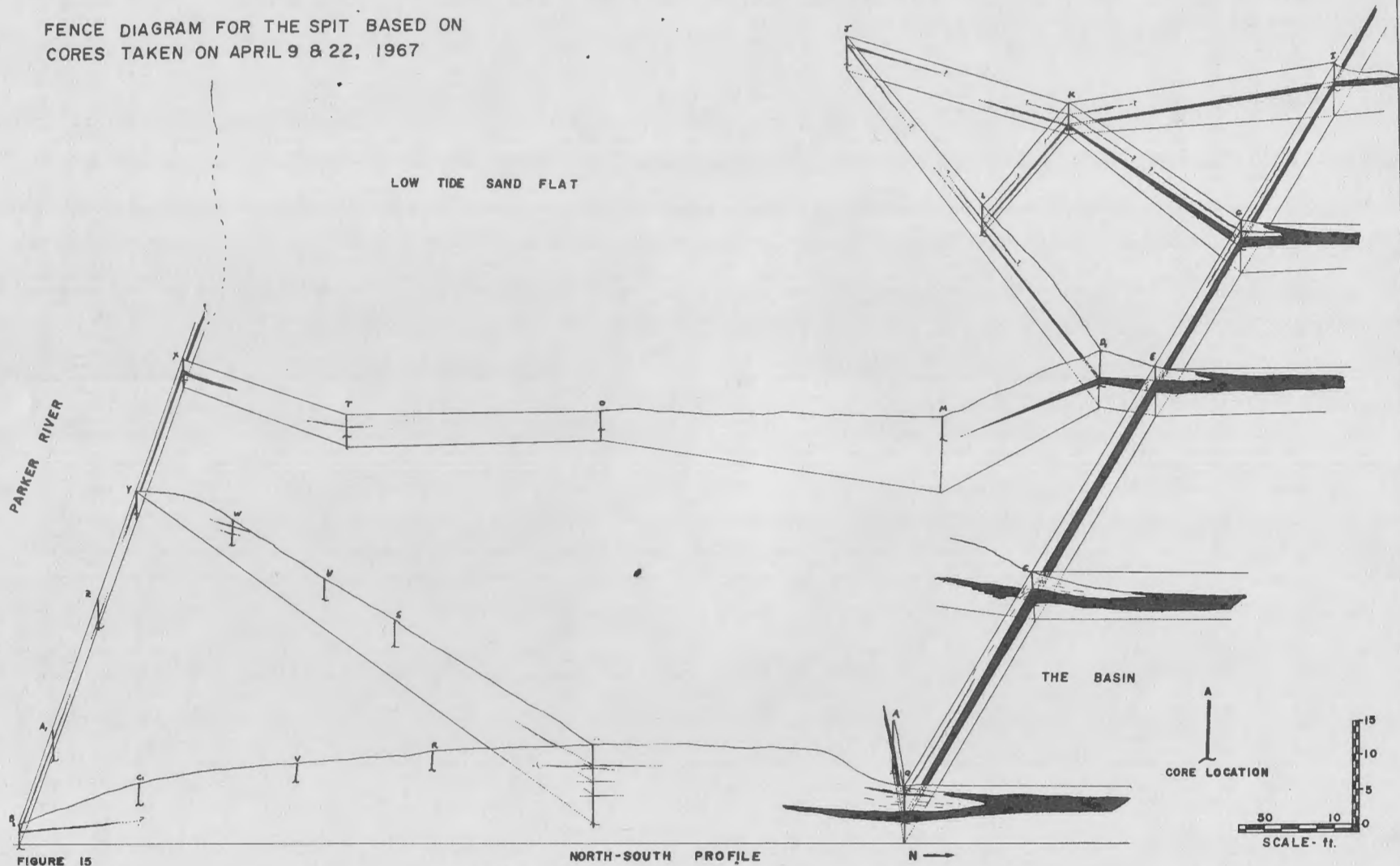


FIGURE 15

NORTH-SOUTH PROFILE

N →

A  
CORE LOCATION

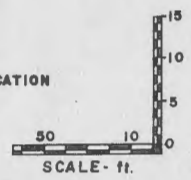


Figure 15. Composite fence diagram constructed from trenches and 25 short sand cores taken April, 1967. The organic mat (represented by black lenses) extended out in front of the spit under the sand flat and was shown to be thinner yet continuous with that being deposited in the basin.

## HOLOCENE SEDIMENTS OF THE PARKER RIVER ESTUARY

Joan M. DaBoll

Abstract: The Parker River estuary, which is situated behind Plum Island, Massachusetts, contains a large meandering main channel, a complex flood-tidal delta system, and large point bars on the meander loops. Numerous tributary creeks branch off the main body of the estuary. Hydrographic data show that the estuary is predominantly horizontally and vertically mixed, with varying tendencies toward very slight salinity stratification, the maximum difference between the surface and bottom water being 4<sup>0</sup>/oo. Ebb currents are stronger than flood currents in the main channel, whereas flood currents are stronger than ebb currents in flood bifurcations off the main channel and over the tidal flats.

Large bedforms (sand waves) are abundant in the sandy areas. They are generally ebb-oriented in the main channel and flood-oriented in flood bifurcations and on most of the sand flats.

In general, grain size decreases toward the head of the estuary. On any one traverse across the main body of the estuary, however, the coarsest sediment is present on the topographic highs. This pattern is reversed in the tributary creeks, where sediment tends to be coarser in the channels and finer on the topographic highs. In the main body of the estuary, sediment tends to be well to moderately well sorted and nearly symmetrical to coarse skewed. Graphic means of samples range from 1.25 to 2.90 $\phi$ . In the tributary creeks the sediment is generally poorly sorted and fine skewed. Samples from these areas have graphic means between 3.00 and 7.25 $\phi$ .

### INTRODUCTION

The Parker River estuary is a large estuarine system with a main body, 4 miles long and 3/4 of a mile wide, fed by four rivers and many small creeks. These rivers and creeks, however, have very low discharges. The discharge of the Parker River, the largest tributary, averages only 33cfs (U.S.G.S., Water Resources Data, 1967).

Hydrographic data were taken throughout one complete tidal cycle at 16 locations in the estuary. Bedforms exposed on the flats at low tide

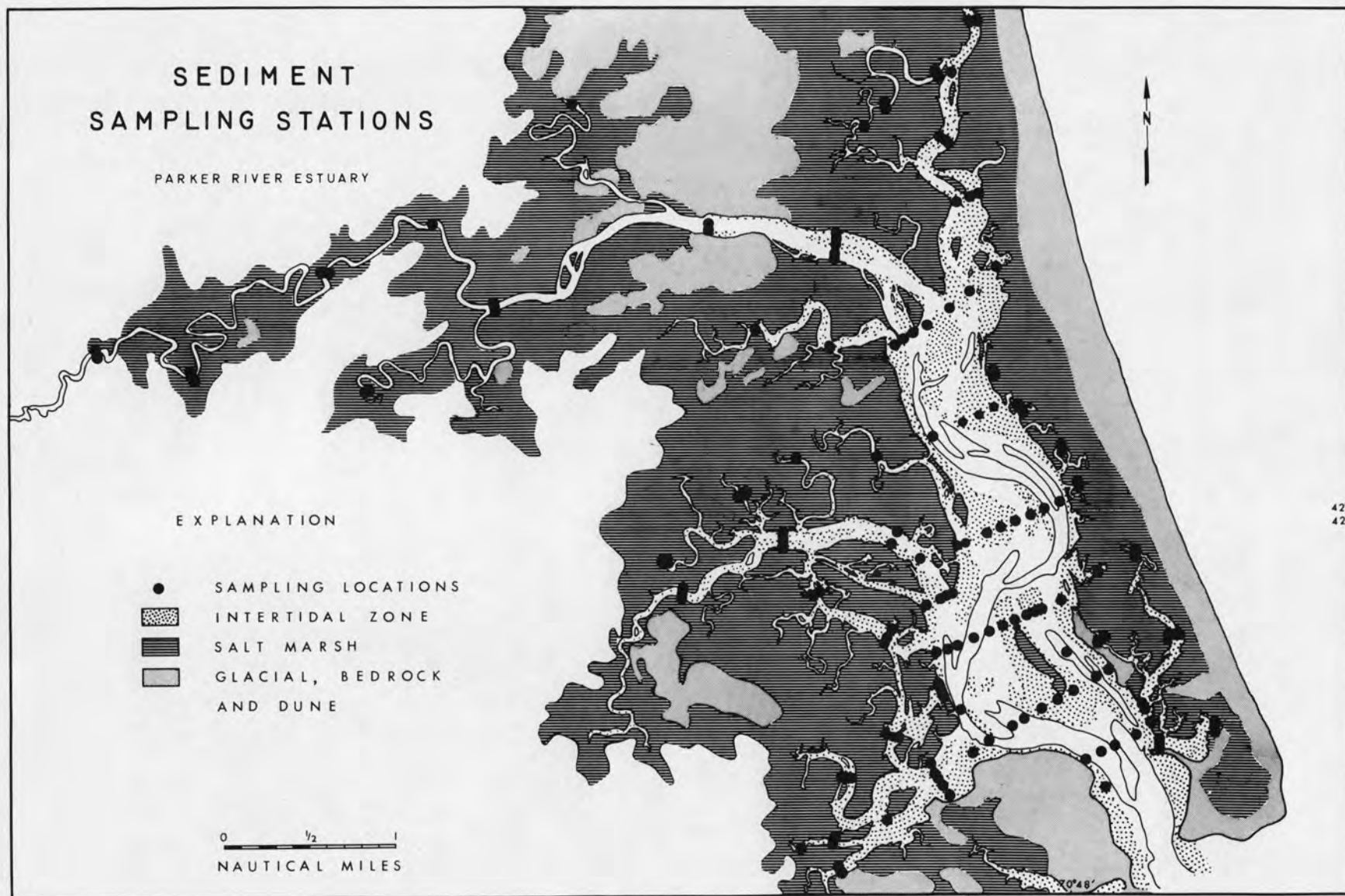


FIGURE 1

were measured directly and, in the channels, several diving observations supplemented data from fathometer profiles. Two hundred and twenty-five sediment samples were analyzed, 167 from a general sampling grid of the estuary as a whole (Fig. 1), and 58 from various areas of detailed study. Seventy-five box samples and 80 core samples were taken from flats exposed at low tide. These were studied for internal structures and the results of this study will be published later.

#### HYDROGRAPHY

The Parker River estuary falls most nearly into the type D classification of Pritchard (1955), horizontally and vertically mixed, due to the ratio of its low fresh water discharge versus high tidal influx. At mean low water the volume of the estuary is 4.5 billion gallons, but at mean high water it is 14.5 billion gallons (Jerome and others, 1968). This large volume change leads to near homogeneity. The salt water overwhelms and mixes with the fresh water so that there is only very slight horizontal salinity stratification during the flood period and slightly greater stratification during ebb tide when a maximum vertical salinity variation of 4<sup>0</sup>/oo occurs in the upper part of the estuary (Fig. 2).

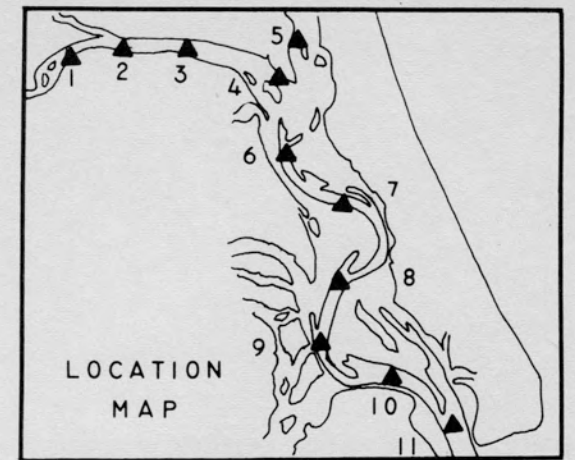
Current patterns in the estuary show several significant features. Flood currents have maximum velocities near the top of the water column, whereas ebb currents are more uniform throughout the column (Fig. 3). In the main channel, ebb currents reach greater velocities than flood and are very asymmetric, reaching the greatest velocities near the low water point of the tidal curve (Fig. 4). In the flood bifurcations off the main channel and over the flats the pattern is reversed. Flood currents are stronger than ebb currents and are asymmetric, reaching maximum velocities between mid-tide and high water (Fig. 4). The fact that flood currents reach maximum velocities late in the flood period and near the tops of the water columns shows that these currents play a major role on the flats, whereas ebb currents reach maximum velocities late in the ebb period after the flow is more confined to the main channel.

---

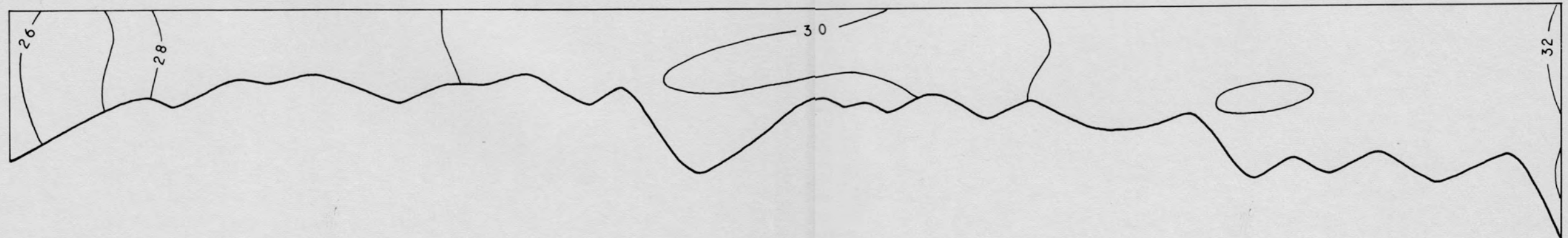
Figure 1. Sediment sampling location map of the Parker River estuary.

# MAIN CHANNEL SALINITY

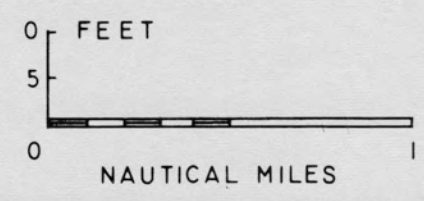
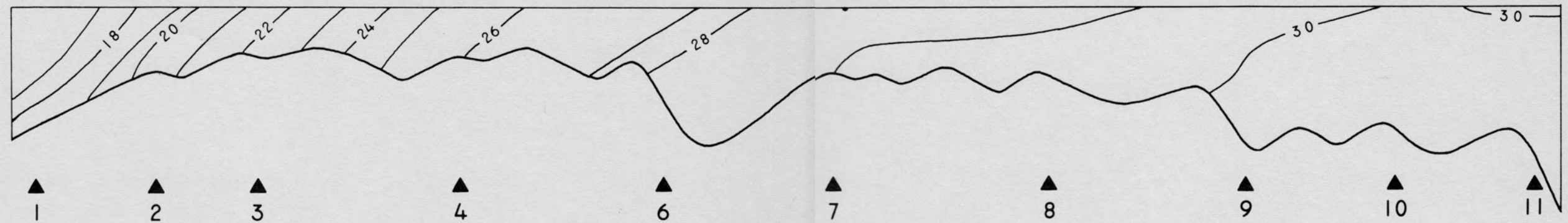
## PARKER RIVER ESTUARY



THREE-QUARTERS FLOOD



THREE-QUARTERS EBB



SALINITY ‰

FIGURE 2

## MAIN ESTUARINE BODY

### Sedimentary Structures

In the main body of the estuary the sediment is, in general, coarse enough to allow the formation of large bedforms. These bedforms are controlled by the hydrographic pattern to a great extent. In the main channel, where ebb currents dominate, large ebb-oriented sand waves have formed, with wavelengths up to 450 feet and heights up to 8 feet. Fathometer profiles (Fig. 5) show that the sand waves are largest near the mouth of the estuary, where ebb currents are strongest, and that they gradually decrease in length and height up the estuary. In the flood bifurcations off the main channel, flood-oriented sand waves have formed with maximum wave lengths of 225 feet and heights of 8 feet. These also are largest near the mouth of the estuary and decrease in size up the channel. On the flats, flood-oriented sand waves dominate, governed by two factors. The first factor is the pattern of flood-current asymmetry and maximum velocity over the flats, and the second factor is the shape of the flats. Most of the flats rise gradually to a well-defined high ridge on the up-stream side. This ridge acts as a shield against ebb currents. The small sand body located northeast of Middle Ground has a particularly well developed ebb shield (Fig. 6). The flood current flows through the central flood channel and over the flat. The shield that has built up on the up-current margin, however, forces the ebb current to flow around the flat. This restriction means that the two currents flow to different areas of the flat, accounting for the sand wave pattern (Fig. 6). Well-developed ebb shields are also found on the southeastern and southwestern sides of Middle Ground (see STOP 16, this guidebook) and on sections of the point bars. Sand-wave size and orientation throughout the estuary are summarized in Figure 7, which shows the areal domination of flood-oriented sand waves and the confining, in general, of ebb-oriented sand waves to the main channel.

Ripples are ubiquitous throughout the study area, but do not show consistent trends. Their form and orientation vary greatly over small distances, reflecting variations in current patterns. In general,

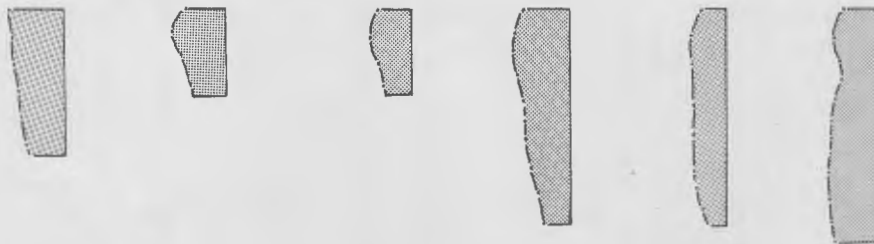
---

Figure 2. Longitudinal salinity profiles of the main channel of the Parker River estuary. During the flood period, the estuary is mixed. During the ebb period, slight horizontal stratification occurs, being most pronounced in the upper reaches of the estuary.

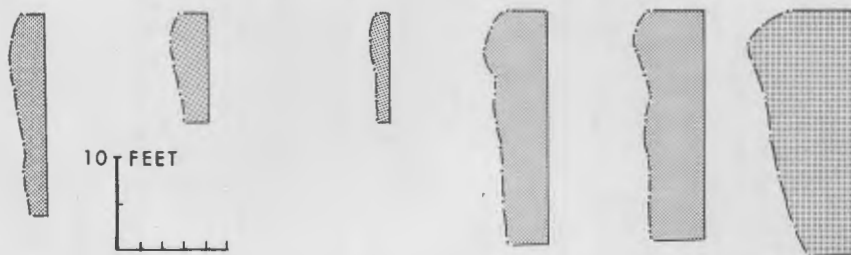
# CURRENT VELOCITY

PARKER RIVER ESTUARY

ONE-QUARTER FLOOD



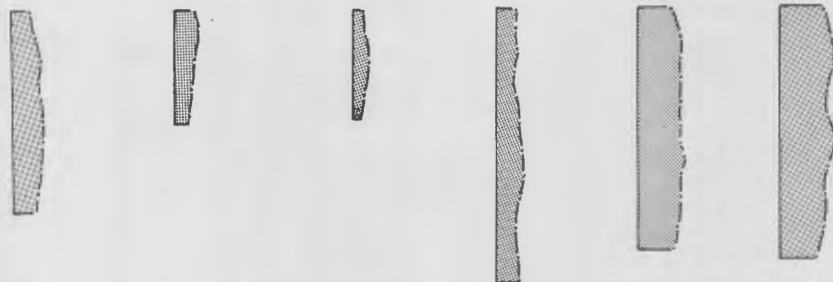
THREE-QUARTERS FLOOD



10 FEET

0 FT/SEC 5

ONE-QUARTER EBB



THREE-QUARTERS EBB

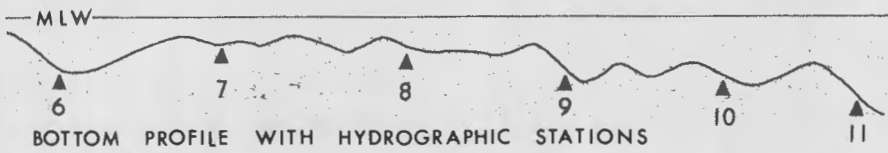
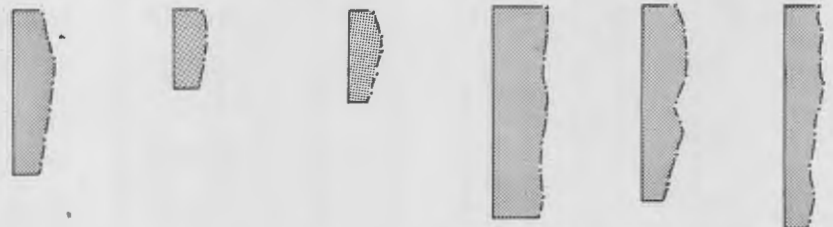


FIGURE 3

however, the ripples are ebb-oriented at mean low water with the exception of the southern end of Middle Ground, where a large field of linear flood ripples has formed. Thus, in most areas, ripples change their orientation with the changing tide.

#### GRAIN SIZE

The sediment of this estuary is supplied mostly from Plum Island and offshore areas, due to the dominance of tidal currents and the lack of a supply of coarse sediment from any of the small tributaries of the estuary. Therefore, grain size is coarsest near the mouth of the estuary and gradually decreases toward the head. However, on any one traverse across the main body of the estuary, the grain size is coarsest on the topographic highs and decreases toward the lows (Fig. 8). The hydrographic pattern is partly responsible for this. With the maximum flood velocity exceeding the ebb velocity over the flats, fine material is winnowed from the sediment, concentrating the coarser fractions on the higher elevations. The relationship between water depth and velocity is another important factor. Over the flats, currents are high during flood (up to 3 ft./sec.) but depths are small so the Froude number (hence, transporting capacity) is considerably higher than for similar velocities in the deep channels. Winnowing is also accomplished by wave action in the estuary where there is a long enough fetch to permit the formation of waves.

An exception to the pattern of gradual grain-size decrease results from the configuration of the estuary. Along the eastern edge of Middle Ground a large flood-bifurcation channel bypasses the first meander loop of the main channel. This allows sediment to take a short route over the tidal-delta system. This sediment is dumped into the main channel just below the second meander loop, creating an abrupt increase in grain size at the point of dumping. Thus, there is a sudden jump of one phi unit in graphic mean in the main channel samples at this location. On the bifurcation route, grain size gradually increases over the tidal-delta system because the coarser fraction is concentrated on the topographic highs until

---

Figure 3. Current velocity profiles from representative stations in the main channel of the Parker River estuary. During flood, the greatest velocities are reached near the top of the water column. During ebb, velocities are vertically uniform.

# CURRENT VELOCITY ASYMMETRY

PARKER RIVER ESTUARY

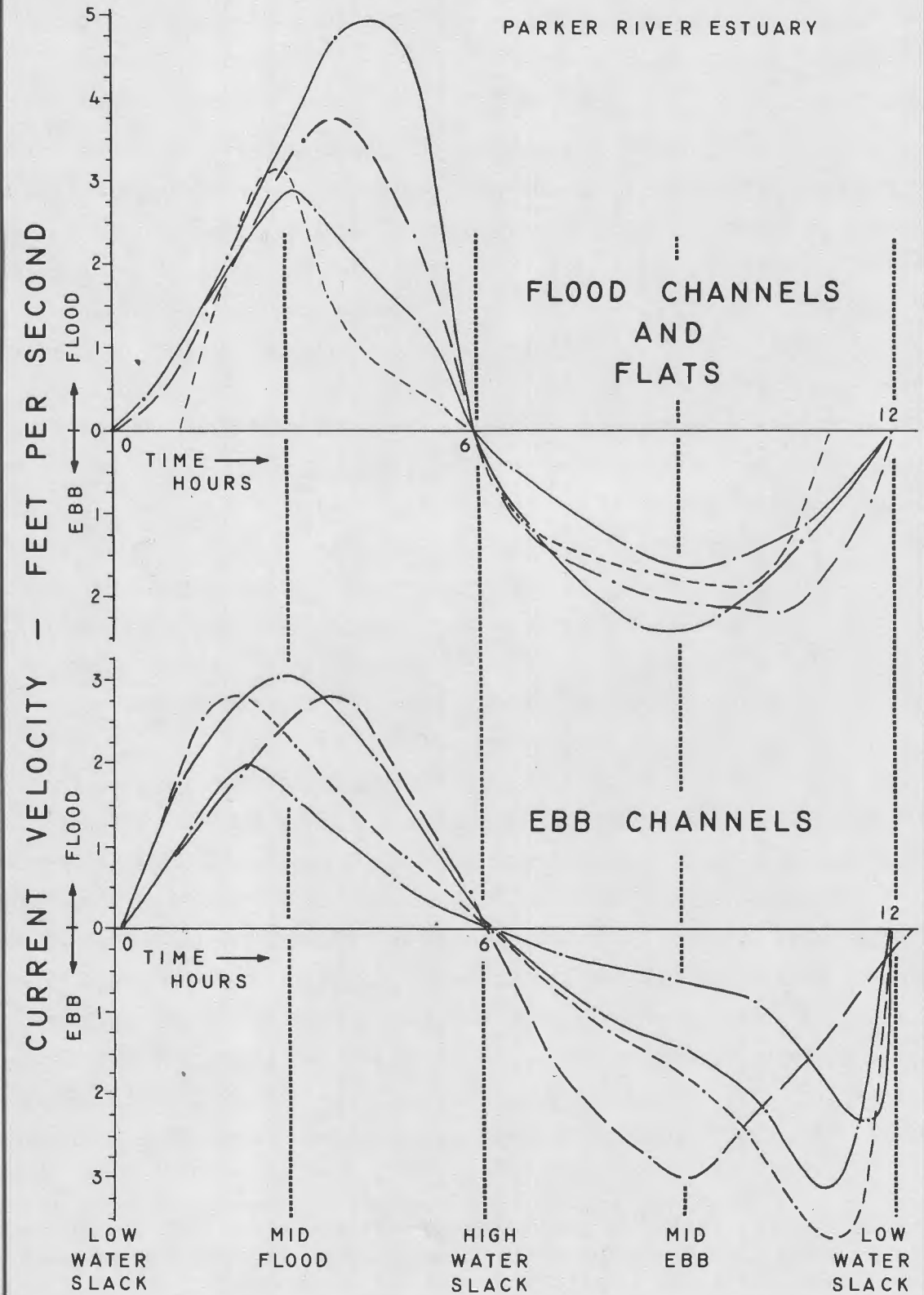


FIGURE 4

the bifurcation rejoins the main channel. The graphic means of samples from both the main channel route and the flood bifurcation are shown in Figure 9.

Sorting, skewness, and kurtosis values in the main body of the estuary vary widely, depending on many factors. In general, however, the sediment is moderately well sorted, nearly symmetrical to coarse-skewed and mesokurtic (using graphic measures of Folk and Ward, 1957).

## TIDAL CREEKS

### Sedimentary Structures

In the tidal creeks which are tributary to the main estuarine body, the sediment is, in general, too fine grained to allow the formation of sand waves. The small meandering channels, which are sometimes devoid of water at low tide, have bordering flats of very fine-grained material. The flats are broad and very gently sloping in the large tidal creeks (Fig. 1, STOP 9) and gradually become narrower and steeper as the creeks decrease in size. Commonly the flats are dissected by small drainage channels. The surfaces of the flats are slightly undulating and usually covered with small irregularities. In a few places the sediment is coarse enough to allow the formation of ripples. At low water the ripples are usually ebb-oriented, but on some of the flats in the broad tidal creeks, wave action has generated symmetrical ripples.

## GRAIN SIZE

The sediments of the tidal creeks tend to decrease in size toward the heads, but in these areas, on any one traverse, the coarsest sediment is in the channel and the sediment on the topographic highs is finer. This is a reversal of the pattern across the main body of the estuary because in

---

Figure 4. Graphs illustrating time-velocity asymmetry of flood and ebb tidal currents. Flood currents reach maximum velocities late in the flood period and ebb currents reach their maximum velocities late in the ebb period. Over the flats and in the flood bifurcations off the main channel, flood currents are stronger than ebb currents and the time-velocity curves for the ebb currents are not asymmetric. In the ebb channels, ebb current velocities are greater than flood current velocities and time-velocity curves for the flood currents are not asymmetric.

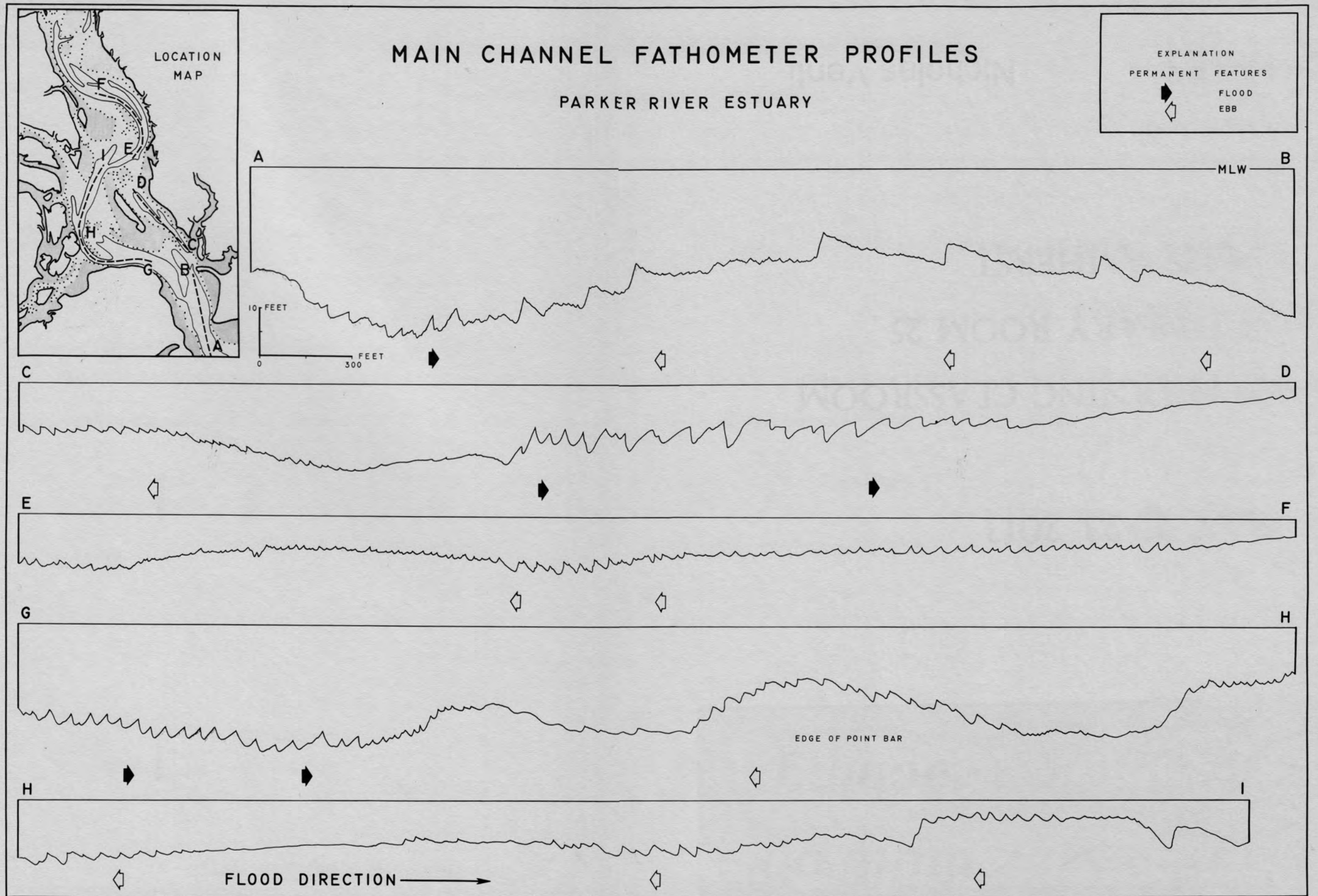


FIGURE 5

these areas winnowing is done by ebb currents at the very end of the ebb period when the channels are draining. At this time in the tidal cycle the current velocity is high enough and the water depth small enough that effective transportation in these areas is accomplished. Sorting, skewness, and kurtosis values from these areas show greater variation than they do in the main body. Sediments are usually poorly to very poorly sorted. Skewness values range from strongly fine to fine-skewed and kurtosis values from mesokurtic to leptokurtic.

#### SUMMARY

The Parker River estuary is a horizontally and vertically mixed estuary in which tidal currents play the dominant role. Flood currents reach maximum velocities near the end of the flood period and over the flats, whereas ebb currents reach maximum velocities near the end of the ebb period and in the main channels.

The sediment of the estuary falls into two populations, one in the main body of the estuary and the other in the tidal creeks. Plots of textural parameters (Figs. 10 and 11) illustrate differences between these two populations. Samples from the main channel, point bars, and tidal delta fall into a cluster with graphic means between 1.25 and 2.90 $\phi$ , sorting values between .75 and .25, and skewness between +.1 and -.35. The more scattered tidal creek population branches from this well-defined main body cluster with some samples from the large tidal creeks interspersed with the population from the main body. All of the overlapping samples come from the mouths of the large tidal creeks which generally have small deposits of coarser sediment extending a few hundred feet into them.

This division of the sediment into two populations is marked in the field by the abrupt change in sedimentary structures from sand waves in the main body to smooth mud flats in the tidal creeks.

---

Figure 5. Fathometer profiles from selected areas of the main channels. Flood-oriented sand waves dominate the flood bifurcations and ebb-oriented sand waves dominate the main channel. Bedforms are largest near the mouth of the estuary where currents are strongest.

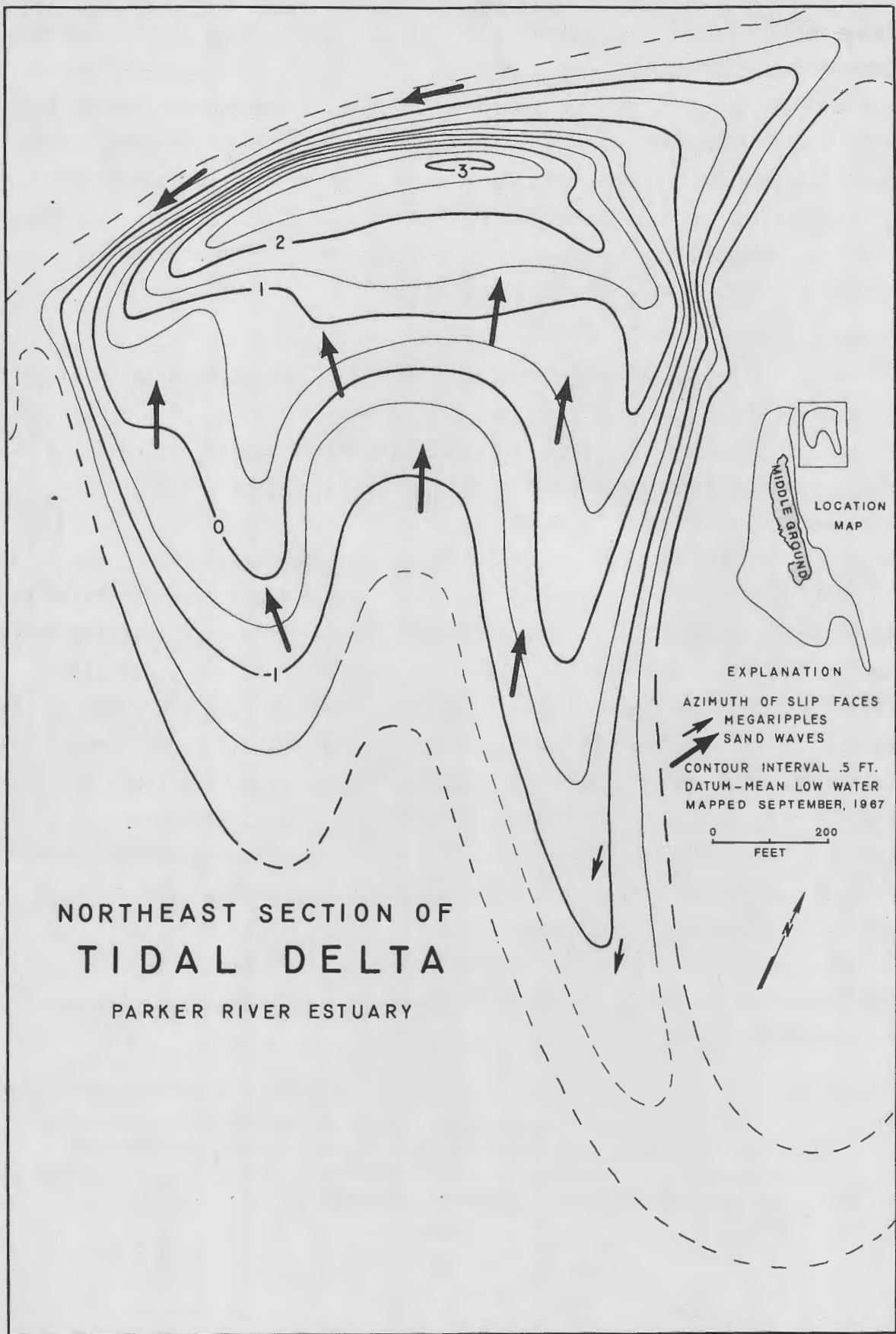


FIGURE 6

# SAND-WAVE DISTRIBUTION

PARKER RIVER ESTUARY

## EXPLANATION

-  INTERTIDAL ZONE
-  DEPTH AT MLW 0-6 FT

 MEGARIPPLES

## LENGTH OF SAND WAVES

-  15 - 30 FEET
-  30 - 60
-  60 - 120
-  > 120

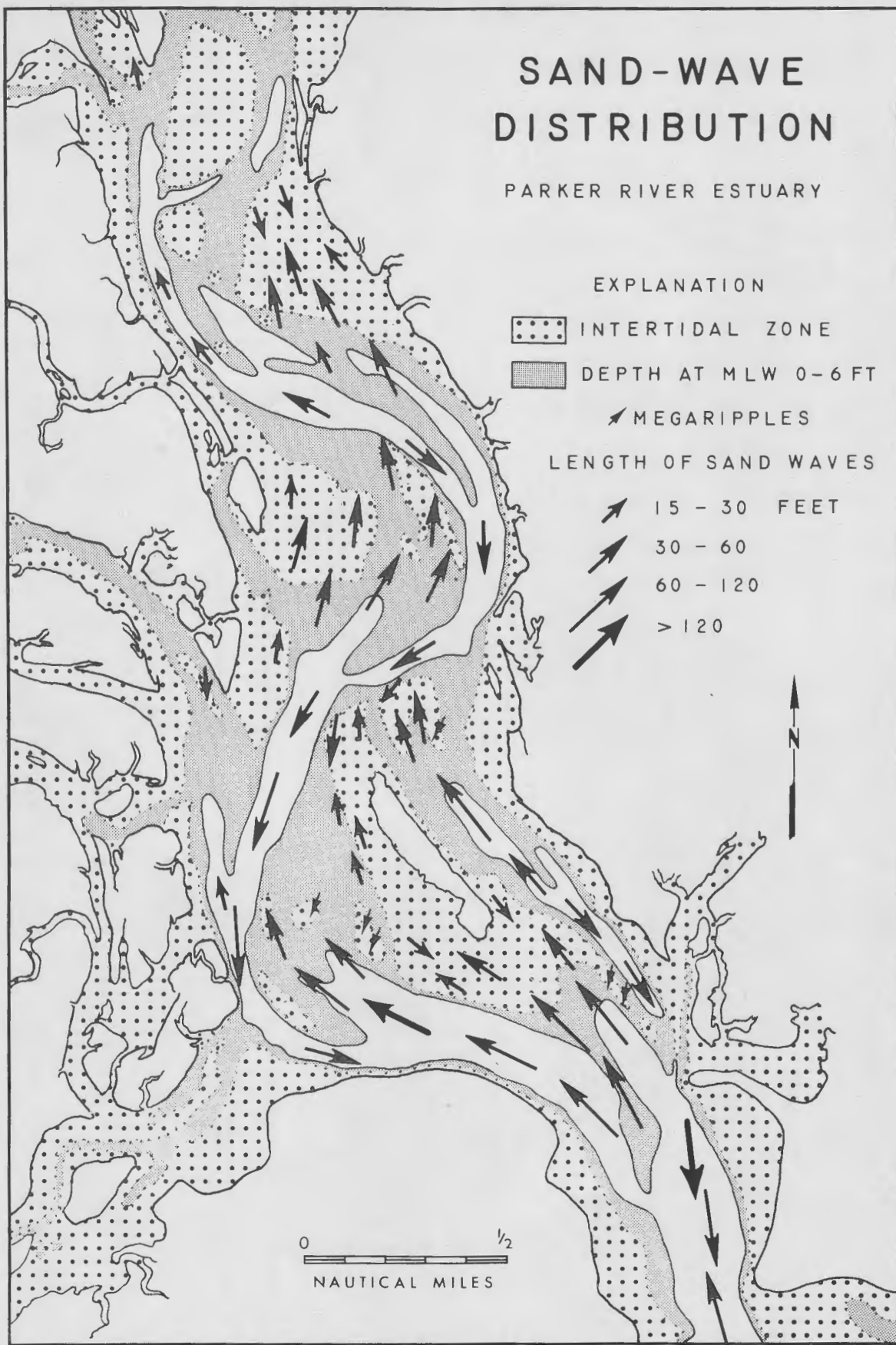


FIGURE 7

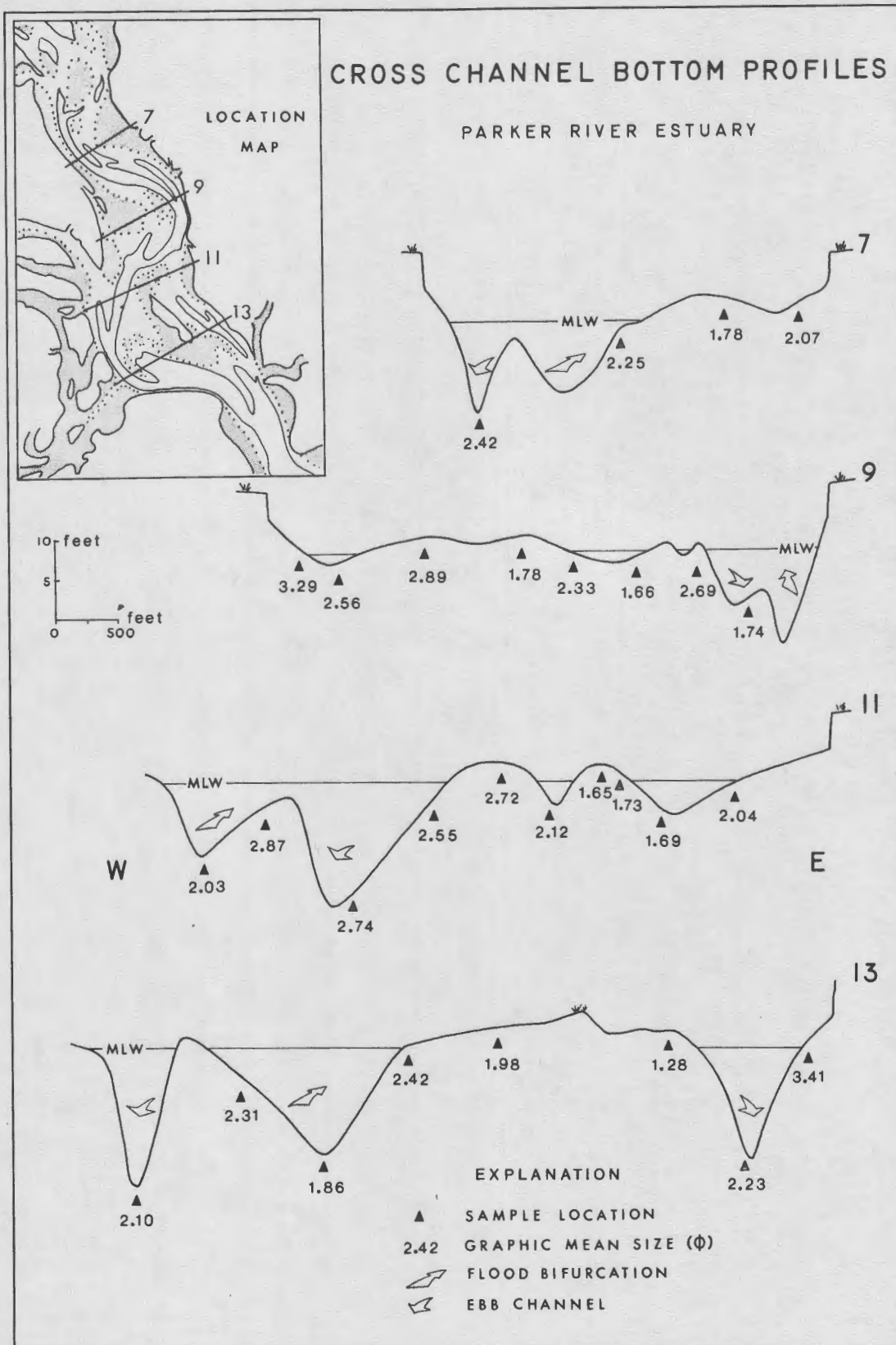


FIGURE 8

Figure 6. Contour map of the northeast section of the flood-tidal delta system in the Parker River estuary. Note the well-developed ebb shield on the northern margin and the central flood channel. Ebb currents, forced to flow around the flat, have formed long ebb spits. The sand wave orientation pattern (dip direction of slip faces) is superimposed on the map. See Figure 25-1, p.184 of this guidebook, for an aerial photograph of the flat.

Figure 7. Map of the Parker River estuary showing the areal distribution and orientation of sand waves. Note the dominance of flood-oriented features.

Figure 8. Bottom profiles across the estuary showing the graphic means of sediment samples. The sediment is coarsest on the topographic highs and in the flood bifurcations off the main channel.

# CHANNEL BOTTOM SEDIMENT

PARKER RIVER ESTUARY

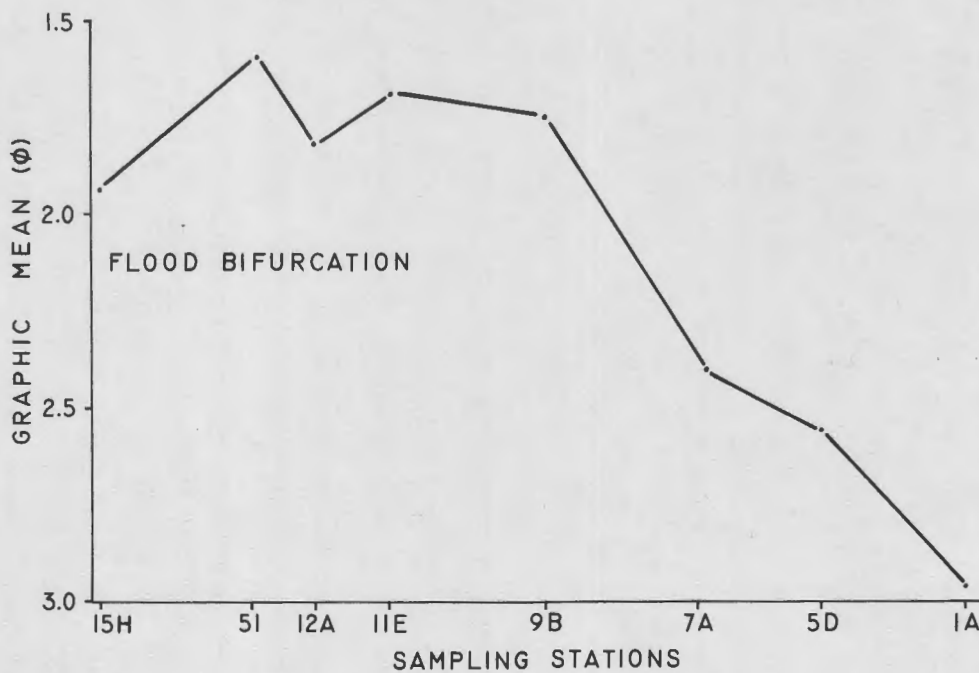
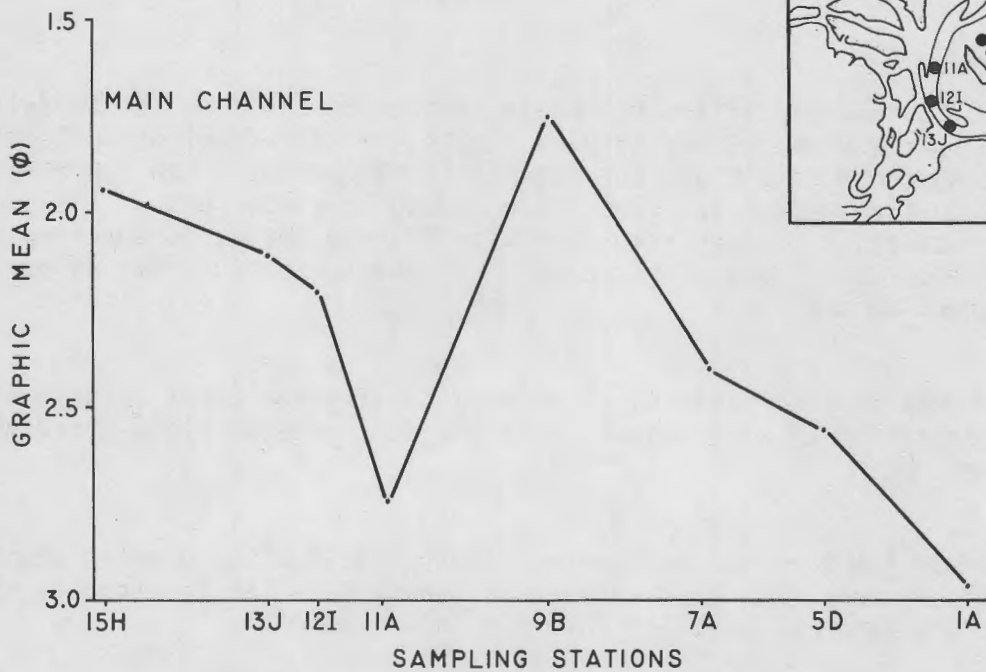
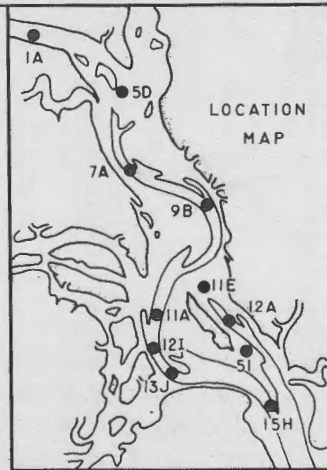


FIGURE 9

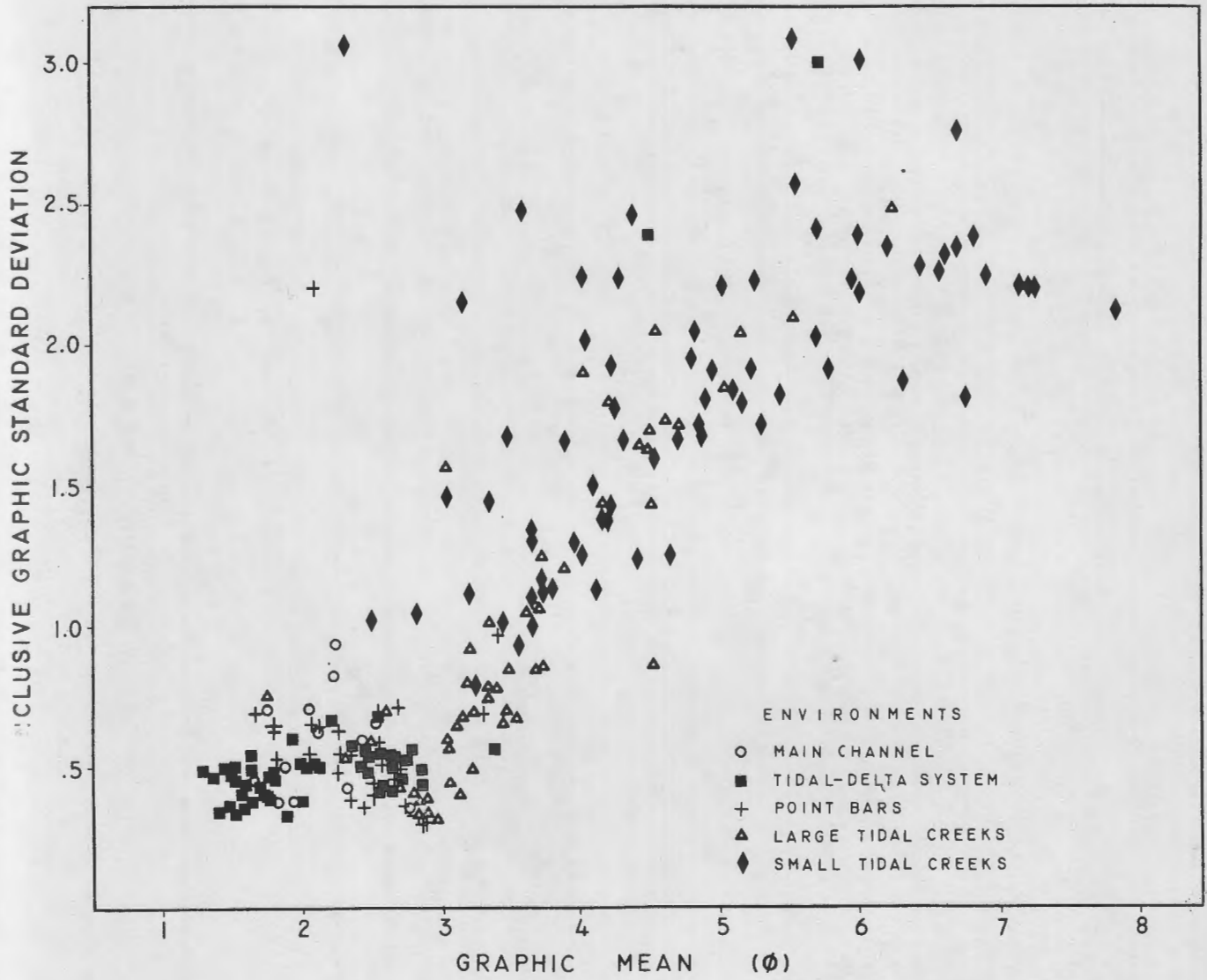


FIGURE 10

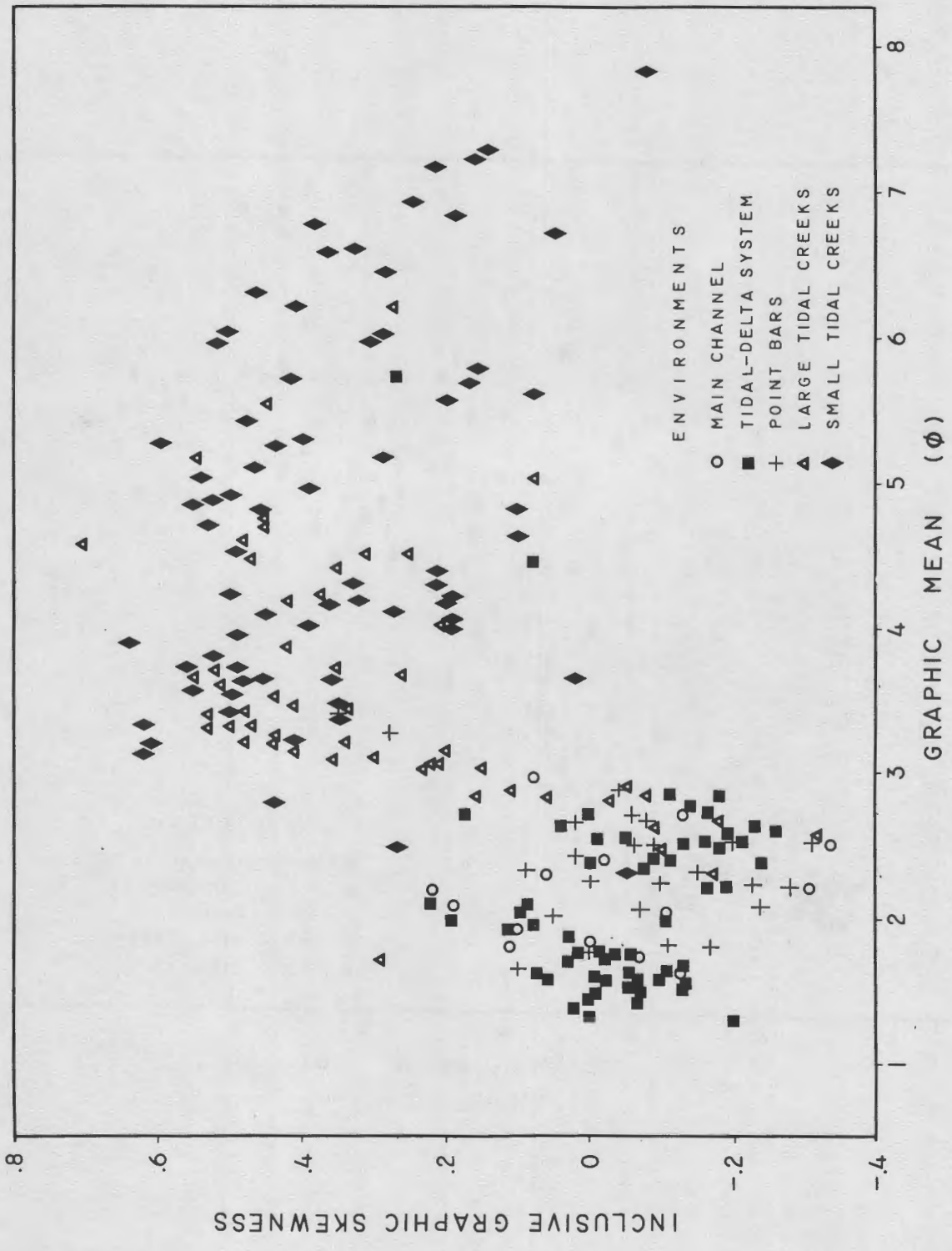


FIGURE II

Figure 9. Plots of the changes in graphic means of mid-channel bottom samples along the main channel and the bifurcation east of Middle Ground. Samples from the main channel decrease in size upstream to the second meander loop where an abrupt increase occurs. This size increase results from the dumping of coarser sediment, which has followed the shorter bifurcation route, into the main channel.

Figure 10. Graph of sorting (inclusive graphic standard deviation) versus graphic mean for 225 surface sediment samples from the Parker River estuary. The samples fall into two populations, one from the main body of the estuary and one from the tidal creeks. In the main body, graphic means range between 1.25 and 2.90 $\phi$ . Sorting values range from very well to moderately sorted. Samples from the tidal creeks are fine-grained, 3.0 to 7.5 $\phi$ , and poorly to very poorly sorted.

Figure 11. Graph of sample graphic means versus inclusive graphic skewness. The main channel population is nearly symmetrical to coarse skewed and the tidal creek population is fine skewed.

EOLIAN SAND TRANSPORT ON  
PLUM ISLAND, MASSACHUSETTS

Frederick D. Larsen

Abstract: North-south trending physiographic units on Plum Island are defined as: (1) beach, (2) foredune ridge, (3) interdune area, (4) back-dune ridge, (5) wooded area with low, stabilized dunes and (6) salt-water marsh.

Measurement of the movement of active slip faces indicated that dominant winds were from the northwest in November, 1966. A sand trap designed to collect sand from eight points of the compass was buried in the interdune area from December 4 to 28, 1966. The trap collected saltating sand grains moved by winds with northerly components.

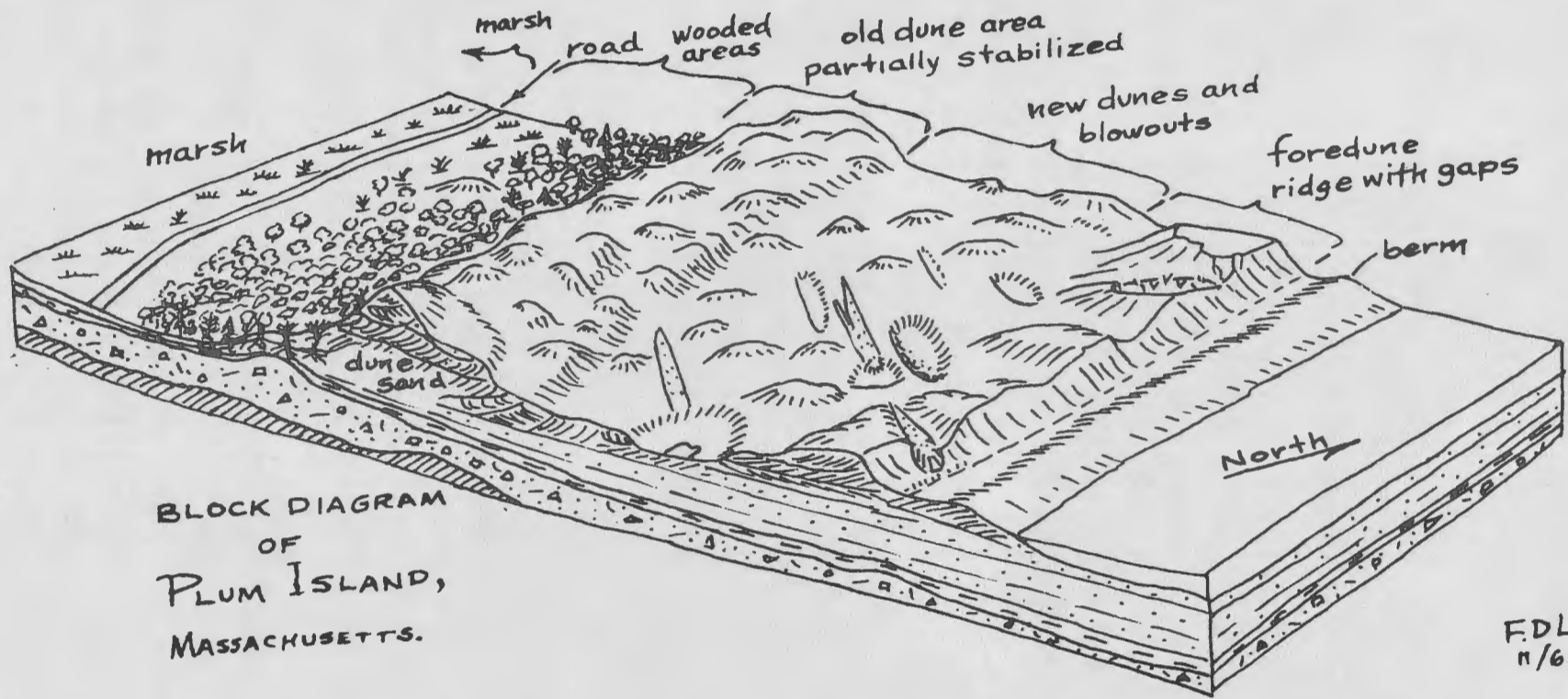
The eolian history of Plum Island parallels that of coastal dune areas in Europe and at Cape Cod where once-stable forest-covered dunes have been deforested by man's activities. The fact that these dunes are not easily and quickly stabilized by natural and artificial planting may support the idea that the climate today is drier than it was several thousand years ago.

#### INTRODUCTION

The purpose of this study was to contribute to the overall geomorphic history of Plum Island by measuring the orientation of active slip faces and the movement of sand by present-day dominant winds. The study area is located south and west of reference station PLC, which is located 4.75 miles south of the Plum Island Coast Guard station.

#### PHYSIOGRAPHY

Plum Island consists of several physiographic zones that trend parallel to the present shoreline (Fig. 1). The zones are: (1) the present beach, with its berm, beach face, and low-tide terrace; (2) a foredune ridge 30 to 35 feet in elevation with gaps formed by blowouts, slip faces, and new dunes; (3) an interdune area; (4) a discontinuous backdune ridge, partially stabilized, with elevations over 50 feet in places; (5) a low wooded



BLOCK DIAGRAM  
 OF  
 PLUM ISLAND,  
 MASSACHUSETTS.

F.D. Larsen  
 n/66

FIGURE I

area with small stabilized dunes; and (6) a tidal salt-marsh flat with some windblown sand. This study is not concerned further with the beach, the wooded area, and the salt marsh.

#### The Foredune Ridge

The foredune ridge is an erosional remnant of a line of phyto-genic dunes. The foredunes are asymmetrical in shape, with a steep east-facing slope and a gentle west-facing slope. The east-facing slope is a wave-cut cliff in eolian sand. As a result of storm-wave erosion, east-facing slopes are usually devoid of vegetation. In contrast, west-facing slopes are stable, with thick growths of American dune grass, seaside goldenrod, and other plants. The internal structure of the foredune ridge consists mainly of gently westward-dipping layers of eolian sand, but in many places high-angle, seaward-dipping crossbedding is present (M.O.Hayes, oral communication, 1969; see Fig. 11b-1, p.78 in this guidebook). Some layers marked with plant remains and root zones indicate the phytogenic origin of the foredunes.

#### Interdune Area

The low interdune area between the foredune ridge and the back-dune ridge displays a strong northwest-southeast lineation on aerial photos. On the ground the lineation is seen to coincide with the long axes of blow-outs and is therefore due to deflation by northwest winds. A variety of dune forms is found in this area, including actively moving lobes with slip faces which are building into the northwest sides of depressions. Other characteristic dunes include low, rounded phyto-genic dunes and conical erosional dunes.

#### Backdune Ridge

A discontinuous backdune ridge presents the highest elevations

---

Figure 1. Block diagram of a portion of Plum Island, Massachusetts. Location is about 5.0 miles south of U.S. Coast Guard Station.

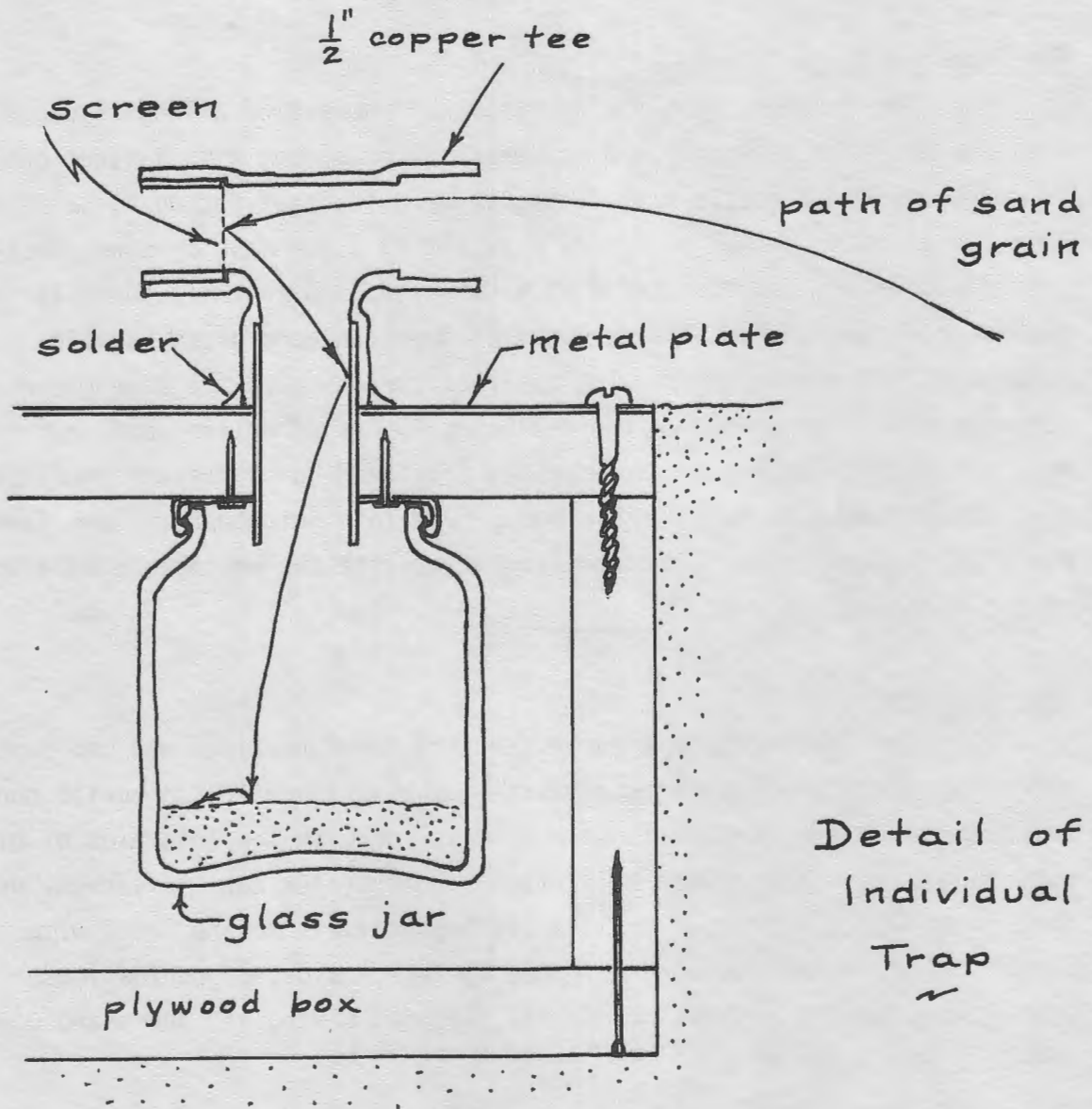


FIGURE 2

on Plum Island. On the west, the backdune ridge has an active slip face which is moving slowly into a heavily forested area. The crests of the higher dunes are well stabilized by branches of bushes and trees and reach elevations over 50 feet. In spite of the fact that many of the forms are erosional and assume a conical form, crossbedding is not commonly observed in the backdune area. The backdune ridge is missing for a distance of one-half mile north of the detailed study area at the site of a possible washover fan.

## SAND MOVEMENT

### Active Slip Faces

Evidence that the wind is actively moving sand on Plum Island at the present time comes from the presence of active slip faces that have angles of repose of between 30 and 32 degrees. On November 4, 1966, two stakes were placed in front of an active slip face in the study area southwest of PLC. In 31 days, the slip face moved 0.4 and 0.5 feet closer to the stakes.

### Multidirectional Sand Trap

A multidirectional sand trap was constructed in order to evaluate the direction of sand-transporting winds on Plum Island. The trap consists of eight one-half inch copper tees, each screened at one end and arranged radially to trap sand from eight directions (Fig. 2). The center of the trap opening is 0.9 inches above ground level and allows saltating sand grains to enter the tee, strike the screen and drop into a removable glass container below.

---

Figure 2. Diagram of individual sand trap. Eight of these mounted radially form the multidirectional sand trap.

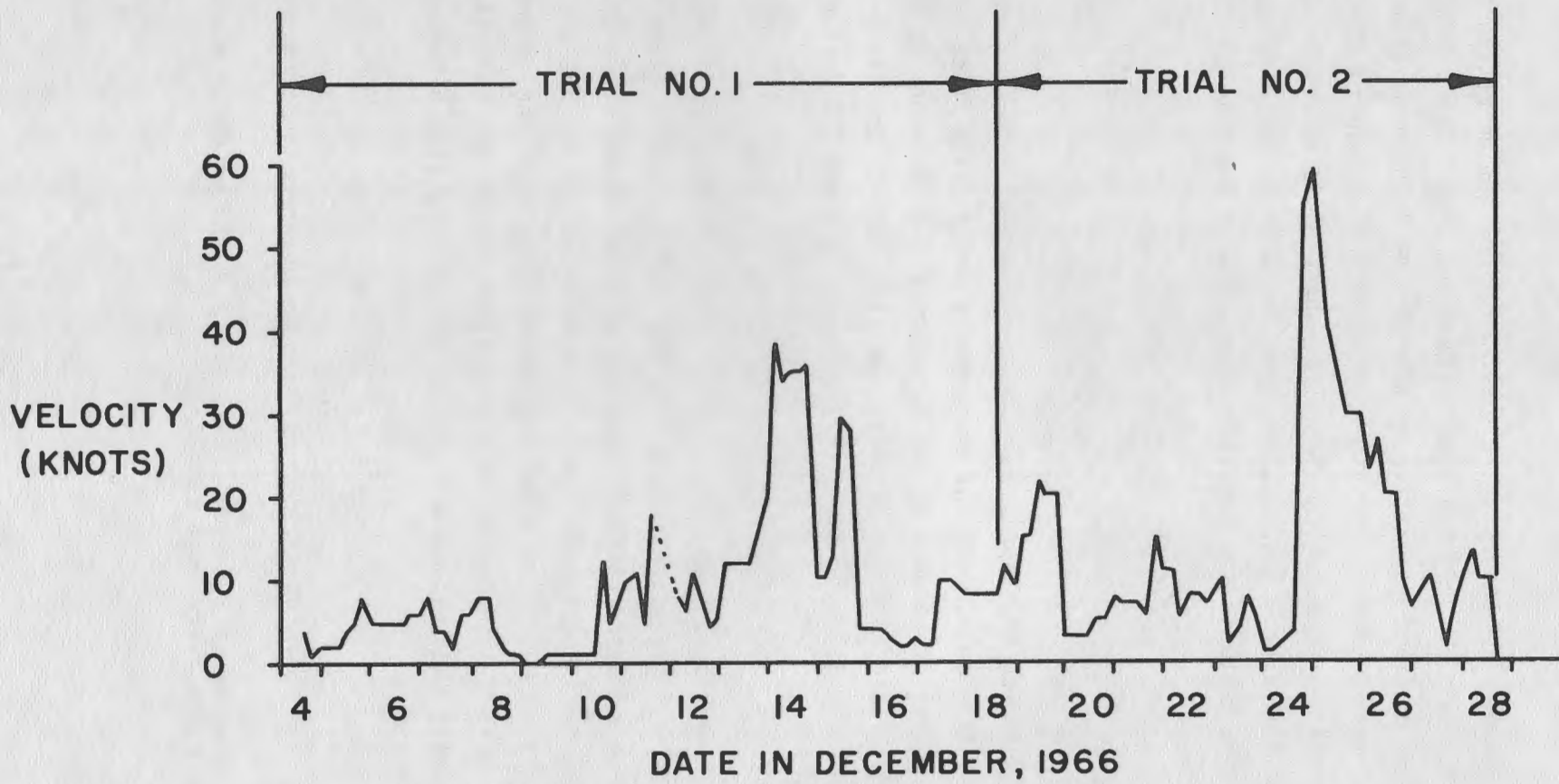


FIGURE 3

On December 4, 1966, the trap was buried on a flat sandy surface in the interdune area. The nearest vegetation was 25 feet south-southeast. The backdune ridge rose 10 to 15 feet about 60 feet west of the trap. Loose sand was available for transport from all directions. Sand was collected from the trap two weeks later on December 18, 1966 (Table 1, Trial No. 1). Sand was also collected from the trap on December 28, 1966 (Table 1, Trial No. 2), following a heavy snowstorm on December 25, 1966, which completely clogged the trap openings.

Wind data for the two trial periods were obtained from the six daily weather observations at the U.S. Coast Guard Station 5.05 miles north of the trap. Data for the two trial periods are given in Table 2 and are presented in graphic form in Figures 3 and 4.

Wind roses are presented in Figure 4 in an effort to correlate wind data with amounts of sand collected from the multidirectional wind trap. Figure 4a represents the total number of times that wind was recorded from a particular direction. During Trial No. 1 the wind blew from all directions, with northwest winds prevailing slightly.

The quantity of sand transported by the wind in a dune area varies as the cube of the velocity of the wind over a particular threshold value (Bagnold, 1954). The threshold value for the movement of Plum Island sand was not determined during this study. The trap was designed to catch a small portion of the sand moved by the wind, that is, the saltating particles. Because the trap openings are mounted nearly an inch above the ground they catch an exponentially reduced fraction of the total amount of sand moved by the wind.

Wind roses based on the cube of the velocity of the winds over 9 knots (approximate threshold value, Bagnold, 1954) during the two trial periods are greatly exaggerated and do not compare well with rose diagrams

---

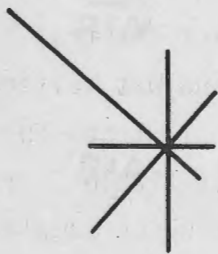
Figure 3. Wind velocity curve for December, 1966. Data from U.S. Coast Guard Station on Plum Island.

(A)

SCALE: 1" = 20 TIMES

TRIAL NO. 1

TRIAL NO. 2

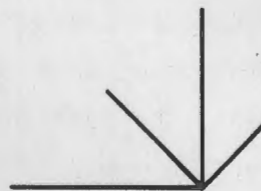


(B)

SCALE: 1" = 20 KNOTS

TRIAL NO. 1

TRIAL NO. 2



(C)

SCALE: 1" = 50 GRAMS

TRIAL NO. 1

TRIAL NO. 2

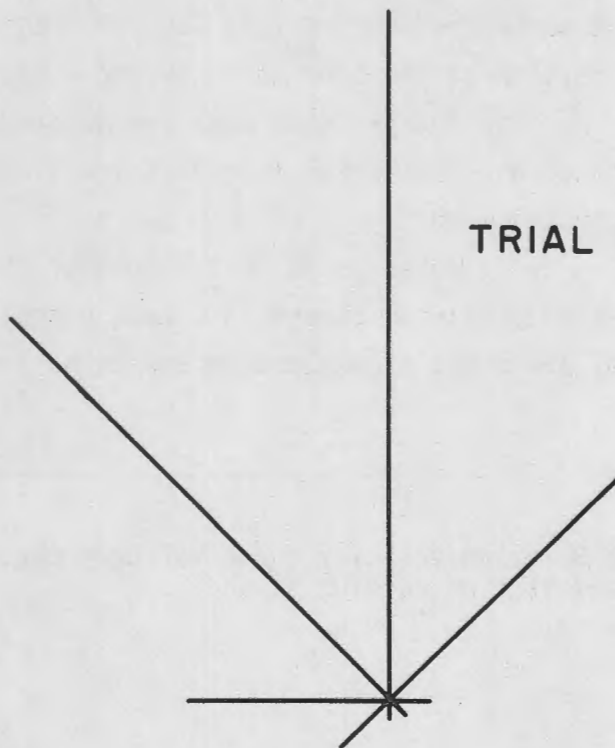
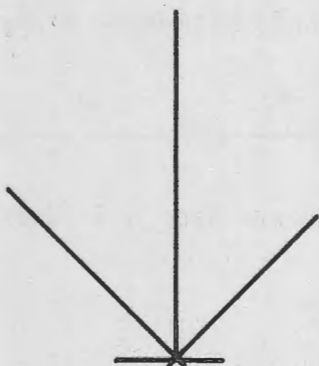


FIGURE 4

based on the weight of sand collected (Fig. 4c) and are not shown here. The wind roses in Figure 4b are based on values determined simply by adding up the values of the velocities of winds over 9 knots. The rose for Trial No. 1 in Figure 4c is smaller than the rose for Trial No. 2, in part because the sand was wet during part of Trial No. 1. Evidence for wet sand was the presence of water in individual traps and conical piles of wet sand formed in the jars during entrapment.

The plugging of trap openings during the storm of December 25, 1966, which had wind velocities up to 60 knots, has already been cited. This is the reason why the rose diagram based on the weight of sand for Trial No. 2 in Figure 4c has poorer westerly development than the wind rose for Trial No. 2 in Figure 4b.

The limitations of the multidirectional sand trap are many; however, it does present a general correlation between recorded wind direction and amount of sand trapped. Before the history of sand movement on Plum Island is inferred from the U.S. Coast Guard wind data more trial periods should be completed. An accurate calibration of the sand trap under controlled conditions in a wind tunnel would lend more credence to the concept of correlation between weight of sand trapped and wind data.

#### HISTORY OF THE PLUM ISLAND DUNES

Upon retreat of the Wisconsin ice sheet the northeast coast of Massachusetts was depressed by the weight of the ice so that marine water covered the land west of Plum Island to a height of 80 feet above the present mean tide (Sammel, 1963). In the Salem quadrangle to the southwest, Oldale (1961) has found evidence that the sea stood at least 50 feet above

- 
- Figure 4. Rose diagrams comparing wind data with amounts of sand trapped.
- A. Number of times that wind from a particular direction was recorded by the U.S. Coast Guard Station.
  - B. Wind roses representing the total velocity of winds over 9 knots as recorded by the U.S. Coast Guard Station.
  - C. Rose diagrams based on weight of sand collected by the multidirectional sand trap.

present mean tide. Marine clams buried in blue-gray clay that was deposited in Maine during this encroachment of the sea have been radiocarbon-dated at 11,800 yrs. B.P. (Bloom, 1960). At that time, no part of the present Plum Island stood above the waves.

Radiocarbon dates reported by McIntire and Morgan (1963) indicate that Plum Island was initiated as a transgressive barrier island about 6300 years ago. Although dunes may have been formed earlier in northeast Massachusetts from glacial deposits, this is the earliest that dunes could have formed on Plum Island itself. However, if dunes did form 6300 years ago, they underwent 22 feet of submergence and reworking by wind and waves as the area subsided due to tectonism and eustatic rise of sea level. McIntire and Morgan (1963) reported that the Plum Island coast was undergoing subsidence at the rate of 0.30 feet per century.

The first humans to walk on Plum Island were Indians who left a record of their life and culture in shell heaps. The Indians were not numerous and probably had little effect upon the dunes compared to the white man who followed them.

"...on the East an Ile of two or three leagues in length [Plum Island], the one halfe plaine marish ground, fit for pasture or salt ponds, with many faire high groves of mulberry trees and Gardens; there is also Oakes, Pines, Walnuts and other wood to make this place an excellent habitation...". This first description of a pristine Plum Island by John Smith in 1616 (Currier, 1902) implies a fairly well-developed vegetative cover. The early settlers placed livestock on the island for the winter and allowed them to fend for themselves. On March 7, 1663, the town selectmen ordered that "all horses and dry cattle should be cleared out of Plum Island or a fine would be imposed". We can only guess that the reason for the selectmen's order in 1663 was due to over-grazing of cattle and destruction of the forest cover by settlers.

The presence of a buried soil horizon in the interdune area supports the contention that a vegetative cover has been destroyed at some time in the recent past. A similar occurrence of buried soils has been reported by Westgate (1904), who noted a widespread rejuvenation of dunes on Cape Cod due to the destruction of forest and pasturage by settlers. The deforestation of Plum Island may have occurred during the middle of the

17th century. Since then storm activity has been responsible for piling up sand as a discontinuous backdune ridge where sand moved into a forested area. With the passage of successive storms, sand zigzags back and forth across the interdune area and moves slowly southward. The dominant winds, that is, the winds responsible for moving sand, are those with northerly components.

Table 1

Weight of sand in grams for two trial periods

TRAP DIRECTION	TRIAL NO. 1 (12/4/66-12/18/66)	TRIAL NO. 2 (12/18/66-12/28/66)
S	0.6	4.0
SW	1.2	17.9
W	14.0	51.6
NW	59.9	139.1
N	87.1	180.4
NE	44.2	84.6
E	6.6	11.0
SE	0.7	5.2

Table 2

Wind Data for the Two Collection Periods (U. S. Coast Guard)

Date	Dec 4	Dec 5	Dec 6	Dec 7	Dec 8	Dec 9	Dec 10
0000hrs	----	WNW 2	SW 5	SE 6	SE 6	ENE 1	N 1
0400hrs	----	WSW 2	WSW 5	S 8	S 8	NNW 0	NE 1
0800hrs	----	WSW 2	NW 5	NW 4	S 8	NW 0	E 1
1200hrs	----	SSW 4	WNW 5	W 4	W 4	N 1	SE 1
1600hrs	NNW 4	SSW 5	NW 5	NE 2	NE 2	NNE 1	S 13
2000hrs	WNW 1	SSW 8	SE 6	SE 6	ENE 1	N 1	S 4

Date	Dec 11	Dec 12	Dec 13	Dec 14	Dec 15	Dec 16	Dec 17
0000hrs	S 7	----	NW 6	ENE 20	NW 10	NW 4	NW 3
0400hrs	S 10	NW 8	NW 12	NNE 39	NW 10	NW 4	WSW 2
0800hrs	S 11	NW 6	N 12	NNE 34	NW 12	NW 4	WSW 2
1200hrs	WNW 4	NW 11	NNE 12	NNE 35	N 30	WNW 3	SW 10
1600hrs	NW 18	NW 8	E 12	NNE 35	N 28	S 2	SW 10
2000hrs	---	WNW 4	E 15	NNE 36	N 4	NW 2	SSW 9

Date	Dec 18	Dec 19	Dec 20	Dec 21	Dec 22	Dec 23	Dec 24
0000hrs	SW 8	NW 9	NE 3	NNE 8	NNW 11	N 8	NE 1
0400hrs	SW 8	NW 15	NE 3	NNE 7	NW 11	NE 10	NE 1
0800hrs	SW 8	NW 15	NE 3	NNE 7	NNW 5	W 2	NE 2
1200hrs	SW 8	N 22	NE 3	NNE 7	NNW 8	W 4	NE 3
1600hrs	WSW 8	N 20	NE 5	N 6	NW 8	WNW 8	NE 4
2000hrs	W 12	N 20	NE 5	NNW 15	N 7	WNW 5	NNE 55

Date	Dec 25	Dec 26	Dec 27	Dec 28
0000hrs	NNE 60	W 30	NW 6	W 10
0400hrs	NNE 50	W 23	W 8	WNW 13
0800hrs	NNW 40	WNW 27	WNW 10	W 10
1200hrs	NW 35	WNW 20	W 8	NNW 10
1600hrs	W 30	W 20	WSW 1	NNW 0
2000hrs	W 30	WNW 9	WNW 7	---

Wind velocities are in knots.

Collection Period No. 1 = 1600hrs, Dec 4, 1966 to 1600hrs, Dec 18, 1966.

Collection Period No. 2 = 1600hrs, Dec 18, 1966 to 1600hrs, Dec 28, 1966.

HOLOCENE STRATIGRAPHY OF THE MARSHES AT  
PLUM ISLAND, MASSACHUSETTS

C. Larry McCormick\*

Abstract: The salt marshes landward of Plum Island, Massachusetts, are cut by an anastomosing network of tidal channels. The salt marsh itself, which has a planar surface at the level of mean high water, is subdivided into: (1) the high salt marsh; (2) channel margin marsh; (3) salt pannes; and (4) rotten spots. On the basis of physiographic breaks and grain size, the tidal channel zone is subdivided into: (1) peat scarps; (2) mud flats; (3) sand flats; and (4) deep channels.

From fifty-two cores, the stratigraphic sequence within the marsh was found to consist of: (1) a layer of high salt marsh peat; (2) a thin bed of Spartina alterniflora peat; (3) a silty layer analogous to present day mud flat deposits; (4) a thin bed of black peat containing fresh-water plant remains; and (5) a layer of late Pleistocene glaciomarine blue clay with a weathered zone at its upper contact. In some areas the Spartina alterniflora peat was underlain by sandy deposits believed to be analogous to material presently being deposited on the sand flats of the major tidal channels.

The geometry of these deposits and the radiocarbon data (of McIntire and Morgan, 1963) indicate that there was an offshore barrier in the vicinity of Plum Island as early as 6000 B.P. Fine-grained sediment was deposited in the open bay behind the barrier and a fresh to brackish water marsh fringed the bay. As sea level rose, the mud flat deposits of the bay

---

\*Present address:

8100 North Robinson  
Oklahoma City, Oklahoma 73114

transgressed landward over the plant remains of the fringing marsh. About 4000 B.P. there was a reduction in rate of sea level rise allowing the fringing marsh to expand and transgress seaward over mud flats of the open bay. The result of this transgression was to transform the original open bay to the present system of tidal channels.

This picture was complicated by the movement of the axis of the major tidal channel landward, eroding previously deposited peat and mud flat sediment. It left behind a thick sheet of fine sand which has been veneered by a thin layer of peat in the past few hundred years. Radiocarbon dates from opposite sides of the present channel support this premise.

## INTRODUCTION

Work on the stratigraphy of the salt marshes landward of Plum Island, Massachusetts, was conducted during the two-year period, 1965-1966. The landward edge of Plum Island forms the eastern boundary of the marshes considered in this study. The western boundary is marked by an abrupt change in slope and a conspicuous change in flora. The study area is bordered on the north by the Merrimack River and on the south by the Eagle Hill River (Fig. RL-1; p. 7 of this guidebook). Plum Island is one segment of a barrier island system which extends south from Plaice Cove, New Hampshire, to the bedrock promontory of Cape Ann, Massachusetts.

The primary purpose of this investigation is to chronicle the history of the deposition of Holocene sediments underlying the salt marshes at Plum Island. An attempt is made to define the stratigraphic relationships of Holocene units at Plum Island so that they may be compared with similar ancient deposits and with other recent marsh deposits.

The record of land-sea movements for the Plum Island area has been established by McIntire and Morgan (1963). Their history of sea level changes is based on radiocarbon dates of samples collected from a thin layer of fresh-to-brackish water peat which forms the lower boundary of the Holocene deposits. The radiocarbon dates published in their paper supply good control on sea level changes from 6280 B.P., but information on earlier sea level changes is based only on stratigraphic evidence (the details of sea level changes in this area are given on

page of this guidebook).

#### ACKNOWLEDGMENTS

My thanks to the National Science Foundation for the award of two summer fellowships which helped defray many of the field expenses for this project. In addition, I would like to thank the Society of Sigma Xi and the Geological Society of America for grants which made the first year of my field work possible. The laboratory work was supported by the Office of Naval Research (Geography Branch) Contract N00014-67-A-0230-0001.

#### PHYSIOGRAPHY

The study area can be divided into two major physiographic units, the salt marsh zone and tidal channel zone. The salt marsh zone is the densely vegetated area occurring at, or very near, the level of mean high tide. It occupies approximately seventy percent of the total study area and is thoroughly dissected by a system of tidal channels. The eastern margin of the marsh is a fairly smooth line formed by the intersection of the back slope of Plum Island and the nearly planar surface of the marsh. Its landward limit is a line defined by the intersection of the hummocky Pleistocene topography and the marsh surface, as such it is essentially a contour line drawn at mean high water. Except for the interruptions created by tidal channels and the Merrimack River, the salt marsh zone extends continuously from Coffin Beach, Massachusetts, to Plaice Cove, New Hampshire. Four physiographic subdivisions of the salt marsh zone are recognized: (1) the high salt marsh; (2) channel margin marsh; (3) salt pannes, and (4) rotten spots (Fig. 1).

#### High Salt Marsh

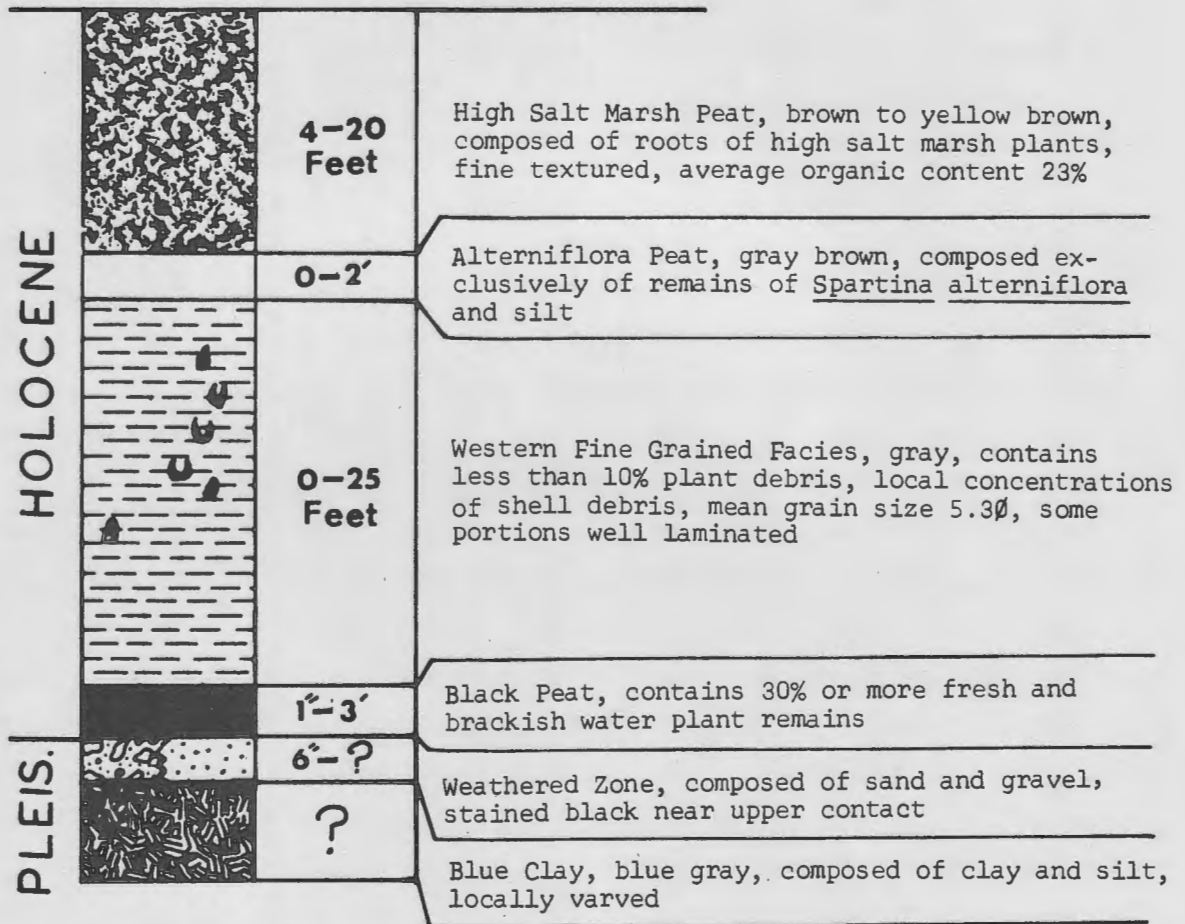
The high salt marsh stands slightly higher than mean high tide

---

Figure 1. Typical stratigraphic section of Holocene sediments in the Parker River estuary. In much of the eastern half of the study area, the western fine-grained facies is replaced by a zone of coarse, sandy sediment (eastern coarse-grained facies).

Figure 1

### Columnar Section



and is very densely populated by salt marsh grasses. It is flooded only during spring tides or high storm tides. According to data assembled by McIntire and Morgan (1963), mean high water is exceeded by one foot on the average of about twelve times a year.

The grasses, which form a dense mat of vegetation over the entire surface of the high marsh, most commonly include Spartina patens, Juncus gerardi, Distichlis spicata and a depauperate form of Spartina alterniflora. Another grass, believed to be Glyceria melicaria is present in fair abundance in the northern one-fourth of the study area. It is usually mixed with gerardi and patens. The stunted form of alterniflora rarely exceeds one foot in height and all parts of the plant are proportionately smaller than the more hardy variety that populates the channel margin environment. On a quantitative basis, Scirpus americanus, Salicornia europaea and Triglochin maritima are of minor importance. However, Triglochin maritima occurs in abundance in a few small areas east of the Plum Island River.

The high salt marsh is the most nearly planar surface in the marsh environment and the most densely populated with floral elements. By contrast, it is the most barren of faunal elements. It has been referred to as a salt meadow, which seems a good descriptive term, particularly in the spring when the broad flat expanses of the high salt marsh are colored a bright green with the re-growth of a new crop of salt grass.

#### Channel Margin Marsh

The channel margin marsh occurs as a fringe around the upper edges of the tidal channels and represents a transition from the high salt marsh to the channels. It occupies a vertical zone extending from mean high water to minus 2½ feet mean high water. Along most of the channels it comprises a strip about ten yards across, which slopes gently toward the tidal channels. There is a general tendency for the slope to increase toward the channel, with fissures six inches to a foot wide occurring in the substratum near the channel edge. The cracks are often found on the outside of meander bends as a result of undercutting and subsequent slumping. The channel margin marsh ends abruptly at the sharp break in slope defining the edge of the tidal channel. It is always characterized by a thick growth of alterniflora, otherwise known as common salt thatch. This plant has the ability to withstand extended periods of submergence, and according to

Hinde (1954) it may be submerged for 17 hours/day at its lower limit and 2.5 hours/day at its upper limit. As a result of its ability to stand prolonged periods of wetting, alterniflora is nearly the only plant that populates the channel margin marsh. It forms a thick growth which can attain a height of about four feet at maturity. The only other plant that inhabits this zone in any abundance is Salicornia europaea, which is found growing around the stalks of the common salt thatch. The rhizomes and roots of alterniflora are not as closely packed as are the roots of the high salt marsh plants, producing peat that is much more silty than that of the high salt marsh.

The channel margin marsh as here defined does not correspond to the Spartina glabra zone, alterniflora zone or thatch line of other writers [Johnson and York (1915), Miller and Egler (1950), and Redfield (1965)]. These zones cover the entire vertical range of alterniflora which extends considerably below the sharp break in slope defining the channel edge. The channel margin subenvironment, thus defined, represents a distinct physiographic unit which falls inside the vertical range of the common salt thatch.

#### Salt Pannes

Salt pannes are locally depressed areas distributed randomly over the surface of the high salt marsh. In this study I have restricted the use of the term salt panne to those areas slightly depressed in elevation relative to the surrounding high salt marsh that are constantly filled with water. They are the Ruppia pools of Miller and Egler (1950). Salt pannes range in size from a few inches to 70 feet. Most tend to be roughly circular in outline but some have an irregular shape. The margins of the salt pannes are usually very sharp as a result of the encroachment of tussock-forming plants. Chapman (1960) proposed two basic modes of formation for these features: (1) the result of irregular colonization of plants on a previously unpopulated tract of estuarine sediment; and (2) the result of an interruption in the normal growth of the high salt marsh plants with subsequent sinking of the effected area. Most of the pannes on the Plum Island marsh are believed to have been formed by the second mechanism.

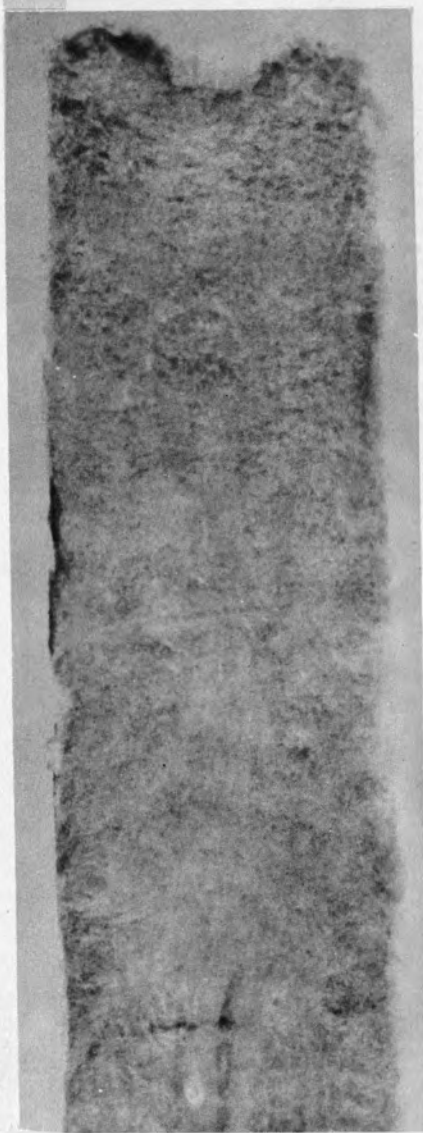
## METHODS OF STUDY

Fifty-two cores were extracted from the marsh using a fixed-piston coring device; the core locations were spaced approximately one half mile apart. An attempt was made to take all cores to the Pleistocene or bedrock foundation of the Holocene deposits. Of the fifty-two cores, nineteen completely penetrated the Holocene deposits; the other thirty-three cores bottomed in sandy or silty Holocene material. Sediment samples were collected from the surface of the marsh and from the mud flat and sand flat zones for comparison with core samples. In the laboratory, mud and sand samples were analyzed for grain size using standard pipette and sieving techniques. Organic content of the cores was determined by means of a special optical method that is discussed in detail elsewhere (McCormick, 1968). Every foot of core collected was X-rayed with the General Electric Mobile 90-II unit and radiographs were studied for variations in internal structures. Radiographs of the marsh sediment exhibited sharp contrasts as a result of the high percent of organic material contained within the deposits. Bedding and lamination were obvious in radiographs of many cores that appeared homogeneous on solid surfaces. Clay minerals were identified by means of x-ray diffraction.

## STRATIGRAPHIC SEQUENCE

The stratigraphic sequence of recent deposits at Plum Island varies considerably as a function of each specific locality and its history. However, the sequence is consistent enough to allow the construction of an idealized stratigraphic column (Fig. 1).

The high salt marsh peat occurs as a blanket of tightly woven organic debris over the entire surface of the marsh. It is interrupted only by tidal channels and exhibits a general tendency to thicken west of Plum Island Sound and Plum Island River. The S. alterniflora peat is a thin unit (0-2 ft. thick) that grades upward into high salt marsh peat and downward into the western fine-grained facies. Inasmuch as S. alterniflora peat records the vertical transition from the western fine-grained facies to the high salt marsh peat deposits, the S. alterniflora peat and **western** fine-grained facies are always found together. In areas where the latter

**A****B****C****FIGURE 2**

two units are missing, the high salt marsh peat rests directly on top of the black peat. The western fine-grained facies forms an irregular wedge of clastic material pinching out westward toward the mainland and northward toward the Merrimack River. Its sharply truncated eastern boundary lies along the west side of Plum Island Sound and Plum Island River. The black peat is a thin layer underlying the western fine-grained facies and high salt marsh peat. Below the black peat is a sandy or gravelly layer representing a weathered zone. This unit, though thin in places, occurs everywhere at the base of the Holocene deposits. The lowermost unit is a plastic blue glaciomarine clay (McIntire and Morgan, 1963) which displays the same wide distribution as the weathered zone above it.

#### High Salt Marsh Peat

The high salt marsh peat is composed of roots of high salt marsh plants and silt and clay-sized terrigenous particles. The major contributors include S. patens, D. spicata, J. gerardi, and the dwarf form of S. alterniflora. The growth of these plants produces roots that do not usually exceed 2 or 3 mm in diameter. Therefore, the peat produced on the high salt marsh is fine textured. An exception is the roots of S. alterniflora which, even though depauperate, produces roots and rhizomes up to 5 mm in diameter. It was not possible to identify specific contributors to the peat although it is obvious that the peat was formed by plants presently populating the high salt marsh (Fig. 2A). An exception occurs where a pure stand of S. patens has given rise to very fine-textured homogeneous peat (Fig. 2B).

---

Figure 2. A. Typical X-ray radiograph of high salt marsh peat, light areas are remains of the depauperate form of S. alterniflora, and dark bands are areas enriched in terrigenous material.

B. X-ray radiograph of high salt marsh peat consisting entirely of S. patens; note fine texture of peat.

C. X-ray radiograph of a typical section of S. alterniflora peat. Light areas are the coarse roots and rhizomes of S. alterniflora.

The lower boundary of the high salt marsh peat is gradational into either black peat or S. alterniflora peat. Where it grades downward into black peat, the typical brown or yellow-brown color of the high salt marsh changes to black and the organic content increases with a coincident increase of fresh-water plant debris. The change from high salt marsh peat downward into S. alterniflora peat is recorded by an increase in the amount of terrigenous material and by the complete disappearance of the fine textured roots of the high salt marsh plants (Fig. 2C).

Bedding and lamination are common in the high salt marsh peat. Individual layers average about 2 inches thick but may vary from less than one-quarter inch to a foot in thickness. Many of these units are not discernible in sawed sections of the peat, but are clearly shown on radiographs (Fig. 2A, 2C). The layering is the result of rapid changes in the proportions of organic detritus and terrigenous material. The upper and lower boundaries of these units are not always clearly defined because of disruption of the units by plant roots. Attempts to correlate these units among cores were unsuccessful and it is concluded that they arise from local variations in depositional conditions. Part of this layering is due to the deposition of mud sediments by rafted ice blocks during storm tides or exceptional spring tides (Hayes, personal communication, 1969).

#### Spartina Alterniflora Peat

S. alterniflora peat occurs as a thin layer overlying terrigenous deposits and underlying the high salt marsh peat. It consists of silt, clay, and the coarse roots and rhizomes of S. alterniflora (Fig. 2C). It is deposited in the intertidal zone during the transition from tidal flats to high salt marsh vegetation. Except for plant remains, this unit is structureless and has poorly defined upper and lower boundaries.

#### Western Fine-grained Facies

The western fine-grained facies are deposits that occur west of the dashed line on Figure 3. They abut coarser grained, more recently deposited sediment on the east, and pinch out landward.

Grain-size analyses of thirty-two samples selected from this unit show an overall mean grain size of  $5.3\phi$  (0.025 mm), with a range of means

from 3.4 to 7.22 $\phi$  (using graphic measures of Folk and Ward, 1957). Clay minerals in three samples were identified as poorly crystallized illite and kaolinite.

The shells of marine gastropods and a clam, or Mya arenaria, were found in growth position in many of the cores, indicating an intertidal environment of deposition.

### Black Peat

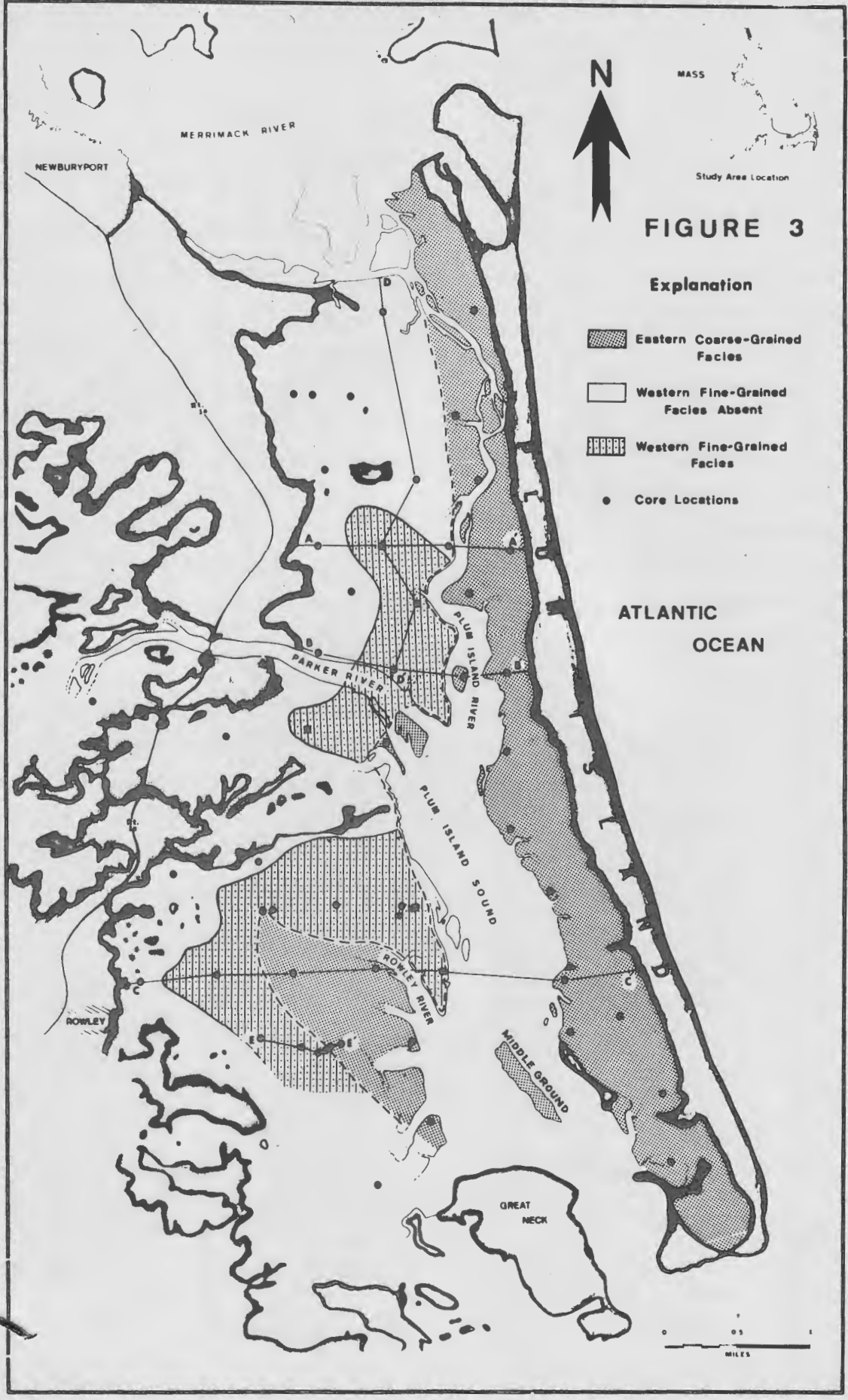
The black peat occurs as a thin layer at the base of the Holocene deposits. It varies in thickness from 6 inches to 3 feet and is readily recognizable due to the color contrast to underlying beds. It grades upward into either the western fine-grained facies or high salt marsh peat and downward into bituminous, poorly sorted sand or gravel. It contains less than 70% inorganic material and appears as a homogeneous, light-grey unit on radiographs. The organic remains are a mixture of broad-leaf fresh-water plants and high salt marsh plants. Black peat has been noted in many of the New England marshes (Johnson, 1925; Davis, 1910; Bloom, 1964) and has been variously termed "fresh-water peat," "sedge peat," and "brackish-water peat." Regardless of the name used, all workers agree that it represents an accumulation of fresh- and salt-water plants deposited in the zone of transition from the salt marsh to normal highland vegetation.

### Weathered Zone - Blue Clay

Below the black peat is a layer of sand or gravel stained dark brown by the overlying layer of peat. It grades downward into a bed of

---

Figure 3. Areal distribution of the eastern coarse-grained facies, western fine-grained facies, and location of cross sections shown in Figure 4. Unshaded areas indicate absence of the western fine-grained facies. The dashed line represents the sharp boundary between the eastern coarse-grained facies and older deposits which they meet to the west.



silty blue clay of unknown thickness. The sand and gravel is believed to represent a weathered horizon that developed on the surface of the blue clay after sea level dropped at the close of the Pleistocene, and as such, it is the "basement deposit" for the Holocene sediment.

The blue clay that underlies the weathered zone is believed to be of glaciomarine origin. According to McIntire and Morgan (1963), it is thought to have been deposited during a high stand of sea level in the late Pleistocene. It has been correlated northward with similar deposits occurring along the coast of Maine (Oldale, 1961, p. 60), but correlation with clays in the Boston area is in doubt. According to Oldale, the glaciomarine clay deposits in the Plum Island area extend inland along the valleys from sea level to an altitude of 50 feet. The fine-grained marine clay grades landward into till, ice contact stratified drift, and outwash. X-ray analysis of one sample of the blue clay indicates that the clay fraction is composed of well-crystallized kaolinite, illite, chlorite, and quartz.

## STRATIGRAPHIC RELATIONSHIPS

### High Salt Marsh Peat

Except for interruptions caused by tidal channels and creeks, the high salt marsh deposit blankets the entire study area. In cross sections B, C, and D, Figure 3, it forms an open V-shaped wedge of sediment. The lowest point of the "V" corresponds approximately with a line formed by the landward limit of the western fine-grained facies; the peat thins both landward and seaward of this line (compare Figures 1, 4 and 5). Landward and north of this line the high salt marsh peat is underlain by a thin layer of black peat. The thickness of the high salt marsh peat in this area is determined by the configuration of the buried Pleistocene topography which, though irregular, shallows to the north and west (Fig.5). East of the line formed by the pinchout of the western fine-grained facies, the high salt marsh peat thins gradually to five feet and this thickness remains constant to the eastern boundary of the marsh.

### Western Fine-Grained Facies

As mentioned earlier, the western fine-grained facies abuts

coarser grained more recently deposited sediment to the east. These two units were distinguished on the basis of differing grain-size characteristics, primary structures, and differences in thickness of the overlying beds. Those deposits west of the dashed line on Figure 4 are overlain by a thickness of high salt marsh peat and S. alterniflora peat that varies from 5 to 20 feet. They are underlain everywhere by a thin layer of black peat (Fig. 3). The eastern coarse-grained facies is overlain by a thin veneer (usually less than 6 feet thick) of high salt marsh peat and S. alterniflora peat. Attempts to penetrate this unit were unsuccessful and the occurrence of black peat at its base is a matter of conjecture. The western fine-grained facies is commonly well laminated, contains shell debris and often contains up to 10% organic debris, while the eastern coarse-grained facies is structureless, contains no large shell fragments, and never contains more than 5% organic material.

The coring device will not penetrate sediment coarser than very fine sand and, as a result, the degree of penetration furnishes a rough measure of grain size. Cores that penetrate the western fine-grained facies extend to the Pleistocene "basement" or to a minimum depth of 20 feet, but cores to the east of the dashed line (Fig. 4) reach a maximum depth of only 10 feet. To quantify this apparent difference, size distributions were prepared for forty-two samples collected from cores east and west of the dashed line. The summary results of these analyses indicate that sediment east of the line is coarser and better sorted than on the west (Fig. 6). The transition from fine to coarse-grained sediments is abrupt, as indicated by a cross section prepared from several closely spaced cores (Fig. 7).

---

Figure 4. Cross sections along lines shown on Figure 3. Note the open "V" shape of the high salt marsh peat deposit in cross sections B, C, and D. The intersection of the black peat and S. alterniflora peat forms a point in all cross sections which record the change from landward transgression of the western fine-grained facies to seaward transgression of the high salt marsh peat over western fine-grained facies.

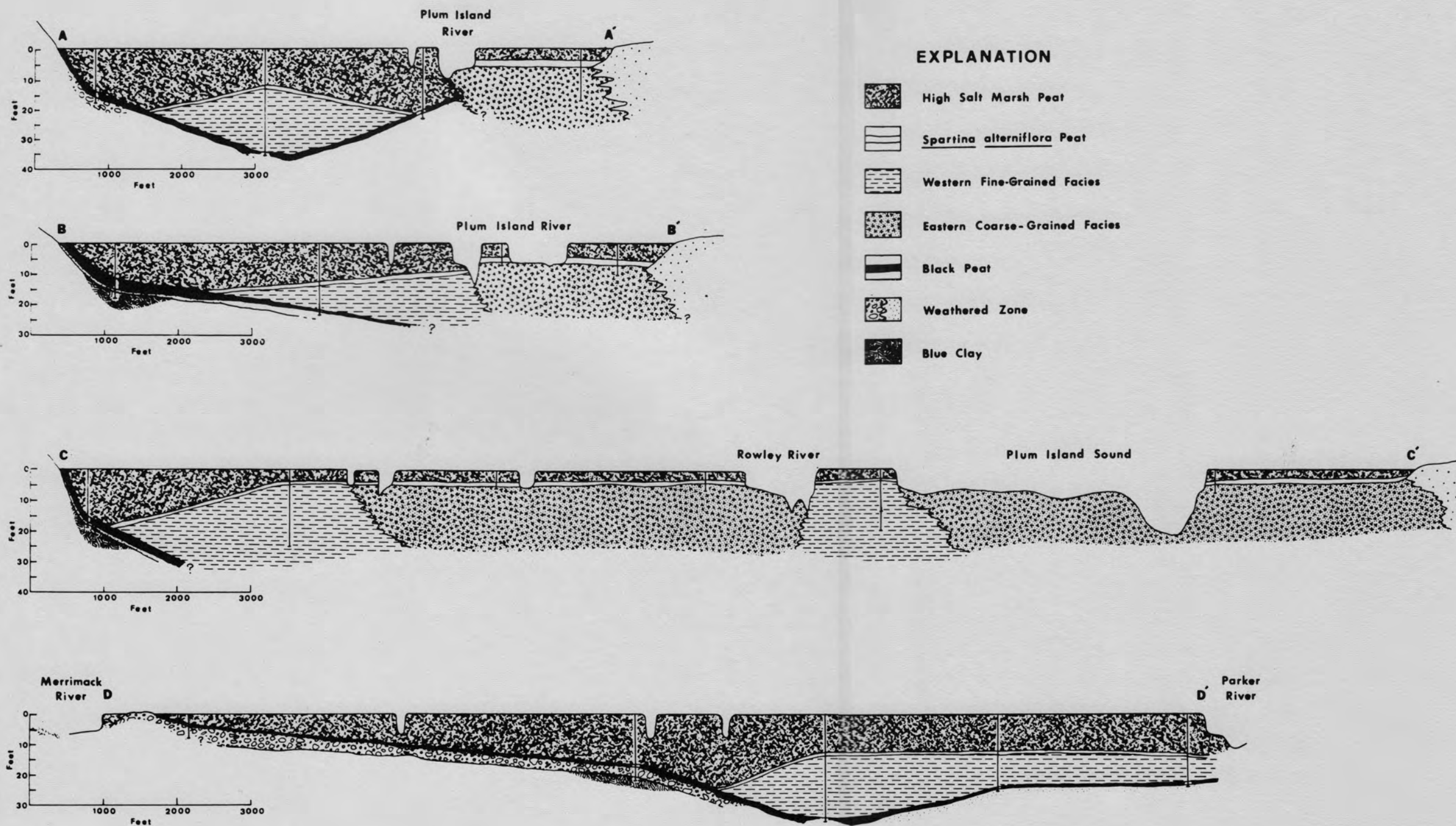


**FIGURE 4**

The wedge of sediment forming the western fine-grained facies thickens eastward and southward of the zero isopach line and is terminated by sandy deposits to the east (Fig. 8). The upper surface of the wedge slopes gently upward away from the zero isopach line complementary to the thinning peat above. The slope of the lower surface is determined by the character of the buried Pleistocene topography and, to a much lesser extent, by the thickness of the black peat.

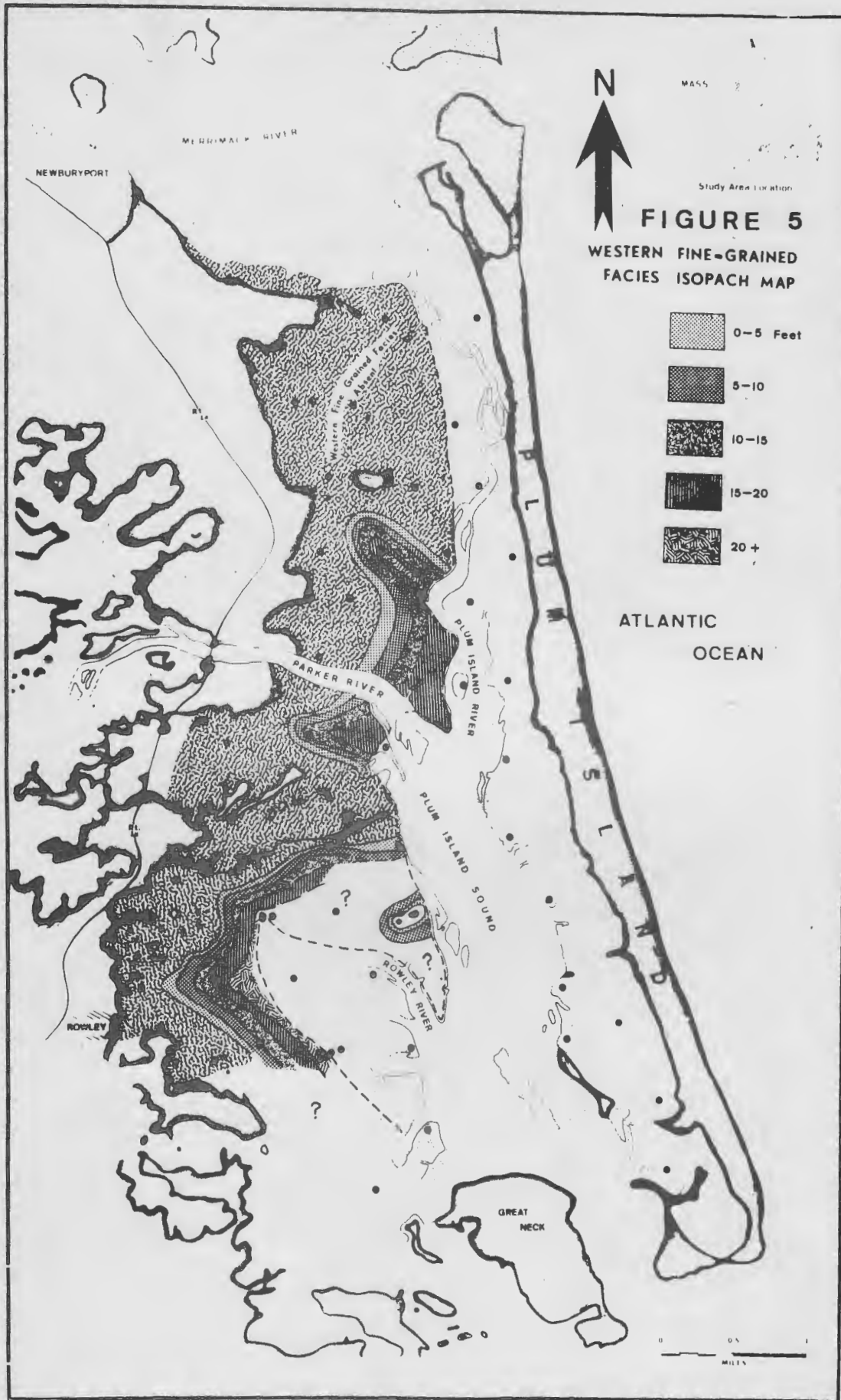
#### Eastern Coarse-Grained Facies

The coarse-grained facies to the east was never completely penetrated, so little can be said of its geometry. Deep borings made by McIntire and Morgan (1963) adjacent to Plum Island indicate a general thickening seaward. The upper contact is a nearly planar surface occurring at a depth of about 5 feet mean high water, or in other words, at the level of the present sand and mud flats. The simple north-south linear trend of this deposit is broken by a projection which extends northeast from Plum Island Sound into the area of the Rowley River and its tributaries.

In summary, the belt of deposits west of the dashed line (Fig. 5) consists of a basal layer of black peat, a wedge of fine-grained sediment pinching out landward, and a layer of high salt marsh peat that thins landward over the black peat and seaward over the western fine-grained facies. The fine-grained facies is truncated by a deposit of fine sand along the western margin of Plum Island River and Plum Island Sound, but the high salt marsh peat continues eastward as a thin veneer to the margin

---

Figure 5. Isopach map of the western fine-grained facies shows general thickening seaward. The western fine-grained facies is truncated sharply to the east along the dashed line. The areal distribution of this deposit roughly outlines the shape of the bay before encroachment of the high salt marsh.



of Plum Island.

#### DISCUSSION AND CONCLUSIONS

The earliest radiocarbon date (6280 B.P.) obtained by McIntire and Morgan (1963) was prepared from a sample of black peat obtained at a depth of 41 feet. This date records the minimum time that a barrier has been in existence in the vicinity of the present Plum Island.

The broad areal extent of the shell-bearing fine-grained facies indicates that early in its development the area west of the barrier was a shallow open bay, probably analogous to the present situation at Plymouth Bay, Massachusetts. The thin layer of black peat that underlies the mud flat sediments suggests that a narrow marsh fringed the edges of the bay. As relative sea level rose, the mud flat deposits of the bay were extended landward, burying previously deposited remnants of the fringing marsh and thickening the wedge of fine-grained sediments. Landward expansion of the fine-grained facies is terminated by seaward growth of the high salt marsh deposits, as indicated in the cross section (Fig. 3). This reversal takes place at an approximate depth of 15 feet and is correlated with the depth at which the rise in relative sea level slowed from 1.2 feet/century to 0.6 feet/century.

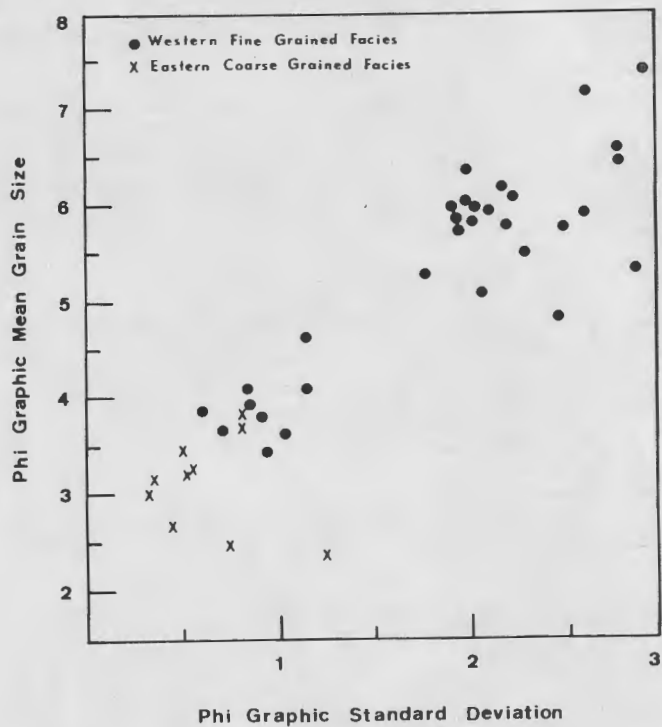
The radiocarbon data of McIntire and Morgan (1963) indicate that the rapid rise in sea level (1.2 feet/century) occurred during the period between 6280 and 4225 B.P. As it is known that the change in

---

Figure 6. Comparison of samples from the western fine-grained facies and eastern coarse-grain facies indicates overall coarser grain size and better sorting in the eastern coarse-grained facies.

Figure 7. Cross section along line E - E' (Fig. 4). This cross section shows the abrupt change from western fine-grained facies to eastern coarse-grained facies. The distance between cores 30 and 31 is only ten yards and there is a slight difference in elevation of the surface of the marsh between these two cores.

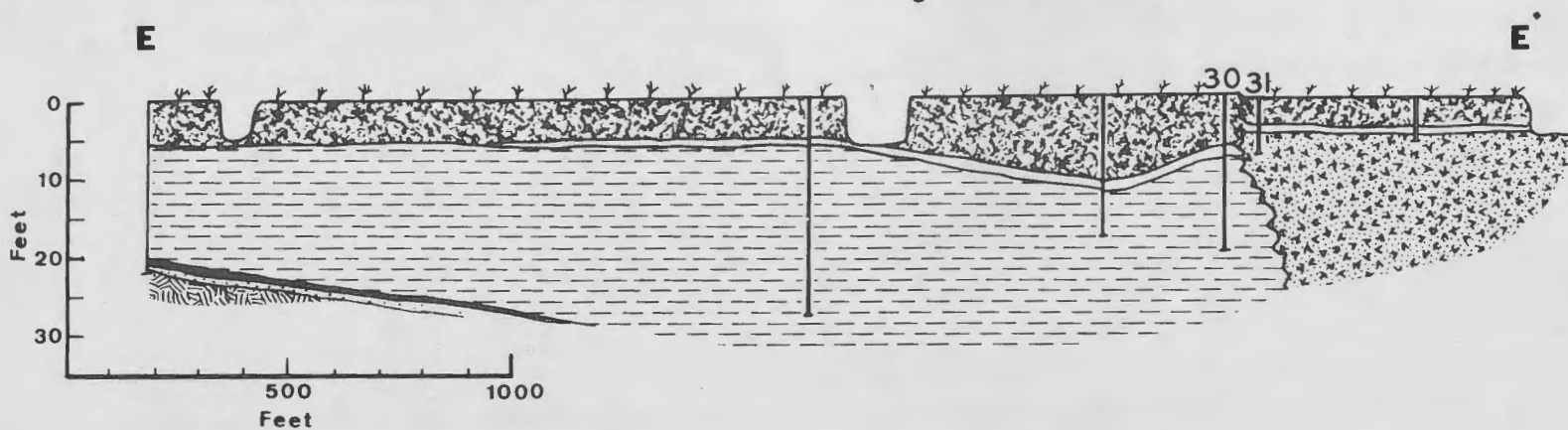
Fig. 6



EXPLANATION

-  High Salt Marsh Peat
-  *Spartina alterniflora* Peat
-  Western Fine Grained Facies
-  Eastern Coarse Grained Facies
-  Black Peat
-  Weathered Zone
-  Blue Clay

Figure 7



in rate of sea level rise occurred in the period of 4225 to 3550 B.P., the 4225 B.P. date represents the earliest possible time that a change in rate could have occurred. It is concluded that during a 2000 year period of rapid sea level rise, 25 feet of sediment was deposited in a shallow open bay that probably consisted of a system of deep channels separated by broad mud flats. The landward margin of the bay was fringed by a narrow band of brackish to fresh-water marsh.

The change in rate of sea level rise between 4225 and 3550 B.P. corresponds in depth to 15 and 10 feet respectively. The approximate 15-foot depth of the zero isopach line for the western fine-grained facies suggests a connection between the change in rate of sea level rise and the transgression of high salt marsh peat over the previously deposited sediment of the western fine-grained facies. I propose that the relative pressure of the fringing marsh against the margin of the open bay was increased by a decrease in the rate of relative sea level rise. The result was encroachment of salt marsh seaward, away from the Pleistocene upland. Bloom and Stuiver (1963) reached essentially the same conclusion regarding the Connecticut coastal marshes. However, the change in rate of sea level rise appears to have occurred at a shallower depth in the Connecticut marshes than at Plum Island. The continued rise in sea level, accompanied by further reduction in the rate of sea level rise, has allowed the marsh to restrict the once open bay to the present system of channels which are entirely bounded by high salt marsh and peat scarps.

From the time that the high salt marsh began to transgress seaward over previously deposited mud flat material, marsh development at Plum Island follows closely the theory of marsh growth proposed by

---

Figure 8. Isopach map of the high salt marsh peat and Spartina alterniflora peat. The two peat types exhibit seaward thickening to a line which corresponds roughly with the landward limit of the western fine-grained facies (compare Figs 4 and 3). Seaward from this line the peat thins to five feet and this thickness is maintained to the edge of Plum Island.

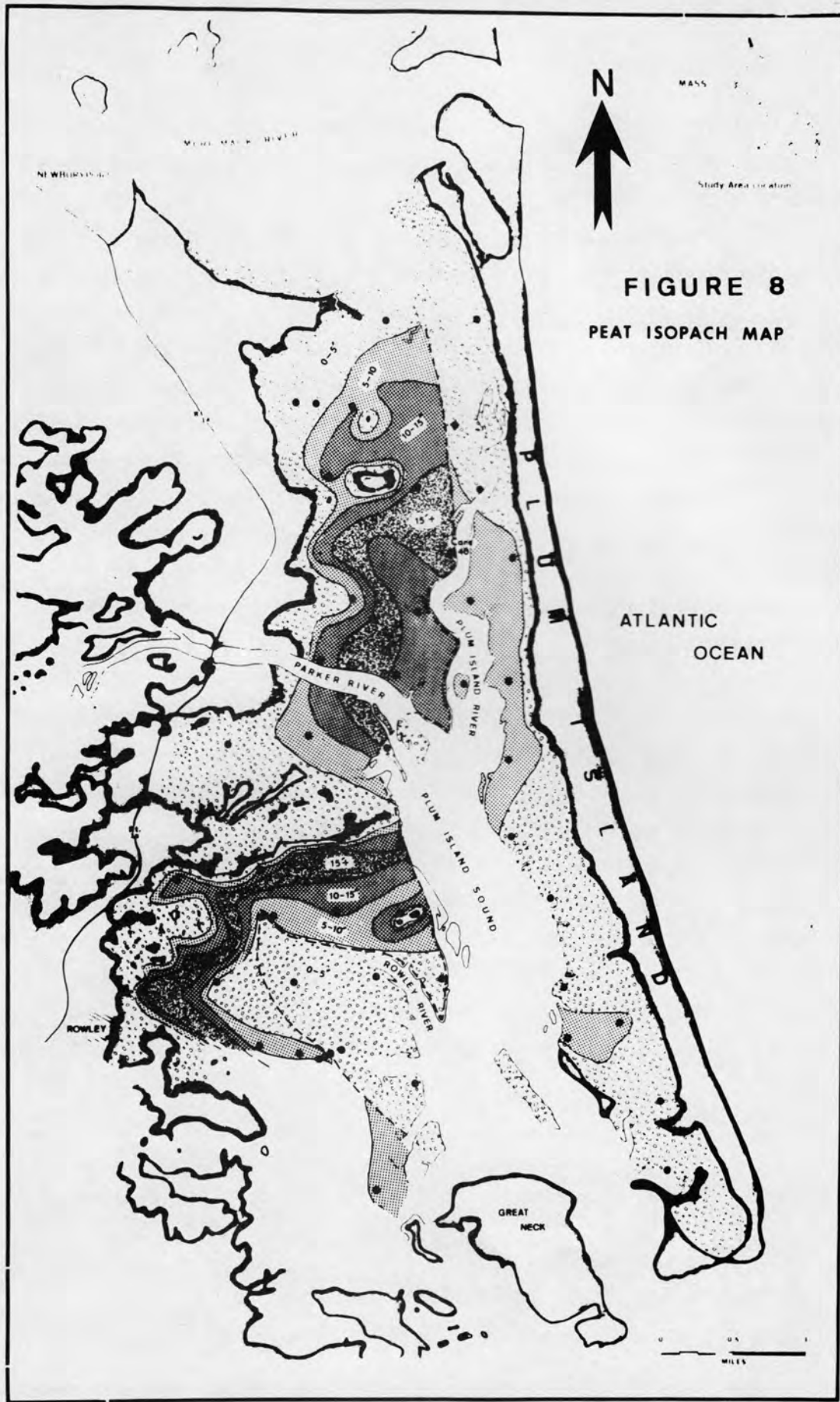


**FIGURE 8**  
**PEAT ISOPACH MAP**

A.C. Redfield (1965). It is not known whether the earlier stages of the development of the Holocene stratigraphy at Barnstable are analogous to those at Plum Island.

The simple picture presented above for infilling of a bay in response to rising sea level has been modified by fairly recent changes in the position of the major tidal channels. Apparently the present axis of Plum Island Sound has shifted westward eroding the high salt marsh peat and fine-grained sediment on the west and leaving in its path a thick sheet of sand. As the channel moved westward, the sand flats left behind became populated first by S. alterniflora and then by high salt marsh grasses which have developed into the thin veneer of peat east of Plum Island Sound. Movement of the channel westward and deposition of fine sand to the east accounts for the coarser-grained sediment that truncate the western fine-grained facies. If this sequence of events is correct, the peat east of Plum Island Sound should be younger than the peat west of the Sound. McIntire and Morgan (1963) dated samples from the same depth on opposite sides of the channel and found that although there was only a one foot depth difference in the two borings below the marsh surface, there was an 1800 years differential in time. I believe that westward channel migration and subsequent marsh growth to the east of the channel explains the contrasting depositional histories between the two points and the difference in age of the peat.

In the area north of Plum Island Sound along the Plum Island River, the eastern coarse-grained facies forms a narrow band that represents an earlier and wider channel that once connected the Merrimack

---

Figure 9. Aerial photograph at high tide (4-4-65) showing inundation of the recently filled Rowley River area. The dark flooded area (populated by S. alterniflora) has not yet built up to the level of the surrounding high salt marsh. Compare this area to the coarse-grained facies in the Rowley River area, Figure 4.

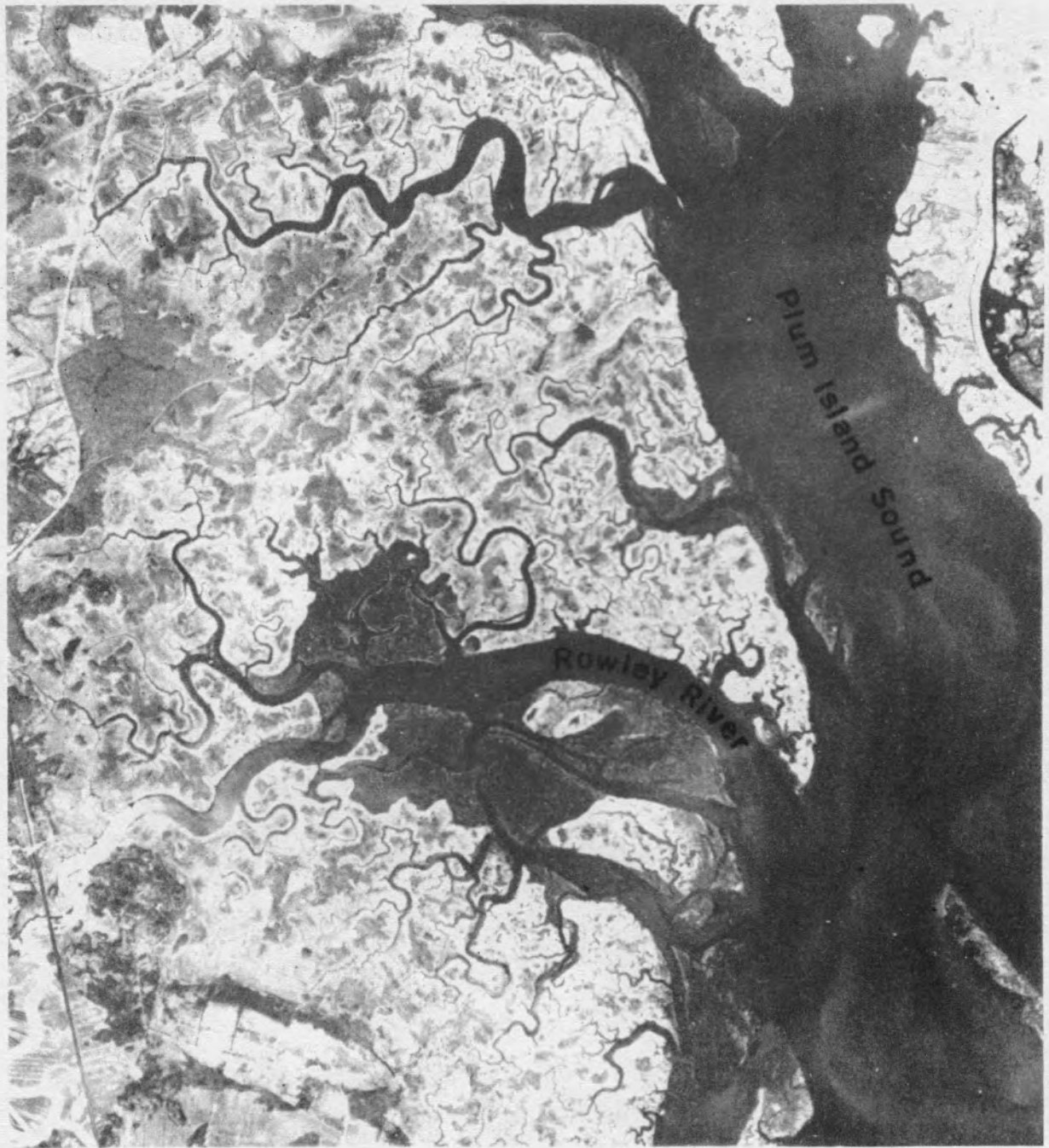


FIGURE 9

River and Plum Island Sound (Fig. 4). Similarly, the Rowley River appears to be the remnant of a much wider sound that extended roughly northwest from Plum Island Sound. Before encroachment of the marsh, it must have been much like the present sound to the southeast, occupied by broad sand flats, broken by occasional deep tidal channels, and bordered on either side by peat scarps. So recent is the filling of the Rowley River area that much of the surface has not built up to the level where typical high salt marsh plants can establish themselves. Broad fields of S. alterniflora populate much of the area. The recently deposited fill of the original channel is slightly lower in elevation than the older high salt marsh (Fig. 9).

POST-STORM PROFILE AND PARTICLE-SIZE  
CHANGES OF A NEW HAMPSHIRE GRAVEL  
BEACH: A PRELIMINARY REPORT

Barry S. Timson

Abstract: Preliminary studies on a New Hampshire gravel beach indicate rapid recovery of the beach profile following storm erosion.

Profile measurements and particle-size analyses show that the storm beach is characterized by a smooth concave-upward profile and uniform distribution of relatively small-sized particles. The post-storm recovery beach is characterized by a convex-upward profile and uneven distribution of constituent particles.

Coarse particles are removed and transported south during storm conditions. Recovery initiates the rapid return of the coarse mode to the south end of the beach.

#### INTRODUCTION

Rye Gravel Beach, which lies just south of Rye Harbor, New Hampshire (Fig. RL-2, p.18 ), is a ridge of gravel connecting a small, isolated headland to the northern edge of Straw Point. A minor amount of coarse sand is isolated at the north end of the beach. The gravel ridge is approximately 600 feet in length and 120 to 150 feet wide. The gravel deposit is backed by a large Holocene marsh which is still actively prograding into Rye Harbor. The ridge in front faces a small reentrant paved with large cobbles and boulders. Sources of the gravel and coarse sand are most likely the Pleistocene till-covered bedrock headlands of Straw Point and the aforementioned isolated ledge to the north. Both the till and metasedimentary bedrock contribute gravel to the beach, but the source of the coarse sand is limited to the till veneer on the isolated ledge. Gravel eroded from the till, which presumably once filled the shallow reentrant, probably constitutes the bulk of the present beach deposit.

## DISCUSSION OF THE PROBLEM

Extensive previous work on beach gravel grain size parameters and their geologic interpretation (Emery, 1955; Fleming, 1964; Jolliffe, 1964; Krumbein, 1941a, 1941b; Krumbein and Griffith, 1938; Marshall, 1929; Van Andel, Wiggers and Maarleveld, 1954; and Blatt, 1959), abrasion and hydrodynamic response of beach gravels (Jolliffe, 1964; Kidson, Clarence and Carr, 1959; Krumbein, 1941a, 1941b; Kuenen, 1956, 1964; Landon, 1930; and Marshall, 1927), and evolution of gravel beach morphology (Bagnold, 1940; Fleming, 1964; Lewis, 1931; and Bluck, 1967) provide a basis for interpreting this gravel deposit. The nature of gravel beach deposits and their changes are still not yet completely understood, however.

Although observations of the sediments and morphology of this particular gravel beach have been made since 1966 (Miles O. Hayes, oral communication, 1969), intensive study did not begin until late winter in 1969. It is the purpose of this reconnaissance study to ascertain the relationships between hydrographic conditions during and following storm periods, sediment-particle behavior, and storm beach ridge morphology. Rye Gravel Beach provides a unique set of depositional conditions. The small areal extent of the basin and close proximity of the source areas to the site of deposition allow for strict study controls on particle shape morphogenesis, particle hydrodynamic response, and mechanics of gravel ridge formation.

## PROCEDURE

Initial observations indicated that the gravel beach morphological features changed rapidly in response to climate variation. Particle-size and shape variation in the beach forms (i.e., berms, cusps, etc.) indicated a strong genetic relationship between the beach forms and particle behavior. Profile measurements obtained on different days were correlated with sediment samples collected on the same dates to ascertain the relationship between changes in morphology and changes in grain size and shape parameters.

# Rye Gravel Profile

Fall 1968-Spring 1969

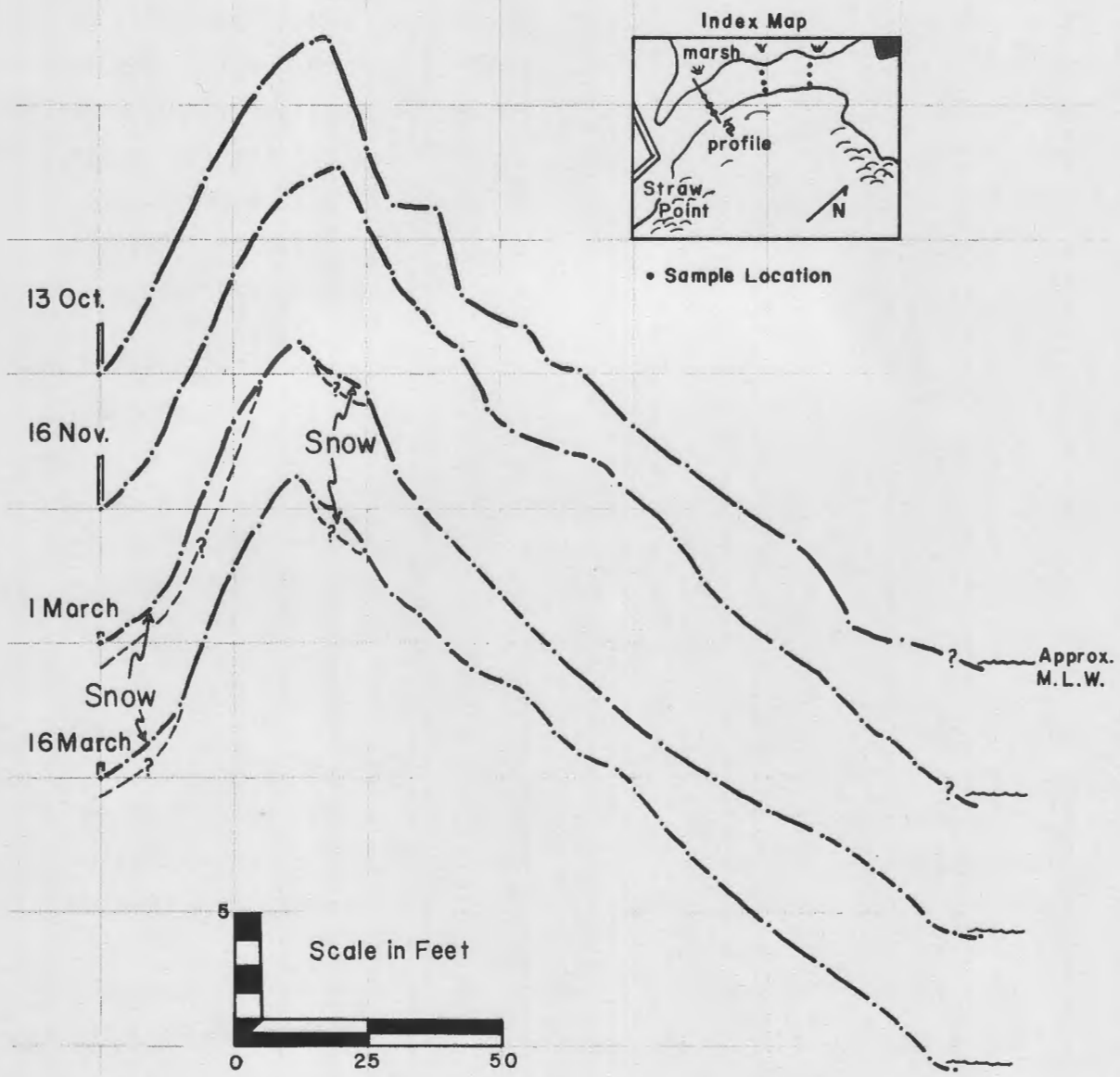


FIGURE 1

## Field Procedures

Profiles. Two profile measurements were obtained on March 1 and 16, 1969, respectively. The March 1 profile immediately followed intense beach erosion incurred during a strong northeasterly storm which lasted from February 25 to 27. The second profile was measured on March 16 after two weeks of recovery. The profile measuring method used is a slight modification of the technique developed by Emery (1961). Five-foot profile intervals were measured except where boundaries of morphological features dictated larger or smaller intervals. Ten foot intervals were measured where the degree of slope allowed. All profiles were traversed perpendicular to the beach strike; the profile locality (Fig. 1) was permanently maintained by driving a large marker stake into the marsh at the landward end of the profile traverse. The profile is approximately 225 feet from the north end of Straw Point.

Sediment Samples. Nine sample localities were established on March 1 (Figs. 1 and 3). The localities were chosen to indicate sediment distribution over the beach face seaward of the storm ridge. Samples were collected from the same localities on March 16. All samples were surface samples and incorporated a surficial lag population with the depositional sediment layer beneath. At least seventy-five particles were sampled, but in most samples more were taken.

## Laboratory Procedure

All profiles (Fig. 1) were plotted on graph paper using a five to one vertical exaggeration. Profiles measured at approximately the same traverse on October 13 and November 16, 1968 by the Coastal Processes Class of the University of Massachusetts were also plotted for comparison.

All eighteen sediment samples were separated into quarter  $\phi$  intervals by sieving. Particles with intermediate diameters greater than

---

Figure 1. Measured profiles of a traverse on Rye Gravel Beach on four successive dates. The November 16 profile was measured several days after a storm of moderate intensity.



FIGURE 2-A



FIGURE 2-B



FIGURE 2-C

-2.50 $\phi$  were individually passed through the sieves. Size statistics were then calculated by computer using the graphic measures of Folk and Ward (1957). The individual graphic measures for each sample were plotted on a fence diagram to illustrate the changes over the entire beach as well as at each sampling locality. Mean values for each statistical parameter were tabulated and compared for the two sampling data sets. Graphs of graphic mean versus inclusive graphic standard deviation and inclusive graphic skewness were constructed in order to compare parameter changes.

## RESULTS

### Effect of Storm Conditions and Recovery on the Ridge Profile

The intense storm wave action of February 25 - 27, 1969 produced a marked concave-up profile which remained, unchanged, on March 1 (Fig. 2a). Large waves accompanying storm-surge tides cut 9 feet back into the large gravel storm ridge. A small but conspicuous storm-ridge terrace positioned high on the ridge escarpment occurred along the south end of the ridge. The size of this ridge terrace diminished northward and ceased to exist where the ridge scarp was entirely erosional. The position and variation of size of the ridge terrace suggested that during storms, (a) erosion occurs at the north end of the beach, (b) particles are transported in a southerly direction, and (c) deposition occurs at the south end of the beach. Particle transport and deposition seaward of the beach probably occurs as well. On March 1, the ridge scarp graded seaward into a long, smooth, concave-up beach face which continued to the beach step (Figs. 1 and 2a).

Two weeks of post-storm recovery initiated the development of two berms on the original beach face and progradation of the beach step 15 feet seaward (Figs. 1 and 2b). Both berms, which were cusped, decreased

---

Figure 2. Views illustrating changes in the morphology and grain-size character of Rye Gravel Beach: a. March 1, 1969; b. March 16, 1969; c. October 13, 1968.

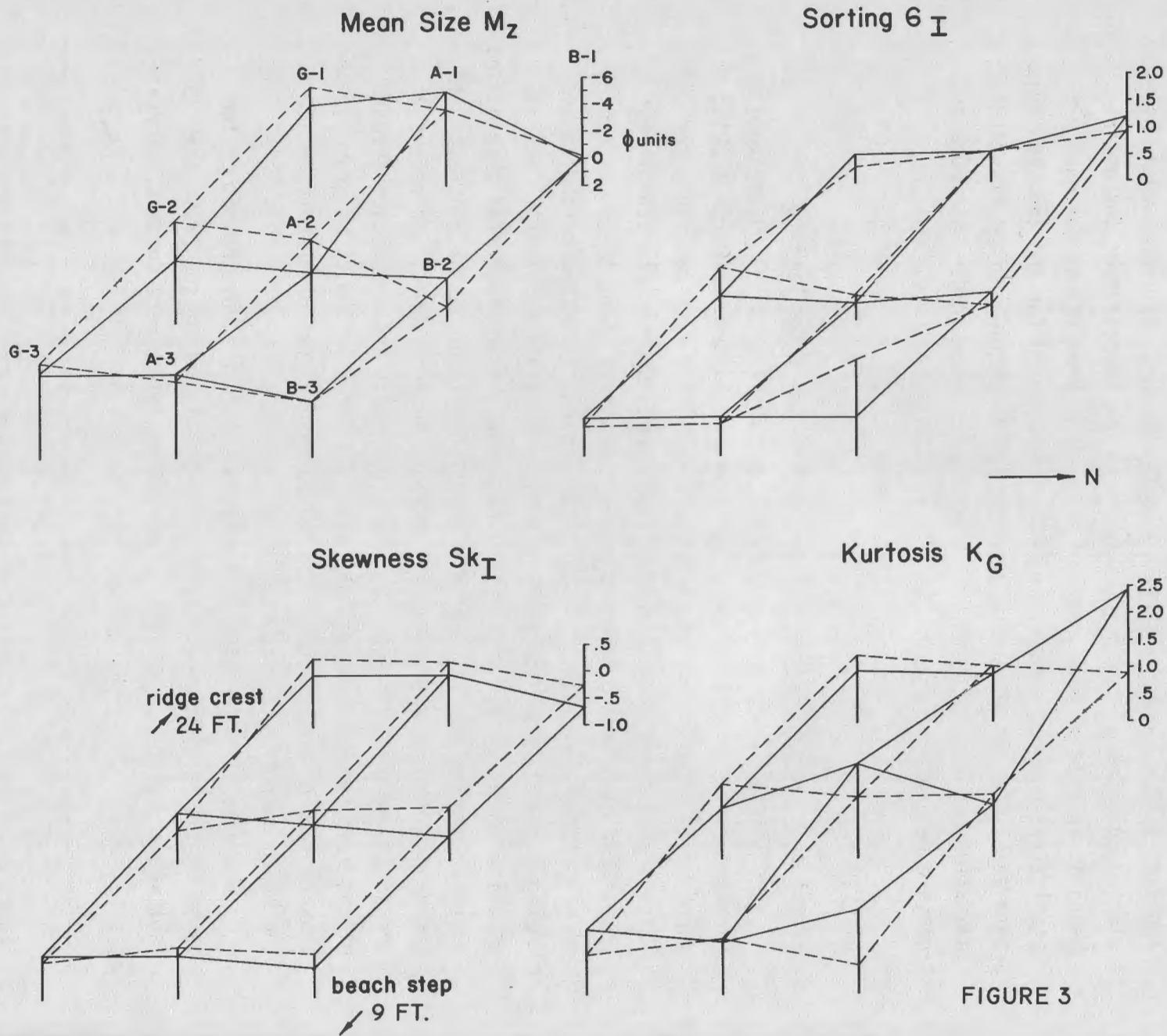


FIGURE 3

in size toward the north and ceased to exist approximately 360 feet from the north end of the beach. The north end of the beach remained unchanged from the conditions of March 1 - a smooth, concave-up beach face of sand and gravel-sized constituents.

The profiles of March 1 and 16 can be profitably compared with beach development on October 13, 1968 (see Figs. 1 and 2). The October 13 profile is typical of New Hampshire gravel beach morphology after an extended period of calm weather. Three cusped berms extended the entire length of the beach. The north end of the beach, which is usually composed of coarse sand, was covered by small to medium-sized pebbles on October 13. Recovery beyond March 16 should be exemplified by further accretion with resultant morphology similar to the October 13 profile.

#### Effect of Storm Conditions and Recovery on Particle Size

Three colinear zones of different particle size paralleled the beach strike on March 1. Three samples were taken along the beach strike in each zone. The three samples from the lowest zone on the profile average  $-2.96\phi$ , those from the middle zone  $-1.87\phi$ , and those from the upper zone  $-3.6\phi$ . The fine-grained median zone is probably the result of retention of large disc-shaped particles high on the beach face and the reworking of similar-sized spheres and rod-shaped particles by swash action until they are deposited on the lower portion of the beach face. This leaves the mid-portion of the beach face free of coarse particles.

Samples collected on March 16 show marked grain size parameter differences from those collected on March 1 (Fig. 3). Mean size decreases north along the beach strike for both sample sets. The conspicuous size increase at the G-2 and A-2 localities on March 16 reflect the construction of a neap berm composed of large, disc-shaped pebbles. Size changes varied

---

Figure 3. Graphic grain-size statistics at the nine sample localities. Solid lines join values for March 1 samples, and dashed lines join values of samples taken on March 16. The lines intersect the vertical "posts" at the attained values. The "posts" mark relative positions of sample localities. The B-1 post shows scale for each diagram.

little along Traverse B, which reflects the lack of construction or change at the north end of the beach. The decrease in mean size at station B-2 is interpreted as removal of a significant amount of the surface lag population by swash action.

Sorting values remain constant throughout the profile for both sample sets. The sorting value increase from 0.6 to 1.7 at B-3 on March 16 is due to the addition of coarse lag derived from a scarp higher up on the beach face.

All samples were negatively skewed except those collected at the G-1 and A-1 localities on March 16. Slumping and deposition of storm ridge particles at G-1 added a coarser particle population to those areas than would normally be expected. The storm ridge population is characterized by a framework of large disc pebbles. The framework pore spaces are filled with smaller-sized particles which normally yields a positive skewness value to an otherwise normally distributed population. The removal of a significant portion of the coarse tail from the sediment at locality A-1 produced a positive skewness value on March 16. A decrease in values of coarse skewness along the B traverse is also attributed to removal of portions of the coarse lag population by swash reworking.

Samples collected on the G and A traverses yield mesokurtic or leptokurtic values of kurtosis. The changes at B-1 and B-3 on March 16 reflect the removal of portions of the coarse lag from high on the beach-face with subsequent deposition at B-3.

Comparisons of the mean values of the various grain size parameters for the two sample sets show little marked variation (Table 1), but indicate the deposition of coarse particles during the recovery or accretion-period. The skewness value changes indicate the beginning of a return to the coarse pebble population that occurs on this beach under normal conditions.

Scatter plots of mean grain size versus skewness and sorting, respectively, (Fig. 4) illustrate a textural variation between the two sample sets. The close proximity of plotted samples for March 1 indicates a tendency towards greater textural homogeneity than do the plots for March 16. The removal of large-sized particles during storm conditions

Table 1. Average of the graphic grain-size parameters for the nine samples collected during the two sampling periods. The third column is the average of the parameters of all eighteen samples combined.

	$M_Z$	$G_I$	$SK_I$	$K_G$
March 1, 1969	-2.829 $\phi$	.6314	-.2456	1.309
March 16, 1969	-3.286 $\phi$	.7261	-.0829	1.017
Average	-3.058 $\phi$	.6787	-.1642	1.163

leaves a beach face of fairly uniform fine- to medium-grained texture. The subsequent return of coarse particles to the south portion of the beach during recovery created greater inhomogeneity of texture along the beach strike.

#### CONCLUSIONS

Intense storm wave conditions produce a concave-upward profile on Rye Gravel Beach. Coarse pebble particles are removed and transported south by strong beach drift. A minor amount of transported particles are deposited in the form of a ridge terrace at the south end of the beach. Removal of the coarse particle mode leaves a smooth beach face consisting of uniformly distributed, small-sized particles.

Post-storm recovery is characterized by rapid deposition of coarse pebbles along the south end of the gravel beach. Accretion on this portion of the beach suggests onshore transport and redeposition of the particles eroded during the storm. The limited extent of accretion produces a beach surface of heterogeneous texture and morphology. The recovery profile is characteristically convex-up due to the formation of spring and neap berms. The north end of the beach, however, remained unchanged during initial recovery.

Observations on the nature of a fully-recovered profile suggest



that most of the coarse mode eroded during the storm should return to the beach. Minor amounts of new material may originate from offshore, but these source relationships are little understood at present.

---

Figure 4. Scatter plots of mean grain size versus skewness and standard deviation. The broken line encloses a field occupied by values attained for March 1 samples. Sample B-1, not included in the field, is believed to be anomalous due to contamination of the normally fine-grained post-storm beach sediment by large-grained particles that fell from a wave-cut cliff (near crest of gravel ridge) onto the profile at sampling station B-1. Plot indicates textural uniformity of the post-storm beach in comparison to that of the recovery beach.

SEDIMENTARY MINERALOGY  
OF THE  
HAMPTON HARBOR ESTUARY,  
NEW HAMPSHIRE AND MASSACHUSETTS

Sharon A. Greer

Abstract: Sedimentary deposits of the Hampton Harbor estuary include distinctly separate bodies of yellow and gray feldspathic sediments. Both the yellow feldspar of the yellow suite and the gray feldspar of the gray suite are similar in composition, and the quartz associated with both types is similar. The yellow feldspathic sand is being eroded from the barrier beaches and transported into the inlet where it is mixed with the gray feldspathic sand, which may be derived locally. The mineralogical similarity of the two feldspar types indicates that they were derived from similar source material, either glacial drift or bedrock. Two possibilities exist to explain the two feldspar suites: (1) both are from the same source except that one of the feldspars has changed color in the interval between initial erosion and final deposition, or (2) there are two sources, each yielding feldspar of a different color -- the yellow feldspar being unavailable to the Hampton Harbor drainage, and the gray feldspar unavailable to the Merrimack River drainage.

#### INTRODUCTION

The intertidal sediments of the Hampton Harbor estuary range from gravel to clay with medium- to fine-grained sand being the most abundant type. The fine-grained sand of the small tidal channels and large sand flats is nearly 100 percent quartz, whereas the coarser sand of the large tidal channels and the inlet is feldspathic, containing approximately 5-15 percent feldspar.

A large part of the coarse-grained feldspathic sand is derived from the barrier beach complex that separates the estuary from the Gulf of Maine (Fig. 1). Tidal currents and wave action have eroded the barrier

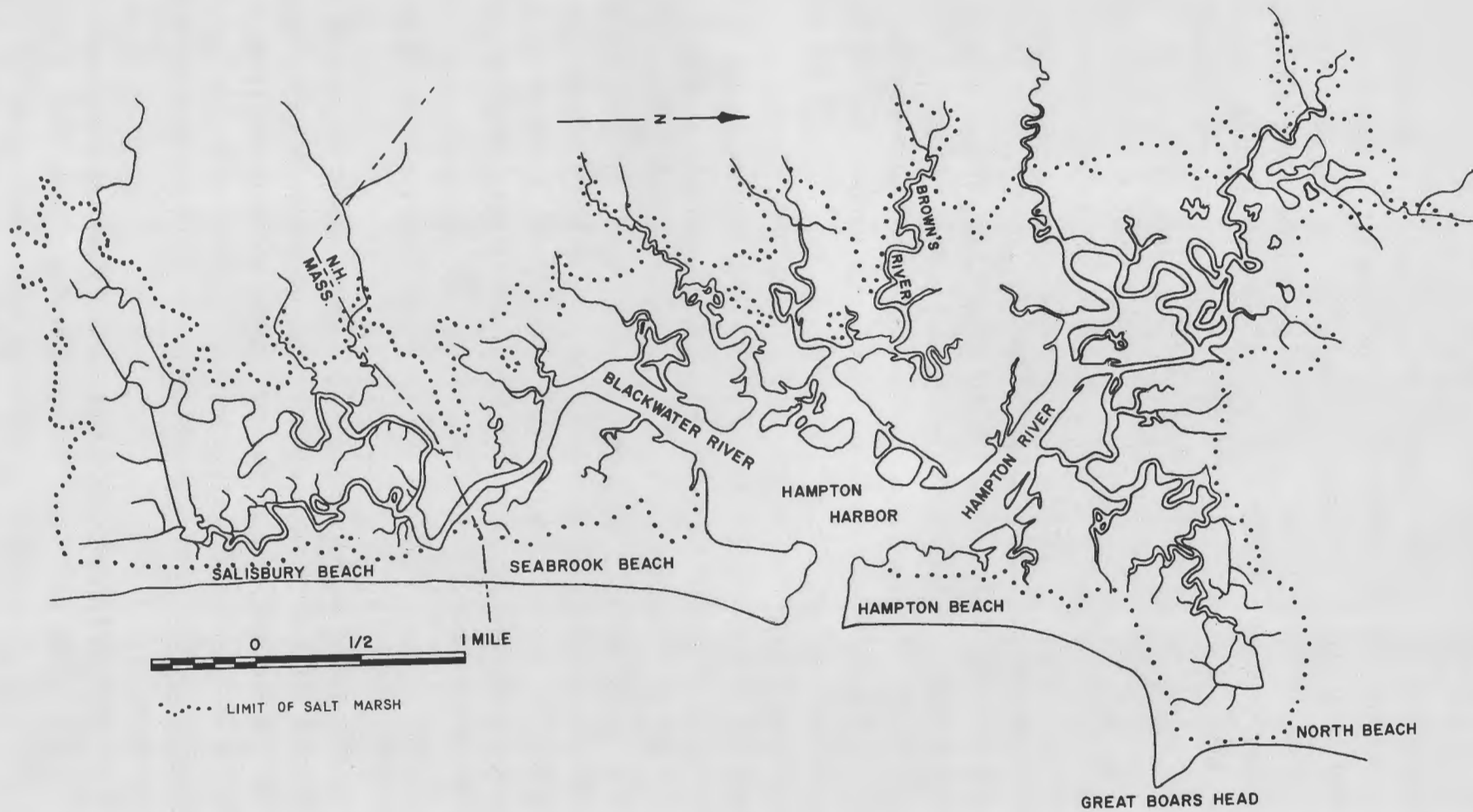


FIGURE 1

sediments and transported them into the estuary as well as offshore.

The coarse feldspathic sand of the inlet has a distinctive yellow-brown color due to a high percentage of yellow feldspar. Landward from the inlet, in the main tidal channels, the yellow feldspar is replaced by gray feldspar. Figure 2 shows the progressive change in mineralogy up the main tidal channels; Hampton River to the north, Blackwater River to the south, and Brown's River to the west.

The original source for the sediment is bedrock, but the immediate source is glacial drift of Pleistocene age, which is being reworked and distributed along the coastline. The glacial material probably has been eroded from the igneous and metamorphic complexes west and northwest of the New Hampshire shoreline and carried south and east, first by the glaciers and later by glacial melt water during the retreat of the ice.

#### PETROGRAPHIC STUDY

The sediment is composed of common igneous and metamorphic minerals. The constituents are feldspar, quartz, muscovite, garnet, tourmaline, zircon, and igneous and metamorphic rock fragments. There is no indication that any of these minerals have been derived from sedimentary rocks and are in their second cycle of deposition.

During the processes of reworking, the glacial drift has undergone selective sorting by wave and current action. This selective sorting has concentrated certain minerals in some deposits, giving a false impression of the total mineralogy in a sample that has a narrow range of grain sizes. To eliminate this potential bias, the study was done on sediments with a size range from  $-1.0$  to  $+4.0\phi$ . Twenty-three selected samples were sieved and point-counted at  $0.5\phi$  intervals.

Most of the selected samples were from the floor of the inlet and the center of the main tidal channels. The percentage of yellow vs. gray feldspar for the  $0.0\phi$  size is shown in Figure 3. The results show

---

Figure 1. Location map for Hampton Harbor estuary, New Hampshire and Massachusetts.

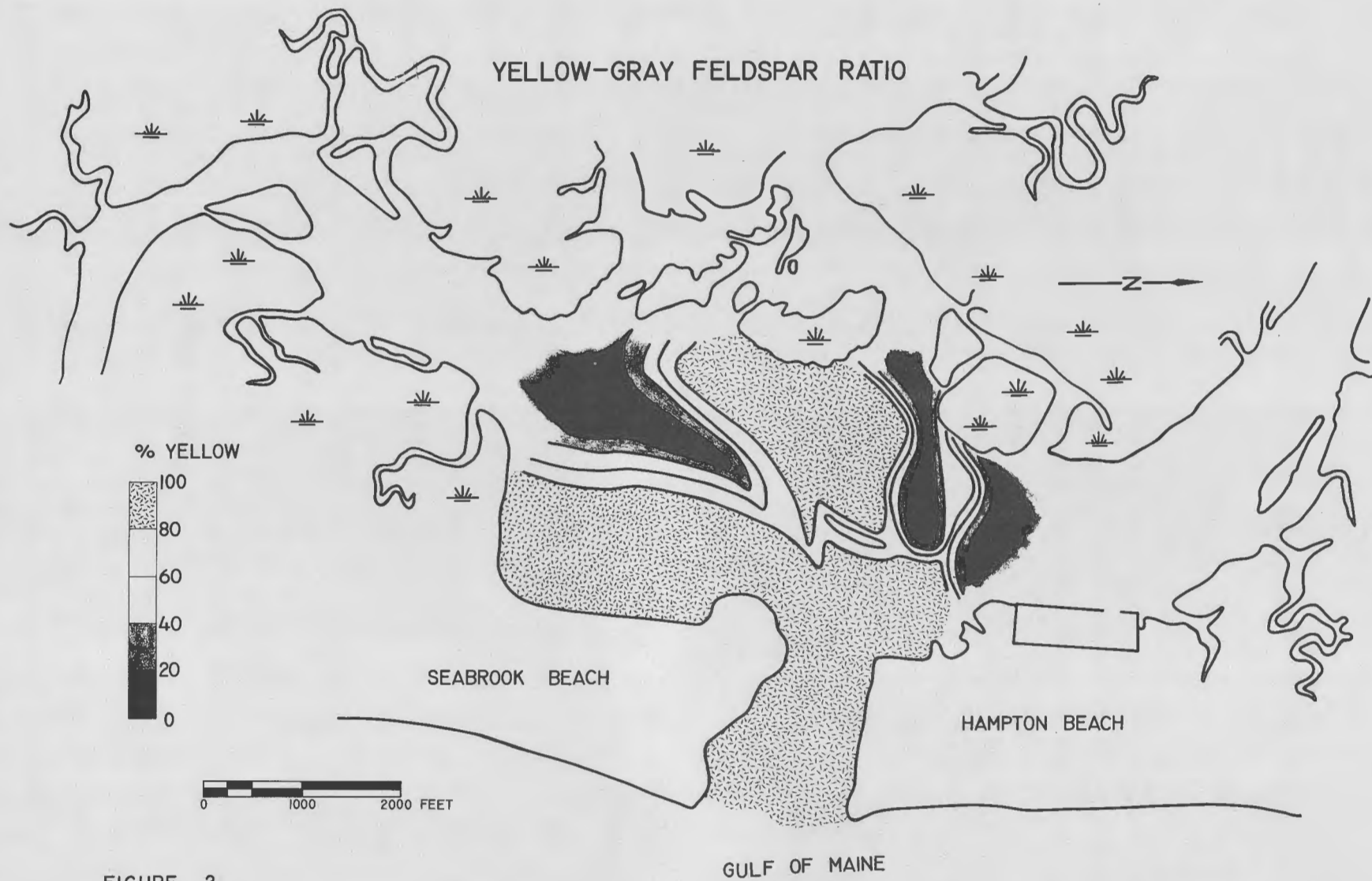


FIGURE 2

three categories can be recognized on the basis of feldspar types; yellow, gray, and mixed.

#### Yellow Feldspathic Sand

The yellow feldspathic sediment is concentrated in the inlet where it comprises the bulk of the flood tidal delta, a large flood-oriented bar, and the floor of the flood dominated inlet. Clearly this sediment is being brought into the estuary from the Gulf of Maine.

Chemical composition of the yellow feldspar is variable. Some is perthite, some is microcline, but the majority is plagioclase of oligoclase composition. It is devoid of inclusions but is partially altered, thus it has a dull, cloudy appearance in plane polarized light. The quartz is subangular, polished, and for the most part monocrystalline. It commonly contains fluid inclusions and inclusions of a green acicular mineral, probably an amphibole. The remaining bulk of the sediment is composed of rock fragments that are mostly coarse grained. In some samples, phyllite and schists form the pebble size fraction. Another common constituent of the pebble sizes is a brown or green amorphous transparent substance with conchoidal fracture, which is localized near a favorite fishing hole. The heavy minerals compose the remaining fraction of the sediment. They are predominantly garnet and magnetite but small amounts of amphibole, tourmaline, zircon, and apatite also are present. The heavy minerals are restricted to the 3.0-4.0 $\phi$  size, thus in zones of high turbulence the heavy mineral content is low. The histograms in Figure 4 give the mineralogy-grain size relationship of a typical yellow feldspathic sand.

#### Gray Feldspathic Sand

The mineral composition of the gray feldspathic sand and the yellow feldspathic sand are nearly the same. The only difference between

---

Figure 2. Map showing progressive change in yellow-gray feldspar content within the estuary.

# CHANGE IN FELDSPAR MINERALOGY WITH DISTANCE FROM INLET

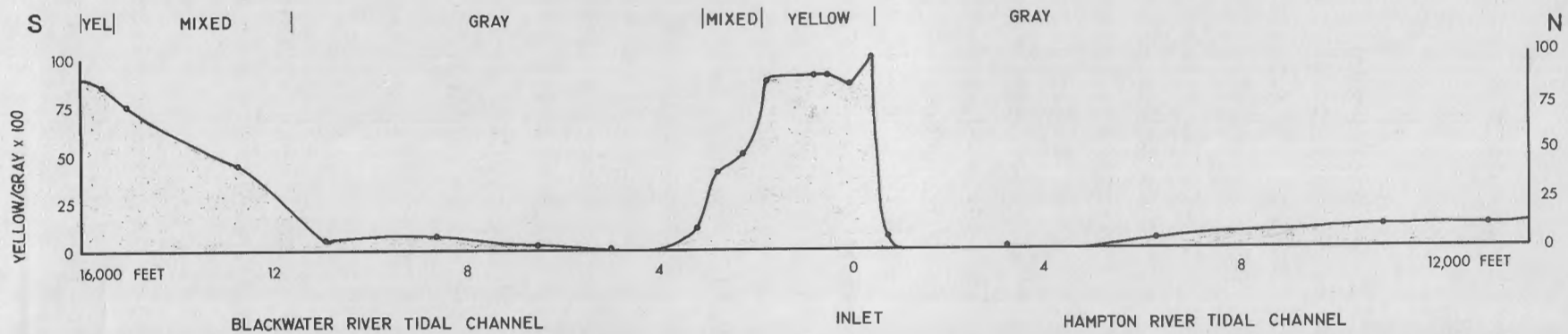


FIGURE 3

the two is that the gray sand is in a slightly lower energy environment and commonly has the fine fractions of 3.0-4.0 $\phi$ , which give it a higher heavy mineral content. The gray feldspar has the same composition as the yellow, the same degree of alteration, and the same lack of inclusions. The quartz is the same in both types of sediment, containing fluid inclusions and abundant green acicular inclusions. Figure 5 is a representative sample of the gray feldspathic sand.

#### Mixed Feldspathic Sand

Where the yellow and gray feldspars are mixed, the total feldspar content remains approximately the same as in the sediments containing only one feldspar (Fig. 6). A mixed zone (Fig. 2) is present in the Blackwater River in two places, one near the inlet and one approximately three miles from the inlet. The mixed zone near the inlet results from the yellow sands that are brought in the inlet and mixed with gray sand brought down the ebb-dominated tidal channels. The second mixed zone results from currents distributing sand from a local yellow sand source. The local source is a body of coarse sand and gravel that is exposed beneath the salt marsh. This sand deposit is very poorly sorted, coarse grained, shows no bedding, and has an unusually high heavy mineral content. The yellow sand body was probably deposited when the barrier beach was washed over during storms. Large quantities of barrier beach sediment were dumped into the marsh or into an open lagoon behind the barrier (McIntire and Morgan, 1963). The washover fan deposit has since been overgrown by salt marsh and later exposed when the tidal channel meandered into it. This apparently has happened recently, because the sediment has not been dispersed much and a meander that was cut off when the channel meandered into the sand body has not yet been filled.

The mixed zone is absent in the Hampton River channel. An abrupt change occurs at the margin of a large migrating body of yellow

---

Figure 3. Longitudinal profile from the inlet up the Hampton River and Blackwater River tidal channels showing percentage of yellow feldspar vs. gray feldspar for the 0.0 $\phi$  size class.

# YELLOW FELDSPATHIC SAND

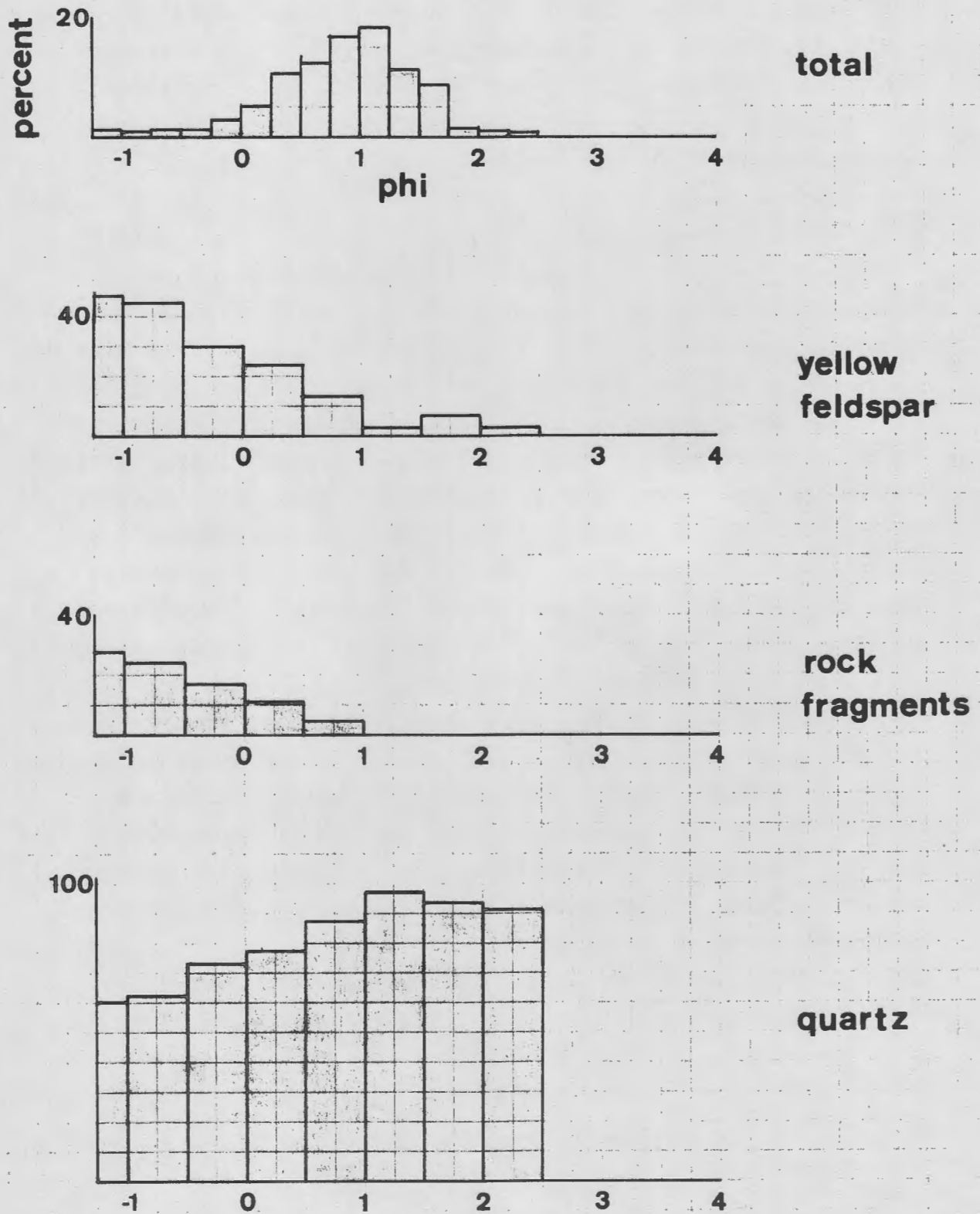


FIGURE 4

sand that is moving from the inlet up the main channel. It has an active slip face 18 feet high and approximately 500 feet long, which is migrating over the gray sand floor of the channel.

#### CONCLUSIONS

From the sediment distribution shown in Figures 2 and 3, it is evident that the yellow feldspathic sand is coming into the inlet and mixing with the gray sand of the estuary. From this relationship one would assume that the gray sand is derived from local glacial drift and is slowly being covered by the transgressing barrier beach sand, which has been derived from yet another source. However, the situation may be more complex than this.

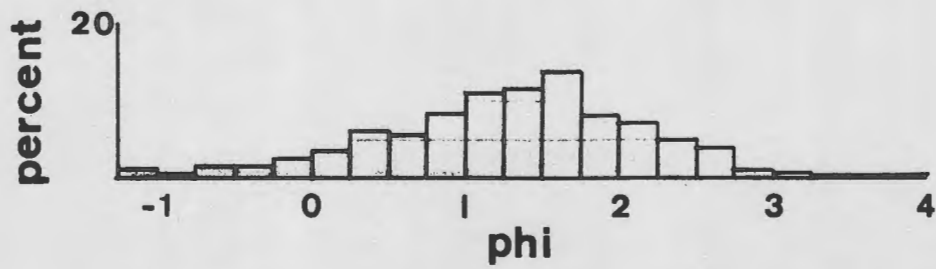
All present data indicate that the yellow barrier beach sand has been brought into the coastal system by the Merrimack River. The barrier beach sediments become progressively finer away from the river's mouth, and coarse yellow sand is found for some distance up into the channel. During Wisconsin time, the Merrimack River apparently transported great quantities of sand out onto the continental shelf. Sea level rose quickly (Bloom, 1968), and marine clay was deposited during the transgression. Isostatic rebound lifted the clay above sea level and also brought the shelf sand deposit up to wave base, where it could be moved ashore and built into the barrier beach complex when sea level became relatively stable, around 3000 to 5000 B.P. (McIntire and Morgan, 1963).

Keeping the above late Pleistocene and Holocene history in mind, one can consider two possible explanations for the two feldspar suites. The first possibility is that the two suites are not only from similar sources but are from the same source. Possibly the Merrimack River and Hampton Harbor drainage areas were covered by a veneer of gray

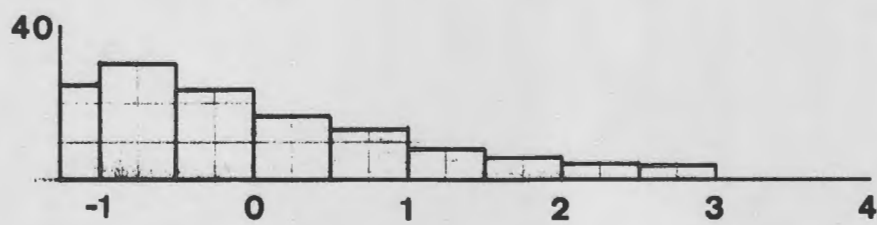
---

Figure 4. Histograms of a typical sample from the yellow feldspathic sand suite. First histogram is total grain-size distribution, others are grain-size distribution of a specific component.

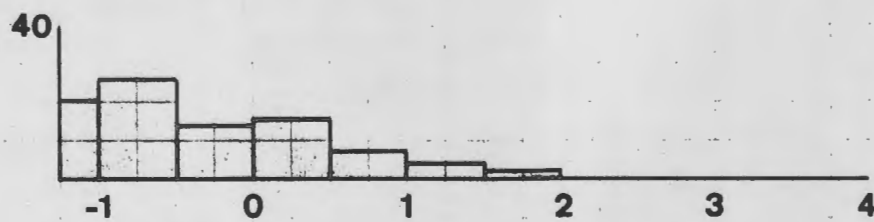
# GRAY FELDSPATHIC SAND



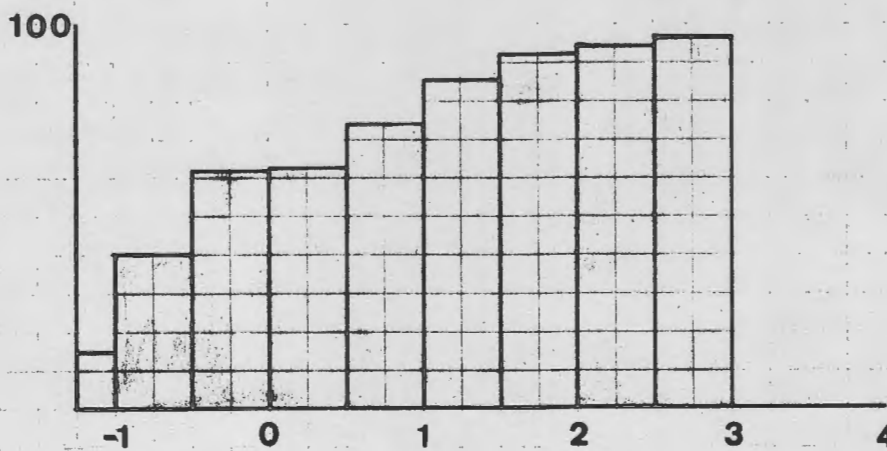
total



gray  
feldspar



rock  
fragments



quartz

FIGURE 5

feldspathic sand, which the Merrimack River transported out onto the shelf where it was oxidized to its present yellow color. The yellow sand is now transgressing the gray sand, which was trapped in the low area around Hampton Harbor and was not transported onto the shelf. This explanation would be applicable if the Merrimack River had large quantities of coarse gray feldspathic sand available to it during Pleistocene.

The second possibility is that there are two mineralogically similar but separate source areas, one supplying yellow feldspar and the other, gray. Sediment sampling of the Merrimack River drainage by Favez Anan (personal communication, 1969) indicates that the tributaries are supplying primarily a coarse yellow feldspathic sand; one minor tributary is probably supplying a small quantity of gray sand.

If the Merrimack River were transporting only yellow sand out onto the shelf, then the gray sand of the estuary necessarily must be derived from local drift or bedrock. The bedrock of the area is gray quartz diorite with basalt dikes (Newburyport Quartz Diorite). This rock unit could easily supply the gray feldspar for the Hampton Harbor gray feldspathic sand.

In order to verify one of the above explanations, the exact mineralogy of the glacial drift in the Merrimack River and Hampton Harbor drainage basins must be determined.

---

Figure 5. Histogram of a typical sample from the gray feldspathic sand suite. First histogram is total grain-size distribution, others are grain-size distribution of a specific component. Heavy mineral content not included.

Figure 6. Histogram of a typical sample from the mixed feldspathic sand suite. First histogram is total grain-size distribution, others are grain-size distribution of a specific component. Heavy mineral content not included.

# MIXED FELDSPATHIC SAND

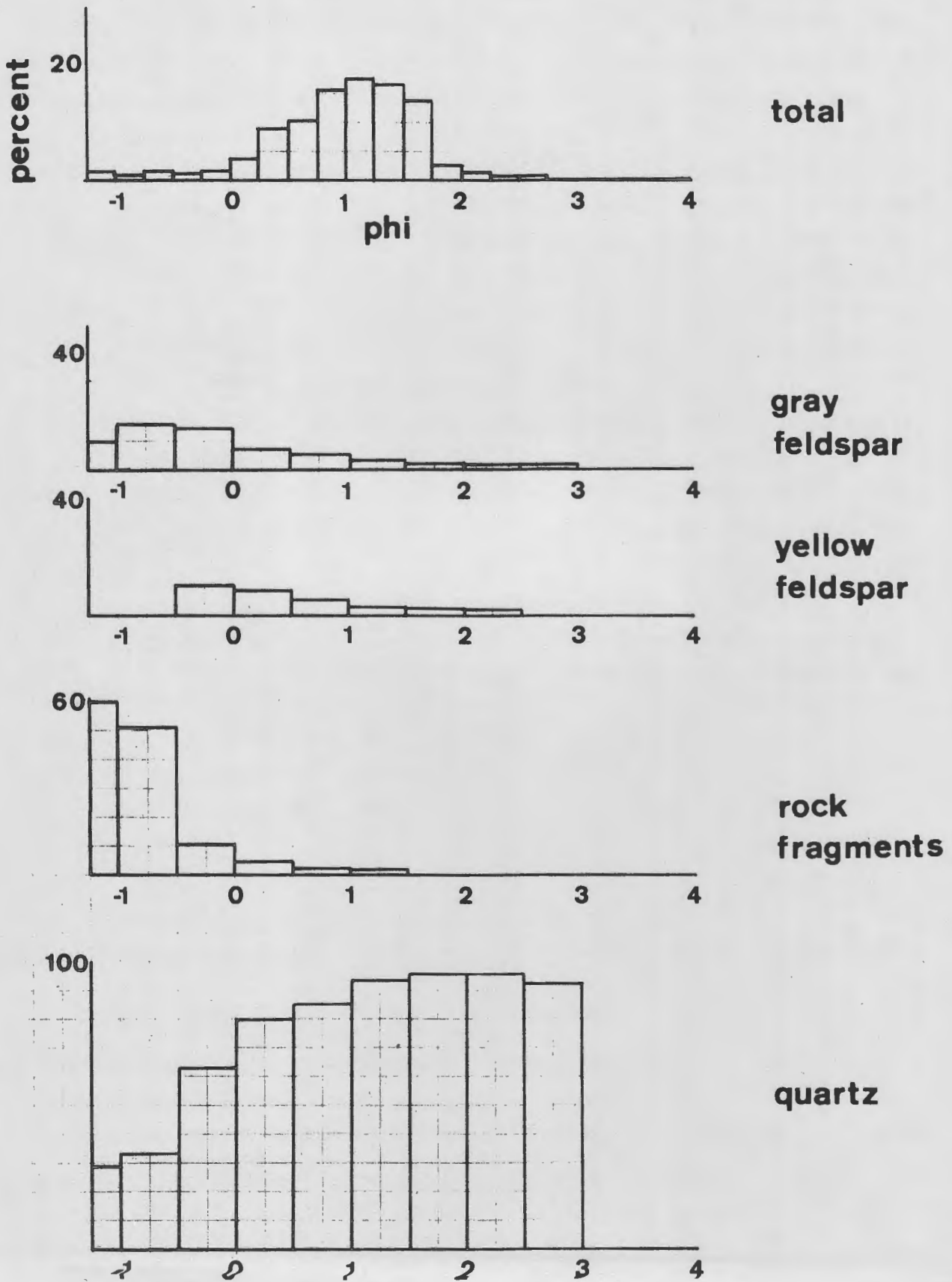


FIGURE 6

## DIAGNOSTIC PRIMARY STRUCTURES OF ESTUARINE SAND BODIES

Miles O. Hayes

Jon C. Boothroyd

Albert C. Hine

**Abstract:** Estuarine sand bodies assume complex morphologies in response to multidirectional tidal currents and wave action. Studies in eight New England estuaries show, however, that the major forms are repetitive from estuary to estuary and that they display diagnostic suites of primary structures.

Sand accumulation around the seaward margin of the major inlets takes the form of ridge-and-runnel systems and recurved spits attached to the barrier beaches, large swash bars offshore, and submerged ebb-dominated sand sheets. Wave-generated flow over the intertidal bars creates an abundance of large-scale (up to 20 ft. thick), planar crossbeds oriented landward.

Tidal deltas inside the inlets consist mainly of sand flats covered with flood-oriented sand waves [ $>20$  ft. wave lengths ( $\lambda$ )]. Margins of the deltas (ebb shields and ebb spits) contain predominantly ebb-oriented megaripples ( $\lambda = 2-20$  ft.) which produce festoon crossbedding. In places, the deltas are cut by spillover lobes formed by ebb currents. Thus, zones of flood dominance are differentiated from zones of ebb dominance by distinct differences in scale and type of crossbedding formed.

Major tidal channels are floored with large sand waves that may be ebb- or flood-oriented or bidirectional, depending on relation of bottom topography to current flow.

With respect to primary structures, a preserved regressive sequence of estuarine sand bodies would begin with large-scale, bimodal crossbedding at the base that would grade upward into broad zones of flood-oriented, planar crossbeds interfingering with linear zones of small-scale, ebb-oriented festoon crossbeds. The sequence would be capped by burrowed sand (clam flats), mud (mud flats), and peat (salt marsh).

## FORMS OF SAND ACCUMULATION IN ESTUARIES

Miles O. Hayes

Abstract: Studies in eight New England estuaries reveal the occurrence of several distinct forms of sand accumulation in each estuary. The most common types are ebb deltas (subdivided into swash bars, ebb sand sheets, and submarine lunate bars), flood deltas (made up of clam flats, spillover lobes, ebb shields, ebb spits, and sand flats covered with flood-oriented sand waves), channel-bottom sand wave fields, mid-channel bars and point bars. Smaller forms, such as sand waves [wave length ( $\lambda$ ) = >20 ft.], megaripples ( $\lambda$  = 2-20 ft.), and asymmetric ripples ( $\lambda$  = < 2 ft.), abound on the surfaces of these features. Four factors: time-velocity asymmetry of tidal currents, topographic shielding, vertical position with reference to mean low water, and residual ebb currents in major channels, are the primary controls of the type, abundance, and orientation of these smaller bed forms on the larger sand bodies.

Of major importance is the prominence of flood currents as sand-transporting agents. Most of the intertidal sandy areas are dominated by flood-formed features; therefore, the dominant transport direction is landward with resultant infilling of the estuaries from barrier beaches and/or offshore sources.

HYDRAULIC CONDITIONS CONTROLLING  
THE FORMATION OF ESTUARINE BEDFORMS

Jon C. Boothroyd

**Abstract:** Bedforms in estuaries form in response to complex variations in flow conditions. The sequence of bedforms formed under increasing strengths of flow in the lower flow regime is: linear ripples, lunate-linguoid ripples, sand waves, linear megaripples, scour-megaripples, and planed-off megaripples. Bedforms formed under upper flow regime conditions are rare. Crossbedding formed by bedform migration also changes in form with change in flow conditions, varying from small-scale festoon, to planar, to large-scale festoon crossbedding under increasing flow strengths.

INTRODUCTION

Flume experimentation has shown that bedforms in alluvial channels change in response to variations in slope, depth, velocity, and other variables. Flow conditions were first divided into upper and lower flow regimes by Simons, Richardson, and Albertston (1961), and a sequence of bedforms was described for increasing strengths of flow (Table 1 and Fig. 1). A summary of data on Colorado State flume experiments can be

TABLE 1. CLASSIFICATION OF FLOW REGIME  
(from Simons, Richardson, and Nordin, 1965, p. 36)

Flow Regime	Bed Form	Mode of Sediment Transport	Type of Roughness	Phase Relation Between Bed & Water Surface
Lower Regime	Ripples	Discrete Steps	Form Roughness Predominates	Out of Phase
	Ripples on Dunes			
Transition	Dunes		Variable	
	Washed out Dunes			
Upper Regime	Plane Beds Antidunes Chutes & Pools	Continuous	Grain Roughness Predominates	In Phase

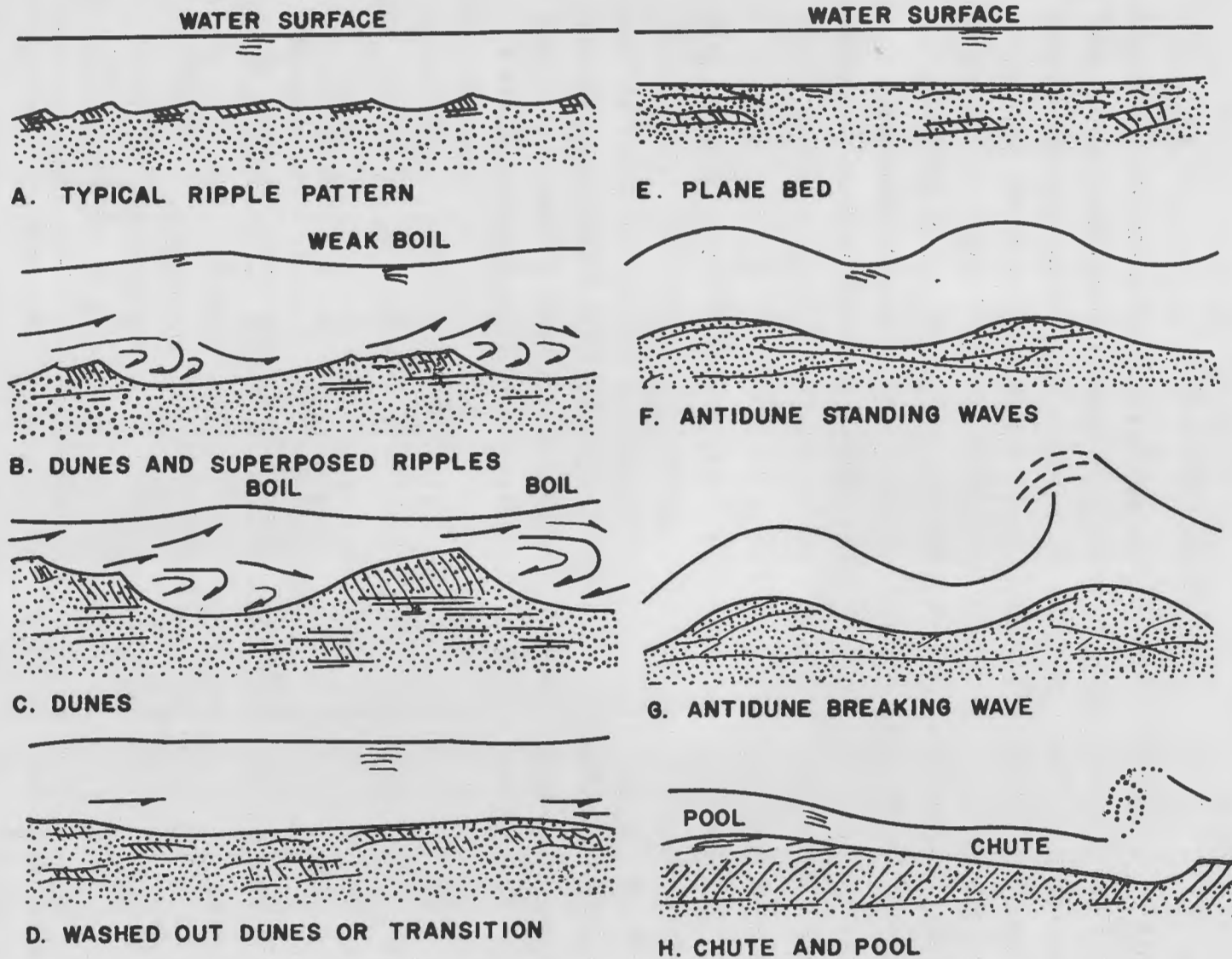


**FIGURE I**

found in Guy, Simons, and Richardson (1966).

An interpretation of flow conditions in estuaries can be made by study of intertidal and subtidal bedforms. Harms and Fahnestock (1965) set the major precedent for interpretation of stream power and flow regime through analysis of bedforms in their study on the Rio Grande.

Perhaps the main problem is projecting flume data to the field is the size of the flume in which the original experiment was done. A small flume does not allow a bedform to develop fully in its third dimension, width, and limited heights of sidewalls do not allow a large range of depths of flow. The most realistic simulation of real conditions has been at Colorado State University, in a large flume that measures 150 feet long by 8 feet wide and allows flow depths of as much as two feet. But even this large flume is not wide enough and does not have enough flow depth to develop fully what Simons and Richardson (1962) term "bars" and what our Coastal Research Group calls "sand waves".

#### BEDFORM TYPES

Both linear and lunate-linguoid ripples are found in northern New England estuaries (Figs. 2 and 3). Harms (1969) shows that linear ripples develop in response to lower strengths of flow than do lunate-linguoid ripples. Liu (1957) indicates that at the beginning of bedload movement linear ripples form first and then break into a lunate-linguoid pattern almost at once. Most estuarine ripples are lunate-linguoid, especially those associated with higher flow regime bedforms.

Most estuarine megaripples ( $\lambda = 2$  to 20 ft.) in the study area have a well-developed scour pit in front of the slip face and hence are termed "scour-megaripples". The bedforms that Simons and Richardson (1962) call dunes are scour-megaripples in our classification. Dunes formed in smaller flumes tend to extend from sidewall to sidewall and are incomplete forms of a fully developed scour-megaripple.

In northern New England estuaries, sand waves ( $\lambda = > 20$  feet)

---

Figure 1. Sequence of bedforms with increase in flow regime conditions. From Simons and Richardson (1962).



FIGURE 2

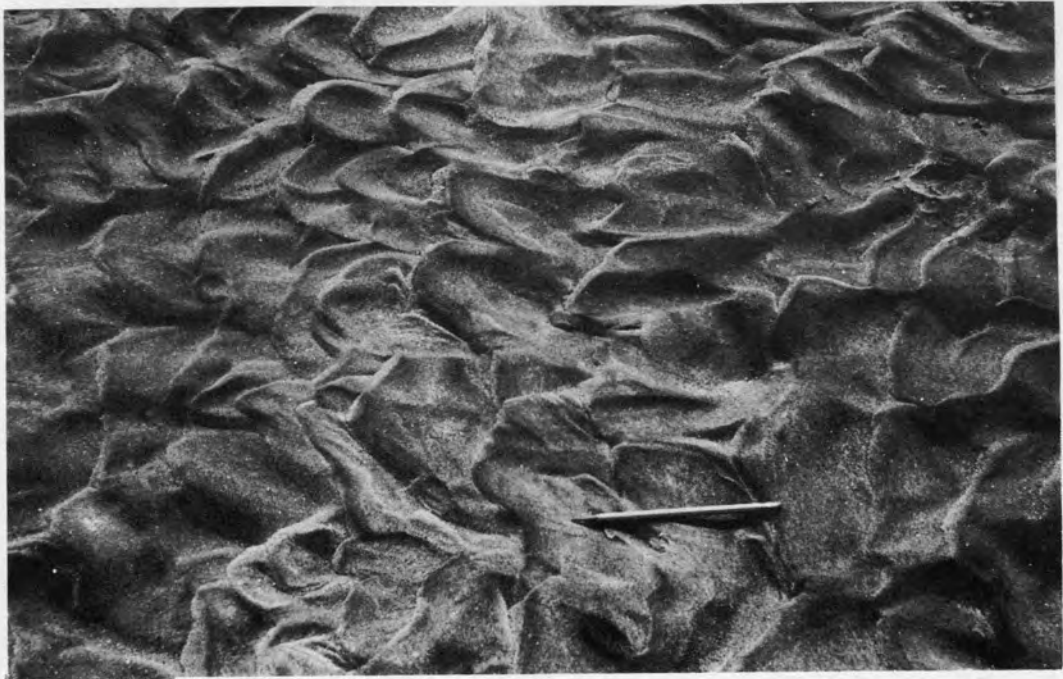


FIGURE 3

exist in areas of deeper water and lower flow velocities than scour-megaripples and thus form at lower Froude values. Sand waves tend to have straight to somewhat sinuous crests with well-developed lunate-linguoid ripples on their backs. Sand waves commonly have no pits in front of their slip faces but they do tend to develop shallow scour pits at times of higher velocity flow, for example, during spring tides. Crests also tend to become more sinuous in response to greater flow strengths.

With the above ideas in mind, one can classify strengths of flow in the lower flow regime on the basis of 3-dimensional bedforms. Table 2 and Figures 4 and 5 present some preliminary data on strengths of flow versus large-scale bedform type. Scour-megaripples are formed under greater strengths of flow ( $F_r = .36$ ) and sand waves under lower strengths ( $F_r = .22$ ), but both under "dune" conditions in the sequence of Simons and others. Megaripples with linear crests occur in some localities under special flow conditions, but they are not common. They are interpreted as having formed during flow conditions intermediate between scour-megaripples and sand waves. Transition bedforms are found in areas of higher flow strengths (p.121, this guidebook), but upper flow regime bedforms are rare in estuaries. Upper flow regime bed configurations will be discussed in sections of this guidebook dealing with the beach environment.

#### CROSSBEDDING

Lunate-linguoid ripples form small-scale festoon crossbedding; in a cut horizontal to the bedding surface, troughs can be seen that can be used as an indicator of current direction (Fig. 6). Crossbedding in linear ripples is poorly defined and interpretation is a problem.

---

Figure 2. Linear ripples on the upper part of the Hampton tidal delta, Hampton Harbor estuary. These ripples developed in response to very low energy flood tidal currents.

Figure 3. Lunate-linguoid ripples on a small sand flat at the south end of Plum Island. The ripples are ebb-oriented, having developed in shallow water during late-stage draining of the sand flat.

TABLE 2. HYDRAULIC FLOW CONDITIONS FOR SAND WAVE AND MEGARIPPLE FIELDS. MEASUREMENTS TAKEN DURING TIDAL CYCLE OBSERVATIONS, AUGUST, 1968, BY HAYES, GREER, AND BOOTHROYD. NOTE THE FROUDE NUMBER DIFFERENCES FOR FLOOD AND EBB FLOW OVER THE SAND WAVES, AND CONTINUING HIGH FROUDE VALUES AS THE MEGARIPPLES ARE UNCOVERED.

BEDFORM	AVG. $\lambda$ (FT.)	AVG. AMP. (FT.)	CURRENT VELOCITY (FT/SEC)	DEPTH (FT.)	FROUDE NUMBER	TIDE STAGE	TIME OF MEASUREMENT
Sand waves	38.0	1.15	3.05	5.8	0.22	Flood	Mid-flood
			1.50	8.0	0.094	Ebb	1.5 hr. past high tide
Megaripples	7.6	.77	2.99	2.8	0.32	Flood	Mid-flood
			3.81	5.5	0.29	Ebb	2.0 hrs. past high tide
			3.29	2.6	0.36	Ebb	Mid-ebb
			1.67	0.8	0.33	Ebb	4.0 hrs. past high tide

Sand-wave migration forms planar crossbedding of greater amplitude than that generally formed by scour-megaripples. However, this crossbedding is extremely difficult to see in the field. Tentatively, then, "dune" crossbedding type can be correlated with flow regime in the following manner. With increasing strength of flow, "dune" crossbedding goes from planar to a combination of planar and festoon. At still greater strengths of flow, scour-megaripples decrease in amplitude, increase in wavelength, and form concave slip faces (see p. this guidebook). At this stage of flow (upper part of lower flow regime), well-developed festoon crossbedding is formed (illustrated by Figures 17-7 and 17-8, p. 121, this guidebook).

#### CONCLUSIONS

A sequence of bedforms and crossbedding types can be correlated with increasing strength of flow. Harms and Fahnestock (1965, Plate 1) give a general sequence of bedforms and crossbedding formed with increase in flow regime. Figure 7 of this paper is a further refinement of that sequence for lower flow regime bedforms and crossbedding. In addition, estuarine depositional environments where the different bedforms occur are indicated in the summary diagram (Fig. 7).

Figure 4. Sand waves on the central clam flat, Essex estuary. These bedforms are flood-oriented with wavelengths of 30 to 50 feet. Note the well-developed lunate-linguoid ripples on the backs of the sand waves.

Figure 5. Megaripples on the Plum Island ebb spit. The megaripples show an ebb orientation. Note the well-developed scour pits and fair linearity of crests.

Figure 6. Small-scale festoon crossbedding formed by lunate-linguoid ripples (ebb-oriented) on a sand flat at the south end of Plum Island. Cut is horizontal to bedding surface. Current direction is from upper-left center to lower-right center of the photograph.

Figure 7. Sequence of bedforms and crossbedding with increasing strengths of flow in the lower flow regime. Based on work by the Coastal Research Group, University of Massachusetts, in New England estuaries. Some depositional environments in the estuary where each bedform may occur are indicated.



FIGURE 4



FIGURE 5

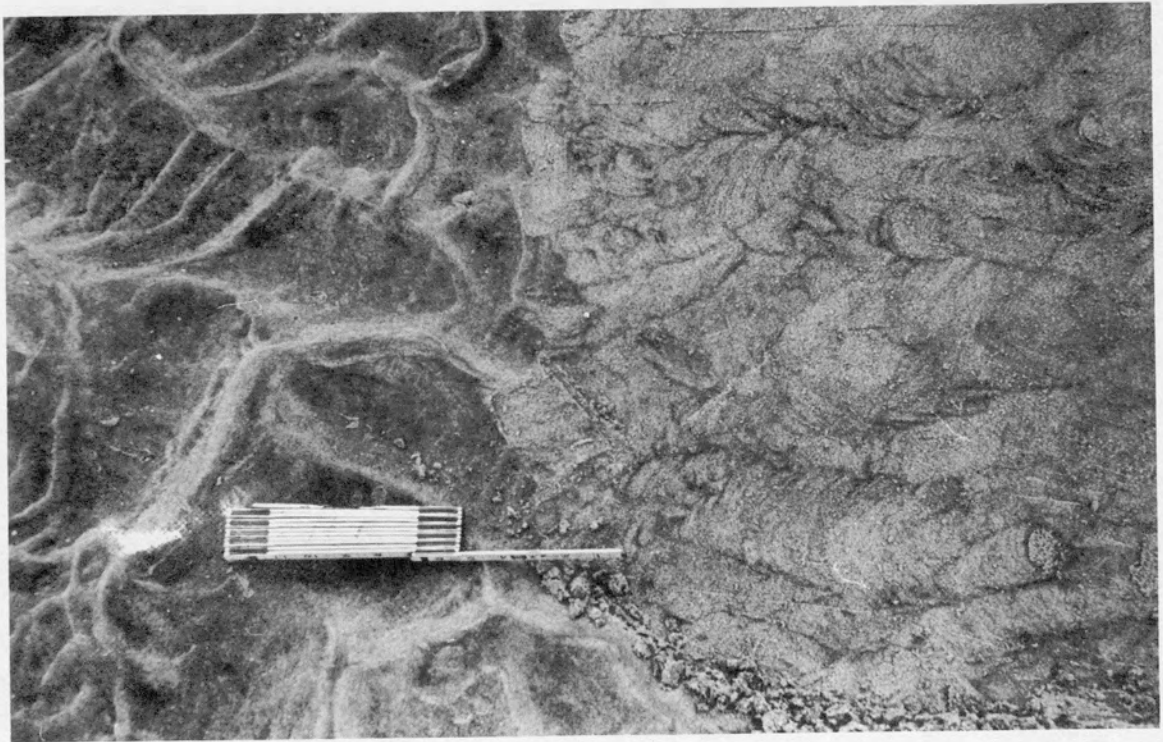


FIGURE 6

## SEQUENCE OF BEDFORMS AND CROSSBEDDING IN THE LOWER FLOW REGIME

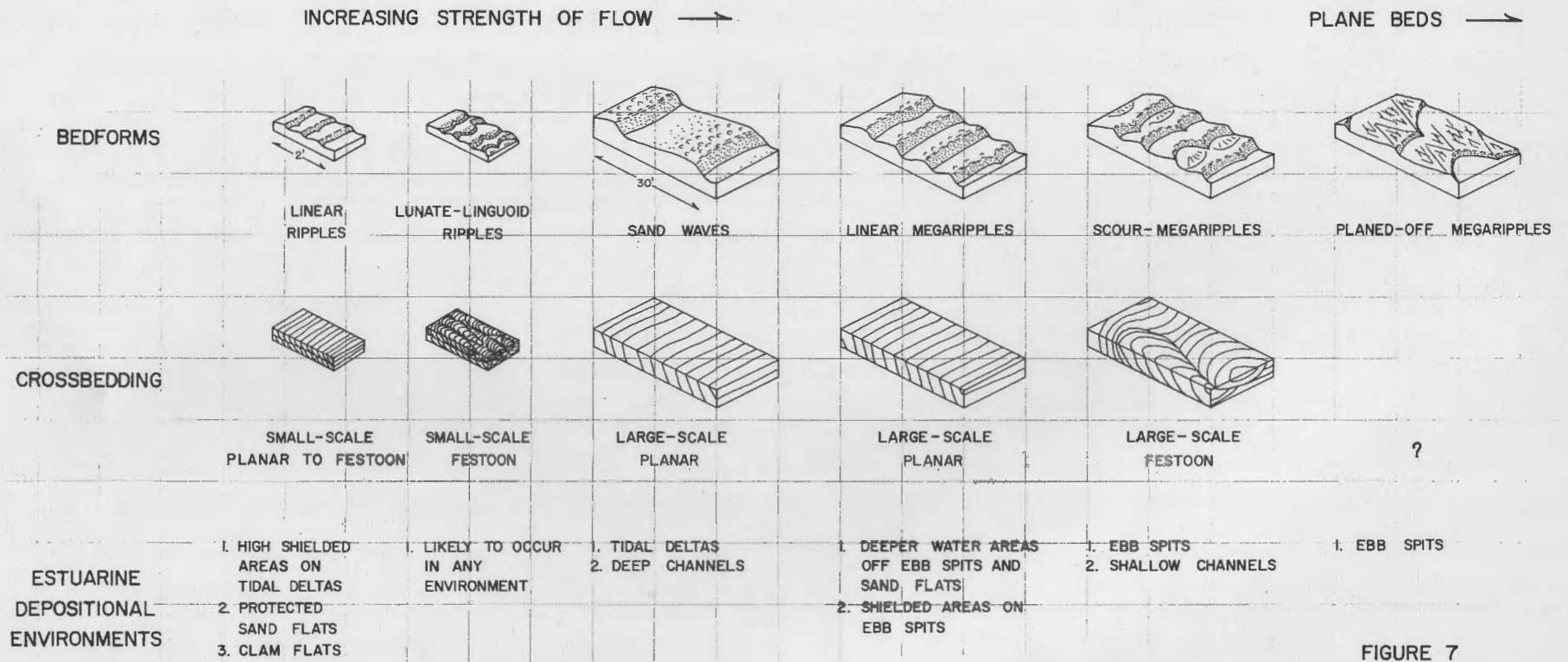


FIGURE 7

HOLOCENE STRATIGRAPHY OF THE MARSHES  
OF THE MERRIMACK RIVER ESTUARY,  
MASSACHUSETTS

Allan D. Hartwell

Abstract: A series of 17 cores from the marshes of the Merrimack River estuary reveals a general stratigraphic sequence from top to bottom of: (1) living high salt marsh dominated by Spartina patens, (2) high salt marsh peat, (3) sandy to muddy low salt marsh peat with abundant roots of Spartina alterniflora, (4) gray silty to sandy intertidal facies believed to be analogous to the clam-flat and tidal-channel sediments in the present estuary, and (5) black peat composed of fresh- to brackish-water plant material. As early as 6000 B.P. an offshore barrier island was present in the vicinity of Plum Island. Fine-grained sediment accumulated behind the island in an open bay environment with a fringing fresh- to brackish-water marsh. With rising sea-level, these sand-flat and mud-flat sediments transgressed landward over the black peat. About 3000 B.P. the rate of sea-level rise decreased enough to allow the fringing S. alterniflora marsh to accrete seaward over the open bay sediments. Once the marshes grew above the intertidal zone, high salt marsh plants such as S. patens were able to establish themselves. As a result of this regression of marsh deposits, the original open bay environment was transformed into the present marsh system with tidal channels and islands.

INTRODUCTION

Recent work by McIntire and Morgan (1963) and McCormick (1968) has revealed many details of the marsh morphology, Holocene stratigraphy, and sea-level changes in the marshes of the Plum Island, Massachusetts, area south of the Plum Island River Bridge (see Fig. 4 of Plum Island Marsh paper by McCormick in this guidebook). Because little work has been done on the marshes of the Merrimack River estuary, in August, 1968, the author undertook a study of the structure and Holocene stratigraphy of the Salisbury, Woodbridge Island, Newbury, and Town Creek marshes (Figs. 3-5). This paper is a summary of the data obtained from 17 cores and 458 probe rod stations.

Using an aluminum rod 3.3 M. (10 ft.) long, all of the marshes were probed to determine peat thickness and to locate potential coring sites. A total of 17 cores, 5cm. in diameter and averaging 2.5 M. in length, were obtained with a piston coring rig similar to that used by McCormick (1968). Details of core lithology are shown in Figures 1 and 2 (for core locations refer to Figs. 3 to 5).

#### MARSH STRATIGRAPHY

The Holocene stratigraphy of the Merrimack marshes is similar to that observed by McCormick (1968) in the Parker River area. Almost everywhere the marsh is topped by a zone of living high salt marsh, dominated by S. patens. This layer is generally underlain by a thick deposit of high salt marsh peat. In most of the cores this grades into a sandy to muddy low-salt marsh peat with abundant roots of S. alterniflora. Many of the cores bottomed in a gray silty to sandy intertidal facies believed to be analogous to the clam-flat and tidal-channel sediments in the present estuary. Cores H, I, O, and P (Figs. 1 and 2) all had layers of dark brown to black peat believed to be deposited by fresh- to brackish-water plants. This peat is analogous to that found under the Parker River Marshes (McCormick, 1958, p. 66) and in many of the New England marshes (Bloom, 1964; Davis, 1910; Johnson, 1925; McIntire and Morgan, 1963; and Redfield and Rubin, 1962). All workers agree that this peat represents an accumulation of fresh- to brackish-water sedge-type plants, deposited in the zone of transition from salt marsh to normal highland vegetation at or very near mean high water level. The base of core C consisted of 50 cm of blue-gray clay believed to be intertidal tide-channel sediment. McIntire and Morgan (1963) and McCormick (1968) found late Pleistocene glaciomarine blue clay below the Parker River marshes but because of limited coring capability the author was unable to confirm its

---

Figure 1. Lithology of cores A-I. Locations for these cores are given on Figures 3 and 4.

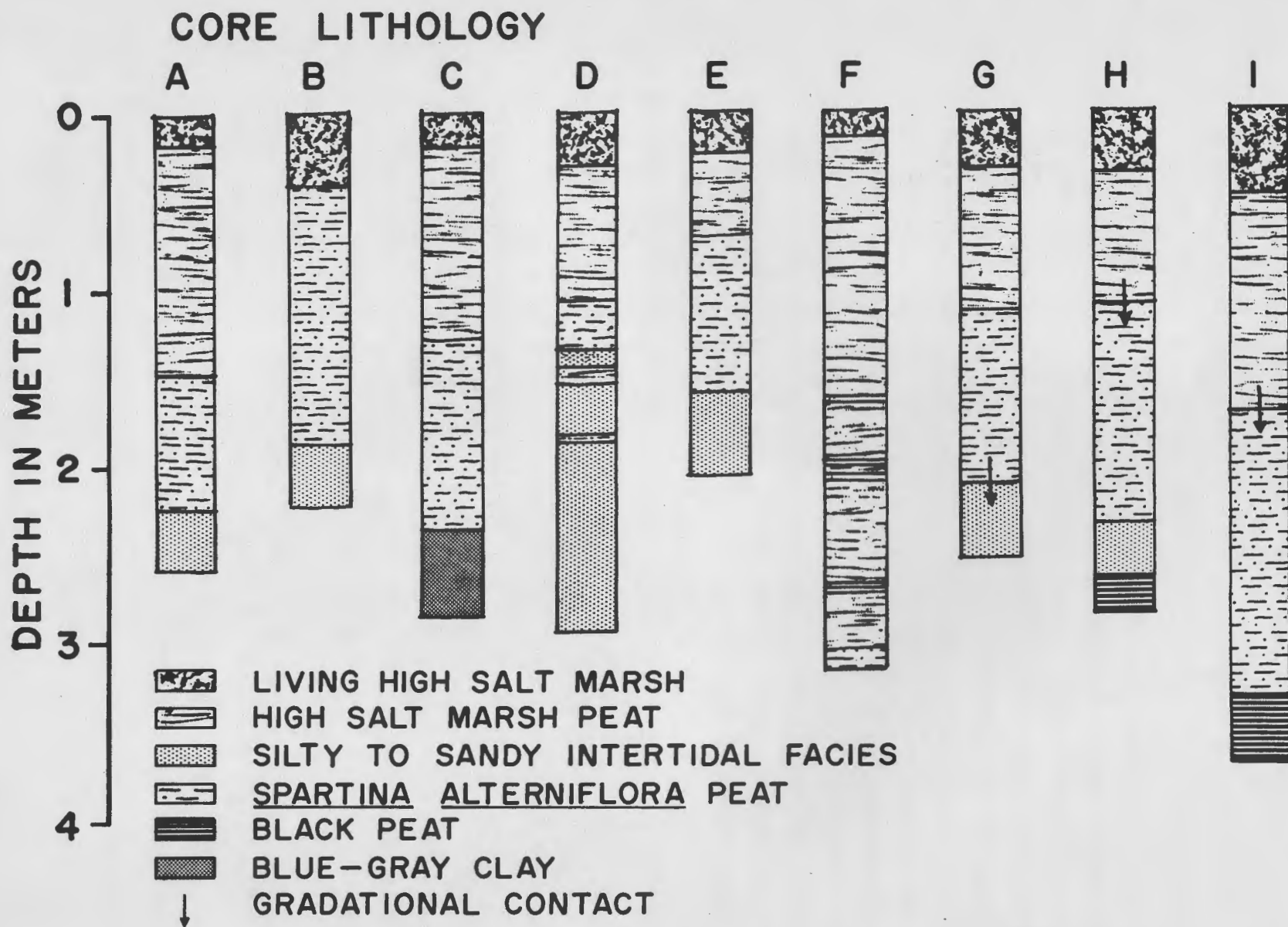


FIGURE 1

presence here.

#### PALEOGEOGRAPHY OF THE LOWER ESTUARY

The observed stratigraphy is evidence of a gradual marine transgression and rising sea-level since about 6300 B.P. According to McIntire and Morgan (1963), the blue clay was deposited during late Pleistocene in an estuarine area at or near sea level. By 10,500 years B.P., the ice had retreated and the land was rebounding more rapidly than sea level was rising. About 7500 B.P. the land reached its maximum uplift while sea level reached maximum regression. By 6300 B.P. the land began to subside and the sea started transgressing over the glaciomarine blue clay. Apparently the black peat was deposited as a time-transgressive unit in response to relative sea-level rise. At about 3000 years B.P. a marked decrease in the rate of sea-level rise occurred along much of the New England coast (McIntire and Morgan, 1963, and Bloom and Stuiver, 1963). Since then sea-level appears to have reached stillstand while crustal downwarping in the Plum Island area continues at a rate of about 9.1 cm. per century (McIntire and Morgan, 1963).

As early as 6000 B.P. an offshore barrier island was present in the vicinity of Plum Island. Fine-grained sediment accumulated behind the island in an open bay environment with a fringing fresh- to brackish-water marsh along the landward margin. With the gradual marine transgression the gray silty to sandy intertidal facies overlapped the fringing black peat, but sedimentation was unable to keep pace with submergence. At approximately 3000 B.P. the rate of sea level rise changed such that the marsh sediments encroached over the open bay deposits. This accreting marsh sequence consists of S. alterniflora peat at the base and S. patens peat at the top (see Figs. 6 and 7). This interpretation is in agreement with that of Bloom (1968) for the marshes of Connecticut, Redfield (1965) for the Barnstable, Massachusetts, marsh, and McCormick (1968)

---

Figure 2. Lithology of cores J-Q. Locations for these cores are given on Figures 3, 4, and 5.

# CORE LITHOLOGY

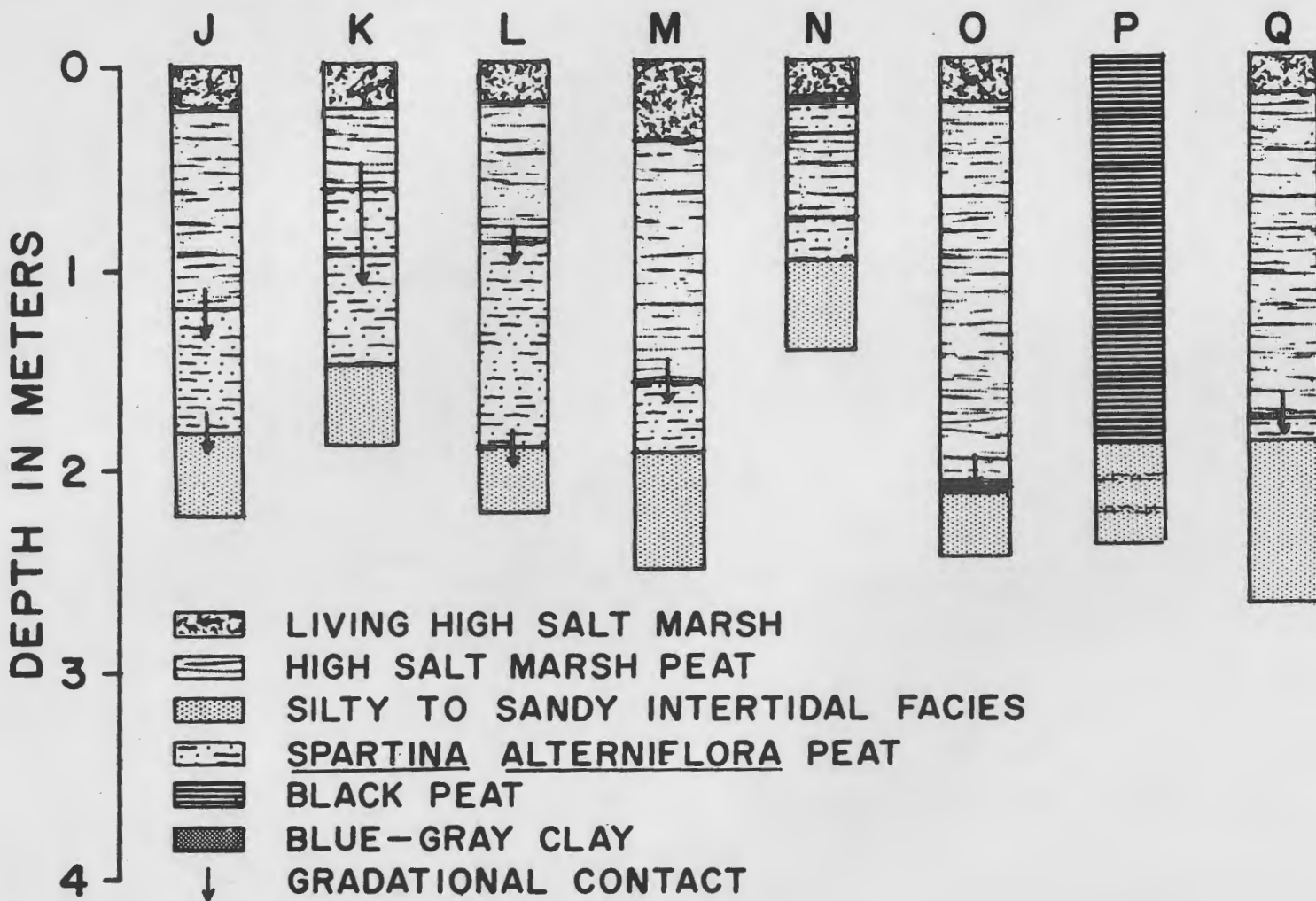


Figure 3. Peat isopach map of Salisbury marsh. Note bedrock pinnacles in the northwest and the thickest peat extending northeast to southwest.

Figure 4. Peat isopach map of Newbury marsh. Note sand body under north end of Woodbridge Island.

Figure 5. Peat isopach map of Town Creek marsh. Note abundant bedrock outcrops of Newburyport Quartz Diorite and thick fresh- to brackish-water peat.

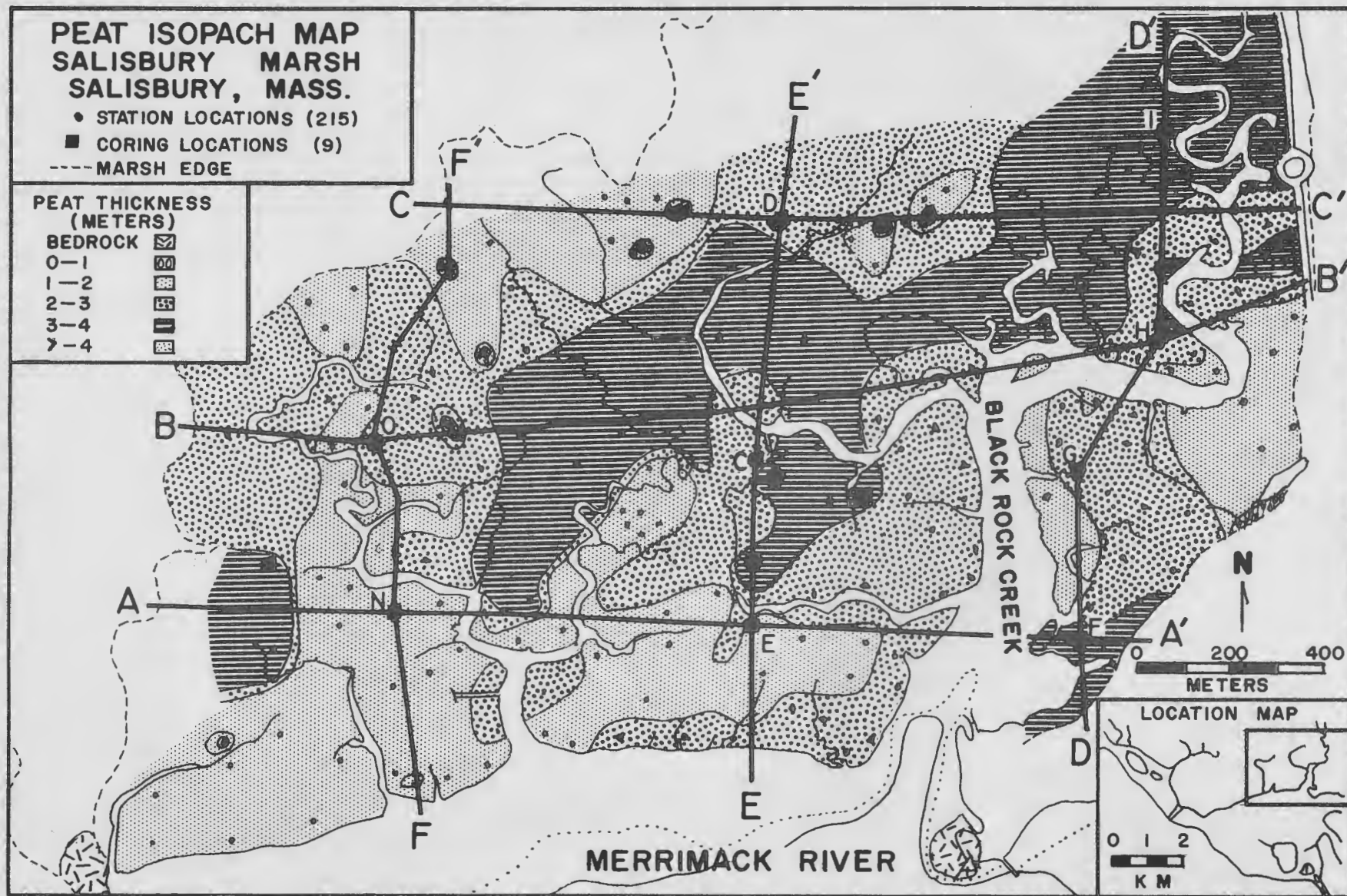


FIGURE 3

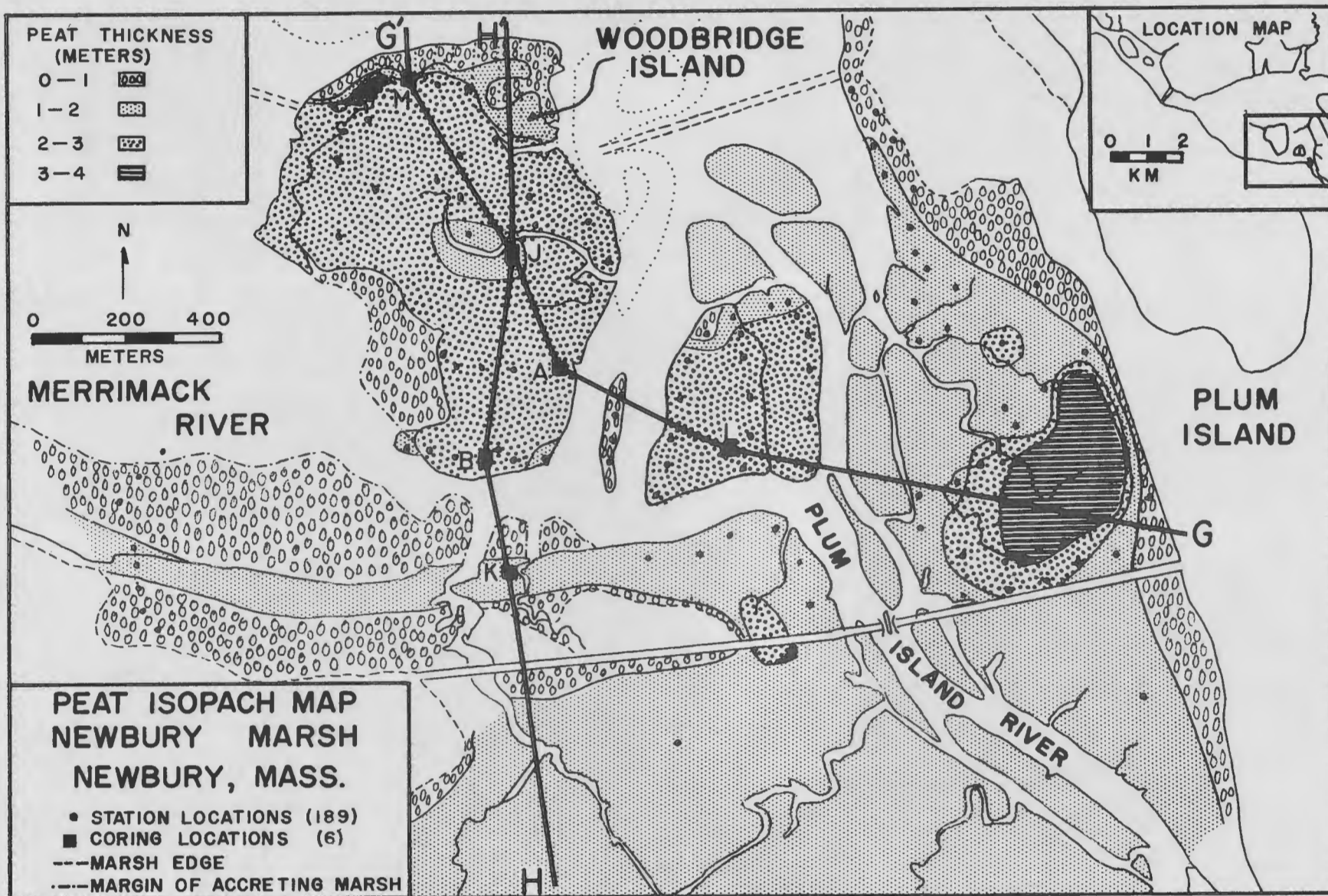


FIGURE 4

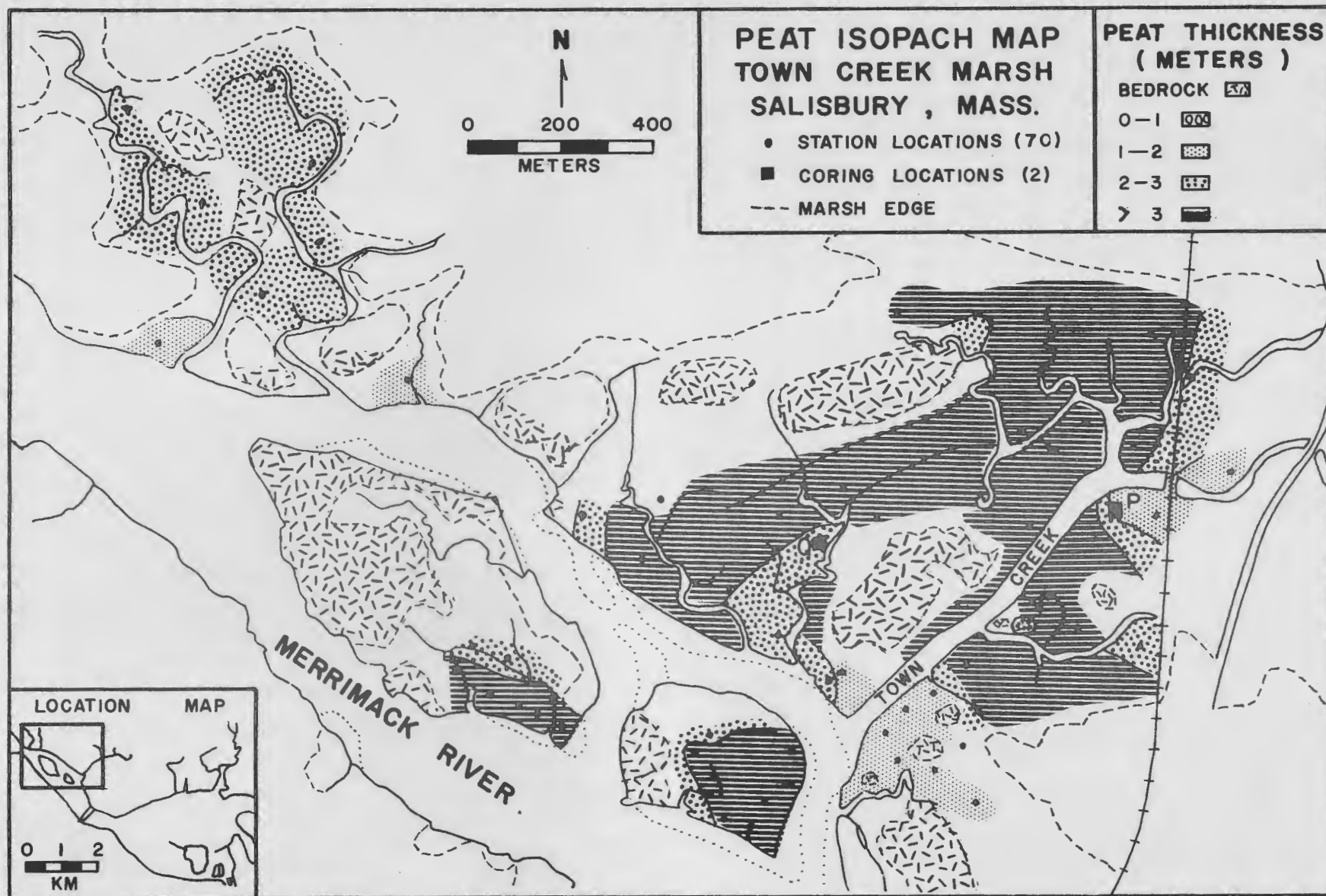


FIGURE 5

for the marshes of the Parker River.

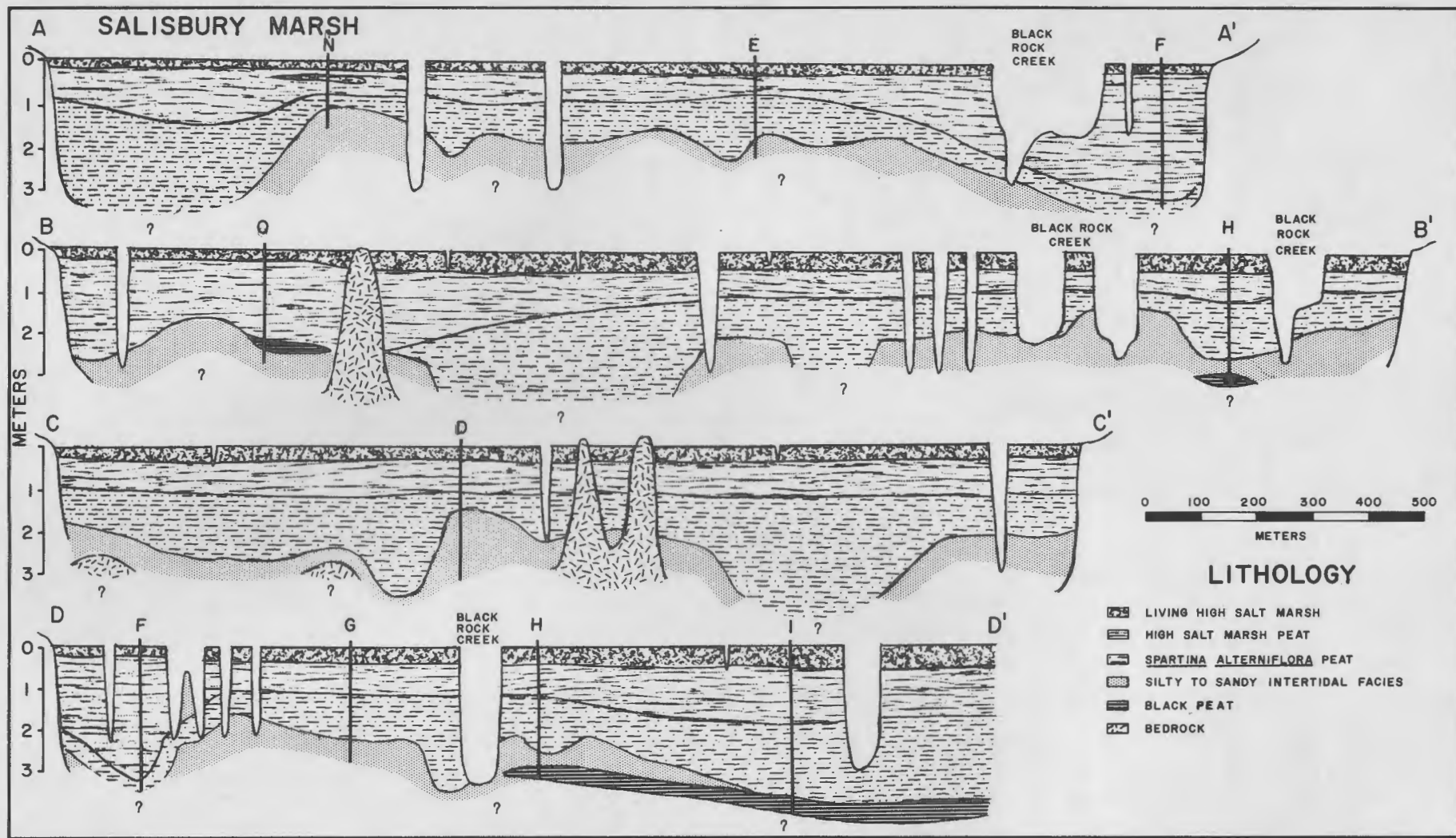
Details of the geometry of the marsh deposits are revealed in peat isopach maps (Figs. 3-5) and in stratigraphic cross sections (Figs. 6 and 7). In Salisbury Marsh (Fig. 3), a belt of peat 3-4 M thick extends from the northeast across most of the marsh, nearly parallel to a series of bedrock pinnacles in the northwest. Cores H and I bottom in black peat of the fringing fresh- to brackish-water marsh facies while most of the other cores bottom in the silty to sandy intertidal facies (Figs. 1 and 2). Core H reveals the general transgressive Holocene stratigraphy of black peat overlain by the intertidal facies and the S. alterniflora to S. patens marsh sequence. The presence of the silty to sandy intertidal facies under most of the S. alterniflora peat suggest that the latter did not develop until the sand- and mud-flats of the former open bay environment built up to mid-tide level about 3000 B.P. This interpretation is in agreement with Bloom (1968) for the marshes of Connecticut.

A similar stratigraphic sequence is evident in the Newbury marsh (Figs. 4 and 7). The thickest peat is west of Plum Island. At the south end of Woodbridge Island high salt marsh peat is absent, reflecting rapid infilling of the existing channel. The north end of the Island is underlain by an elongate curving sand body (Fig. 23-1) composed of reworked glaciofluvial sediment similar to that found under the marshes south of the Plum Island Turnpike. Angular cobbles were unearthed in several holes and probe rod data suggest a possible bedrock pinnacle at depth. Origin of this sand mass is still uncertain. It could be either an old tidal delta complex built when the river mouth was further south than at present or a deposit of glaciofluvial material which was reworked into a curved spit complex by wave action as sea level rose.

The Town Creek marsh reveals a slightly different stratigraphy (Fig. 2). Much of the marsh is underlain by a thick peat section (Fig. 5),

---

Figure 6. Stratigraphic cross sections of the Salisbury marsh.



but this material is largely fresh- to brackish-water peat (Core P). This area has relatively little salt influence and only along the Merrimack channel is S. alterniflora abundant. These marshes are in an early stage of marine transgression.

#### CONCLUSION

The stratigraphy and geometry of the marsh deposits of the Merrimack River estuary are evidence of a gradual rise in sea level and accompanying marine transgression since late Pleistocene. A barrier island complex appeared in the vicinity of Plum Island as early as 6000 B.P. (McIntire and Morgan, 1963). Fine-grained sediment accumulated behind the island in an open bay environment with a fringing fresh- to brackish-water marsh. With rising sea level the gray silty to sandy intertidal facies overlapped the fringing black peat, but sedimentation was unable to keep pace with submergence. About 3000 B.P. the rate of sea-level rise slowed down enough to allow sediment accumulation in the open bay and the fringing S. alterniflora marsh was able to accrete seaward. Once the marshes grew above the intertidal zone, high salt marsh species such as S. patens were able to establish themselves. As a result of this regression of marsh deposits, the original open bay environment was transformed into the present marsh system with tidal channels and islands.

---

Figure 7. Stratigraphic cross sections of the Salisbury and Newbury marshes.

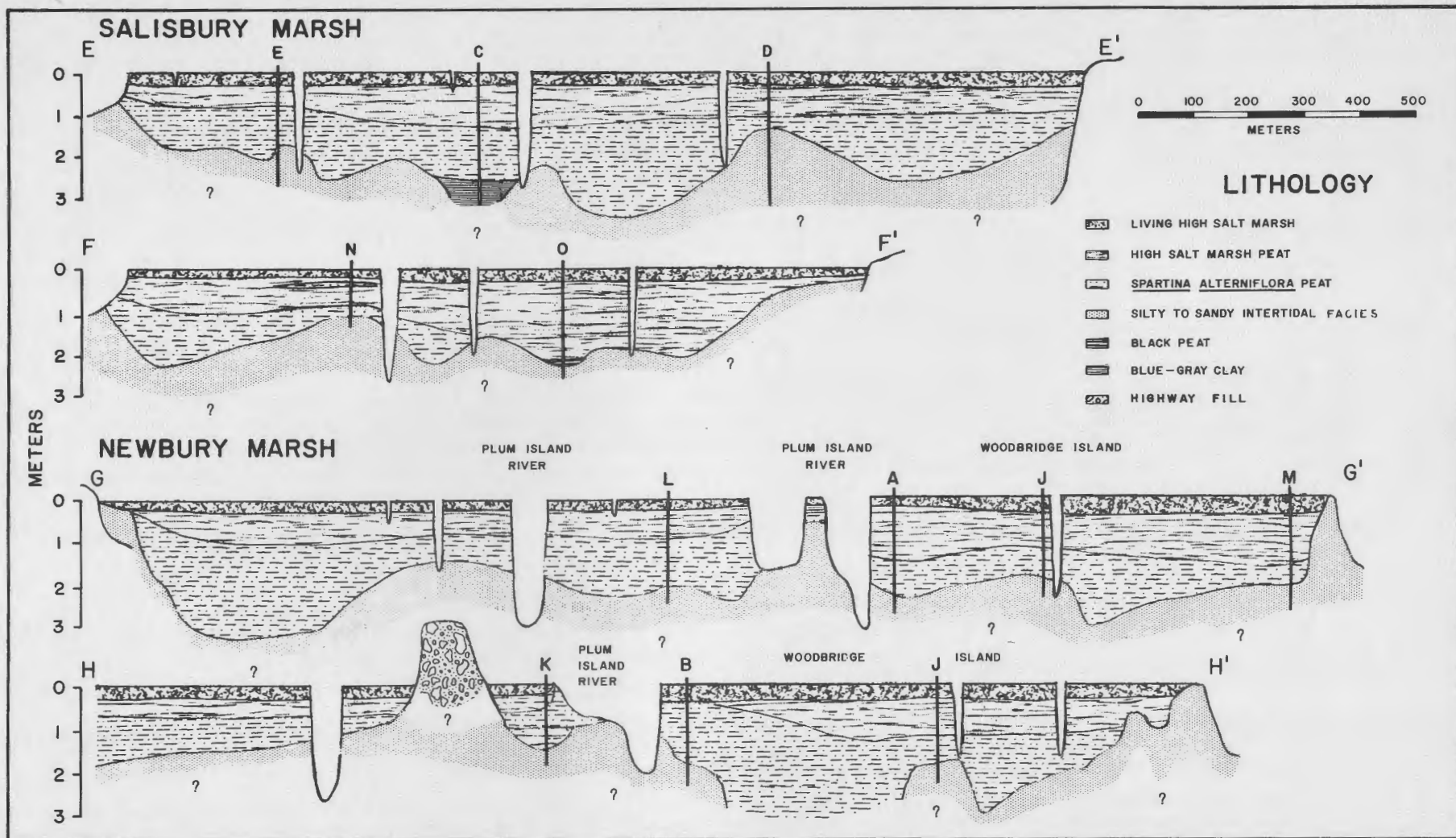


FIGURE 7

GLOSSARY OF PRIMARY SEDIMENTARY STRUCTURES  
OF THE INTERTIDAL ZONE

Fayez S. Anan  
Stewart C. Farrell  
Miles O. Hayes  
Sharon A. Greer

The 18 photographs in this compilation were selected to demonstrate the complexity of primary sedimentary structures that can develop in the intertidal zone. Photographs were taken by various members of the Coastal Research Group. These photographs do not represent all the structures present in this area.

The terminology presented here, which has been developed by the Coastal Research Group, is tentative.

1. Antidunes in a runnel outlet. Second wave from left is breaking. Current from right to left. At station PLB, Plum Island, April, 1966.
2. Antidunes on low-tide terrace formed by the return of wave uprush. Notice the extremely wide low-tide terrace. At Hampton Beach, N. H., July, 1968.
3. Swash marks on beach face at station PLA, Plum Island, January, 1966.
4. Rhomboid ripples. Current from left to right. Scale is one foot long, August, 1968.
5. Rhomboid marks on a ridge surface. At Small Point Beach, Maine, October, 1965.
6. Grain lineation in the swash zone oriented perpendicular to the coast line. Formed under upper flow-regime sheet flow. This feature corresponds to parting-plane lineation found in many ancient sediments.
7. Scour around a small pebble on the low-tide terrace producing isolate imbrication. Note the grain lineation (right) and the bird-foot print (upper left). Current from right to left. At station PLB, Plum Island, June, 1968.
8. Ladder-back ripples in the intertidal zone. They formed as a result of a shift in current direction during different stages of the tide. At Nauset Beach, Massachusetts, August, 1968.
9. Ladder-back ripples formed on a mid-channel bar in the Blackwater River channel of the Hampton Harbor estuary, N. H. The larger ripple set, oriented toward the bottom of the photographs,

was formed by ebb currents. The smaller, superimposed set was formed by waves generated by strong northwesterly winds (from the right).

10. Wave-generated, asymmetric ripples in a runnel outlet. At station PLB, Plum Island, 1966.
11. Rill marks formed at base of beach face by seeping ground water during low tide. At Seabrook, N. H., July, 1966.
12. Ladder-back ripples. The larger ridges are wave-generated ripples. As the tide receded, water flowed parallel to the large ripple crests, producing the smaller set. Late stage wave action planed-off the ripple tops. At Crane Beach, August, 1966.
13. Rill marks formed at base of beach face by seeping ground water during low tide. At station PLD, Plum Island, March, 1966.
14. Rill marks near base of beach face. Note the micro-deltas formed by rill drainage into the runnel. At station PLB, Plum Island, February, 1968.
15. Ebb-oriented crossbedding in scour-megaripples formed on the ebb spit at the southern end of Plum Island. Scale is one foot. August, 1968.
16. Ebb-oriented megaripples. Wave length is six to eight feet. From Hampton Harbor, N. H., bridge, November, 1965.
17. Lunate-linguoid ripples. Current flowing toward the bottom of the picture. Photographed in a drainage channel on the sand flat at the southern end of Plum Island, July, 1968.
18. Ripples of granule-sized sand moving over foredune crossbedding exposed by erosion during a northeaster. Rod is five feet long. Plum Island, winter, 1965.



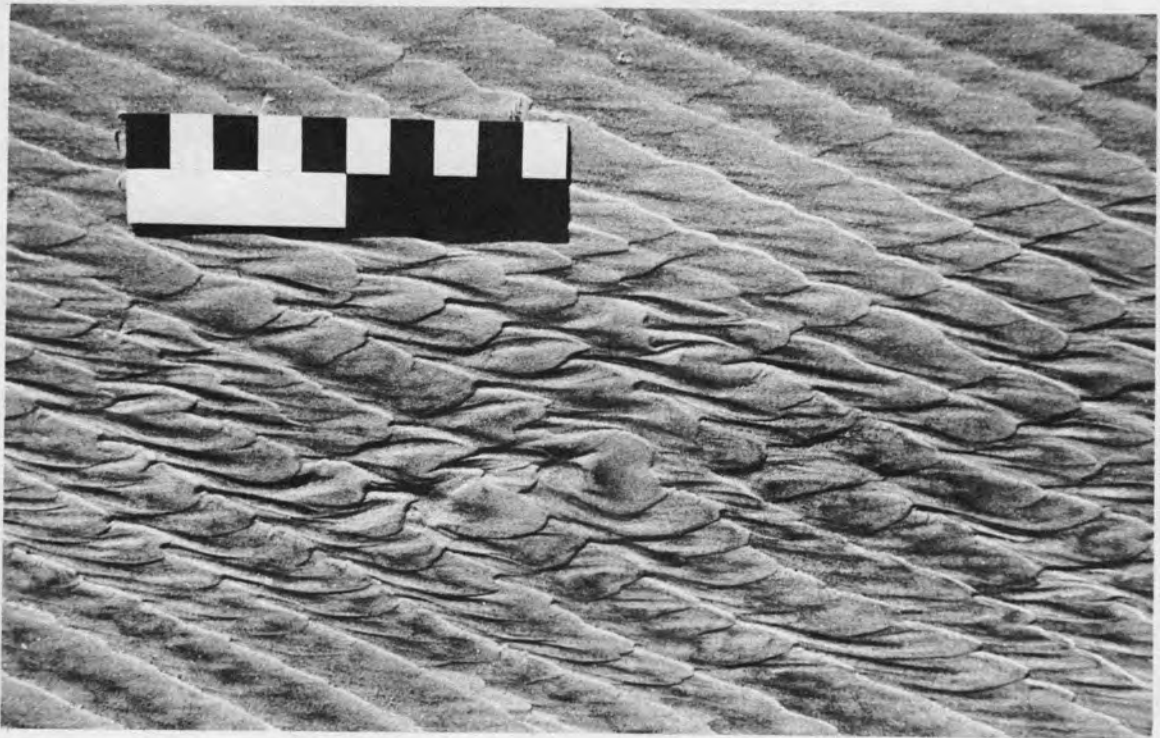
1



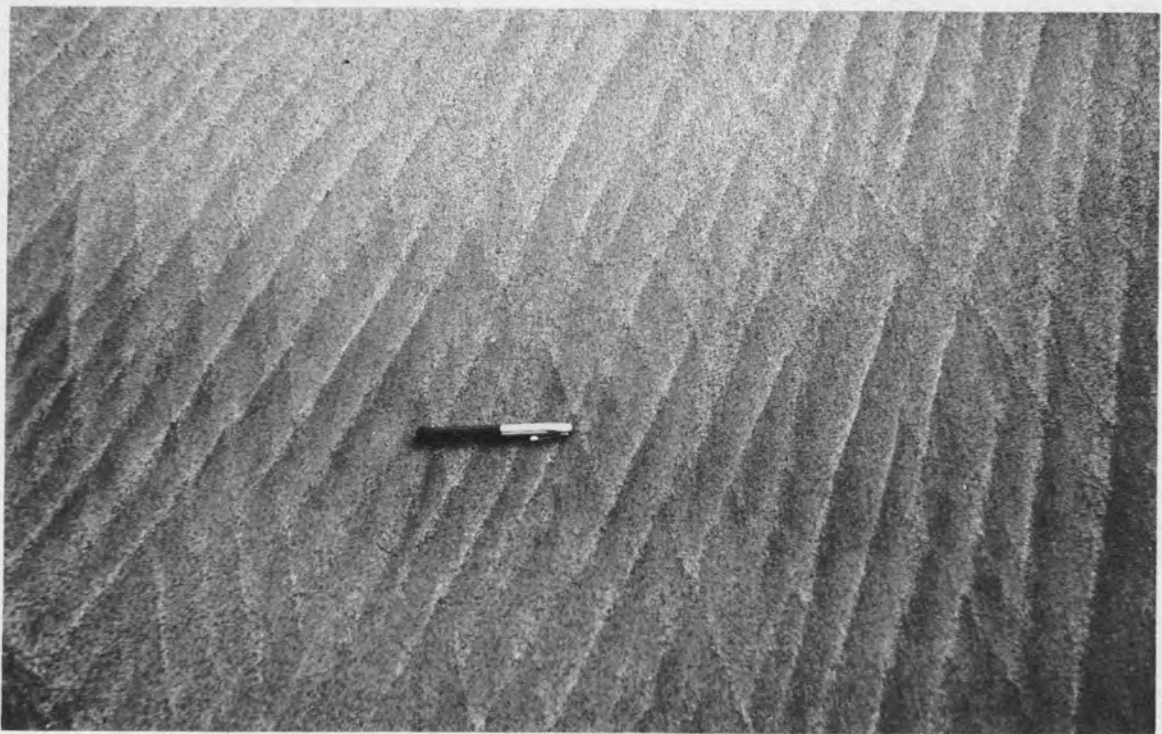
2



3



4



5



6



7

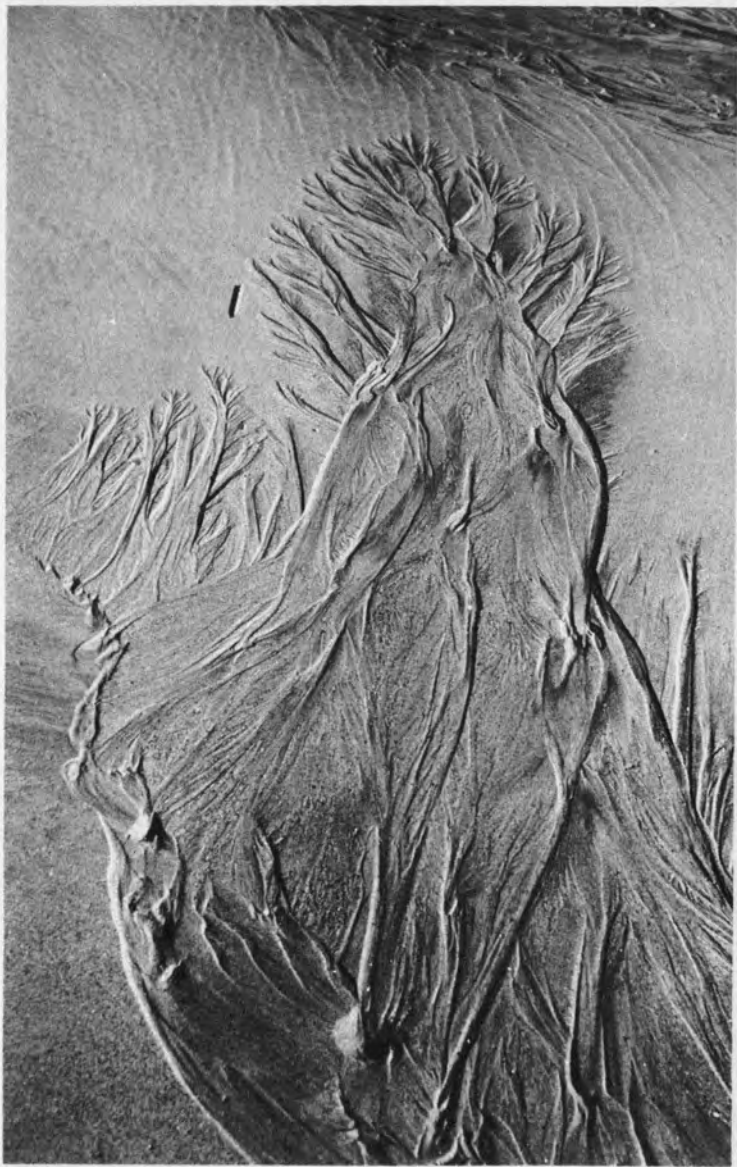


8



9

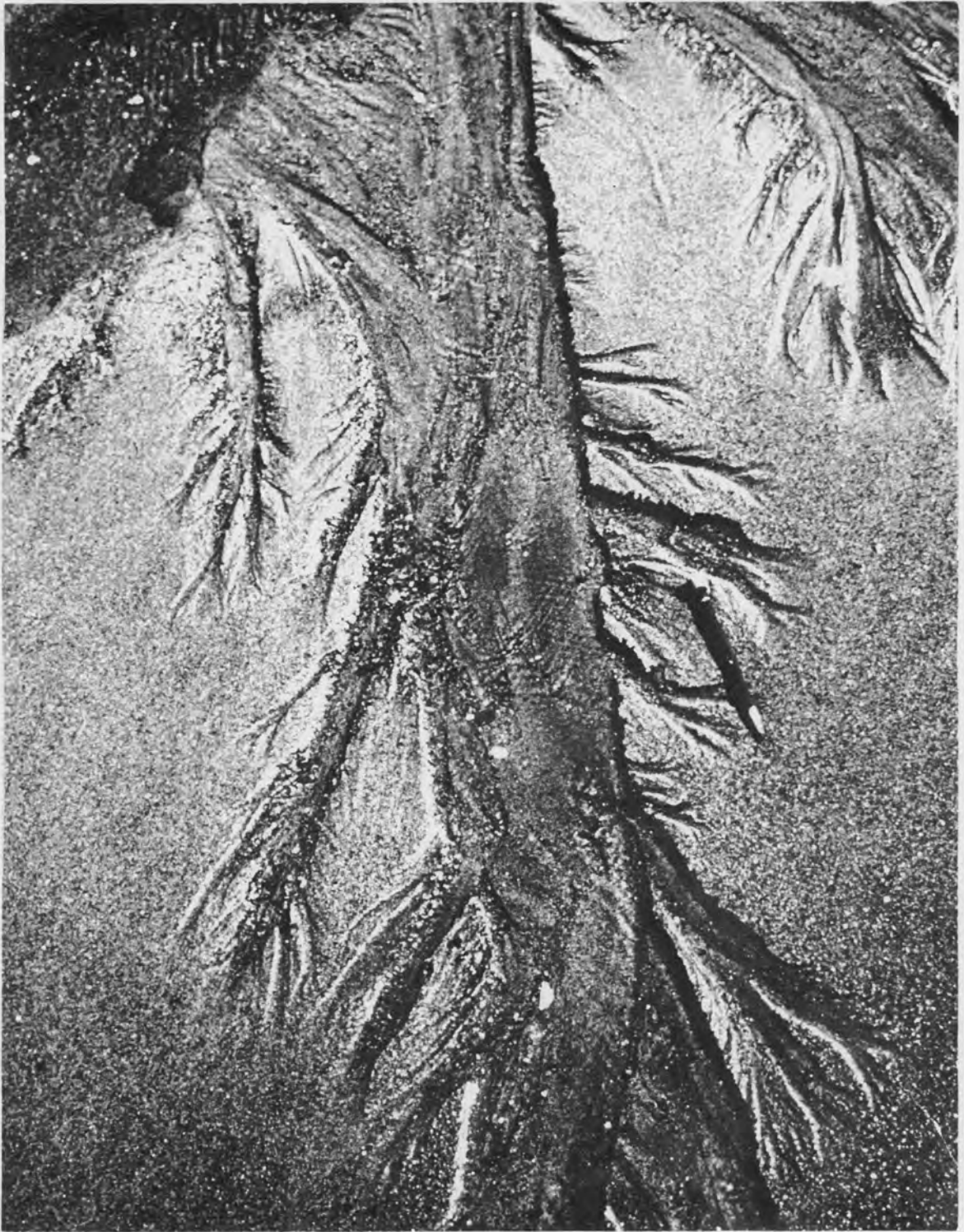




11



12



13



14



15







18

## GLOSSARY OF TERMS

Because of the ambiguity of some of the terminology applied to coastal features, and because of the uniqueness of some of the features found in this area, it has been necessary for us to establish a working system of nomenclature. These terms are very tentative at the present time; we are open to suggestions for improvements.

### Beach Features

Berm: A linear sand body parallel to the shore that occurs on the landward portion of the beach profile. It has a triangular cross-section with a horizontal to slightly landward-dipping top surface and a more steeply-dipping seaward surface. This definition incorporates the berm and the beach face in Wiegell's (1953) classification.

Beach face: The seaward-dipping face of the berm. The zone ordinarily traversed by the uprush and backrush of waves as the tide rises and falls.

Berm crest: Point of intersection between the beach face and the top surface of the berm.

Neap berm: A berm formed with its crest near the neap high-water mark. It forms very rapidly, within a few tidal cycles, during neap tide. It usually appears as a secondary linear feature in the middle of the beach face.

Ridge-and-runnel system: Combination of a swash bar (in terminology of King, 1961) and a trough that develops between the landward-dipping slip face of the bar and the beach face. The ridge is a tabular body of sand that develops on the low-tide terrace during constructional periods.

Berm-ridge: A modified ridge that develops characteristics of a berm on its seaward margin. This normally happens during neap tides (see example in Figure 19-11).

Low-tide terrace: Broad flat area located seaward of the beach face. Its boundaries are a topographic break at the base of the beach face (zone where water table intersects beach profile) and mean low water (MLW).

Beach face terrace: Broad, gently sloping terrace that connects the middle to upper portion of the normal beach face with some point on the low-tide terrace.

### Bedforms

The sequence of bedforms that develop under conditions of increasing flow regime are:

Ripples: Asymmetric bedforms formed by unidirectional flow. Wavelength less than two feet.

Lunate-linguoid ripples: Asymmetric bedforms with both slip faces and scour pits concave down current.

Sand waves: Wavelength greater than twenty feet.

Megaripples: Wavelength between two and twenty feet.

Linear-megaripples: Megaripples with straight crests.

Scour-megaripples: Megaripples with undulatory to cusped crests and well-developed scour pits in front of the slip faces.

Plane beds: Flat bedding surface upon which parallel laminations are deposited.

Antidunes: Symmetrical trochoid-shaped bedform in phase with water surface. Produce low-angle, bi-directional crossbedding.

### Tidal deltas

Flood-tidal delta: Sediment accumulation formed inside an inlet by flood-tidal currents.

Ebb-tidal delta: Sediment accumulation seaward of a tidal inlet. Deposited by ebb-tidal currents.

Ebb spit: Spit formed in an estuary as a result of ebb currents. Commonly found attached to the borders of flood-tidal deltas.

Ebb shield: Topographically high rim or margin around a sand body that protects portions of the sand body from modification by ebb-currents.

Spillover lobe: Following the definition of Ball (1967), a lobate ridge of sediment formed by unidirectional currents. The most common examples in the field trip area are formed by ebb currents cutting through ebb-shielded areas.

## REFERENCES CITED

- Allen, J. R. L., 1966, On bed forms and paleocurrents: *Sedimentology*, v. 6, p. 153-190
- Bagnold, R. A., 1940, Beach formation by waves; some model experiments in a wave tank: *Jour. Inst. Civil Engineers*, v. 15, p. 27-52
- \_\_\_\_\_, 1954, *The physics of blown sand and desert dunes*: London, Methuen Limited, 265 p.
- Ball, M. M., 1967, Carbonate sand bodies of Florida and the Bahamas: *Jour. Sed. Petrology*, v. 37, p. 556-591
- Blatt, H., 1959, Effect of size and genetic quartz type on sphericity and form of beach sediments, northern New Jersey: *Jour. Sed. Petrology*, v. 29, p. 197-206
- Bloom, A. L., 1960, Late Pleistocene changes of sea level in southwestern Maine: *Maine Geol Survey*, 143 p.
- \_\_\_\_\_, 1964, Peat accumulation and compaction in a Connecticut coastal marsh: *Jour. Sed. Petrology*, v. 34, p. 599-603
- \_\_\_\_\_, 1968, Postglacial stratigraphy and morphology of central Connecticut, p. A-1-1 - A-1-7, in Orville, P. M., Editor, *Guidebook for field trips in Connecticut*, New England Intercollegiate Geological Conference, 305 p.
- Bloom, A. L., and Stuiver, M., 1963, Submergence of the Connecticut coast: *Science*, v. 139, p. 332-334
- Bluck, B. J., 1967, Sedimentation of beach gravels: Examples from South Wales: *Jour. Sed. Petrology*, v. 37, p. 128-156
- Blumenstock, D. I., Fosberg, F. R., and Johnson, C. G., 1961, The re-survey of typhoon effects on Jaluit Atoll in the Marshall Islands: *Nature*, v. 189, p. 618-620
- Byrne, V., 1966, Artificial processes vs. natural processes at Hampton Beach, New Hampshire: Class report for Coastal Processes, Geology 756, Univ. of Mass., 21 p. (unpublished)
- Chapman, V. J., 1960, *Salt marshes and salt deserts of the world*: London, Interscience Publishers, 392 p.
- Chappell, J., 1967, Recognizing fossil strand lines from grain-size analysis: *Jour. Sed. Petrology*, v. 37, p. 157-165
- Chute, N. E., and Nichols, R. L., 1941, *Geology of Northeastern Massachusetts*: Mass. Dept. Public Works and U. S. Geol. Survey Cooperative Geology Project, Bull. 7, 48 p.
- Currier, J. J., 1902, *History of Newbury, Massachusetts*: Newbury, Mass. (Copy available at the public library in Newburyport)
- Davis, C. A., 1910, Salt marsh formation near Boston and its geological significance: *Econ. Geol.*, v. 5, p. 623-639
- Doeglas, D. J., 1946, Interpretation of the results of mechanical analysis: *Jour. Sed. Petrology*, v. 16, p. 19-40
- Duane, D. B., 1964, Significance of skewness in recent sediments, Western Pamlico Sound, North Carolina: *Jour. Sed. Petrology*, v. 34, p. 864-874
- Emery, K. O., 1955, Grain size of marine gravels: *Jour. Geology*, v. 63, p. 39-49
- Fleming, N. C., 1964, Tank experiments on the sorting of beach material during cusp formation: *Jour. Sed. Petrology*, v. 34, p. 112-122
- Folk, R. L., and Ward, W. C., 1957, Brazos River bar: A study in the significance of grain size parameters: *Jour. Sed. Petrology*, v. 27, p. 3-26
- Friedman, G. M., 1961, Distinction between dune, beach, and river sands from their textural characteristics: *Jour. Sed. Petrology*, v. 31, p. 514-529

- Gees, R. A., 1965, Moment measures in relation to the depositional environments of sands: *Eclogae Geol. Helv.*, v. 58, p. 209-213
- Guy, H. P., Simons, D. B., and Richardson, E. V., 1966, Summary of alluvial channel data from flume experiments, 1956-61: U. S. Geol. Survey Prof. Paper 462-I, 96 p.
- Hails, J. R., 1967, Significance of statistical parameters for distinguishing sedimentary environments in New South Wales, Australia: *Jour. Sed. Petrology*, v. 37, p. 1059-1069
- Harms, J. C., 1969, Hydraulic significance of some sand ripples: *Geol. Soc. America Bull.*, v. 80, p. 363-396
- Harms, J. C., and Fahnestock, R. K., 1965, Stratification, bed forms, and flow phenomena (with an example from the Rio Grande): p. 84-115 in Middleton, G. V., Editor, *Primary sedimentary structures and their hydrodynamic interpretation*, Soc. Econ. Paleontologists and Mineralogists Spec. Pub. 12, 265 p.
- Harms, J. C., MacKenzie, D. B., and McCubbin, D. G., 1963, Stratification in modern sands of the Red River, Louisiana: *Jour. Geology*, V. 71, p. 566-580
- Harris, S. A., 1959, The mechanical composition of some intertidal sands: *Jour. Sed. Petrology*, v. 29, p. 412-424
- Hayes, M. O., 1965, Sedimentation in a semiarid wave-dominated coast (South Texas) with an emphasis on hurricane effects: Ph. D. thesis, Univ. of Texas, 350 p. (unpublished)
- \_\_\_\_\_, 1967, Hurricanes as geological agents - case studies of Hurricanes Carla, 1961, and Cindy, 1963: Report of Investigations no. 61, Bureau of Economic Geology, Univ. of Texas, Austin, Texas, 54 p.
- Haven, D. S., and Morales - Alamo, R., 1969, Biodeposition as a factor in estuarine sedimentary processes: Abstracts with programs for 1969, part 4, Southeastern Section, 18<sup>th</sup> Annual Meeting, Geol. Soc. America, p. 33
- Inman, D. L., 1952, Measures for describing the size distribution of sediments: *Jour. Sed. Petrology*, v. 22, p. 125-145
- Inman, D. L., and Chamberlain, T. K., 1955, Particle-size distribution in nearshore sediments: in Hough, J. L., and Menard, H. W., Editors, *Finding ancient shorelines*, Soc. Econ. Paleontologists and Mineralogists Spec. Pub. 3, p. 106-129
- Jerome, W. C., Jr., Chesmore, A. P., Anderson, C. O., Jr., and Grice, F., 1965, A study of the marine resources of the Merrimack River Estuary: Division of Marine Fisheries, Mono. Ser. no. 1, Mass. Div. Marine Fisheries, 90 p.
- \_\_\_\_\_, 1968, A study of the marine resources of the Parker River - Plum Island Sound Estuary: Division of Marine Fisheries, Mono. Ser. no. 6, Mass. Div. Marine Fisheries, 79 p.
- Johnson, D. S., and York, H. H., 1915, The relation of plants to tide levels: *Carnegie Inst. Wash.*, Publ. 206, 162 p.
- Johnson, D. W., 1925, *New England Acadian shoreline*: New York, John Wiley Co., 608 p.
- Jolliffe, I. P., 1964, An experiment designed to compare the relative rates of movement of different sizes of beach pebbles: *Proc. Geol. Assoc. London*, v. 75, p. 67-86
- Jopling, A. V., 1965, Hydraulic factors controlling the slope of laminae in laboratory deltas: *Jour. Sed. Petrology*, v. 35, p. 777-791

- Keulegan, G. H., 1948, An experimental study of submarine sand bars: Tech. Report no. 3, Beach Erosion Board, Department of the Army, Corps of Engineers, 40 p.
- Kidson, C., and Carr, A. P., 1959, The movement of shingle over the sea bed close inshore: *Geog. Jour.*, v. 125, p. 380-389
- King, C. A. M., 1961, *Beaches and coasts*: London, Edward Arnold Limited., 403 p.
- King, C. A. M., and Williams, W. W., 1949, The formation and movement of sand bars by wave action: *Geog. Jour.*, v. 113, p. 70-85
- Klein, G. deV., 1967, Paleocurrent analysis in relation to modern marine sediment dispersal patterns: *Am. Assoc. Petroleum Geologists Bull.*, v. 51, p. 366-382
- Krumbein, W. C., 1941a, The effect of abrasion on the size, shape and roundness of rock fragments: *Jour. Geology*, v. 49, p. 482-520
- \_\_\_\_\_, 1941b, Measurement and geological significance of shape and roundness of sedimentary particles: *Jour. Sed. Petrology*, v. 11, p. 64-72
- Krumbein, W. C., and Griffith, J. S., 1938, Beach environment in Little Sister Bay, Wisconsin: *Geol. Soc. America Bull.*, v. 59, p. 510-522
- Kuenen, Ph., 1956, Experimental abrasion of pebbles: 2. Rolling by current: *Jour. Geology*, v. 64, p. 336-368
- \_\_\_\_\_, 1964, Experimental abrasion: 6. Surf action: *Sedimentology*, v. 3, p. 29-34
- Landon, R. E., 1930, An analysis of beach pebble abrasion and transportation: *Jour. Geology*, v. 38, p. 437-446
- Lewis, M. V., 1931, The effect of wave incidence on the configuration of a shingle beach: *Geog. Jour.*, v. 78, p. 129-148
- Liu, H. K., 1957, Mechanics of sediment-ripple formation: *Jour. Hydraul. Div., Amer. Soc. Civil Eng. Proc.*, v. 83, No. HY2, p. 1-23
- Marshall, P., 1927, The wearing of beach gravels: *New Zealand Inst. Trans.*, v. 58, p. 507-532
- Mason, C. C., and Folk, R. L., 1958, Differentiation of beach, dune, and aeolian flat environments by size analysis, Mustang Island, Texas: *Jour. Sed. Petrology*, v. 28, p. 211-226
- McCormick, C. L., 1968, Holocene stratigraphy of the marshes at Plum Island, Massachusetts: Ph. D. thesis, Univ. of Mass., 104 p. (unpublished)
- McIntire, W. G., and Morgan, J. P., 1963, Recent geomorphic history of Plum Island, Massachusetts, and adjacent coasts: *Louisiana State Univ., Coastal Studies*, No. 8, 44p.
- Miller, W. R., and Egler, F. E., 1950, Vegetation of the Wequetequock - Pawcatuck tidal-marshes, Conn.: *Ecol. Monog.*, v. 20, p. 143-172
- Moiola, R. J., and Weiser, D., 1968, Textural parameters: An evaluation: *Jour. Sed. Petrology*, v. 38, p. 45-53
- Nichols, R. L., 1964, Northeastern Massachusetts geomorphology - Trip A, p. 3-40, in Skehan, S. J., Editor, *Guidebook to field trips in the Boston area and vicinity*, New England Intercollegiate Geological Conference, 120 p.
- Oldale, R. N., 1961, Late-glacial marine deposits in the Salem quadrangle, Massachusetts: *U. S. Geol. Survey Prof. Paper* 424-C, p. C-59
- Otto, G. H., 1939, A modified logarithmic probability graph for the interpretation of mechanical analysis of sediments: *Jour. Sed. Petrology*, v. 9, p. 62-76

- Postma, H., 1967, Sediment transport and sedimentation in the estuarine environment: p. 158-179, in Lauff, G. H., Editor, Estuaries, Amer. Assoc. for the Advancement of Science, Washington, D. C., 757 p.
- Price, W. A., 1963, Patterns of flow and channeling in tidal inlets: Jour. Sed. Petrology, v. 33, p. 279-290
- Pritchard, D. W., 1955, Estuarine circulation patterns: Am. Soc. Civil Engineers, Proc., 81, 717/1-717/11
- Redfield, A. C., 1965, Ontogeny of a salt marsh estuary: Science, V. 147, p. 50-55
- Redfield, A. C., and Rubin, M., 1962, The age of salt marsh peat and its relation to recent changes in sea level at Barnstable, Mass.: Proc. Nat'l. Acad. Sci., v. 48, p. 1728-1734
- Reineck, H. E., 1963, Sedimentgefüge im Bereich der südlichen Nordsee: Abhandl. Senckenberg, Naturforsch, Ges., 505, p. 1-136
- Reineck, H. E., Gutmann, W. F., and Hertweck, G., 1967, Das Schlickgebiet südlich Helgoland als Beispiel rezenter Schelfablagerungen: Senckenbergiana Lethaea, v. 48, p. 219-275
- Sammel, E. A., 1962, Parker and Rowley River basins: U. S. Geol. Survey, Massachusetts Basic-Data Rept. no. 4, Ground Water Series, 33p.
- \_\_\_\_\_, 1963, Surficial geology of the Ipswich quadrangle, Massachusetts: U. S. Geol. Survey Geol. Quad. Map GQ-189
- Schlee, J., Uchupi, E., and Trumbull, J. V. A., 1964, Statistical parameters of Cape Cod beach and eolian sands: U. S. Geol. Survey Prof. Paper 501-D, p. D118-D122
- Shepard, F. P., 1950, Longshore bars and longshore troughs: Tech. Mono. no. 15, Beach Erosion Board, Department of the Army, Corps of Engineers, 32, p.
- Shepard, F. P., and Young, R., 1961, Distinguishing between beach and dune sands: Jour. Sed. Petrology, v. 31, p. 196-214
- Simons, D. B., and Richardson, E. V., 1962, Resistance to flow in alluvial channels: Amer. Soc. Civil Eng. Trans., v. 127, p. 927-1006
- Simons, D. B., Richardson, E. V., and Albertson, M. L., 1961, Flume studies using medium sand (0.45 mm): U. S. Geol. Survey Water-Supply Paper 1498-A, 76 p.
- Simons, D. B., Richardson, E. V., and Nordin, C. F., Jr., 1965, Sedimentary structures generated by flow in alluvial channels: in Middleton, C. V., Editor, Primary sedimentary structures and their hydrodynamic interpretation; Soc. Econ. Paleontologists and Mineralogists Spec. Pub. 12, p. 34-52
- Sonu, C. J., McCloy, J. M., and McArthur, D. S., 1966, Longshore currents and nearshore topographies: Proc. of the Tenth Conference of Coastal Engineering, Tokyo, Japan, v. 1, p. 525-549
- Stoddart, D. R., 1962, Catastrophic storm effects of the British Honduras reefs and cays: Nature, v. 196, p. 515-515
- Udden, J. A., 1914, Mechanical composition of clastic sediments: Geol. Soc. America Bull., v. 25, p. 655-744
- U. S. Army Corps of Engineers, 1953, Beach erosion control study, Plum Island, Massachusetts: House Document no. 243, 41 p.
- \_\_\_\_\_, 1954, Beach erosion control study, Hampton Beach, New Hampshire: House Document no. 325
- \_\_\_\_\_, 1955, Beach erosion control study, shore of the state of New Hampshire: House Document no. 416
- \_\_\_\_\_, 1967, Small beach erosion control project, Plum Island, Massachusetts - preliminary study: Waltham, Massachusetts, Department of the Army, New England Division, Corps of Engineers, 53 p.

- U. S. Geological Survey, 1968, Water resources data for Massachusetts, New Hampshire, Rhode Island, Vermont - 1967: Water Resources Division, U. S. Geological Survey, Department of the Interior, 305 p.
- Van Andel, Th., Wiggers, A. J., and Maarleveld, G., 1954, Roundness and shape of marine gravels from Urk (Netherlands): a comparison of several methods of investigation: Jour. Sed. Petrology, v. 24, p. 100-116.
- Wentworth, C. K., 1929, Method of computing mechanical composition types in sediments: Geol. Soc. America., v. 40, p. 771-790
- Westgate, J. M., 1904, Reclamation of Cape Cod sand dunes: U. S. Department of Agriculture, Bur. Plant Ind., Bull. 65, 26 p.
- Wiegel, R. L., 1953, Waves, tides, currents and beaches - glossary of terms and list of standard symbols: Council on Wave Research, The Engineering Foundation, 113 p.
- \_\_\_\_\_, 1964, Oceanographic engineering: Englewood Cliffs, N. J., Prentice-Hall, 532 p.
- Wiesnet, D. R., and Cotton, J. E., 1967, Use of infrared imagery in circulation studies of the Merrimack River Estuary, Massachusetts: U. S. Geological Survey open-file report, 11 p., (reprinted as National Aeronautics and Space Administration Tech. Letter NASA - 78)
- Williams, G. E., 1968, Formation of large-scale trough cross-stratification in a fluvial environment: Jour. Sed. Petrology, v. 38, p. 136-140

